

Научном већу Института за физику у Београду  
Београд, 31. јануар 2017.

**ПРЕДМЕТ:**

**Молба за покретање поступка за стицање звања виши научни  
сарадник**

Молим Научно веће Института за физику да у складу са Правилником о поступку и начину вредновања и квантитативном исказивању научно-истраживачких резултата истраживача покрене поступак за мој избор у звање виши научни сарадник.

У прилогу достављам:

- Мишљење руководиоца пројекта са предлогом чланова комисије
- Биографске податке
- Преглед научне активности
- Елементе за квалитативну оцену научног доприноса
- Елементе за квантитативну оцену научног доприноса
- Списак објављених радова и њихове копије
- Податке о цитираности
- Фотокопију решења о претходном избору у звање
- Додатке

С поштовањем,  
др Ивана Васић

**ИНСТИТУТ ЗА ФИЗИКУ**

ПРИМЉЕНО: 19-01-2017			
Рад. јед.	б р о	Арх. шифра	Прилог
0801	48/1		

## Научном већу Института за физику у Београду

Београд, 19. јануар 2017. године

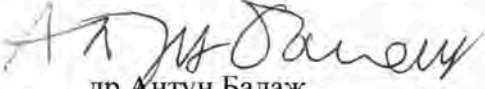
**Предмет: Мишљење руководиоца пројекта о избору др Иване Васић у звање виши научни сарадник**

Др Ивана Васић је запослена у Лабораторији за примену рачунара у науци, у оквиру Националног центра изузетних вредности за изучавање комплексних система Института за физику у Београду и ангажована је на пројекту основних истраживања Министарства просвете, науке и технолошког развоја Републике Србије ОН171017, под називом "Моделирање и нумеричке симулације сложених вишечестичних физичких система". На поменутом пројекту ради на темама везаним за проучавање ултрахладних квантних гасова. С обзиром да испуњава све предвиђене услове у складу са Правилником о поступку, начину вредновања и квантитативном исказивању научноистраживачких резултата истраживача МПНТР, сагласан сам са покретањем поступка за избор др Иване Васић у звање виши научни сарадник.

За састав комисије за избор др Иване Васић у звање виши научни сарадник предлажем:

- (1) др Антун Балаж, научни саветник, Институт за физику у Београду
- (2) др Милица Миловановић, научни саветник, Институт за физику у Београду
- (3) проф. др Зоран Радовић, дописни члан САНУ, редовни професор у пензији Физичког факултета Универзитета у Београду

Руководилац пројекта

  
др Антун Балаж  
научни саветник

## 2 БИОГРАФСКИ ПОДАЦИ КАНДИДАТКИЊЕ

Ивана Васић (девојачко Видановић) је рођена 1983. године у Јагодини, где је завршила основну школу. Као средњошколац била је Ђак Математичке гимназије у Београду. Школовање наставља на Физичком факултету Универзитета у Београду, где је студирала теоријску физику и стекла основну диплому 2006. године и мастер диплому 2007. године. Добитница је стипендије Краљевске Норвешке амбасаде у Београду, награде и стипендије "Проф. др Ђорђе Живановић" и награде "Проф. др Љубомир Тирковић" за најбољи дипломски рад из физике. Од стране Универзитета у Београду проглашена је за студента генерације Физичког факултета. У току 2007. године била је стипендиста Министарства науке Републике Србије. Докторску тезу под насловом "Нумеричко проучавање хладних квантних гасова" урадила је под руководством др Антуна Балажа и одбранила је 2011. године на Физичком факултету Универзитета у Београду. Добитница је и годишње награде Института за физику у Београду за најбољу докторску дисертацију. Након завршених докторских студија, у периоду од јуна 2012. до септембра 2014. године, др Ивана Васић је радила као постдокторски истраживач у групи проф. др Валтера Хофштетера на Институту за теоријску физику Гете универзитета у Франкфурту.

Ивана Васић је запослена у Лабораторији за примену рачунара у науци Института за физику у Београду од 1. јануара 2008. године на националном пројекту "Моделирање и нумеричке симулације комплексних физичких система" (ОИ 141035). Активно је учествовала на билатералном српско-немачком пројекту "Fast Converging Path Integral Approach to Bose-Einstein Condensation", у периоду 2009.-2010. године и у раду европског Центра изврсности за компјутерско моделирање комплексних система (СХ-СМCS). У звање научног сарадника изабрана је 18. јула 2012. године. У току боравка на Гете универзитету, кандидаткиња је била ангажована на престижном пројекту "DFG-Research Unit 801" финансираном од стране Немачке истраживачке фондације (DFG), који је представљао колаборацију шест водећих немачких експерименталних и теоријских група из области хладних атома. По завршетку постдокторског усавршавања у септембру 2014. године, Ивана се вратила на Институт за физику у Београду, где сада ради на националном пројекту "Моделирање и нумеричке симулације сложених вишечестичних система" (ОН 171017) као руководилац потпројекта "Ефикасно израчунавање функционалних интеграла са применом на ултрахладне квантне гасове". Такође је и руководилац билатералног српско-немачког пројекта "Квантне фазе бозонског Кејн-Меле-Хабард модела (ВКМН)" за период 2016.-2017. година, и билатералног српског-хрватског пројекта "Тополошка својства оптичких и фотонских решетки" за период 2016.-2017. година.

Главне теме њеног истраживања су колективне ексцитације хладних бозонских гасова, особине бозонских гасова у оптичким решеткама и бозонске фазе у присуству вештачких магнетних поља. Она је коаутор 20 научних радова у међународним часописима, од којих је 10 радова објављено у Physical Review часописима. Заједно са проф. др Хофштетером, била је руководилац два дипломска рада и два мастер рада. У току боравка на Гете универзитету, била је асистент на предмету Статистичка физика и организовала рачунске вежбе за курсеве Квантна механика, Рачунарска физика и Физика ултрахладних квантних гасова. Тренутно је ментор за израду докторске дисертације Ане Худомал на Физичком факултету Универзитета у Београду.

### 3 ПРЕГЛЕД НАУЧНЕ АКТИВНОСТИ

Др Ивана Васић се бави теоријским проучавањем хладних квантних гасова у циљу описа модерних експеримената у овој области. Вишедеценијска потрага за чистом експерименталном реализацијом Бозе-Ајнштајн кондензације је довела системе хладних атома на нанокелвинским температурама у први план савремене физике. Данас ови системи заиста представљају дуго очекиване Фајнманове квантне симулаторе: експериментално добро контролисане системе описане законима квантне механике и квантне статистике. Пуно разумевање експеримената захтева детаљно поређење са одговарајућим теоријским резултатима и у том циљу кандидаткиња је радила на следећим истраживачким темама:

- развој ефикасног нумеричког метода за решавање својственог проблема Хамилтонијана,
- испитивање особина идеалних бозона у систему са анхармонијским потенцијалом,
- детаљан опис динамике бозонског кондензата,
- проучавање ефеката дисипације на бозонске фазе,
- одређивање фазног дијаграма и основних ексцитација бозона у присуству синтетичких магнетних поља.

У наредним секцијама су укратко приказани главни научни резултати добијени у оквиру ових тема.

#### 3.1 Нумерички метод за решавање својственог проблема применом ефективних дејстава

Као докторанд, кандидаткиња је увела и детаљно испитала нумерички метод базиран на дијагонализацији еволуционог оператора. Кључни елемент метода су ефективна дејства, раније уведена у истој истраживачкој групи, која омогућавају прецизно и ефикасно рачунање одговарајућих амплитуда прелаза. Аналитички је показано да дискретизациона грешка овог приступа има супериорно понашање у односу на друге стандардне методе. Метод је примењен на неколико једнодимензионалних и дводимензионалних модела и показано је да се на нумерички ефикасан начин може добити информација о великом броју енергетских нивоа. Ови резултати су представљени у следећим радовима:

- Fast Convergence of Path Integrals for Many-Body Systems  
A. Bogojević, **I. Vidanović**, A. Balaž, and A. Belić  
Phys. Lett. A **372**, 3341 (2008),
- Recursive Schrödinger Equation Approach to Faster Converging Path Integrals  
A. Balaž, A. Bogojević, **I. Vidanović**, and A. Pelster  
Phys. Rev. E **79**, 036701 (2009),
- Properties of Quantum Systems Via Diagonalization of Transition Amplitudes. I. Discretization Effects  
**I. Vidanović**, A. Bogojević, and A. Belić  
Phys. Rev. E **80**, 066705 (2009),
- Properties of Quantum Systems Via Diagonalization of Transition Amplitudes. II. Systematic Improvements of Short-time Propagation  
**I. Vidanović**, A. Bogojević, A. Balaž, and A. Belić  
Phys. Rev. E **80**, 066706 (2009),

- Fast Converging Path Integrals for Time-Dependent Potentials: II. Generalization to Many-Body Systems and Real-Time Formalism  
A. Balaž, **I. Vidanović**, A. Bogojević, A. Belić, and A. Pelster  
J. Stat. Mech. P03005 (2011),
- Fast Converging Path Integrals for Time-Dependent Potentials: I. Recursive Calculation of Short-Time Expansion of the Propagator  
A. Balaž, **I. Vidanović**, A. Bogojević, A. Belić, and A. Pelster  
J. Stat. Mech. P03004 (2011).

### 3.2 Особине идеалних бозона у анхармонијском потенцијалу

После обимног тестирања, претходни метод је примењен за одређивање особина идеалних бозона у случају спољашњег анхармонијског потенцијала. Најчешће, хладни бозони се налазе у хармонијској потенцијалној замци, коју производи спољашње електрично или магнетно поље. За овај најчешћи случај температура на којој долази до макроскопске насељености основног стања, односно до Бозе-Ајнштајн кондензације, је добро позната. Међутим, одређени експерименти захтевају употребу додатног конфинирајућег потенцијала. Конкретно, у релевантном случају оствареном у експерименту, брзо ротирајући кондензат је смештен у потенцијал који је комбинација квадратног и квартичног члана. Наши нумерички резултати показују како промена спољашњег потенцијала утиче на температуру на којој долази до Бозе-Ајнштајн кондензације, на расподелу честица у замци и на резултате експерименталних мерења разлетања атома по искључивању замке (time of flight). За ово је на кључан начин коришћен SPEEDUP нумерички код, у чијем развоју је кандидаткиња такође учествовала. Истраживања су објављена у:

- SPEEDUP Code for Calculation of Transition Amplitudes Via the Effective Action Approach  
A. Balaž, **I. Vidanović**, D. Stojiljković, D. Vudragović, A. Belić, and A. Bogojević  
Commun. Comput. Phys. **11**, 739 (2012),
- Ultra-Fast Converging Path-Integral Approach for Rotating Ideal Bose-Einstein Condensates  
A. Balaž, **I. Vidanović**, A. Bogojević, and A. Pelster  
Phys. Lett. A **374**, 1539 (2010).

### 3.3 Динамика бозонског кондензата

Динамички одговор Бозе-Ајнштајн кондензата на спољашње пертурбације је најдиректнији и најчешћи начин мерења ових система. Типично, динамика се побуђује малом пертурбацијом хармонијског потенцијала и мере се резултујуће фреквенције осцилација положаја центра масе или ширине кондензата, које у линеарном режиму одговарају колективним модама. У новијем експерименту, употребом технике Фешбах резонанци, ефективна међуатомска интеракција је периодично осцилована и при одређеним примењеним фреквенцијама, примећен је резонантни одговор кондензата. На довољно ниским температурама и при slabим интеракцијама, за опис динамике кондензата се може користити временски зависна Грос-Питаевски једначина. Овај ефективни опис је нелинеаран и у одређеном режиму нелинеарни ефекти постају експериментално значајни. Нумеричким симулацијама Грос-Питаевски једначине и применом аналитичке Поенкаре-Линдштет методе, кандидаткиња је идентификовала нелинеарне ефекте који се јављају у близини резонанци, као што су линеарне комбинације основних ексцитација, побуђивање виших хармоника и помераји побуђених фреквенција у односу на вредности добијене у линеарном режиму. Такође, показано је да интензитет нелинеарних ефеката постаје јачи при одређеној конфигурацији хармонијског потенцијала. Осим употребе Фешбах резонанци, атомске интеракције се могу контролисати и променом атомских стања. Често коришћен динамички протокол је да се делу почетног кондензата атомско стање промени применом одговарајућег ласерског пулса. У тој ситуацији, систем описују (бар) две константе

интеракција и детаљи резултујуће динамике јако зависе од њиховог односа. Обимним нумеричким симулацијама и одговарајућом анализом у линеарном одзиву, кандидаткиња је класификовала могуће динамичке одговоре система при овом често коришћеном протоколу. Ова истраживања су довела и до развоја ефикасних нумеричких кодова који су објављени независно. Најважнији радови су

- Nonlinear Bose-Einstein-condensate Dynamics Induced by a Harmonic Modulation of the s-wave Scattering Length  
**I. Vidanović**, A. Balaž, H. Al-Jibbouri, and A. Pelster  
Phys. Rev. A **84**, 013618 (2011),
- Parametric and Geometric Resonances of Collective Oscillation Modes in Bose-Einstein Condensates  
**I. Vidanović**, H. Al-Jibbouri, A. Balaž, and A. Pelster  
Phys. Scr. T **149**, 014003 (2012),
- C Programs for Solving the Time-dependent Gross-Pitaevskii Equation in a Fully Anisotropic Trap  
D. Vudragović, **I. Vidanović**, A. Balaž, P. Muruganandam, and S. K. Adhikari  
Comput. Phys. Commun. **183**, 2021 (2012),
- Geometric Resonances in Bose-Einstein Condensates with Two- and Three-body Interactions  
H. Al-Jibbouri, **I. Vidanović**, A. Balaž, and A. Pelster  
J. Phys. B: At. Mol. Opt. Phys. **46**, 065303 (2013),
- Spin Modulation Instabilities and Phase Separation Dynamics in Trapped Two-component Bose Condensates  
**I. Vidanović**, N. J. van Druten, and M. Haque  
New J. Phys. **15**, 035008 (2013).

### 3.4 Ефекти дисипације на бозонске фазе

Примена контролисане дисипације пружа нов начин мерења особина и понашања хладних атомских система. На пример, у експериментима групе проф. Хервига Ота (Технички универзитет у Кајзерслаутерну, Немачка), јако фокусиран електронски снап се усмерава на облак хладних атома, а услед нееластичних судара електрона и атома формирају се јони, који напуштају систем и касније се детектују.

Мотивисана овим експериментом, кандидаткиња је разматрала динамику хладних бозона која је изазвана локализованом дисипацијом у дводимензионалној оптичкој решетки. Основни модел којим се описују бозони у оптичкој решетки је Бозе-Хабард модел који садржи чланове који одговарају тунелирању између најближих чворова решетке и локалној репулзивној интеракцији. Динамика система је описана Линдбладовом мастер једначином која даје временску еволуцију матрице густине. Основна апроксимација која је коришћена при решавању ове једначине је Гуцвилерова теорија средњег поља. Добијени резултати показују да при слабој дисипацији укупни губици директно одсликавају почетну локалну густину атома и расту са појачањем примењене дисипације. Много интересантнији је режим јаке дисипације у ком је уочен квантни Зенонов ефекат при ком мерење успорава унитарну еволуцију система и ефективни губици опадају са појачањем примењене дисипације. У овом режиму ефективни губици одсликавају вредности микроскопских параметара система (као што су јачина тунелирања и интеракција), што значи да овакво мерење пружа додатне важне информације о систему. Истраживање је објављено у раду:

- Dissipation through Localized Loss in Bosonic Systems with Long-range Interactions  
**I. Vidanović**, D. Cocks, and W. Hofstetter  
Phys. Rev. A **89**, 053614 (2014).

Други важна експериментална поставка која се описује дисипативним Бозе-Хабард моделом је дата низовима спрегнутих фотонских шупљина. Неизбежни губици се компензују применом спољашњег ласера и у овом отвореном квантном систему се проучавају стационарна стања која настају балансом губитака и додатне експитације. Циљ једног од дипломских радова којима је кандидаткиња руководила је било испитивање стационарних стања у којима постоје коначне фотонске струје. Конкретно, анализирано је како на фотонске струје утичу спољашњи параметри, као што су интензитет и фреквенција ласерске пумпе, стопе губитка, као и физички параметри ефективног Бозе-Хабард модела. Транспортна мерења ће бити природни први експерименти које треба урадити у овим системима да би се утврдило како интеракције утичу на простирање фотона, а теоријски резултати су објављени у раду:

- Photonic currents in driven and dissipative resonator lattices  
T. Mertz, **I. Vasić**, M. J. Hartmann, and W. Hofstetter  
Phys. Rev. A **94**, 013809 (2016).

### 3.5 Особине бозона у присуству синтетичких магнетних поља

Кључни модели физике чврстог стања, Хофштатеров и Холдејнов модел, су успешно реализовани у најновијим експериментима са хладним атомима у оптичким решеткама. На овај искорак се дуго чекало, јер атоми не поседују наелектрисање и нема њиховог директног спрезања са спољашњим магнетним пољем. Основни предуслов за реализацију је вештачки калибрациони ("gauge") потенцијал, тј. нетривијална фаза при тунелирању атома између два суседна чвора решетке, што је ефективно постигнуто или осциловањем читаве решетке или употребом додатних ласера. Мотивисана отвореним питањима о могућим новим бозонским фазама и расположивим експерименталним могућностима, кандидаткиња је увела и проучавала бозонски Холдејн-Хабард модел на хексагоналној решетки при концентрацији од једног атома по чвору оптичке решетке. Модел укључује: тунелирање између најближих суседа решетке, комплексно тунелирање између следећих најближих суседа и локалне интеракције. Сваки од ових чланова преферира различиту фазу: доминатно тунелирање између најближих суседа даје суперфлуидну фазу, комплексно тунелирање између првих следећих суседа води киралном суперфлуиду са неуниформним параметрима уређења, док доминантне локалне интеракције производе Мот изолатор фазу.

Применом бозонске динамичке теорије средњег поља мапиран је комплетан фазни дијаграм у функцији амплитуда тунелирања и локалних интеракција. Идентификован је реентратни прелаз другог реда у Мот изолатор стање као ефекат ван домања основне теорије средњег поља. За сваку од фаза су одређене особине локалних струја и флукуације локалне густине. Ове величине су експериментално доступне и користе се за идентификацију различитих фаза. Посебно, у разматраном случају, локалне струје се појављују и у Мот фази, што је аналитички аргументовано. Посебно интересантна је кирална суперфлуидна фаза – у овом случају теорија средњег поља предвиђа независну кондензацију атома две подрешетке хексагоналне решетке. Међутим, детаљном анализом квантних флукуација око конфигурација које даје теорија средњег поља, утврђено је да ефекат уређења услед флукуација доводи до спрезања фаза параметара поретка две подрешетке. Резултати су приказани у раду:

- Chiral Bosonic Phases on the Haldane Honeycomb Lattice  
**I. Vasić**, A. Petrescu, K. Le Hur, and W. Hofstetter  
Phys. Rev. B **91**, 094502 (2015).

Експериментална реализација ефективног спин-орбит спрезања у системима хладних атома је посебно значајна за бозонске системе за које не постоје директне аналогиије у физици кондензоване материје. Неколико теоријских радова је разматрало могућност спрезања спина и ангуларног момента у режиму Бозе-Ајнштајн кондензата. Са експерименталне тачке гледишта, физички систем

би се састојао од два различита атомска стања, која заправо чине псеудоспин, и пара супротно пропадајућих ласера који носе ангуларни моменат и спрежу два поменута атомска стања. У зависности од јачине спрезања и јачине интеракција, утврђено је да основно стање система може бити или тополошки полускирмион или вортекс-антивортекс пар.

Кандидаткиња је одредила најниже ексцитације овог система, које експериментално могу да се испитају у будућим експериментима. Конкретно, испитан је одговор система на две пертурбације хармонијске замке које се стандардно примењују у експериментима: дишућа (breathing) мода се побуђује променом јачине замке, док се диполна мода уводи померањем минимума хармонијског потенцијала. Директним нумеричким решавањем Грос-Питаевски једначине и применом проширене методе Богољубова утврђено је да две фазе дају потпуно различита понашања на побуде и да су ефекти интеракција најизраженији на прелазу између две фазе. Нумеричке симулације су показале да је одговор полускирмионске фазе на померање минимума замке комплексан и карактеристичан на више начина. Пре свега, услед присуства спин-орбит спрезања у систему, Конова теорема више не важи, па померај у једном правцу резултује дводимензионалним кретањем центра масе система које укључује више фреквенција. Услед дегенерације основног стања овај резултат се мора интерпретирати применом дегенерисане пертурбативне теорије. Резултати су објављени у раду:

- Excitation Spectra of a Bose-Einstein Condensate with an Angular Spin-orbit Coupling  
**I. Vasić** and A. Balaž  
Phys. Rev. A **94**, 033627 (2016).



## 4 ЕЛЕМЕНТИ ЗА КВАЛТИТАТИВНУ ОЦЕНУ НАУЧНОГ ДОПРИНОСА КАНДИДАТА

### 4.1 Квалитет научних резултата

#### 4.1.1 Научни ниво и значај резултата, утицај научних радова

Др Ивана Васић је у свом досадашњем раду дала кључни допринос у укупно 20 радова у међународним часописима са ISI листе. Од тога је 6 у M21a категорији (међународни часописи изузетних вредности), 12 у M21 категорији (врхунски међународни часописи) и 2 у M22 категорији.

У периоду након одлуке Научног већа о предлогу за стицање претходног научног звања, др Ивана Васић је објавила 9 радова у часописима са ISI листе. Од тога је 3 у M21a категорији (међународни часописи изузетних вредности) и 5 у M21 категорији (врхунски међународни часописи). Одржала је више предавања на научним скуповима, од којих три по позиву.

Као најзначајнијих пет радова кандидаткиње могу се узети:

1. **I. Vasić**, A. Petrescu, K. Le Hur, and W. Hofstetter  
*Chiral Bosonic Phases on the Haldane Honeycomb Lattice*  
Phys. Rev. B **91**, 094502 (2015), *Editors' Suggestion*, M21, цитиран 15 пута,
2. **I. Vidanović**, D. Cocks, and W. Hofstetter  
*Dissipation through Localized Loss in Bosonic Systems with Long-range Interactions*  
Phys. Rev. A **89**, 053614 (2014), M21a, цитиран 14 пута,
3. **I. Vidanović**, N. J. van Druten, and M. Haque  
*Spin Modulation Instabilities and Phase Separation Dynamics in Trapped Two-component Bose Condensates*  
New J. Phys. **15**, 035008 (2013), M21a, цитиран 7 пута,
4. **I. Vidanović**, A. Balaž, H. Al-Jibbouri, and A. Pelster  
*Nonlinear Bose-Einstein-condensate Dynamics Induced by a Harmonic Modulation of the s-wave Scattering Length*  
Phys. Rev. A **84**, 013618 (2011), M21a, цитиран 33 пута,
5. **I. Vidanović**, A. Vogojević, and A. Belić  
*Properties of Quantum Systems Via Diagonalization of Transition Amplitudes. I. Discretization Effects*  
Phys. Rev. E **80**, 066705 (2009), M21, цитиран 10 пута.

У првом раду уведен је и детаљно испитан нови модел чија се експериментална реализација очекује у текућим експериментима са хладним атомима у вештачким магнетним пољима. Показано је да се у присуству интеракција и вештачких магнетних поља могу појавити нестандартне бозонске фазе и анализирани су њихове конкретне експерименталне карактеристике. Рад је по објављивању издвојен ознаком *Editors' Suggestion*, и на основу овог рада кандидаткиња је одржала два предавања по позиву. Резултате су као уводна предавања представили и други коаутори на водећим конференцијама у овој области. Истраживања започета у овом раду настављају докторанди на Гете универзитету у Франкфурту, на Ecole Polytechnique, CNRS у Паризу, и на Институту за физику у Београду. Такође, на основу овог рада кандидаткиња и њен докторанд Ана Худомал из Београда су сараднице на новом престижном пројекту "FOR 2414: Artificial Gauge Fields and Interacting Topological Phases in Ultracold Atoms" финансираном од стране Немачке истраживачке фондације (DFG), који представља колаборацију десет водећих европских група у области хладних атома.

Други рад је инспирисан сарадњом теоријске групе са Гете универзитета у Франкфурту и експерименталне групе Хервига Ота са Техничког универзитета у Кајзерслаутерну, која је објавила

прва мерења бозонског кондензата применом контролисане локализоване дисипације. Наш теоријски рад разматра аналогна мерења у режиму јаких интеракција и даје конкретно, нумерички проверено предвиђање за пун опсег примењеног интензитета дисипације. Посебно су интересантни резултати за режим јаке дисипације у ком се јавља тзв. квантни Зенонов ефекат, где смо показали како микроскопски параметри Хамилтонијана утичу на експериментално доступне величине. Ове резултате кандидаткиња је представила на интерном састанку колаборативног немачког пројекта SFB/TR49.

У трећем и четвртном раду теоријски је проучавана динамика атомског Бозе-Ајнштајн кондензата са фокусом на експериментално доступне динамичке протоколе. Велика контролабилност система хладних атома је њихова главна предност и то се јасно илуструје чињеницом да се чак и ефективне међуатомске интеракције могу динамички мењати у овим експериментима. У поменутиим радовима кандидаткиња је разматрала одговор система на периодично осциловање интензитета и на изненадну промену интензитета ефективне интеракције. Детаљно су анализирани нелинеарни ефекти и услови у којима је почетно стање нестабилно на примењену пертурбацију и води комплексној динамици.

У петом раду уведен је и анализиран нумерички метод који на ефикасан начин пружа информацију о спектру квантног система. Овај метод је касније коришћен за прецизно одређивање температуре Бозе-Ајнштајн кондензације у анхармонијском потенцијалу.

#### 4.1.2 Позитивна цитираност научних радова кандидата

Према ISI Web of Science бази радови кандидаткиње су цитирани укупно 315 пута, док је број цитата без аутоцитата 271. Према истој бази h-индекс кандидаткиње је 11.

Прилог: подаци о цитираности са интернет странице ISI Web of Science.

#### 4.1.3 Параметри квалитета часописа

Битан елемент за процену квалитета научних резултата је и квалитет часописа у којима су радови објављени, односно њихов импакт фактор – ИФ. У категорији M21a, M21 и M22 кандидаткиња је објавила радове у следећим часописима, где су подвучени они часописи у којима је кандидаткиња објављивала у периоду након одлуке Научног већа о предлогу за стицање претходног научног звања:

- 1 рад у New Journal of Physics (ИФ = 4,177),
- 1 рад у Computer Physics Communications (ИФ = 3,268),
- 4 рада у Physical Review A (ИФ = 2,866 за 1 рад, ИФ = 3,042 за 1 рад и ИФ = 2,991 за 2 рада),
- 3 рада у Physical Review B (ИФ = 3,475 за 1 рад, ИФ = 3,774 за 1 рад и ИФ = 3,736 за 1 рад),
- 3 рада у Physical Review E (ИФ = 2,508 за 3 рада),
- 2 рада у Journal of Statistical Mechanics (ИФ = 2,67 за 2 рада),
- 1 рад у Communications in Computational Physics (ИФ = 1,863),
- 1 рад у Journal of Physics B (ИФ = 2,031),
- 2 рада у Physics Letters A (ИФ = 2,174 за 2 рада),
- 1 рад у The European Physical Journal B (ИФ = 1,575),
- 1 рад у Physica Scripta (ИФ = 1,204).

Укупан фактор утицаја радова кандидаткиње је 54.205, а у периоду након одлуке Научног већа о предлогу за стицање претходног научног звања тај фактор је 27.214. Часописи у којима је кандидаткиња објављивала радове су по свом угледу цењени и водећи у областима којима припадају. Посебно се међу њима истичу: *New Journal of Physics*, *Computer Physics Communications*, *Physical Review A*, *Physical Review B* и *Physical Review E*.

#### 4.1.4 Степен самосталности и степен учешћа у реализацији радова у научним центрима у земљи и иностранству

Кандидаткиња је водећи аутор девет радова, други аутор осам публикација и трећи аутор три публикације.

На радовима који су објављени у периоду након одлуке Научног већа о предлогу за стицање претходног научног звања, кандидаткиња је водећи аутор пет публикација и други аутор три рада. При изради свих ових публикација кандидаткиња је учествовала у конкретној формулацији проблема, у његовом решавању применом обимних нумеричких симулација и апроксимативних аналитичких техника, и у завршном писању. У радовима где је кандидаткиња други аутор, у једном случају први аутор је студент чијим дипломским радом је кандидаткиња директно руководила, а у друга два случаја први аутори су докторанди са којима је сарађивала.

Током израде докторске дисертације на Институту за физику у Београду, у сарадњи са др Антонином Балажем и др Акселом Пелстером са Универзитета у Дуизбургу, кандидаткиња је започела са нумеричким симулацијама хладних бозонских атома у режиму слабих интеракција применом Грос-Питаевски једначине. У току постдокторског истраживања кандидаткиња се бавила проучавањем особина јако интерагујућих бозона у оптичким решеткама, испитивањем ефеката дисипације на бозонске фазе, као и одређивањем особина бозонских фаза у присуству синтетичких магнетних поља. Ово су веома актуелне теме, које се истражују у најновијим експериментима са хладним атомима. За њихово успешно проучавање неопходне су напредне нумеричке технике, које је кандидаткиња усавршила као постдокторанд у Франкфурту и затим то знање пренела на Институт за физику.

Кандидаткиња има активну сарадњу са истраживачким групама проф. Валтера Хофштетера, Франкфурт, Немачка, проф. Карин Ле Хур, Париз, Француска, проф. Масуд Хаке, Даблин, Ирска и проф. Хрвоје Буљан, Загреб, Хрватска.

#### 4.1.5 Награде

Кандидаткиња је добитница годишње награде Института за физику у Београду за најбољу докторску дисертацију за 2012. годину.

## 4.2 Ангажованост у формирању научних кадрова

Кандидаткиња је тренутно ментор на изради докторске дисертације Ане Худомал на Физичком факултету Универзитета у Београду.

Поред тога, блиско је сарађивала и помагала студентима докторандима Хамиду Ал-Џибурију (Hamid Jabber Naziran Al-Jibbouri) на Free University, у Берлину, Немачка, чија докторска теза је одбрањена септембра 2013. и Андреасу Гајслеру (Andreas Geissler) на Гете универзитету у Франкфурту, Немачка, чија одбрана се очекује ове године.

Кандидаткиња је као коментор учествовала у изради два мастер рада

- *Phase transitions of the coherently coupled two-component Bose gas in a 2D Optical Lattice*  
Студент: Улрике Борнхајмер (Ulrike Bornheimer)  
Гете универзитет, Франкфурт, Немачка, децембар 2014. године  
Ментори: Валтер Хофштетер, Ивана Васић,

- *Phase Diagram of the Bosonic Kane-Mele-Hubbard Model*  
Студент: Раџбир Нирван (Rajbir Nirwan)  
Гете универзитет, Франкфурт, Немачка, септембар 2016. године  
Ментори: Валтер Хофштетер, Ивана Васић,

и два дипломска рада

- *Transport and Dynamics of Interacting Bosons with Dissipation*  
Студент: Томас Мерц (Thomas Mertz)  
Гете универзитет, Франкфурт, Немачка, септембар 2014.  
Ментори: Валтер Хофштетер, Ивана Васић,
- *Superfluid Phases in the Presence of Artificial Gauge Fields*  
Раџбир-Синг Нирван (Rajbir-Singh Nirwan)  
Гете универзитет, Франкфурт, Немачка, октобар 2014.  
Ментори: Валтер Хофштетер, Ивана Васић.

У току постдокторског боравка на Гете универзитету, кандидаткиња је активно учествовала у настави на основним студијама Физичког факултета. Била је асистент-тутор на вежбама из Статистичке физике, као и асистент који припрема материјале, испите и координише рад асистената-тутора на предметима Квантна механика, Рачунарска физика, Квантне информације и ултрахладни квантни гасови.

Прилог: потврда о менторству руководиоца пројекта, извештај о раду истраживача докторанда, захвалница докторске тезе Хамида Ал-Џибурија, насловне стране наведених мастер и дипломских радова.

#### 4.3 Нормирање броја коауторских радова, патената и техничких решења

Сви радови кандидаткиње објављени у периоду након одлуке Научног већа о предлогу за стицање претходног научног звања су базирани на комплексним нумеричким симулацијама и имају пет или мање аутора, тако да улазе са пуном тежином у односу на број коаутора.

#### 4.4 Руковођење пројектима, потпројектима и пројектним задацима

Кандидаткиња руководи:

- пројектом "Квантне фазе бозонског Кејн-Меле Хабард модела (ВКМН)" у оквиру Програма билатералне научне и технолошке сарадње између Министарства просвете, науке и технолошког развоја Републике Србије и Немачке агенције за академску размену (DAAD) за период 2016.-2017. година,
- пројектом "Тополошка својства оптичких и фотонских решетки" у оквиру Програма билатералне научне и технолошке сарадње између Министарства просвете, науке и технолошког развоја Републике Србије и Министарства знаности, образовања и спорта Републике Хрватске за период 2016.-2017. година,
- потпројектом "Ефикасно израчунавање функционалних интеграла са применом на ултрахладне квантне гасове" у оквиру пројекта основних истраживања ОН171017 "Моделирање и нумеричке симулације сложених вишечестичних система" Министарства просвете, науке и технолошког развоја Републике Србије.

У току постдокторског боравка на Гете универзитету, кандидаткиња је била ангажована на престижном пројекту "DFG-Research Unit 801 - Strong Correlations in Multiflavor Ultracold Quantum

Gases" финансираном од стране Немачке истраживачке фондације (DFG), који је представљао ко-лаборацију шест водећих немачких експерименталних и теоријских група из области хладних атома.

Прилог: званична писма обавештења о одобреним билатералним пројектима, потврда руководиоца пројекта о руковођењу потпројектом.

#### 4.5 Активност у научним и научно-стручним друштвима

Кандидаткиња је члан Одсека за физику кондензоване материје и статистичку физику Друштва физичара Србије, члан Оптичког друштва Србије и Немачког друштва физичара. Учествовала је у раду Државне комисије за такмичења из физике за ученике средњих школа Друштва физичара Србије при прегледању задатака на Државном такмичењу 2016. године.

Рецензент је за часописе *Physical Review Letters*, *Physical Review A* и *Physical Review B* Америчког друштва физичара. Била је члан организационог комитета конференције *Turkish Physical Society 32 nd International Physics Congress – TPS32*, Бодрум, Турска, 6.-9. септембар, 2016. године, организоване од стране Турског друштва физичара.

Прилог: писмо уредништва рецензенту, званични позив за чланство у организационом комитету.

#### 4.6 Утицајност научних резултата

Утицај научних резултата кандидаткиње је наведен у одељку 4.1. овог документа. Пун списак радова и цитата је у прилогу.

#### 4.7 Конкретан допринос кандидата у реализацији радова у научним центрима у земљи и иностранству

Кандидаткиња је значајно допринела сваком раду на коме је учествовала. Од девет радова у часописима у периоду након одлуке Научног већа о предлогу за стицање претходног научног звања, један је комплетно урађен на Институту за физику у Београду, шест у сарадњи са колегама у иностранству, а два су комплетно реализована у иностранству (док је кандидаткиња била на постдокторском усавршавању). У овим публикацијама кандидаткиња је имала кључни допринос, па је водећи аутор 5 публикација и други аутор 3 публикације. Конкретно, кандидаткиња је била покретач истраживања, радила је на конкретном решавању проблема применом нумеричких симулација, координисала је сарадњу свих коаутора, писала рад и била у комуникацији са уредником часописа при слању рада за објављивање.

Нова истраживачка тема коју је кандидаткиња покренула на Институту за физику у Београду су особине јако интерагујућих хладних бозонских атома у оптичким решеткама. За рад на овој теми потребни су напредни нумерички методи и кандидаткиња је успешно пренела своје познавање бозонске динамичке теорије средњег поља које је стекла на постдокторском усавршавању.

#### 4.8 Уводна предавања на конференцијама и друга предавања

Након претходног избора у звање, кандидаткиња је одржала следећа предавања:

- **I. Vasić**, A. Petrescu, K. Le Hur and W. Hofstetter  
*Bosonic phases on the Haldane honeycomb lattice*  
Conference Topological effects and synthetic gauge/magnetic fields for atoms and photons, Zagreb, Croatia, 29 September 2015 – 1 October 2015, M32
- **I. Vasić**, A. Petrescu, K. Le Hur and W. Hofstetter  
*Bosonic phases on the Haldane honeycomb lattice*  
The 19th Symposium on Condensed Matter Physics, Belgrade, Serbia, 7–11 September 2015, M32

- **I. Vasić**, A. Petrescu, K. Le Hur, and W. Hofstetter  
*Chiral Bosonic Phases on the Haldane Honeycomb Lattice*  
Osma radionica fotonike, Kopaonik, Serbia, 8–12 March 2015, M62
- **I. Vasić**  
*Hladni bozonski atomi u optičkim rešetkama*  
Seminar Fizičkog fakulteta u Beogradu, Belgrade, Serbia, 10. June 2015
- **I. Vasić**  
*Bozonski gasovi u optičkim rešetkama*  
Predavanje u okviru predmeta Seminari savremene fizike, Fizički fakultet, Belgrade, Serbia, 20. April 2015
- **I. Vidanović**  
*Dissipation induced bosonic dynamics and hybrid quantum simulations*  
International conference on Strong Correlations in Ultracold Quantum Gases – Munich 2013, Munich, Germany, 22-25 October 2013
- **I. Vidanović**, D. Cocks, W. Hofstetter  
*Dissipation through localised loss in bosonic systems with long-range interactions*  
7th Annual Retreat of the SFB/TR 49, Bensheim, Germany, 19–20 September 2013

Прилог: позивна писма за учешће на конференцијама, izvodi iz knjiga apstrakata.

## 5 ЕЛЕМЕНТИ ЗА КВАНТИТАТИВНУ ОЦЕНУ НАУЧНОГ ДОПРИНОСА КАНДИДАТА

Остварени резултати у периоду након одлуке Научног већа о предлогу за стицање претходног научног звања:

Категорија	М бодова по раду	Број радова	Укупно М бодова
M21a	10	3	<b>30</b>
M21	8	5	<b>40</b>
M22	5	1	<b>5</b>
M32	1.5	2	<b>3</b>
M34	0.5	16	<b>8</b>
M62	1	1	<b>1</b>

Поређење са минималним квантитативним условима за избор у звање виши научни сарадник:

Минималан број М бодова		Остварено
Укупно	50	<b>87</b>
M10+M20+M31+M32+M33+M41+M42	40	<b>78</b>
M11+M12+M21+M22+M23+M24	30	<b>75</b>

Према ISI Web of knowledge бази укупан број цитата радова кандидаткиње је 315, док је број цитата без ауоцитата 271. Према истој бази h-индекс кандидаткиње је 11.

## 6 СПИСАК РАДОВА ДР ИВАНЕ ВАСИЋ

### Радови у међународним часописима изузетних вредности (M21a)

#### Радови објављени након претходног избора у звање

1. **I. Vidanović**, D. Cocks, and W. Hofstetter  
*Dissipation through Localized Loss in Bosonic Systems with Long-range Interactions*  
Phys. Rev. A **89**, 053614 (2014), ИФ = 3.042 за 2012. год.
2. **I. Vidanović**, N. J. van Druten, and M. Haque  
*Spin Modulation Instabilities and Phase Separation Dynamics in Trapped Two-component Bose Condensates*  
New J. Phys. **15**, 035008 (2013), ИФ = 4.177 за 2011. год.

#### Радови објављени између два избора у звање

1. D. Vudragović, **I. Vidanović**, A. Balaž, P. Muruganandam, and S. K. Adhikari  
*C Programs for Solving the Time-dependent Gross-Pitaevskii Equation in a Fully Anisotropic Trap*  
Comput. Phys. Commun. **183**, 2021 (2012), ИФ = 3.268 за 2011. год.

#### Радови објављени пре претходног избора у звање

1. **I. Vidanović**, A. Balaž, H. Al-Jibbouri, and A. Pelster  
*Nonlinear Bose-Einstein-condensate Dynamics Induced by a Harmonic Modulation of the s-wave Scattering Length*  
Phys. Rev. A **84**, 013618 (2011), ИФ = 2.866 за 2009. год.
2. A. Balaž, **I. Vidanović**, A. Bogojević, A. Belić, and A. Pelster  
*Fast Converging Path Integrals for Time-Dependent Potentials: II. Generalization to Many-Body Systems and Real-Time Formalism*  
J. Stat. Mech. P03005 (2011), ИФ = 2.670 за 2009. год.
3. A. Balaž, **I. Vidanović**, A. Bogojević, A. Belić, and A. Pelster  
*Fast Converging Path Integrals for Time-Dependent Potentials: I. Recursive Calculation of Short-Time Expansion of the Propagator*  
J. Stat. Mech. P03004 (2011), ИФ = 2.670 за 2009. год.

### Радови у врхунским међународним часописима (M21)

#### Радови објављени након претходног избора у звање

1. **I. Vasić** and A. Balaž  
*Excitation Spectra of a Bose-Einstein Condensate with an Angular Spin-orbit Coupling*  
Phys. Rev. A **94**, 033627 (2016), ИФ = 2.991 за 2013. год.
2. T. Mertz, **I. Vasić**, M. J. Hartmann, and W. Hofstetter  
*Photonic currents in driven and dissipative resonator lattices*  
Phys. Rev. A **94**, 013809 (2016), ИФ = 2.991 за 2013. год.
3. **I. Vasić**, A. Petrescu, K. Le Hur, and W. Hofstetter  
*Chiral Bosonic Phases on the Haldane Honeycomb Lattice*  
Phys. Rev. B **91**, 094502 (2015), *Editors' Suggestion*, ИФ = 3.736 за 2014. год.



4. H. Al-Jibbouri, **I. Vidanović**, A. Balaž, and A. Pelster  
*Geometric Resonances in Bose-Einstein Condensates with Two- and Three-body Interactions*  
J. Phys. B: At. Mol. Opt. Phys. **46**, 065303 (2013), ИФ = 2.031 за 2012. год.

**Радови објављени између два избора у звање**

1. N. Moran, A. Sterdyniak, **I. Vidanović**, N. Regnault, and M. V. Milovanović  
*Topological D-wave Pairing Structures in Jain States*  
Phys. Rev. B **85**, 245307 (2012), *Editors' Suggestion*, ИФ = 3.774 за 2010. год.

**Радови објављени пре претходног избора у звање**

1. A. Balaž, **I. Vidanović**, D. Stojiljković, D. Vudragović, A. Belić, and A. Bogojević  
*SPEEDUP Code for Calculation of Transition Amplitudes Via the Effective Action Approach*  
Commun. Comput. Phys. **11**, 739 (2012), ИФ = 1.863 за 2012. год.
2. A. Balaž, **I. Vidanović**, A. Bogojević, and A. Pelster  
*Ultra-Fast Converging Path-Integral Approach for Rotating Ideal Bose-Einstein Condensates*  
Phys. Lett. A **374**, 1539 (2010), ИФ = 2.174 за 2008. год.
3. **I. Vidanović**, A. Bogojević, A. Balaž, and A. Belić  
*Properties of Quantum Systems Via Diagonalization of Transition Amplitudes.*  
*II. Systematic Improvements of Short-time Propagation*  
Phys. Rev. E **80**, 066706 (2009), ИФ = 2.508 за 2008. год.
4. **I. Vidanović**, A. Bogojević, and A. Belić  
*Properties of Quantum Systems Via Diagonalization of Transition Amplitudes.*  
*I. Discretization Effects*  
Phys. Rev. E **80**, 066705 (2009), ИФ = 2.508 за 2008. год.
5. M. V. Milovanović, T. Jolicoeur, and **I. Vidanović**  
*Modified Coulomb Gas Construction of Quantum Hall States from Nonunitary Conformal Field Theories*  
Phys. Rev. B **80**, 155324 (2009), ИФ = 3.475 за 2009. год.
6. A. Balaž, A. Bogojević, **I. Vidanović**, and A. Pelster  
*Recursive Schrödinger Equation Approach to Faster Converging Path Integrals*  
Phys. Rev. E **79**, 036701 (2009), ИФ = 2.508 за 2008. год.
7. A. Bogojević, **I. Vidanović**, A. Balaž, and A. Belić  
*Fast Convergence of Path Integrals for Many-Body Systems*  
Phys. Lett. A **372**, 3341 (2008), ИФ = 2.174 за 2008. год.

**Радови у истакнутим међународним часописима (M22)**

**Радови објављени између два избора у звање**

1. **I. Vidanović**, H. Al-Jibbouri, A. Balaž, and A. Pelster  
*Parametric and Geometric Resonances of Collective Oscillation Modes in Bose-Einstein Condensates*  
Phys. Scr. T **149**, 014003 (2012), ИФ = 1.204 за 2011. год.

### Радови објављени пре претходног избора у звање

1. **I. Vidanović**, S. Arsenijević, and S. Elezović-Hadžić  
*Force-induced Desorption of Self-avoiding Walks on Sierpinski Gasket Fractals*  
Eur. Phys. J. B **81**, 291 (2011), ИФ = 1.575 за 2010. год.

### Предавања по позиву са међународних скупова штампана у изводу (M32)

#### Радови објављени након претходног избора у звање

1. **I. Vasić**, A. Petrescu, K. Le Hur and W. Hofstetter  
*Bosonic phases on the Haldane honeycomb lattice*  
The 19th Symposium on Condensed Matter Physics, Belgrade, Serbia, 7–11 September 2015, p. 61 (2015)
2. **I. Vasić**, A. Petrescu, K. Le Hur and W. Hofstetter  
*Bosonic phases on the Haldane honeycomb lattice*  
Topological effects and synthetic gauge/magnetic fields for atoms and photons, Zagreb, Croatia, 29 September 2015 - 1 October 2015, p. 20 (2015)

### Саопштења са међународних скупова штампана у целини (M33)

#### Радови објављени пре претходног избора у звање

1. A. Balaž, **I. Vidanović**, A. Bogojević, and A. Belić  
*Accelerated Path-Integral Calculations via Effective Actions*  
Proceedings of the Path Integrals – New Trends and Perspectives PI07 Conference, Dresden, Germany, 23–28 September 2007, p. 86 (2008)
2. **I. Vidanović**, A. Balaž, A. Bogojević, and A. Belić  
*Systematic Speedup of Energy Spectra Calculations for Many-Body Systems*  
Proceedings of the Path Integrals – New Trends and Perspectives PI07 Conference, Dresden, Germany, 23–28 September 2007, p. 92 (2008)
3. A. Balaž, **I. Vidanović**, and A. Bogojević  
*Accelerated Path Integral Calculations for Many-body Systems*  
Proceedings of the QTS-5 Conference, Valladolid, Spain, 22-28 July 2007  
J. Phys. Conf. Ser. **128**, 012048 (2008)

### Саопштења са међународних скупова штампана у изводу (M34)

#### Радови објављени након претходног избора у звање

1. **I. Vasić** and A. Balaž  
*Excitations of a Bose-Einstein condensate with angular spin-orbit coupling*  
Proceedings of the Conference on Ultracold Quantum Gases–Current Trends and Future Perspectives, Bad Honnef, Germany, 18–20 April 2016, P35 (2016)
2. R. Nirwan, **I. Vasić**, A. Petrescu, K. Le Hur, and W. Hofstetter  
*The Bosonic Kane-Mele Hubbard model*  
Proceedings of the APS March Meeting 2016, Baltimore, Maryland U.S.A, 14–18 March 2016, #L50.010 (2016)

3. **I. Vasić** and A. Balaž  
*Excitations of a Bose-Einstein condensate with angular spin-orbit coupling*  
Proceedings of the DPG-2016 Conference, Hannover, Germany, 29 February 2016 – 4 March 2016, Q-27.8 (2016)
4. **I. Vasić**, D. Cocks and W. Hofstetter  
*Dissipation through localised loss in lattice bosonic systems*  
Proceedings of the V International School and Conference on Photonics, Belgrade, Serbia, 24–28 August 2015 p. 39, (2015)
5. **I. Vasić**, A. Petrescu, K. Le Hur, and W. Hofstetter  
*Chiral Bosonic Phases on the Haldane Honeycomb Lattice*  
Proceedings of the APS March Meeting 2015, San Antonio, Texas, U.S.A, 2–6 March 2015, #J36.013 (2015)
6. T. Mertz, **I. Vasić**, D. Cocks, and W. Hofstetter  
*Steady State Currents in the Driven Dissipative Bose-Hubbard Model*  
Proceedings of the DPG-2015 Conference, Heidelberg, Germany, 23–27 March 2015, Q-15.30 (2015)
7. R. Nirwan, **I. Vasić**, A. Petrescu, K. Le Hur, and W. Hofstetter  
*Superfluid Phases in the Presence of Artificial Gauge Field*  
Proceedings of the DPG-2015 Conference, Heidelberg, Germany, 23–27 March 2015, Q-15.31 (2015)
8. A. Geissler, M. Barbier, **I. Vasić**, and W. Hofstetter  
*Dynamical Mean-Field Theory of Rydberg-dressed quantum gases in optical lattices*  
Proceedings of the DPG-2015 Conference, Heidelberg, Germany, 23–27 March 2015, Q-62.6 (2015)
9. **I. Vasić**, A. Petrescu, K. Le Hur, and W. Hofstetter  
*Superfluid - Mott transition in the presence of artificial gauge fields*  
Proceedings of the 45th Annual Meeting of the APS Division of Atomic, Molecular, and Optical Physics, Madison, Wisconsin, U.S.A, 2–6 June 2014, K1.00144 (2014)
10. U. Bornheimer, **I. Vidanović**, and W. Hofstetter  
*Coherently coupled two-component ultracold bosons*  
Proceedings of the DPG-2014 Conference, Berlin, Germany, 17–21 March 2014, A-34.21 (2014)
11. **I. Vidanović**, D. Cocks, and W. Hofstetter  
*Dissipation through localised loss in bosonic systems with long-range interactions*  
Proceedings of the DPG-2014 Conference, Berlin, Germany, 17–21 March 2014, Q-32.37 (2014)
12. T. Mertz, **I. Vidanović**, D. Cocks, and W. Hofstetter  
*Steady State Currents in the Driven Dissipative Bose-Hubbard Model*  
Proceedings of the DPG-2014 Conference, Berlin, Germany, 17–21 March 2014, Q-32.38 (2014)
13. A. Geissler, **I. Vidanović**, and W. Hofstetter  
*Dynamical Mean-Field Theory of Rydberg-dressed quantum gases in optical lattices*  
Proceedings of the DPG-2014 Conference, Berlin, Germany, 17–21 March 2014, Q-32.75 (2014)
14. **I. Vidanović**, A. Petrescu, K. Le Hur, and W. Hofstetter  
*Superfluid - Mott transition in the presence of artificial gauge fields*  
Proceedings of the DPG-2014 Conference, Berlin, Germany, 17–21 March 2014, Q-57.4 (2014)
15. **I. Vidanović**, U. Bissbort, and W. Hofstetter  
*Collective modes of interacting bosons in artificial gauge fields*  
Proceedings of the Workshop on Ultracold Atoms and Gauge Theories, Trieste, Italy, 13–17 May 2013, p. 45 (2013)

16. **I. Vidanović**, U. Bissbort, and W. Hofstetter  
*Collective modes of interacting bosons in artificial gauge fields*  
Proceedings of the DPG-2013 Conference, Hannover, Germany, 18–22 March 2013, Q-31.4 (2013)

#### **Радови објављени пре претходног избора у звање**

1. **I. Vidanović**, H. Al-Jibbouri, A. Balaž, and A. Pelster  
*Parametric and Geometric Resonances of Collective Oscillation Modes in Bose-Einstein Condensates*  
Proceedings of the III International School and Conference on Photonics, Photonica 2011, Belgrade, Serbia, 29 August–2 September 2011, p. 56 (2011)
2. **I. Vidanović**, A. Balaž, H. Al-Jibbouri, and A. Pelster  
*Nonlinear Bose-Einstein-condensate Dynamics Induced by a Harmonic Modulation of the s-wave Scattering Length*  
Proceedings of the DPG-2011 Conference, Dresden, Germany, 13–18 March 2011, Q-57.3 (2011)
3. A. Balaž, **I. Vidanović**, A. Bogojević, and A. Pelster  
*Fast Converging Path Integrals for Time-Dependent Potentials*  
Proceedings of the DPG-2010 Conference, Regensburg, Germany, 22–27 March 2010, DY-1.3 (2010)
4. A. Balaž, **I. Vidanović**, A. Bogojević, and A. Pelster  
*Short-time Effective Action Approach for Numerical Studies of Rotating Ideal BECs*  
Proceedings of the Conference on Research Frontiers in Ultra-Cold Atoms, ICTP, Trieste, Italy, 4–8 May 2009, P2030-4 (2009)
5. A. Balaž, **I. Vidanović**, A. Bogojević, and A. Pelster  
*Ultra-fast Converging Path Integral Approach for Rotating Ideal Bose Gases*  
Proceedings of the DPG-2009 Conference, Dresden, Germany, 22–27 March 2009, DY-1.4 (2009)
6. **I. Vidanović**, A. Balaž, A. Bogojević, and A. Pelster  
*Calculation of  $T_c$  of  $^{87}\text{Rb}$  BEC using High-order Effective Actions*  
Proceedings of the Quo Vadis BEC? Conference, Bad Honnef, Germany, 29-31 October 2008, P2 (2008)
7. A. Balaž, **I. Vidanović**, A. Bogojević, and A. Pelster  
*Path Integrals Without Integrals*  
Proceedings of the DPG-2008 Conference, Berlin, Germany, 25–29 February 2008, DY-29.16 (2008)
8. **I. Vidanović**, A. Bogojević, and A. Balaž  
*Effective Action Approach for Improved Many-Body Path Integral Calculations*  
Proceedings of the V International Student Conference of the Balkan Physical Union, Bodrum, Turkey, 21–24 August 2007, p. 82 (2007)

**Предавања по позиву са скупова националног значаја штампана у изводу (M62)**

#### **Радови објављени након претходног избора у звање**

1. **I. Vasić**, A. Petrescu, K. Le Hur, and W. Hofstetter  
*Chiral Bosonic Phases on the Haldane Honeycomb Lattice*  
Osma radionica fotonike, Kopaonik, Serbia, 8–12 March 2015, p. 41 (2015)

Саопштење са скупа националног значаја штампано у целини (M63)

**Радови објављени пре претходног избора у звање**

1. **I. Vidanović**, A. Balaž, A. Bogojević, and A. Belić  
*Effective Actions for Path Integral Monte Carlo*  
Proceedings of the XVII National Symposium on Condensed Matter Physics, SFKM 2007, Vršac, Serbia, 16–20 September 2007, S3P010, p. 201 (2007)
2. **I. Vidanović** and S. Elezović-Hadžić  
*Force-Induced Desorption of a Linear Polymer Adsorbed on a Boundary of the Sierpinski Gasket Fractal*  
Proceedings of the XVII National Symposium on Condensed Matter Physics, SFKM 2007, Vršac, Serbia, 16–20 September 2007, S3P002, p. 172 (2007)

Саопштење са скупа националног значаја штампано у изводу (M64)

**Радови објављени пре претходног избора у звање**

1. **I. Vidanović**, A. Balaž, H. Al-Jibbouri, and A. Pelster  
*Nonlinear Bose-Einstein-condensate Dynamics Induced by a Harmonic Modulation of the s-wave Scattering Length*  
Book of Abstracts of the XVIII National Symposium on Condensed Matter Physics, SFKM 2011, Belgrade, Serbia, 18–22 April 2011, p. 55 (2011)

**Citation Report: 24**

(from Web of Science Core Collection)

You searched for: **AUTHOR:** (vasic i\*) OR **AUTHOR:** (vidanovic i\*)

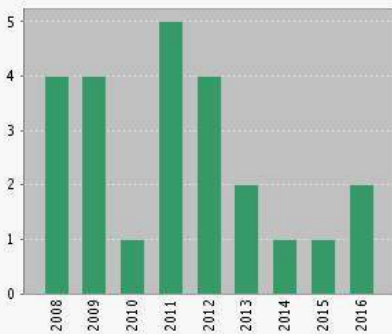
**Refined by:** [excluding] **SOURCE TITLES:** ( SWISS MEDICAL WEEKLY OR CHEST OR ALLERGY OR INTERNATIONAL JOURNAL OF CLINICAL PHARMACY OR TREE GENETICS GENOMES )

**Timespan:** All years. **Indexes:** SCI-EXPANDED, SSCI, A&HCI, CPCI-S, CPCI-SSH, ESCI.

[...Less](#)

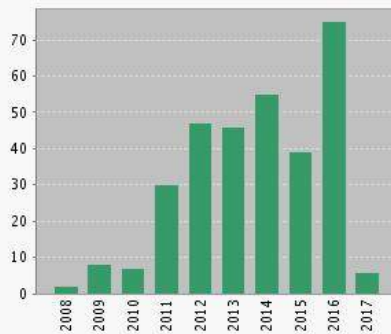
This report reflects citations to source items indexed within Web of Science Core Collection. Perform a Cited Reference Search to include citations to items not indexed within Web of Science Core Collection.

**Published Items in Each Year**



The latest 20 years are displayed.

**Citations in Each Year**



The latest 20 years are displayed.

Results found:	24
Sum of the Times Cited [?]:	315
Sum of Times Cited without self-citations [?]:	271
Citing Articles [?]:	194
Citing Articles without self-citations [?]:	179
Average Citations per Item [?]:	13.12
h-index [?]:	11

Sort by: Times Cited -- highest to lowest

Page 1 of 3

	2013	2014	2015	2016	2017	Total	Average Citations per Year
Use the checkboxes to remove individual items from this Citation Report or restrict to items published between 1996 and 2017 Go	46	55	39	75	6	315	31.50
1. <b>C programs for solving the time-dependent Gross-Pitaevskii equation in a fully anisotropic trap</b> By: Vudragovic, Dusan; Vidanovic, Ivana; Balaz, Antun; et al. COMPUTER PHYSICS COMMUNICATIONS Volume: 183 Issue: 9 Pages: 2021-2025 Published: SEP 2012	17	19	16	28	2	85	14.17
2. <b>Nonlinear Bose-Einstein-condensate dynamics induced by a harmonic modulation of the s-wave scattering length</b> By: Vidanovic, Ivana; Balaz, Antun; Al-Jibbouri, Hamid; et al. PHYSICAL REVIEW A Volume: 84 Issue: 1 Article Number: 013618 Published: JUL 27 2011	4	10	3	0	1	33	4.71
3. <b>Ultra-fast converging path-integral approach for rotating ideal Bose-Einstein condensates</b> By: Balaz, Antun; Vidanovic, Ivana; Bogojevic, Aleksandar; et al. PHYSICS LETTERS A Volume: 374 Issue: 13-14 Pages: 1539-1549 Published: MAR 29 2010	3	2	2	5	0	19	2.38
4. <b>Geometric resonances in Bose-Einstein condensates with two- and three-body interactions</b> By: Al-Jibbouri, Hamid; Vidanovic, Ivana; Balaz, Antun; et al. JOURNAL OF PHYSICS B-ATOMIC MOLECULAR AND OPTICAL PHYSICS Volume: 46 Issue: 6 Article Number: 065303 Published: MAR 28 2013	4	4	1	8	0	18	3.60
5. <b>Recursive Schrodinger equation approach to faster converging</b>	0	1	1	2	0	18	2.00

**path integrals**

By: Balaz, Antun; Bogojevic, Aleksandar; Vidanovic, Ivana; et al.  
 PHYSICAL REVIEW E Volume: 79 Issue: 3 Article Number: 036701 Part: 2  
 Published: MAR 2009

6. **Fast converging path integrals for time-dependent potentials: I. Recursive calculation of short-time expansion of the propagator**

By: Balaz, Antun; Vidanovic, Ivana; Bogojevic, Aleksandar; et al.  
 JOURNAL OF STATISTICAL MECHANICS-THEORY AND EXPERIMENT  
 Article Number: P03004 Published: MAR 2011

7. **Fast converging path integrals for time-dependent potentials: II. Generalization to many-body systems and real-time formalism**

By: Balaz, Antun; Vidanovic, Ivana; Bogojevic, Aleksandar; et al.  
 JOURNAL OF STATISTICAL MECHANICS-THEORY AND EXPERIMENT  
 Article Number: P03005 Published: MAR 2011

8. **Properties of quantum systems via diagonalization of transition amplitudes. II. Systematic improvements of short-time propagation**

By: Vidanovic, Ivana; Bogojevic, Aleksandar; Balaz, Antun; et al.  
 PHYSICAL REVIEW E Volume: 80 Issue: 6 Article Number: 066706 Part: 2  
 Published: DEC 2009

9. **Fast convergence of path integrals for many-body systems**

By: Bogojevic, A.; Vidanovic, I.; Balaz, A.; et al.  
 PHYSICS LETTERS A Volume: 372 Issue: 19 Pages: 3341-3349 Published:  
 MAY 5 2008

10. **Chiral bosonic phases on the Haldane honeycomb lattice**

By: Vasic, Ivana; Petrescu, Alexandru; Le Hur, Karyn; et al.  
 PHYSICAL REVIEW B Volume: 91 Issue: 9 Article Number: 094502  
 Published: MAR 3 2015

4	4	1	0	0	17	2.43
4	4	1	1	0	17	2.43
3	2	1	2	0	16	1.78
1	1	1	2	0	16	1.60
0	0	3	11	1	15	5.00

Select Page



Save to Text File



Sort by: Times Cited -- highest to lowest

Page 1 of 3

24 records matched your query of the 36,843,663 in the data limits you selected.

**Citation Report: 24**

(from Web of Science Core Collection)

You searched for: **AUTHOR:** (vasic i\*) **OR AUTHOR:** (vidanovic i\*)

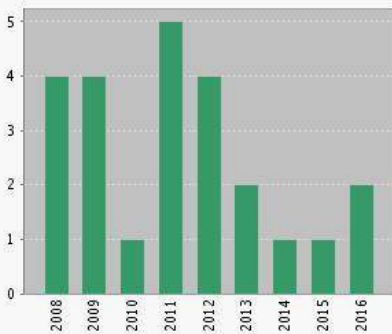
**Refined by:** [excluding] **SOURCE TITLES:** ( SWISS MEDICAL WEEKLY OR CHEST OR ALLERGY OR INTERNATIONAL JOURNAL OF CLINICAL PHARMACY OR TREE GENETICS GENOMES )

**Timespan:** All years. **Indexes:** SCI-EXPANDED, SSCI, A&HCI, CPCI-S, CPCI-SSH, ESCI.

[...Less](#)

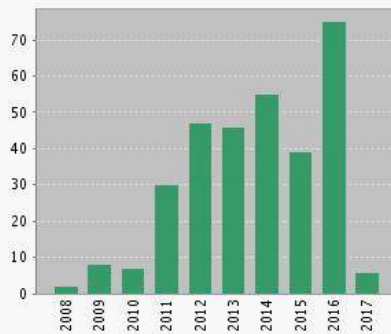
This report reflects citations to source items indexed within Web of Science Core Collection. Perform a Cited Reference Search to include citations to items not indexed within Web of Science Core Collection.

**Published Items in Each Year**



The latest 20 years are displayed.

**Citations in Each Year**



The latest 20 years are displayed.

Results found:	24
Sum of the Times Cited [?]:	315
Sum of Times Cited without self-citations [?]:	271
Citing Articles [?]:	194
Citing Articles without self-citations [?]:	179
Average Citations per Item [?]:	13.12
h-index [?]:	11

Sort by: **Times Cited -- highest to lowest**

Page 2 of 3

	2013	2014	2015	2016	2017	Total	Average Citations per Year
Use the checkboxes to remove individual items from this Citation Report or restrict to items published between 1996 and 2017 Go	46	55	39	75	6	315	31.50
11. <b>Dissipation through localized loss in bosonic systems with long-range interactions</b> By: Vidanovic, Ivana; Cocks, Daniel; Hofstetter, Walter PHYSICAL REVIEW A Volume: 89 Issue: 5 Article Number: 053614 Published: MAY 12 2014	0	2	5	6	1	14	3.50
12. <b>Modified Coulomb gas construction of quantum Hall states from nonunitary conformal field theories</b> By: Milovanovic, M. V.; Jolicoeur, Th.; Vidanovic, I. PHYSICAL REVIEW B Volume: 80 Issue: 15 Article Number: 155324 Published: OCT 2009	0	2	0	1	0	11	1.22
13. <b>Properties of quantum systems via diagonalization of transition amplitudes. I. Discretization effects</b> By: Vidanovic, Ivana; Bogojevic, Aleksandar; Belic, Aleksandar PHYSICAL REVIEW E Volume: 80 Issue: 6 Article Number: 066705 Part: 2 Published: DEC 2009	1	1	1	0	0	10	1.11
14. <b>Spin modulation instabilities and phase separation dynamics in trapped two-component Bose condensates</b> By: Vidanovic, Ivana; van Druuten, N. J.; Haque, Masudul NEW JOURNAL OF PHYSICS Volume: 15 Article Number: 035008 Published: MAR 6 2013	0	1	1	4	1	7	1.40
15. <b>Topological d-wave pairing structures in Jain states</b>	1	2	0	1	0	5	0.83



By: Moran, N.; Sterdyniak, A.; Vidanovic, I.; et al.  
**PHYSICAL REVIEW B** Volume: 85 Issue: 24 Article Number: 245307  
 Published: JUN 13 2012

16. **SPEEDUP Code for Calculation of Transition Amplitudes via the Effective Action Approach**

By: Balaz, Antun; Vidanovic, Ivana; Stojiljkovic, Danica; et al.  
**COMMUNICATIONS IN COMPUTATIONAL PHYSICS** Volume: 11 Issue: 3  
 Pages: 739-755 Published: MAR 2012

17. **Parametric and geometric resonances of collective oscillation modes in Bose-Einstein condensates**

By: Vidanovic, Ivana; Al-Jibbouri, Hamid; Balaz, Antun; et al.  
 Conference: 3rd International School and Conference on Photonics Location: Belgrade, SERBIA Date: AUG 29-SEP 02, 2011  
**PHYSICA SCRIPTA** Volume: T149 Article Number: 014003 Published: APR 2012

18. **Excitation spectra of a Bose-Einstein condensate with an angular spin-orbit coupling**

By: Vasic, Ivana; Balaz, Antun  
**PHYSICAL REVIEW A** Volume: 94 Issue: 3 Article Number: 033627  
 Published: SEP 21 2016

19. **Photonic currents in driven and dissipative resonator lattices**

By: Mertz, Thomas; Vasic, Ivana; Hartmann, Michael J.; et al.  
**PHYSICAL REVIEW A** Volume: 94 Issue: 1 Article Number: 013809  
 Published: JUL 5 2016

20. **Force-induced desorption of self-avoiding walks on Sierpinski gasket fractals**

By: Vidanovic, I.; Arsenijevic, S.; Elezovic-Hadzic, S.  
**EUROPEAN PHYSICAL JOURNAL B** Volume: 81 Issue: 3 Pages: 291-302  
 Published: SEP 2011

1	0	1	1	0	5	0.83
2	0	1	0	0	3	0.50
0	0	0	2	0	2	1.00
0	0	0	1	0	1	0.50
1	0	0	0	0	1	0.14

Select Page



Save to Text File

Sort by: **Times Cited -- highest to lowest**

Page 2 of 3

24 records matched your query of the 36,843,663 in the data limits you selected.

**Citation Report: 24**

(from Web of Science Core Collection)

You searched for: **AUTHOR:** (vasic i\*) **OR AUTHOR:** (vidanovic i\*)

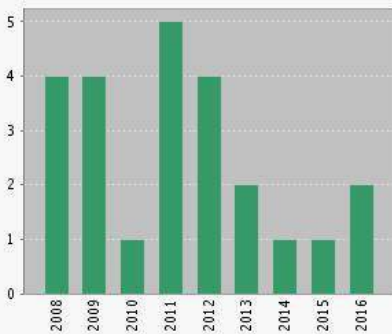
**Refined by:** [excluding] **SOURCE TITLES:** ( SWISS MEDICAL WEEKLY OR CHEST OR ALLERGY OR INTERNATIONAL JOURNAL OF CLINICAL PHARMACY OR TREE GENETICS GENOMES )

**Timespan:** All years. **Indexes:** SCI-EXPANDED, SSCI, A&HCI, CPCI-S, CPCI-SSH, ESCI.

[...Less](#)

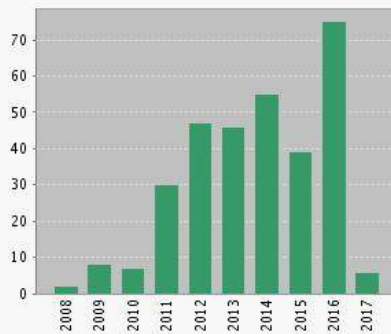
This report reflects citations to source items indexed within Web of Science Core Collection. Perform a Cited Reference Search to include citations to items not indexed within Web of Science Core Collection.

**Published Items in Each Year**



The latest 20 years are displayed.

**Citations in Each Year**



The latest 20 years are displayed.

Results found:	24
Sum of the Times Cited [?]	315
Sum of Times Cited without self-citations [?]	271
Citing Articles [?]	194
Citing Articles without self-citations [?]	179
Average Citations per Item [?]	13.12
h-index [?]	11

Sort by: **Times Cited -- highest to lowest**

Page 3 of 3

	2013	2014	2015	2016	2017	Total	Average Citations per Year
Use the checkboxes to remove individual items from this Citation Report or restrict to items published between <input type="text" value="1996"/> and <input type="text" value="2017"/> <input type="button" value="Go"/>	46	55	39	75	6	315	31.50
21. <b>Accelerated path integral calculations for many-body systems</b> By: Balaz, A.; Vidanovic, I.; Bogojevic, A. Book Author(s): Arratia, O; Calzada, JA; GomezCubillo, F; et al. Conference: 5th International Symposium on Quantum Theory and Symmetries Location: Univ Valladolid, Valladolid, SPAIN Date: JUL 22-28, 2007 5TH INTERNATIONAL SYMPOSIUM ON QUANTUM THEORY AND SYMMETRIES QTS5 Book Series: Journal of Physics Conference Series Volume: 128 Article Number: 012048 Published: 2008	0	0	0	0	0	1	0.10
22. <b>ACCELERATED PATH-INTEGRAL CALCULATIONS VIA EFFECTIVE ACTIONS</b> By: Balaz, A.; Vidanovic, I.; Bogojevic, A.; et al. Edited by: Janke, W; Pelster, A Conference: 9th International Conference on Path Integrals Location: Max Planck Inst Phys Complex Syst, Dresden, GERMANY Date: SEP 23-28, 2007 Sponsor(s): German Sci Fdn; Wilhelm & Else Heraeus Fdn PATH INTEGRALS: NEW TRENDS AND PERSPECTIVES, PROCEEDINGS Pages: 86-91 Published: 2008	0	0	0	0	0	1	0.10
23. <b>Faraday Waves and Collective Modes in Bose-Einstein Condensates</b> By: Nicolin, Alexandru I.; Vidanovic, Ivana; Balaz, Antun Edited by: Kocarev, L Conference: 3rd International Conference on ICT Innovations Location: Macedonian Acad Sci & Art, Skopje, MACEDONIA Date: SEP 14-16, 2011 ICT INNOVATIONS 2011 Book Series: Advances in Intelligent and Soft	0	0	0	0	0	0	0.00

Computing Volume: 150 Pages: 247-+ Published: 2011

24. **SYSTEMATIC SPEEDUP OF ENERGY SPECTRA CALCULATIONS FOR MANY-BODY SYSTEMS**

By: Vidanovic, I.; Balaz, A.; Bogojevic, A.; et al.

Edited by: Janke, W; Pelster, A

Conference: 9th International Conference on Path Integrals Location: Max Planck

Inst Phys Complex Syst, Dresden, GERMANY Date: SEP 23-28, 2007

Sponsor(s): German Sci Fdn; Wilhelm & Else Heraeus Fdn

PATH INTEGRALS: NEW TRENDS AND PERSPECTIVES, PROCEEDINGS

Pages: 92-+ Published: 2008

0	0	0	0	0	0	0.00

Select Page



Save to Text File



Sort by: Times Cited -- highest to lowest

Page 3 of 3

24 records matched your query of the 36,843,663 in the data limits you selected.

Web of Science™ InCites™ Journal Citation Reports® Essential Science Indicators™ EndNote™
Sign In Help English

# WEB OF SCIENCE™

Search
Return to Search Results
My Tools Search History Marked List

### Citing Articles: 82

*(from Web of Science Core Collection)*

**For:** C programs for solving the time-dependent Gross-Pitaevskii equation in a fully anisotropic trap ...[Less](#)

**Times Cited Counts**

85 in All Databases

85 in Web of Science Core Collection

1 in BIOSIS Citation Index

0 in Chinese Science Citation Database

0 data sets in Data Citation Index

0 publication in Data Citation Index

0 in Russian Science Citation Index

0 in SciELO Citation Index

[View Additional Times Cited Counts](#)

---

### Refine Results

**Web of Science Categories**

- OPTICS (40)
- PHYSICS ATOMIC MOLECULAR CHEMICAL (34)
- PHYSICS MATHEMATICAL (25)
- COMPUTER SCIENCE INTERDISCIPLINARY APPLICATIONS (16)
- PHYSICS APPLIED (9)

[more options / values...](#)

Refine

---

**Document Types**

- ARTICLE (80)
- PROCEEDINGS PAPER (2)
- BOOK CHAPTER (1)

[more options / values...](#)

Refine

---

**Research Areas**

---

**Authors**

---

**Group Authors**

---

**Editors**

---

**Source Titles**

Sort by: Publication Date -- newest to oldest
Page 1 of 2

Select Page
Save to EndNote online
Add to Marked List

Analyze Results
Create Citation Report

- 1. Statics and dynamics of a self-bound dipolar matter-wave droplet**

By: Adhikari, S. K.  
**LASER PHYSICS LETTERS** Volume: 14 Issue: 2 Article Number: 025501 Published: FEB 2017

View Abstract

**Times Cited: 0**  
*(from Web of Science Core Collection)*

**Usage Count** ▼
- 2. Vortex-bright solitons in a spin-orbit-coupled spin-1 condensate**

By: Gautam, Sandeep; Adhikari, S. K.  
**PHYSICAL REVIEW A** Volume: 95 Issue: 1 Article Number: 013608 Published: JAN 9 2017

View Abstract

**Times Cited: 0**  
*(from Web of Science Core Collection)*

**Usage Count** ▼
- 3. A finite-element toolbox for the stationary Gross-Pitaevskii equation with rotation**

By: Vergez, Guillaume; Danaila, Ionut; Auliac, Sylvain; et al.  
**COMPUTER PHYSICS COMMUNICATIONS** Volume: 209 Pages: 144-162 Published: DEC 2016

Full Text from Publisher
View Abstract

**Times Cited: 0**  
*(from Web of Science Core Collection)*

**Usage Count** ▼
- 4. OpenMP, OpenMP/MPI, and CUDA/MPI C programs for solving the time-dependent dipolar Gross-Pitaevskii equation**

By: Loncar, Vladimir; Young-S, Luis E.; Skrbic, Srdjan; et al.  
**COMPUTER PHYSICS COMMUNICATIONS** Volume: 209 Pages: 190-196 Published: DEC 2016

Full Text from Publisher
View Abstract

**Times Cited: 2**  
*(from Web of Science Core Collection)*

**Usage Count** ▼
- 5. Modulation instability in quasi-two-dimensional spin-orbit coupled Bose-Einstein condensates**

By: Bhuvanewari, S.; Nithyanandan, K.; Muruganandam, P.; et al.  
**JOURNAL OF PHYSICS B-ATOMIC MOLECULAR AND OPTICAL PHYSICS** Volume: 49 Issue: 24 Article Number: 245301 Published: NOV 25 2016

View Abstract

**Times Cited: 0**  
*(from Web of Science Core Collection)*

**Usage Count** ▼
- 6. Challenges and constraints of dynamically emerged source and sink in atomtronic circuits: From closed-system to open-system approaches**

By: Lai, Chen-Yen; Chien, Chih-Chun  
**SCIENTIFIC REPORTS** Volume: 6 Article Number: 37256 Published: NOV 16 2016

Full Text from Publisher
View Abstract

**Times Cited: 0**  
*(from Web of Science Core Collection)*

**Usage Count** ▼
- 7. Polariton condensation threshold investigation through the numerical resolution of the generalized Gross-Pitaevskii equation**

By: Gargoubi, Hamis; Guillet, Thierry; Jaziri, Sihem; et al.  
**PHYSICAL REVIEW E** Volume: 94 Issue: 4 Article Number: 043310 Published: OCT 18 2016

**Times Cited: 0**  
*(from Web of Science Core Collection)*

**Usage Count** ▼

Book Series Titles	◀
Conference Titles	◀
Publication Years	◀
Organizations-Enhanced	◀
Funding Agencies	◀
Languages	◀
Countries/Territories	◀
ESI Top Papers	◀
Open Access	◀

For advanced refine options, use

Analyze Results

- [View Abstract](#)
8. **Elastic collision and molecule formation of spatiotemporal light bullets in a cubic-quintic nonlinear medium**  
 By: Adhikari, S. K.  
**PHYSICAL REVIEW E** Volume: 94 Issue: 3 Article Number: 032217 Published: SEP 26 2016  
[View Abstract](#) Times Cited: 0  
(from Web of Science Core Collection)  
Usage Count
9. **Elements of Vortex-Dipole Dynamics in a Nonuniform Bose-Einstein Condensate**  
 By: Sakhel, Roger R.; Sakhel, Asaad R.  
**JOURNAL OF LOW TEMPERATURE PHYSICS** Volume: 184 Issue: 5-6 Pages: 1092-1113 Published: SEP 2016  
[View Abstract](#) Times Cited: 1  
(from Web of Science Core Collection)  
Usage Count
10. **Faraday and resonant waves in binary collisionally-inhomogeneous Bose-Einstein condensates**  
 By: Sudharsan, J. B.; Radha, R.; Raportaru, Mihaela Carina; et al.  
**JOURNAL OF PHYSICS B-ATOMIC MOLECULAR AND OPTICAL PHYSICS** Volume: 49 Issue: 16 Article Number: 165303 Published: AUG 28 2016  
[View Abstract](#) Times Cited: 0  
(from Web of Science Core Collection)  
Usage Count
11. **Three-dimensional vortex structures in a rotating dipolar Bose-Einstein condensate**  
 By: Kumar, Ramavarmaraja Kishor; Sriraman, Thangarasu; Fabrelli, Henrique; et al.  
**JOURNAL OF PHYSICS B-ATOMIC MOLECULAR AND OPTICAL PHYSICS** Volume: 49 Issue: 15 Article Number: 155301 Published: AUG 14 2016  
[View Abstract](#) Times Cited: 1  
(from Web of Science Core Collection)  
Usage Count
12. **Dynamics of trapped interacting vortices in Bose-Einstein condensates: a role of breathing degree of freedom**  
 By: Nakamura, Katsuhiro; Babajanov, Doniyor; Matrasulov, Davron; et al.  
**JOURNAL OF PHYSICS A-MATHEMATICAL AND THEORETICAL** Volume: 49 Issue: 31 Article Number: 315102 Published: AUG 5 2016  
[View Abstract](#) Times Cited: 0  
(from Web of Science Core Collection)  
Usage Count
13. **Two-dimensional bright and dark-in-bright dipolar Bose-Einstein condensate solitons on a one-dimensional optical lattice**  
 By: Adhikari, S. K.  
**LASER PHYSICS LETTERS** Volume: 13 Issue: 8 Article Number: 085501 Published: AUG 2016  
[View Abstract](#) Times Cited: 2  
(from Web of Science Core Collection)  
Usage Count
14. **OpenMP Fortran and C programs for solving the time-dependent Gross-Pitaevskii equation in an anisotropic trap**  
 By: Young-S., Luis E.; Vudragovic, Dugan; Muruganandam, Paulsamy; et al.  
**COMPUTER PHYSICS COMMUNICATIONS** Volume: 204 Pages: 209-213 Published: JUL 2016  
[Full Text from Publisher](#) [View Abstract](#) Times Cited: 10  
(from Web of Science Core Collection)  
Usage Count
15. **Analytical and numerical study of dirty bosons in a quasi-one-dimensional harmonic trap**  
 By: Khellil, Tama; Balaz, Antun; Pelster, Axel  
**NEW JOURNAL OF PHYSICS** Volume: 18 Article Number: 063003 Published: JUN 2 2016  
[Full Text from Publisher](#) [View Abstract](#) Times Cited: 7  
(from Web of Science Core Collection)  
Usage Count

16. **Statics and dynamics of quasi one-dimensional Bose-Einstein condensate in harmonic and dimple trap**  
By: Akram, Javed; Pelster, Axel  
**LASER PHYSICS** Volume: 26 Issue: 6 Article Number: 065501 Published: JUN 2016  
[View Abstract](#)  
**Times Cited: 1**  
*(from Web of Science Core Collection)*  
**Usage Count**
17. **ATUS-PRO: A FEM-based solver for the time-dependent and stationary Gross-Pitaevskii equation**  
By: Marojevic, Zelimir; Goeklue, Ertan; Laemmerzahl, Claus  
**COMPUTER PHYSICS COMMUNICATIONS** Volume: 202  
Pages: 216-232 Published: MAY 2016  
[Full Text from Publisher](#) [View Abstract](#)  
**Times Cited: 1**  
*(from Web of Science Core Collection)*  
**Usage Count**
18. **Quasi one-dimensional Bose-Einstein condensate in a gravito-optical surface trap**  
By: Akram, Javed; Girodias, Benjamin; Pelster, Axel  
**JOURNAL OF PHYSICS B-ATOMIC MOLECULAR AND OPTICAL PHYSICS** Volume: 49 Issue: 7 Article Number: 075302 Published: APR 14 2016  
[View Abstract](#)  
**Times Cited: 2**  
*(from Web of Science Core Collection)*  
**Usage Count**
19. **Conditions for order and chaos in the dynamics of a trapped Bose-Einstein condensate in coordinate and energy space**  
By: Sakhel, Roger R.; Sakhel, Asaad R.; Ghassib, Humam B.; et al.  
**EUROPEAN PHYSICAL JOURNAL D** Volume: 70 Issue: 3  
Article Number: 66 Published: MAR 24 2016  
[View Abstract](#)  
**Times Cited: 2**  
*(from Web of Science Core Collection)*  
**Usage Count**
20. **Manipulating localized matter waves in multicomponent Bose-Einstein condensates**  
By: Manikandan, K.; Muruganandam, P.; Senthilvelan, M.; et al.  
**PHYSICAL REVIEW E** Volume: 93 Issue: 3 Article Number: 032212 Published: MAR 10 2016  
[View Abstract](#)  
**Times Cited: 4**  
*(from Web of Science Core Collection)*  
**Usage Count**
21. **Numerical study of localized impurity in a Bose-Einstein condensate**  
By: Akram, Javed; Pelster, Axel  
**PHYSICAL REVIEW A** Volume: 93 Issue: 3 Article Number: 033610 Published: MAR 4 2016  
[View Abstract](#)  
**Times Cited: 3**  
*(from Web of Science Core Collection)*  
**Usage Count**
22. **Geometry-Induced Memory Effects in Isolated Quantum Systems: Cold-Atom Applications**  
By: Lai, Chen-Yen; Chien, Chih-Chun  
**PHYSICAL REVIEW APPLIED** Volume: 5 Issue: 3 Article Number: 034001 Published: MAR 3 2016  
[View Abstract](#)  
**Times Cited: 3**  
*(from Web of Science Core Collection)*  
**Usage Count**
23. **Stable and mobile two-dimensional dipolar ring-dark-in-bright Bose-Einstein condensate soliton**  
By: Adhikari, S. K.  
**LASER PHYSICS LETTERS** Volume: 13 Issue: 3 Article Number: 035502 Published: MAR 2016  
[View Abstract](#)  
**Times Cited: 2**  
*(from Web of Science Core Collection)*  
**Usage Count**
24. **CUDA programs for solving the time-dependent dipolar Gross-Pitaevskii equation in an anisotropic trap**  
By: Loncar, Vladimir; Balaz, Antun; Boojevic, Aleksandar; et al.  
**COMPUTER PHYSICS COMMUNICATIONS** Volume: 200  
Pages: 406-410 Published: MAR 2016  
[Full Text from Publisher](#) [View Abstract](#)  
**Times Cited: 14**  
*(from Web of Science Core Collection)*  
 **Highly Cited Paper**  
**Usage Count**
25. **Hybrid OpenMP/MPI programs for solving the**  
**Times Cited: 17**

**time-dependent Gross-Pitaevskii equation in a fully anisotropic trap**

By: Sataric, Bogdan; Slavnic, Vladimir; Belic, Aleksandar; et al.  
 COMPUTER PHYSICS COMMUNICATIONS Volume: 200  
 Pages: 411-417 Published: MAR 2016

[Full Text from Publisher](#)[View Abstract](#)*(from Web of Science Core Collection)* **Highly Cited Paper****Usage Count** 26. **Sculpting quasi-one-dimensional Bose-Einstein condensate to generate calibrated matter waves**

By: Akram, Javed; Pelster, Axel  
 PHYSICAL REVIEW A Volume: 93 Issue: 2 Article Number:  
 023606 Published: FEB 1 2016

[View Abstract](#)**Times Cited: 4**  
*(from Web of Science Core Collection)***Usage Count** 27. **Fractional-charge vortex in a spinor Bose-Einstein condensate**

By: Gautam, Sandeep; Adhikari, S. K.  
 PHYSICAL REVIEW A Volume: 93 Issue: 1 Article Number:  
 013630 Published: JAN 29 2016

[View Abstract](#)**Times Cited: 3**  
*(from Web of Science Core Collection)***Usage Count** 28. **Disorder-induced vortex lattice melting in a Bose-Einstein condensate**

By: Mithun, T.; Porsezian, K.; Dey, Bishwajyoti  
 PHYSICAL REVIEW A Volume: 93 Issue: 1 Article Number:  
 013620 Published: JAN 22 2016

[View Abstract](#)**Times Cited: 4**  
*(from Web of Science Core Collection)***Usage Count** 29. **STUDY ON THE STABILIZATION OF ATTRACTIVE BOSE-EINSTEIN CONDENSATES USING PROJECTION OPERATOR METHOD**

By: Sabari, S.; Porsezian, K.; Muruganandam, P.  
 ROMANIAN REPORTS IN PHYSICS Volume: 68 Issue: 3  
 Pages: 990-1003 Published: 2016

[View Abstract](#)**Times Cited: 0**  
*(from Web of Science Core Collection)***Usage Count** 30. **On the phase-correlation and phase-fluctuation dynamics of a strongly excited Bose gas**

By: Sakhel, Roger R.; Sakhel, Asaad R.; Ghassib, Humam B.  
 PHYSICA B-CONDENSED MATTER Volume: 478 Pages:  
 68-76 Published: DEC 1 2015

[Full Text from Publisher](#)[View Abstract](#)**Times Cited: 4**  
*(from Web of Science Core Collection)***Usage Count** 31. **Stable multiple vortices in collisionally inhomogeneous attractive Bose-Einstein condensates**

By: Sudharsan, J. B.; Radha, R.; Fabrelli, H.; et al.  
 PHYSICAL REVIEW A Volume: 92 Issue: 5 Article Number:  
 053601 Published: NOV 3 2015

[View Abstract](#)**Times Cited: 4**  
*(from Web of Science Core Collection)***Usage Count** 32. **Stable spatial and spatiotemporal optical soliton in the core of an optical vortex**

By: Adhikari, S. K.  
 PHYSICAL REVIEW E Volume: 92 Issue: 4 Article Number:  
 042926 Published: OCT 29 2015

[View Abstract](#)**Times Cited: 6**  
*(from Web of Science Core Collection)***Usage Count** 33. **Fortran and C programs for the time-dependent dipolar Gross-Pitaevskii equation in an anisotropic trap**

By: Kumar, R. Kishor; Young-S, Luis E.; Vudragovic, Dusan; et al.  
 COMPUTER PHYSICS COMMUNICATIONS Volume: 195  
 Pages: 117-128 Published: OCT 2015

[Full Text from Publisher](#)[View Abstract](#)**Times Cited: 27**  
*(from Web of Science Core Collection)***Usage Count** 34. **Stable matter-wave solitons in the vortex core of a uniform condensate**

By: Adhikari, S. K.  
 JOURNAL OF PHYSICS B-ATOMIC MOLECULAR AND

**Times Cited: 3**  
*(from Web of Science Core Collection)*

OPTICAL PHYSICS Volume: 48 Issue: 16 Special Issue: SI  
Article Number: 165303 Published: AUG 28 2015

[View Abstract](#)

Usage Count 

35. **Analytic models for the density of a ground-state spinor condensate**

By: Gautam, Sandeep; Adhikari, S. K.  
PHYSICAL REVIEW A Volume: 92 Issue: 2 Article Number:  
023616 Published: AUG 12 2015

[View Abstract](#)

Times Cited: **4**  
(from Web of Science Core Collection)

Usage Count 

36. **Vector solitons in a spin-orbit-coupled spin-2 Bose-Einstein condensate**

By: Gautam, Sandeep; Adhikari, S. K.  
PHYSICAL REVIEW A Volume: 91 Issue: 6 Article Number:  
063617 Published: JUN 15 2015

[View Abstract](#)

Times Cited: **9**  
(from Web of Science Core Collection)

Usage Count 

37. **Mobile vector soliton in a spin-orbit coupled spin-1 condensate**

By: Gautam, Sandeep; Adhikari, S. K.  
LASER PHYSICS LETTERS Volume: 12 Issue: 4 Article  
Number: 045501 Published: APR 2015

[View Abstract](#)

Times Cited: **7**  
(from Web of Science Core Collection)

Usage Count 

38. **Evolution and dynamical properties of Bose-Einstein condensate dark matter stars**

By: Madarassy, Eniko J. M.; Toth, Viktor T.  
PHYSICAL REVIEW D Volume: 91 Issue: 4 Article Number:  
044041 Published: FEB 24 2015

[View Abstract](#)

Times Cited: **12**  
(from Web of Science Core Collection)

Usage Count 

39. **Localization of a two-component Bose-Einstein condensate in a one-dimensional random potential**

By: Xi, Kui-Tian; Li, Jinbin; Shi, Da-Ning  
PHYSICA B-CONDENSED MATTER Volume: 459 Pages: 6-11  
Published: FEB 15 2015

[Full Text from Publisher](#)

[View Abstract](#)

Times Cited: **4**  
(from Web of Science Core Collection)

Usage Count 

40. **A G-FDTD scheme for solving multi-dimensional open dissipative Gross-Pitaevskii equations**

By: Moxley, Frederick Ira, III; Byrnes, Tim; Ma, Baoling; et al.  
JOURNAL OF COMPUTATIONAL PHYSICS Volume: 282  
Pages: 303-316 Published: FEB 1 2015

[Full Text from Publisher](#)

[View Abstract](#)

Times Cited: **6**  
(from Web of Science Core Collection)

Usage Count 

41. **Spontaneous symmetry breaking in a spin-orbit-coupled f=2 spinor condensate**

By: Gautam, Sandeep; Adhikari, S. K.  
PHYSICAL REVIEW A Volume: 91 Issue: 1 Article Number:  
013624 Published: JAN 23 2015

[View Abstract](#)

Times Cited: **9**  
(from Web of Science Core Collection)

Usage Count 

42. **Modulational instability windows in the nonlinear Schrodinger equation involving higher-order Kerr responses**

By: Novoa, David; Tommasini, Daniele; Novoa-Lopez, Jose A.  
PHYSICAL REVIEW E Volume: 91 Issue: 1 Article Number:  
012904 Published: JAN 6 2015

[View Abstract](#)

Times Cited: **3**  
(from Web of Science Core Collection)

Usage Count 

43. **Modeling and Computation of Bose-Einstein Condensates: Stationary States, Nucleation, Dynamics, Stochasticity**









By: Antoine, Xavier; Duboscq, Romain  
Edited by: Besse, C; Garreau, JC  
NONLINEAR OPTICAL AND ATOMIC SYSTEMS: AT THE  
INTERFACE OF PHYSICS AND MATHEMATICS Book Series:

Times Cited: **5**  
(from Web of Science Core Collection)

Usage Count 




Lecture Notes in Mathematics Volume: 2146 Pages: 49-145  
Published: 2015

44. **BOSE-EINSTEIN CONDENSATION: TWENTY YEARS AFTER**  
By: Bagnato, V. S.; Frantzeskakis, D. J.; Kevrekidis, P. G.; et al.  
**ROMANIAN REPORTS IN PHYSICS** Volume: 67 Issue: 1  
Pages: 5-50 Published: 2015  
[View Abstract](#)  
**Times Cited: 52**  
*(from Web of Science Core Collection)*  
 **Highly Cited Paper**  
**Usage Count** 
45. **EFFECTIVE LOW-DIMENSIONAL POLYNOMIAL EQUATIONS FOR BOSE-EINSTEIN CONDENSATES**  
By: Nicolin, Alexandru I.; Raportaru, Mihaela C.; Balaz, Antun  
**ROMANIAN REPORTS IN PHYSICS** Volume: 67 Issue: 1  
Pages: 143-157 Published: 2015  
[View Abstract](#)  
**Times Cited: 10**  
*(from Web of Science Core Collection)*  
**Usage Count** 
46. **Manipulating matter rogue waves and breathers in Bose-Einstein condensates**  
By: Manikandan, K.; Muruganandam, P.; Senthilvelan, M.; et al.  
**PHYSICAL REVIEW E** Volume: 90 Issue: 6 Article Number: 062905  
Published: DEC 2 2014  
[View Abstract](#)  
**Times Cited: 12**  
*(from Web of Science Core Collection)*  
**Usage Count** 
47. **Stable and mobile excited two-dimensional dipolar Bose-Einstein condensate solitons**  
By: Adhikari, S. K.  
**JOURNAL OF PHYSICS B-ATOMIC MOLECULAR AND OPTICAL PHYSICS** Volume: 47 Issue: 22 Article Number: 225304  
Published: NOV 28 2014  
[View Abstract](#)  
**Times Cited: 5**  
*(from Web of Science Core Collection)*  
**Usage Count** 
48. **Multicomponent long-wave-short-wave resonance interaction system: Bright solitons, energy-sharing collisions, and resonant solitons**  
By: Sakkaravarthi, K.; Kanna, T.; Vijayajayanthi, M.; et al.  
**PHYSICAL REVIEW E** Volume: 90 Issue: 5 Article Number: 052912  
Published: NOV 14 2014  
[View Abstract](#)  
**Times Cited: 8**  
*(from Web of Science Core Collection)*  
**Usage Count** 
49. **Bright dipolar Bose-Einstein-condensate soliton mobile in a direction perpendicular to polarization**  
By: Adhikari, S. K.  
**PHYSICAL REVIEW A** Volume: 90 Issue: 5 Article Number: 055601  
Published: NOV 10 2014  
[View Abstract](#)  
**Times Cited: 6**  
*(from Web of Science Core Collection)*  
**Usage Count** 
50. **GPELab, a Matlab toolbox to solve Gross-Pitaevskii equations I: Computation of stationary solutions**  
By: Antoine, Xavier; Duboscq, Romain  
**COMPUTER PHYSICS COMMUNICATIONS** Volume: 185 Issue: 11 Pages: 2969-2991  
Published: NOV 2014  
[Full Text from Publisher](#) [View Abstract](#)  
**Times Cited: 20**  
*(from Web of Science Core Collection)*  
**Usage Count** 

Select Page



[Save to EndNote online](#) 

[Add to Marked List](#)

Sort by: **Publication Date -- newest to oldest** 

◀ Page 1 of 2 ▶

Show: **50 per page** 

82 records matched your query of the 36,843,663 in the data limits you selected.

Web of Science™ InCites™ Journal Citation Reports® Essential Science Indicators™ EndNote™
Sign In Help English

# WEB OF SCIENCE™

Search
Return to Search Results
My Tools Search History Marked List

### Citing Articles: 82

(from Web of Science Core Collection)

**For:** C programs for solving the time-dependent Gross-Pitaevskii equation in a fully anisotropic trap [...More](#)

**Times Cited Counts**

85 in All Databases

85 in Web of Science Core Collection

1 in BIOSIS Citation Index

0 in Chinese Science Citation Database

0 data sets in Data Citation Index

0 publication in Data Citation Index

0 in Russian Science Citation Index

0 in SciELO Citation Index

[View Additional Times Cited Counts](#)

---

### Refine Results

**Web of Science Categories**

- OPTICS (40)
- PHYSICS ATOMIC MOLECULAR CHEMICAL (34)
- PHYSICS MATHEMATICAL (25)
- COMPUTER SCIENCE INTERDISCIPLINARY APPLICATIONS (16)
- PHYSICS APPLIED (9)

[more options / values...](#)

Refine

**Document Types**

- ARTICLE (80)
- PROCEEDINGS PAPER (2)
- BOOK CHAPTER (1)

[more options / values...](#)

Refine

**Research Areas**

**Authors**

**Group Authors**

**Editors**

**Source Titles**

Sort by: Publication Date -- newest to oldest

Page 2 of 2

Select Page
Save to EndNote online
Add to Marked List

[Analyze Results](#)

[Create Citation Report](#)

**Times Cited: 11**  
(from Web of Science Core Collection)

**Usage Count**

---

**Times Cited: 3**  
(from Web of Science Core Collection)

**Usage Count**

---

**Times Cited: 3**  
(from Web of Science Core Collection)

**Usage Count**

---

**Times Cited: 0**  
(from Web of Science Core Collection)

**Usage Count**

---

**Times Cited: 10**  
(from Web of Science Core Collection)

**Usage Count**

---

**Times Cited: 3**  
(from Web of Science Core Collection)

**Usage Count**









---

**Times Cited: 6**  
(from Web of Science Core Collection)

**Usage Count**

Book Series Titles			
Conference Titles			
Publication Years			
Organizations-Enhanced			
Funding Agencies			
Languages			
Countries/Territories			
ESI Top Papers			
Open Access			
For advanced refine options, use			
<a href="#">Analyze Results</a>			
58.	<b>Faraday waves in collisionally inhomogeneous Bose-Einstein condensates</b> By: Balaz, Antun; Paun, Remus; Nicolin, Alexandru I.; et al. <b>PHYSICAL REVIEW A</b> Volume: 89 Issue: 2 Article Number: 023609 Published: FEB 11 2014 <a href="#">View Abstract</a>	<b>Times Cited: 20</b> <i>(from Web of Science Core Collection)</i> <b>Usage Count</b>	
59.	<b>Demixing and symmetry breaking in binary dipolar Bose-Einstein-condensate solitons</b> By: Adhikari, S. K. <b>PHYSICAL REVIEW A</b> Volume: 89 Issue: 1 Article Number: 013630 Published: JAN 31 2014 <a href="#">View Abstract</a>	<b>Times Cited: 5</b> <i>(from Web of Science Core Collection)</i> <b>Usage Count</b>	
60.	<b>Statics and dynamics of a binary dipolar Bose-Einstein condensate soliton</b> By: Adhikari, S. K.; Young-S, L. E. <b>JOURNAL OF PHYSICS B-ATOMIC MOLECULAR AND OPTICAL PHYSICS</b> Volume: 47 Issue: 1 Article Number: 015302 Published: JAN 14 2014 <a href="#">View Abstract</a>	<b>Times Cited: 4</b> <i>(from Web of Science Core Collection)</i> <b>Usage Count</b>	
61.	<b>Density Waves in Dipolar Bose-Einstein Condensates by Means of Symbolic Computations</b> By: Nicolin, Alexandru I.; Rata, Ionel Edited by: Dulea, M; Karaivanova, A; Oulas, A; et al. Conference: HP-SEE User Forum Location: Natl Lib Serbia, Belgrade, SERBIA Date: OCT 17-19, 2012 Sponsor(s): Inst Phys Belgrade HIGH-PERFORMANCE COMPUTING INFRASTRUCTURE FOR SOUTH EAST EUROPE'S RESEARCH COMMUNITIES: RESULTS OF THE HP-SEE USER FORUM 2012 Book Series: Modeling and Optimization in Science and Technologies Volume: 2 Pages: 15-21 Published: 2014 <a href="#">View Abstract</a>	<b>Times Cited: 3</b> <i>(from Web of Science Core Collection)</i> <b>Usage Count</b>	
62.	<b>ANALYTICAL DESCRIPTION OF THE NONLINEAR DYNAMICS OF BOSE-EINSTEIN CONDENSATES BY MEANS OF GENETIC ALGORITHMS</b> By: Raportaru, Mihaela Carina; Jovanovski, Jane; Jakimovski, Boro; et al. <b>ROMANIAN JOURNAL OF PHYSICS</b> Volume: 59 Issue: 7-8 Pages: 677-685 Published: 2014 <a href="#">View Abstract</a>	<b>Times Cited: 3</b> <i>(from Web of Science Core Collection)</i> <b>Usage Count</b>	
63.	<b>Numerical studies on vortices in rotating dipolar Bose-Einstein condensates</b> By: Kumar, R. Kishor; Muruganandam, P. Book Group Author(s): IOP Conference: 22nd Annual International Laser Physics Workshop (LPHYS) Location: Acad Sci Czech Republ, Inst Phys, Prague, CZECH REPUBLIC Date: JUL 15-19, 2013 Sponsor(s): Czech Tech Univ 22ND INTERNATIONAL LASER PHYSICS WORKSHOP (LPHYS'13) Book Series: Journal of Physics Conference Series Volume: 497 Article Number: 012036 Published: 2014 <a href="#">Full Text from Publisher</a> <a href="#">View Abstract</a>	<b>Times Cited: 3</b> <i>(from Web of Science Core Collection)</i> <b>Usage Count</b>	
64.	<b>GROUND STATE OF BOSE-EINSTEIN CONDENSATES WITH INHOMOGENEOUS SCATTERING LENGTHS</b> By: Nicolin, A. I.; Balaz, A.; Sudharsan, J. B.; et al. <b>ROMANIAN JOURNAL OF PHYSICS</b> Volume: 59 Issue: 3-4 Pages: 204-213 Published: 2014 <a href="#">View Abstract</a>	<b>Times Cited: 8</b> <i>(from Web of Science Core Collection)</i> <b>Usage Count</b>	
65.	<b>Computational methods for the dynamics of the nonlinear Schrodinger/Gross-Pitaevskii equations</b> By: Antoine, Xavier; Bao, Weizhu; Besse, Christophe <b>COMPUTER PHYSICS COMMUNICATIONS</b> Volume: 184 Issue: 12 Pages: 2621-2633 Published: DEC 2013 <a href="#">Full Text from Publisher</a> <a href="#">View Abstract</a>	<b>Times Cited: 47</b> <i>(from Web of Science Core Collection)</i> <b>Usage Count</b>	


66. **Nonequilibrium Dynamics of a Bose-Einstein Condensate Excited by a Red Laser Inside a Power-Law Trap with Hard Walls**  
 By: Sakhel, Roger R.; Sakhel, Asaad R.; Ghassib, Humam B.  
 JOURNAL OF LOW TEMPERATURE PHYSICS Volume: 173  
 Issue: 3-4 Pages: 177-206 Published: NOV 2013  
[View Abstract](#)  
**Times Cited: 9**  
*(from Web of Science Core Collection)*  
**Usage Count**
67. **Stability and collapse of fermions in a binary dipolar boson-fermion Dy-164-Dy-161 mixture**  
 By: Adhikari, S. K.  
 PHYSICAL REVIEW A Volume: 88 Issue: 4 Article Number: 043603  
 Published: OCT 3 2013  
[View Abstract](#)  
**Times Cited: 6**  
*(from Web of Science Core Collection)*  
**Usage Count**
68. **Breakdown of the Kohn theorem near a Feshbach resonance in a magnetic trap**  
 By: Al-Jibbouri, Hamid; Pelster, Axel  
 PHYSICAL REVIEW A Volume: 88 Issue: 3 Article Number: 033621  
 Published: SEP 17 2013  
[View Abstract](#)  
**Times Cited: 6**  
*(from Web of Science Core Collection)*  
**Usage Count**
69. **Vortical and fundamental solitons in dipolar Bose-Einstein condensates trapped in isotropic and anisotropic nonlinear potentials**  
 By: Kumar, R. Kishor; Muruganandam, P.; Malomed, B. A.  
 JOURNAL OF PHYSICS B-ATOMIC MOLECULAR AND OPTICAL PHYSICS Volume: 46 Issue: 17 Article Number: 175302  
 Published: SEP 14 2013  
[View Abstract](#)  
**Times Cited: 9**  
*(from Web of Science Core Collection)*  
**Usage Count**
70. **Collisionally inhomogeneous Bose-Einstein condensates with binary and three-body interactions in a bichromatic optical lattice**  
 By: Sudharsan, J. B.; Radha, R.; Muruganandam, P.  
 JOURNAL OF PHYSICS B-ATOMIC MOLECULAR AND OPTICAL PHYSICS Volume: 46 Issue: 15 Article Number: 155302  
 Published: AUG 14 2013  
[View Abstract](#)  
**Times Cited: 2**  
*(from Web of Science Core Collection)*  
**Usage Count**
71. **Energy eigenfunctions of the 1D Gross-Pitaevskii equation**  
 By: Marojevic, Zelimir; Goeklue, Ertan; Laemmerzahl, Claus  
 COMPUTER PHYSICS COMMUNICATIONS Volume: 184  
 Issue: 8 Pages: 1920-1930 Published: AUG 2013  
[Full Text from Publisher](#) [View Abstract](#)  
**Times Cited: 9**  
*(from Web of Science Core Collection)*  
**Usage Count**
72. **Dipolar Bose-Einstein condensates in weak anisotropic disorder**  
 By: Nikolic, Branko; Balaz, Antun; Pelster, Axel  
 PHYSICAL REVIEW A Volume: 88 Issue: 1 Article Number: 013624  
 Published: JUL 16 2013  
[View Abstract](#)  
**Times Cited: 20**  
*(from Web of Science Core Collection)*  
**Usage Count**
73. **Stability of trapped degenerate dipolar Bose and Fermi gases**  
 By: Adhikari, S. K.  
 JOURNAL OF PHYSICS B-ATOMIC MOLECULAR AND OPTICAL PHYSICS Volume: 46 Issue: 11 Article Number: 115301  
 Published: JUN 14 2013  
[View Abstract](#)  
**Times Cited: 4**  
*(from Web of Science Core Collection)*  
**Usage Count**
74. **NLSEmagic: Nonlinear Schrodinger equation multi-dimensional Matlab-based GPU-accelerated integrators using compact high-order schemes**  
 By: Caplan, R. M.  
 COMPUTER PHYSICS COMMUNICATIONS Volume: 184  
 Issue: 4 Pages: 1250-1271 Published: APR 2013  
[Full Text from Publisher](#) [View Abstract](#)  
**Times Cited: 11**  
*(from Web of Science Core Collection)*  
**Usage Count**

75. **Numerical simulation code for self-gravitating Bose-Einstein condensates**  
 By: Madarassy, Eniko J. M.; Toth, Viktor T.  
 COMPUTER PHYSICS COMMUNICATIONS Volume: 184  
 Issue: 4 Pages: 1339-1343 Published: APR 2013  
 Times Cited: 15  
 (from Web of Science Core Collection)  
 Usage Count   
[Full Text from Publisher](#) [View Abstract](#)
76. **Numerical methods and comparison for computing dark and bright solitons in the nonlinear Schrodinger equation**  
 By: Bao, Weizhu; Tang, Qinglin; Xu, Zhiguo  
 JOURNAL OF COMPUTATIONAL PHYSICS Volume: 235  
 Pages: 423-445 Published: FEB 15 2013  
 Times Cited: 17  
 (from Web of Science Core Collection)  
 Usage Count   
[Full Text from Publisher](#) [View Abstract](#)
77. **Dipolar droplet bound in a trapped Bose-Einstein condensate**  
 By: Young-S, Luis E.; Adhikari, S. K.  
 PHYSICAL REVIEW A Volume: 87 Issue: 1 Article Number: 013618  
 Published: JAN 17 2013  
 Times Cited: 4  
 (from Web of Science Core Collection)  
 Usage Count   
[View Abstract](#)
78. **FARADAY WAVES IN CIGAR-SHAPED BOSE-EINSTEIN CONDENSATES WITH RADIALLY INHOMOGENEOUS SCATTERING LENGTHS**  
 By: Balasubramanian, Sudharsan; Ramaswamy, Radha; Nicolin, A. I.  
 ROMANIAN REPORTS IN PHYSICS Volume: 65 Issue: 3  
 Pages: 820-824 Published: 2013  
 Times Cited: 9  
 (from Web of Science Core Collection)  
 Usage Count   
[View Abstract](#)
79. **DENSITY WAVES IN DIPOLAR BOSE-EINSTEIN CONDENSATES**  
 By: Nicolin, Alexandru I.  
 PROCEEDINGS OF THE ROMANIAN ACADEMY SERIES A-MATHEMATICS PHYSICS TECHNICAL SCIENCES INFORMATION SCIENCE  
 Volume: 14 Issue: 1 Pages: 35-41  
 Published: JAN-MAR 2013  
 Times Cited: 15  
 (from Web of Science Core Collection)  
 Usage Count   
[View Abstract](#)
80. **Study of a degenerate dipolar Fermi gas of Dy-161 atoms**  
 By: Adhikari, S. K.  
 JOURNAL OF PHYSICS B-ATOMIC MOLECULAR AND OPTICAL PHYSICS Volume: 45 Issue: 23 Article Number: 235303  
 Published: DEC 14 2012  
 Times Cited: 5  
 (from Web of Science Core Collection)  
 Usage Count   
[View Abstract](#)
81. **Mixing, demixing, and structure formation in a binary dipolar Bose-Einstein condensate**  
 By: Young-S, Luis E.; Adhikari, S. K.  
 PHYSICAL REVIEW A Volume: 86 Issue: 6 Article Number: 063611  
 Published: DEC 11 2012  
 Times Cited: 14  
 (from Web of Science Core Collection)  
 Usage Count   
[View Abstract](#)
82. **Vortex dynamics of rotating dipolar Bose-Einstein condensates**  
 By: Kumar, R. Kishor; Muruganandam, P.  
 JOURNAL OF PHYSICS B-ATOMIC MOLECULAR AND OPTICAL PHYSICS Volume: 45 Issue: 21 Article Number: 215301  
 Published: NOV 14 2012  
 Times Cited: 14  
 (from Web of Science Core Collection)  
 Usage Count   
[View Abstract](#)

Select Page

[Save to EndNote online](#) [Add to Marked List](#)Sort by: [Publication Date -- newest to oldest](#) 

◀ Page 2 of 2 ▶

Show: [50 per page](#) 

82 records matched your query of the 36,843,663 in the data limits you selected.

Web of Science™ InCites™ Journal Citation Reports® Essential Science Indicators™ EndNote™
Sign In Help English ▾

# WEB OF SCIENCE™

Search
Return to Search Results
My Tools ▾ Search History Marked List

**Citing Articles: 29**  
*(from Web of Science Core Collection)*

**For:** Nonlinear Bose-Einstein-condensate dynamics induced by a harmonic modulation of the s-wave scatterin ...[More](#)

**Times Cited Counts**  
[33 in All Databases](#)

- 33 in Web of Science Core Collection
- 0 in BIOSIS Citation Index
- 2 in Chinese Science Citation Database
- 0 data sets in Data Citation Index
- 0 publication in Data Citation Index
- 0 in Russian Science Citation Index
- 0 in SciELO Citation Index

[View Additional Times Cited Counts](#)

**Refine Results**

**Web of Science Categories** ▾

- OPTICS (15)
- PHYSICS ATOMIC MOLECULAR CHEMICAL (12)
- PHYSICS MULTIDISCIPLINARY (9)
- PHYSICS MATHEMATICAL (2)
- PHYSICS APPLIED (2)

[more options / values...](#)

**Refine**

**Document Types** ▾

- ARTICLE (27)
- REVIEW (1)
- PROCEEDINGS PAPER (1)

[more options / values...](#)

**Refine**

**Research Areas** ▾

**Authors** ▾

**Group Authors** ▾

**Editors** ▾

**Source Titles** ▾

**Book Series Titles** ▾

Sort by: **Publication Date -- newest to oldest** ▾

◀ Page 1 of 1 ▶

Select Page

Save to EndNote online ▾
Add to Marked List

[Analyze Results](#)

[Create Citation Report](#)

1. **Statics and dynamics of a self-bound dipolar matter-wave droplet**

By: Adhikari, S. K.  
[LASER PHYSICS LETTERS](#) Volume: 14 Issue: 2 Article Number: 025501 Published: FEB 2017

[View Abstract](#)
2. **Fortran and C programs for the time-dependent dipolar Gross-Pitaevskii equation in an anisotropic trap**

By: Kumar, R. Kishor; Young-S, Luis E.; Vudragovic, Dusan; et al.  
[COMPUTER PHYSICS COMMUNICATIONS](#) Volume: 195 Pages: 117-128 Published: OCT 2015

[Full Text from Publisher](#)   [View Abstract](#)
3. **Split and overlapped binary solitons in optical lattices**

By: Sekh, Golam Ali; Pepe, Francesco V.; Facchi, Paolo; et al.  
[PHYSICAL REVIEW A](#) Volume: 92 Issue: 1 Article Number: 013639 Published: JUL 31 2015

[View Abstract](#)
4. **Recurrence for motion of solitons of the Bose-Einstein condensate in a dynamic trap**

By: Rosanov, Nikolay N.; Vysotina, Nina V.  
[JOURNAL OF THE OPTICAL SOCIETY OF AMERICA B-OPTICAL PHYSICS](#) Volume: 32 Issue: 5 Pages: B20-B24 Published: MAY 2015

[View Abstract](#)
5. **Beats and expansion of two-component Bose-Einstein condensates in the Thomas-Fermi limit**

By: Quach, James Q.  
[JOURNAL OF PHYSICS B-ATOMIC MOLECULAR AND OPTICAL PHYSICS](#) Volume: 47 Issue: 21 Article Number: 215007 Published: NOV 14 2014

[View Abstract](#)
6. **Tuning the quantum phase transition of bosons in optical lattices via periodic modulation of the s-wave scattering length**

By: Wang, Tao; Zhang, Xue-Feng; Alves dos Santos, Francisco Ednilson; et al.  
[PHYSICAL REVIEW A](#) Volume: 90 Issue: 1 Article Number: 013633 Published: JUL 31 2014

[View Abstract](#)
7. **Parametric resonance in Bose-Einstein condensates with periodic modulation of attractive interaction**

By: Cairncross, William; Pelster, Axel  
[EUROPEAN PHYSICAL JOURNAL D](#) Volume: 68 Issue: 5 Article Number: 106 Published: MAY 7 2014

[View Abstract](#)

**Times Cited: 0**  
*(from Web of Science Core Collection)*

**Usage Count** ▾

**Times Cited: 27**  
*(from Web of Science Core Collection)*

**Usage Count** ▾

**Times Cited: 0**  
*(from Web of Science Core Collection)*

**Usage Count** ▾

**Times Cited: 7**  
*(from Web of Science Core Collection)*

**Usage Count** ▾

**Times Cited: 0**  
*(from Web of Science Core Collection)*

**Usage Count** ▾

**Times Cited: 8**  
*(from Web of Science Core Collection)*

**Usage Count** ▾

**Times Cited: 4**  
*(from Web of Science Core Collection)*

**Usage Count** ▾

Conference Titles		
Publication Years		
Organizations-Enhanced		
Funding Agencies		
Languages		
Countries/Territories		
ESI Top Papers		
Open Access		
For advanced refine options, use		
<a href="#">Analyze Results</a>		
8.	<p><b>Faraday waves in collisionally inhomogeneous Bose-Einstein condensates</b></p> <p>By: Balaz, Antun; Paun, Remus; Nicolin, Alexandru I.; et al.  <b>PHYSICAL REVIEW A</b> Volume: 89 Issue: 2 Article Number: 023609 Published: FEB 11 2014</p> <p><a href="#">View Abstract</a></p>	<p><b>Times Cited: 20</b>  <i>(from Web of Science Core Collection)</i></p> <p><b>Usage Count</b> </p>
9.	<p><b>Nonlinear resonance phenomenon of one-dimensional Bose-Einstein condensate under periodic modulation</b></p> <p>By: Hua Wei; Liu Shi-Xing  <b>CHINESE PHYSICS B</b> Volume: 23 Issue: 2 Article Number: 020309 Published: FEB 2014</p> <p><a href="#">View Abstract</a></p>	<p><b>Times Cited: 3</b>  <i>(from Web of Science Core Collection)</i></p> <p><b>Usage Count</b> </p>
10.	<p><b>Bifurcation response and Melnikov chaos in the dynamic of a Bose-Einstein condensate loaded into a moving optical lattice</b></p> <p>By: Tchatchueng, S.; Siewe, M. Siewe; Kakmeni, F. M. Moukam; et al.  <b>NONLINEAR DYNAMICS</b> Volume: 75 Issue: 3 Pages: 461-474 Published: FEB 2014</p> <p><a href="#">View Abstract</a></p>	<p><b>Times Cited: 2</b>  <i>(from Web of Science Core Collection)</i></p> <p><b>Usage Count</b> </p>
11.	<p><b>Density Waves in Dipolar Bose-Einstein Condensates by Means of Symbolic Computations</b></p> <p>By: Nicolin, Alexandru I.; Rata, Ionel            Edited by: Dulea, M; Karaivanova, A; Oulas, A; et al.            Conference: HP-SEE User Forum Location: Natl Lib Serbia, Belgrade, SERBIA Date: OCT 17-19, 2012            Sponsor(s): Inst Phys Belgrade            HIGH-PERFORMANCE COMPUTING INFRASTRUCTURE FOR SOUTH EAST EUROPE'S RESEARCH COMMUNITIES: RESULTS OF THE HP-SEE USER FORUM 2012 Book Series: Modeling and Optimization in Science and Technologies            Volume: 2 Pages: 15-21 Published: 2014</p> <p><a href="#">View Abstract</a></p>	<p><b>Times Cited: 3</b>  <i>(from Web of Science Core Collection)</i></p> <p><b>Usage Count</b> </p>
12.	<p><b>ANALYTICAL DESCRIPTION OF THE NONLINEAR DYNAMICS OF BOSE-EINSTEIN CONDENSATES BY MEANS OF GENETIC ALGORITHMS</b></p> <p>By: Raportaru, Mihaela Carina; Jovanovski, Jane; Jakimovski, Boro; et al.  <b>ROMANIAN JOURNAL OF PHYSICS</b> Volume: 59 Issue: 7-8 Pages: 677-685 Published: 2014</p> <p><a href="#">View Abstract</a></p>	<p><b>Times Cited: 3</b>  <i>(from Web of Science Core Collection)</i></p> <p><b>Usage Count</b> </p>
13.	<p><b>SPLITTING AND RECOMBINATION OF 2D MATTER-WAVE SOLITONS IN A TRANSIENT TRAP</b></p> <p>By: Kumar, V. Ramesh; Wen, Lin; Radha, R.; et al.  <b>ROMANIAN REPORTS IN PHYSICS</b> Volume: 66 Issue: 2 Pages: 443-454 Published: 2014</p> <p><a href="#">View Abstract</a></p>	<p><b>Times Cited: 0</b>  <i>(from Web of Science Core Collection)</i></p> <p><b>Usage Count</b> </p>
14.	<p><b>GROUND STATE OF BOSE-EINSTEIN CONDENSATES WITH INHOMOGENEOUS SCATTERING LENGTHS</b></p> <p>By: Nicolin, A. I.; Balaz, A.; Sudharsan, J. B.; et al.  <b>ROMANIAN JOURNAL OF PHYSICS</b> Volume: 59 Issue: 3-4 Pages: 204-213 Published: 2014</p> <p><a href="#">View Abstract</a></p>	<p><b>Times Cited: 8</b>  <i>(from Web of Science Core Collection)</i></p> <p><b>Usage Count</b> </p>
15.	<p><b>Breakdown of the Kohn theorem near a Feshbach resonance in a magnetic trap</b></p> <p>By: Al-Jibbouri, Hamid; Pelster, Axel  <b>PHYSICAL REVIEW A</b> Volume: 88 Issue: 3 Article Number: 033621 Published: SEP 17 2013</p> <p><a href="#">View Abstract</a></p>	<p><b>Times Cited: 6</b>  <i>(from Web of Science Core Collection)</i></p> <p><b>Usage Count</b> </p>
16.	<p><b>Super-Bloch oscillations with modulated interaction</b></p> <p>By: Diaz, Elena; Garcia Mena, Alberto; Asakura, Kunihiro; et al.  <b>PHYSICAL REVIEW A</b> Volume: 87 Issue: 1 Article Number:</p>	<p><b>Times Cited: 1</b>  <i>(from Web of Science Core Collection)</i></p>



015601 Published: JAN 17 2013

[View Abstract](#)Usage Count **17. DENSITY WAVES IN DIPOLAR BOSE-EINSTEIN CONDENSATES**

By: Nicolin, Alexandru I.

PROCEEDINGS OF THE ROMANIAN ACADEMY SERIES  
A-MATHEMATICS PHYSICS TECHNICAL SCIENCES  
INFORMATION SCIENCE Volume: 14 Issue: 1 Pages: 35-41  
Published: JAN-MAR 2013[View Abstract](#)**Times Cited: 15**  
*(from Web of Science Core Collection)*Usage Count **18. Beyond mean-field low-lying excitations of dipolar Bose gases**

By: Lima, A. R. P.; Pelster, A.

PHYSICAL REVIEW A Volume: 86 Issue: 6 Article Number:  
063609 Published: DEC 10 2012[View Abstract](#)**Times Cited: 32**  
*(from Web of Science Core Collection)*Usage Count **19. Effects of spatially inhomogeneous atomic interactions on Bose-Einstein condensates in optical lattices**

By: Sekh, Golam Ali

PHYSICS LETTERS A Volume: 376 Issue: 21 Pages:  
1740-1747 Published: APR 23 2012[Full Text from Publisher](#)[View Abstract](#)**Times Cited: 6**  
*(from Web of Science Core Collection)*Usage Count **20. Numerical and variational solutions of the dipolar Gross-Pitaevskii equation in reduced dimensions**

By: Muruganandam, P.; Adhikari, S. K.

LASER PHYSICS Volume: 22 Issue: 4 Pages: 813-820  
Published: APR 2012[View Abstract](#)**Times Cited: 19**  
*(from Web of Science Core Collection)*Usage Count **21. Controlled excitation and resonant acceleration of ultracold few-boson systems by driven interactions in a harmonic trap**

By: Brouzos, Ioannis; Schmelcher, Peter

PHYSICAL REVIEW A Volume: 85 Issue: 3 Article Number:  
033635 Published: MAR 26 2012[View Abstract](#)**Times Cited: 8**  
*(from Web of Science Core Collection)*Usage Count **22. Coupling collective modes in a trapped superfluid**

By: Ramos, E. R. F.; dos Santos, F. E. A.; Caracanhas, M. A.; et al.

PHYSICAL REVIEW A Volume: 85 Issue: 3 Article Number:  
033608 Published: MAR 5 2012[View Abstract](#)**Times Cited: 3**  
*(from Web of Science Core Collection)*Usage Count **23. Variational treatment of Faraday waves in inhomogeneous Bose-Einstein condensates**

By: Nicolin, Alexandru I.

PHYSICA A-STATISTICAL MECHANICS AND ITS  
APPLICATIONS Volume: 391 Issue: 4 Pages: 1062-1067  
Published: FEB 15 2012[Full Text from Publisher](#)[View Abstract](#)**Times Cited: 21**  
*(from Web of Science Core Collection)*Usage Count **24. Faraday waves in binary nonmiscible Bose-Einstein condensates**

By: Balaz, Antun; Nicolin, Alexandru I.

PHYSICAL REVIEW A Volume: 85 Issue: 2 Article Number:  
023613 Published: FEB 9 2012[View Abstract](#)**Times Cited: 46**  
*(from Web of Science Core Collection)*Usage Count **25. Nonlinear quantum interferometry with Bose condensed atoms**

By: Lee, Chaohong; Huang, Jiahao; Deng, Haiming; et al.

FRONTIERS OF PHYSICS Volume: 7 Issue: 1 Pages:  
109-130 Published: FEB 2012**Times Cited: 36**  
*(from Web of Science Core Collection)*Usage Count 

[View Abstract](#)26. **FORMATION OF FARADAY AND RESONANT WAVES IN DRIVEN BOSE-EINSTEIN CONDENSATES**

By: Raportaru, Mihaela-Carina

ROMANIAN REPORTS IN PHYSICS Volume: 64 Issue: 1  
Pages: 105-115 Published: 2012**Times Cited: 8**  
(from Web of Science Core Collection)**Usage Count** [View Abstract](#)27. **Stability and decay of Bloch oscillations in the presence of time-dependent nonlinearity**

By: Gaul, Christopher; Diaz, Elena; Lima, Rodrigo P. A.; et al.

PHYSICAL REVIEW A Volume: 84 Issue: 5 Article Number: 053627  
Published: NOV 23 2011**Times Cited: 9**  
(from Web of Science Core Collection)**Usage Count** [View Abstract](#)28. **Resonant wave formation in Bose-Einstein condensates**


By: Nicolin, Alexandru I.

PHYSICAL REVIEW E Volume: 84 Issue: 5 Article Number: 056202  
Part: 2 Published: NOV 4 2011**Times Cited: 28**  
(from Web of Science Core Collection)**Usage Count** [View Abstract](#)29. **FARADAY WAVES IN BOSE-EINSTEIN CONDENSATES SUBJECT TO ANISOTROPIC TRANSVERSE CONFINEMENT**

By: Nicolin, Alexandru I.

ROMANIAN REPORTS IN PHYSICS Volume: 63 Supplement: S  
Pages: 1329-1337 Published: 2011**Times Cited: 16**  
(from Web of Science Core Collection)**Usage Count** [View Abstract](#)

Select Page

[Save to EndNote online](#) [Add to Marked List](#)Sort by: **Publication Date -- newest to oldest** ◀ Page  of 1 ▶Show: **50 per page** 

29 records matched your query of the 36,843,663 in the data limits you selected.

Web of Science™ InCites™ Journal Citation Reports® Essential Science Indicators™ EndNote™
Sign In Help English

# WEB OF SCIENCE™

Search
Return to Search Results
My Tools Search History Marked List

### Citing Articles: 15

(from Web of Science Core Collection)

**For:** Ultra-fast converging path-integral approach for rotating ideal Bose-Einstein condensates  
[...More](#)

**Times Cited Counts**

19 in All Databases

19 in Web of Science Core Collection

0 in BIOSIS Citation Index

1 in Chinese Science Citation Database

0 data sets in Data Citation Index

0 publication in Data Citation Index

0 in Russian Science Citation Index

0 in SciELO Citation Index

[View Additional Times Cited Counts](#)

---

### Refine Results

**Web of Science Categories**

- PHYSICS MULTIDISCIPLINARY (6)
- PHYSICS ATOMIC MOLECULAR CHEMICAL (6)
- OPTICS (6)
- COMPUTER SCIENCE INTERDISCIPLINARY APPLICATIONS (2)
- PHYSICS MATHEMATICAL (1)

[more options / values...](#)

Refine

---

**Document Types**

- ARTICLE (14)
- PROCEEDINGS PAPER (1)

[more options / values...](#)

Refine

---

**Research Areas**

---

**Authors**

---

**Group Authors**

---

**Editors**

---

**Source Titles**

Sort by: Publication Date -- newest to oldest
Page 1 of 1

Select Page
Save to EndNote online
Add to Marked List

Analyze Results
Create Citation Report

1. **OpenMP, OpenMP/MPI, and CUDA/MPI C programs for solving the time-dependent dipolar Gross-Pitaevskii equation**
Times Cited: 0  
*(from Web of Science Core Collection)*

By: Loncar, Vladimir; Young-S, Luis E.; Skrbic, Srdjan; et al.  
**COMPUTER PHYSICS COMMUNICATIONS** Volume: 209  
Pages: 190-196 Published: DEC 2016

Full Text from Publisher
View Abstract
2. **Thermodynamic properties of a rotating ideal Bose gas in an anisotropic harmonic trap**
Times Cited: 0  
*(from Web of Science Core Collection)*

By: Guo, CuiXian; Xiao, DuanLiang; Pan, Xiao-Yin  
**EUROPEAN PHYSICAL JOURNAL D** Volume: 70 Issue: 10  
Article Number: 223 Published: OCT 25 2016

View Abstract
3. **Faraday and resonant waves in binary collisionally-inhomogeneous Bose-Einstein condensates**
Times Cited: 0  
*(from Web of Science Core Collection)*

By: Sudharsan, J. B.; Radha, R.; Raportaru, Mihaela Carina; et al.  
**JOURNAL OF PHYSICS B-ATOMIC MOLECULAR AND OPTICAL PHYSICS** Volume: 49 Issue: 16 Article Number: 165303  
Published: AUG 28 2016

View Abstract
4. **The particle flow oscillations of rotating non-interacting gases in a two-dimensional harmonic trap**
Times Cited: 0  
*(from Web of Science Core Collection)*

By: Li, Yushan; Gu, Qiang  
**PHYSICS LETTERS A** Volume: 380 Issue: 3 Pages: 353-358  
Published: JAN 28 2016

Full Text from Publisher
View Abstract
5. **Effects of a finite number of particles on the thermodynamic properties of a harmonically trapped ideal charged Bose gas in a constant magnetic field**
Times Cited: 0  
*(from Web of Science Core Collection)*

By: Xiao, Duan-Liang; Lai, Meng-Yun; Pan, Xiao-Yin  
**CHINESE PHYSICS B** Volume: 25 Issue: 1 Article Number: 010307  
Published: JAN 2016

View Abstract
6. **Split and overlapped binary solitons in optical lattices**
Times Cited: 0  
*(from Web of Science Core Collection)*

By: Sekh, Golam Ali; Pepe, Francesco V.; Facchi, Paolo; et al.  
**PHYSICAL REVIEW A** Volume: 92 Issue: 1 Article Number: 013639  
Published: JUL 31 2015

View Abstract
7. **BOSE-EINSTEIN CONDENSATION: TWENTY YEARS AFTER**
Times Cited: 50  
*(from Web of Science Core Collection)*

By: Bagnato, V. S.; Frantzeskakis, D. J.; Kevrekidis, P. G.; et al.  
**ROMANIAN REPORTS IN PHYSICS** Volume: 67 Issue: 1  
Pages: 5-50 Published: 2015

View Abstract
Highly Cited Paper

Usage Count

Book Series Titles	◀
Conference Titles	◀
Publication Years	◀
Organizations-Enhanced	◀
Funding Agencies	◀
Languages	◀
Countries/Territories	◀
ESI Top Papers	◀
Open Access	◀

For advanced refine options, use

Analyze Results

8. **Thermodynamic properties of rotating trapped ideal Bose gases**  
 By: Li, Yushan; Gu, Qiang  
 PHYSICS LETTERS A Volume: 378 Issue: 18-19 Pages: 1233-1238 Published: MAR 28 2014  

Full Text from Publisher
View Abstract

**Times Cited: 6**  
*(from Web of Science Core Collection)*  
**Usage Count** ▼
  
9. **Density Waves in Dipolar Bose-Einstein Condensates by Means of Symbolic Computations**  
 By: Nicolin, Alexandru I.; Rata, Ionel  
 Edited by: Dulea, M; Karaivanova, A; Oulas, A; et al.  
 Conference: HP-SEE User Forum Location: Natl Lib Serbia, Belgrade, SERBIA Date: OCT 17-19, 2012  
 Sponsor(s): Inst Phys Belgrade  
 HIGH-PERFORMANCE COMPUTING INFRASTRUCTURE FOR SOUTH EAST EUROPE'S RESEARCH COMMUNITIES: RESULTS OF THE HP-SEE USER FORUM 2012 Book Series: Modeling and Optimization in Science and Technologies Volume: 2 Pages: 15-21 Published: 2014  

View Abstract

**Times Cited: 3**  
*(from Web of Science Core Collection)*  
**Usage Count** ▼
  
10. **Quantum phase for a system with an arbitrary discrete energy spectrum**  
 By: Arsenovic, Dusan; Buric, Nikola; Davidovic, Dragomir; et al.  
 PHYSICAL REVIEW A Volume: 88 Issue: 2 Article Number: 022117 Published: AUG 19 2013  

View Abstract

**Times Cited: 1**  
*(from Web of Science Core Collection)*  
**Usage Count** ▼
  
11. **DENSITY WAVES IN DIPOLAR BOSE-EINSTEIN CONDENSATES**  
 By: Nicolin, Alexandru I.  
 PROCEEDINGS OF THE ROMANIAN ACADEMY SERIES A-MATHEMATICS PHYSICS TECHNICAL SCIENCES INFORMATION SCIENCE Volume: 14 Issue: 1 Pages: 35-41 Published: JAN-MAR 2013  

View Abstract

**Times Cited: 15**  
*(from Web of Science Core Collection)*  
**Usage Count** ▼
  
12. **Effects of spatially inhomogeneous atomic interactions on Bose-Einstein condensates in optical lattices**  
 By: Sekh, Golam Ali  
 PHYSICS LETTERS A Volume: 376 Issue: 21 Pages: 1740-1747 Published: APR 23 2012  

Full Text from Publisher
View Abstract

**Times Cited: 6**  
*(from Web of Science Core Collection)*  
**Usage Count** ▼
  
13. **Faraday waves in binary nonmiscible Bose-Einstein condensates**  
 By: Balaz, Antun; Nicolin, Alexandru I.  
 PHYSICAL REVIEW A Volume: 85 Issue: 2 Article Number: 023613 Published: FEB 9 2012  

View Abstract

**Times Cited: 46**  
*(from Web of Science Core Collection)*  
**Usage Count** ▼
  
14. **Critical temperature of a Rashba spin-orbit-coupled Bose gas in a harmonic trap**  
 By: Hu, Hui; Liu, Xia-Ji  
 PHYSICAL REVIEW A Volume: 85 Issue: 1 Article Number: 013619 Published: JAN 12 2012  

View Abstract

**Times Cited: 23**  
*(from Web of Science Core Collection)*  
**Usage Count** ▼
  
15. **FORMATION OF FARADAY AND RESONANT WAVES IN DRIVEN BOSE-EINSTEIN CONDENSATES**  
 By: Raportaru, Mihaela-Carina  
 ROMANIAN REPORTS IN PHYSICS Volume: 64 Issue: 1 Pages: 105-115 Published: 2012  

View Abstract

**Times Cited: 8**  
*(from Web of Science Core Collection)*  
**Usage Count** ▼

Select Page



Save to EndNote online ▼

Add to Marked List

Sort by: Publication Date -- newest to oldest ▼

◀ Page 1 of 1 ▶

Show: **50 per page** 

*15 records matched your query of the 36,466,594 in the data limits you selected.*

Web of Science™ InCites™ Journal Citation Reports® Essential Science Indicators™ EndNote™
Sign In Help English

# WEB OF SCIENCE™

Search
Return to Search Results
My Tools Search History Marked List

### Citing Articles: 18

*(from Web of Science Core Collection)*

**For:** Geometric resonances in Bose-Einstein condensates with two- and three-body interactions [...More](#)

**Times Cited Counts**  
18 in All Databases

- 18 in Web of Science Core Collection
- 0 in BIOSIS Citation Index
- 0 in Chinese Science Citation Database
- 0 data sets in Data Citation Index
- 0 publication in Data Citation Index
- 0 in Russian Science Citation Index
- 0 in SciELO Citation Index

[View Additional Times Cited Counts](#)

---

### Refine Results

**Web of Science Categories**

- PHYSICS MULTIDISCIPLINARY (7)
- PHYSICS ATOMIC MOLECULAR CHEMICAL (6)
- OPTICS (6)
- PHYSICS MATHEMATICAL (5)
- COMPUTER SCIENCE INTERDISCIPLINARY APPLICATIONS (3)

[more options / values...](#)

**Refine**

**Document Types**

- ARTICLE (18)

**Refine**

**Research Areas**

**Authors**

- BALAZ A (5)
- MURUGANANDAM P (4)
- PORSEZIAN K (3)
- PELSTER A (3)
- ADHIKARI SK (3)

[more options / values...](#)

**Refine**

**Group Authors**

Sort by: Publication Date -- newest to oldest

Page 1 of 1

Select Page
Save to EndNote online
Add to Marked List

Analyze Results
Create Citation Report

- 1. OpenMP, OpenMP/MPI, and CUDA/MPI C programs for solving the time-dependent dipolar Gross-Pitaevskii equation**

By: Loncar, Vladimir; Young-S, Luis E.; Skrbic, Srdjan; et al.  
**COMPUTER PHYSICS COMMUNICATIONS** Volume: 209  
 Pages: 190-196 Published: DEC 2016

Full Text from Publisher
View Abstract
- 2. Faraday and resonant waves in binary collisionally-inhomogeneous Bose-Einstein condensates**

By: Sudharsan, J. B.; Radha, R.; Raportaru, Mihaela Carina; et al.  
**JOURNAL OF PHYSICS B-ATOMIC MOLECULAR AND OPTICAL PHYSICS** Volume: 49 Issue: 16 Article Number: 165303  
 Published: AUG 28 2016

View Abstract
- 3. OpenMP Fortran and C programs for solving the time-dependent Gross-Pitaevskii equation in an anisotropic trap**

By: Young-S., Luis E.; Vudragovic, Dugan; Muruganandam, Paulsamy; et al.  
**COMPUTER PHYSICS COMMUNICATIONS** Volume: 204  
 Pages: 209-213 Published: JUL 2016

Full Text from Publisher
View Abstract
- 4. Observation of Geometric Parametric Instability Induced by the Periodic Spatial Self-Imaging of Multimode Waves**

By: Krupa, Katarzyna; Tonello, Alessandro; Barthelemy, Alain; et al.  
**PHYSICAL REVIEW LETTERS** Volume: 116 Issue: 18  
 Article Number: 183901 Published: MAY 5 2016

View Abstract
- 5. Hybrid OpenMP/MPI programs for solving the time-dependent Gross-Pitaevskii equation in a fully anisotropic trap**

By: Sataric, Bogdan; Slavnic, Vladimir; Belic, Aleksandar; et al.  
**COMPUTER PHYSICS COMMUNICATIONS** Volume: 200  
 Pages: 411-417 Published: MAR 2016

Full Text from Publisher
View Abstract
- 6. Droplet formation in a Bose-Einstein condensate with strong dipole-dipole interaction**

By: Xi, Kui-Tian; Saito, Hiroki  
**PHYSICAL REVIEW A** Volume: 93 Issue: 1 Article Number: 011604  
 Published: JAN 15 2016

View Abstract

Editors	◀
Source Titles	◀
Book Series Titles	◀
Conference Titles	◀
Publication Years	◀
Organizations-Enhanced	◀
Funding Agencies	◀
Languages	◀
Countries/Territories	◀
ESI Top Papers	◀
Open Access	◀

For advanced refine options, use

[Analyze Results](#)

7. **STUDY ON THE STABILIZATION OF ATTRACTIVE BOSE-EINSTEIN CONDENSATES USING PROJECTION OPERATOR METHOD**  
 By: Sabari, S.; Porsezian, K.; Muruganandam, P.  
 ROMANIAN REPORTS IN PHYSICS Volume: 68 Issue: 3  
 Pages: 990-1003 Published: 2016  
[View Abstract](#)  
 Times Cited: 0  
 (from Web of Science Core Collection)  
 Usage Count
8. **LOCALIZED NONLINEAR MATTER WAVES IN ONE-DIMENSIONAL BOSE-EINSTEIN CONDENSATES WITH SPATIOTEMPORALLY MODULATED TWO- AND THREE-BODY INTERACTIONS**  
 By: Wang, Deng-Shan; Xue, Yushan; Zhang, Zhifei  
 ROMANIAN JOURNAL OF PHYSICS Volume: 61 Issue: 5-6  
 Pages: 827-841 Published: 2016  
[View Abstract](#)  
 Times Cited: 1  
 (from Web of Science Core Collection)  
 Usage Count
9. **Stability of logarithmic Bose-Einstein condensate in harmonic trap**  
 By: Bouharia, Brahim  
 MODERN PHYSICS LETTERS B Volume: 29 Issue: 1  
 Article Number: 1450260 Published: JAN 10 2015  
[Full Text from Publisher](#) [View Abstract](#)  
 Times Cited: 1  
 (from Web of Science Core Collection)  
 Usage Count
10. **One-dimensional Bose-Hubbard model with pure three-body interactions**  
 By: Sowinski, Tomasz  
 CENTRAL EUROPEAN JOURNAL OF PHYSICS Volume: 12  
 Issue: 7 Pages: 473-479 Published: JUL 2014  
[View Abstract](#)  
 Times Cited: 4  
 (from Web of Science Core Collection)  
 Usage Count
11. **Parametric resonance in Bose-Einstein condensates with periodic modulation of attractive interaction**  
 By: Cairncross, William; Pelster, Axel  
 EUROPEAN PHYSICAL JOURNAL D Volume: 68 Issue: 5  
 Article Number: 106 Published: MAY 7 2014  
[View Abstract](#)  
 Times Cited: 3  
 (from Web of Science Core Collection)  
 Usage Count
12. **ANALYTICAL DESCRIPTION OF THE NONLINEAR DYNAMICS OF BOSE-EINSTEIN CONDENSATES BY MEANS OF GENETIC ALGORITHMS**  
 By: Raportaru, Mihaela Carina; Jovanovski, Jane; Jakimovski, Boro; et al.  
 ROMANIAN JOURNAL OF PHYSICS Volume: 59 Issue: 7-8  
 Pages: 677-685 Published: 2014  
[View Abstract](#)  
 Times Cited: 3  
 (from Web of Science Core Collection)  
 Usage Count
13. **GROUND STATE OF BOSE-EINSTEIN CONDENSATES WITH INHOMOGENEOUS SCATTERING LENGTHS**  
 By: Nicolin, A. I.; Balaz, A.; Sudharsan, J. B.; et al.  
 ROMANIAN JOURNAL OF PHYSICS Volume: 59 Issue: 3-4  
 Pages: 204-213 Published: 2014  
[View Abstract](#)  
 Times Cited: 8  
 (from Web of Science Core Collection)  
 Usage Count
14. **A variational approach to the modulational-oscillatory instability of Bose-Einstein condensates in an optical potential**  
 By: Sabari, S.; Wamba, E.; Porsezian, K.; et al.  
 PHYSICS LETTERS A Volume: 377 Issue: 37 Pages: 2408-2415  
 Published: NOV 8 2013  
[Full Text from Publisher](#) [View Abstract](#)  
 Times Cited: 4  
 (from Web of Science Core Collection)  
 Usage Count
15. **Breakdown of the Kohn theorem near a Feshbach resonance in a magnetic trap**  
 By: Al-Jibbouri, Hamid; Pelster, Axel  
 PHYSICAL REVIEW A Volume: 88 Issue: 3 Article Number: 033621  
 Published: SEP 17 2013  
[View Abstract](#)  
 Times Cited: 6  
 (from Web of Science Core Collection)  
 Usage Count

16. **Vortex dynamics in cubic-quintic Bose-Einstein condensates**  
By: Mithun, T.; Porsezian, K.; Dey, Bishwajyoti  
**PHYSICAL REVIEW E** Volume: 88 Issue: 1 Article Number: 012904 Published: JUL 8 2013  
[View Abstract](#)  
**Times Cited: 9**  
*(from Web of Science Core Collection)*  
**Usage Count**
17. **One-dimensional cubic-quintic Gross-Pitaevskii equation for Bose-Einstein condensates in a trap potential**  
By: Trallero-Giner, Carlos; Cipelatti, Rolci; Liew, Timothy C. H.  
**EUROPEAN PHYSICAL JOURNAL D** Volume: 67 Issue: 7 Article Number: 143 Published: JUL 2013  
[View Abstract](#)  
**Times Cited: 9**  
*(from Web of Science Core Collection)*  
**Usage Count**
18. **Beyond mean-field low-lying excitations of dipolar Bose gases**  
By: Lima, A. R. P.; Pelster, A.  
**PHYSICAL REVIEW A** Volume: 86 Issue: 6 Article Number: 063609 Published: DEC 10 2012  
[View Abstract](#)  
**Times Cited: 30**  
*(from Web of Science Core Collection)*  
**Usage Count**

Select Page

[Save to EndNote online](#) [Add to Marked List](#)Sort by: **Publication Date -- newest to oldest**

◀ Page 1 of 1 ▶

Show: **50 per page** *18 records matched your query of the 36,466,594 in the data limits you selected.*



Web of Science™	InCites™	Journal Citation Reports®	Essential Science Indicators™	EndNote™	Sign In ▾	Help	English ▾
-----------------	----------	---------------------------	-------------------------------	----------	-----------	------	-----------

WEB OF SCIENCE™

---

Search
Return to Search Results
My Tools ▾
Search History
Marked List

### Citing Articles: 12

*(from Web of Science Core Collection)*

**For:** Recursive Schrodinger equation approach to faster converging path integrals [...More](#)

**Times Cited Counts**  
18 in All Databases

18 in Web of Science Core Collection

0 in BIOSIS Citation Index

0 in Chinese Science Citation Database

0 data sets in Data Citation Index

0 publication in Data Citation Index

0 in Russian Science Citation Index

0 in SciELO Citation Index

[View Additional Times Cited Counts](#)

---

### Refine Results

**Web of Science Categories** ▾

- PHYSICS MULTIDISCIPLINARY (6)
- PHYSICS MATHEMATICAL (3)
- PHYSICS FLUIDS PLASMAS (2)
- PHYSICS ATOMIC MOLECULAR CHEMICAL (2)
- OPTICS (2)

[more options / values...](#)

Refine

---

**Document Types** ▾

ARTICLE (12)

Refine

---

**Research Areas** ▾

---

**Authors** ▾

---

**Group Authors** ▾

---

**Editors** ▾

---

**Source Titles** ▾

---

**Book Series Titles** ▾

---

**Conference Titles** ▾

Sort by: Publication Date -- newest to oldest ▾
 ◀ Page 1 of 1 ▶

Select Page
 
Save to EndNote online ▾
 Add to Marked List

[Analyze Results](#)
 [Create Citation Report](#)

1. **OpenMP, OpenMP/MPI, and CUDA/MPI C programs for solving the time-dependent dipolar Gross-Pitaevskii equation**

By: Loncar, Vladimir; Young-S, Luis E.; Skrbic, Srdjan; et al.  
**COMPUTER PHYSICS COMMUNICATIONS** Volume: 209  
 Pages: 190-196 Published: DEC 2016

Full Text from Publisher
View Abstract
2. **Faraday and resonant waves in binary collisionally-inhomogeneous Bose-Einstein condensates**

By: Sudharsan, J. B.; Radha, R.; Raportaru, Mihaela Carina; et al.  
**JOURNAL OF PHYSICS B-ATOMIC MOLECULAR AND OPTICAL PHYSICS** Volume: 49 Issue: 16 Article Number: 165303  
 Published: AUG 28 2016

View Abstract
3. **BOSE-EINSTEIN CONDENSATION: TWENTY YEARS AFTER**

By: Bagnato, V. S.; Frantzeskakis, D. J.; Kevrekidis, P. G.; et al.  
**ROMANIAN REPORTS IN PHYSICS** Volume: 67 Issue: 1  
 Pages: 5-50 Published: 2015

View Abstract
4. **ANALYTICAL DESCRIPTION OF THE NONLINEAR DYNAMICS OF BOSE-EINSTEIN CONDENSATES BY MEANS OF GENETIC ALGORITHMS**

By: Raportaru, Mihaela Carina; Jovanovski, Jane; Jakimovski, Boro; et al.  
**ROMANIAN JOURNAL OF PHYSICS** Volume: 59 Issue: 7-8  
 Pages: 677-685 Published: 2014

View Abstract
5. **Effects of spatially inhomogeneous atomic interactions on Bose-Einstein condensates in optical lattices**

By: Sekh, Golam Ali  
**PHYSICS LETTERS A** Volume: 376 Issue: 21 Pages: 1740-1747  
 Published: APR 23 2012

Full Text from Publisher
View Abstract
6. **Variational treatment of Faraday waves in inhomogeneous Bose-Einstein condensates**

By: Nicolin, Alexandru I.  
**PHYSICA A-STATISTICAL MECHANICS AND ITS APPLICATIONS** Volume: 391 Issue: 4 Pages: 1062-1067  
 Published: FEB 15 2012

Full Text from Publisher
View Abstract
7. **Faraday waves in binary nonmiscible Bose-Einstein condensates**

By: Balaz, Antun; Nicolin, Alexandru I.  
**PHYSICAL REVIEW A** Volume: 85 Issue: 2 Article Number: 023613  
 Published: FEB 9 2012

**Times Cited: 0**  
*(from Web of Science Core Collection)*

**Usage Count** ▾

**Times Cited: 0**  
*(from Web of Science Core Collection)*

**Usage Count** ▾

**Times Cited: 50**  
*(from Web of Science Core Collection)*

**Highly Cited Paper**

**Usage Count** ▾

**Times Cited: 3**  
*(from Web of Science Core Collection)*

**Usage Count** ▾

**Times Cited: 6**  
*(from Web of Science Core Collection)*

**Usage Count** ▾

**Times Cited: 21**  
*(from Web of Science Core Collection)*



**Usage Count** ▾

**Times Cited: 46**  
*(from Web of Science Core Collection)*

**Usage Count** ▾

<p><b>Publication Years</b> ◀</p> <p><b>Organizations-Enhanced</b> ◀</p> <p><b>Funding Agencies</b> ◀</p> <p><b>Languages</b> ◀</p> <p><b>Countries/Territories</b> ◀</p> <p><b>ESI Top Papers</b> ◀</p> <p><b>Open Access</b> ◀</p> <p><i>For advanced refine options, use</i></p> <p><b>Analyze Results</b></p>	<p><a href="#">View Abstract</a></p> <p>8. <b>Onset Temperature of Bose-Einstein Condensation in Incommensurate Solid He-4</b></p> <p>By: Rota, R.; Boronat, J.  <b>PHYSICAL REVIEW LETTERS</b> Volume: 108 Issue: 4 Article Number: 045308 Published: JAN 26 2012</p> <p><a href="#">View Abstract</a></p> <p>9. <b>FORMATION OF FARADAY AND RESONANT WAVES IN DRIVEN BOSE-EINSTEIN CONDENSATES</b></p> <p>By: Raportaru, Mihaela-Carina  <b>ROMANIAN REPORTS IN PHYSICS</b> Volume: 64 Issue: 1 Pages: 105-115 Published: 2012</p> <p><a href="#">View Abstract</a></p> <p>10. <b>Resonant wave formation in Bose-Einstein condensates</b></p> <p>By: Nicolin, Alexandru I.  <b>PHYSICAL REVIEW E</b> Volume: 84 Issue: 5 Article Number: 056202 Part: 2 Published: NOV 4 2011</p> <p><a href="#">View Abstract</a></p> <p>11. <b>Development of Grid e-Infrastructure in South-Eastern Europe</b></p> <p>By: Balaz, Antun; Prnjat, Ognjen; Vudragovic, Dusan; et al.  <b>JOURNAL OF GRID COMPUTING</b> Volume: 9 Issue: 2 Special Issue: SI Pages: 135-154 Published: JUN 2011</p> <p><a href="#">View Abstract</a></p> <p>12. <b>Path-integral-expanded-ensemble Monte Carlo method in treatment of the sign problem for fermions</b></p> <p>By: Voznesenskiy, M. A.; Vorontsov-Velyaminov, P. N.; Lyubartsev, A. P.  <b>PHYSICAL REVIEW E</b> Volume: 80 Issue: 6 Article Number: 066702 Part: 2 Published: DEC 2009</p> <p><a href="#">View Abstract</a></p> <p>Select Page       <a href="#">Save to EndNote online</a>   <a href="#">Add to Marked List</a></p> <p>Sort by: <b>Publication Date -- newest to oldest</b> ▼</p> <p>Show: <b>50 per page</b> ▼</p> <p>◀ Page 1 of 1 ▶</p> <p><i>12 records matched your query of the 36,466,594 in the data limits you selected.</i></p>	<p><b>Times Cited: 7</b>  <i>(from Web of Science Core Collection)</i></p> <p><b>Usage Count</b> ▼</p> <p><b>Times Cited: 8</b>  <i>(from Web of Science Core Collection)</i></p> <p><b>Usage Count</b> ▼</p> <p><b>Times Cited: 28</b>  <i>(from Web of Science Core Collection)</i></p> <p><b>Usage Count</b> ▼</p> <p><b>Times Cited: 19</b>  <i>(from Web of Science Core Collection)</i></p> <p><b>Usage Count</b> ▼</p> <p><b>Times Cited: 1</b>  <i>(from Web of Science Core Collection)</i></p> <p><b>Usage Count</b> ▼</p>
---	---	--

Web of Science™	InCites™	Journal Citation Reports®	Essential Science Indicators™	EndNote™	Sign In ▾	Help	English ▾
-----------------	----------	---------------------------	-------------------------------	----------	-----------	------	-----------

---

Search
Return to Search Results
My Tools ▾
Search History
Marked List

**Citing Articles: 14**  
*(from Web of Science Core Collection)*

**For:** Fast converging path integrals for time-dependent potentials: I. Recursive calculation of short-time ...  
[More](#)

**Times Cited Counts**  
[17 in All Databases](#)

17 in Web of Science Core Collection  
0 in BIOSIS Citation Index  
0 in Chinese Science Citation Database  
0 data sets in Data Citation Index  
0 publication in Data Citation Index  
0 in Russian Science Citation Index  
0 in SciELO Citation Index  
[View Additional Times Cited Counts](#)

---

**Refine Results**

**Web of Science Categories** ▾

- PHYSICS MULTIDISCIPLINARY (8)
- PHYSICS MATHEMATICAL (3)
- PHYSICS FLUIDS PLASMAS (2)
- PHYSICS ATOMIC MOLECULAR CHEMICAL (2)
- OPTICS (2)

[more options / values...](#)

[Refine](#)

**Document Types** ▾

- ARTICLE (13)
- PROCEEDINGS PAPER (1)

[more options / values...](#)

[Refine](#)

**Research Areas** ▾

**Authors** ▾

**Group Authors** ▾

**Editors** ▾



**Source Titles** ▾



**Book Series Titles** ▾

Sort by: **Publication Date -- newest to oldest** ▾

Page 1 of 1

---

Select Page
 
Save to EndNote online ▾
Add to Marked List

 [Analyze Results](#)
 [Create Citation Report](#)

1. **BOSE-EINSTEIN CONDENSATION: TWENTY YEARS AFTER**

By: Bagnato, V. S.; Frantzeskakis, D. J.; Kevrekidis, P. G.; et al.  
**ROMANIAN REPORTS IN PHYSICS** Volume: 67 Issue: 1  
Pages: 5-50 Published: 2015

[View Abstract](#)
2. **Path integral Monte Carlo on a lattice: Extended states**

By: O'Callaghan, Mark; Miller, Bruce N.  
**PHYSICAL REVIEW E** Volume: 89 Issue: 4 Published: APR 15 2014

[View Abstract](#)
3. **Faraday waves in collisionally inhomogeneous Bose-Einstein condensates**

By: Balaz, Antun; Paun, Remus; Nicolin, Alexandru I.; et al.  
**PHYSICAL REVIEW A** Volume: 89 Issue: 2 Article Number: 023609 Published: FEB 11 2014

[View Abstract](#)
4. **Density Waves in Dipolar Bose-Einstein Condensates by Means of Symbolic Computations**

By: Nicolin, Alexandru I.; Rata, Ionel  
Edited by: Dulea, M.; Karaivanova, A.; Oulas, A.; et al.  
Conference: HP-SEE User Forum Location: Natl Lib Serbia, Belgrade, SERBIA Date: OCT 17-19, 2012  
Sponsor(s): Inst Phys Belgrade  
HIGH-PERFORMANCE COMPUTING INFRASTRUCTURE FOR SOUTH EAST EUROPE'S RESEARCH COMMUNITIES: RESULTS OF THE HP-SEE USER FORUM 2012 Book Series: Modeling and Optimization in Science and Technologies  
Volume: 2 Pages: 15-21 Published: 2014

[View Abstract](#)
5. **ANALYTICAL DESCRIPTION OF THE NONLINEAR DYNAMICS OF BOSE-EINSTEIN CONDENSATES BY MEANS OF GENETIC ALGORITHMS**


By: Raportaru, Mihaela Carina; Jovanovski, Jane; Jakimovski, Boro; et al.  
**ROMANIAN JOURNAL OF PHYSICS** Volume: 59 Issue: 7-8  
Pages: 677-685 Published: 2014

[View Abstract](#)
6. **Dynamics of one-dimensional tight-binding models with arbitrary time-dependent external homogeneous fields**

By: Hu, W. H.; Jin, L.; Song, Z.  
**QUANTUM INFORMATION PROCESSING** Volume: 12 Issue: 11  
Pages: 3569-3585 Published: NOV 2013

[View Abstract](#)
7. **FARADAY WAVES IN CIGAR-SHAPED BOSE-EINSTEIN CONDENSATES WITH RADIALLY INHOMOGENEOUS**

**Times Cited: 50**  
*(from Web of Science Core Collection)*

 **Highly Cited Paper**

**Usage Count** ▾

**Times Cited: 1**  
*(from Web of Science Core Collection)*

**Usage Count** ▾

**Times Cited: 20**  
*(from Web of Science Core Collection)*

**Usage Count** ▾

**Times Cited: 3**  
*(from Web of Science Core Collection)*

**Usage Count** ▾

**Times Cited: 3**  
*(from Web of Science Core Collection)*

**Usage Count** ▾

**Times Cited: 4**  
*(from Web of Science Core Collection)*

**Usage Count** ▾

**Times Cited: 9**  
*(from Web of Science Core Collection)*

Conference Titles	◀
Publication Years	◀
Organizations-Enhanced	◀
Funding Agencies	◀
Languages	◀
Countries/Territories	◀
ESI Top Papers	◀
Open Access	◀

For advanced refine options, use

[Analyze Results](#)

**SCATTERING LENGTHS**

By: Balasubramanian, Sudharsan; Ramaswamy, Radha; Nicolin, A. I.  
 ROMANIAN REPORTS IN PHYSICS Volume: 65 Issue: 3  
 Pages: 820-824 Published: 2013

[View Abstract](#)

Collection)

**Usage Count** ▼

8. **DENSITY WAVES IN DIPOLAR BOSE-EINSTEIN CONDENSATES**

By: Nicolin, Alexandru I.  
 PROCEEDINGS OF THE ROMANIAN ACADEMY SERIES A-MATHEMATICS PHYSICS TECHNICAL SCIENCES INFORMATION SCIENCE Volume: 14 Issue: 1 Pages: 35-41  
 Published: JAN-MAR 2013

[View Abstract](#)

**Times Cited: 15**  
 (from Web of Science Core Collection)

**Usage Count** ▼

9. **Geometric-phase-propagator approach to time-dependent quantum systems**

By: Diakonou, F. K.; Kaloizoumis, P. A.; Karanikas, A. I.; et al.  
 PHYSICAL REVIEW A Volume: 85 Issue: 6 Article Number: 062110  
 Published: JUN 18 2012

[View Abstract](#)

**Times Cited: 3**  
 (from Web of Science Core Collection)

**Usage Count** ▼

10. **Effects of spatially inhomogeneous atomic interactions on Bose-Einstein condensates in optical lattices**

By: Sekh, Golam Ali  
 PHYSICS LETTERS A Volume: 376 Issue: 21 Pages: 1740-1747  
 Published: APR 23 2012

[Full Text from Publisher](#)

[View Abstract](#)

**Times Cited: 6**  
 (from Web of Science Core Collection)

**Usage Count** ▼

11. **Variational treatment of Faraday waves in inhomogeneous Bose-Einstein condensates**

By: Nicolin, Alexandru I.  
 PHYSICA A-STATISTICAL MECHANICS AND ITS APPLICATIONS Volume: 391 Issue: 4 Pages: 1062-1067  
 Published: FEB 15 2012

[Full Text from Publisher](#)

[View Abstract](#)

**Times Cited: 21**  
 (from Web of Science Core Collection)

**Usage Count** ▼

12. **FORMATION OF FARADAY AND RESONANT WAVES IN DRIVEN BOSE-EINSTEIN CONDENSATES**

By: Raportaru, Mihaela-Carina  
 ROMANIAN REPORTS IN PHYSICS Volume: 64 Issue: 1  
 Pages: 105-115 Published: 2012

[View Abstract](#)

**Times Cited: 8**  
 (from Web of Science Core Collection)

**Usage Count** ▼

13. **Resonant wave formation in Bose-Einstein condensates**

By: Nicolin, Alexandru I.  
 PHYSICAL REVIEW E Volume: 84 Issue: 5 Article Number: 056202 Part: 2  
 Published: NOV 4 2011

[View Abstract](#)

**Times Cited: 28**  
 (from Web of Science Core Collection)

**Usage Count** ▼

14. **FARADAY WAVES IN BOSE-EINSTEIN CONDENSATES SUBJECT TO ANISOTROPIC TRANSVERSE CONFINEMENT**

By: Nicolin, Alexandru I.  
 ROMANIAN REPORTS IN PHYSICS Volume: 63 Supplement: S  
 Pages: 1329-1337 Published: 2011

[View Abstract](#)

**Times Cited: 16**  
 (from Web of Science Core Collection)

**Usage Count** ▼

Select Page



[Save to EndNote online](#) ▼

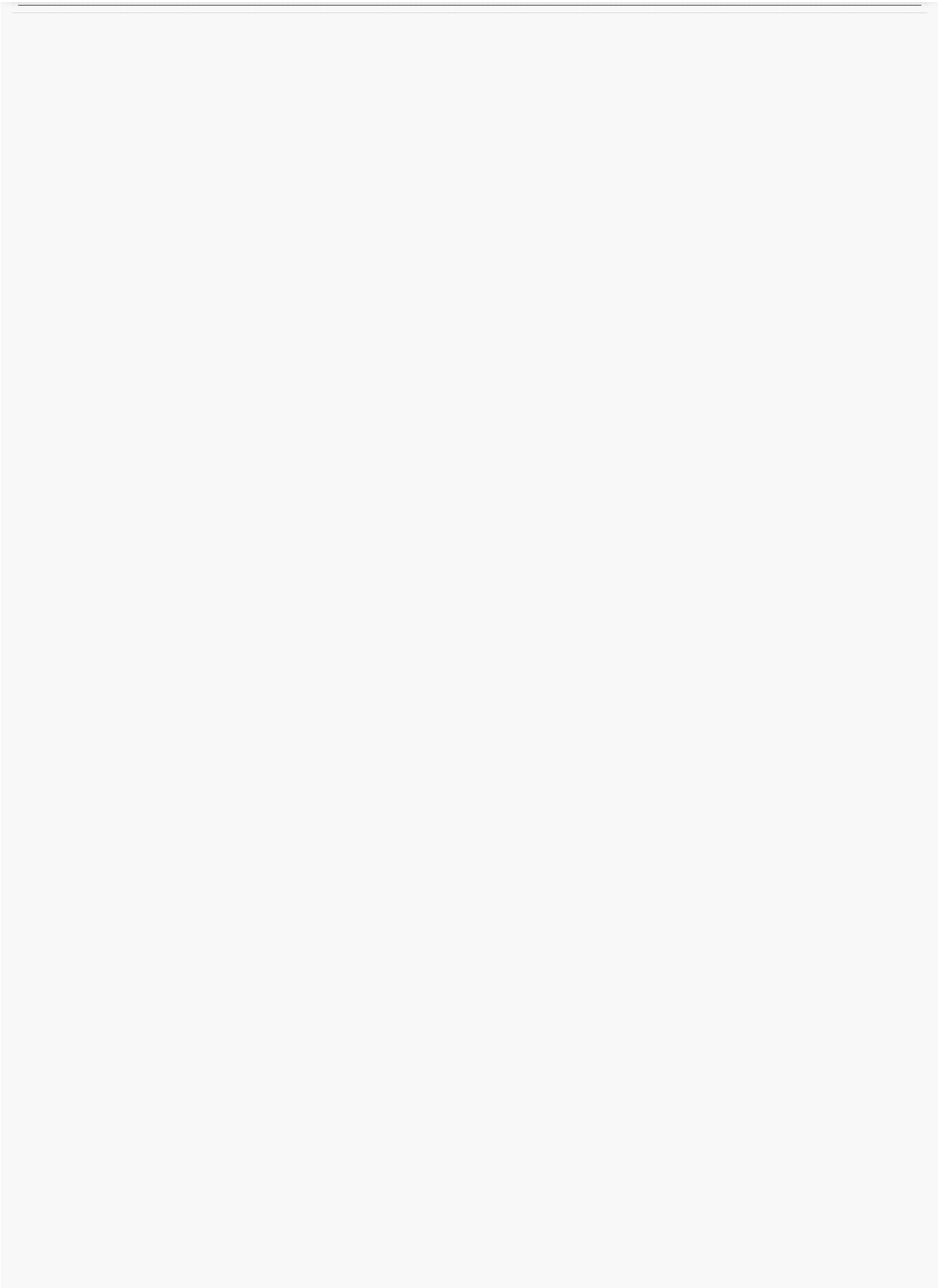
[Add to Marked List](#)

Sort by: **Publication Date -- newest to oldest** ▼

◀ Page 1 of 1 ▶

Show: **50 per page** ▼

14 records matched your query of the 36,466,594 in the data limits you selected.



Web of Science™	InCites™	Journal Citation Reports®	Essential Science Indicators™	EndNote™	Sign In ▾	Help	English ▾
-----------------	----------	---------------------------	-------------------------------	----------	-----------	------	-----------

# WEB OF SCIENCE™

Search
Return to Search Results
My Tools ▾ Search History Marked List

### Citing Articles: 15

*(from Web of Science Core Collection)*

**For:** Fast converging path integrals for time-dependent potentials: II. Generalization to many-body system  
[...More](#)

**Times Cited Counts**

17 in All Databases

17 in Web of Science Core Collection

0 in BIOSIS Citation Index

0 in Chinese Science Citation Database

0 data sets in Data Citation Index

0 publication in Data Citation Index

0 in Russian Science Citation Index

0 in SciELO Citation Index

[View Additional Times Cited Counts](#)

---

### Refine Results

**Web of Science Categories** ▾

- PHYSICS MULTIDISCIPLINARY (9)
- PHYSICS MATHEMATICAL (3)
- PHYSICS FLUIDS PLASMAS (2)
- PHYSICS ATOMIC MOLECULAR CHEMICAL (2)
- OPTICS (2)

[more options / values...](#)

Refine

---

**Document Types** ▾

- ARTICLE (14)
- PROCEEDINGS PAPER (1)

[more options / values...](#)

Refine

---

**Research Areas** ▾

---

**Authors** ▾

---

**Group Authors** ▾

---

**Editors** ▾

---

**Source Titles** ▾

---

**Book Series Titles** ▾

Sort by: Publication Date -- newest to oldest ▾
 Page 1 of 1

Select Page


Save to EndNote online ▾
 Add to Marked List

1. **Exact solution of Schrodinger equation for two state problem with time dependent coupling**  
 By: Diwaker; Panda, Bandhan; Chakraborty, Aniruddha  
 PHYSICA A-STATISTICAL MECHANICS AND ITS APPLICATIONS Volume: 442 Pages: 380-387 Published: JAN 15 2016  

Full Text from Publisher
View Abstract
2. **BOSE-EINSTEIN CONDENSATION: TWENTY YEARS AFTER**  
 By: Bagnato, V. S.; Frantzeskakis, D. J.; Kevrekidis, P. G.; et al.  
 ROMANIAN REPORTS IN PHYSICS Volume: 67 Issue: 1 Pages: 5-50 Published: 2015  

View Abstract
3. **Path integral Monte Carlo on a lattice: Extended states**  
 By: O'Callaghan, Mark; Miller, Bruce N.  
 PHYSICAL REVIEW E Volume: 89 Issue: 4 Published: APR 15 2014  

View Abstract
4. **Faraday waves in collisionally inhomogeneous Bose-Einstein condensates**  
 By: Balaz, Antun; Paun, Remus; Nicolin, Alexandru I.; et al.  
 PHYSICAL REVIEW A Volume: 89 Issue: 2 Article Number: 023609 Published: FEB 11 2014  

View Abstract
5. **Density Waves in Dipolar Bose-Einstein Condensates by Means of Symbolic Computations**  
 By: Nicolin, Alexandru I.; Rata, Ionel  
 Edited by: Dulea, M.; Karaivanova, A.; Oulas, A.; et al.  
 Conference: HP-SEE User Forum Location: Natl Lib Serbia, Belgrade, SERBIA Date: OCT 17-19, 2012  
 Sponsor(s): Inst Phys Belgrade  
 HIGH-PERFORMANCE COMPUTING INFRASTRUCTURE FOR SOUTH EAST EUROPE'S RESEARCH COMMUNITIES: RESULTS OF THE HP-SEE USER FORUM 2012 Book Series: Modeling and Optimization in Science and Technologies  
 Volume: 2 Pages: 15-21 Published: 2014  

View Abstract
6. **ANALYTICAL DESCRIPTION OF THE NONLINEAR DYNAMICS OF BOSE-EINSTEIN CONDENSATES BY MEANS OF GENETIC ALGORITHMS**  
 By: Raportaru, Mihaela Carina; Jovanovski, Jane; Jakimovski, Boro; et al.  
 ROMANIAN JOURNAL OF PHYSICS Volume: 59 Issue: 7-8 Pages: 677-685 Published: 2014  

View Abstract
7. **Dynamics of one-dimensional tight-binding models with arbitrary time-dependent external homogeneous**

≡ [Analyze Results](#)  
≡ [Create Citation Report](#)

**Times Cited: 0**  
*(from Web of Science Core Collection)*

**Usage Count** ▾

---

**Times Cited: 50**  
*(from Web of Science Core Collection)*

**Highly Cited Paper**

**Usage Count** ▾

---

**Times Cited: 1**  
*(from Web of Science Core Collection)*

**Usage Count** ▾

---

**Times Cited: 20**  
*(from Web of Science Core Collection)*

**Usage Count** ▾

---

**Times Cited: 3**  
*(from Web of Science Core Collection)*

**Usage Count** ▾

---

**Times Cited: 3**  
*(from Web of Science Core Collection)*

**Usage Count** ▾

---

**Times Cited: 4**  
*(from Web of Science Core Collection)*

Conference Titles	◀
Publication Years	◀
Organizations-Enhanced	◀
Funding Agencies	◀
Languages	◀
Countries/Territories	◀
ESI Top Papers	◀
Open Access	◀

For advanced refine options, use

Analyze Results

- fields**
- By: Hu, W. H.; Jin, L.; Song, Z.  
**QUANTUM INFORMATION PROCESSING** Volume: 12 Issue: 11 Pages: 3569-3585 Published: NOV 2013  
[View Abstract](#)
8. **FARADAY WAVES IN CIGAR-SHAPED BOSE-EINSTEIN CONDENSATES WITH RADIALLY INHOMOGENEOUS SCATTERING LENGTHS**  
 By: Balasubramanian, Sudharsan; Ramaswamy, Radha; Nicolin, A. I.  
**ROMANIAN REPORTS IN PHYSICS** Volume: 65 Issue: 3 Pages: 820-824 Published: 2013  
[View Abstract](#)
9. **DENSITY WAVES IN DIPOLAR BOSE-EINSTEIN CONDENSATES**  
 By: Nicolin, Alexandru I.  
 PROCEEDINGS OF THE ROMANIAN ACADEMY SERIES A-MATHEMATICS PHYSICS TECHNICAL SCIENCES INFORMATION SCIENCE Volume: 14 Issue: 1 Pages: 35-41 Published: JAN-MAR 2013  
[View Abstract](#)
10. **Geometric-phase-propagator approach to time-dependent quantum systems**  
 By: Diakonov, F. K.; Kaloizoumis, P. A.; Karanikas, A. I.; et al.  
**PHYSICAL REVIEW A** Volume: 85 Issue: 6 Article Number: 062110 Published: JUN 18 2012  
[View Abstract](#)
11. **Effects of spatially inhomogeneous atomic interactions on Bose-Einstein condensates in optical lattices**  
 By: Sekh, Golam Ali  
**PHYSICS LETTERS A** Volume: 376 Issue: 21 Pages: 1740-1747 Published: APR 23 2012  
[Full Text from Publisher](#) [View Abstract](#)
12. **Variational treatment of Faraday waves in inhomogeneous Bose-Einstein condensates**  
 By: Nicolin, Alexandru I.  
**PHYSICA A-STATISTICAL MECHANICS AND ITS APPLICATIONS** Volume: 391 Issue: 4 Pages: 1062-1067 Published: FEB 15 2012  
[Full Text from Publisher](#) [View Abstract](#)
13. **FORMATION OF FARADAY AND RESONANT WAVES IN DRIVEN BOSE-EINSTEIN CONDENSATES**  
 By: Raportaru, Mihaela-Carina  
**ROMANIAN REPORTS IN PHYSICS** Volume: 64 Issue: 1 Pages: 105-115 Published: 2012  
[View Abstract](#)
14. **Resonant wave formation in Bose-Einstein condensates**  
 By: Nicolin, Alexandru I.  
**PHYSICAL REVIEW E** Volume: 84 Issue: 5 Article Number: 056202 Part: 2 Published: NOV 4 2011  
[View Abstract](#)
15. **FARADAY WAVES IN BOSE-EINSTEIN CONDENSATES SUBJECT TO ANISOTROPIC TRANSVERSE CONFINEMENT**  
 By: Nicolin, Alexandru I.  
**ROMANIAN REPORTS IN PHYSICS** Volume: 63 Supplement: S Pages: 1329-1337 Published: 2011  
[View Abstract](#)
- Collection)
- Usage Count ▼
- Times Cited: 9  
(from Web of Science Core Collection)
- Usage Count ▼
- Times Cited: 15  
(from Web of Science Core Collection)
- Usage Count ▼
- Times Cited: 3  
(from Web of Science Core Collection)
- Usage Count ▼
- Times Cited: 6  
(from Web of Science Core Collection)
- Usage Count ▼
- Times Cited: 21  
(from Web of Science Core Collection)
- Usage Count ▼
- Times Cited: 8  
(from Web of Science Core Collection)
- Usage Count ▼
- Times Cited: 28  
(from Web of Science Core Collection)
- Usage Count ▼
- Times Cited: 16  
(from Web of Science Core Collection)
- Usage Count ▼

Select Page



Save to EndNote online ▼

Add to Marked List

Sort by: **Publication Date -- newest to oldest** ▼

◀ Page 1 of 1 ▶

Show: **50 per page** ▼

*15 records matched your query of the 36,466,594 in the data limits you selected.*



Web of Science™	InCites™	Journal Citation Reports®	Essential Science Indicators™	EndNote™	Sign In ▾	Help	English ▾
-----------------	----------	---------------------------	-------------------------------	----------	-----------	------	-----------

WEB OF SCIENCE™

---

**Search**
Return to Search Results
My Tools ▾
Search History
Marked List

**Citing Articles: 10**  
*(from Web of Science Core Collection)*

**For:** Properties of quantum systems via diagonalization of transition amplitudes. II. Systematic improve...  
[...More](#)

**Times Cited Counts**  
[16 in All Databases](#)

16 in Web of Science Core Collection

0 in BIOSIS Citation Index

0 in Chinese Science Citation Database

0 data sets in Data Citation Index

0 publication in Data Citation Index

0 in Russian Science Citation Index

0 in SciELO Citation Index

[View Additional Times Cited Counts](#)

---

**Refine Results**

**Web of Science Categories** ▾

- PHYSICS MULTIDISCIPLINARY (3)
- PHYSICS ATOMIC MOLECULAR CHEMICAL (3)
- OPTICS (3)
- COMPUTER SCIENCE INTERDISCIPLINARY APPLICATIONS (2)
- MATHEMATICS APPLIED (1)

[more options / values...](#)

Refine

---

**Document Types** ▾

- ARTICLE (9)
- PROCEEDINGS PAPER (1)

[more options / values...](#)

Refine

---

**Research Areas** ▾

---

**Authors** ▾

---

**Group Authors** ▾

---

**Editors** ▾

---

**Source Titles** ▾

Sort by: Publication Date -- newest to oldest ▾
 ◀ Page 1 of 1 ▶

Select Page
 
Save to EndNote online ▾
 Add to Marked List

[Analyze Results](#)
 [Create Citation Report](#)

1. **OpenMP, OpenMP/MPI, and CUDA/MPI C programs for solving the time-dependent dipolar Gross-Pitaevskii equation**

By: Loncar, Vladimir; Young-S, Luis E.; Skrbic, Srdjan; et al.  
**COMPUTER PHYSICS COMMUNICATIONS** Volume: 209  
 Pages: 190-196 Published: DEC 2016

Full Text from Publisher
View Abstract
2. **Faraday and resonant waves in binary collisionally-inhomogeneous Bose-Einstein condensates**

By: Sudharsan, J. B.; Radha, R.; Raportaru, Mihaela Carina; et al.  
**JOURNAL OF PHYSICS B-ATOMIC MOLECULAR AND OPTICAL PHYSICS** Volume: 49 Issue: 16 Article Number: 165303  
 Published: AUG 28 2016

View Abstract
3. **BOSE-EINSTEIN CONDENSATION: TWENTY YEARS AFTER**

By: Bagnato, V. S.; Frantzeskakis, D. J.; Kevrekidis, P. G.; et al.  
**ROMANIAN REPORTS IN PHYSICS** Volume: 67 Issue: 1  
 Pages: 5-50 Published: 2015

View Abstract
4. **Faraday waves in collisionally inhomogeneous Bose-Einstein condensates**

By: Balaz, Antun; Paun, Remus; Nicolin, Alexandru I.; et al.  
**PHYSICAL REVIEW A** Volume: 89 Issue: 2 Article Number: 023609  
 Published: FEB 11 2014

View Abstract
5. **Density Waves in Dipolar Bose-Einstein Condensates by Means of Symbolic Computations**

By: Nicolin, Alexandru I.; Rata, Ionel  
 Edited by: Dulea, M.; Karaivanova, A; Oulas, A; et al.  
 Conference: HP-SEE User Forum Location: Natl Lib Serbia, Belgrade, SERBIA Date: OCT 17-19, 2012  
 Sponsor(s): Inst Phys Belgrade  
 HIGH-PERFORMANCE COMPUTING INFRASTRUCTURE FOR SOUTH EAST EUROPE'S RESEARCH COMMUNITIES: RESULTS OF THE HP-SEE USER FORUM 2012 Book Series: Modeling and Optimization in Science and Technologies  
 Volume: 2 Pages: 15-21 Published: 2014

View Abstract
6. **FARADAY WAVES IN CIGAR-SHAPED BOSE-EINSTEIN CONDENSATES WITH RADIALLY INHOMOGENEOUS SCATTERING LENGTHS**

By: Balasubramanian, Sudharsan; Ramaswamy, Radha; Nicolin, A. I.  
**ROMANIAN REPORTS IN PHYSICS** Volume: 65 Issue: 3  
 Pages: 820-824 Published: 2013

View Abstract

**Times Cited: 0**  
*(from Web of Science Core Collection)*

**Usage Count** ▾

**Times Cited: 0**  
*(from Web of Science Core Collection)*

**Usage Count** ▾

**Times Cited: 50**  
*(from Web of Science Core Collection)*

**Highly Cited Paper**

**Usage Count** ▾

**Times Cited: 20**  
*(from Web of Science Core Collection)*



**Usage Count** ▾

**Times Cited: 3**  
*(from Web of Science Core Collection)*

**Usage Count** ▾

**Times Cited: 9**  
*(from Web of Science Core Collection)*

**Usage Count** ▾

<p><b>Book Series Titles</b> ◀</p> <p><b>Conference Titles</b> ◀</p> <p><b>Publication Years</b> ◀</p> <p><b>Organizations-Enhanced</b> ◀</p> <p><b>Funding Agencies</b> ◀</p> <p><b>Languages</b> ◀</p> <p><b>Countries/Territories</b> ◀</p> <p><b>ESI Top Papers</b> ◀</p> <p><b>Open Access</b> ◀</p> <p><i>For advanced refine options, use</i></p> <p><b>Analyze Results</b></p>	<p>7. <b>DENSITY WAVES IN DIPOLAR BOSE-EINSTEIN CONDENSATES</b>                  By: Nicolin, Alexandru I.                  PROCEEDINGS OF THE ROMANIAN ACADEMY SERIES A-MATHEMATICS PHYSICS TECHNICAL SCIENCES INFORMATION SCIENCE Volume: 14 Issue: 1 Pages: 35-41                  Published: JAN-MAR 2013  <a href="#">View Abstract</a>  <b>Times Cited: 15</b>  <i>(from Web of Science Core Collection)</i>  <b>Usage Count</b> ▾</p> <p>8. <b>Faraday waves in binary nonmiscible Bose-Einstein condensates</b>                  By: Balaz, Antun; Nicolin, Alexandru I.                  PHYSICAL REVIEW A Volume: 85 Issue: 2 Article Number: 023613 Published: FEB 9 2012  <a href="#">View Abstract</a>  <b>Times Cited: 46</b>  <i>(from Web of Science Core Collection)</i>  <b>Usage Count</b> ▾</p> <p>9. <b>FORMATION OF FARADAY AND RESONANT WAVES IN DRIVEN BOSE-EINSTEIN CONDENSATES</b>                  By: Raportaru, Mihaela-Carina                  ROMANIAN REPORTS IN PHYSICS Volume: 64 Issue: 1 Pages: 105-115 Published: 2012  <a href="#">View Abstract</a>  <b>Times Cited: 8</b>  <i>(from Web of Science Core Collection)</i>  <b>Usage Count</b> ▾</p> <p>10. <b>Development of Grid e-Infrastructure in South-Eastern Europe</b>                  By: Balaz, Antun; Prnjat, Ognjen; Vudragovic, Dusan; et al.                  JOURNAL OF GRID COMPUTING Volume: 9 Issue: 2 Special Issue: SI Pages: 135-154 Published: JUN 2011  <a href="#">View Abstract</a>  <b>Times Cited: 19</b>  <i>(from Web of Science Core Collection)</i>  <b>Usage Count</b> ▾</p> <p>Select Page       <a href="#">Save to EndNote online</a> ▾   <a href="#">Add to Marked List</a></p> <p>Sort by: <b>Publication Date -- newest to oldest</b> ▾</p> <p>Show: <b>10 per page</b> ▾</p> <p>◀ Page 1 of 1 ▶</p> <p><i>10 records matched your query of the 36,466,594 in the data limits you selected.</i></p>
--	--

Web of Science™ InCites™ Journal Citation Reports® Essential Science Indicators™ EndNote™
Sign In Help English ▾

# WEB OF SCIENCE™

Search
Return to Search Results
My Tools ▾ Search History Marked List

**Citing Articles: 9**  
*(from Web of Science Core Collection)*

**For:** Fast convergence of path integrals for many-body systems  
[...More](#)

**Times Cited Counts**  
16 in All Databases

16 in Web of Science Core Collection

0 in BIOSIS Citation Index

0 in Chinese Science Citation Database

0 data sets in Data Citation Index

0 publication in Data Citation Index

0 in Russian Science Citation Index

0 in SciELO Citation Index

[View Additional Times Cited Counts](#)

---

**Refine Results**

**Web of Science Categories** ▾

- PHYSICS MULTIDISCIPLINARY (4)
- PHYSICS ATOMIC MOLECULAR CHEMICAL (4)
- OPTICS (3)
- PHYSICS MATHEMATICAL (1)
- COMPUTER SCIENCE INTERDISCIPLINARY APPLICATIONS (1)

[more options / values...](#)

Refine

---

**Document Types** ▾

ARTICLE (9)

Refine

---

**Research Areas** ▾

---

**Authors** ▾

---

**Group Authors** ▾

---

**Editors** ▾

---

**Source Titles** ▾

---

**Book Series Titles** ▾

Sort by: Publication Date -- newest to oldest ▾
◀ Page 1 of 1 ▶

Select Page
 
Save to EndNote online ▾
Add to Marked List

[Analyze Results](#)  
 [Create Citation Report](#)

1. **OpenMP, OpenMP/MPI, and CUDA/MPI C programs for solving the time-dependent dipolar Gross-Pitaevskii equation**
**Times Cited: 0**  
*(from Web of Science Core Collection)*

By: Loncar, Vladimir; Young-S, Luis E.; Skrbic, Srdjan; et al.  
**COMPUTER PHYSICS COMMUNICATIONS** Volume: 209  
 Pages: 190-196 Published: DEC 2016

Full Text from Publisher
View Abstract
2. **Faraday and resonant waves in binary collisionally-inhomogeneous Bose-Einstein condensates**
**Times Cited: 0**  
*(from Web of Science Core Collection)*

By: Sudharsan, J. B.; Radha, R.; Raportaru, Mihaela Carina; et al.  
**JOURNAL OF PHYSICS B-ATOMIC MOLECULAR AND OPTICAL PHYSICS** Volume: 49 Issue: 16 Article Number: 165303  
 Published: AUG 28 2016

View Abstract
3. **BOSE-EINSTEIN CONDENSATION: TWENTY YEARS AFTER**
**Times Cited: 50**  
*(from Web of Science Core Collection)*

By: Bagnato, V. S.; Frantzeskakis, D. J.; Kevrekidis, P. G.; et al.  
**ROMANIAN REPORTS IN PHYSICS** Volume: 67 Issue: 1  
 Pages: 5-50 Published: 2015

View Abstract

**Highly Cited Paper**  
Usage Count ▾
4. **Faraday waves in collisionally inhomogeneous Bose-Einstein condensates**
**Times Cited: 20**  
*(from Web of Science Core Collection)*

By: Balaz, Antun; Paun, Remus; Nicolin, Alexandru I.; et al.  
**PHYSICAL REVIEW A** Volume: 89 Issue: 2 Article Number: 023609  
 Published: FEB 11 2014

View Abstract

Usage Count ▾
5. **FARADAY WAVES IN CIGAR-SHAPED BOSE-EINSTEIN CONDENSATES WITH RADIALLY INHOMOGENEOUS SCATTERING LENGTHS**
**Times Cited: 9**  
*(from Web of Science Core Collection)*

By: Balasubramanian, Sudharsan; Ramaswamy, Radha; Nicolin, A. I.  
**ROMANIAN REPORTS IN PHYSICS** Volume: 65 Issue: 3  
 Pages: 820-824 Published: 2013

View Abstract

Usage Count ▾
6. **Effects of spatially inhomogeneous atomic interactions on Bose-Einstein condensates in optical lattices**
**Times Cited: 6**  
*(from Web of Science Core Collection)*

By: Sekh, Golam Ali  
**PHYSICS LETTERS A** Volume: 376 Issue: 21 Pages: 1740-1747  
 Published: APR 23 2012

Full Text from Publisher
View Abstract

Usage Count ▾
7. **Faraday waves in binary nonmiscible Bose-Einstein condensates**
**Times Cited: 46**  
*(from Web of Science Core Collection)*

By: Balaz, Antun; Nicolin, Alexandru I.  
**PHYSICAL REVIEW A** Volume: 85 Issue: 2 Article Number: 023613  
 Published: FEB 9 2012

Usage Count ▾

Conference Titles	<a href="#">View Abstract</a>
Publication Years	8. <b>Many-body Hamiltonian with screening parameter and ionization energy</b> By: Arulsamy, Andrew Das PRAMANA-JOURNAL OF PHYSICS Volume: 74 Issue: 4 Pages: 615-631 Published: APR 2010 Times Cited: <b>14</b> (from Web of Science Core Collection) Usage Count
Organizations-Enhanced	<a href="#">Full Text from Publisher</a> <a href="#">View Abstract</a>
Funding Agencies	9. <b>Extrapolated high-order propagators for path integral Monte Carlo simulations</b> By: Zillich, Robert E.; Mayrhofer, Johannes M.; Chin, Siu A. JOURNAL OF CHEMICAL PHYSICS Volume: 132 Issue: 4 Article Number: 044103 Published: JAN 28 2010 Times Cited: <b>25</b> (from Web of Science Core Collection) Usage Count
Languages	<a href="#">View Abstract</a>
Countries/Territories	Select Page <a href="#">Save to EndNote online</a> <a href="#">Add to Marked List</a>
ESI Top Papers	Sort by: <a href="#">Publication Date -- newest to oldest</a>
Open Access	Show: <a href="#">10 per page</a>
For advanced refine options, use <a href="#">Analyze Results</a>	Page 1 of 1
9 records matched your query of the 36,466,594 in the data limits you selected.	

Web of Science™ InCites™ Journal Citation Reports® Essential Science Indicators™ EndNote™
Sign In Help English

# WEB OF SCIENCE™

Search
Return to Search Results
My Tools Search History Marked List

**Citing Articles: 15**  
*(from Web of Science Core Collection)*

**For:** Chiral bosonic phases on the Haldane honeycomb lattice [...More](#)

**Times Cited Counts**  
[15 in All Databases](#)

15 in Web of Science Core Collection

0 in BIOSIS Citation Index

0 in Chinese Science Citation Database

0 data sets in Data Citation Index

0 publication in Data Citation Index

0 in Russian Science Citation Index

0 in SciELO Citation Index

[View Additional Times Cited Counts](#)

---

**Refine Results**

**Web of Science Categories**

- PHYSICS CONDENSED MATTER (8)
- PHYSICS MULTIDISCIPLINARY (4)
- PHYSICS ATOMIC MOLECULAR CHEMICAL (3)
- OPTICS (3)
- ASTRONOMY ASTROPHYSICS (1)

[more options / values...](#)

[Refine](#)

---

**Document Types**

- ARTICLE (15)

[Refine](#)

---

**Research Areas**

---

**Authors**

- LE HUR K (4)
- PLEKHANOV K (2)
- OWERRE SA (2)
- NAKAFUJI T (2)
- LIU TH (2)

[more options / values...](#)

[Refine](#)

---

**Group Authors**

Sort by: **Publication Date -- newest to oldest**
Page 1 of 1

Select Page
[Save to EndNote online](#)
[Add to Marked List](#)

[Analyze Results](#)
[Create Citation Report](#)

1. **Floquet engineering of Haldane Chern insulators and chiral bosonic phase transitions**

By: Plekhanov, Kirill; Roux, Guillaume; Le Hur, Karyn  
**PHYSICAL REVIEW B** Volume: 95 Issue: 4 Article Number: 045102 Published: JAN 3 2017

**Times Cited: 0**  
*(from Web of Science Core Collection)*

**Usage Count**

[View Abstract](#)
2. **Topological phase transitions and universality in the Haldane-Hubbard model**

By: Giuliani, Alessandro; Jauslin, Ian; Mastropietro, Vieri; et al.  
**PHYSICAL REVIEW B** Volume: 94 Issue: 20 Article Number: 205139 Published: NOV 28 2016

**Times Cited: 0**  
*(from Web of Science Core Collection)*

**Usage Count**

[View Abstract](#)
3. **Triplet FFLO superconductivity in the doped Kitaev-Heisenberg honeycomb model**

By: Liu, Tianhan; Repellin, Cecile; Doucot, Benoit; et al.  
**PHYSICAL REVIEW B** Volume: 94 Issue: 18 Article Number: 180506 Published: NOV 14 2016

**Times Cited: 2**  
*(from Web of Science Core Collection)*

**Usage Count**

[View Abstract](#)
4. **Magnon edge states in the hardcore-Bose-Hubbard model**

By: Owerre, S. A.  
**JOURNAL OF PHYSICS-CONDENSED MATTER** Volume: 28 Issue: 43 Article Number: 436003 Published: NOV 2 2016

**Times Cited: 0**  
*(from Web of Science Core Collection)*

**Usage Count**

[View Abstract](#)
5. **Topological Varma Superfluid in Optical Lattices**

By: Di Liberto, M.; Hemmerich, A.; Smith, C. Morais  
**PHYSICAL REVIEW LETTERS** Volume: 117 Issue: 16 Article Number: 163001 Published: OCT 11 2016

**Times Cited: 1**  
*(from Web of Science Core Collection)*

**Usage Count**

[View Abstract](#)
6. **Many-body quantum electrodynamics networks: Non-equilibrium condensed matter physics with light**

By: Le Hur, Karyn; Henriot, Loic; Petrescu, Alexandru; et al.  
**COMPTES RENDUS PHYSIQUE** Volume: 17 Issue: 8 Pages: 808-835 Published: OCT-NOV 2016

**Times Cited: 4**  
*(from Web of Science Core Collection)*

**Usage Count**

[Full Text from Publisher](#) [View Abstract](#)
7. **Topological hardcore bosons on the honeycomb lattice**

By: Owerre, S. A.  
**CANADIAN JOURNAL OF PHYSICS** Volume: 94 Issue: 9 Pages: 814-820 Published: SEP 2016

**Times Cited: 0**  
*(from Web of Science Core Collection)*

**Usage Count**

[View Abstract](#)
8. **Phase diagram of dipolar hard-core bosons on a honeycomb lattice**

By: Nakafuji, Takashi; Ito, Takeshi; Nagamori, Yuya; et al.  
**PHYSICAL REVIEW A** Volume: 94 Issue: 2 Article Number:

**Times Cited: 0**  
*(from Web of Science Core Collection)*

- Editors
- Source Titles
- Book Series Titles
- Conference Titles
- Publication Years
- Organizations-Enhanced
- Funding Agencies
- Languages
- Countries/Territories
- ESI Top Papers
- Open Access

*For advanced refine options, use*

[Analyze Results](#)

	023613 Published: AUG 11 2016	Usage Count
	<a href="#" style="border: 1px solid #ccc; padding: 2px 5px;">View Abstract</a>	
9.	<p><b>Competing ground states of strongly correlated bosons in the Harper-Hofstadter-Mott model</b></p> <p>By: Natu, Stefan S.; Mueller, Erich J.; Das Sarma, S.  <b>PHYSICAL REVIEW A</b> Volume: 93 Issue: 6 Article Number: 063610 Published: JUN 10 2016</p>	<p><b>Times Cited: 2</b>  <i>(from Web of Science Core Collection)</i></p> <p>Usage Count </p>
	<a href="#" style="border: 1px solid #ccc; padding: 2px 5px;">View Abstract</a>	
10.	<p><b>Realizing topological Mott insulators from the RKKY interaction</b></p> <p>By: Liu, Tianhan; Doucot, Benoit; Le Hur, Karyn  <b>PHYSICAL REVIEW B</b> Volume: 93 Issue: 19 Article Number: 195153 Published: MAY 24 2016</p>	<p><b>Times Cited: 2</b>  <i>(from Web of Science Core Collection)</i></p> <p>Usage Count </p>
	<a href="#" style="border: 1px solid #ccc; padding: 2px 5px;">View Abstract</a>	
11.	<p><b>Mean field study of the topological Haldane-Hubbard model of spin-1/2 fermions</b></p> <p>By: Arun, V. S.; Sohal, R.; Hickey, C.; et al.  <b>PHYSICAL REVIEW B</b> Volume: 93 Issue: 11 Article Number: 115110 Published: MAR 4 2016</p>	<p><b>Times Cited: 2</b>  <i>(from Web of Science Core Collection)</i></p> <p>Usage Count </p>
	<a href="#" style="border: 1px solid #ccc; padding: 2px 5px;">View Abstract</a>	
12.	<p><b>Bosonic edge states in gapped honeycomb lattices</b></p> <p>By: Guo, Huaiming; Niu, Yuekun; Chen, Shu; et al.  <b>PHYSICAL REVIEW B</b> Volume: 93 Issue: 12 Article Number: 121401 Published: MAR 1 2016</p>	<p><b>Times Cited: 5</b>  <i>(from Web of Science Core Collection)</i></p> <p>Usage Count </p>
	<a href="#" style="border: 1px solid #ccc; padding: 2px 5px;">View Abstract</a>	
13.	<p><b>Phase diagrams of the Bose-Hubbard model and the Haldane-Bose-Hubbard model with complex hopping amplitudes</b></p> <p>By: Kuno, Yoshihito; Nakafuji, Takashi; Ichinose, Ikuo  <b>PHYSICAL REVIEW A</b> Volume: 92 Issue: 6 Article Number: 063630 Published: DEC 23 2015</p>	<p><b>Times Cited: 4</b>  <i>(from Web of Science Core Collection)</i></p> <p>Usage Count </p>
	<a href="#" style="border: 1px solid #ccc; padding: 2px 5px;">View Abstract</a>	
14.	<p><b>Excitation band topology and edge matter waves in Bose-Einstein condensates in optical lattices</b></p> <p>By: Furukawa, Shunsuke; Ueda, Masahito  <b>NEW JOURNAL OF PHYSICS</b> Volume: 17 Article Number: 115014 Published: NOV 27 2015</p>	<p><b>Times Cited: 10</b>  <i>(from Web of Science Core Collection)</i></p> <p>Usage Count </p>
	<a href="#" style="border: 1px solid #ccc; padding: 2px 5px;"> Full Text from Publisher</a> <a href="#" style="border: 1px solid #ccc; padding: 2px 5px; margin-left: 10px;">View Abstract</a>	
15.	<p><b>Creating nanostructured superconductors on demand by local current annealing</b></p> <p>By: Baek, Hongwoo; Ha, Jeonghoon; Zhang, Duming; et al.  <b>PHYSICAL REVIEW B</b> Volume: 92 Issue: 9 Article Number: 094510 Published: SEP 17 2015</p>	<p><b>Times Cited: 1</b>  <i>(from Web of Science Core Collection)</i></p> <p>Usage Count </p>
	<a href="#" style="border: 1px solid #ccc; padding: 2px 5px;">View Abstract</a>	

Select Page | | Save to EndNote online  | Add to Marked List

Sort by: Publication Date -- newest to oldest

Show: 50 per page

◀ Page 1 of 1 ▶

15 records matched your query of the 36,843,663 in the data limits you selected.

Web of Science™ InCites™ Journal Citation Reports® Essential Science Indicators™ EndNote™
Sign In Help English

# WEB OF SCIENCE™

Search
Return to Search Results
My Tools
Search History
Marked List

### Citing Articles: 13

(from Web of Science Core Collection)

**For:** Dissipation through localized loss in bosonic systems with long-range interactions ...[More](#)

**Times Cited Counts**  
14 in All Databases

- 14 in Web of Science Core Collection
- 0 in BIOSIS Citation Index
- 0 in Chinese Science Citation Database
- 0 data sets in Data Citation Index
- 0 publication in Data Citation Index
- 0 in Russian Science Citation Index
- 0 in SciELO Citation Index

[View Additional Times Cited Counts](#)

---

### Refine Results

**Web of Science Categories**

- PHYSICS MULTIDISCIPLINARY (7)
- PHYSICS ATOMIC MOLECULAR CHEMICAL (6)
- OPTICS (6)

[more options / values...](#)

Refine

**Document Types**

- ARTICLE (12)
- REVIEW (1)

[more options / values...](#)

Refine

**Research Areas**

**Authors**

**Group Authors**

**Editors**

**Source Titles**

**Book Series Titles**

**Conference Titles**

Sort by: Publication Date -- newest to oldest
Page 1 of 1

Select Page
Save to EndNote online
Add to Marked List

Analyze Results
Create Citation Report

1. **Tailored jump operators for purely dissipative quantum magnetism**
Times Cited: 0  
*(from Web of Science Core Collection)*

By: Weimer, Hendrik  
JOURNAL OF PHYSICS B-ATOMIC MOLECULAR AND OPTICAL PHYSICS Volume: 50 Issue: 2 Article Number: 024001 Published: JAN 28 2017

View Abstract
2. **Non-Hermitian dynamics in the quantum Zeno limit**
Times Cited: 3  
*(from Web of Science Core Collection)*

By: Kozłowski, W.; Caballero-Benitez, S. F.; Mekhov, I. B.  
PHYSICAL REVIEW A Volume: 94 Issue: 1 Article Number: 012123 Published: JUL 29 2016

View Abstract
3. **Collective dynamics of multimode bosonic systems induced by weak quantum measurement**
Times Cited: 4  
*(from Web of Science Core Collection)*

By: Mazzucchi, Gabriel; Kozłowski, Wojciech; Caballero-Benitez, Santiago F.; et al.  
NEW JOURNAL OF PHYSICS Volume: 18 Article Number: 073017 Published: JUL 8 2016

Full Text from Publisher
View Abstract
4. **Bistability in a Driven-Dissipative Superfluid**
Times Cited: 3  
*(from Web of Science Core Collection)*

By: Labouvie, Ralf; Santra, Bodhaditya; Heun, Simon; et al.  
PHYSICAL REVIEW LETTERS Volume: 116 Issue: 23 Article Number: 235302 Published: JUN 10 2016

View Abstract
5. **Quantum measurement-induced dynamics of many-body ultracold bosonic and fermionic systems in optical lattices**
Times Cited: 11  
*(from Web of Science Core Collection)*

By: Mazzucchi, Gabriel; Kozłowski, Wojciech; Caballero-Benitez, Santiago F.; et al.  
PHYSICAL REVIEW A Volume: 93 Issue: 2 Article Number: 023632 Published: FEB 19 2016

View Abstract
6. **Time evolution of open quantum many-body systems**
Times Cited: 6  
*(from Web of Science Core Collection)*

By: Overbeck, Vincent R.; Weimer, Hendrik  
PHYSICAL REVIEW A Volume: 93 Issue: 1 Article Number: 012106 Published: JAN 11 2016

View Abstract
7. **Dynamics of the double-well Bose-Einstein condensate coupled to a dual Markovian reservoirs system**
Times Cited: 1  
*(from Web of Science Core Collection)*

By: Rajagopal, Kalai Kumar; Muniandy, S. V.  
PHYSICA A-STATISTICAL MECHANICS AND ITS APPLICATIONS Volume: 440 Pages: 118-128 Published: DEC 15 2015

Full Text from Publisher
View Abstract

<p><b>Publication Years</b> ◀</p> <p><b>Organizations-Enhanced</b> ◀</p> <p><b>Funding Agencies</b> ◀</p> <p><b>Languages</b> ◀</p> <p><b>Countries/Territories</b> ◀</p> <p><b>ESI Top Papers</b> ◀</p> <p><b>Open Access</b> ◀</p> <p><i>For advanced refine options, use</i></p> <p><b>Analyze Results</b></p>	<p>8. <b>The dissipative Bose-Hubbard model</b>                  By: Kordas, G.; Witthaut, D.; Buonsante, P.; et al.                  EUROPEAN PHYSICAL JOURNAL-SPECIAL TOPICS Volume: 224 Issue: 11 Pages: 2127-2171 Published: NOV 2015  <a href="#">View Abstract</a></p> <p>9. <b>Non-equilibrium dynamics in dissipative Bose-Hubbard chains</b>                  By: Kordas, Georgios; Witthaut, Dirk; Wimberger, Sandro                  ANNALEN DER PHYSIK Volume: 527 Issue: 9-10 Pages: 619-628 Published: OCT 2015  <a href="#">View Abstract</a></p> <p>10. <b>Non-Markovian dynamics of a two-mode Bose-Einstein condensate</b>                  By: Rajagopal, Kalai Kumar; Muniandy, Sithi V.                  PHYSICA A-STATISTICAL MECHANICS AND ITS APPLICATIONS Volume: 434 Pages: 164-170 Published: SEP 15 2015  <a href="#">Full Text from Publisher</a> <a href="#">View Abstract</a></p> <p>11. <b>Dissipative two-mode Bose-Einstein condensate coupled to the environment</b>                  By: Rajagopal, Kalai Kumar                  PHYSICA A-STATISTICAL MECHANICS AND ITS APPLICATIONS Volume: 429 Pages: 231-241 Published: JUL 1 2015  <a href="#">Full Text from Publisher</a> <a href="#">View Abstract</a></p> <p>12. <b>Bose-Hubbard model: Relation between driven-dissipative steady states and equilibrium quantum phases</b>                  By: Le Boite, Alexandre; Orso, Giuliano; Ciuti, Cristiano                  PHYSICAL REVIEW A Volume: 90 Issue: 6 Article Number: 063821 Published: DEC 15 2014  <a href="#">View Abstract</a></p> <p>13. <b>Dissipative phase transitions: Independent versus collective decay and spin squeezing</b>                  By: Lee, Tony E.; Chan, Ching-Kit; Yelin, Susanne F.                  PHYSICAL REVIEW A Volume: 90 Issue: 5 Article Number: 052109 Published: NOV 13 2014  <a href="#">View Abstract</a></p> <p>Select Page       <a href="#">Save to EndNote online</a>   <a href="#">Add to Marked List</a></p> <p>Sort by: <b>Publication Date -- newest to oldest</b> ▼</p> <p>Show: <b>50 per page</b> ▼</p> <p>◀ Page 1 of 1 ▶</p> <p><i>13 records matched your query of the 36,843,663 in the data limits you selected.</i></p>	<p><b>Times Cited: 4</b> <i>(from Web of Science Core Collection)</i></p> <p><b>Usage Count</b> ▼</p> <p><b>Times Cited: 6</b> <i>(from Web of Science Core Collection)</i></p> <p><b>Usage Count</b> ▼</p> <p><b>Times Cited: 0</b> <i>(from Web of Science Core Collection)</i></p> <p><b>Usage Count</b> ▼</p> <p><b>Times Cited: 2</b> <i>(from Web of Science Core Collection)</i></p> <p><b>Usage Count</b> ▼</p> <p><b>Times Cited: 19</b> <i>(from Web of Science Core Collection)</i></p> <p><b>Usage Count</b> ▼</p> <p><b>Times Cited: 6</b> <i>(from Web of Science Core Collection)</i></p> <p><b>Usage Count</b> ▼</p>
---	---	--



Web of Science™	InCites™	Journal Citation Reports®	Essential Science Indicators™	EndNote™	Sign In ▾	Help	English ▾
-----------------	----------	---------------------------	-------------------------------	----------	-----------	------	-----------

WEB OF SCIENCE™
THOMSON REUTERS™

---

Search
Return to Search Results
My Tools ▾
Search History
Marked List

### Citing Articles: 11

*(from Web of Science Core Collection)*

**For:** Modified Coulomb gas construction of quantum Hall states from nonunitary conformal field theories ...[More](#)

**Times Cited Counts**

[11 in All Databases](#)

11 in Web of Science Core Collection

0 in BIOSIS Citation Index

0 in Chinese Science Citation Database

0 data sets in Data Citation Index

0 publication in Data Citation Index

0 in Russian Science Citation Index

0 in SciELO Citation Index

[View Additional Times Cited Counts](#)

---

### Refine Results

**Web of Science Categories** ▾

- PHYSICS CONDENSED MATTER (9)
- PHYSICS MULTIDISCIPLINARY (1)
- PHYSICS MATHEMATICAL (1)
- PHYSICS APPLIED (1)
- COMPUTER SCIENCE THEORY METHODS (1)

[more options / values...](#)

Refine

---

**Document Types** ▾

- ARTICLE (10)
- REVIEW (1)
- PROCEEDINGS PAPER (1)

[more options / values...](#)

Refine

---

**Research Areas** ▾

---

**Authors** ▾

- REGNAULT N (3)
- BERNEVIG BA (3)
- ESTIENNE B (2)
- ARDONNE E (2)
- BALDWIN KW (1)

[more options / values...](#)

Refine

Sort by: Publication Date -- newest to oldest ▾
◀ Page 1 of 1 ▶

Select Page

[Full Text from Publisher](#)

[Save to EndNote online](#) ▾

[Add to Marked List](#)

[Analyze Results](#)

[Create Citation Report](#)

- 1. Quantum Hall State  $\nu=1/3$  and Antilexicographic Order of Partitions**

By: Kusmierz, B.; Wjos, A.

Conference: 45th International School and Conference on the Physics of Semiconductors (Jaszowiec) Location: Szczyrk, POLAND Date: JUN 18-24, 2016

Sponsor(s): Polish Acad Sci, Inst Phys; Univ Warsaw, Inst Expt Phys & Theoret Phys, Fac Phys; Polish Acad Sci, Inst High Pressure Phys; Wroclaw Univ Sci & Technol, Div Expt & Theoret Phys; Inst Electron Technol; Polish Acad Sci, Comm Phys; Fdn Pro Physica; Minist Sci & Higher Educ; Polish Acad Sci; Off Naval Res Global; Int Technol Ctr Atlantic; COMEF; EDWARDS; Oxford Instruments, Labis; LOT Quantum Design; OCI Vacuum Microengineering Inc

[ACTA PHYSICA POLONICA A](#) Volume: 130 Issue: 5 Pages: 1183-1186 Published: NOV 2016

**Times Cited: 0**  
*(from Web of Science Core Collection)*

**Usage Count** ▾

[Full Text from Publisher](#)

[View Abstract](#)
- 2. Solvable models for unitary and nonunitary topological phases**

By: Papić, Z.

[PHYSICAL REVIEW B](#) Volume: 90 Issue: 7 Article Number: 075304 Published: AUG 12 2014

**Times Cited: 7**  
*(from Web of Science Core Collection)*

**Usage Count** ▾

[View Abstract](#)
- 3. Absence of a gap in the Gaffnian state**

By: Jolicœur, Th.; Mizusaki, T.; Lecheminant, Ph.

[PHYSICAL REVIEW B](#) Volume: 90 Issue: 7 Article Number: 075116 Published: AUG 11 2014

**Times Cited: 1**  
*(from Web of Science Core Collection)*

**Usage Count** ▾

[View Abstract](#)
- 4. Spin polarization of the  $\nu=12/5$  fractional quantum Hall state**

By: Zhang, Chi; Huan, Chao; Xia, J. S.; et al.

[PHYSICAL REVIEW B](#) Volume: 85 Issue: 24 Article Number: 241302 Published: JUN 7 2012

**Times Cited: 11**  
*(from Web of Science Core Collection)*

**Usage Count** ▾

[View Abstract](#)
- 5. Structure of spinful quantum Hall states: A squeezing perspective**

By: Ardonne, E.; Regnault, N.

[PHYSICAL REVIEW B](#) Volume: 84 Issue: 20 Article Number: 205134 Published: NOV 21 2011

**Times Cited: 16**  
*(from Web of Science Core Collection)*

**Usage Count** ▾

[View Abstract](#)
- 6. Gapless excitations in the Haldane-Rezayi state: The thin-torus limit**

By: Seidel, Alexander; Yang, Kun

[PHYSICAL REVIEW B](#) Volume: 84 Issue: 8 Article Number: 085122 Published: AUG 24 2011

**Times Cited: 16**  
*(from Web of Science Core Collection)*

**Usage Count** ▾

[View Abstract](#)
- 7. Decomposition of fractional quantum Hall model**

**Times Cited: 29**

<ul style="list-style-type: none"> <li>Group Authors &lt;</li> <li>Editors &lt;</li> <li>Source Titles &lt;</li> <li>Book Series Titles &lt;</li> <li>Conference Titles &lt;</li> <li>Publication Years &lt;</li> <li>Organizations-Enhanced &lt;</li> <li>Funding Agencies &lt;</li> <li>Languages &lt;</li> <li>Countries/Territories &lt;</li> <li>ESI Top Papers &lt;</li> <li>Open Access &lt;</li> </ul> <p style="text-align: center; margin-top: 10px;"><i>For advanced refine options, use</i></p> <div style="border: 1px solid #ccc; padding: 5px; width: fit-content; margin: 0 auto;">Analyze Results</div>	<p><b>states: Product rule symmetries and approximations</b>                  By: Thomale, Ronny; Estienne, Benoit; Regnault, Nicolas; et al.                  PHYSICAL REVIEW B Volume: 84 Issue: 4 Article Number: 045127 Published: JUL 19 2011</p> <div style="border: 1px solid #ccc; padding: 2px; width: fit-content; margin: 0 auto;">View Abstract</div>	<p><i>(from Web of Science Core Collection)</i></p> <p><b>Usage Count</b> ▾</p>
	<p>8. <b>From irrational to nonunitary: Haffnian and Haldane-Rezayi wave functions</b>                  By: Hermanns, M.; Regnault, N.; Bernevig, B. A.; et al.                  PHYSICAL REVIEW B Volume: 83 Issue: 24 Article Number: 241302 Published: JUN 10 2011</p> <div style="border: 1px solid #ccc; padding: 2px; width: fit-content; margin: 0 auto;">View Abstract</div>	<p><b>Times Cited: 8</b>  <i>(from Web of Science Core Collection)</i></p> <p><b>Usage Count</b> ▾</p>
	<p>9. <b>Development of Grid e-Infrastructure in South-Eastern Europe</b>                  By: Balaz, Antun; Prnjat, Ognjen; Vudragovic, Dusan; et al.                  JOURNAL OF GRID COMPUTING Volume: 9 Issue: 2 Special Issue: SI Pages: 135-154 Published: JUN 2011</p> <div style="border: 1px solid #ccc; padding: 2px; width: fit-content; margin: 0 auto;">View Abstract</div>	<p><b>Times Cited: 19</b>  <i>(from Web of Science Core Collection)</i></p> <p><b>Usage Count</b> ▾</p>
	<p>10. <b>LAUGHLIN'S WAVE FUNCTION AND ANGULAR MOMENTUM</b>                  By: Shrivastava, Keshav N.                  INTERNATIONAL JOURNAL OF MODERN PHYSICS B Volume: 25 Issue: 10 Pages: 1301-1357 Published: APR 20 2011</p> <div style="border: 1px solid #ccc; padding: 2px; width: fit-content; margin: 0 auto;">Full Text from Publisher</div> <div style="border: 1px solid #ccc; padding: 2px; width: fit-content; margin: 0 auto; margin-left: 20px;">View Abstract</div>	<p><b>Times Cited: 7</b>  <i>(from Web of Science Core Collection)</i></p> <p><b>Usage Count</b> ▾</p>
	<p>11. <b>Electron-quasihole duality and second-order differential equation for Read-Rezayi and Jack wave functions</b>                  By: Estienne, Benoit; Bernevig, B. Andrei; Santachiara, Raoul                  PHYSICAL REVIEW B Volume: 82 Issue: 20 Article Number: 205307 Published: NOV 8 2010</p> <div style="border: 1px solid #ccc; padding: 2px; width: fit-content; margin: 0 auto;">View Abstract</div>	<p><b>Times Cited: 6</b>  <i>(from Web of Science Core Collection)</i></p> <p><b>Usage Count</b> ▾</p>

Select Page
 
Save to EndNote online ▾
Add to Marked List

Sort by: Publication Date -- newest to oldest ▾
◀ Page 1 of 1 ▶

Show: 50 per page ▾

11 records matched your query of the 36,466,594 in the data limits you selected.

Web of Science™ InCites™ Journal Citation Reports® Essential Science Indicators™ EndNote™ Sign In Help English

**WEB OF SCIENCE™** THOMSON REUTERS™

Search Return to Search Results My Tools Search History Marked List

**Citing Articles: 5**  
(from Web of Science Core Collection)

**For:** Properties of quantum systems via diagonalization of transition amplitudes. I. Discretization effect  
...More

**Times Cited Counts**  
10 in All Databases  
10 in Web of Science Core Collection  
0 in BIOSIS Citation Index  
0 in Chinese Science Citation Database  
0 data sets in Data Citation Index  
0 publication in Data Citation Index  
0 in Russian Science Citation Index  
0 in SciELO Citation Index  
[View Additional Times Cited Counts](#)

**Refine Results**

Search within results for...

**Web of Science Categories**

- PHYSICS ATOMIC MOLECULAR CHEMICAL (1)
- OPTICS (1)
- MULTIDISCIPLINARY SCIENCES (1)
- MATHEMATICS APPLIED (1)
- COMPUTER SCIENCE THEORY METHODS (1)

[more options / values...](#) **Refine**

**Document Types**

- ARTICLE (4)
- PROCEEDINGS PAPER (1)

[more options / values...](#) **Refine**

**Research Areas**

**Authors**

**Group Authors**

**Editors**

**Source Titles**

**Book Series Titles**

Sort by: **Publication Date -- newest to oldest** Page 1 of 1

Select Page **Save to EndNote online** **Add to Marked List**

**Analyze Results**  
**Create Citation Report**

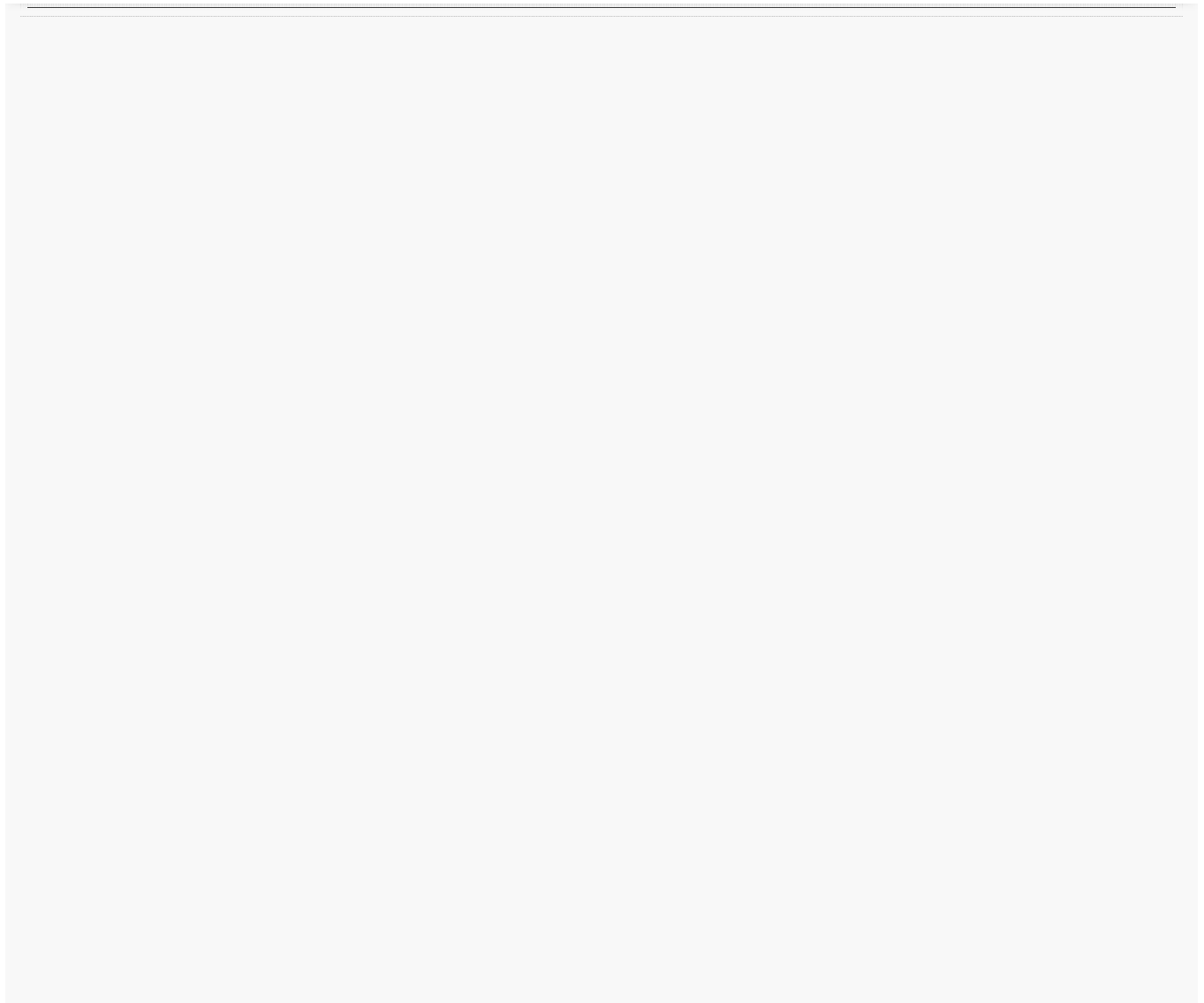
- BOSE-EINSTEIN CONDENSATION: TWENTY YEARS AFTER**  
By: Bagnato, V. S.; Frantzeskakis, D. J.; Kevrekidis, P. G.; et al.  
**ROMANIAN REPORTS IN PHYSICS** Volume: 67 Issue: 1  
Pages: 5-50 Published: 2015  
[View Abstract](#)  
**Times Cited: 50**  
(from Web of Science Core Collection)  
**Highly Cited Paper**  
**Usage Count**
- Density Waves in Dipolar Bose-Einstein Condensates by Means of Symbolic Computations**  
By: Nicolin, Alexandru I.; Rata, Ionel  
Edited by: Dulea, M; Karaivanova, A; Oulas, A; et al.  
Conference: HP-SEE User Forum Location: Natl Lib Serbia, Belgrade, SERBIA Date: OCT 17-19, 2012  
Sponsor(s): Inst Phys Belgrade  
HIGH-PERFORMANCE COMPUTING INFRASTRUCTURE FOR SOUTH EAST EUROPE'S RESEARCH COMMUNITIES: RESULTS OF THE HP-SEE USER FORUM 2012 Book Series: Modeling and Optimization in Science and Technologies  
Volume: 2 Pages: 15-21 Published: 2014  
[View Abstract](#)  
**Times Cited: 3**  
(from Web of Science Core Collection)  
**Usage Count**
- DENSITY WAVES IN DIPOLAR BOSE-EINSTEIN CONDENSATES**  
By: Nicolin, Alexandru I.  
**PROCEEDINGS OF THE ROMANIAN ACADEMY SERIES A-MATHEMATICS PHYSICS TECHNICAL SCIENCES INFORMATION SCIENCE** Volume: 14 Issue: 1 Pages: 35-41  
Published: JAN-MAR 2013  
[View Abstract](#)  
**Times Cited: 15**  
(from Web of Science Core Collection)  
**Usage Count**
- Faraday waves in binary nonmiscible Bose-Einstein condensates**  
By: Balaz, Antun; Nicolin, Alexandru I.  
**PHYSICAL REVIEW A** Volume: 85 Issue: 2 Article Number: 023613  
Published: FEB 9 2012  
[View Abstract](#)  
**Times Cited: 46**  
(from Web of Science Core Collection)  
**Usage Count**
- Development of Grid e-Infrastructure in South-Eastern Europe**  
By: Balaz, Antun; Prnjat, Ognjen; Vudragovic, Dusan; et al.  
**JOURNAL OF GRID COMPUTING** Volume: 9 Issue: 2  
Special Issue: SI Pages: 135-154 Published: JUN 2011  
[View Abstract](#)  
**Times Cited: 19**  
(from Web of Science Core Collection)  
**Usage Count**

Select Page **Save to EndNote online** **Add to Marked List**



Sort by: **Publication Date -- newest to oldest** Page 1 of 1  
Show: **10 per page**

5 records matched your query of the 36,466,594 in the data limits you selected.

Conference Titles	◀
Publication Years	◀
Organizations-Enhanced	◀
Funding Agencies	◀
Languages	◀
Countries/Territories	◀
ESI Top Papers	◀
Open Access	◀
<i>For advanced refine options, use</i>	
<a href="#">Analyze Results</a>	



Web of Science™	InCites™	Journal Citation Reports®	Essential Science Indicators™	EndNote™	Sign In ▾	Help	English ▾
-----------------	----------	---------------------------	-------------------------------	----------	-----------	------	-----------

---

Search
Return to Search Results
My Tools ▾
Search History
Marked List

### Citing Articles: 7

*(from Web of Science Core Collection)*

**For:** Spin modulation instabilities and phase separation dynamics in trapped two-component Bose condensate  
[...More](#)

**Times Cited Counts**

7 in All Databases

7 in Web of Science Core Collection

0 in BIOSIS Citation Index

0 in Chinese Science Citation Database

0 data sets in Data Citation Index

0 publication in Data Citation Index

0 in Russian Science Citation Index

0 in SciELO Citation Index

[View Additional Times Cited Counts](#)

---

### Refine Results

**Web of Science Categories** ▾

- PHYSICS MATHEMATICAL (3)
- PHYSICS ATOMIC MOLECULAR CHEMICAL (3)
- OPTICS (3)
- COMPUTER SCIENCE INTERDISCIPLINARY APPLICATIONS (2)
- MECHANICS (1)

[more options / values...](#)

[Refine](#)

---

**Document Types** ▾

ARTICLE (7)

[Refine](#)

---

**Research Areas** ▾

---

**Authors** ▾

- BALAZ A (3)
- MURUGANANDAM P (2)
- ADHIKARI SK (2)
- HIRANO T (1)
- ETO Y (1)

[more options / values...](#)

[Refine](#)

---

**Group Authors** ▾

Sort by: **Publication Date -- newest to oldest** ▾
 ◀ Page 1 of 1 ▶

Select Page


Save to EndNote online ▾
Add to Marked List

1. **Chaos-assisted formation of immiscible matter-wave solitons and self-stabilization in the binary discrete nonlinear Schrodinger equation**  
 By: Makarov, D. V.; Uleysky, M. Yu.  
 COMMUNICATIONS IN NONLINEAR SCIENCE AND NUMERICAL SIMULATION Volume: 43 Pages: 227-238  
 Published: FEB 2017  

Full Text from Publisher
View Abstract
2. **Faraday and resonant waves in binary collisionally-inhomogeneous Bose-Einstein condensates**  
 By: Sudharsan, J. B.; Radha, R.; Raportaru, Mihaela Carina; et al.  
 JOURNAL OF PHYSICS B-ATOMIC MOLECULAR AND OPTICAL PHYSICS Volume: 49 Issue: 16 Article Number: 165303 Published: AUG 28 2016  

View Abstract
3. **Nonequilibrium dynamics induced by miscible-immiscible transition in binary Bose-Einstein condensates**  
 By: Eto, Yujiro; Takahashi, Masahiro; Kunimi, Masaya; et al.  
 NEW JOURNAL OF PHYSICS Volume: 18 Article Number: 073029 Published: JUL 14 2016  

Full Text from Publisher
View Abstract
4. **OpenMP Fortran and C programs for solving the time-dependent Gross-Pitaevskii equation in an anisotropic trap**  
 By: Young-S., Luis E.; Vudragovic, Dugan; Muruganandam, Paulsamy; et al.  
 COMPUTER PHYSICS COMMUNICATIONS Volume: 204 Pages: 209-213 Published: JUL 2016  

Full Text from Publisher
View Abstract
5. **Hybrid OpenMP/MPI programs for solving the time-dependent Gross-Pitaevskii equation in a fully anisotropic trap**  
 By: Sataric, Bogdan; Slavnic, Vladimir; Belic, Aleksandar; et al.  
 COMPUTER PHYSICS COMMUNICATIONS Volume: 200 Pages: 411-417 Published: MAR 2016  

Full Text from Publisher
View Abstract
6. **Modulational instability in binary spin-orbit-coupled Bose-Einstein condensates**  
 By: Bhat, Ishfaq Ahmad; Mithun, T.; Malomed, B. A.; et al.  
 PHYSICAL REVIEW A Volume: 92 Issue: 6 Article Number: 063606 Published: DEC 2 2015  

View Abstract
7. **Equilibration of a finite-temperature binary Bose gas formed by population transfer**

[Analyze Results](#)

[Create Citation Report](#)

**Times Cited: 0**  
*(from Web of Science Core Collection)*

**Usage Count** ▾

---

**Times Cited: 0**  
*(from Web of Science Core Collection)*

**Usage Count** ▾

---

**Times Cited: 1**  
*(from Web of Science Core Collection)*

**Usage Count** ▾

---

**Times Cited: 7**  
*(from Web of Science Core Collection)*

**Usage Count** ▾

---

**Times Cited: 15**  
*(from Web of Science Core Collection)*

**Highly Cited Paper**

**Usage Count** ▾



---

**Times Cited: 1**  
*(from Web of Science Core Collection)*

**Usage Count** ▾

---

**Times Cited: 3**  
*(from Web of Science Core Collection)*

<b>Editors</b> ◀	By: Pattinson, R. W.; Proukakis, N. P.; Parker, N. G. <span style="float: right;">Usage Count ▾</span>
<b>Source Titles</b> ◀	<a href="#">PHYSICAL REVIEW A</a> Volume: 90 Issue: 3 Article Number: 033625 Published: SEP 24 2014
<b>Book Series Titles</b> ◀	<a href="#">View Abstract</a>
<b>Conference Titles</b> ◀	Select Page     <a href="#">Save to EndNote online</a> ▾ <a href="#">Add to Marked List</a>
<b>Publication Years</b> ◀	Sort by: <a href="#">Publication Date -- newest to oldest</a> ▾ <span style="float: right;">◀ Page 1 of 1 ▶</span>
<b>Organizations-Enhanced</b> ◀	Show: <a href="#">50 per page</a> ▾
<b>Funding Agencies</b> ◀	<i>7 records matched your query of the 36,466,594 in the data limits you selected.</i>
<b>Languages</b> ◀	
<b>Countries/Territories</b> ◀	
<b>ESI Top Papers</b> ◀	
<b>Open Access</b> ◀	
<i>For advanced refine options, use</i>	
<a href="#">Analyze Results</a>	

Web of Science™ InCites™ Journal Citation Reports® Essential Science Indicators™ EndNote™
Sign In Help English ▾

# WEB OF SCIENCE™

Search
Return to Search Results
My Tools ▾ Search History Marked List

**Citing Articles: 5**  
*(from Web of Science Core Collection)*

**For:** Topological d-wave pairing structures in Jain states ...[More](#)

**Times Cited Counts**  
[5 in All Databases](#)

5 in Web of Science Core Collection  
0 in BIOSIS Citation Index  
0 in Chinese Science Citation Database  
0 data sets in Data Citation Index  
0 publication in Data Citation Index  
0 in Russian Science Citation Index  
0 in SciELO Citation Index

[View Additional Times Cited Counts](#)

---

**Refine Results**

**Web of Science Categories** ▾

- PHYSICS CONDENSED MATTER (4)
- PHYSICS PARTICLES FIELDS (1)
- PHYSICS NUCLEAR (1)

[more options / values...](#)

**Refine**

**Document Types** ▾

- ARTICLE (5)

**Refine**

**Research Areas** ▾

**Authors** ▾

**Group Authors** ▾

**Editors** ▾

**Source Titles** ▾

**Book Series Titles** ▾

**Conference Titles** ▾

**Publication Years** ▾

Sort by: Publication Date -- newest to oldest ▾
◀ Page 1 of 1 ▶

Select Page

Save to EndNote online ▾
Add to Marked List

[Analyze Results](#)

[Create Citation Report](#)

1. **Phase diagram of  $nu=1/2+1/2$  bilayer bosons with interlayer couplings**

By: Liu, Zhao; Vaezi, Abolhassan; Repellin, Cecile; et al.  
**PHYSICAL REVIEW B** Volume: 93 Issue: 8 Article Number: 085115 Published: FEB 9 2016

View Abstract
2. **Z(2) fractional topological insulators in two dimensions**

By: Repellin, C.; Bernevig, B. Andrei; Regnault, N.  
**PHYSICAL REVIEW B** Volume: 90 Issue: 24 Article Number: 245401 Published: DEC 1 2014

View Abstract
3. **Composite particles within the Faddeev-Jackiw framework. Nonequivalence between the Dirac and Faddeev-Jackiw formalisms**

By: Manavella, Edmundo C.  
**INTERNATIONAL JOURNAL OF MODERN PHYSICS A** Volume: 29 Issue: 15 Article Number: 1450076 Published: JUN 20 2014

Full Text from Publisher View Abstract
4. **Quantum Hall effect of two-component bosons at fractional and integral fillings**

By: Wu, Ying-Hai; Jain, Jainendra K.  
**PHYSICAL REVIEW B** Volume: 87 Issue: 24 Article Number: 245123 Published: JUN 24 2013

View Abstract
5. **Coexistence of antiferromagnetism and d plus id superconducting correlations in the graphene bilayer**

By: Milovanovic, M. V.; Predin, S.  
**PHYSICAL REVIEW B** Volume: 86 Issue: 19 Article Number: 195113 Published: NOV 8 2012

View Abstract

Select Page

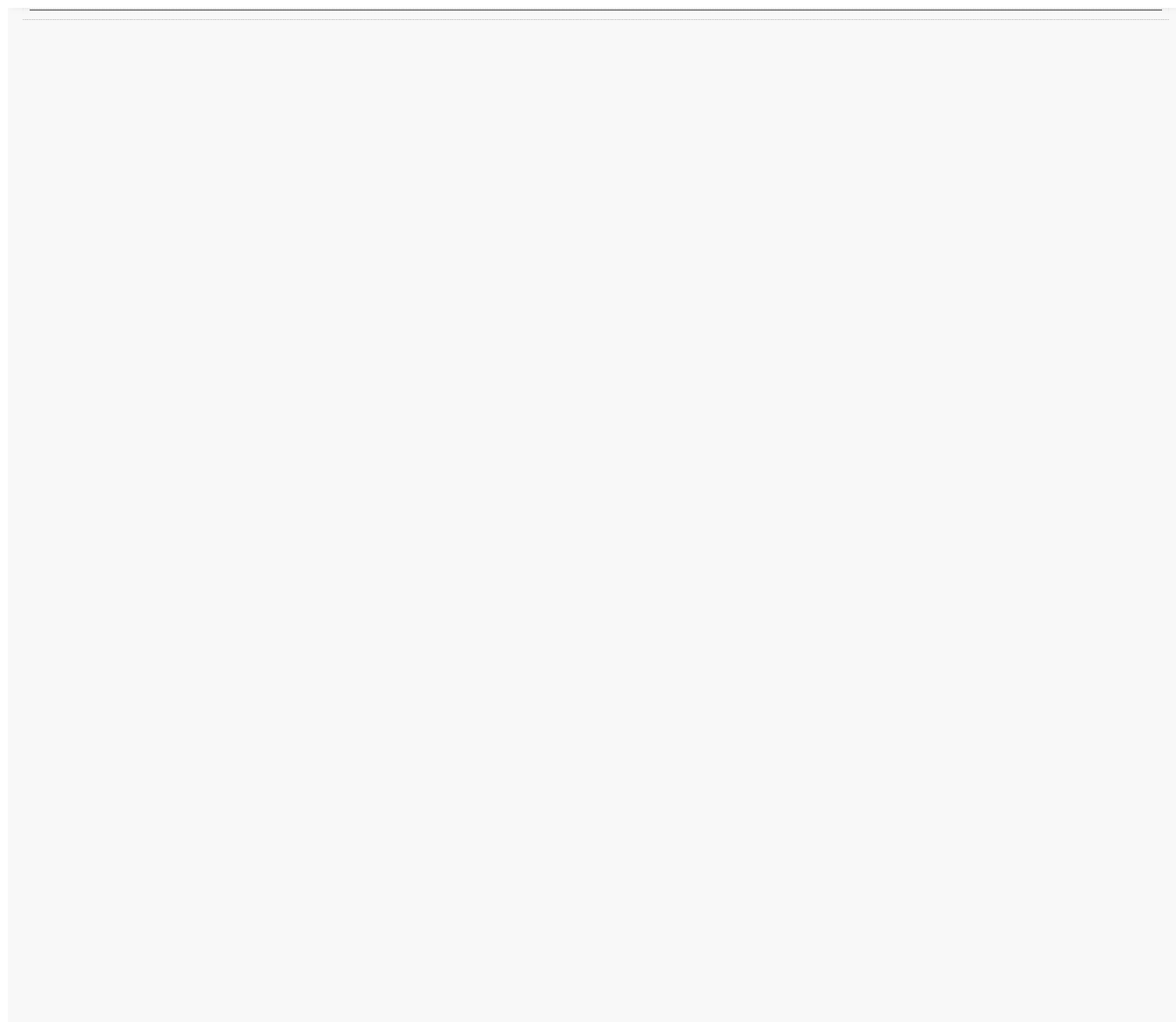
Save to EndNote online ▾
Add to Marked List

Sort by: Publication Date -- newest to oldest ▾
◀ Page 1 of 1 ▶

Show: 50 per page ▾

5 records matched your query of the 36,466,594 in the data limits you selected.

<b>Organizations-Enhanced</b> ◀
<b>Funding Agencies</b> ◀
<b>Languages</b> ◀
<b>Countries/Territories</b> ◀
<b>ESI Top Papers</b> ◀
<b>Open Access</b> ◀
<i>For advanced refine options, use</i> <a href="#">Analyze Results</a>





Web of Science™ InCites™ Journal Citation Reports® Essential Science Indicators™ EndNote™
Sign In Help English

# WEB OF SCIENCE™

Search
Return to Search Results
My Tools Search History Marked List

### Citing Articles: 4

(from Web of Science Core Collection)

**For:** SPEEDUP Code for Calculation of Transition Amplitudes via the Effective Action Approach ...[More](#)

**Times Cited Counts**  
5 in All Databases

- 5 in Web of Science Core Collection
- 0 in BIOSIS Citation Index
- 0 in Chinese Science Citation Database
- 0 data sets in Data Citation Index
- 0 publication in Data Citation Index
- 0 in Russian Science Citation Index
- 0 in SciELO Citation Index

[View Additional Times Cited Counts](#)

---

### Refine Results

**Web of Science Categories**

- PHYSICS MULTIDISCIPLINARY (2)
- PHYSICS CONDENSED MATTER (2)
- MATERIALS SCIENCE MULTIDISCIPLINARY (1)
- ENGINEERING ELECTRICAL ELECTRONIC (1)

[more options / values...](#)

Refine

**Document Types**

- ARTICLE (4)

Refine

**Research Areas**

**Authors**

**Group Authors**

**Editors**

**Source Titles**

**Book Series Titles**

**Conference Titles**

Sort by: Publication Date -- newest to oldest

Page 1 of 1

Select Page   Save to EndNote online Add to Marked List

[Analyze Results](#)

[Create Citation Report](#)

1. **Random networks of carbon nanotubes optimized for transistor mass-production: searching for ultimate performance**

By: Zezelj, M.; Stankovic, I.  
SEMICONDUCTOR SCIENCE AND TECHNOLOGY Volume: 31 Issue: 10 Article Number: 105015 Published: OCT 2016

View Abstract
2. **BOSE-EINSTEIN CONDENSATION: TWENTY YEARS AFTER**

By: Bagnato, V. S.; Frantzeskakis, D. J.; Kevrekidis, P. G.; et al.  
ROMANIAN REPORTS IN PHYSICS Volume: 67 Issue: 1 Pages: 5-50 Published: 2015

View Abstract
3. **From percolating to dense random stick networks: Conductivity model investigation**

By: Zezelj, Milan; Stankovic, Igor  
PHYSICAL REVIEW B Volume: 86 Issue: 13 Article Number: 134202 Published: OCT 8 2012

View Abstract
4. **Effects of spatially inhomogeneous atomic interactions on Bose-Einstein condensates in optical lattices**

By: Sekh, Golam Ali  
PHYSICS LETTERS A Volume: 376 Issue: 21 Pages: 1740-1747 Published: APR 23 2012

Full Text from Publisher View Abstract

Select Page   Save to EndNote online Add to Marked List

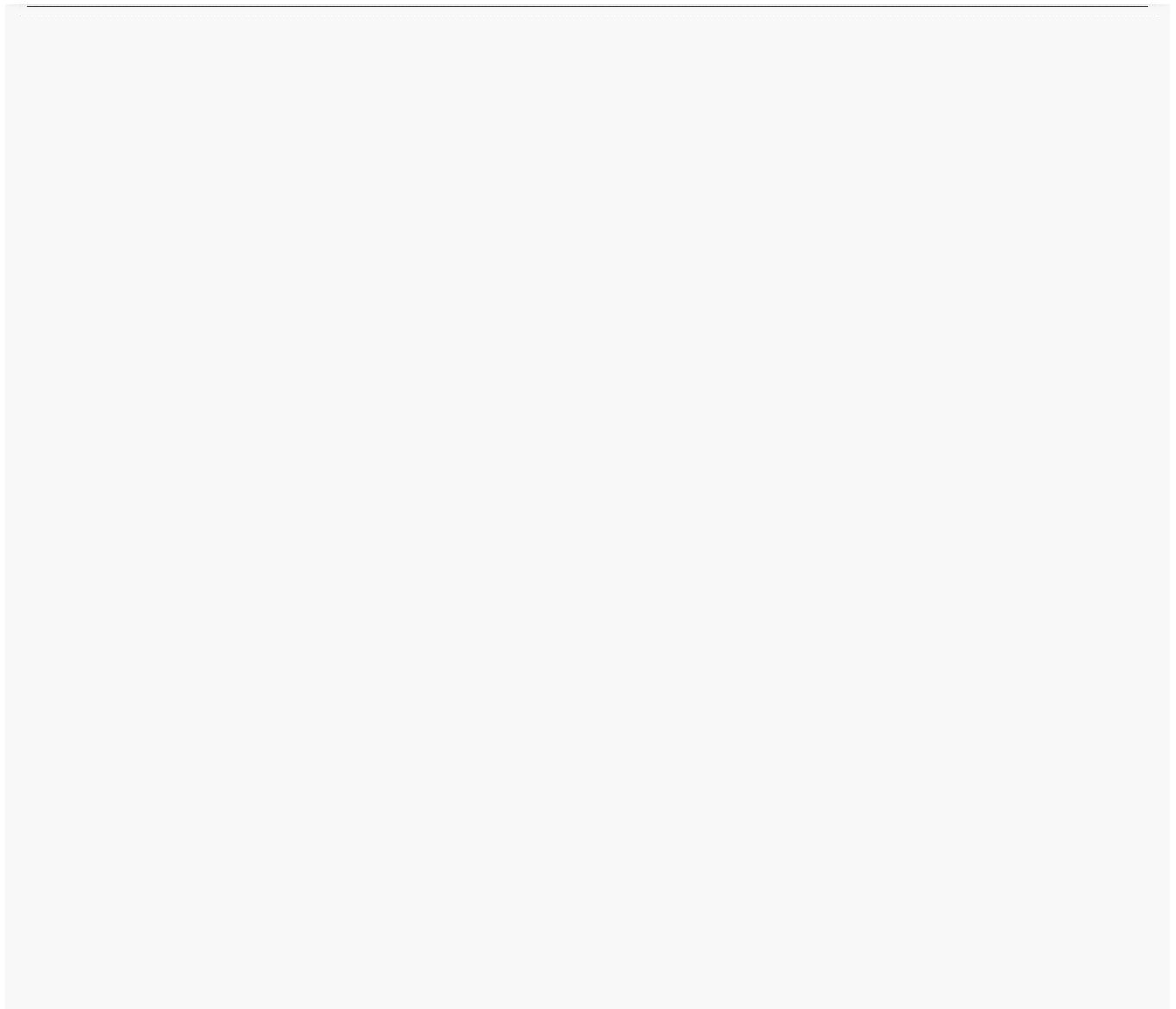
Sort by: Publication Date -- newest to oldest

Show: 10 per page

Page 1 of 1

4 records matched your query of the 36,466,594 in the data limits you selected.

<b>Publication Years</b> ◀
<b>Organizations-Enhanced</b> ◀
<b>Funding Agencies</b> ◀
<b>Languages</b> ◀
<b>Countries/Territories</b> ◀
<b>ESI Top Papers</b> ◀
<b>Open Access</b> ◀
<i>For advanced refine options, use</i> <a href="#">Analyze Results</a>



Web of Science™ InCites™ Journal Citation Reports® Essential Science Indicators™ EndNote™ Sign In Help English

**WEB OF SCIENCE™** THOMSON REUTERS™

Search Return to Search Results My Tools Search History Marked List

**Citing Articles: 2**  
*(from Web of Science Core Collection)*

**For:** Parametric and geometric resonances of collective oscillation modes in Bose-Einstein condensates  
[...More](#)

**Times Cited Counts**  
[3 in All Databases](#)

- 3 in Web of Science Core Collection
- 0 in BIOSIS Citation Index
- 0 in Chinese Science Citation Database
- 0 data sets in Data Citation Index
- 0 publication in Data Citation Index
- 0 in Russian Science Citation Index
- 0 in SciELO Citation Index

[View Additional Times Cited Counts](#)

---

**Refine Results**

Search within results for...

**Web of Science Categories**

- OPTICS (2)
- PHYSICS ATOMIC MOLECULAR CHEMICAL (1)
- PHYSICS APPLIED (1)

[more options / values...](#)

**Refine**

**Document Types**

- ARTICLE (2)

**Refine**

**Research Areas**

**Authors**

**Group Authors**

**Editors**

**Source Titles**

**Book Series Titles**

**Conference Titles**

**Publication Years**

Sort by: **Publication Date -- newest to oldest**

Page 1 of 1

Select Page **Save to EndNote online** **Add to Marked List**

[Analyze Results](#)  
[Create Citation Report](#)

1. **Controlled generation of nonlinear resonances through sinusoidal lattice modes in Bose-Einstein condensate**  
By: Das, Priyam; Panigrahi, Prasanta K.  
**LASER PHYSICS** Volume: 25 Issue: 12 Article Number: 125501 Published: DEC 2015  
[View Abstract](#)
2. **Breakdown of the Kohn theorem near a Feshbach resonance in a magnetic trap**  
By: Al-Jibbouri, Hamid; Pelster, Axel  
**PHYSICAL REVIEW A** Volume: 88 Issue: 3 Article Number: 033621 Published: SEP 17 2013  
[View Abstract](#)

Times Cited: 5  
*(from Web of Science Core Collection)*  
Usage Count

Times Cited: 6  
*(from Web of Science Core Collection)*  
Usage Count

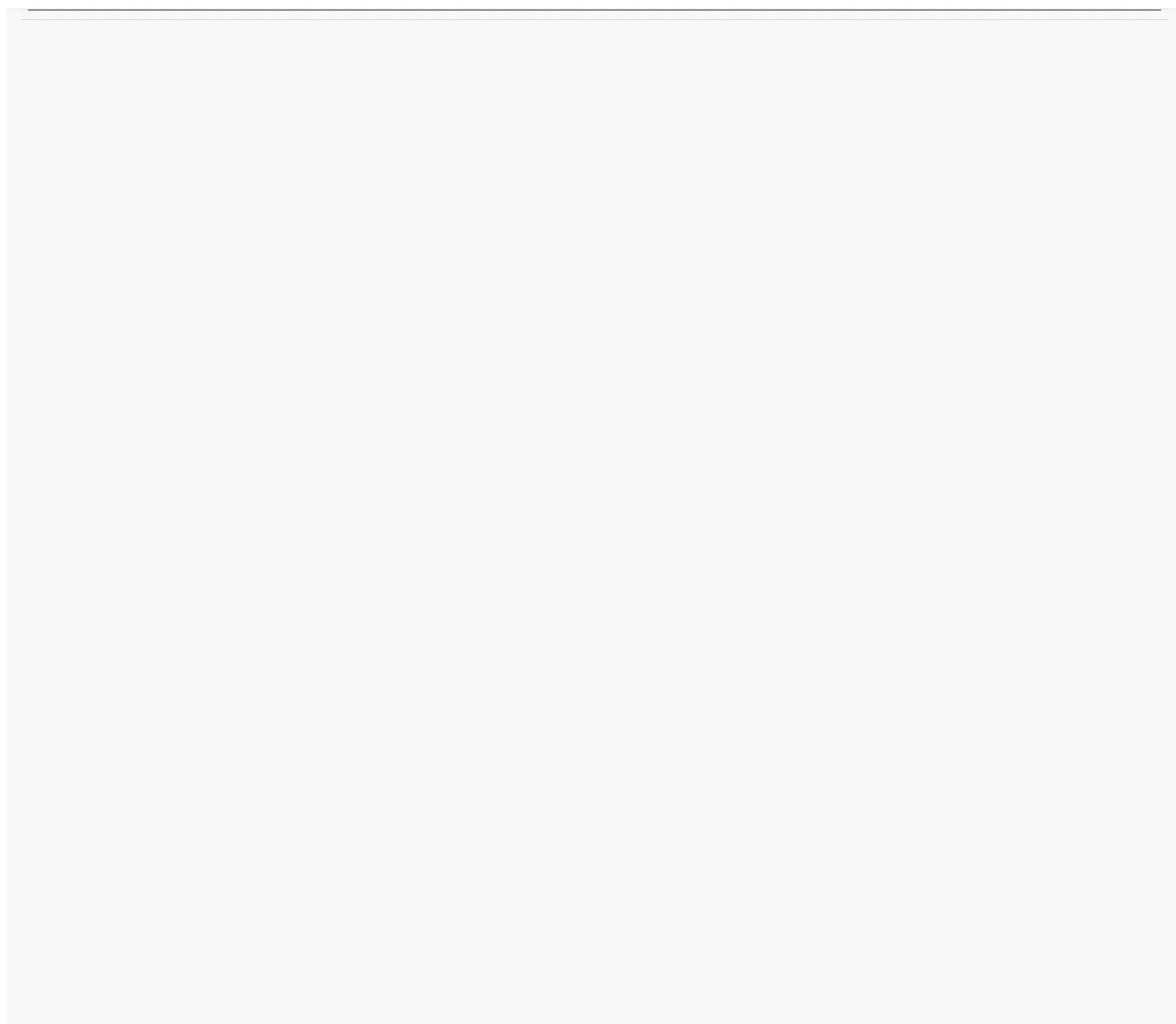
Select Page **Save to EndNote online** **Add to Marked List**

Sort by: **Publication Date -- newest to oldest**

Show: **10 per page**

2 records matched your query of the 36,466,594 in the data limits you selected.

<b>Organizations-Enhanced</b> ◀
<b>Funding Agencies</b> ◀
<b>Languages</b> ◀
<b>Countries/Territories</b> ◀
<b>ESI Top Papers</b> ◀
<b>Open Access</b> ◀
<i>For advanced refine options, use</i> <a href="#">Analyze Results</a>



Web of Science™ InCites™ Journal Citation Reports® Essential Science Indicators™ EndNote™ Sign In Help English

**WEB OF SCIENCE™** THOMSON REUTERS™

Search Return to Search Results My Tools Search History Marked List

**Citing Articles: 2**  
(from Web of Science Core Collection)

**For:** Excitation spectra of a Bose-Einstein condensate with an angular spin-orbit coupling ...[More](#)

**Times Cited Counts**  
2 in All Databases

- 2 in Web of Science Core Collection
- 0 in BIOSIS Citation Index
- 0 in Chinese Science Citation Database
- 0 data sets in Data Citation Index
- 0 publication in Data Citation Index
- 0 in Russian Science Citation Index
- 0 in SciELO Citation Index

[View Additional Times Cited Counts](#)

**Refine Results**

Search within results for...

**Web of Science Categories**

- PHYSICS MATHEMATICAL (2)
- COMPUTER SCIENCE
- INTERDISCIPLINARY APPLICATIONS (2)

[more options / values...](#)

**Refine**

**Document Types**

- ARTICLE (2)

**Refine**

**Research Areas**

**Authors**

**Group Authors**

**Editors**

**Source Titles**

**Book Series Titles**

**Conference Titles**

**Publication Years**

Sort by: **Publication Date -- newest to oldest** Page 1 of 1

Select Page **Save to EndNote online** **Add to Marked List**

**Analyze Results**  
**Create Citation Report**

**Times Cited: 0**  
(from Web of Science Core Collection)

**Usage Count**

1. **OpenMP, OpenMP/MPI, and CUDA/MPI C programs for solving the time-dependent dipolar Gross-Pitaevskii equation**  
By: Loncar, Vladimir; Young-S, Luis E.; Skrbic, Srdjan; et al.  
[COMPUTER PHYSICS COMMUNICATIONS](#) Volume: 209  
Pages: 190-196 Published: DEC 2016

**Full Text from Publisher** **View Abstract**

2. **OpenMP Fortran and C programs for solving the time-dependent Gross-Pitaevskii equation in an anisotropic trap**  
By: Young-S., Luis E.; Vudragovic, Dugan; Muruganandam, Paulsamy; et al.  
[COMPUTER PHYSICS COMMUNICATIONS](#) Volume: 204  
Pages: 209-213 Published: JUL 2016

**Full Text from Publisher** **View Abstract**

**Times Cited: 7**  
(from Web of Science Core Collection)

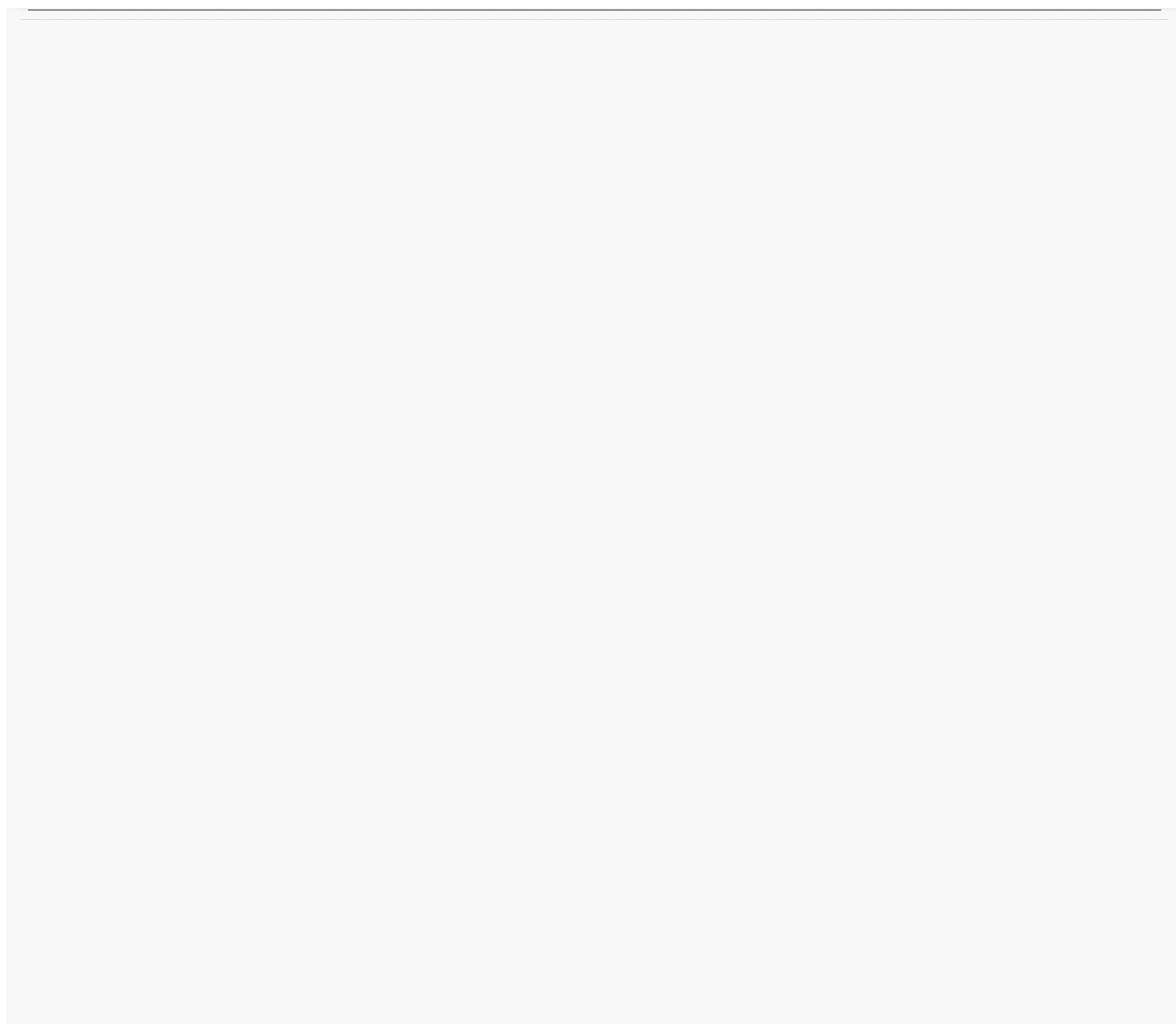
**Usage Count**

Select Page **Save to EndNote online** **Add to Marked List**

Sort by: **Publication Date -- newest to oldest** Show: **50 per page** Page 1 of 1

2 records matched your query of the 36,466,594 in the data limits you selected.

<b>Organizations-Enhanced</b> ◀
<b>Funding Agencies</b> ◀
<b>Languages</b> ◀
<b>Countries/Territories</b> ◀
<b>ESI Top Papers</b> ◀
<b>Open Access</b> ◀
<i>For advanced refine options, use</i> <a href="#">Analyze Results</a>



Citing Articles: 1 (from Web of Science Core Collection)

For: Photonic currents in driven and dissipative resonator lattices ...More

Times Cited Counts

- 1 in All Databases
1 in Web of Science Core Collection
0 in BIOSIS Citation Index
0 in Chinese Science Citation Database
0 data sets in Data Citation Index
0 publication in Data Citation Index
0 in Russian Science Citation Index
0 in SciELO Citation Index

View Additional Times Cited Counts

Refine Results

Search within results for...

Web of Science Categories: PHYSICS ATOMIC MOLECULAR CHEMICAL (1), OPTICS (1). Refine

Document Types: ARTICLE (1). Refine

Research Areas

Authors

Group Authors

Editors

Source Titles

Book Series Titles

Conference Titles

Publication Years

Organizations-Enhanced

Sort by: Publication Date -- newest to oldest Page 1 of 1

Select Page Save to EndNote online Add to Marked List

- 1. Nonlinear transport in an out-of-equilibrium single-site Bose-Hubbard model: Scaling, rectification, and time dynamics

By: Purkayastha, Archak; Dhar, Abhishek; Kulkarni, Manas PHYSICAL REVIEW A Volume: 94 Issue: 5 Article Number: 052134 Published: NOV 28 2016

View Abstract

Analyze Results Create Citation Report

Times Cited: 0 (from Web of Science Core Collection)

Usage Count

Select Page Save to EndNote online Add to Marked List

Sort by: Publication Date -- newest to oldest Page 1 of 1

Show: 50 per page

1 records matched your query of the 36,466,594 in the data limits you selected.

<b>Funding Agencies</b> ◀
<b>Languages</b> ◀
<b>Countries/Territories</b> ◀
<b>ESI Top Papers</b> ◀
<b>Open Access</b> ◀
<i>For advanced refine options, use</i> <a href="#">Analyze Results</a>



Web of Science™ InCites™ Journal Citation Reports® Essential Science Indicators™ EndNote™
Sign In Help English

# WEB OF SCIENCE™

Search
Return to Search Results
My Tools Search History Marked List

### Citing Articles: 1

*(from Web of Science Core Collection)*

**For:** Force-induced desorption of self-avoiding walks on Sierpinski gasket fractals [...More](#)

**Times Cited Counts**  
[1 in All Databases](#)  
 1 in Web of Science Core Collection  
 0 in BIOSIS Citation Index  
 0 in Chinese Science Citation Database  
 0 data sets in Data Citation Index  
 0 publication in Data Citation Index  
 0 in Russian Science Citation Index  
 0 in SciELO Citation Index  
[View Additional Times Cited Counts](#)

---

### Refine Results

**Web of Science Categories** ▼

PHYSICS ATOMIC MOLECULAR CHEMICAL (1)

CHEMISTRY PHYSICAL (1)

[more options / values...](#)

**Refine**

**Document Types** ▼

ARTICLE (1)

**Refine**

Research Areas ▲

Authors ▲

Group Authors ▲

Editors ▲

Source Titles ▲

Book Series Titles ▲

Conference Titles ▲

Publication Years ▲

Organizations-Enhanced ▲

Sort by: Publication Date -- newest to oldest
◀ Page 1 of 1 ▶

Select Page

Save to EndNote online
Add to Marked List

1. **Exact solution of the Zwanzig-Lauritzen model of polymer crystallization under tension**

By: Samanta, Himadri S.; Thirumalai, D.  
**JOURNAL OF CHEMICAL PHYSICS** Volume: 138 Issue: 10  
 Article Number: 104901 Published: MAR 14 2013

View Abstract

Select Page

Save to EndNote online
Add to Marked List

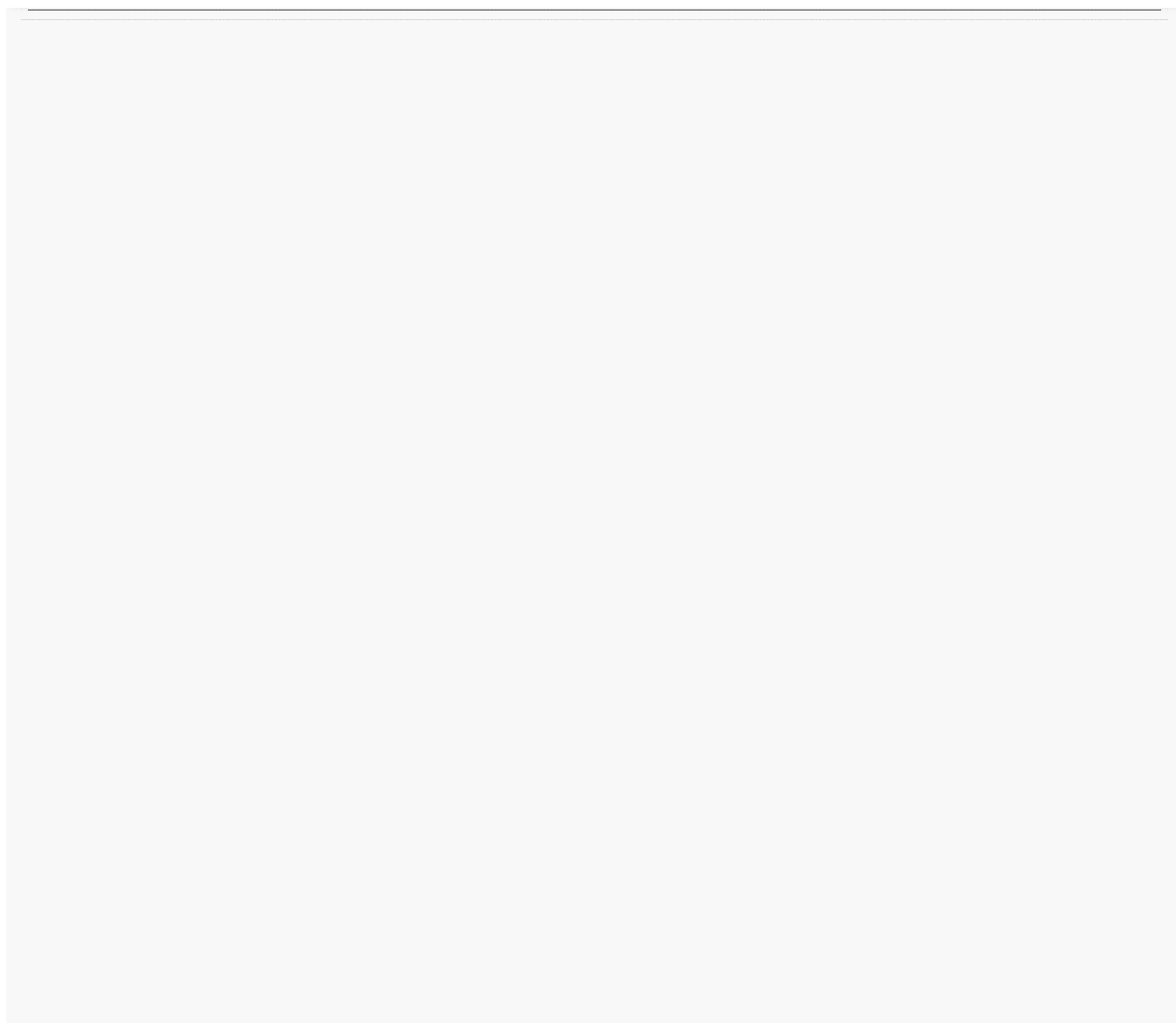
≡ Analyze Results  
▮ Create Citation Report  
**Times Cited: 2**  
*(from Web of Science Core Collection)*  
**Usage Count** ▼

Sort by: Publication Date -- newest to oldest
◀ Page 1 of 1 ▶

Show: 50 per page

1 records matched your query of the 36,466,594 in the data limits you selected.

<b>Funding Agencies</b> ◀
<b>Languages</b> ◀
<b>Countries/Territories</b> ◀
<b>ESI Top Papers</b> ◀
<b>Open Access</b> ◀
<i>For advanced refine options, use</i> <a href="#">Analyze Results</a>



Web of Science™ InCites™ Journal Citation Reports® Essential Science Indicators™ EndNote™
Sign In Help English

WEB OF SCIENCE™

**THOMSON REUTERS™**

Search
Return to Search Results
My Tools Search History Marked List

### Citing Articles: 1

(from Web of Science Core Collection)

**For:** Accelerated path integral calculations for many-body systems  
[...More](#)

**Times Cited Counts**  
1 in All Databases

- 1 in Web of Science Core Collection
- 0 in BIOSIS Citation Index
- 0 in Chinese Science Citation Database
- 0 data sets in Data Citation Index
- 0 publication in Data Citation Index
- 0 in Russian Science Citation Index
- 0 in SciELO Citation Index

[View Additional Times Cited Counts](#)

---

### Refine Results

**Web of Science Categories**

- PHYSICS MATHEMATICAL (1)
- PHYSICS APPLIED (1)
- MATHEMATICS APPLIED (1)

[more options / values...](#)

Refine

**Document Types**

- PROCEEDINGS PAPER (1)

Refine

- Research Areas
- Authors
- Group Authors
- Editors
- Source Titles
- Book Series Titles
- Conference Titles
- Publication Years

Sort by: Publication Date -- newest to oldest
Page 1 of 1

Select Page


Save to EndNote online
Add to Marked List

Analyze Results  
Create Citation Report

**Times Cited: 0**  
*(from Web of Science Core Collection)*

**Usage Count**

1. **Energy levels and expectation values via accelerated path integral Monte Carlo**

By: Stojiljkovic, D.; Bogojevic, A.; Balaz, A.  
 Book Author(s): Arratia, O; Calzada, JA; GomezCubillo, F; et al.  
 Conference: 5th International Symposium on Quantum Theory and Symmetries Location: Univ Valladolid, Valladolid, SPAIN  
 Date: JUL 22-28, 2007  
 5TH INTERNATIONAL SYMPOSIUM ON QUANTUM THEORY AND SYMMETRIES QTS5 Book Series: Journal of Physics Conference Series Volume: 128 Article Number: 012062  
 Published: 2008

Full Text from Publisher
View Abstract

Select Page

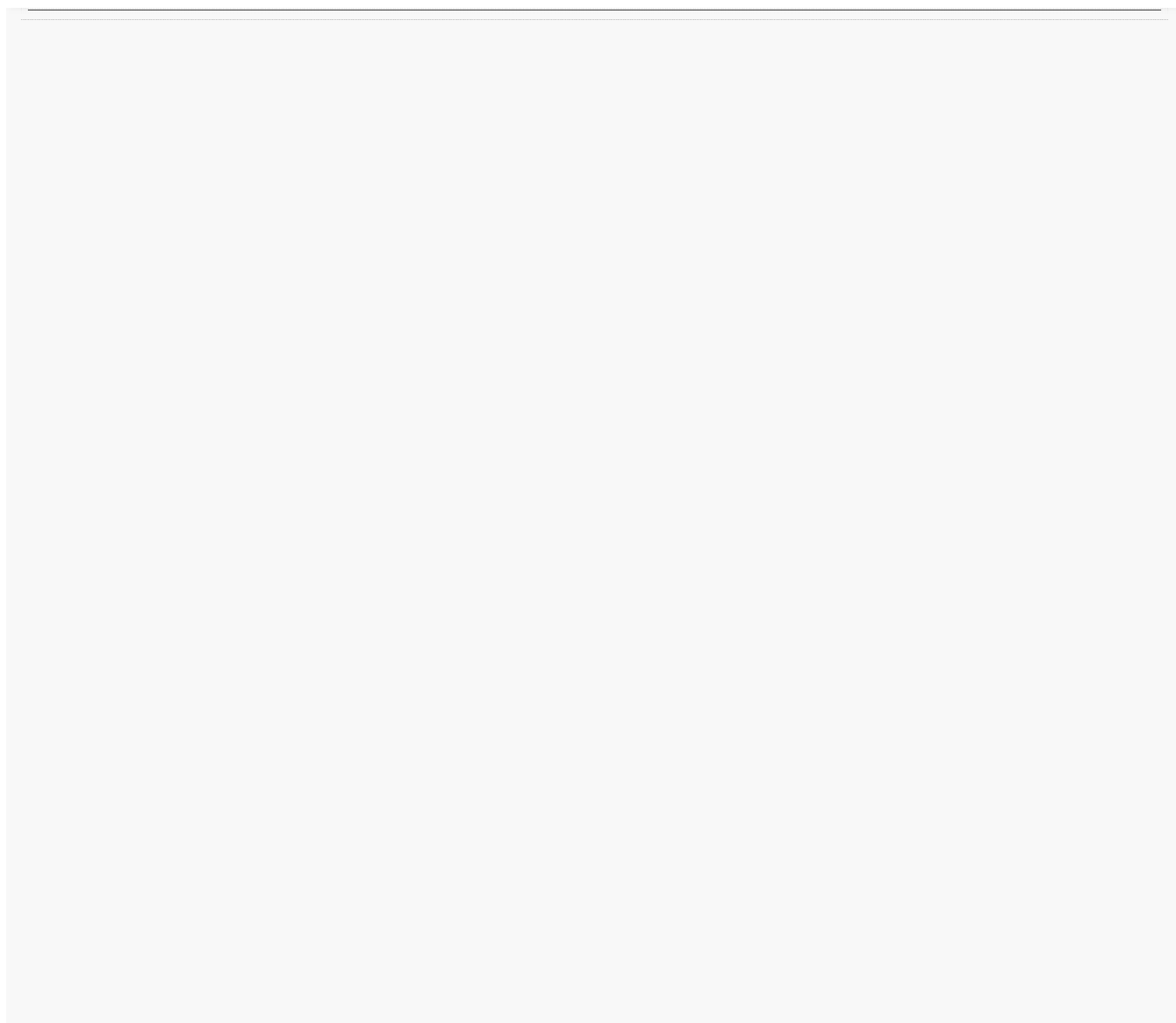

Save to EndNote online
Add to Marked List

Sort by: Publication Date -- newest to oldest
Page 1 of 1

Show: 50 per page

1 records matched your query of the 36,466,594 in the data limits you selected.

<b>Organizations-Enhanced</b> ◀
<b>Funding Agencies</b> ◀
<b>Languages</b> ◀
<b>Countries/Territories</b> ◀
<b>ESI Top Papers</b> ◀
<b>Open Access</b> ◀
<i>For advanced refine options, use</i> <a href="#">Analyze Results</a>



Република Србија  
МИНИСТАРСТВО ПРОСВЕТЕ  
И НАУКЕ  
Комисија за стицање научних звања

Број:06-00-75/833  
18.07.2012. године  
Београд

МИНИСТАРСТВО ПРОСВЕТЕ И НАУКЕ			
С. 24-08-2012			
Рад. д.	број	датум	прилог
06/1	1034/1		

На основу члана 22. става 2. члана 70. став 5. Закона о научноистраживачкој делатности ("Службени гласник Републике Србије", број 110/05 и 50/06 – исправка и 18/10), члана 2. става 1. и 2. тачке 1 – 4.(прилози) и члана 38. Правилника о поступку и начину вредновања и квантитативном исказивању научноистраживачких резултата истраживача ("Службени гласник Републике Србије", број 38/08) и захтева који је поднео

*Инстџиџуџ за физику у Београду*

Комисија за стицање научних звања на седници одржаној 18.07.2012. године, донела је

**ОДЛУКУ  
О СТИЦАЊУ НАУЧНОГ ЗВАЊА**

*Др Ивана Видановић*

стиче научно звање  
*Научни сарадник*

у области природно-математичких наука - физика

**О Б Р А З Л О Ж Е Њ Е**

*Инстџиџуџ за физику у Београду*

утврдио је предлог број 376/1 од 03.04.2012. године на седници научног већа Института и поднео захтев Комисији за стицање научних звања број 448/1 од 20.04.2012. године за доношење одлуке о испуњености услова за стицање научног звања *Научни сарадник*.

Комисија за стицање научних звања је по предходно прибављеном позитивном мишљењу Матичног научног одбора за физику на седници одржаној 18.07.2012. године разматрала захтев и утврдила да именована испуњава услове из члана 70. став 5. Закона о научноистраживачкој делатности ("Службени гласник Републике Србије", број 110/05 и 50/06 – исправка и 18/10), члана 2. става 1. и 2. тачке 1 – 4.(прилози) и члана 38. Правилника о поступку и начину вредновања и квантитативном исказивању научноистраживачких резултата истраживача ("Службени гласник Републике Србије", број 38/08) за стицање научног звања *Научни сарадник*, па је одлучила као у изреци ове одлуке.

Доношењем ове одлуке именована стиче сва права која јој на основу ње по закону припадају.

Одлуку доставити подносиоцу захтева, именованој и архиви Министарства просвете и науке у Београду.

**ПРЕДСЕДНИК КОМИСИЈЕ**

др Станислава Стошић-Грујичић,  
научни саветник

*С. Станислава Стошић-Грујичић*

**МИНИСТАР**  
Проф. др Жарко Обрадовић  
*Жарко Обрадовић*



## Institut za fiziku u Beogradu

Na osnovu obrazloženog predloga Naučnog saveta dodeljuje

# STUDENTSKU NAGRADU INSTITUTA ZA FIZIKU ZA 2012. GODINU

**dr Ivani Vidanović**

za istraživački rad vezan za numeričke studije kvantnih gasova na niskim temperaturama i rezultujuću doktorsku tezu istog naziva

A handwritten signature in blue ink that reads 'B. Marinković'.

dr Bratislav Marinković  
predsednik  
Naučnog saveta



Beograd  
8. maj 2012.

A handwritten signature in blue ink that reads 'Aleksandar Belić'.

dr Aleksandar Belić  
direktor  
Instituta za fiziku



## ПОТВРДА О МЕНТОРСТВУ

Овим потврђујем да је научни сарадник **др Ивана Васић**, за коју се покреће избор у звање виши научни сарадник, у оквиру Лабораторије за примену рачунара у науци Националног центра изузетних вредности за изучавање комплексних система Института за физику у Београду, односно у оквиру пројекта ОН171017 „Моделирање и нумеричке симулације сложених вишечестичних система“, ментор за докторску тезу Ане Худомал, која је студент докторских студија на Физичком факултету Универзитета у Београду, и чија израда докторске тезе је у току.

Ана Худомал је од октобра 2015. године ангажована у нашој Лабораторији, када је и уписала докторске студије. На пројекту ОН171017 је запослена од марта 2016. године. Од октобра 2015. године њеним научним радом руководи др Ивана Васић, која је на Физичком факултету Универзитета у Београду пријављена за ментора приликом уписа докторских студија. Поред тога, Ана Худомал је ангажована на два билатерална пројекта, са Универзитетом у Франкфурту, Немачка и са Универзитетом у Загребу, Хрватска, којима руководи др Ивана Васић.

Београд, 19. јануар 2017. године



др Антун Балаж  
научни саветник

Руководилац пројекта ОН171017

Руководилац Центра за изучавање комплексних  
система Института за физику у Београду

# Collective Excitations in Bose-Einstein Condensates



im Fachbereich Physik der  
Freien Universität Berlin  
eingereichte Dissertation

von

Hamid Jabber Haziran Al-Jibbouri

September 2013



# Acknowledgments

First and foremost, I would like to express my sincere gratitude to my supervisor Priv.-Doz. Dr. Axel Pelster for his supervision and helpful advices throughout the study, as well as his sound mathematical education, his permanent desire to explain and, not at least, his everlasting good mood are a few characteristics, which are of great value for a PhD student. He is always happy to discuss new ideas, and has a wonderful ability of pointing out the important and interesting aspects of a scientific work.

The opportunity to work in the group of Prof. Dr. h.c. mult. Hagen Kleinert has been both an honor and a privilege. His wide interest in physics is responsible for creating an intense interchange of ideas.

Most deeply, I would like to acknowledge the help from my co-advisor, Prof. Dr. Jürgen Bosse. In particular, I would like to mention his critical reading of this manuscript, as well as the support letters for extending the PhD scholarship.

I would also like to express grateful thanks to my collaborators, Dr. Antun Balaž and Dr. Ivana Vidanović from the Scientific Computer Laboratory (SCL) Institute of Physics, University of Belgrade, Serbia for their substantial help and contribution to various numerical aspects of my studies.

I am greatly indebted to Jürgen Dietel, Aristeu Lima, Victor Bezerra, Ednilson Santos, Mohammad Mobarak, Mahmoud Ghabour, Christine Gruber, Javed Akram, and Branko Nikolić. I really would like to thank them.

I would like to acknowledge the financial support from German Academic Exchange Service and Ministry of Higher Education and Scientific Research Iraq (DAAD/MoHESRI). I am specially indebted to Ms. Sandra Wojciechowski for her kind help throughout the period of the DAAD-scholarship. I would like to express my sincere gratitude to the Iraqi cultural attaché in Berlin. I would like to thank, Department of Chemistry, College of Science, Al-Qadisiyah University, Iraq, for all the help they rendered me during my study.

I would like to thank my parents, who have given me more love, support and affection than I ever deserved, I hope this thesis evidences that all these years spent thousands of miles from home have been spent somehow wisely. Most deeply, I am grateful to my dear wife Shurooq. I would like to say that your love makes everything worthwhile.

# Phase transitions of the coherently coupled two-component Bose gas in a 2D Optical Lattice

Master Thesis

Ulrike Bornheimer

Institute for Theoretical Physics  
Goethe University of Frankfurt am Main  
December 2014



first advisor and referee: Prof. Dr. W. Hofstetter

second referee: Prof. Dr. P. Kopietz

second advisor: Dr. I. Vasić

# Acknowledgements

First and foremost, I thank Professor Hofstetter for giving me the opportunity to complete my Bachelor's and my Master's thesis in his group at Goethe university Frankfurt am Main and thus in the inspiring field of cold atoms. I highly appreciate the support he gave me, both for the theses I worked on in his group and for general issues concerning institute, university and career. I also value the effort he puts into his lectures, which also motivated me for his research field.

Furthermore, I thank the whole quantum matter theory group for lively discussions, generous help - especially in proof reading - and nourishing Thai days. Special thanks are given to Ivana Vasić, who supervised the present thesis. I thank her for good ideas, long hours of bug search and very detailed comments on the content of this thesis. More thanks are given to Agnieszka Cichy and Ulf Bissbort in that respect.

In my time at the department of physics at the Goethe university I was able to enjoy numerous valuable and inspiring lectures and to participate as a tutor later. Next to Professor Hofstetter, I thank Professor Valenti, Professor Rezzolla, Professor Maruhn, Professor Rischke, Professor Reifarh and Professor Kopietz for their dedication. I also thank Professor Kopietz for the grading of this thesis.

Moreover, I thank all my friends for their time, their affection and their encouragement. I am especially happy about all the great people, that I was allowed to meet during my time in Frankfurt. I would like to mention the fellow students of my semester Annika, Lisa and Markus, who were great company in lectures and laboratory, the members of the Fachschaft Patricia, Eva, Alex and Gunnar, who I spent long hours of meetings, discussions and conferences with, my housemates Miriam and Diana and finally the great Ultimate Frisbee teams of Eintracht Frankfurt for making me forget all the little problems of everyday life.

Ending this long list of acknowledgements, I want to thank my family Gudrun, Albert, Christian, Helga and Ulf, for being the most loving and supportive family I can imagine. I cannot sufficiently appreciate the possibilities you offered to me, not only with respect to my education.

---

# Phase Diagram of the Bosonic Kane-Mele-Hubbard Model

---

MASTER'S THESIS

*Author:*  
Rajbir-Singh NIRWAN

Institute of Theoretical Physics  
Goethe-University Frankfurt am Main

*First referee and supervisor:*  
Prof. Dr. Walter HOFSTETTER

*Second referee:*  
Prof. Dr. Roser VALENTÍ

*Second supervisor:*  
Dr. Ivana VASIĆ

September 2016



# Transport and Dynamics of Interacting Bosons with Dissipation

Thomas Mertz

Bachelor's Thesis

Institute for Theoretical Physics (ITP)  
Goethe University of Frankfurt am Main

September 2014

First supervisor and first referee: Prof. Dr. Walter Hofstetter  
Second referee: Prof. Dr. Roser Valentí  
Second supervisor: Dr. Ivana Vasić



---

# Superfluid Phases in the Presence of Artificial Gauge Fields

---

BACHELOR'S THESIS

*Author:*  
Rajbir-Singh NIRWAN

Institute of Theoretical Physics  
Goethe-University Frankfurt am Main

*First referee and supervisor:*  
Prof. Dr. Walter HOFSTETTER

*Second referee:*  
Prof. Dr. Roser VALENTÍ

*Second supervisor:*  
Dr. Ivana VASIĆ

October 2014



Република Србија  
МИНИСТАРСТВО ПРОСВЕТЕ,  
НАУКЕ И ТЕХНОЛОШКОГ  
РАЗВОЈА  
Број: 451-03-01038/2015-09/3  
Датум: 27.01.2016.  
Београд, Немањина 22-26

ИНСТИТУТ ЗА ФИЗИКУ			
ПРИМЉЕНО:			
д.в.д.	б.р.ој	Арх.шифра	Прилог
04	177/1	04	02 2016

Институт за физику  
- Ивана Васић -

Прегревица 118  
11 080 Београд

Поштована госпођо Васић,

Обавештавамо Вас да је у оквиру Програма билатералне научне и технолошке сарадње између Министарства просвете, науке и технолошког развоја Републике Србије и Немачке службе за академску размену (ДААД), а на основу спроведених процедура оцене пројеката у обе државе, усвојена листа за финансирање пројеката у двогодишњем периоду са почетком реализације од 1. јануара 2016. године.

Са задовољством Вас обавештавамо да је Ваш пројекат *“Квантне фазе бозонског Кејн-Меле Хабард модела”* одобрен за финансирање.

Желимо да напоменемо да сврха боравка истраживача у Републици Србији, односно Савезној Републици Немачкој, по овом Јавном позиву, треба да допринесе даљем унапређењу сарадње и конституисању пројектног тима, уз учешће младих истраживача, и генерисању новог пројектног предлога којим би се конкурисало у програму HORIZON 2020 или другим програмима са међународним финансирањем.

Захтеви за рефундацију трошкова путовања српских истраживача, односно трошкова боравка немачких истраживача, достављају се на обрасцу који можете преузети на интернет адреси Министарства, у огранку међународна научна сарадња, уз одговарајућу пратећу документацију.

Руководиоци одобрених пројеката за финансирање, дужни су да доставе годишњи и завршни извештај о реализацији пројекта, у року од 15 дана након завршетка пројектне године, односно након завршетка пројекта, у форми која се такође, налази на интернет адреси Министарства. Саставни део извештаја су и прилози који садрже резултате билатералног пројекта: листу учесника заједничке радионице и агенду; радну верзију апстракта пројекта са листом учесника, називом пројекта и називом потенцијалног програма или јавног позива на који се аплицира са овом темом; радну верзију или копију објављеног рада у међународном часопису.

Информација о свим одобреним пројектима објављена је на интернет страници Министарства просвете, науке и технолошког развоја.

Истовремено бих желео да Вам честитам на одобреном пројекту и пожелим успешну реализацију пројектних активности.

С поштовањем,

 **МИНИСТАР**  
*Beđan*  
**Др Срђан Вербић**





Република Србија  
МИНИСТАРСТВО ПРОСВЕТЕ,  
НАУКЕ И ТЕХНОЛОШКОГ РАЗВОЈА

Број: 451-03-40/2016-09/41

Датум: 24.6.2016.

Београд  
Немањина 22-26

ИНСТИТУТ ЗА ФИЗИКУ

ПРИМЉЕНО: 06-07-2016

Рад.јед.	б р о ј	Арх.шифра	Прилог
0801	4195/1		

Институт за физику, Универзитет у Београду  
Др Ивана Васић

Прегревица 118, Земун  
Београд

Поштована госпођо Васић,

Обавештавамо Вас да је на петом заседању Мешовите комисије између Републике Србије и Републике Хрватске, које је одржано у Београду, 22. марта 2016. године, Ваш пројекат „Тополошка својства оптичких и фотонских решетки” одобрен за финансирање у оквиру програма научно-технолошке сарадње између две земље. Информација о свим одобреним пројектима је постављена на интернет презентацији Министарства [www.mprn.gov.rs](http://www.mprn.gov.rs) одмах након одржаног заседања Мешовите комисије у Београду.

Реализација четвртог циклуса билатералних пројеката траје од 1. априла. 2016. до 31. децембра 2017. године и подразумева размену истраживача као што је одобрено на заседању Мешовите комисије.

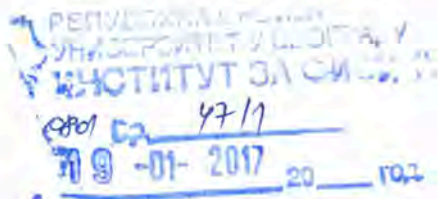
Министарство просвете, науке и технолошког развоја Републике Србије ће суфинансирати путне трошкове истраживача из Србије (без трошкова боравка) као и трошкове боравка истраживача из Хрватске (без путних трошкова) у укупном износу до 1500 евра (у динарској противвредности) по једној години реализације пројекта.

На основу благовремено достављене профактуре за путовање, односно најаве посете хрватских истраживача, потписане од руководиоца пројекта и директора/декана института/факултета, могућа је уплата средстава унапред, у складу са буџетским могућностима и обавезама Министарства. Руководиоци пројеката су дужни да поднесу стручни и финансијски извештај институцијама надлежним за спровођење програма сарадње у својој земљи, по завршетку прве и друге истраживачке године.

Истовремено бих желео да Вам честитам на одобреном пројекту и пожелим успешну реализацију планираних активности.

С поштовањем,





## ПОТВРДА О РУКОВОЂЕЊУ ПОТПРОЈЕКТОМ

Овим потврђујем да научни сарадник **др Ивана Васић** за коју се покреће избор у звање виши научни сарадник, у оквиру Лабораторије за примену рачунара у науци Националног центра изузетних вредности за изучавање комплексних система Института за физику у Београду, односно у оквиру пројекта ОН171017 „Моделирање и нумеричке симулације сложених вишечестичних система“ руководи потпројектом: „Ефикасно израчунавање функционалних интеграла са применом на ултра-хладне квантне гасове“. На поменутом потпројекту су ангажовани следећи истраживачи: др Ивана Васић, др Антун Балаж, др Александар Белић, др Александар Богојевић, Владимир Вељић, Душан Вудраговић, Владимир Лончар, Владимир Славнић и Ана Худомал.

Београд, 19. јануар 2017. године

др Антун Балаж  
научни саветник

Руководилац пројекта ОН171017  
Руководилац Центра за изучавање комплексних  
система Института за физику у Београду

## DFG-Research Unit 801 | DFG-Forschergruppe 801

### Welcome to the DFG-Research Unit 801 Strong Correlations in Multiflavor Ultracold Quantum Gases

Strong correlations have been studied for many decades, particularly in condensed matter and nuclear physics. They play a crucial role in understanding complex phenomena like superconductivity, metal-insulator transitions or the excitation spectra of nuclei. Building on the achievement of Bose-Einstein-Condensation (BEC) and degenerate Fermi gases in ultracold atomic vapors, strong correlation phenomena have recently been shown to appear even in such dilute gases. This has opened a new chapter in atomic and molecular physics, where interactions rather than single particle physics are at center stage.

Two of the major tools which allow to enter the regime of strong correlations in cold gases are optical lattices and Feshbach resonances. Together they allow for an almost perfect tunability of the effective interaction strength, providing an ideal realization of most of the basic models in many body physics. Prominent examples are Bosons on an optical lattice or attractive Fermions near a Feshbach resonance. They exhibit a superfluid-insulator transition or an intermediate regime between a BCS- and a BEC-type superfluid, phenomena which have never before been accessible in condensed matter physics. Here we propose to study strong correlations in cold gases with internal (spinor) degrees of freedom, in mixtures of Bose and Fermi gases and in degenerate gases subject to static disorder potentials. These systems have hardly been explored so far and are expected to display a number of complex phenomena, which are among the most challenging and still poorly understood problems in many body physics.

The experimental groups in Hamburg, Mainz and Munich will realize and investigate degenerate gases, in particular spinor gases and Bose-Fermi and Fermi-Fermi mixtures, both with and without optical lattices. Using two component systems allows realizing static short-range potentials for one of the components. In a coordinated effort, the theoretical description will be provided by the theory groups in Aachen, Frankfurt and Munich, using both analytical and numerical techniques. The close collaboration between theory and experiment offers a unique possibility to explore fundamental issues in many body physics, like the competition between Anderson- and Mott-insulating phases in perfectly well defined and tunable systems.

### Events

---

no news in this list.

### Contact

---

#### **Ludwig-Maximilians- University**

Quantum Optics Chair/  
Fakultät für Physik

[✉ Prof. Immanuel Bloch](mailto:immanuel.bloch@lmu-munich.de)

Schellingstr. 4  
80799 Munich, Germany

Phone: +49 (0)89 2180 - 6130

Fax: +49 (0)89 2180 - 63851

## DFG-Research Unit 801 | DFG-Forschergruppe 801

### Dr. Ivana Vidanovic

#### **Sub-Project T2**

[Disorder versus Interaction in Ultracold Atom Systems](#)

#### **Universität Frankfurt/Institut für Theoretische Physik**

Room: 01.136

Max-von-Laue-Str. 1

60438 Frankfurt/Main

Phone: +49 (0)69 798 47822

Fax: +49 (0)69 798 47881

✉ [vidanovic\(at\)itp.uni-frankfurt.de](mailto:vidanovic(at)itp.uni-frankfurt.de)

▶ [back](#)





Türk Fizik Derneđi  
1950  
Turkish Physical Society

**Turkish Physical Society**  
**32nd International Physics Congress**

**6-9 September 2016**  
**Bodrum - TURKEY**

**Dr. Ivana Vasic**  
**Institute of Physics Belgrade**  
**Serbia**

17/03/2016

**Dear Dr. Ivana Vasic,**

Turkish Physical Society, is greatly honoured that you have accepted our invitation to be a member of the Organizing Committee at the “**Turkish Physical Society 32<sup>nd</sup> International Physics Congress – TPS32**” which will be organized by Turkish Physical Society and hosted by Bodrum Municipality in Bodrum / Muđla between **September 06 – 09, 2016**.

Please do not hesitate to contact Organizing Committee of the Congress by [tfd@turkfizikdernegi.org](mailto:tfd@turkfizikdernegi.org) e-mail address.

We are looking forward to seeing you in Bodrum.  
Yours sincerely,

Prof. Dr. Baki AKKUŞ  
President of TPS-32 Organizing Committee

**Subject** Referee update Vasic (Vidanovic) 824617  
**From** <office@aps.org>  
**To** <ivana.vasic@ipb.ac.rs>  
**Date** 2016-09-15 10:04



---

Dr. Ivana Vasic (Vidanovic)  
Scientific Computing Laboratory  
Institute of Physics Belgrade  
Pregrevica 118  
11080 Belgrade  
SERBIA  
[ivana.vasic@ipb.ac.rs](mailto:ivana.vasic@ipb.ac.rs)

Dear Dr. Vasic (Vidanovic),

Thank you for your help as a referee for the Physical Review journals and Reviews of Modern Physics. We understand that your time is valuable and have therefore made your record available via our referee server (<https://referees.aps.org/>) so that you can make changes quickly and easily at any time.

We recognize that your availability to review manuscripts may fluctuate throughout the year and suggest that you visit this site whenever necessary to update your relevant information. Please be reminded that to access our referee server you will need to have an active APS Journal account. For more information and to create an account please go to <https://journals.aps.org/signup>.

Providing us with up to date and accurate information helps the refereeing process run smoothly and ensures that we only ask you to review appropriate material, when you are able to, and that we do not contact you unnecessarily.

Thank you for your assistance.

Sincerely,

Pierre Meystre  
Editor in Chief  
American Physical Society

**Subject** Invitation to a Workshop in Zagreb  
**From** Hrvoje Buljan <hbuljan@phy.hr>  
**To** <ivanavi@ipb.ac.rs>  
**Cc** <hbuljan@phy.hr>  
**Reply-To** <hbuljan@phy.hr>  
**Date** 2015-06-18 22:33  
**Priority** Normal



---

Dear Dr. Ivana Vasić,

Prof. Moti Segev and I are putting together a workshop titled "Topological effects and synthetic gauge/magnetic fields for atoms and photons", please see [synthetic.ifs.hr](http://synthetic.ifs.hr)

We would like to cordially invite you to present an invited talk at the workshop, and we hope that you will be able to accept this invitation.

Time: 29 September - October 1, 2015

Venue: Zagreb, Croatia.

Zagreb is the Capital of Croatia easy to reach from many European destinations. The charms of Zagreb have been recognized by ever increasing number of visitors: the al fresco cafe tables, the classic Austro-Hungarian architecture, the rows of fashionable boutiques and bars, restaurants, and lively night life. Before/after the workshop we suggest visiting the unspoiled natural beauty of Plitvice Lakes National Park ( <http://www.np-plitvicka-jezera.hr/en/> , just two hour drive ) or the Adriatic Sea. In fact if there will be interest we will organize an excursion with hiking or swimming after the workshop.

Topics:

Synthetic gauge fields / synthetic magnetism, topological phases and topological effects, physics of the Hall effect, topologically protected edge states, have been of great interest to the communities in optics and photonics and ultracold atomic gases. A flurry of papers is being published in most prestigious journals on these topics. However, we believe that both communities could benefit by having stronger links in understanding the methods from the other side, experimental difficulties, new possibilities and ideas. This workshop is intended to bring together a few most distinguished scientists and interested young scientists together to discuss these topics. We aim at having 50-70 people in the workshop.

Funding:

As an invited speaker you will not have to pay for the conference fee, and we will provide accommodation for you.

In the name of the organizing committee,  
Hrvoje Buljan

Organized by:



Department of Physics  
Faculty of Science,  
University of Zagreb

UNITY THROUGH  
KNOWLEDGE FUND



Institute of Physics,  
Zagreb

INSTITUT ZA FIZIKU

29 September – 1 October 2015

Zagreb, Croatia

Topological effects and synthetic gauge/magnetic fields for atoms and photons

**Invited speakers:**

Demetrios Christodoulides  
Klaus Sengstock  
Gennady Shvets  
Michael Fleischhauer  
Francesca Ferlino  
Gediminas Juzeliunas  
Fabrice Gerbier  
Alex Szameit  
Darrick Chang  
Mikael Rechtsman  
Zhigang Chen  
Thomas Pohl  
Marcello Dalmonte  
Thomas Gasenzer  
Netanel Lindner  
Giorgos Tsironis  
Ivana Vasić  
Gregor Jotzu

**Scientific organizing committee:**

Hrvoje Buljan  
Mordechai Segev  
Marin Soljačić

**Local organizing committee:**

Hrvoje Buljan  
Ticijana Ban  
Damir Aumiler  
Robert Pezer  
Karlo Lelas  
Neven Šantić  
Tena Dubček

*synthF*  
Zagreb

[synthetic.ifs.hr](http://synthetic.ifs.hr)





# Bosonic Phases On The Haldane Honeycomb Lattice

Vasić, I (1); Petrescu, A (2,3); Le Hur, K (2); Hofstetter, W (4);

Contact: ivana.vasic@ipb.ac.rs

(1) *Scientific Computing Laboratory, Institute of Physics Belgrade, University of Belgrade, Belgrade, Serbia*

(2) *Centre de Physique Theorique, Ecole Polytechnique, CNRS, 91128 Palaiseau Cedex, France*

(3) *Department of Physics, Yale University, New Haven, Connecticut 06520, USA*

(4) *Institute of Theoretical Physics, Goethe University, Frankfurt/Main, Germany*

Recent experiments [1] in ultracold atoms have reported the implementation of artificial gauge fields in lattice systems. Motivated by such advances, we investigate the Haldane honeycomb lattice tight-binding model [2], for bosons with local interactions at the average filling of one boson per site. We analyze the ground state phase diagram and uncover three distinct phases: a uniform superfluid, a chiral superfluid and a plaquette Mott insulator with local current loops. Nearest-neighbor and next-nearest neighbor currents distinguish CSF from SF, and the phase transition between them is first order. We apply bosonic dynamical mean field theory and exact diagonalization to obtain the phase diagram, complementing numerics with calculations of excitation spectra in strong and weak coupling perturbation theory. The characteristic density fluctuations and excitation spectra can be probed in future experiments.

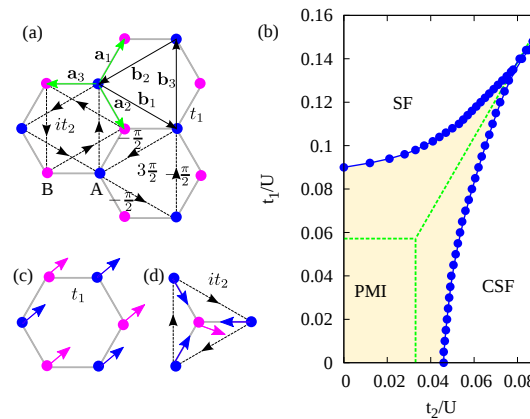


Figure 2.2: a) Lattice vectors and hopping integrals of the Haldane model. b) Phase diagram of the model at unit filling, containing plaquette Mott insulator (PMI), uniform superfluid (SF) and chiral superfluid (CSF) phases. c) Local condensate order parameter in the uniform superfluid; d) In CSF the condensate order parameters on sublattices A and B are determined up to a relative phase.

## References

- [1] G. Jotzu, M. Messer, R. Desbuquois, M. Lebrat, T. Uehlinger, D. Greif, T. Esslinger, *Nature (London)* **515**, 237 (2014).
- [2] I. Vasić, A. Petrescu, K. Le Hur, W. Hofstetter, *Phys. Rev. B* **91**, 094502 (2015).

**Subject** Invitation from SFKM 2015  
**From** Leonardo Golubovic <Leonardo.Golubovic@mail.wvu.edu>  
**To** ivana.vidanovic@scl.rs <ivana.vidanovic@scl.rs>  
**Date** 2015-01-16 07:41



Faculty of Physics University of Belgrade  
Institute of Physics Belgrade  
Institute for Nuclear Sciences "Vinca" Belgrade  
Serbian Academy of Sciences and Arts

**Dr. Ivana Vasic**  
Scientific Computing Laboratory  
Institute of Physics Belgrade  
Pregrevica 118  
11080 Belgrade, Serbia

Dear Dr. Vasic,

On behalf of the Organizing and Program Committees and my own, it is my privilege and pleasure to offer you to give an invited talk at the **19th Symposium on Condensed Matter Physics - SFKM 2015**, to be held in Belgrade, Serbia, September 7-11, 2015.

We are hoping that you can accept the invitation and are looking forward to your response. More information about the conference can be found posted at <http://www.sfkm.ac.rs>

We would be very grateful if you could send us a tentative title or subject of your talk at your earliest convenience, as this would be very helpful for our planning the conference sessions.

We are looking forward to meeting you in Belgrade in September.

Sincerely yours,

SFKM 2015 Chair  
Prof. Leonardo Golubovic  
West Virginia University, USA

XIX Symposium on  
Condensed Matter Physics  
SFKM 2015

---

**Book of Abstracts**

---



# Bosonic Phases On The Haldane Honeycomb Lattice

I. Vasić<sup>a</sup>, A. Petrescu<sup>bc</sup>, K. Le Hur<sup>b</sup> and W. Hofstetter<sup>d</sup>

<sup>a</sup>Scientific Computing Laboratory, Institute of Physics, University of Belgrade, Belgrade, Serbia

<sup>b</sup>Centre de Physique Theorique, Ecole Polytechnique, CNRS, 91128 Palaiseau Cedex, France

<sup>c</sup>Department of Physics, Yale University, New Haven, Connecticut 06520, USA

<sup>d</sup>Institute of Theoretical Physics, Goethe University, Frankfurt/Main, Germany

**Abstract.** Recent experiments [1] in ultracold atoms have reported the implementation of artificial gauge fields in lattice systems. Motivated by such advances, we investigate the Haldane honeycomb lattice tight-binding model [2], for bosons with local interactions at the average filling of one boson per site. We analyze the ground state phase diagram and uncover three distinct phases: a uniform superfluid, a chiral superfluid and a plaquette Mott insulator with local current loops. We apply bosonic dynamical mean field theory and exact diagonalization to obtain the phase diagram, complementing numerics with calculations of excitation spectra in strong and weak coupling perturbation theory. The characteristic density fluctuations and excitation spectra can be probed in future experiments.

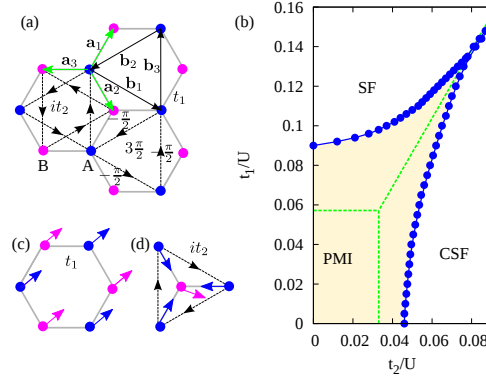


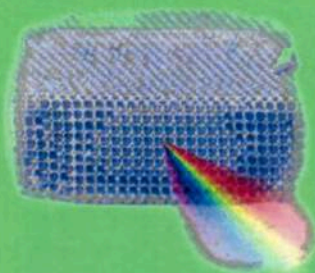
**FIGURE 1.** a) Lattice vectors and hopping integrals the Haldane model. b) Phase diagram of the model at unit filling, containing plaquette Mott insulator (PMI), uniform superfluid (SF) and chiral superfluid (CSF) phases. c) Local condensate order parameter in the uniform superfluid; d) In CSF the condensate order parameters on sublattices A and B are determined up to a relative phase.

## REFERENCES

1. Jotzu, G., Messer, M., Desbuquois, R., Lebrat, M., Uehlinger, T., Greif, D., and Esslinger, T., *Nature (London)* **515**, 237-240 (2014).
2. Haldane, F. D. M., *Phys. Rev. Lett.* **61**, 2015 (1988).
3. Vasić, I., Petrescu, A., Le Hur, K., and Hofstetter, W., *Phys. Rev. B* **91**, 094502 (2015).

UNIVERZITET U BEOGRADU

Institut za fiziku



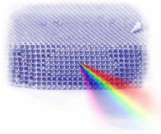
Konferencija

# Osma radionica fotonike (2015)

Zbornik apstrakata



Kopaonik, 8.–12. marta 2015.



## RADIONICA FOTONIKE

8. radionica: Kopaonik, 8–12. 3. 2015.

Naslovna stranica

Program

Teme

Predavanja

Arhiva

Mesto

Smeštaj

O prijavljivanju

Prijava i pristup

Apstrakti

Odbori

Druženje

Doprinos

Kontakt

Ostale radionice

IF

INN "Vinča"

FF

ETF

IHTM

Photonica09

Photonica 2011  
Photonica 2011 - III  
International School and  
Conference on Photonics

IFS

Optela

MNP

Facebook

Predavanja >>

Pošalji link prijatelju

2015-03-05

### Predavači

Specijalno i uvodna predavanja.

### Posebna prezentacija / *Special presentation*

- **Ljupčo Hadžievski**
  - *International year of light 2015*

### Uvodna predavanja / *Introductory lectures*

- **Pavle Andjus**
  - *Distribution of mutant SOD1 in reactive glial cells on the ALS animal model - 3D analysis of confocal images with IMARIS*
- **Srdjan Antić (USA)**
  - *Branch Specific and Spike-order Specific Action Potential Invasion in Basal, Oblique and Apical Dendrites of Cortical Pyramidal Neurons*
- **Marios Barberoglou (Greece)**
  - *Femtosecond laser micro/nano structuring of solid surfaces: fundamentals and applications*
- **Francesco Saverio Cataliotti (Italia)**
  - *Atom-Chip for Quantum Control*
- **Miroslav Dramićanin**
  - *Luminescence of rare earth and transition metal doped titanates*
- **Torsten Goltz (Germany)**
  - *Electro-Optical Sampling of THz packets: from THz spectroscopy to THz control*
- **Zoran Jakšić**
  - *Localized plasmon resonance for photonic infrared detectors*
- **Lars Klimaschewski (Austria)**
  - *Receptor trafficking in human glioma cells - in-depth analysis by fluorescence microscopy*
- **Aleksandar Krmpot**
  - *Multifocal Functional Fluorescence Microscopy Imaging*
- **Ivanka Marković**
  - *The role of alpha-synuclein Parkinson's disease: methods in deciphering molecular mechanisms of neurodegeneration*
- **Dejan Pantelić**
  - *Super-rezoluione fazne tehnike u optičkoj mikroskopiji*
- **Jovana Petrović**
  - *Characterization of Optical Sensors Using Fisher Information*
- **Dragomir Stamenković**
  - *Nanophotonics and the damaging effects of light in ophthalmology*
- **George Tserevelakis (Greece)**
  - *Hybrid multiphoton and optoacoustic label-free microscopy*
- **Ivana Vasić**
  - *Chiral Bosonic Phases on the Haldane Honeycomb Lattice*

2015-03-05

### VAŽNI DATUMI

- Prijava:
  - 29.1.2015.
  - 30.1.2015.
  - 20.2.2015.
- Podnošenje apstrakta:
  - 19.2.2015.
  - 20.2.2015.

### SPONZORI



### ORGANIZATORI



### MREŽE



## Chiral Bosonic Phases on the Haldane Honeycomb Lattice

Ivana Vasic<sup>1</sup>, Alex Petrescu<sup>2</sup>, Karyn Le Hur<sup>3</sup>, Walter Hofstetter<sup>4</sup>

<sup>1</sup>Scientific Computing Laboratory, Institute of Physics, Pregrevica 118, 11080 Belgrade, Serbia

<sup>2</sup>Department of Physics, Yale University, New Haven CT 06520, USA

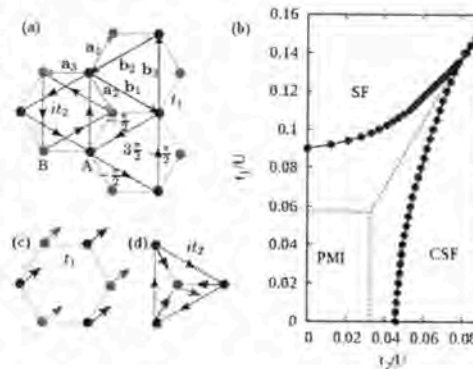
<sup>3</sup>Centre de Physique Theorique, Ecole Polytechnique, CNRS, 91128 Palaiseau Cedex, France

<sup>4</sup>ITP, Goethe University, 60438 Frankfurt/Main, Germany

Contact: I. Vasic (ivanavi@ipb.ac.rs)

**Abstract.** Recent experiments in ultracold atoms [1] and photonic analogs have reported the implementation of artificial gauge fields in lattice systems, facilitating the realization of topological phases. Motivated by such advances, we investigate the Haldane honeycomb lattice tight-binding model, for bosons with local interactions at the average filling of one boson per site [2]. We analyze the ground state phase diagram and uncover three distinct phases: a uniform superfluid *SF*, a chiral superfluid *CSF* and a plaquette Mott insulator with local current loops *PMI*. Nearest-neighbor and next-nearest neighbor currents distinguish *CSF* from *SF*, and the phase transition between them is first order. We apply bosonic dynamical mean field theory and exact diagonalization to obtain the phase diagram, complementing numerics with calculations of excitation spectra in strong and weak coupling perturbation theory. The characteristic density fluctuations, current correlation functions, and excitation spectra are measurable in ultracold atom experiments

Figure 1. **a)** Lattice vectors on the honeycomb lattice and hopping integrals the Haldane model. **b)** Phase diagram of the model at unit filling, containing plaquette Mott insulator (*PMI*), uniform superfluid (*SF*) and chiral superfluid (*CSF*) phases. Solid (dashed) lines represent DMFT (Gutzwiller mean-field) results. **c)** Local condensate order parameter in the uniform superfluid; **d)** In *CSF* the condensate order parameters on sublattices A and B are determined up to a relative phase.



### REFERENCES

- [1] G. Jotzu, M. Messer, R. Desbuquois, M. Lebrat, T. Uehlinger, D. Greif, and T. Esslinger, *Nature* (London) **515** (2014), 237.
- [2] I. Vasic, A. Petrescu, K. Le Hur, W. Hofstetter, arXiv: 1408.1411

# 7<sup>th</sup> Annual Retreat of the SFB/TR 49, Bensheim, September 19 – 20, 2013

## Programme

### Thursday, September 19, 2013

<b>1. Ultracold Gases &amp; Cold Ion Crystals</b>		A. Widera / H. Ott
09:15 (5)	Michael Lang	<i>Welcome</i>
09:20 (12+8)	Ivana Vidanovic (A3)	<i>Dissipation induced bosonic dynamics an hybrid quantum simulations</i>
09:40 (12+8)	Michael Fleischhauer (A5)	<i>Adiabatic preparation of Wigner crystals of photons in Rydberg gases</i>
10:00 (12+8)	Elena Gorelik (A6)	<i>Quantum magnetism of ultracold fermions on optical lattices with novel geometries</i>
10:20 (12+8)	Herwig Ott (A9)	<i>Strong interactions in mesoscopic Rydberg gases</i>
10:40 (20)	<b>Coffee Break</b>	
11:00 (12+8)	René Gerritsma (A10)	<i>Quantum simulations with atoms and ions</i>
11:20 (12+8)	Nicholas Sedlmayr (A11)	<i>When is a bath a bath? Relaxation dynamics and thermalization in a fermionic chain</i>
11:40 (12+8)	Artur Widera (A12)	<i>Polarons in cold bosonic gases</i>
12:00 (60)	<b>Lunch</b>	

<b>2. Quantum Spin Systems</b>		J. Sirker / S. Eggert
13:00 (12+8)	Ulrich Tutsch (B1)	<i>Field-induced Berezinskii-Kosterlitz-Thouless scenario in a 2-dimensional spin-dimer system</i>
13:20 (12+8)	Harald Jeschke (B2)	<i>Spin liquid systems herbertsmithite and <math>\text{EtMe}_3\text{Sb}[\text{Pd}(\text{dmit})_2]_2</math>: Detailed investigation of the underlying Hamiltonians</i>
13:40 (12+8)	Sebastian Eggert (B3)	<i>Spin liquid versus dimer phases in an anisotropic <math>J_1</math>-<math>J_2</math> frustrated square antiferromagnet</i>
14:00 (12+8)	Natalija van Well (B4)	<i>Single crystal growth of tunable quantum critical materials</i>
14:20 (9+6)	Prince Ravat (B5)	<i>Tuning the Magnetic Exchange Interaction in Antiferromagnetically Coupled Biradicals</i>
14:35 (10)	<b>Break</b>	





## Topological $d$ -wave pairing structures in Jain states

N. Moran,<sup>1</sup> A. Sterdyniak,<sup>1</sup> I. Vidanović,<sup>2</sup> N. Regnault,<sup>1,3</sup> and M. V. Milovanović<sup>2</sup>

<sup>1</sup>*Laboratoire Pierre Aigrain, ENS and CNRS, 24 Rue Lhomond, 75005 Paris, France*

<sup>2</sup>*Scientific Computing Laboratory, Institute of Physics Belgrade, University of Belgrade, Pregrevica 118, 11 080 Belgrade, Serbia*

<sup>3</sup>*Department of Physics, Princeton University, Princeton, New Jersey 08544, USA*

(Received 17 May 2012; revised manuscript received 30 May 2012; published 13 June 2012)

We discuss  $d$ -wave topological (broken time-reversal symmetry) pairing structures in unpolarized and polarized Jain states. We demonstrate pairing in the Jain spin-singlet state by rewriting it in an explicit pairing form, in which we can recognize  $d$ -wave weak pairing of underlying quasiparticles—composite fermions. We find and describe the root configuration of the Jain spin-singlet state and its connection with neutral excitations of the Haldane-Rezayi state, and study the transition between these states via exact diagonalization. We find high overlaps with the Jain spin-singlet state upon a departure from the hollow-core model for which the Haldane-Rezayi state is the exact ground state. Due to a proven algebraic identity we are able to extend the analysis of topological  $d$ -wave pairing structures to polarized Jain states and integer quantum Hall states and discuss its consequences.

DOI: [10.1103/PhysRevB.85.245307](https://doi.org/10.1103/PhysRevB.85.245307)

PACS number(s): 05.30.Pr, 73.43.–f

### I. INTRODUCTION

Fractional quantum Hall (FQH) states are strongly correlated many-body states which in certain cases have an effective description in terms of weakly interacting quasiparticles. An important example is the Jain states<sup>1</sup> which are composed of weakly interacting composite fermion quasiparticles, which themselves form underlying integer quantum Hall (IQH) states. In other important examples these underlying states of quasiparticles may be superconducting with broken time-reversal symmetry, as in the famous Pfaffian (Moore-Read) state<sup>2</sup> with  $p$ -wave superconducting pairing of composite fermion quasiparticles. The paired states in the FQH effect (FQHE) are often discussed in connection with systems with extra degrees of freedom such as spin. The first paired state proposed was the spin-singlet  $d$ -wave Haldane-Rezayi (HR) state.<sup>3</sup> It has served as inspiration and as a prototype for other paired states, despite initial confusion about its compressibility. Initially it was believed to be an incompressible state—a spin-singlet state at filling factor  $1/2$ . However, in Ref. 4 the HR state was identified as a critical (gapless) state of a  $d$ -wave superconductor with broken time reversal symmetry. In the same reference it was shown that the gapped phase that is on the weak-pairing side of the transition for which the HR state is critical possesses some universal properties of the Jain spin-singlet (JSS) state at half filling.<sup>5</sup> Therefore the JSS state may represent a weakly paired  $d$ -wave topological superconductor of composite fermion quasiparticles and may be related to the gapless HR  $d$ -wave state. On the other hand, recent developments in the theory of the FQHE have demonstrated exceptional similarities between polarized Jain states and a nonunitary series of states [connected with nonunitary conformal field theories (CFTs)] with gapless behavior.<sup>6–10</sup>

In this paper we focus on  $d$ -wave topological pairing structures in unpolarized and polarized Jain states. First we discuss further the connection between the JSS state and topological  $d$ -wave superconductors, and the implied connection between HR and JSS states. Due to an algebraic identity we recover the exact pairing (structure) in the JSS

wave function. The root configuration of the same state is also presented. These results improve our understanding of the role of paired composite fermions in the HR and JSS states, and the transition that is expected to occur between these states. In order to confirm its existence in the presence of specific interactions we study this transition by way of exact diagonalization. Due to the spin degree of freedom our studies are limited in the system sizes treated compared to studies without spin. In the systems we could treat we demonstrate high overlaps with the JSS state upon departing from the pure hollow-core model for which the HR state is the exact ground state. Due to the proven identity we are able to show that the pairing structures also exist even in polarized Jain states, as a consequence of the underlying multicomponent nature of the FQH states. Furthermore, we demonstrate a connection, based on the proven identity, between the IQH states with Chern number equal to 2 (Refs. 11–13) and the  $d$ -wave superconducting states with broken time-reversal symmetry. This connection is enabled by the extremely weak pairing in the  $d$ -wave superconductor. We will discuss the connection on the level of many-body wave functions; it was introduced previously on the level of Hamiltonians by Laughlin in Ref. 14.

The paper is organized as follows: Sec. II introduces the HR and JSS model wave functions and reviews their most relevant properties, Sec. III shows how to see hidden pairing structure in the JSS state, Sec. IV discusses the HR and JSS states in terms of their root partitions, Sec. V presents results from numerical calculations, Sec. VI extends the pairing structure arguments to the spin-polarized case, and finally Sec. VII presents conclusions.

### II. MODEL WAVE FUNCTIONS

To understand better the topological nature of Jain states and their relationship to the nonunitary states, we will first discuss the JSS state and the related HR state. The JSS state at  $\nu = \frac{1}{2}$  is defined as

$$\Psi_{\text{JSS}} = \mathcal{P}_{\text{LLL}}(\chi_2 \chi_{110} \chi_1) \quad (1)$$

in the usual Jain notation.  $\mathcal{P}_{\text{LLL}}$  is the projector operator to the lowest Landau level (LLL).  $\chi_2$  denotes the wave function of two filled Landau levels (LLs) of all particles. As shown in Ref. 15, in a condensed form  $\chi_2$  can be expressed as

$$\chi_2 = \mathcal{A} \left\{ \prod_{i=1}^M z_i^* \times \prod_{i < j; i, j \leq M} (z_i - z_j) \times \prod_{k < l; M < k, l \leq N} (z_k - z_l) \right\}, \quad (2)$$

where  $N$ , the total number of particles, is assumed even, and  $M = N/2$ .  $\mathcal{A}$  denotes the antisymmetrization operator over the  $N$  particles. Here and below we suppress the omnipresent Gaussian factors, characteristic of the disk geometry. In this section we look for long-distance properties of wave functions, and use the expression (2) or (7) below.  $\chi_1$  denotes the wave function of the filled LLL of all particles,

$$\chi_1 = \prod_{i < j}^N (z_i - z_j), \quad (3)$$

and  $\chi_{110}$  denotes the wave function with Jastrow-Laughlin factors only between particles with the same spin,

$$\chi_{110} = \prod_{i < j}^{\frac{N}{2}} (z_i^\uparrow - z_j^\uparrow) \prod_{i < j}^{\frac{N}{2}} (z_i^\downarrow - z_j^\downarrow), \quad (4)$$

where  $z_i^\uparrow$  ( $z_i^\downarrow$ ) are the positions of the particles with spin up (down). Where no spin index is given, the product is over all particles irrespective of spin.

The HR state<sup>3</sup> is a fermionic spin-singlet state defined as

$$\Psi_{\text{HR}} = \det \left( \frac{1}{(z_i^\uparrow - z_j^\downarrow)^2} \right) \prod_{i < j} (z_i - z_j)^2. \quad (5)$$

This state is the unique densest zero-energy ground state of a hollow-core two-body interaction Hamiltonian. Two-body interaction Hamiltonians can be expressed in terms of the Haldane pseudopotential coefficients<sup>16</sup>  $V_m$  as

$$H = \sum_{m \geq 0} \left( V_m \sum_{i < j} \mathcal{P}_{ij}^{(m)} \right), \quad (6)$$

where  $V_m$  is the pseudopotential coefficient for relative angular momentum  $m$  and  $\mathcal{P}_{ij}^{(m)}$  projects a particle pair onto relative angular momentum  $m$ . The hollow-core interaction corresponds to setting the  $V_1$  coefficient to a finite value while the rest are set to zero. For the HR state the counting of zero modes with and without quasiholes can be deduced from a generalized Pauli principle.<sup>17,18</sup>

We will examine in detail the transition induced by changing  $V_0$  (the interaction pseudo-potential for particles with relative angular momentum zero) that is believed to represent the transition from the HR to the JSS state. We are especially interested in identifying the JSS state and its universal properties on the weak-pairing side of the transition. This will also entail better examination of the JSS state along with its root configuration.

### III. PAIRING STRUCTURE

From the expression for the JSS state in Eq. (1) we will illustrate the basic pairing structure that is hidden in the usual definition of Jain states. We will prove an algebraic identity in this case that directly relates the JSS wave function and the long-distance form of the ground state of a  $d$ -wave topological superconductor in its weak-pairing phase.

The projection to the LLL is made by replacing complex conjugate coordinates  $z_i^*$ ,  $i = 1, \dots, N$ , in the two-LLs-filled wave function  $\chi_2$  with derivatives  $\partial/(\partial z_i)$ ,  $i = 1, \dots, N$ . When attempting to construct this state numerically we found that changing the order of application of the projection operator to reduce the computational complexity is no longer applicable here as it is in the spinless case.<sup>19,20</sup> For further details see the Appendix. We will use expression (2) for  $\chi_2$ , derived in Ref. 15, which assumes even numbers of particles,  $N = 2M$ . It is important to notice that in the equivalent but more common definition of  $\chi_2$ ,

$$\chi_2 = \begin{vmatrix} 1 & \cdots & 1 & \cdots & 1 \\ z_1 & \cdots & z_i & \cdots & z_N \\ z_1^2 & \cdots & z_i^2 & \cdots & z_N^2 \\ \vdots & & \vdots & & \vdots \\ z_1^{M-1} & \cdots & z_i^{M-1} & \cdots & z_N^{M-1} \\ z_1^* & \cdots & z_i^* & \cdots & z_N^* \\ z_1^* z_1 & \cdots & z_i^* z_i & \cdots & z_N^* z_N \\ z_1^* z_1^2 & \cdots & z_i^* z_i^2 & \cdots & z_N^* z_N^2 \\ \vdots & & \vdots & & \vdots \\ z_1^* z_1^{M-1} & \cdots & z_i^* z_i^{M-1} & \cdots & z_N^* z_N^{M-1} \end{vmatrix}, \quad (7)$$

due to the asymmetry of the determinant, any exchange of two particles amounts only to a change of sign as for the wave function of a filled LLL, expression (3). If we use these expressions for two groups of particles as in the case of states with spin assignment, which particles are up or down becomes irrelevant (as far as the correlations are concerned), as these expressions have equal correlations for up-up, down-down, and up-down correlators. It is important to notice that spin is not fixed in a given LL [in  $\chi_2$  in the definition, expression (2) or (7)], and each LL may contain any distribution of up and down spins. In the following we will extract (under derivatives due to the LLL projection) from each term in  $\chi_2$  the correlator that is between the two definite groups with the same numbers of particles equal to  $M$ ; the first group will be among particles to which we assign spin up and the second group will be among particles with spin down. Therefore we have

$$\Psi_{\text{JSS}} = \mathcal{A} \left[ \partial_{z_1} \cdots \partial_{z_M} \times \frac{\prod_{i < j; i, j \leq M} (z_i - z_j) \prod_{k < l; M < k, l \leq N} (z_k - z_l)}{\prod_{p, q} (z_{p\uparrow} - z_{q\downarrow})} \times \prod_{p, q} (z_{p\uparrow} - z_{q\downarrow}) \right] \chi_{110} \chi_1. \quad (8)$$

Only if the division into two groups under  $\mathcal{A}$  coincides with division between up and down particles can we use the Cauchy identity

$$\frac{\prod_{i < j} (z_{i\uparrow} - z_{j\uparrow}) \prod_{l < m} (z_{l\downarrow} - z_{m\downarrow})}{\prod_{p,q} (z_{p\uparrow} - z_{q\downarrow})} = \det \left( \frac{1}{z_{p\uparrow} - z_{q\downarrow}} \right),$$

where the resulting determinant has antisymmetry among same-spin particles. This gives us a clue about what the expression in the square brackets in Eq. (8),

$$\mathcal{A}[\partial_{z_1} \cdots \partial_{z_M} \frac{\prod_{i < j; i, j \leq M} (z_i - z_j) \prod_{k < l; M < k, l \leq N} (z_k - z_l)}{\prod_{p,q} (z_{p\uparrow} - z_{q\downarrow})}], \quad (9)$$

should be.

The expression

(a) should not carry macroscopic flux (the filling factor is determined by  $[\prod_{p,q} (z_{p\uparrow} - z_{q\downarrow})] \chi_{110} \chi_1 = \chi_1^2$ ),

(b) should preserve the same total power ( $N/2 = M$ ) of derivatives,

(c) should be antisymmetric under exchange of same-spin particles,

(d) should be invariant under total (when all particles participate) exchange between opposite-spin particles due to the factor  $\prod_{p,q} (z_{p\uparrow} - z_{q\downarrow})$  that already encodes a definite symmetry of  $\chi_2$  under the total exchange equal to the parity of  $M^2$ , i.e.,  $(-1)^{M^2} = (-1)^M$  between opposite-spin particles,

(f) and should be invariant under translation (as  $\chi_2$  is).

This is achieved by the following pairing function:

$$\Psi_d = \det \left( \frac{z_{p\uparrow}^* - z_{q\downarrow}^*}{z_{p\uparrow} - z_{q\downarrow}} \right), \quad (10)$$

to which the projection to the LLL has to be applied when considering the JSS state.

To see that the function is invariant under any total exchange between up and down particles, we start with a general expression,

$$\Psi = \sum_{p \in \mathcal{S}_M} f_{1,p(2)} \cdots f_{2M-1,p(2M)} \text{sgn}(p), \quad (11)$$

for a pairing function of  $M$  pairs.  $\mathcal{S}_M$  is the symmetric group over a set of  $M$  elements and  $\text{sgn}(p)$  is the signature of the permutation  $p$ . Each pair is invariant under the exchange of its constituents, i.e.,  $f_{i,j} = f_{j,i}$ . Any total exchange between two kinds (even and odd) of particles is defined by a single permutation  $s$  on  $M$  numbers. The transformed wave function  $\mathcal{E}\Psi$  can be expressed as

$$\begin{aligned} \mathcal{E}\Psi &= \sum_p f_{s^{-1}p(2),s(1)} \cdots f_{s^{-1}p(2M),s(2M-1)} \text{sgn}(p) \\ &= \sum_p f_{s(1),s^{-1}p(2)} \cdots f_{s(2M-1),s^{-1}p(2M)} \text{sgn}(p) \\ &= \sum_p f_{1,s^{-2}p(2)} \cdots f_{2M-1,s^{-2}p(2M)} \text{sgn}(p) \\ &= \sum_\sigma f_{1,\sigma(2)} \cdots f_{2M-1,\sigma(2M)} \text{sgn}(\sigma) = \Psi, \quad (12) \end{aligned}$$

i.e., we have proved that the pairing function is invariant under any total exchange  $\mathcal{E}$  between (ups and downs) even- and odd-number particles.

Thus we have

$$\begin{aligned} \Psi_{\text{JSS}} &= \det \left( \frac{\partial_{z_\uparrow} - \partial_{z_\downarrow}}{z_\uparrow - z_\downarrow} \right) \left[ \prod_{i,j} (z_{i\uparrow} - z_{j\downarrow}) \right] \chi_{110} \chi_1 \\ &= \det \left( \frac{\partial_{z_\uparrow} - \partial_{z_\downarrow}}{z_\uparrow - z_\downarrow} \right) \chi_1^2. \quad (13) \end{aligned}$$

The existence and uniqueness of the pairing function that satisfies the listed conditions lead to the equality of the expressions. While we do not have a proof of the uniqueness of the pairing wave function, we checked that the following identity:

$$\chi_2 = \Psi_d \prod_{i,j} (z_{i\uparrow} - z_{j\downarrow}), \quad (14)$$

and thus Eq. (13), hold true up to  $N \leq 8$ . Interestingly we came to an expression for  $\chi_2$  that includes the division into two groups of particles, but as we emphasized previously this does not select any particular two groups in the definition of  $\chi_2$  as long as we do not assign spin. But in the definition of the JSS wave function we do, and it is then natural to decompose  $\chi_2$  in a way that respects this spin assignment.

#### IV. ROOT PARTITIONS

In the following we will describe another characteristic of the JSS state, its root configuration. It has been established<sup>21</sup> that many model FQH states can be written exactly as Jack polynomials or as the product of a Jack polynomial and some power of Vandermonde determinants. Jack polynomials are characterized by a dominant partition which reflects the vanishing properties of the state. A partition  $\lambda$  can be represented as an occupation-number configuration  $n(\lambda) = \{n_m(\lambda), m = 0, 1, 2, \dots\}$  of each of the LLL orbitals. A ‘‘squeezing rule’’ connects configurations  $n(\lambda) \rightarrow n(\mu)$ . This is a two-particle operation that moves a particle from orbital  $m_1$  to  $m'_1$  and another from  $m_2$  to  $m'_2$  with  $m_1 < m'_1 \leq m'_2 < m_2$  and  $m_1 + m_2 = m'_1 + m'_2$ . A configuration  $\lambda$  dominates a configuration  $\mu$  if  $n(\mu)$  can be derived from  $n(\lambda)$  by applying a sequence of squeezing operations. When FQH wave functions, equivalent to Jack polynomials, are expanded in the occupation-number basis, the only configurations with nonzero weight are the dominant configuration and those derived from this via squeezing operations. This is also true of FQH states which are equivalent to the product of Jack polynomials and some power of Vandermonde determinants. Recent work<sup>18,22</sup> has focused on the form of squeezing operations required for dealing with spinful states.

As a consequence of the pairing structure that we described in Sec. III we will demonstrate that the difference between the HR and JSS ground states can be described by an excitation of two neutral fermions of opposite spins at total momentum  $k = 0$  in the corresponding root configurations. Here we use the term ‘‘neutral fermions’’ in place of ‘‘composite fermions’’ to stress that, at  $\nu = 1/2$ , these excitations are due to unpaired particles in the BCS states, i.e., neutral fermions.<sup>4</sup> We can start from the neutral excitation spectrum of the JSS state in the thermodynamic limit with a quasiparticle-quasihole minimum as sketched on the left of Fig. 1. The spectrum is completely

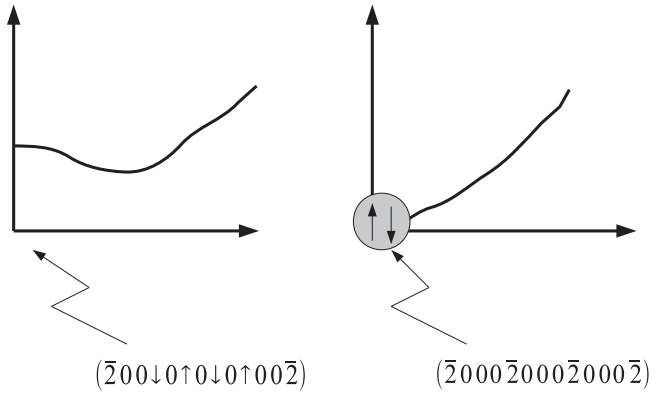


FIG. 1. Sketches of the excitation spectra of the Jain spin-singlet (left panel) and Haldane-Rezayi (right panel) states with the respective root configurations of the ground states.

gapped from the ground state, Eq. (1), with root configuration on a sphere given by  $(\bar{2}00\downarrow 0\uparrow 0\downarrow \dots 0\uparrow 00\bar{2})$ . By  $\bar{2}$  we denote a spin-singlet pair on a single orbital. The relationship of flux to particle number ( $N_\phi/N$ ) is  $N_\phi = 2N - 4$ . We expect that by changing (decreasing) the  $V_0$  component of the pseudopotential series  $\{V_0, V_1, 0, 0, \dots\}$ ,  $V_0, V_1 > 0$ , the system will become gapless and will be described at  $V_0 = 0$  by the HR state with excitation spectrum sketched on the right of Fig. 1, with root configuration  $(\bar{2}000\bar{2}000\bar{2}000\bar{2})$  with the same relationship of flux to number of particles. As we know from the previous analysis,<sup>4</sup> the branch of gapless excitations of the HR state is described by neutral fermions (excitations due to unpaired particles in the BCS state). Neutral fermions exist<sup>4</sup> in the JSS state, and it is this gapped branch around  $k = 0$  that becomes gapless at the critical point. It is thus to be expected that at the transition the pair of neutral fermions of opposite spins, each of momentum  $k = 0$ , become part of the ground-state configuration and description. Indeed, we can convince ourselves by looking at the root configurations of the JSS and HR states that they differ by the excitation of two neutral fermions with opposite spins. Each bulk spin-singlet pair in the HR state becomes set apart by one orbital in the root configuration of the JSS state. Opposite spins thus carry opposite momenta, but due to the requirement of inversion symmetry with respect to the equator and the constraint on the ratio of flux to number of particles (charge neutrality), the boundary configurations do not change and the difference between the two states may appear to us as some kind of boundary excitation in a uniform state (the JSS state). But as we already explained, essentially the difference between the HR and JSS phases can be described by the state of two neutral fermion bulk excitations in their respective ground states.

### V. NUMERICAL CALCULATIONS

To verify that the state on the weak-pairing side of the transition (HR state) is indeed a JSS state we obtain the ground state of the relevant interaction Hamiltonian and compare this to the explicitly constructed JSS state. The two-body interaction here consists of a hollow-core interaction ( $V_1 = 1$ ) along with a varying strength hard-core interaction ( $V_0 > 0$ ). Constructing the JSS wave function is very computationally

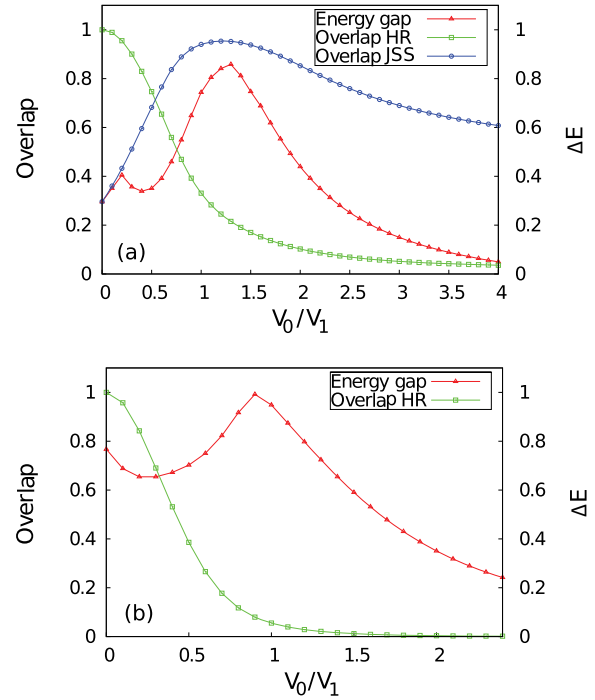


FIG. 2. (Color online) Excitation gap and overlaps of the ground state for a two-body interaction Hamiltonian for different  $V_0/V_1$  for (a)  $N = 10$  and (b)  $N = 12$  (see Ref. 5 for plots of the  $N = 8$  case). No overlap data are available for the JSS for  $N = 12$ .

intensive and  $N = 10$  was the largest we could construct. This is somewhat smaller than what has been achieved for spin-polarized systems. This is because changing the order of application of the projection operator no longer results in a good approximation as it does in the spin-polarized case (see the Appendix). Figure 2 shows the results of these calculations for the  $N = 10$  and  $N = 12$  cases. As expected, as  $V_0$  is increased the overlap with the HR state decays. For  $N = 10$  where we could construct the JSS state we see that as  $V_0$  is increased the overlap with this state increases to almost unity before starting to decay. This is a strong indication that this is indeed the JSS state on the weak-pairing side of the transition. In both cases the energy gap also shows a peak near where we expect the JSS state to be, which is consistent with this picture. Note that the Coulomb ground state in the lowest or the second Landau level has a zero overlap with the HR or JSS state for  $N = 10$  and  $N = 12$ , because of the different quantum numbers.

### VI. SPIN-POLARIZED CASE

In the following we will discuss spin-polarized Jain states and their relationship to the nonunitary states. This subject is well studied, especially for the case of bosons at filling factor  $2/3$  and the related nonunitary state, the Gaffnian state,<sup>23,24</sup> and our focus here will be the underlying pairing structures in these states. The root configurations of these two states, Jain and Gaffnian, are well known<sup>8</sup> and their pairing structure can be probed. We will see that in this case also, as the difference of the two states, two neutral excitations exist that are spread out over the whole system. Due to the equivalence of north

and south poles on the sphere (with a magnetic monopole in its center), i.e., symmetry under inversion on the finite interval of angular momentum states of any quantum Hall state, and as a consequence of the bulk neutral excitations, “edge decorations”—special decorations on the ends (north and south poles)—appear, as we find in the case for the JSS state. This neutral rearrangement and the edge decorations can be seen in the root configuration of the Jain state (2010110102) compared to that of the Gaffnian state (2002002002) (for the sake of simplicity we display the root configurations for only eight particles). This can also be seen in Jain states that need more than two LLs for their construction. Each new LL contributes a new pair of neutral excitations with respect to nonunitary partner states.<sup>8</sup> To understand the origin of this behavior, which may stem from a pairing structure in Jain states, we begin with the definition of the Gaffnian wave function of bosons at  $2/3$ :

$$\Psi_{Gf} = \mathcal{S} \left[ \Psi_{221} \text{perm} \left( \frac{1}{z_{\uparrow} - z_{\downarrow}} \right) \right]. \quad (15)$$

In constructing this state we first divide the electrons into two groups of up ( $\uparrow$ ) and down ( $\downarrow$ ) pseudospins. In the definition Eq. (15), “perm” denotes the permanent which for an  $M \times M$  matrix is  $\text{perm}(\mathcal{M}) = \sum_{p \in \mathcal{S}_M} \prod_{k=1}^M \mathcal{M}_{k,p(k)}$ .  $\Psi_{221}$  is the well-known notation of Halperin states for which we have

$$\Psi_{221} = \prod_{i < j} (z_{i\uparrow} - z_{j\uparrow})^2 \prod_{l < m} (z_{l\downarrow} - z_{m\downarrow})^2 \prod_{p < q} (z_{p\uparrow} - z_{q\downarrow}). \quad (16)$$

In the following we will use

$$(z_{\sigma} - z_{\sigma'})^m, \quad (17)$$

where  $m$  can be a fraction and  $(\sigma, \sigma') = (\uparrow, \uparrow), (\downarrow, \downarrow)$ , or  $(\uparrow, \downarrow)$  as a shorthand notation for any of the three factors in Eq. (16). The overall symmetrization operator  $\mathcal{S}$  in Eq. (15) is necessary to produce a state of polarized bosons.

To display the pairing structure related to the previous discussion of the HR state we will separate out the charge part, i.e., the part unaffected by pseudospin:

$$\Psi_{Gf} = \mathcal{S} \left[ \prod (z - z)^{3/2} (z_{\uparrow} - z_{\uparrow})^{1/2} (z_{\downarrow} - z_{\downarrow})^{1/2} \times \frac{1}{(z_{\uparrow} - z_{\downarrow})^{1/2}} \text{perm} \left( \frac{1}{(z_{\uparrow} - z_{\downarrow})} \right) \right], \quad (18)$$

where  $\prod (z - z)^{3/2}$  denotes the product of all possible pairs:

$$\prod (z - z)^{3/2} = (z_{\uparrow} - z_{\uparrow})^{3/2} (z_{\downarrow} - z_{\downarrow})^{3/2} (z_{\uparrow} - z_{\downarrow})^{3/2}. \quad (19)$$

Due to the equality given in Ref. 3,

$$\Psi_{11-1} \text{perm} \left( \frac{1}{z_{\uparrow} - z_{\downarrow}} \right) = \det \left( \frac{1}{(z_{\uparrow} - z_{\downarrow})^2} \right), \quad (20)$$

we can rewrite the Gaffnian as

$$\Psi_{Gf} = \mathcal{S} \left[ \prod (z - z)^{3/2} \frac{(z_{\uparrow} - z_{\downarrow})^{1/2}}{(z_{\uparrow} - z_{\uparrow})^{1/2} (z_{\downarrow} - z_{\downarrow})^{1/2}} \times \det \left( \frac{1}{(z_{\uparrow} - z_{\downarrow})^2} \right) \right]. \quad (21)$$

Thus a possible interpretation of the Gaffnian state is that it represents a HR pairing state of neutral semions, semions because we have taken in front the factor  $\prod (z - z)^{3/2}$  that describes the charge part. The original semions that paired by way of a permanent in the usual definition [Eq. (18)] have relative fermionic statistics with respect to the new semions of Eq. (21).

We can try to extend our pairing arguments from spin-singlet HR and Jain states to Gaffnian and Jain states at  $2/3$  filling ( $2/5$  in the case of fermions). We expect that the Jain state at  $2/3$  filling can be viewed as an underlying state of weakly paired semions as in the following expression (we neglect the projection to the LLL in the following):

$$\Psi_{\text{Jain}} = \mathcal{S} \left[ \prod (z - z)^{3/2} \frac{(z_{\uparrow} - z_{\downarrow})^{1/2}}{(z_{\uparrow} - z_{\uparrow})^{1/2} (z_{\downarrow} - z_{\downarrow})^{1/2}} \times \det \left( \frac{z_{\uparrow}^* - z_{\downarrow}^*}{z_{\uparrow} - z_{\downarrow}} \right) \right]. \quad (22)$$

Due to the previously proven identity [Eq. (14)]

$$\chi_2 = \frac{\chi_1}{\chi_{110}} \det \left( \frac{z_{\uparrow}^* - z_{\downarrow}^*}{z_{\uparrow} - z_{\downarrow}} \right), \quad (23)$$

we can rewrite Eq. (22) as

$$\Psi_{\text{Jain}} = \mathcal{S} \left[ \prod (z - z)^{3/2} \frac{(z_{\uparrow} - z_{\downarrow})^{1/2}}{(z_{\uparrow} - z_{\uparrow})^{1/2} (z_{\downarrow} - z_{\downarrow})^{1/2}} \frac{\chi_2 \chi_{110}}{\chi_1} \right] = \mathcal{S}(\chi_1 \chi_2) = \chi_1 A(\chi_2) = \chi_1 \chi_2, \quad (24)$$

as we anticipated. The last identity, in which  $A$  is the antisymmetrizer, follows from the antisymmetry already encoded in  $\chi_2$  under exchange of any  $i$  and  $j$ . Moreover, we can start from the definition of the bosonic Jain state,

$$\Psi_{\text{Jain}} = \chi_2 \chi_1, \quad (25)$$

use the same identity in Eq. (23), and conclude that

$$\Psi_{\text{Jain}} = \det \left( \frac{z_{\uparrow}^* - z_{\downarrow}^*}{z_{\uparrow} - z_{\downarrow}} \right) \times (z_{\uparrow} - z_{\uparrow})(z_{\downarrow} - z_{\downarrow})(z_{\uparrow} - z_{\downarrow})^2, \quad (26)$$

i.e., come to an expression for  $\Psi_{\text{Jain}}$  in terms of two groups of particles. As we emphasized below Eq. (14), the division between ups and downs in Eq. (26) is arbitrary and we do not have a regular paired state with a charge part clearly separated from a pairing function. As before, but without the need for the symmetrizer  $\mathcal{S}$ , we have

$$\Psi_{\text{Jain}} = \prod (z - z)^{3/2} \frac{(z_{\uparrow} - z_{\downarrow})^{1/2}}{(z_{\uparrow} - z_{\uparrow})^{1/2} (z_{\downarrow} - z_{\downarrow})^{1/2}} \times \det \left( \frac{z_{\uparrow}^* - z_{\downarrow}^*}{z_{\uparrow} - z_{\downarrow}} \right). \quad (27)$$

Therefore we conclude that the Jain state at  $2/3$  filling can be (to a certain degree) viewed as a topological superconductor of anyons in a weak-pairing phase. The physical consequences of such a statement are not obvious. The pairing is very much disguised. We may also talk about neutral fermions and their pairing, but there is no simple relationship between them and the underlying particles—in this case bosons.

Edge decorations in the root configuration of the Jain state in comparison with the Gaffnian clearly point to the presence of neutral excitations that follow from pair breaking. To understand better how edge decorations are connected with the pairing structure in Gaffnian and Jain states that we demonstrated previously in Eqs. (18), (21), (22), and (24), we will take out  $\mathcal{S}$  (symmetrizer) in the definition of the Gaffnian [Eq. (15)]. As a result we get a spinful state with root configuration  $(\bar{2}00\bar{2}00\bar{2}00\bar{2})$  where  $\bar{2}$  represents a spin singlet on a single orbital. (This is analogous to the HR case.) We may imagine pair-breaking neutral excitations with spin which would lead to root configurations of the form  $(\bar{2}0\uparrow 0\downarrow\uparrow 0\downarrow 0\bar{2})$ , but this would be too restrictive to describe the root configuration of a Jain state which is ferromagnetically ordered with the total projection along the quantization axis equal to zero in the pseudospin space: (2010110102). We can convince ourselves of this particular ferromagnetic ordering by analyzing the expression Eq. (22) for the Jain state. Nevertheless, we see the similarity between pair-breaking neutral excitations that carry spin and quasiparticle-quasihole excitations<sup>25</sup> on both ends of the Jain state. Here quasiparticle-quasihole excitations correspond to neutral fermions in the HR and JSS case. Instead of a pair of neutral fermions of opposite spins in the polarized Jain case we have a quadrupolar<sup>26</sup> excitation, two quasiparticle-quasihole pairs that are spread out over the ground state. Namely, we need two (neutral) dipoles of corresponding but opposite momenta to make a  $k = 0$  excitation that decreases in energy when we are approaching the critical Gaffnian state. The situation is similar to the spin-singlet HR and JSS case with opposite-spin neutral fermions as sketched in Fig. 1.

With all that we have said about Jain states, we can expect that IQH effect (IQHE) wave functions that describe noninteracting fermions can be described as some kind of weakly paired topological superconductors where the extremely weak pairing of a time-reversal-symmetry-breaking  $d$  wave, which is just a phase, changes into the description of fermionic correlations between different LLs. As we already demonstrated the Slater determinant of two filled LLs can be written as

$$\chi_2 = \det \begin{pmatrix} z_{\uparrow}^* & -z_{\downarrow}^* \\ z_{\uparrow} & -z_{\downarrow} \end{pmatrix} (z_{\uparrow} - z_{\downarrow}). \quad (28)$$

We emphasize that the division between ups and downs is arbitrary; the only requirement is an equal number of ups and downs, i.e., an even total number of fermionic particles. The factor  $(z_{\uparrow} - z_{\downarrow})$ , similar to the Jastrow-Laughlin factor but not the same, carries the information about the filling factor, i.e., from the number of flux quanta that particles experience,  $N_{\phi}^{\uparrow} = N_{\phi}^{\downarrow} = N/2 - 2$ , we can read off the filling factor,  $\nu = 2$ .

The interesting question concerns the relationship between weakly paired  $d$ -wave superconductors and the topological

insulator, i.e., the IQHE with Chern number equal to 2. This question is highly relevant in the context of fractional Chern insulators<sup>27</sup> (i.e., the FQHE without a magnetic field) with Chern number larger than 1.<sup>11–13</sup> Besides the relationship between bulk Hamiltonians defined on a lattice as demonstrated in Ref. 14, there is obvious similarity in the edge theories: Both are made up of two Dirac fermions,<sup>4</sup> which, expressed as Majoranas, represent a theory with  $SO(4)$  symmetry which is equivalent to  $SU(2) \times SU(2)$  symmetry. We may ask what is the symmetry of bulk  $d$ -wave Hamiltonians in order to identify the degrees of freedom which are transformed under the symmetry. First there is obvious spin rotation symmetry,  $SU(2)_{\text{spin}}$ , due to the underlying spin degree of freedom in the Hamiltonian; the ground-state wave function

$$\Psi_d = \det \begin{pmatrix} z_{\uparrow}^* & -z_{\downarrow}^* \\ z_{\uparrow} & -z_{\downarrow} \end{pmatrix} \quad (29)$$

is a spin-singlet eigenstate of  $SU(2)_{\text{spin}}$  since it is a collection of BCS spin-singlet pairs. Second, besides particle-hole symmetry, there is no additional internal symmetry in the BCS Hamiltonian. Only in its ground-state wave function is the number of complex conjugated and the number of nonconjugated variables (“LL index”) expected to be the same or, expressed in an equivalent way, their difference should be conserved. Hence we may talk about an internal  $U(1)$  symmetry. What we can conclude is that the symmetry that is present in the bulk is enlarged at the edge to  $SU(2)_{\text{spin}} \times SU(2)_{\text{internal}}$ .

On the other hand, in the case of the IQHE at  $\nu = 2$ , at the edge we may talk certainly about a symmetry that acts on the LL index in parallel with the spin symmetry on the edge of  $d$ -wave superconductors. Therefore on the edge we have an  $SU(2)_{\text{LL index}} \times SU(2)_{\text{internal}}$  symmetry. [Note that here  $SU(2)_{\text{internal}}$  should not be identified with that in the context of the  $d$ -wave superconductor.] There are no explicit degrees of freedom in the bulk that would correspond to or lead to  $SU(2)_{\text{internal}}$  symmetry on the edge. Interestingly, the bulk ground-state wave function has the form which can be seen in Eq. (28)—it is invariant under arbitrary assignment of ups and downs. Equation (28) relates the ground-state wave function of  $d$ -wave superconductors and the IQHE at  $\nu = 2$  and therefore indicates a pairing structure in IQHE wave functions. There is no pseudospin degree of freedom in the IQHE (Hamiltonian) in the bulk, but the ground-state wave function looks as if there is an additional ferromagnetically ordered pseudospin degree of freedom next to the LL index. And the symmetries related to these structures exist on the edge.

Therefore IQHE and polarized FQHE states underlie a pairing construction which incorporates the “right” mutual statistics of constituents that is achieved by their  $d$ -wave pairing. At the same time their construction incorporates an explicit projection to a ferromagnetic, i.e., one-component, state so that the paired nature is suppressed. In this way latent pseudospin degrees of freedom that are paired in the ground-state wave functions appear in the root configurations of the model wave functions and on the edge by way of enlarged symmetry.

## VII. CONCLUSIONS

Haldane-Rezayi and Jain spin-singlet states are canonical examples of  $d$ -wave pairing of FQHE wave functions. We explicitly showed  $d$ -wave pairing in the case of the JSS state. The root configuration of the JSS state was derived; in it we could recognize the role of composite (neutral) fermion pairs in the transition from the JSS to the HR state. We demonstrated this transition in an exact diagonalization study. Besides its intrinsic interest the study enabled us to draw parallels and conclusions concerning polarized FQHE and IQHE states. We found the presence of  $d$ -wave pairing in these states although it is suppressed due to their one-component nature.

## ACKNOWLEDGMENTS

We thank V. Gurarie for useful discussions. A.S. thanks Princeton University for generous hosting. A.S. was supported by a Keck grant and N. R. was supported by NSF Grant No. CAREER DMR-095242, ONR Grant No. N00014-11-1-0635, the Packard Foundation, and a Keck grant. I.V. and M.V.M. were supported by the Serbian Ministry of Education and Science under Project No. ON171017. The authors also acknowledge support from the bilateral MES-CNRS-2011/12 program. This research was supported in part by the National Science Foundation under Grant No. NSF PHY11-25915. M.V.M. acknowledges the hospitality of KITP, Santa Barbara.

## APPENDIX: NUMERICAL CONSTRUCTION OF COMPOSITE FERMION WAVE FUNCTIONS

First we discuss the construction of lowest-Landau-level spin-polarized composite fermion (CF) wave functions of the form

$$\phi = \mathcal{P}_{\text{LLL}}[\chi_1^{2p} \chi_n].$$

In Ref. 19 it was demonstrated that when constructing wave functions of this form the Jastrow factor  $\chi_1^{2p}$  can be moved

inside the determinant coming from  $\chi_n$ . The LLL projection can then be performed before taking the determinant. In addition, analytical expressions for the application for the LLL projection operator can be derived. In this manner the computational cost of constructing such wave functions is dramatically reduced.

Extending this, it was discovered that this method can be applied even for cases where the wave function in question does not have this form. For example, the bosonic wave functions considered in Ref. 20 that are associated with the CF state at filling factor  $\nu = \frac{n}{n+1}$  fall into this category:

$$\phi_B = \mathcal{P}_{\text{LLL}}[\chi_1 \chi_n].$$

It was shown that this wave function can be approximated well with

$$\phi'_B = \chi_1^{-1} \mathcal{P}_{\text{LLL}}[\chi_1^2 \chi_n],$$

which is amenable to the technique from Ref. 19. The overlap for  $N = 8$  is  $|\langle \phi_B | \phi'_B \rangle|^2 = 0.9820$ .<sup>20</sup>

In the case of the JSS wave function it was hoped that a similar method could be applied. We constructed the wave functions

$$\phi'_{\text{JSS}} = \chi_{001}^{-1} \mathcal{P}_{\text{LLL}}[\chi_1^2 \chi_2]$$

and

$$\phi''_{\text{JSS}} = \chi_{110} \mathcal{P}_{\text{LLL}}[\chi_1 \chi_2].$$

However, it was found that these do not offer good approximations of the JSS state even for small systems. The overlaps with the JSS state for  $N = 8$  are  $|\langle \phi_{\text{JSS}} | \phi'_{\text{JSS}} \rangle|^2 = 0.790$  and  $|\langle \phi_{\text{JSS}} | \phi''_{\text{JSS}} \rangle|^2 = 0.792$ . Note that for  $\phi''_{\text{JSS}}$  the term inside the projection is not of the form  $\chi_1^{2p} \chi_2$  and thus is not amenable to the technique described in Ref. 19. However, this wave function is still less computationally intensive to construct than  $\phi_{\text{JSS}}$  [Eq. (1)] since the application of the projection operator before performing the product operation makes this operation much less demanding.

<sup>1</sup>J. Jain, *Composite Fermions* (Cambridge University Press, Cambridge, 2007).

<sup>2</sup>G. Moore and N. Read, *Nucl. Phys. B* **360**, 362 (1991).

<sup>3</sup>F. D. M. Haldane and E. H. Rezayi, *Phys. Rev. Lett.* **60**, 956 (1988).

<sup>4</sup>N. Read and D. Green, *Phys. Rev. B* **61**, 10267 (2000).

<sup>5</sup>L. Belkhir, X. G. Wu, and J. K. Jain, *Phys. Rev. B* **48**, 15245 (1993).

<sup>6</sup>S. H. Simon, E. H. Rezayi, N. R. Cooper, and I. Berdnikov, *Phys. Rev. B* **75**, 075317 (2007).

<sup>7</sup>N. Regnault, M. Goerbig, and T. Jolicoeur, *Phys. Rev. Lett.* **101**, 066803 (2008).

<sup>8</sup>N. Regnault, B. A. Bernevig, and F. D. M. Haldane, *Phys. Rev. Lett.* **103**, 016801 (2009).

<sup>9</sup>B. A. Bernevig and F. D. M. Haldane, *Phys. Rev. Lett.* **101**, 246806 (2008).

<sup>10</sup>B. A. Bernevig, V. Gurarie, and S. H. Simon, *J. Phys. A* **42**, 245206 (2009).

<sup>11</sup>M. Barkeshli and X. L. Qi, [arXiv:1112.3311](https://arxiv.org/abs/1112.3311).

<sup>12</sup>F. Wang and Y. Ran, *Phys. Rev. B* **84**, 241103(R) (2011).

<sup>13</sup>Y. F. Wang, H. Yao, C. D. Gong, and D. N. Sheng, [arXiv:1204.1697](https://arxiv.org/abs/1204.1697).

<sup>14</sup>R. B. Laughlin, *Phys. Rev. Lett.* **80**, 5188 (1998).

<sup>15</sup>T. H. Hansson, C.-C. Chang, J. K. Jain, and S. Viefers, *Phys. Rev. B* **76**, 075347 (2007).

<sup>16</sup>F. D. M. Haldane, *Phys. Rev. Lett.* **51**, 605 (1983).

<sup>17</sup>N. Read and E. Rezayi, *Phys. Rev. B* **54**, 16864 (1996).

<sup>18</sup>E. Ardonne and N. Regnault, *Phys. Rev. B* **84**, 205134 (2011).

<sup>19</sup>J. K. Jain and R. K. Kamilla, *Int. J. Mod. Phys. B* **11**, 2621 (1997).

<sup>20</sup>C. Chang, N. Regnault, T. Jolicoeur, and J. K. Jain, *Phys. Rev. A* **72**, 013611 (2005).

<sup>21</sup>B. A. Bernevig and F. D. M. Haldane, *Phys. Rev. Lett.* **100**, 246802 (2008).

<sup>22</sup>B. Estienne, and B. A. Bernevig, *Nucl. Phys. B* **857**, 185 (2012).

<sup>23</sup>D. Yoshioka, A. H. MacDonald, and S. M. Girvin, *Phys. Rev. B* **38**, 3636 (1988).

<sup>24</sup>S. H. Simon, E. H. Rezayi, N. R. Cooper, and I. Berdnikov, *Phys. Rev. B* **75**, 075317 (2007).

<sup>25</sup>B. A. Bernevig and F. D. M. Haldane, *Phys. Rev. Lett.* **102**, 06802 (2009).

<sup>26</sup>S. C. Zhang, *Int. J. Mod. Phys. B* **6**, 25 (1992).

<sup>27</sup>F. D. M. Haldane, *Phys. Rev. Lett.* **61**, 2015 (1988).



## C programs for solving the time-dependent Gross–Pitaevskii equation in a fully anisotropic trap<sup>☆</sup>

Dušan Vudragović<sup>a</sup>, Ivana Vidanović<sup>a</sup>, Antun Balaž<sup>a,\*</sup>, Paulsamy Muruganandam<sup>b</sup>, Sadhan K. Adhikari<sup>c</sup>

<sup>a</sup> Scientific Computing Laboratory, Institute of Physics Belgrade, University of Belgrade, Pregrevica 118, 11080 Belgrade, Serbia

<sup>b</sup> School of Physics, Bharathidasan University, Palkalaiperur Campus, Tiruchirappalli – 620024, Tamil Nadu, India

<sup>c</sup> Instituto de Física Teórica, UNESP – Universidade Estadual Paulista, 01.140-70 São Paulo, São Paulo, Brazil

### ARTICLE INFO

#### Article history:

Received 2 March 2012

Accepted 21 March 2012

Available online 21 April 2012

#### Keywords:

Bose–Einstein condensate

Gross–Pitaevskii equation

Split-step Crank–Nicolson scheme

Real- and imaginary-time propagation

C program

OpenMP

Partial differential equation

### ABSTRACT

We present C programming language versions of earlier published Fortran programs (Muruganandam and Adhikari (2009) [1]) for calculating both stationary and non-stationary solutions of the time-dependent Gross–Pitaevskii (GP) equation. The GP equation describes the properties of dilute Bose–Einstein condensates at ultra-cold temperatures. C versions of programs use the same algorithms as the Fortran ones, involving real- and imaginary-time propagation based on a split-step Crank–Nicolson method. In a one-space-variable form of the GP equation, we consider the one-dimensional, two-dimensional, circularly-symmetric, and the three-dimensional spherically-symmetric harmonic-oscillator traps. In the two-space-variable form, we consider the GP equation in two-dimensional anisotropic and three-dimensional axially-symmetric traps. The fully-anisotropic three-dimensional GP equation is also considered. In addition to these twelve programs, for six algorithms that involve two and three space variables, we have also developed threaded (OpenMP parallelized) programs, which allow numerical simulations to use all available CPU cores on a computer. All 18 programs are optimized and accompanied by makefiles for several popular C compilers. We present typical results for scalability of threaded codes and demonstrate almost linear speedup obtained with the new programs, allowing a decrease in execution times by an order of magnitude on modern multi-core computers.

#### New version program summary

**Program title:** GP-SCL package, consisting of: (i) *imagtime1d*, (ii) *imagtime2d*, (iii) *imagtime2d-th*, (iv) *imagtimecir*, (v) *imagtime3d*, (vi) *imagtime3d-th*, (vii) *imagtimeaxial*, (viii) *imagtimeaxial-th*, (ix) *imagtimesph*, (x) *realttime1d*, (xi) *realttime2d*, (xii) *realttime2d-th*, (xiii) *realttimecir*, (xiv) *realttime3d*, (xv) *realttime3d-th*, (xvi) *realttimeaxial*, (xvii) *realttimeaxial-th*, (xviii) *realttimesph*.

**Catalogue identifier:** AEDU\_v2\_0.

**Program Summary URL:** [http://cpc.cs.qub.ac.uk/summaries/AEDU\\_v2\\_0.html](http://cpc.cs.qub.ac.uk/summaries/AEDU_v2_0.html).

**Program obtainable from:** CPC Program Library, Queen's University of Belfast, N. Ireland.

**Licensing provisions:** Standard CPC licence, <http://cpc.cs.qub.ac.uk/licence/licence.html>.

**No. of lines in distributed program, including test data, etc.:** 180 583.

**No. of bytes in distributed program, including test data, etc.:** 1 188 688.

**Distribution format:** tar.gz.

**Programming language:** C and C/OpenMP.

**Computer:** Any modern computer with C language compiler installed.

**Operating system:** Linux, Unix, Mac OS, Windows.

**RAM:** Memory used with the supplied input files: 2–4 MB (i, iv, ix, x, xiii, xvi, xvii, xviii), 8 MB (xi, xii), 32 MB (vii, viii), 80 MB (ii, iii), 700 MB (xiv, xv), 1.2 GB (v, vi).

**Number of processors used:** For threaded (OpenMP parallelized) programs, all available CPU cores on the computer.

**Classification:** 2.9, 4.3, 4.12.

<sup>☆</sup> D.V., I.V., and A.B. acknowledge support by the Ministry of Education and Science of the Republic of Serbia under projects No. ON171017 and NAD-BEC, by DAAD - German Academic and Exchange Service under project NAD-BEC, and by the European Commission under EU FP7 projects PRACE-1IP, PRACE-2IP, HP-SEE, and EGI-InSPIRE. P.M. acknowledges support by DST and CSIR of India. S.K.A. acknowledges support by FAPESP and CNPq of Brazil.

\* Corresponding author.

E-mail address: [antun@ipb.ac.rs](mailto:antun@ipb.ac.rs) (A. Balaž).



*Catalogue identifier of previous version:* AEDU\_v1\_0.

*Journal reference of previous version:* Comput. Phys. Commun. 180 (2009) 1888.

*Does the new version supersede the previous version?:* No.

*Nature of problem:* These programs are designed to solve the time-dependent Gross–Pitaevskii (GP) nonlinear partial differential equation in one-, two- or three-space dimensions with a harmonic, circularly-symmetric, spherically-symmetric, axially-symmetric or fully anisotropic trap. The GP equation describes the properties of a dilute trapped Bose–Einstein condensate.

*Solution method:* The time-dependent GP equation is solved by the split-step Crank–Nicolson method by discretizing in space and time. The discretized equation is then solved by propagation, in either imaginary or real time, over small time steps. The method yields solutions of stationary and/or non-stationary problems.

*Reasons for the new version:* Previous Fortran programs [1] are used within the ultra-cold atoms [2–11] and nonlinear optics [12,13] communities, as well as in various other fields [14–16]. This new version represents translation of all programs to the C programming language, which will make it accessible to the wider parts of the corresponding communities. It is well known that numerical simulations of the GP equation in highly experimentally relevant geometries with two or three space variables are computationally very demanding, which presents an obstacle in detailed numerical studies of such systems. For this reason, we have developed threaded (OpenMP parallelized) versions of programs *imagtime2d*, *imagtime3d*, *imagtimeaxial*, *realtime2d*, *realtime3d*, *realtimeaxial*, which are named *imagtime2d-th*, *imagtime3d-th*, *imagtimeaxial-th*, *realtime2d-th*, *realtime3d-th*, *realtimeaxial-th*, respectively. Fig. 1 shows the scalability results obtained for OpenMP versions of programs *realtime2d* and *realtime3d*. As we can see, the speedup is almost linear, and on a computer with the total of 8 CPU cores we observe in Fig. 1(a) a maximal speedup of around 7, or roughly 90% of the ideal speedup, while on a computer with 12 CPU cores we find in Fig. 1(b) that the maximal speedup is around 9.6, or 80% of the ideal speedup. Such a speedup represents significant improvement in the performance.

*Summary of revisions:* All Fortran programs from the previous version [1] are translated to C and named in the same way. The structure of all programs is identical. We have introduced the use of comprehensive input files, where all parameters are explained in detail and can be set by a user. We have also included makefiles with tested and verified settings for GNU's gcc compiler, Intel's icc compiler, IBM's xlc compiler, PGI's pgcc compiler, and Oracle's suncc (former Sun's) compiler. In addition to this, 6 new threaded (OpenMP parallelized) programs are supplied (*imagtime2d-th*, *imagtime3d-th*, *imagtimeaxial-th*, *realtime2d-th*, *realtime3d-th*, *realtimeaxial-th*) for algorithms involving two or three space variables. They are written by OpenMP-parallelizing the most computationally demanding loops in functions performing time evolution (*calcnu*, *calclux*, *calcluy*, *calcluz*), normalization (*calcnorm*), and calculation of physical quantities (*calcmuen*, *calcrms*). Since some of the dynamically allocated array variables are used within such loops, they had to be made private for each thread. This was done by allocating matrices instead of arrays, with the first index in all such matrices corresponding to a thread number.

*Additional comments:* This package consists of 18 programs, see Program title above, out of which 12 programs (i, ii, iv, v, vii, ix, x, xi, xiii, xiv, xvi, xviii) are serial, while 6 programs (iii, vi, viii, xii, xv, xvii) are threaded (OpenMP parallelized). For the particular purpose of each program, please see descriptions below.

*Running time:* All running times given in descriptions below refer to programs compiled with gcc on quad-core Intel Xeon X5460 at 3.16 GHz (CPU1), and programs compiled with icc on quad-core Intel Nehalem E5540 at 2.53 GHz (CPU2). With the supplied input files, running times on CPU1 are: 5 min (i, iv, ix, xii, xiii, xvii, xviii), 10 min (viii, xvi), 15 min (iii, x, xi), 30 min (ii, vi, vii), 2 h (v), 4 h (xv), 15 h (xiv). On CPU2, running times are: 5 min (i, iii, iv, viii, ix, xii, xiii, xvi, xvii, xviii), 10 min (vi, x, xi), 20 min (ii, vii), 1 h (v), 2 h (xv), 12 h (xiv).

© 2012 Elsevier B.V. All rights reserved.

### **New version program summary (i)**

*Program title:* *imagtime1d*.

*Title of electronic files:* *imagtime1d.c*, *imagtime1d.h*.

*Computer:* Any modern computer with C language compiler installed.

*Maximum RAM memory:* 4 MB.

*Programming language used:* C.

*Typical running time:* 2 min (CPU1), 1 min (CPU2).

*Nature of physical problem:* This program is designed to solve the time-dependent GP nonlinear partial differential equation in one space dimension with a harmonic trap. The GP equation describes the properties of a dilute trapped Bose–Einstein condensate.

*Method of solution:* The time-dependent GP equation is solved by the split-step Crank–Nicolson method by discretizing in space and time. The discretized equation is then solved by propagation in imaginary time over small time steps. The method yields solutions of stationary problems.

### **New version program summary (ii)**

*Program title:* *imagtime2d*.

*Title of electronic files:* *imagtime2d.c*, *imagtime2d.h*.

*Computer:* Any modern computer with C language compiler installed.

*Maximum RAM memory:* 80 MB.

*Programming language used:* C.

*Typical running time:* 30 min (CPU1), 20 min (CPU2).

*Nature of physical problem:* This program is designed to solve the time-dependent GP nonlinear partial differential equation in two space dimensions with an anisotropic trap. The GP equation describes the properties of a dilute trapped Bose–Einstein condensate.

*Method of solution:* The time-dependent GP equation is solved by the split-step Crank–Nicolson method by discretizing in space and time. The discretized equation is then solved by propagation in imaginary time over small time steps. The method yields solutions of stationary problems.

**New version program summary (iii)**

*Program title:* imagtime2d-th.

*Title of electronic files:* imagtime2d-th.c, imagtime2d-th.h.

*Computer:* Any modern computer with C language compiler installed.

*Maximum RAM memory:* 80 MB.

*Programming language used:* C/OpenMP.

*Typical running time:* 15 min (CPU1), 5 min (CPU2).

*Nature of physical problem:* This program is designed to solve the time-dependent GP nonlinear partial differential equation in two space dimensions with an anisotropic trap. The GP equation describes the properties of a dilute trapped Bose–Einstein condensate.

*Method of solution:* The time-dependent GP equation is solved by the split-step Crank–Nicolson method by discretizing in space and time. The discretized equation is then solved by propagation in imaginary time over small time steps. The method yields solutions of stationary problems.

**New version program summary (iv)**

*Program title:* imagtimecir.

*Title of electronic files:* imagtimecir.c, imagtimecir.h.

*Computer:* Any modern computer with C language compiler installed.

*Maximum RAM memory:* 2 MB.

*Programming language used:* C.

*Typical running time:* 2 min (CPU1), 1 min (CPU2).

*Nature of physical problem:* This program is designed to solve the time-dependent GP nonlinear partial differential equation in two space dimensions with a circularly-symmetric trap. The GP equation describes the properties of a dilute trapped Bose–Einstein condensate.

*Method of solution:* The time-dependent GP equation is solved by the split-step Crank–Nicolson method by discretizing in space and time. The discretized equation is then solved by propagation in imaginary time over small time steps. The method yields solutions of stationary problems.

**New version program summary (v)**

*Program title:* imagtime3d.

*Title of electronic files:* imagtime3d.c, imagtime3d.h.

*Computer:* Any modern computer with C language compiler installed.

*Maximum RAM memory:* 1.2 GB.

*Programming language used:* C.

*Typical running time:* 1.5 h (CPU1), 1 h (CPU2).

*Nature of physical problem:* This program is designed to solve the time-dependent GP nonlinear partial differential equation in three space dimensions with an anisotropic trap. The GP equation describes the properties of a dilute trapped Bose–Einstein condensate.

*Method of solution:* The time-dependent GP equation is solved by the split-step Crank–Nicolson method by discretizing in space and time. The discretized equation is then solved by propagation in imaginary time over small time steps. The method yields solutions of stationary problems.

**New version program summary (vi)**

*Program title:* imagtime3d-th.

*Title of electronic files:* imagtime3d-th.c, imagtime3d-th.h.

*Computer:* Any modern computer with C language compiler installed.

*Maximum RAM memory:* 1.2 GB.

*Programming language used:* C/OpenMP.

*Typical running time:* 25 min (CPU1), 10 min (CPU2).

*Nature of physical problem:* This program is designed to solve the time-dependent GP nonlinear partial differential equation

in three space dimensions with an anisotropic trap. The GP equation describes the properties of a dilute trapped Bose–Einstein condensate.

*Method of solution:* The time-dependent GP equation is solved by the split-step Crank–Nicolson method by discretizing in space and time. The discretized equation is then solved by propagation in imaginary time over small time steps. The method yields solutions of stationary problems.

**New version program summary (vii)**

*Program title:* imagtimeaxial.

*Title of electronic files:* imagtimeaxial.c, imagtimeaxial.h.

*Computer:* Any modern computer with C language compiler installed.

*Maximum RAM memory:* 32 MB.

*Programming language used:* C.

*Typical running time:* 30 min (CPU1), 20 min (CPU2).

*Nature of physical problem:* This program is designed to solve the time-dependent GP nonlinear partial differential equation in three space dimensions with an axially-symmetric trap. The GP equation describes the properties of a dilute trapped Bose–Einstein condensate.

*Method of solution:* The time-dependent GP equation is solved by the split-step Crank–Nicolson method by discretizing in space and time. The discretized equation is then solved by propagation in imaginary time over small time steps. The method yields solutions of stationary problems.

**New version program summary (viii)**

*Program title:* imagtimeaxial-th.

*Title of electronic files:* imagtimeaxial-th.c, imagtimeaxial-th.h.

*Computer:* Any modern computer with C language compiler installed.

*Maximum RAM memory:* 32 MB.

*Programming language used:* C/OpenMP.

*Typical running time:* 10 min (CPU1), 5 min (CPU2).

*Nature of physical problem:* This program is designed to solve the time-dependent GP nonlinear partial differential equation in three space dimensions with an axially-symmetric trap. The GP equation describes the properties of a dilute trapped Bose–Einstein condensate.

*Method of solution:* The time-dependent GP equation is solved by the split-step Crank–Nicolson method by discretizing in space and time. The discretized equation is then solved by propagation in imaginary time over small time steps. The method yields solutions of stationary problems.

**New version program summary (ix)**

*Program title:* imagtimesph.

*Title of electronic files:* imagtimesph.c, imagtimesph.h.

*Computer:* Any modern computer with C language compiler installed.

*Maximum RAM memory:* 2.5 MB.

*Programming language used:* C.

*Typical running time:* 2 min (CPU1), 1 min (CPU2).

*Nature of physical problem:* This program is designed to solve the time-dependent GP nonlinear partial differential equation in three space dimensions with a spherically-symmetric trap. The GP equation describes the properties of a dilute trapped Bose–Einstein condensate.

*Method of solution:* The time-dependent GP equation is solved by the split-step Crank–Nicolson method by discretizing in space and time. The discretized equation is then solved by propagation in imaginary time over small time steps. The method yields solutions of stationary problems.

#### **New version program summary (x)**

*Program title:* realtime1d.

*Title of electronic files:* realtime1d.c, realtime1d.h.

*Computer:* Any modern computer with C language compiler installed.

*Maximum RAM memory:* 4 MB.

*Programming language used:* C.

*Typical running time:* 15 min (CPU1), 10 min (CPU2).

*Nature of physical problem:* This program is designed to solve the time-dependent GP nonlinear partial differential equation in one space dimension with a harmonic trap. The GP equation describes the properties of a dilute trapped Bose–Einstein condensate.

*Method of solution:* The time-dependent GP equation is solved by the split-step Crank–Nicolson method by discretizing in space and time. The discretized equation is then solved by propagation in real time over small time steps. The method yields solutions of stationary and non-stationary problems.

#### **New version program summary (xi)**

*Program title:* realtime2d.

*Title of electronic files:* realtime2d.c, realtime2d.h.

*Computer:* Any modern computer with C language compiler installed.

*Maximum RAM memory:* 8 MB.

*Programming language used:* C.

*Typical running time:* 15 min (CPU1), 10 min (CPU2).

*Nature of physical problem:* This program is designed to solve the time-dependent GP nonlinear partial differential equation in two space dimensions with an anisotropic trap. The GP equation describes the properties of a dilute trapped Bose–Einstein condensate.

*Method of solution:* The time-dependent GP equation is solved by the split-step Crank–Nicolson method by discretizing in space and time. The discretized equation is then solved by propagation in real time over small time steps. The method yields solutions of stationary and non-stationary problems.

#### **New version program summary (xii)**

*Program title:* realtime2d-th.

*Title of electronic files:* realtime2d-th.c, realtime2d-th.h.

*Computer:* Any modern computer with C language compiler installed.

*Maximum RAM memory:* 8 MB.

*Programming language used:* C/OpenMP.

*Typical running time:* 5 min (CPU1), 2 min (CPU2).

*Nature of physical problem:* This program is designed to solve the time-dependent GP nonlinear partial differential equation in two space dimensions with an anisotropic trap. The GP equation describes the properties of a dilute trapped Bose–Einstein condensate.

*Method of solution:* The time-dependent GP equation is solved by the split-step Crank–Nicolson method by discretizing in space and time. The discretized equation is then solved by propagation in real time over small time steps. The method yields solutions of stationary and non-stationary problems.

#### **New version program summary (xiii)**

*Program title:* realtimecir.

*Title of electronic files:* realtimecir.c, realtimecir.h.

*Computer:* Any modern computer with C language compiler installed.

*Maximum RAM memory:* 3 MB.

*Programming language used:* C.

*Typical running time:* 5 min (CPU1), 5 min (CPU2).

*Nature of physical problem:* This program is designed to solve the time-dependent GP nonlinear partial differential equation in two space dimensions with a circularly-symmetric trap. The GP equation describes the properties of a dilute trapped Bose–Einstein condensate.

*Method of solution:* The time-dependent GP equation is solved by the split-step Crank–Nicolson method by discretizing in space and time. The discretized equation is then solved by propagation in real time over small time steps. The method yields solutions of stationary and non-stationary problems.

#### **New version program summary (xiv)**

*Program title:* realtime3d.

*Title of electronic files:* realtime3d.c, realtime3d.h.

*Computer:* Any modern computer with C language compiler installed.

*Maximum RAM memory:* 700 MB.

*Programming language used:* C.

*Typical running time:* 15 h (CPU1), 12 h (CPU2).

*Nature of physical problem:* This program is designed to solve the time-dependent GP nonlinear partial differential equation in three space dimensions with an anisotropic trap. The GP equation describes the properties of a dilute trapped Bose–Einstein condensate.

*Method of solution:* The time-dependent GP equation is solved by the split-step Crank–Nicolson method by discretizing in space and time. The discretized equation is then solved by propagation in real time over small time steps. The method yields solutions of stationary and non-stationary problems.

#### **New version program summary (xv)**

*Program title:* realtime3d-th.

*Title of electronic files:* realtime3d-th.c, realtime3d-th.h.

*Computer:* Any modern computer with C language compiler installed.

*Maximum RAM memory:* 700 MB.

*Programming language used:* C/OpenMP.

*Typical running time:* 4 h (CPU1), 1.8 h (CPU2).

*Nature of physical problem:* This program is designed to solve the time-dependent GP nonlinear partial differential equation in three space dimensions with an anisotropic trap. The GP equation describes the properties of a dilute trapped Bose–Einstein condensate.

*Method of solution:* The time-dependent GP equation is solved by the split-step Crank–Nicolson method by discretizing in space and time. The discretized equation is then solved by propagation in real time over small time steps. The method yields solutions of stationary and non-stationary problems.

#### **New version program summary (xvi)**

*Program title:* realtimeaxial.

*Title of electronic files:* realtimeaxial.c, realtimeaxial.h.

*Computer:* Any modern computer with C language compiler installed.

*Maximum RAM memory:* 4 MB.

*Programming language used:* C.

*Typical running time:* 10 min (CPU1), 5 min (CPU2).

*Nature of physical problem:* This program is designed to solve the time-dependent GP nonlinear partial differential equation in three space dimensions with an axially-symmetric trap. The GP equation describes the properties of a dilute trapped Bose–Einstein condensate.

*Method of solution:* The time-dependent GP equation is solved by the split-step Crank–Nicolson method by discretizing in space and time. The discretized equation is then solved by propagation in real time over small time steps. The method yields solutions of stationary and non-stationary problems.

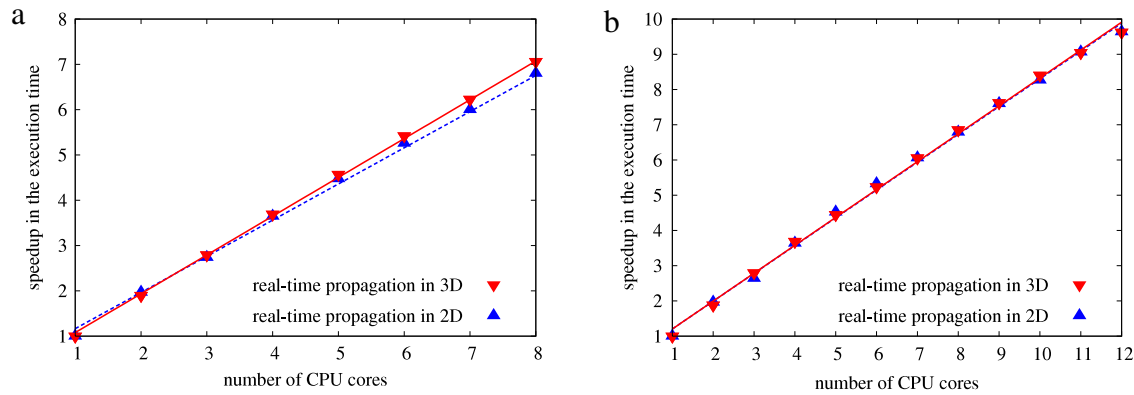


**Fig. 1.** (Colour online) Speedup in the execution time of realtime2d-th and realtime3d-th threaded (OpenMP parallelized) programs as a function of the number of CPU cores used. The results are obtained: (a) on an 8-core machine with  $2 \times$  quad-core Intel Nehalem E5540 CPU at 2.53 GHz, using the icc compiler, (b) on a 12-core machine with  $2 \times$  six-core Intel Nehalem X5650 CPU at 2.66 GHz, using the pgcc compiler. The spatial grid sizes used are  $2000 \times 2000$  (realtime2d-th) and  $1000 \times 1000 \times 300$  (realtime3d-th).

### New version program summary (xvii)

*Program title:* realtimeaxial-th.

*Title of electronic files:* realtimeaxial-th.c, realtimeaxial-th.h.

*Computer:* Any modern computer with C language compiler installed.

*Maximum RAM memory:* 4 MB.

*Programming language used:* C/OpenMP.

*Typical running time:* 5 min (CPU1), 1 min (CPU2).

*Nature of physical problem:* This program is designed to solve the time-dependent GP nonlinear partial differential equation in three space dimensions with an axially-symmetric trap. The GP equation describes the properties of a dilute trapped Bose–Einstein condensate.

*Method of solution:* The time-dependent GP equation is solved by the split-step Crank–Nicolson method by discretizing in space and time. The discretized equation is then solved by propagation in real time over small time steps. The method yields solutions of stationary and non-stationary problems.

### New version program summary (xviii)

*Program title:* reallimesph.

*Title of electronic files:* reallimesph.c, reallimesph.h.

*Computer:* Any modern computer with C language compiler installed.

*Maximum RAM memory:* 2.5 MB.

*Programming language used:* C.

*Typical running time:* 5 min (CPU1), 5 min (CPU2).

*Nature of physical problem:* This program is designed to solve the time-dependent GP nonlinear partial differential equation in three space dimensions with a spherically-symmetric trap. The GP equation describes the properties of a dilute trapped Bose–Einstein condensate.

*Method of solution:* The time-dependent GP equation is solved by the split-step Crank–Nicolson method by discretizing in space and time. The discretized equation is then solved by propagation in real time over small time steps. The method yields solutions of stationary and non-stationary problems.

## References

- [1] P. Muruganandam, S.K. Adhikari, Fortran programs for the time-dependent Gross–Pitaevskii equation in a fully anisotropic trap, *Comput. Phys. Commun.* 180 (2009) 1888.
- [2] G. Mazzarella, L. Salasnich, Collapse of triaxial bright solitons in atomic Bose–Einstein condensates, *Phys. Lett. A* 373 (2009) 4434.
- [3] Y. Cheng, S.K. Adhikari, Symmetry breaking in a localized interacting binary Bose–Einstein condensate in a bichromatic optical lattice, *Phys. Rev. A* 81 (2010) 023620; S.K. Adhikari, H. Lu, H. Pu, Self-trapping of a Fermi superfluid in a double-well potential in the Bose–Einstein-condensate-unity crossover, *Phys. Rev. A* 80 (2009) 063607.
- [4] S. Gautam, D. Angom, Rayleigh–Taylor instability in binary condensates, *Phys. Rev. A* 81 (2010) 053616; S. Gautam, D. Angom, Ground state geometry of binary condensates in axisymmetric traps, *J. Phys. B* 43 (2010) 095302; S. Gautam, P. Muruganandam, D. Angom, Position swapping and pinching in Bose–Fermi mixtures with two-color optical Feshbach resonances, *Phys. Rev. A* 83 (2011) 023605.
- [5] S.K. Adhikari, B.A. Malomed, L. Salasnich, F. Toigo, Spontaneous symmetry breaking of Bose–Fermi mixtures in double-well potentials, *Phys. Rev. A* 81 (2010) 053630.
- [6] G.K. Chaudhary, R. Ramakumar, Collapse dynamics of a  $(176)\text{Yb}-(174)\text{Yb}$  Bose–Einstein condensate, *Phys. Rev. A* 81 (2010) 063603.
- [7] S. Sabari, R.V.J. Raja, K. Porsezian, P. Muruganandam, Stability of trapless Bose–Einstein condensates with two- and three-body interactions, *J. Phys. B* 43 (2010) 125302.
- [8] L.E. Young-S, L. Salasnich, S.K. Adhikari, Dimensional reduction of a binary Bose–Einstein condensate in mixed dimensions, *Phys. Rev. A* 82 (2010) 053601.
- [9] I. Vidanović, A. Balaž, H. Al-Jibbouri, A. Pelster, Nonlinear Bose–Einstein-condensate dynamics induced by a harmonic modulation of the  $s$ -wave scattering length, *Phys. Rev. A* 84 (2011) 013618.
- [10] R.R. Sakhel, A.R. Sakhel, H.B. Ghassib, Self-interfering matter-wave patterns generated by a moving laser obstacle in a two-dimensional Bose–Einstein condensate inside a power trap cut off by box potential boundaries, *Phys. Rev. A* 84 (2011) 033634.
- [11] A. Balaž, A.I. Nicolin, Faraday waves in binary nonmiscible Bose–Einstein condensates, *Phys. Rev. A* 85 (2012) 023613; A.I. Nicolin, Variational treatment of Faraday waves in inhomogeneous Bose–Einstein condensates, *Physica A* 391 (2012) 1062; A.I. Nicolin, Resonant wave formation in Bose–Einstein condensates, *Phys. Rev. E* 84 (2011) 056202; A.I. Nicolin, Faraday waves in Bose–Einstein condensates subject to anisotropic transverse confinement, *Rom. Rep. Phys.* 63 (2011) 1329; A.I. Nicolin, M.C. Raportaru, Faraday waves in high-density cigar-shaped Bose–Einstein condensates, *Physica A* 389 (2010) 4663.
- [12] S. Yang, M. Al-Amri, J. Evers, M.S. Zubairy, Controllable optical switch using a Bose–Einstein condensate in an optical cavity, *Phys. Rev. A* 83 (2011) 053821.
- [13] W. Hua, X.-S. Liu, Dynamics of cubic and quintic nonlinear Schrödinger equations, *Acta Phys. Sinica* 60 (2011) 110210.
- [14] Z. Sun, W. Yang, An exact short-time solver for the time-dependent Schrödinger equation, *J. Chem. Phys.* 134 (2011) 041101.
- [15] A. Balaž, I. Vidanović, A. Bogojević, A. Belić, A. Pelster, Fast converging path integrals for time-dependent potentials: I. Recursive calculation of short-time expansion of the propagator, *J. Stat. Mech. Theory Exp.* (2011) P03004.
- [16] W.B. Cardoso, A.T. Avelar, D. Bazeia, One-dimensional reduction of the three-dimensional Gross–Pitaevskii equation with two- and three-body interactions, *Phys. Rev. E* 83 (2011) 036604.

# Parametric and geometric resonances of collective oscillation modes in Bose–Einstein condensates

Ivana Vidanović<sup>1</sup>, Hamid Al-Jibbouri<sup>2</sup>, Antun Balaž<sup>1</sup> and Axel Pelster<sup>3,4</sup>

<sup>1</sup> Scientific Computing Laboratory, Institute of Physics Belgrade, University of Belgrade, Pregrevica 118, 11080 Belgrade, Serbia

<sup>2</sup> Free University of Berlin, Arnimallee 14, 14195 Berlin, Germany

<sup>3</sup> University of Duisburg–Essen, Lotharstrasse 1, 47048 Duisburg, Germany

<sup>4</sup> University of Bielefeld, Universitätsstrasse 25, 33501 Bielefeld, Germany

E-mail: [antun@ipb.ac.rs](mailto:antun@ipb.ac.rs)

Received 4 September 2011

Accepted for publication 11 November 2011

Published 27 April 2012

Online at [stacks.iop.org/PhysScr/T149/014003](http://stacks.iop.org/PhysScr/T149/014003)

## Abstract

We analytically and numerically study nonlinear dynamics in Bose–Einstein condensates (BECs) induced either by a harmonic modulation of the interaction or by the geometry of the trapping potential. To analytically describe BEC dynamics, we use a perturbative expansion based on the Poincaré–Lindstedt analysis of a Gaussian variational ansatz, whereas in the numerical approach we use numerical solutions of both a variational system of equations and the full time-dependent Gross–Pitaevskii equation. The harmonic modulation of the atomic s-wave scattering length of a BEC of <sup>7</sup>Li was achieved recently via Feshbach resonance, and such a modulation leads to a number of nonlinear effects, which we describe within our approach: mode coupling, higher harmonics generation and significant shifts in the frequencies of collective modes. In addition to the strength of atomic interactions, the geometry of the trapping potential is another key factor for the dynamics of the condensate, as well as for its collective modes. The asymmetry of the confining potential leads to important nonlinear effects, including resonances in the frequencies of collective modes of the condensate. We study in detail such geometric resonances and derive explicit analytic results for frequency shifts for the case of an axially symmetric condensate with two- and three-body interactions. Analytically obtained results are verified by extensive numerical simulations.

PACS numbers: 03.75.Kk, 03.75.Nt, 67.85.De

(Some figures may appear in colour only in the online journal)

## 1. Introduction

Collective oscillation modes of various physical systems provide important insights into their behavior and represent a valuable source of information about their properties. Collective modes are usually easily accessible experimentally, and a comparison of the measured values of their frequencies with corresponding analytical results obtained from a linear stability analysis provides an essential tool for quantitative assessment of the theoretical description of a given physical system. In Bose–Einstein condensate (BEC) systems [1, 2], collective oscillation modes were among the first properties

to be measured [3, 4] and compared with theoretical results [5–9]. However, the prominent nonlinear features of BECs open up a rich variety of phenomena, such as solitons [10] or Faraday waves [11–15] that arise in different experimental setups. This is most dramatically seen through a resonant behavior, but a number of other phenomena are also observed. For instance, mode coupling due to nonlinearities is always present, and even when we excite only one given collective oscillation mode, in the realistic experimental setup other modes will also be excited eventually. Furthermore, resonances and pronounced nonlinear effects can also be caused purely by the geometry of the trapping potential, thus

making the study of nonlinear effects quite important even for the design of BEC experiments. Therefore, a detailed theoretical and numerical description of nonlinear phenomena is of significant interest and analytic results, which we derive from the Poincaré–Lindstedt analysis, can contribute to a better understanding of them.

In this paper, following the approach introduced in [16], we study nonlinear effects in a BEC due to the harmonic modulation of the *s*-wave scattering length [17], as well as due to the geometry of the trap, where geometric resonances emerge. In section 2, we briefly introduce the mean-field description and the Gaussian variational approach for BEC with two- and three-body contact interactions. We present in section 3 our results on frequency shifts due to the modulation of two-body interactions and due to the geometry of the trap, whereas in section 4, we summarize our main results and give a brief outlook for future research on this topic.

## 2. Variational approach

If we take into account two- and three-body contact interactions, the dynamics of a BEC at zero temperature is described by the generalized Gross–Pitaevskii equation [18]

$$i\hbar \frac{\partial}{\partial t} \Psi(\mathbf{r}, t) = \left\{ -\frac{\hbar^2}{2m} \Delta + V(\mathbf{r}) + g_2 |\Psi(\mathbf{r}, t)|^2 + g_3 |\Psi(\mathbf{r}, t)|^4 \right\} \Psi(\mathbf{r}, t), \quad (1)$$

where  $\Psi(\mathbf{r}, t)$  is a condensate wave function, the trapping potential is considered to be axially symmetric  $V(\mathbf{r}) = \frac{1}{2}m\omega_\rho^2(\rho^2 + \lambda^2 z^2)$  with anisotropy  $\lambda$ , while  $g_2$  and  $g_3$  are two- and three-body interaction strengths, respectively.

In order to obtain analytic results on the low-lying collective modes of a BEC, we use the Gaussian variational ansatz for the ground state [7, 8]

$$\psi^G(\rho, z, t) = \mathcal{N}(t) \exp \left[ -\frac{1}{2} \frac{\rho^2}{u_\rho(t)^2} + i\rho^2 \phi_\rho(t) \right] \times \exp \left[ -\frac{1}{2} \frac{z^2}{u_z(t)^2} + iz^2 \phi_z(t) \right], \quad (2)$$

with the normalization factor  $\mathcal{N}(t) = (\pi^{\frac{3}{2}} u_\rho^2 u_z)^{-1/2}$ . Here  $u_\rho(t)$ ,  $u_z(t)$ ,  $\phi_z(t)$  and  $\phi_\rho(t)$  are variational parameters with a straightforward interpretation:  $u_\rho(t)$  and  $u_z(t)$  correspond to the radial and the axial condensate width, while  $\phi_\rho(t)$  and  $\phi_z(t)$  represent the corresponding phases. After minimization of the Lagrangian corresponding to the Gross–Pitaevskii equation, we arrive at the following nonlinear system of ordinary differential equations for condensate widths, which is our variational description of a BEC:

$$\ddot{u}_\rho(t) + u_\rho(t) - \frac{1}{u_\rho(t)^3} - \frac{p}{u_\rho(t)^3 u_z(t)} - \frac{k}{u_\rho(t)^5 u_z(t)^2} = 0, \quad (3)$$

$$\ddot{u}_z(t) + \lambda^2 u_z(t) - \frac{1}{u_z(t)^3} - \frac{p}{u_\rho(t)^2 u_z(t)^2} - \frac{k}{u_\rho(t)^4 u_z(t)^3} = 0, \quad (4)$$

where

$$p = \frac{g_2 N}{(2\pi)^{3/2} \hbar \omega_\rho \ell^3} \quad \text{and} \quad k = \frac{2g_3 N^2}{9\sqrt{3}\pi^3 \omega_\rho \hbar \ell^6}$$

are dimensionless two- and three-body interaction strengths and  $\ell = \sqrt{\hbar/m\omega_\rho}$  denotes the harmonic oscillator length. Through extensive numeric simulations in [16], it was shown that the above Gaussian variational ansatz can be successfully used for describing the real-time dynamics of BEC systems with parameters similar to the experimental ones from [17].

## 3. Results

Nonlinear terms in the underlying Gross–Pitaevskii equation (1) and consequently in the variational system of equations (3) and (4) lead to a number of interesting effects in the properties of collective modes of a BEC. First we consider the important case of a harmonic modulation of the two-body interaction [17],

$$p(t) = p_0 + q \cos \Omega t, \quad (5)$$

and neglect three-body effects. As we can see from figure 1(a) for a spherically symmetric trap, i.e.  $\lambda = 1$ , when the two-body interaction strength is harmonically modulated with the external driving frequency  $\Omega$ , collective modes exhibit a resonant behavior. The resonant frequencies correspond to collective modes calculated from the linear stability analysis and their higher harmonics. Close to resonances, frequencies of collective modes exhibit shifts from the corresponding linear stability results. By performing a Poincaré–Lindstedt perturbative expansion [19, 20] in the small modulation amplitude  $q$ , we can calculate this shift, which stems from secular terms in solving the hierarchy of equations obtained in the perturbation theory. It turns out that the first correction to the linear stability frequencies is quadratic in the modulation amplitude  $q$  and reads for the quadrupole mode

$$\omega_Q = \omega_{Q0} + q^2 \frac{C_Q}{2\omega_{Q0} A_Q} + \dots \quad (6)$$

Similar results can also be obtained for the breathing mode frequency. The coefficients  $A_Q$  and  $C_Q$  are calculated using the Mathematica code<sup>5</sup>. The structure of the coefficient  $A_Q$  shows that the quadrupole mode frequency contains poles at  $\omega_{Q0}$ ,  $2\omega_{Q0}$ ,  $\omega_{B0} - \omega_{Q0}$ ,  $\omega_{B0}$  and  $\omega_{Q0} + \omega_{B0}$  to second order of perturbation theory. Higher-order calculations would lead to additional poles, which are, indeed, observed numerically [16]. Figure 1(b) compares the analytic result for the frequency shift (6) for an axially symmetric BEC at  $\lambda = 0.3$  with the numerical results obtained by solving the nonlinear variational equations (3)–(4) and performing their Fourier analysis. As we can see, even the first analytically calculated correction to the frequencies of collective oscillation modes is in excellent agreement with the full numerical results.

Next, we consider the interplay between the geometry of the trap, which is represented by the anisotropy  $\lambda$ , and

<sup>5</sup> SCL BEC MATHEMATICA codes, <http://www.scl.rs/speedup>

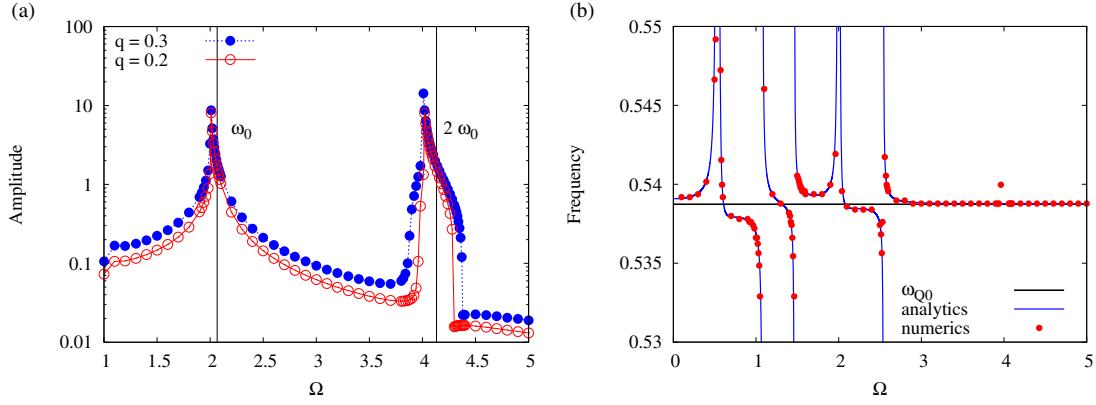


**Figure 1.** (a) Oscillation amplitude  $(u_{\max} - u_{\min})/2$  versus driving frequency  $\Omega$  for  $p_0 = 0.4$ ,  $k = 0$  for a spherically symmetric BEC. The shape and value of a resonance occur at a driving frequency  $\Omega$ , which differs from the linear stability frequency  $\omega_0$ , and depends on the modulation amplitude  $q$ . (b) Frequency of the quadrupole mode  $\omega_Q$  versus driving frequency  $\Omega$  for  $p_0 = 1$ ,  $q = 0.2$  and  $k = 0$  for an axially symmetric BEC with anisotropy  $\lambda = 0.3$ .

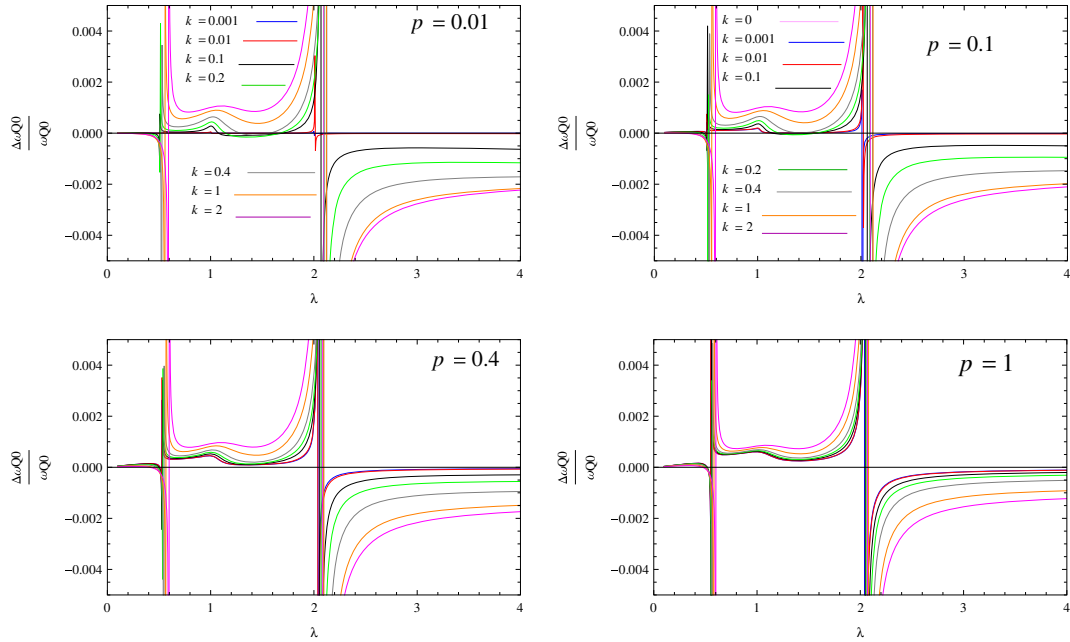


**Figure 2.** Relative frequency shift of the quadrupole oscillation mode versus the trap aspect ratio  $\lambda$  for values of the dimensionless two-body interaction  $p = 0.01, 0.1, 0.4$  and  $1$  and for several values of the dimensionless three-body interaction  $k$ .

nonlinearities due to interactions. In the case of two-body interactions, this was studied within the hydrodynamic approach of [21] and more recently in other formalisms [22, 23]. Here we also consider three-body contact interactions, and describe the BEC system by the variational set of equations (3) and (4). Linear stability analysis yields the frequencies of collective modes:

$$\omega_{B0,Q0} = \left( \frac{m_1 + m_3 \pm \sqrt{(m_1 - m_3)^2 + 8m_2^2}}{2} \right)^{1/2}, \quad (7)$$

$$m_1 = 1 + \frac{3}{u_{\rho 0}^4} + \frac{3p}{u_{\rho 0}^4 u_{z 0}} + \frac{5k}{u_{\rho 0}^6 u_{z 0}^2}, \quad (8)$$

$$m_2 = \frac{p}{u_{\rho 0}^3 u_{z 0}^2} + \frac{2k}{u_{\rho 0}^5 u_{z 0}^3}, \quad (9)$$

$$m_3 = \lambda^2 + \frac{3}{u_{z 0}^4} + \frac{2p}{u_{\rho 0}^2 u_{z 0}^3} + \frac{3k}{u_{\rho 0}^4 u_{z 0}^4}, \quad (10)$$

and  $u_{\rho 0}$  and  $u_{z 0}$  are equilibrium widths, obtained as stationary solutions.

To study nonlinear effects in real-time dynamics, we consider a BEC in the initial state corresponding to the stationary ground state with a small perturbation proportional to the eigenvector of the quadrupole mode. This perturbation, proportional to the small parameter  $\epsilon$ , leads to quadrupole mode oscillations. However, due to nonlinear effects in a BEC, the breathing mode is also excited eventually, as well as other, higher harmonics, which include linear combinations of both modes. The frequency of collective modes depends on the anisotropy  $\lambda$  and, as was shown in [21], exhibit resonances for specific values of  $\lambda$ . For trap geometries with anisotropies close to resonant values, frequencies of collective

oscillation modes are significantly shifted from their linear stability analysis values. If we take into account three-body interactions and apply a Poincaré–Lindstedt perturbative expansion [19, 20] in the small parameter  $\epsilon$ , we obtain the frequency shift of the quadrupole mode in the form

$$\omega_Q = \omega_{Q0} + \epsilon^2 \frac{f(\omega_{Q0}, \omega_{B0}, u_{\rho 0}, u_{z0}, p, k, \lambda)}{2\omega_{Q0}^2(\omega_{B0} - 2\omega_{Q0})(\omega_{B0} + 2\omega_{Q0})}. \quad (11)$$

From this, we can immediately read off poles for the values of  $\lambda$  determined by the condition  $\omega_{B0} = 2\omega_{Q0}$ . Similar results are obtained for the breathing mode. The frequency shifts for the quadrupole mode are illustrated in figure 2 for various values of dimensionless two- and three-body interaction strengths. As we can see from the graphs, for small values of the two-body interaction, the three-body interaction can have a significant effect on the frequency of collective modes. Furthermore, we see that the trap anisotropy can be fine-tuned in such a way that the frequency shift is completely removed. However, as two-body interactions increase, three-body interaction effects become less important and eventually just represent a small correction to the leading two-body behavior.

#### 4. Conclusions

In this paper, we have studied prominent nonlinear effects that arise in BECs due to two- and three-body contact interactions. We have used a Gaussian variational approach which was shown to well describe BEC systems in the range of parameters that are relevant for current experimental setups [16]. Using the Poincaré–Lindstedt perturbation theory, we have calculated frequency shifts due to a harmonic modulation of the s-wave scattering length, motivated by a recent experiment [17]. We have also studied in detail the delicate interplay between nonlinear effects due to two- and three-body interactions and the trap geometry. Within the variational approach and the Poincaré–Lindstedt method, we have calculated frequency shifts and identified the geometric resonances of collective modes of axially symmetric BEC systems. We have also shown that the observed geometric resonances can be eliminated if two- and three-body interactions can be appropriately fine-tuned.

We plan to extend this research and further study the interplay of two- and three-body interactions by considering the case of attractive three-body interaction, when competing effects between repulsive two-body and attractive three-body interactions may give rise to interesting phenomena. We also plan to study mode coupling and energy transfer between quadrupole and breathing oscillation mode due to nonlinear effects.

#### Acknowledgments

This work was supported in part by the Ministry of Education and Science of the Republic of Serbia under project numbers ON171017 and NAD-BEC, by DAAD—German Academic and Exchange Service under the project NAD-BEC, and by the European Commission under the EU FP7 projects PRACE-IIP, HP-SEE and EGI-InSPIRE.

#### References

- [1] Pitaevskii L and Stringari S 2004 *Bose–Einstein Condensation* (Oxford: Clarendon)
- [2] Pethick C J and Smith H 2008 *Bose–Einstein Condensation in Dilute Gases* 2nd edn (Cambridge: Cambridge University Press)
- [3] Jin D S, Ensher J R, Matthews M R, Wieman C E and Cornell E A 1996 *Phys. Rev. Lett.* **77** 420
- [4] Mewes M O, Andrews M R, van Druten N J, Kurn D M, Durfee D S, Townsend C G and Ketterle W 1996 *Phys. Rev. Lett.* **77** 988
- [5] Edwards M, Ruprecht P A, Burnett K, Dodd R J and Clark C W 1996 *Phys. Rev. Lett.* **77** 5320
- [6] Stringari S 1996 *Phys. Rev. Lett.* **77** 2360
- [7] Pérez-García V M, Michinel H, Cirac J I, Lewenstein M and Zoller P 1996 *Phys. Rev. Lett.* **77** 2360
- [8] Pérez-García V M, Michinel H, Cirac J I, Lewenstein M and Zoller P 1997 *Phys. Rev. A* **56** 1424
- [9] Hutchinson D A W, Zaremba E and Griffin A 1997 *Phys. Rev. Lett.* **78** 1842
- [10] Malomed B 2006 *Soliton Management in Periodic Systems* (New York: Springer)
- [11] Nicolin A I, Carretero-González R and Kevrekidis P G 2007 *Phys. Rev. A* **76** 063609
- [12] Nicolin A I and Raportaru M C 2010 *Physica A* **389** 4663
- [13] Nicolin A I and Raportaru M C 2011 *Proc. Rom. Acad. Ser. A* **12** 209
- [14] Nicolin A I 2011 *Rom. Rep. Phys.* **63** 1329
- [15] Nicolin A I 2011 *Phys. Rev. E* **84** 056202  
Nicolin A I 2012 *Physica A* **391** 1062  
Balaž A and Nicolin A I 2012 *Phys. Rev. A* **85** 023613
- [16] Vidanović I, Balaž A, Al-Jibbouri H and Pelster A 2011 *Phys. Rev. A* **84** 013618
- [17] Pollack S E, Dries D, Hulet R G, Magalhães K M F, Henn E A L, Ramos E R F, Caracanhas M A and Bagnato V S 2010 *Phys. Rev. A* **81** 053627
- [18] Yong W-M, Wei X-F, Zhou X-Y and Xue J-K 2009 *J. Commun. Theor. Phys.* **51** 433
- [19] Bogoliubov N N and Mitropolsky Y A 1961 *Asymptotic Methods in the Theory of Non-Linear Oscillations* (New York: Gordon and Breach)
- [20] Pelster A, Kleinert H and Schanz M 2003 *Phys. Rev. E* **67** 016604
- [21] Dalfovo F, Minniti C and Pitaevskii L P 1997 *Phys. Rev. A* **56** 4855
- [22] Adhikari S K 2003 *J. Phys. B: At. Mol. Opt. Phys.* **36** 1109
- [23] Filatrella G, Malomed B A and Salasnich L 2009 *Phys. Rev. A* **79** 045602



# Geometric resonances in Bose–Einstein condensates with two- and three-body interactions

Hamid Al-Jibbouri<sup>1</sup>, Ivana Vidanović<sup>2,3</sup>, Antun Balaz̃<sup>2,4</sup>  
and Axel Pelster<sup>4,5</sup>

<sup>1</sup> Institut für Theoretische Physik, Freie Universität Berlin, Arnimallee 14, D-14195 Berlin, Germany

<sup>2</sup> Scientific Computing Laboratory, Institute of Physics Belgrade, University of Belgrade, Pregrevica 118, 11080 Belgrade, Serbia

<sup>3</sup> Institut für Theoretische Physik, Johann Wolfgang Goethe-Universität, D-60438 Frankfurt am Main, Germany

<sup>4</sup> Hanse-Wissenschaftskolleg, Lehmkuhlenbusch 4, D-27733 Delmenhorst, Germany

<sup>5</sup> Fachbereich Physik und Forschungszentrum OPTIMAS, Technische Universität Kaiserslautern, D-67663 Kaiserslautern, Germany

E-mail: [antun@ipb.ac.rs](mailto:antun@ipb.ac.rs)

Received 9 October 2012, in final form 18 January 2013

Published 7 March 2013

Online at [stacks.iop.org/JPhysB/46/065303](http://stacks.iop.org/JPhysB/46/065303)

## Abstract

We investigate geometric resonances in Bose–Einstein condensates by solving the underlying time-dependent Gross–Pitaevskii equation for systems with two- and three-body interactions in an axially symmetric harmonic trap. To this end, we use a recently developed analytical method (Vidanović *et al* 2011 *Phys. Rev. A* **84** 013618), based on both a perturbative expansion and a Poincaré–Lindstedt analysis of a Gaussian variational approach, as well as a detailed numerical study of a set of ordinary differential equations for variational parameters. By changing the anisotropy of the confining potential, we numerically observe and analytically describe strong nonlinear effects: shifts in the frequencies and mode coupling of collective modes, as well as resonances. Furthermore, we discuss in detail the stability of a Bose–Einstein condensate in the presence of an attractive two-body interaction and a repulsive three-body interaction. In particular, we show that a small repulsive three-body interaction is able to significantly extend the stability region of the condensate.

(Some figures may appear in colour only in the online journal)

## 1. Introduction

The experimental discovery of Bose–Einstein condensation [1–6] has instigated extensive experimental and theoretical studies of ultracold atoms and molecules. In particular, many experiments have focused on collective excitations of harmonically trapped Bose–Einstein condensates (BECs), as their frequencies can be measured to the order of a few per mill [7–10] and calculated analytically [11–17], and thus provide a reliable method for extracting ultracold system parameters.

A wide variety of interesting nonlinear phenomena are observed in collective excitations of BECs, including frequency shifts [18, 19], mode coupling [18, 20, 21], damping [9, 22], nonlinear interferometry [23], as well as collapse and

revival of oscillations [18, 24, 25]. The collective oscillation modes can be induced in a BEC by modulating the external potential trap [7, 8, 18, 26–39], the s-wave scattering length [19, 40–43] or three-body interactions [42, 44].

Resonant coupling between collective modes in a BEC was experimentally observed [20, 45], and it was shown that, when the parity quadrupole mode is excited by changing the trap anisotropy parameter above a certain value, it is possible to achieve an energy transfer between modes at a rate [21] which is comparable to the collective mode frequency. In [18], the frequency shift of collective modes due to the trap anisotropy in a generic axially symmetric geometry was studied, and it was shown that the collective modes exhibit a resonant

behaviour for specific values of the trap anisotropy, which are called geometric resonances, and that the strong effects can be observed even for oscillations of relatively small amplitude. The excitations and coupling of quadrupole and scissor modes in two-component BECs were investigated in [46]. Recently, also a coupling of the dipole, breathing and quadrupole modes close to a Feshbach resonance was analysed in [47].

In this paper, we study geometric resonances and resonant mode coupling in BECs with two- and three-body contact interactions. Theoretical studies of collective excitations are usually focused on two-body contact interactions due to the diluteness of quantum gases [10, 18–21, 41, 48]. However, the experimental progress with BECs in atomic waveguides and on the surface of atomic chips, which involve a strong increase in the density of BECs, also necessitates the study of three-body interactions [49–51]. Theoretical and experimental studies [49, 52, 53] for a BEC of  $^{87}\text{Rb}$  atoms indicated that the real part of the three-body interaction term can be  $10^3$ – $10^4$  times larger than the imaginary part. The imaginary part, which arises from three-body recombinations, limits the lifetime of the condensate. However, even for a small strength of the three-body interaction, the region of stability for the condensate can be extended considerably according to [54–57]. We study this in more detail and provide a phase diagram which demonstrates the significantly enhanced stability of BECs due to three-body interactions.

Due to the three-body interaction, the density profile [56], the excitation spectrum of the collective oscillations [59, 58] as well as the modulation instability of a trapped BEC [60] is modified. The effects of the three-body interaction were furthermore studied in ultracold bosonic atoms in an optical lattice [51, 61–68], BCS-BEC crossover [69], complex solitons BEC [70] and vortex BEC [71]. In addition, an extensive work was done on the study of cubic–quintic nonlinear equations, most notably in the context of nonlinear optics and superfluid helium. Even though these studies were done in uniform systems, many of the results are quite relevant for trapped systems as well. In particular, we mention studies of cavitation [72], droplets [73], as well as dynamics, solitary waves and vortex nucleation [74]. The transition temperature, the depletion of the condensate atoms and the collective excitations of a BEC with two- and three-body interactions in an anharmonic trap at finite temperature are studied in [75]. Reference [76] shows that the frequency of the collective excitation is also significantly affected by the strength of the three-body interaction and the anharmonicity of the potential. In [77], the authors investigated the collective excitations and the stability of a BEC in a one-dimensional trapping geometry for the case of repulsive or attractive three-body and repulsive two-body interactions.

Motivated by this, we study here the dynamics of the condensate with both two- and three-body contact interactions in general and its collective oscillation modes in particular by changing the geometry of the trapping potential. Within a Gaussian variational approach, the partial differential equation of Gross and Pitaevskii is transformed in section 2 into a set of ordinary differential equations for the condensate widths. We then discuss in detail in section 3 the resulting stability of the

condensate. First, we consider the case of an attractive two-body interaction and a vanishing three-body interaction, and afterwards the case of attractive two-body and repulsive three-body interactions. In section 4, we study geometric resonances and derive explicit analytic results for the frequency shifts for the case of an axially symmetric condensate based on a perturbative expansion and a Poincaré–Lindstedt method. This frequency shift is calculated for a quadrupole mode in subsection 4.1, for a breathing mode in subsection 4.2 and the derived analytical results are then compared with the results of numerical simulations in subsection 4.3. In that subsection, we also compare results of numerical simulations for radial and longitudinal condensate widths and the corresponding excitations spectra with the analytical results obtained using perturbation theory. Then, in section 5, we analyse the resonant mode coupling and the generation of second harmonics of the collective modes. Finally, in section 6 we summarize our findings and present our conclusions.

## 2. Variational approach

The dynamics of a Bose–Einstein-condensed gas in a trap at zero temperature is well described by the time-dependent Gross–Pitaevskii (GP) equation [76–81]. Usually, only two-body contact interactions are considered due to the diluteness of the gas. In this paper, however, we study systems where also three-body contact interactions have to be taken into account [82, 52]. In that case, the GP equation has the form

$$i\hbar \frac{\partial}{\partial t} \psi(\mathbf{r}, t) = \left[ -\frac{\hbar^2}{2m} \Delta + V(\mathbf{r}) + g_2 N |\psi(\mathbf{r}, t)|^2 + g_3 N^2 |\psi(\mathbf{r}, t)|^4 \right] \psi(\mathbf{r}, t), \quad (1)$$

where  $\psi(\mathbf{r}, t)$  denotes a condensate wavefunction normalized to unity and  $N$  is the total number of atoms in the condensate. On the right-hand side of the above equation, we have a kinetic energy term, an external axially symmetric harmonic trap potential  $V(\mathbf{r}) = \frac{1}{2} m \omega_\rho^2 (\rho^2 + \lambda^2 z^2)$  with the anisotropy parameter  $\lambda = \omega_z / \omega_\rho$ , while the parameters  $g_2$  and  $g_3$  account for the strength of two-body and three-body contact interactions, respectively. The two-body interaction strength  $g_2 = 4\pi \hbar^2 a / m$  is proportional to the s-wave scattering length  $a$ , where  $m$  denotes the mass of the corresponding atomic species.

The three-body interaction strength  $g_3$  becomes important not only for large values of the s-wave scattering length, but also for small values of  $a$  close to the ideal gas regime. It is well known that the stability against the collapse of  $^{85}\text{Rb}$  cannot be described by using only the two-body scattering [83]. The three-body scattering also plays an essential role in understanding the Efimov physics, where three bosons form a bound state [84, 85]. Braaten and Nieto [86] have used an effective field theory to calculate the strength of the three-body interaction, which effectively arises from the two-body interaction, and obtained the result  $g_3(\kappa) = 384\pi (4\pi - 3\sqrt{3}) [\ln \kappa a + B] \hbar^2 a^4 / m$ , where  $\kappa$  is an arbitrary wave number and  $B$  is a complex constant, both being suitably fixed in [86]. Thus, in general, the effective three-body coupling

strength represents a complex number, where its imaginary part describes recombination effects. However, its real part turns out to be much larger, and the fit to experimental data for  $^{85}\text{Rb}$  and  $^{87}\text{Rb}$  gives typical values for  $\text{Re}(g_3)/\hbar$  of the order of  $10^{-27}$  to  $10^{-26} \text{ cm}^6 \text{ s}^{-1}$  [87, 75, 88].

Equation (1) can be cast into a variational problem, which corresponds to the extremization of the action defined by the Lagrangian  $L(t) = \int \mathcal{L}(\mathbf{r}, t) \mathbf{dr}$ , with the Lagrangian density

$$\mathcal{L}(\mathbf{r}, t) = \frac{i\hbar}{2} \left( \psi^* \frac{\partial \psi}{\partial t} - \psi \frac{\partial \psi^*}{\partial t} \right) - \frac{\hbar^2}{2m} |\nabla \psi|^2 - V(\mathbf{r}) |\psi|^2 - \frac{g_2 N}{2} |\psi|^4 - \frac{g_3 N^2}{3} |\psi|^6. \quad (2)$$

In order to analytically study the dynamics of BEC systems with two- and three-body interactions, we use the Gaussian variational ansatz, which was introduced in [15, 16]. For an axially symmetric trap, this time-dependent ansatz reads

$$\psi^G(\rho, z, t) = \mathcal{N}(t) \exp \left[ -\frac{1}{2} \frac{\rho^2}{u_\rho(t)^2} + i\rho^2 \phi_\rho(t) \right] \times \exp \left[ -\frac{1}{2} \frac{z^2}{u_z(t)^2} + iz^2 \phi_z(t) \right], \quad (3)$$

where  $\mathcal{N}(t) = 1/\sqrt{\pi^{\frac{3}{2}} u_\rho^2(t) u_z(t)}$  is a normalization factor, while  $u_\rho(t)$ ,  $u_z(t)$ ,  $\phi_z(t)$  and  $\phi_\rho(t)$  are variational parameters, representing radial and axial condensate widths and the corresponding phases. The ansatz (3) describes dynamics of the condensate in terms of the time-dependent condensate widths and phases, while no centre-of-mass motion is considered here. A similar variational ansatz including the centre-of-mass motion has been studied in [89], and would be suitable to investigate how the centre-of-mass motion couples to the collective oscillation modes in the presence of three-body interactions.

If we insert the Gaussian ansatz (3) into the Lagrangian (2), we obtain the Lagrange function

$$L(t) = -\frac{\hbar}{2} (2\dot{\phi}_\rho u_\rho^2 + \dot{\phi}_z u_z^2) - \frac{m\omega_\rho^2}{2} \left( u_\rho^2 + \lambda^2 \frac{u_z^2}{2} \right) - \frac{\hbar^2}{2m} \left[ \left( \frac{1}{u_\rho^4} + 4\phi_\rho^2 \right) u_\rho^2 + \left( \frac{1}{u_z^4} + 4\phi_z^2 \right) \frac{u_z^2}{2} \right] - \frac{g_2 N}{2(2\pi)^{3/2} u_\rho^2 u_z} - \frac{g_3 N^2}{9\sqrt{3}\pi^3 u_\rho^4 u_z^2}. \quad (4)$$

From the corresponding Euler–Lagrange equations, we obtain the equations of motion for all variational parameters. The phases  $\phi_\rho$  and  $\phi_z$  can be expressed explicitly in terms of first derivatives of the widths  $u_\rho$  and  $u_z$  according to

$$\phi_\rho = \frac{m\dot{u}_\rho}{2\hbar u_\rho}, \quad \phi_z = \frac{m\dot{u}_z}{2\hbar u_z}. \quad (5)$$

Inserting equations (5) into the Euler–Lagrange equations for the widths, we obtain the second-order differential equation for  $u_\rho$  and  $u_z$ . After introducing the dimensionless parameters

$$\tilde{\omega}_i = \omega_i/\omega_\rho, \quad \tilde{u}_i = u_i/\ell, \quad \tilde{t} = \omega_\rho t \quad (6)$$

with the oscillator length  $\ell = \sqrt{\hbar/m\omega_\rho}$ , we obtain a system of two second-order differential equations for  $u_\rho$  and  $u_z$  in the

dimensionless form

$$\ddot{u}_\rho + u_\rho - \frac{1}{u_\rho^3} - \frac{p}{u_\rho^3 u_z} - \frac{k}{u_\rho^5 u_z^2} = 0, \quad (7)$$

$$\ddot{u}_z + \lambda^2 u_z - \frac{1}{u_z^3} - \frac{p}{u_\rho^2 u_z^2} - \frac{k}{u_\rho^4 u_z^3} = 0, \quad (8)$$

where, for simplicity, we drop the tilde sign in the dimensionless widths. In the above equations,

$$p = \frac{g_2 N}{(2\pi)^{3/2} \hbar \omega_\rho \ell^3} = \sqrt{\frac{2}{\pi}} \frac{Na}{\ell} \quad (9)$$

denotes the dimensionless two-body interaction strength, while the parameter

$$k = \frac{4g_3 N^2}{9\sqrt{3}\pi^3 \hbar \omega_\rho \ell^6} \quad (10)$$

is the dimensionless three-body interaction strength, which can also be expressed in terms of  $p$  as

$$k = \frac{32}{9\sqrt{3}} \frac{g_3 \hbar \omega_\rho}{g_2^2} p^2. \quad (11)$$

For  $N = 10^5$  atoms of  $^{87}\text{Rb}$  [45, 51] in a trap with  $\omega_\rho = 2\pi \times 112 \text{ Hz}$ , the two-body interaction strength is  $g_2 = 5\hbar \times 10^{-11} \text{ cm}^3 \text{ s}^{-1}$ , yielding  $p = 426$ . The three-body interaction is of the order of  $g_3 \approx \hbar \times 10^{-26} \text{ cm}^6 \text{ s}^{-1}$  [51], which gives the dimensionless three-body interaction value  $k = 1050$ .

Although the value of  $k$  is larger than that of  $p$ , the corresponding terms in equations (7) and (8), i.e.  $k/u_\rho^5 u_z^2$  and  $k/u_\rho^4 u_z^3$ , are suppressed by the factor  $u_\rho^2 u_z$  compared to the respective  $p$ -terms. The value of this factor can be estimated by taking into account the equilibrium positions  $u_{\rho 0}$  and  $u_{z 0}$ , which are obtained by solving the stationary equations

$$u_{\rho 0} = \frac{1}{u_{\rho 0}^3} + \frac{p}{u_{\rho 0}^3 u_{z 0}} + \frac{k}{u_{\rho 0}^5 u_{z 0}^2}, \quad (12)$$

$$\lambda^2 u_{z 0} = \frac{1}{u_{z 0}^3} + \frac{p}{u_{\rho 0}^2 u_{z 0}^2} + \frac{k}{u_{\rho 0}^4 u_{z 0}^3}. \quad (13)$$

For the anisotropy  $\lambda = 3/2$ , one numerically obtains  $u_{\rho 0} \approx 3.69$  and  $u_{z 0} \approx 2.47$ , yielding the value  $u_{\rho 0}^2 u_{z 0} \approx 33.6$ . This shows that the terms proportional to  $k$  have the effective coupling  $k/33.6 \approx 31.2$ , which makes them small corrections of the order of 7% to the leading two-body interaction terms. However, if the system exhibits resonances, this may no longer be true, and three-body interactions can play a significant role for the system dynamics. In this paper, we study geometric resonances, where it turns out to be necessary to take into account effects of three-body interactions. The s-wave scattering length can be tuned to any value, large or small, positive or negative, by applying an external magnetic field, using the Feshbach resonance technique [90, 91]. Therefore, in this paper we will consider a range of experimentally realistic values for dimensionless interaction strengths  $p$  and  $k$ .

Using the Gaussian approximation enables us to analytically estimate frequencies of the low-lying collective modes [15, 16, 19]. This is done by linearizing equations (7)

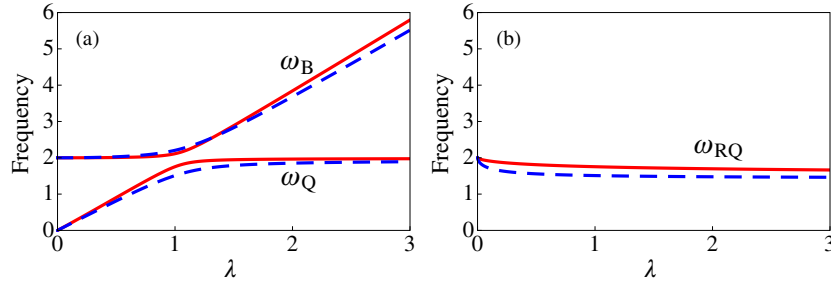


**Figure 1.** Frequencies (in units of  $\omega_\rho$ ) of collective oscillation modes for (a) breathing and quadrupole modes and (b) the radial quadrupole mode versus the trap aspect ratio  $\lambda$  for  $p = 1, k = 0.001$  (solid red lines) and  $p = 10, k = 0.1$  (dashed blue lines).

and (8) around the equilibrium positions. If we expand the condensate widths as  $u_\rho(t) = u_{\rho 0} + \delta u_\rho(t)$  and  $u_z(t) = u_{z 0} + \delta u_z(t)$ , insert these expressions into the corresponding equations and expand them around the equilibrium widths by keeping only linear terms, we immediately obtain the frequencies of the breathing and the quadrupole modes,

$$\omega_{B,Q}^2 = \frac{m_1 + m_3 \pm \sqrt{(m_1 - m_3)^2 + 8m_2^2}}{2}, \quad (14)$$

where the abbreviations  $m_1, m_2$  and  $m_3$  are given by

$$\begin{aligned} m_1 &= 4 + \frac{2k}{u_{\rho 0}^6 u_{z 0}^2}, & m_2 &= \frac{p}{u_{\rho 0}^3 u_{z 0}^2} + \frac{2k}{u_{\rho 0}^5 u_{z 0}^3}, \\ m_3 &= 4\lambda^2 - \frac{p}{u_{\rho 0}^2 u_{z 0}^3}, \end{aligned} \quad (15)$$

and the corresponding breathing and quadrupole mode eigenvectors are given by

$$\mathbf{u}_{B,Q} = \frac{1}{\sqrt{m_2^2 + (\omega_{B,Q}^2 - m_1)^2}} \begin{pmatrix} m_2 \\ \omega_{B,Q}^2 - m_1 \end{pmatrix}. \quad (16)$$

The quadrupole mode has a lower frequency and is characterized by out-of phase radial and axial oscillations, while in-phase oscillations correspond to the breathing mode. Another low-lying collective excitation is the radial quadrupole mode, which is characterized by out-of-phase oscillations in the  $x$  and  $y$  directions, while in the  $z$  direction there are no oscillations. As this mode breaks the cylindrical symmetry, it can only be calculated by using the three-dimensional equations of motion. The frequency turns out to be

$$\omega_{RQ}^2 = 2 + \frac{2}{u_{\rho 0}^4}, \quad (17)$$

and the corresponding three-dimensional eigenvector is

$$\mathbf{u}_{RQ} = \frac{1}{\sqrt{2}} \begin{pmatrix} 1 \\ -1 \\ 0 \end{pmatrix}. \quad (18)$$

Figure 1 shows the frequencies of all collective oscillation modes as functions of the trap aspect ratio  $\lambda$ . We see that the collective mode frequencies depend relatively strongly on the trap anisotropy, whereas a variation of the dimensionless interaction strengths  $p$  and  $k$  yields only marginal changes.

### 3. Stability diagram

In this section, we discuss the stability of a BEC in the mean-field framework for systems with two- and three-body contact interaction in an axially symmetric harmonic trap. It is well known that BEC systems with an attractive two-body interaction are unstable against collapse above the critical number of atoms (i.e. for a sufficiently large negative value of  $p$ ) in the condensate [80, 81]. For smaller numbers of atoms, the zero-point kinetic energy is able to counter the attractive inter-atomic interactions; however, when the number of atoms sufficiently increases, this is no longer possible, and the system collapses to the centre of the trapping potential.

We find that, for a pure two-body interaction, the condensate is stable only above a critical stability line  $p_c(\lambda)$ , while the presence of even a small repulsive three-body interaction leads to the stabilization of the condensate. On the other hand, we find that an attractive three-body interaction further destabilizes the condensate.

To study in detail the effects of the three-body interaction on the stability of BEC systems, we consider several cases of interest: repulsive and attractive pure two-body interactions, attractive two-body and repulsive three-body interactions, and attractive two- and three-body interactions. If the corresponding system of equations does (not) have positive and bounded solutions of equations (7) and (8) in the vicinity of positive equilibrium widths determined by equations (12) and (13), then the condensate is considered stable (unstable). This is equivalent to performing a linear stability analysis and determining the stability of positive equilibrium widths by examining frequencies of the corresponding collective oscillation modes (14) and (17). The solution is only stable if frequencies of all low-lying collective modes are found to be real; otherwise the solution is unstable.

For the case of a pure repulsive two-body interaction, we will immediately see that the condensate is always stable. For the case of an attractive two-body interaction, the situation is quite different: the above system of equations can have no equilibrium, or it could have up to three equilibrium solutions. The results of a detailed numerical analysis are summarized in figure 2.

The dashed red line in figure 2(a) represents the critical stability line as a function of the trap aspect ratio  $\lambda$  for a pure two-body interaction ( $k = 0$ ). Below the critical stability line, there are no stable solutions and the system is unstable.

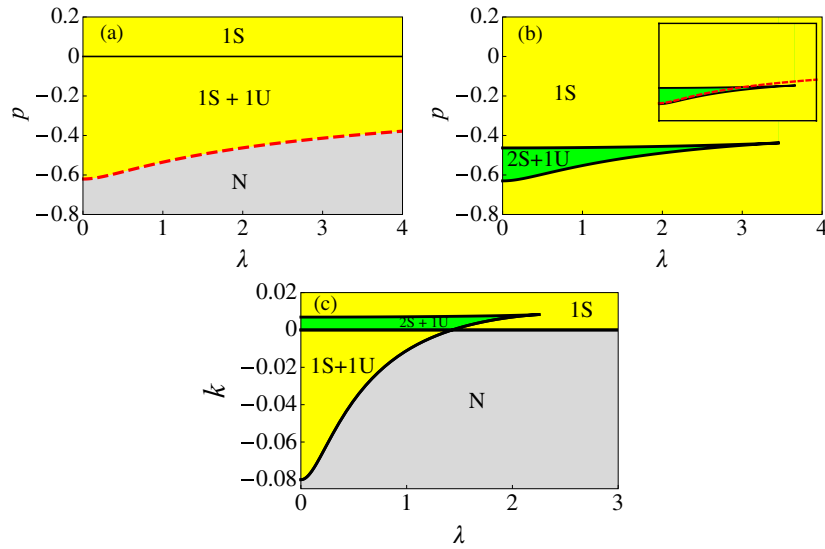


**Figure 2.** Stability diagram of a BEC as a function of a trap aspect ratio  $\lambda$  for different values of dimensionless two-body and three-body contact interaction strengths  $p$  and  $k$ . (a)  $\lambda$ - $p$  stability diagram for  $k = 0$ , where the dashed red line represents the critical stability line, below which there are no solutions (N). Above this line, for  $p < 0$ , there is one stable and one unstable solution (1S+1U), while for  $p \geq 0$  there is only one stable solution (1S). (b)  $\lambda$ - $p$  stability diagram for  $k = 0.005$ , where two cases exist: the small region with two stable and one unstable solution (2S+1U), while otherwise only one stable solution exists (1S). For comparison, in the inset we combine the critical stability line for  $k = 0$  with the stability diagram for  $k = 0.005$ . (c)  $\lambda$ - $k$  stability diagram for  $p = -0.5$ . For  $k \leq 0$ , there are two regions: the one without solutions (N), and the one with one stable and one unstable solution (1S+1U). For  $k > 0$ , there are also two regions: the small region with two stable solutions and one unstable solution (2S+1U), while otherwise there is only one stable solution (1S). As we can see, a non-vanishing value of the three-body interaction  $k$  substantially enhances the stability of a condensate.

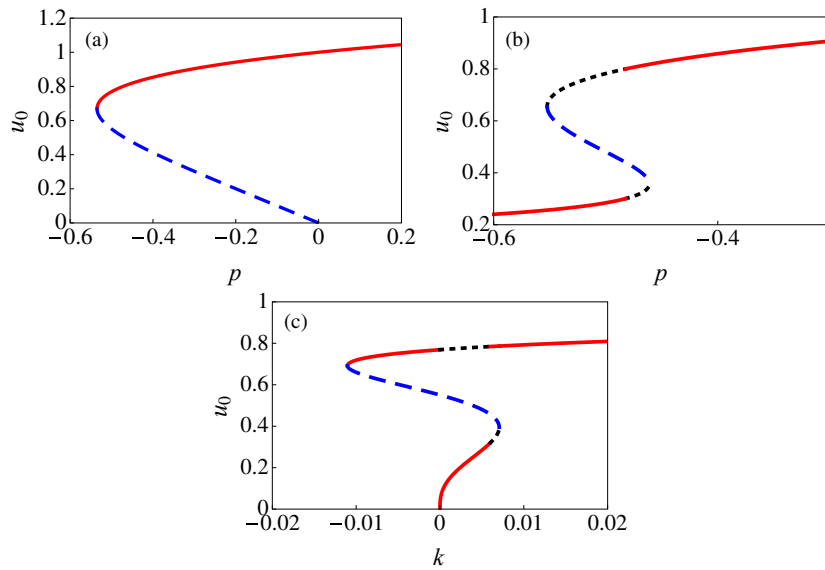


**Figure 3.** Condensate width  $u_{\rho 0} = u_{z 0} = u_0$  for  $\lambda = 1$  and (a)  $k = 0$ , as a function of  $p$ ; (b)  $k = 0.005$ , as a function of  $p$ ; (c)  $p = -0.5$ , as a function of  $k$ . The solid red lines represent the stable solution with minimal energy, the dotted black lines represent another stable solution and the dashed blue lines represent the unstable solution.

Above the critical stability line, the system has one stable and one unstable solution for an attractive two-body interaction ( $p < 0$ ), and only one stable solution for a repulsive two-body interaction ( $p \geq 0$ ). For  $\lambda = 0$ , which corresponds to the limit of a cigar-shaped condensate, we have the critical value of two-body interactions  $p_c = -0.6204$ , which coincides precisely with the value from [16]. For the isotropic case, when  $\lambda = 1$ , the critical value is  $p_c = -0.535$ , which again coincides with

the value from the literature [6, 16, 87, 57]. Figure 3(a) shows solutions for the isotropic condensate as a function of  $p$ .

Now, if we consider the case of an attractive two-body interaction and a small repulsive three-body interaction, then the results of the stability analysis are quite different. The system can either have one or three solutions, as shown in figure 2(b). The presence of a positive three-body interaction  $k$ , however small, leads to the existence of at least one stable

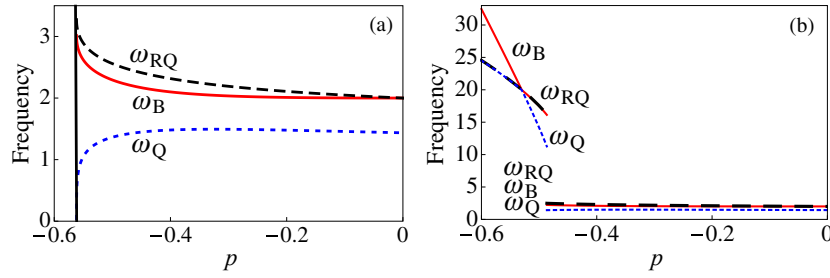


**Figure 4.** Frequencies (in units of  $\omega_\rho$ ) of low-lying collective excitation modes: breathing (B), radial quadrupole (RQ) and quadrupole (Q), as functions of an attractive two-body interaction  $p$  for the trap anisotropy  $\lambda = 117/163$  and (a)  $k = 0$ , (b)  $k = 0.005$ .

solution in the whole range of values of  $\lambda$  and  $p$ . In the small area designated by 2S+1U in figure 2(b), two stable solutions and one unstable solution exist. Out of these two stable solutions, only the one with the minimal energy is physically relevant and could be realized in an experiment. Figure 3(b) shows solutions for  $\lambda = 1, k = 0.005$  as a function of  $p$ . As we can see, a minimal-energy stable solution exists for any value of  $p$ . However, for large negative values of  $p$  this solution tends to zero, which practically represents a collapsed condensate. Therefore, although within the given mathematical model the condensate is always stable, physically this is valid only up to a critical number of atoms, which has to be determined by considering in detail the corresponding condensate density. However, as we can see from figure 3(b), the dependence  $u_0(p)$  for large negative values of  $p$  is quite flat, which means that the stability region can be significantly extended in the presence of a small positive value of  $k$  compared to the case of pure two-body interaction.

We also analyse the stability of a BEC system as a function of the three-body interaction  $k$ . Figure 2(c) shows the corresponding stability diagram for an attractive two-body interaction  $p = -0.5$ . For a repulsive three-body interaction ( $k > 0$ ), as expected, we see a small region with two stable solutions and one unstable solution (2S+1U), as well as a region with only one stable solution (1S), similar to figure 2(b). For an attractive three-body interaction ( $k < 0$ ), the stability region with one stable and one unstable solution (1S+1U), which corresponds to the 1S+1U region in figure 2(a), gradually shrinks until it disappears as  $k$  becomes sufficiently negative. Therefore, we see that an attractive three-body interaction has the same destabilizing effect on a BEC as an attractive two-body interaction. This can also be seen in figure 3(c), where the stable minimal-energy solution for  $p = -0.5$  exists only for a limited range of negative values of  $k$ .

To further illustrate the findings of the above stability analysis, we plot in figure 4 the frequencies of the low-lying collective excitation modes as functions of an attractive two-body interaction for the trap anisotropy  $\lambda = 117/163$  [3]. Figure 4(a) corresponds to the case when three-body interactions are neglected, i.e.  $k = 0$ , and we can see that the condensate collapses for  $p_c = -0.561$ , when the expression for  $\omega_Q^2$  from equation (14) becomes negative. For a small repulsive three-body interaction  $k = 0.005$ , figure 4(b) shows the frequencies corresponding to stable minimum-energy solutions. From figure 3(b) we see that for  $p_c = -0.486$

there is a jump from one to another solution branch due to the minimal energy condition, which is reflected in figure 4(b) by a corresponding jump in the frequencies of the collective modes.

#### 4. Shifts in frequencies of collective modes

Close to geometric resonances, the nonlinear structure of the GP equation (1) leads to shifts in the frequencies of collective oscillation modes compared to the respective values in equation (14), which are calculated using a linear stability analysis. Here we apply the standard Poincaré–Lindstedt method [92–95, 19] in order to develop a perturbation theory and calculate these frequency shifts.

##### 4.1. Quadrupole mode

We start with working out a perturbation theory for the BEC dynamic, which is based on the set of ordinary differential equations (7)–(8), by expanding the condensate widths in the series

$$u_\rho(t) = u_{\rho 0} + \varepsilon u_{\rho 1}(t) + \varepsilon^2 u_{\rho 2}(t) + \varepsilon^3 u_{\rho 3}(t) + \dots, \quad (19)$$

$$u_z(t) = u_{z 0} + \varepsilon u_{z 1}(t) + \varepsilon^2 u_{z 2}(t) + \varepsilon^3 u_{z 3}(t) + \dots, \quad (20)$$

where the smallness parameter  $\varepsilon$  stems from the respective initial conditions. Here we study the system dynamics with the initial conditions in the form

$$\mathbf{u}(0) = \mathbf{u}_0 + \varepsilon \mathbf{u}_Q, \quad \dot{\mathbf{u}}(0) = \mathbf{0}, \quad (21)$$

when the system is close to the equilibrium position  $\mathbf{u}_0$ , and is perturbed in the direction of the quadrupole oscillation mode eigenvector  $\mathbf{u}_Q$ , determined by equation (16). By inserting expansions (19) and (20) into equations (7) and (8), we obtain the following system of linear differential equations:

$$\ddot{u}_{\rho n}(t) + m_1 u_{\rho n}(t) + m_2 u_{zn}(t) = \chi_{\rho n}(t), \quad (22)$$

$$\ddot{u}_{zn}(t) + 2m_2 u_{\rho n}(t) + m_3 u_{zn}(t) = \chi_{zn}(t), \quad (23)$$

where the index  $n$  takes integer values  $n = 1, 2, 3, \dots$ , and the quantities  $m_1, m_2$  and  $m_3$  are already defined by expressions (15). The functions  $\chi_{\rho n}(t)$  and  $\chi_{zn}(t)$  depend only on the solutions  $u_{\rho i}(t)$  and  $u_{zi}(t)$  of lower orders  $i$ , i.e. those corresponding to  $i < n$ . Therefore, the above system of equations can be solved hierarchically, and at each level  $n$  of this procedure, we use the initial conditions from equations (21).

In order to decouple the system of equations (22)–(23), we use the linear transformation

$$u_{\rho n}(t) = x_n(t) + y_n(t), \quad (24)$$

$$u_{zn}(t) = c_1 x_n(t) + c_2 y_n(t) \quad (25)$$

with the coefficients

$$c_{1,2} = \frac{m_3 - m_1 \mp \sqrt{(m_3 - m_1)^2 + 8m_2^2}}{2m_2}, \quad (26)$$

which leads to two independent linear second-order differential equations:

$$\ddot{x}_n(t) + \omega_Q^2 x_n(t) + \frac{c_2 \chi_{\rho n}(t) - \chi_{zn}(t)}{c_1 - c_2} = 0, \quad (27)$$

$$\ddot{y}_n(t) + \omega_B^2 y_n(t) + \frac{\chi_{zn}(t) - c_1 \chi_{\rho n}(t)}{c_1 - c_2} = 0. \quad (28)$$

From this we see that  $x_n(t)$  and  $y_n(t)$  correspond to quadrupole and breathing mode oscillations, respectively. Although the system is initially perturbed only in the direction of the quadrupole mode eigenvector, due to the nonlinearity of the system, the breathing mode is excited as well. The solutions of the above equations depend essentially on the nature of the inhomogeneous terms, which are given by polynomials of harmonic functions of  $\omega_Q t$ ,  $\omega_B t$  and their linear combinations  $(k\omega_Q + m\omega_B)t$ . Therefore, compared to linear systems, the important difference here is that higher harmonics and linear combinations of the modes emerge due to the structure of the GP equation.

A careful analysis also reveals the important conclusion that secular terms will start appearing at the level  $n = 3$ . As usual, they can be absorbed by a shift in the quadrupole mode frequency [19, 92–95]. At level  $n = 3$ , equations (22)–(23) can be written as

$$\ddot{\mathbf{u}}_3(t) + \mathcal{M}\mathbf{u}_3(t) + \mathbf{I}_{Q,3} \cos \omega_Q t + \dots = 0, \quad (29)$$

with the matrix  $\mathcal{M}$  defined as

$$\mathcal{M} = \begin{pmatrix} m_1 & m_2 \\ 2m_2 & m_3 \end{pmatrix}, \quad (30)$$

and the dots represent the inhomogeneous part of the equation, which does not contain linear terms proportional to harmonic functions in  $\omega_Q t$ . The expression for  $\mathbf{I}_{Q,n}$  can be calculated systematically in the *Mathematica* software package [96].

The frequency shift of the quadrupole mode is found to be quadratic in  $\varepsilon$ :

$$\omega_Q(\varepsilon) = \omega_Q + \Delta\omega_Q = \omega_Q - \varepsilon^2 \frac{(\mathbf{u}_Q^L)^T \mathbf{I}_{Q,3}}{2\omega_Q}, \quad (31)$$

where  $\mathbf{u}_Q^L$  is the left-hand quadrupole mode eigenvector of the matrix  $\mathcal{M}$ . After a detailed calculation, the frequency shift of a quadrupole mode to lowest order in  $\varepsilon$  is found to be

$$\Delta\omega_Q = -\varepsilon^2 \frac{f_{Q,3}(\omega_Q, \omega_B, u_{\rho 0}, u_{z0}, p, k, \lambda)}{2\omega_Q(\omega_B - 2\omega_Q)(\omega_B + 2\omega_Q)}, \quad (32)$$

where  $f_{Q,3}$  is a regular function, without poles for real values of its arguments. The above expression (32) has a pole for  $\omega_B = 2\omega_Q$ . Taking into account the fact that  $\omega_Q < \omega_B$ , as

we can see from equation (14) and figure 1, as well as the fact that collective frequencies depend on the trap aspect ratio  $\lambda$ , the condition  $\omega_B = 2\omega_Q$  can, in principle, be satisfied. This is denoted as a geometric resonance, since it is obtained by simply tuning the geometry of the experiment through  $\lambda$ . Higher-order corrections to  $\Delta\omega_Q$  in  $\varepsilon$  could, in principle, be obtained systematically by using the developed perturbation theory.

#### 4.2. Breathing mode

In a similar manner, we also study the dynamics of a cylindrically symmetric BEC system when initially only the breathing mode is excited,

$$\mathbf{u}(0) = \mathbf{u}_0 + \varepsilon \mathbf{u}_B, \quad \dot{\mathbf{u}}(0) = \mathbf{0}. \quad (33)$$

Applying again the Poincaré–Lindstedt perturbation theory, we calculate the breathing mode frequency shift,

$$\omega_B(\varepsilon) = \omega_B + \Delta\omega_B = \omega_B - \varepsilon^2 \frac{(\mathbf{u}_B^L)^T \mathbf{I}_{B,3}}{2\omega_B}, \quad (34)$$

where again the expression  $(\mathbf{u}_B^L)^T \mathbf{I}_{B,3}$  is calculated in *Mathematica*. In this way, we finally yield the following analytic formula for the frequency shift of the breathing mode

$$\Delta\omega_B = -\varepsilon^2 \frac{f_{B,3}(\omega_Q, \omega_B, u_{\rho 0}, u_{z0}, p, k, \lambda)}{2\omega_B(2\omega_B - \omega_Q)(2\omega_B + \omega_Q)}, \quad (35)$$

where the function  $f_{B,3}$  is a regular function of its arguments. Naively looking at this expression, one would say that it exhibits a pole for  $2\omega_B = \omega_Q$ . However, from equation (14) and figure 1 we see that  $\omega_Q < \omega_B$ , and, therefore, the condition  $2\omega_B = \omega_Q$  is never satisfied. In the following subsection, we numerically demonstrate that a geometric resonance does not occur, and verify the analytical result for the frequency shift of the breathing mode.

#### 4.3. Comparison with numerical results

In order to verify our analytical results, we perform high-precision numerical simulations [97–105]. At first we focus on a description of the BEC dynamics, and compare our analytical results for the radial and longitudinal widths of the condensate obtained perturbatively to the direct numerical solutions of equations (7)–(8). To this end, we consider a BEC in the initial state corresponding to the perturbed equilibrium position, where the small perturbation is proportional to the eigenvector of the quadrupole mode according to equations (21). Examples of the condensate dynamics are shown in figure 5 for a pure two-body interaction  $p = 1$ ,  $k = 0$  with  $\varepsilon = 0.1$ , and in figure 6 for  $p = 1$ ,  $k = 0.001$ ,  $\varepsilon = 0.1$ .

In both figures, we plot analytical and numerical solutions for  $u_\rho$  and  $u_z$  as functions of the dimensionless time parameter  $\omega_\rho t$  for different values of the trap aspect ratio  $\lambda$ . Analytical solutions are calculated using the third-order perturbation theory developed in subsection 4.1. We can see in figure 5 that the agreement is excellent, not only for the non-resonant value of the trap aspect ratio  $\lambda = 2.3$  (top panels), but also for  $\lambda = 0.55$  (bottom panels), which is close to a geometric resonance, as we will see later in figure 8(a). For

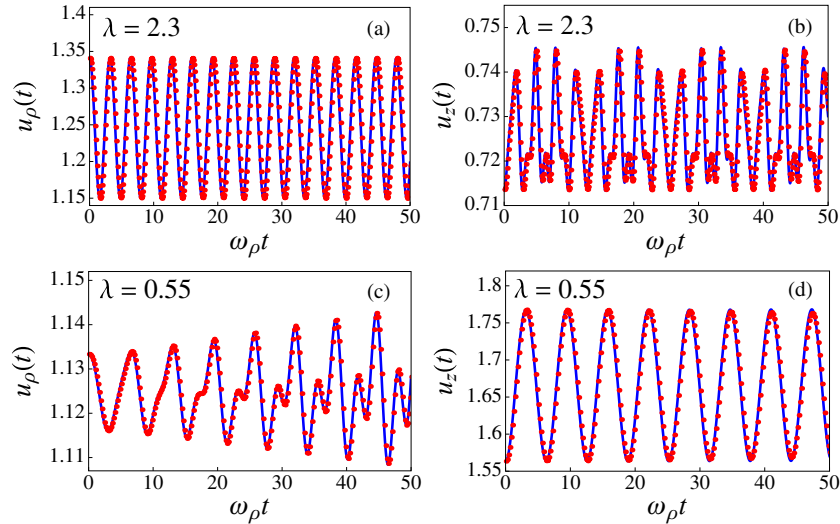


**Figure 5.** A comparison of analytic (solid blue lines) and numeric (red dots) results for a BEC dynamics with a pure repulsive two-body interaction  $p = 1$ ,  $k = 0$  and  $\varepsilon = 0.1$ . The top panels show dynamics of (a) radial and (b) longitudinal condensate widths for the trap aspect ratio  $\lambda = 2.3$  as a function of the dimensionless time  $\omega_\rho t$ ; the bottom panels show dynamics of (c) radial and (d) longitudinal BEC widths for  $\lambda = 0.55$ .

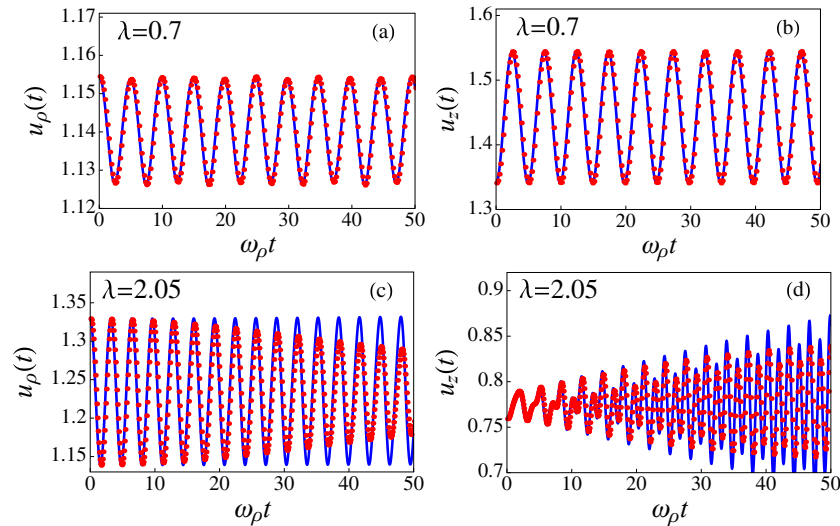


**Figure 6.** A comparison of analytic (solid blue lines) and numeric (red dots) results for BEC dynamics for a repulsive two-body interaction  $p = 1$  and a repulsive three-body interaction  $k = 0.001$ , with  $\varepsilon = 0.1$ . The top panels show dynamics of (a) radial and (b) longitudinal condensate widths for the trap aspect ratio  $\lambda = 0.7$  as a function of the dimensionless time  $\omega_\rho t$ ; the bottom panels show dynamics of (c) radial and (d) longitudinal BEC widths for  $\lambda = 2.05$ .

these values of parameters, the relative shift in the quadrupole mode frequency is of the order of 0.3%, and therefore third-order perturbation theory yields a quite accurate description of the system dynamics. The same applies to the top panels of figure 6, where  $\lambda = 0.7$  is far from any resonance. However, for  $\lambda = 2.05$  (bottom panels), we observe some disagreement, which increases with propagation time. This is due to the fact that  $p = 1$ ,  $k = 0.001$ ,  $\lambda = 2.05$  is close to a geometric resonance, as we will see in figure 8(b). In this case, the perturbatively calculated shift in the quadrupole mode frequency is much larger than that for the bottom panels of figure 5. For this reason, after a long enough time the third-order perturbation theory is not sufficiently accurate. Although it gives a qualitatively correct description of the behaviour of the system, one would have to go to higher orders in

perturbation theory to get more accurate agreement with the numerical results. Such a behaviour in the bottom panels of figure 6 is just a telltale of the occurrence of a geometric resonance, and a subsequent analysis of frequency shifts is the only proper way to identify these resonances in a more quantitative way.

However, before we present this analysis, we show in figure 7 the excitation spectra of the BEC dynamics which corresponds to the initial conditions (21) for  $p = 1$ ,  $k = 0.001$  and two values of the trap aspect ratio,  $\lambda = 1.9$  and  $\lambda = 0.5$ . For the parameter values in figure 7(a), the linear stability analysis yields breathing and quadrupole mode frequencies (14) with  $\omega_B = 3.65$  and  $\omega_Q = 1.96$ , while for the parameters in figure 7(b), we obtain  $\omega_B = 2.01$  and  $\omega_Q = 0.905$ , all expressed in units of  $\omega_\rho$ . In both graphs, we



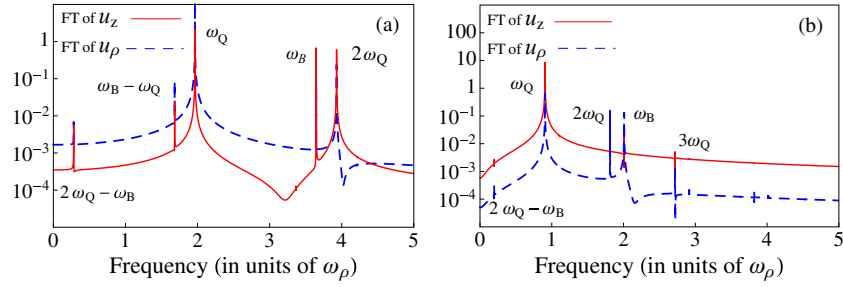


**Figure 7.** Fourier spectra of the BEC dynamics obtained by numerically solving the system of equations (7) and (8) for a repulsive two-body interaction  $p = 1$ , a repulsive three-body interaction  $k = 0.001$ , and  $\varepsilon = 0.1$  for (a)  $\lambda = 1.9$  and (b)  $\lambda = 0.5$ . Each graph shows spectra of both longitudinal and radial condensate widths. The locations of all peaks are identified as linear combinations of the quadrupole and the breathing mode frequencies, in correspondence with the analysis based on the developed perturbation theory.

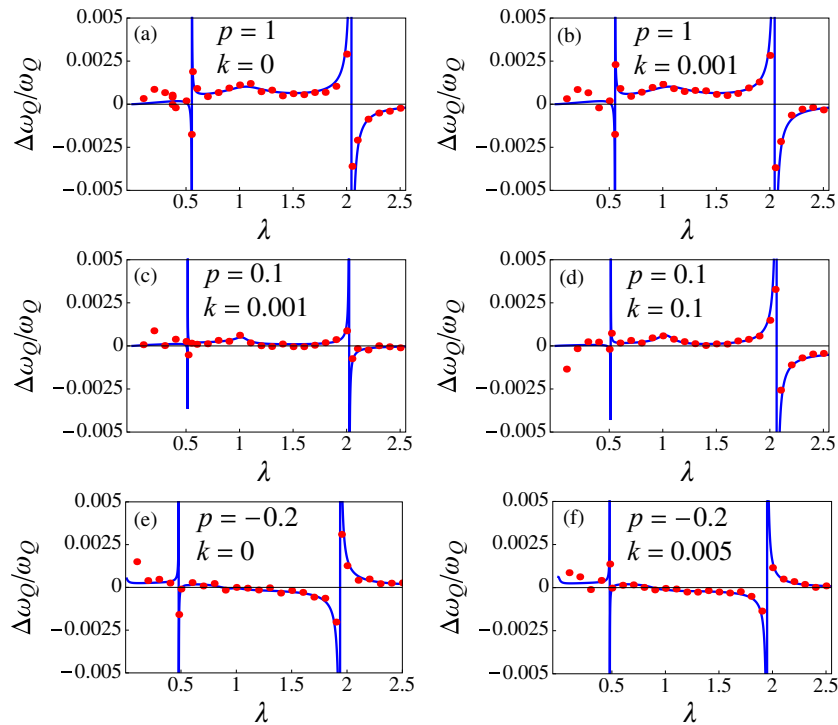


**Figure 8.** Relative frequency shift of the quadrupole mode as a function of the trap aspect ratio  $\lambda$  for  $\varepsilon = 0.1$  and different values of two-body and three-body interaction strengths: (a)  $p = 1, k = 0$ , (b)  $p = 1, k = 0.001$ , (c)  $p = 0.1, k = 0.001$ , (d)  $p = 0.1, k = 0.1$ , (e)  $p = -0.2, k = 0$ , (f)  $p = -0.2, k = 0.005$ . The solid lines represent the analytical result (32), while dots are obtained by a numerical analysis of the corresponding excitation spectrum for each value of  $\lambda$ , as described in figure 7.

can see that the Fourier spectra contain two basic modes,  $\omega_Q$  and  $\omega_B$ , whose values agree well with those obtained from the linear stability analysis in equation (14), and a multitude of higher order harmonics, which are linear combinations of the two modes, as pointed out in subsection 4.1.

Now we compare the derived analytical results for the frequency shifts of the quadrupole and the breathing modes with the results of numerical simulations for the BEC systems with two- and three-body contact interactions in a cylindrical trap. In particular, we note that the calculated frequency shifts close to geometric resonances reveal poles, which are an artefact of the perturbative approach. Indeed, our detailed numerical calculations show that the observed frequencies remain finite through the whole geometric resonance. In figures 8 and 9, we present the comparison of analytic (solid lines) and numeric (dots) values of relative frequency shifts as

functions of the trap aspect ratio  $\lambda$ . The analytical results are calculated from equations (32) and (35), respectively, while the numerical data are obtained from a Fourier analysis of the excitation spectrum, i.e. for each value of  $\lambda$  we have calculated the corresponding Fourier spectra, as in figure 7, and then extracted the frequency values of the quadrupole and the breathing mode.

In figure 8(a), we show a special case of a pure two-body interaction, when  $k = 0$ . The condition for a geometric resonance  $\omega_B = 2\omega_Q$  yields the trap aspect ratios  $\lambda_1 = 0.555$  and  $\lambda_2 = 2.056$ , which is in good agreement with the numerical data, as we can see from the graph. The existence of a geometric resonance at  $\lambda_1 = 0.555$  is responsible for a violent dynamics seen in the bottom panels of figure 5, as we have pointed out earlier. However, by analysing the frequency shifts we can conclusively show that, indeed, the geometric

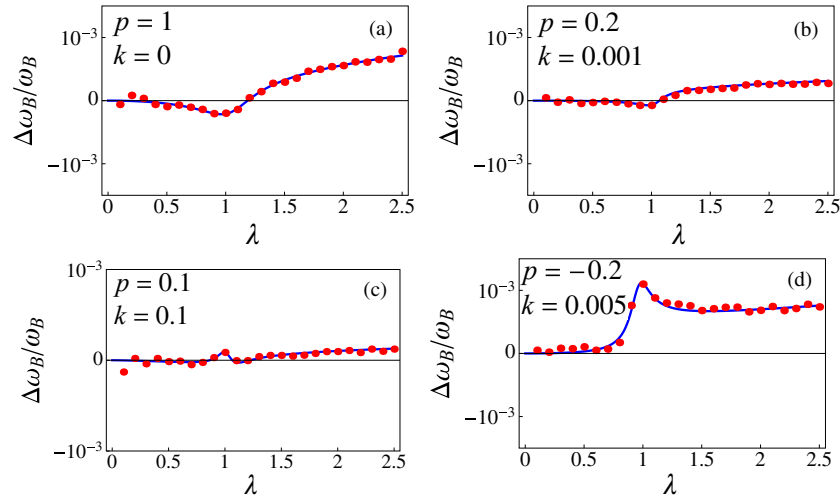


**Figure 9.** Relative frequency shift of the breathing mode as a function of the trap aspect ratio  $\lambda$  for  $\varepsilon = 0.1$  and different values of two-body and three-body interaction strengths: (a)  $p = 1, k = 0$ , (b)  $p = 0.2, k = 0.001$ , (c)  $p = 0.1, k = 0.1$ , (d)  $p = -0.2, k = 0.005$ . The solid lines represent the analytical result (35), while dots are obtained by a numerical analysis of the corresponding excitation spectrum for each value of  $\lambda$ , as described in figure 7.

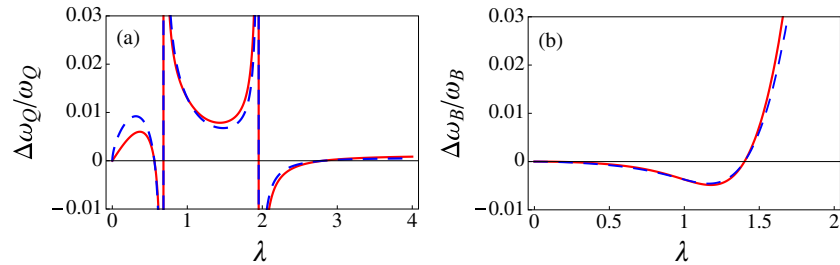


**Figure 10.** Comparison of the analytical results for the relative frequency shifts of (a) quadrupole and (b) breathing modes in the Thomas–Fermi limit from [18] derived using the parabolic variational ansatz (solid red lines) and the analytical results derived here using the Poincaré–Lindstedt perturbation theory with the Gaussian variational ansatz (dashed blue lines).

resonance is present. In further graphs, we see that the excellent agreement between analytical and numerical results also holds for other values of  $p$  and  $k$ , including the case of an attractive two-body interaction  $p = -0.2$ , which is still within the BEC stability region. It is interesting to note the observation that the asymptotic approach to geometric resonances for the case of an attractive two-body interaction is reversed compared to the case of a repulsive two-body interaction. For instance, we can see in figure 8(d) that  $\Delta\omega_Q/\omega_Q \rightarrow \infty$  when  $\lambda \rightarrow \lambda_2^-$ , and  $\Delta\omega_Q/\omega_Q \rightarrow -\infty$  when  $\lambda \rightarrow \lambda_2^+$ , while for an attractive  $p = -0.2$  in figure 8(f) we see that the situation is reversed.

In figure 9, we compare analytic and numeric results for a frequency shift of the breathing mode. As for the quadrupole mode, the agreement is excellent for both repulsive and attractive two-body interactions. As pointed out in subsection 4.2, there are no geometric resonances for the breathing mode frequency, since the corresponding condition  $\omega_Q = 2\omega_B$  cannot be satisfied.

Finally, we compare our derived analytic results with those from [18], where frequency shifts of collective modes were calculated in the Thomas–Fermi (TF) limit using a hydrodynamic approach. In terms of our variational approach, the TF limit corresponds to the limit  $p \rightarrow \infty$ , so that

equation (14) for the frequencies of the breathing and the quadrupole mode reduces to

$$\omega_{B,Q}^2 = 2 + \frac{3}{2}\lambda^2 \pm \frac{1}{2}\sqrt{16 - 16\lambda^2 + 9\lambda^4}, \quad (36)$$

which is in agreement with [18]. The condition for a geometric resonance  $\omega_B = 2\omega_Q$  thus yields trap aspect ratios  $\lambda_{1,2} = (\sqrt{125} \pm \sqrt{29})/\sqrt{72}$ , i.e.  $\lambda_1 \approx 0.683$  and  $\lambda_2 \approx 1.952$ .

Figure 10 gives a comparison of the relative frequency shifts in the TF limit calculated in [18] using a hydrodynamic approach, and our analytical results obtained using the Poincaré–Lindstedt perturbation theory. Despite the good agreement, we observe small differences, which are due to the fact that [18] uses a parabolic variational ansatz for the condensate wavefunction, while we use the Gaussian ansatz in equation (3). We have confirmed that, when applied to the parabolic variational ansatz, our perturbative approach yields frequency shifts in perfect agreement with [18].

## 5. Resonant mode coupling

In this section, we study the phenomenon of nonlinearity-induced resonant mode coupling. As already pointed out, even if a BEC system is excited precisely along the quadrupole or, equivalently, the breathing mode, the emerging dynamics

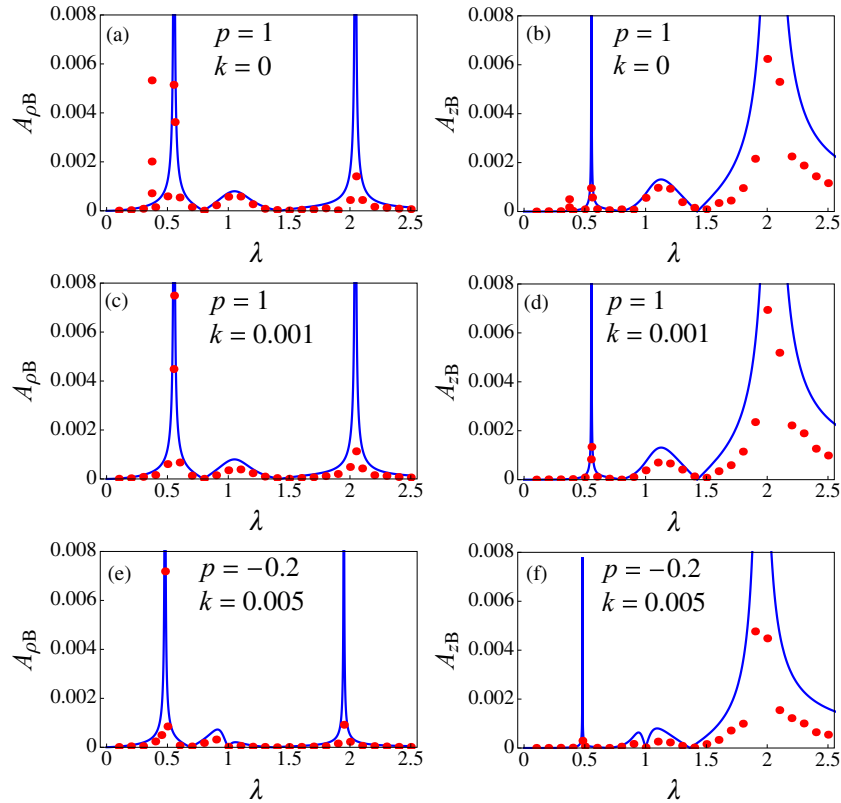


**Figure 11.** Amplitudes of the breathing mode emerging in the second order of the perturbation theory from BEC dynamics after initially only the quadrupole mode is excited, given as functions of the trap aspect ratio  $\lambda$  for  $\varepsilon = 0.1$  and different values of two-body and three-body interaction strengths  $p$  and  $k$ . The amplitudes  $A_{\rho B}$  and  $A_{zB}$  from equations (40) and (41) correspond to the radial and the longitudinal condensate widths of the emerging breathing mode dynamics.

will lead to small oscillations which initially involve only the corresponding mode, but then the other collective mode will eventually step in, as well as higher harmonics of the two modes and their linear combinations will appear. If the trap confinement of the system allows a geometric resonance, this could greatly enhance the mode coupling and speed up the emergence of those modes which are initially not excited, and therefore we designate it as a resonant mode coupling. We focus on the experimentally most studied case of a repulsive two-body interaction, although all derived analytical results are also valid for the case of an attractive interaction. As effects of three-body interactions are usually small, and their main contribution is related to a stabilization/destabilization of the condensate, we focus on the emergence of a resonant mode coupling due to geometric resonances.

To demonstrate this phenomenon, we use the perturbative solution of equations (7) and (8) with the initial conditions defined by equations (21), for which the initial state coincides with the equilibrium with a small perturbation proportional to the quadrupole mode eigenvector. The second-order perturbative solution can then be written as

$$\mathbf{u}_0 + \begin{pmatrix} A_{\rho Q} \\ A_{zQ} \end{pmatrix} \cos \omega_Q t + \begin{pmatrix} A_{\rho B} \\ A_{zB} \end{pmatrix} \cos \omega_B t + \dots, \quad (37)$$

where dots represent higher harmonics and the respective amplitudes are given by

$$A_{\rho Q} = \varepsilon u_{\rho Q} + \varepsilon^2 \mathcal{A}_{\rho Q2} \frac{u_{\rho Q}^2}{\omega_Q^2}, \quad (38)$$

$$A_{zQ} = c_1 A_{\rho Q}, \quad (39)$$

$$A_{\rho B} = \varepsilon^2 \mathcal{A}_{\rho B2} \frac{u_{\rho Q}^2 (\omega_B^2 - 2\omega_Q^2)}{\omega_B^2 (\omega_B^2 - 4\omega_Q^2)}, \quad (40)$$

$$A_{zB} = c_2 A_{\rho B}. \quad (41)$$

Note that the absence of terms linear in  $\varepsilon$  in expressions for  $A_{\rho B}$  and  $A_{zB}$  is due to the initial condition, i.e. the fact that, initially, we only excite the quadrupole mode. The constants  $c_{1,2}$  in the above expressions are defined by equation (26), while  $\mathcal{A}_{\rho Q2}$  and  $\mathcal{A}_{\rho B2}$  are calculated to be

$$\mathcal{A}_{\rho Q2} = \frac{c_2 \gamma_\rho + c_1 c_2 \alpha + c_1^2 c_2 \beta - \alpha - 4c_1 \beta - c_1^2 \gamma_z}{3(c_1 - c_2)}, \quad (42)$$

$$\mathcal{A}_{\rho B2} = \frac{-c_1^3 \beta + \alpha - c_1 \gamma_\rho + 4c_1 \beta - c_1^2 \alpha + c_1^2 \gamma_z}{c_1 - c_2}, \quad (43)$$

with  $\alpha, \beta, \gamma_\rho, \gamma_z$  defined as

$$\alpha = \frac{3p}{u_{\rho 0}^4 u_{z 0}^2} + \frac{10k}{u_{\rho 0}^6 u_{z 0}^3}, \quad \beta = \frac{p}{u_{\rho 0}^3 u_{z 0}^3} + \frac{3k}{u_{\rho 0}^5 u_{z 0}^4}, \quad (44)$$

$$\gamma_\rho = \frac{6}{u_{\rho 0}^5} + \frac{6p}{u_{\rho 0}^5 u_{z 0}} + \frac{15k}{u_{\rho 0}^7 u_{z 0}^2}, \quad \gamma_z = \frac{6}{u_{z 0}^5} + \frac{3p}{u_{\rho 0}^2 u_{z 0}^4} + \frac{6k}{u_{\rho 0}^4 u_{z 0}^5} \quad (45)$$

In figure 11, we see the comparison of the derived analytical results, which emerge in the second order, and

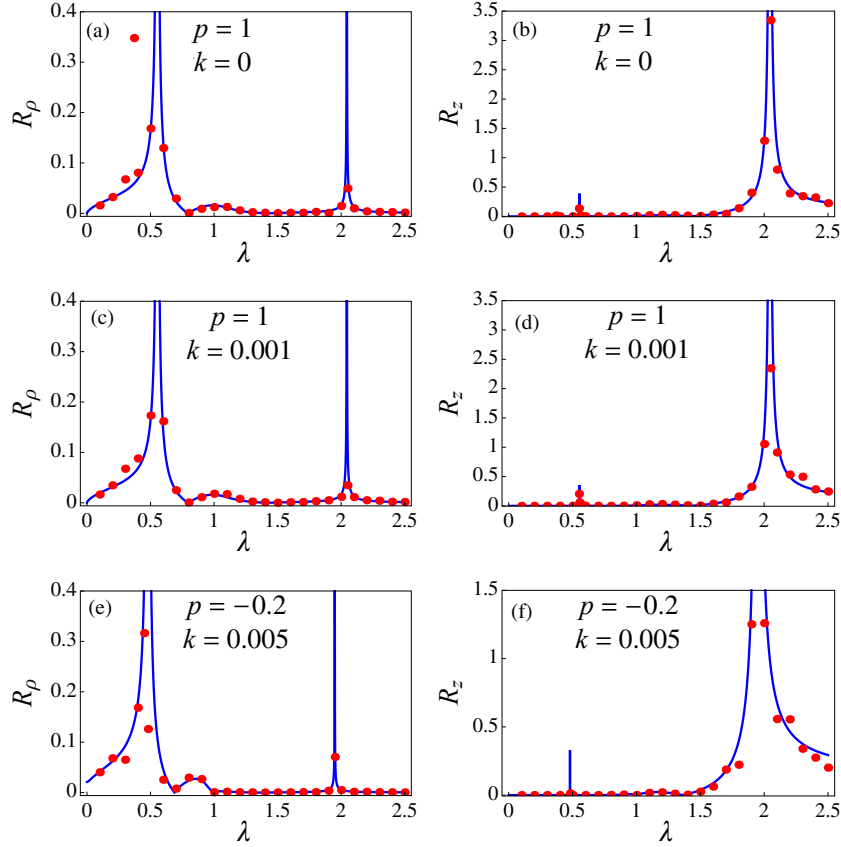


**Figure 12.** Ratios of breathing and quadrupole mode amplitudes emerging in the second order of the perturbation theory after initially only the quadrupole mode is excited, given as functions of the trap aspect ratio  $\lambda$  for  $\varepsilon = 0.1$  and different values of two-body and three-body interaction strengths  $p$  and  $k$ . The quantities  $R_\rho$  and  $R_z$  from equations (46) and (47) correspond to ratios of amplitudes of the breathing and the quadrupole mode in the radial and longitudinal condensate widths.

corresponding numerical simulations for the amplitudes of the breathing mode. The numerical results are obtained, as before, by extracting the amplitude of the breathing mode from the Fourier excitation spectra of the system for each value of the trap aspect ratio  $\lambda$ . The agreement is quite good, and we see again a resonant behaviour, which occurs at the same trap aspect ratios as for the frequency shift of the quadrupole mode. From equations (40) and (41), we actually see that the resonances occur when the condition  $\omega_B = 2\omega_Q$  is satisfied, which is precisely the same condition as for the frequency shift. This is not surprising, since amplitudes are expressed in terms of frequencies of the collective modes, and a resonant behaviour of the quadrupole mode frequency leads to resonances in the amplitudes for the same values of  $\lambda$ . Therefore, geometric resonances are not only reflected in the resonances of frequency shifts of collective modes, but also in the resonant mode coupling.

In addition to the absolute values of the breathing mode amplitudes, which are excited through the resonant mode coupling, it is also interesting to look at their relative values, compared to the quadrupole mode amplitudes, i.e.

$$R_\rho = \frac{A_{\rho B}}{A_{\rho Q}} \propto \frac{\omega_B^2 - 2\omega_Q^2}{\omega_B^2 - 4\omega_Q^2}, \quad (46)$$

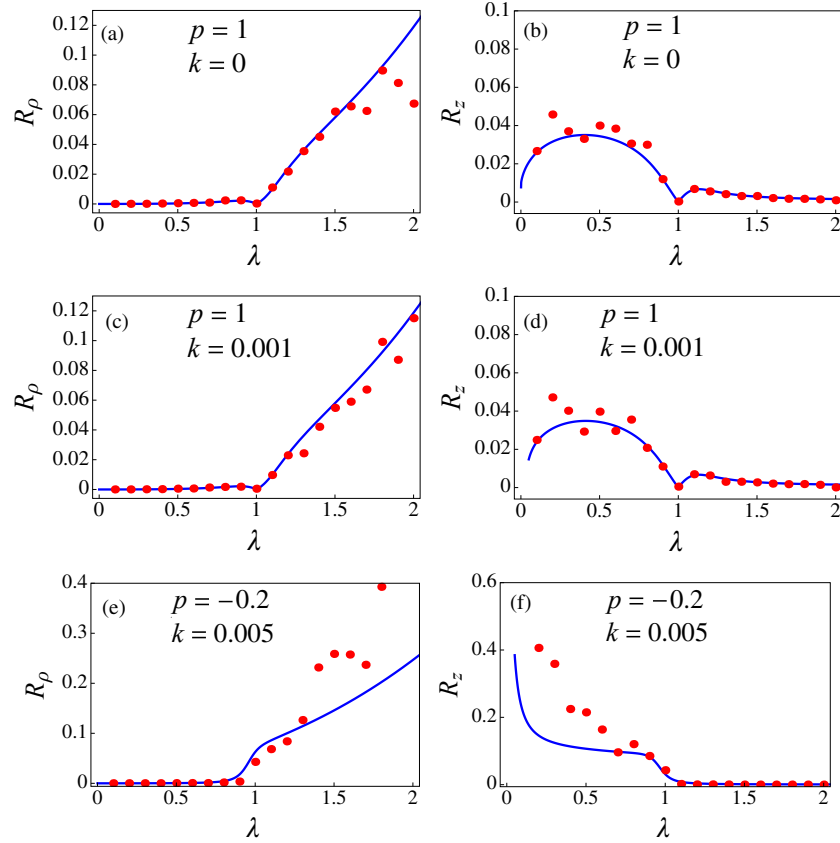
$$R_z = \frac{A_{zB}}{A_{zQ}} \propto \frac{\omega_B^2 - 2\omega_Q^2}{\omega_B^2 - 4\omega_Q^2}. \quad (47)$$

Figure 12 shows the comparison of analytical and numerical results for the relative ratio of amplitudes of the resonance-excited breathing mode. Due to the geometric resonances, we see that the trap aspect ratio can be tuned in such a way that the resonant mode coupling excites the breathing mode with an amplitude far larger than that of the quadrupole mode, which serves as the source of excitation.

Furthermore, from equations (40) and (41) we see that, if the geometry of the trap is tuned such that  $\omega_B = \omega_Q\sqrt{2}$ , then the amplitudes of the breathing mode vanish simultaneously, i.e.  $A_{\rho B} = A_{zB} = 0$ . Although this is true only in the second-order perturbation theory, it still represents a condition for a significant suppression of the resonant mode coupling. Therefore, the tunability of the trap aspect ratio offers a unique tool for enhancing and suppressing the mode coupling in a BEC, which might be of broad experimental interest.

In a similar way, we can initially excite only the breathing mode, which corresponds to equations (7) and (8) with initial conditions defined in equations (33). The solution in the second-order perturbation theory has again the form

$$\mathbf{u}_0 + \begin{pmatrix} A_{\rho B} \\ A_{zB} \end{pmatrix} \cos \omega_B t + \begin{pmatrix} A_{\rho Q} \\ A_{zQ} \end{pmatrix} \cos \omega_Q t + \dots, \quad (48)$$



**Figure 13.** Ratios of quadrupole and breathing mode amplitudes emerging in the second order of the perturbation theory after initially only the breathing mode is excited, given as functions of the trap aspect ratio  $\lambda$  for  $\varepsilon = 0.1$  and different values of two-body and three-body interaction strengths  $p$  and  $k$ . The quantities  $R_\rho$  and  $R_z$  from equations (55) and (56) correspond to ratios of amplitudes of the breathing and the quadrupole modes in the radial and longitudinal condensate widths.

but now the respective amplitudes read

$$A_{\rho B} = \varepsilon u_{\rho B} + \varepsilon^2 \mathcal{A}_{\rho B2} \frac{u_{\rho B}^2}{\omega_B^2}, \quad (49)$$

$$A_{zB} = c_2 A_{\rho B}, \quad (50)$$

$$A_{\rho Q} = \varepsilon^2 \mathcal{A}_{\rho Q2} \frac{u_{\rho B}^2 (2\omega_B^2 - \omega_Q^2)}{\omega_Q^2 (4\omega_B^2 - \omega_Q^2)}, \quad (51)$$

$$A_{zQ} = c_1 A_{\rho Q}, \quad (52)$$

and the coefficients  $\mathcal{A}_{\rho B2}$  and  $\mathcal{A}_{\rho Q2}$  are given by

$$\mathcal{A}_{\rho B2} = \frac{-c_1 \gamma_\rho - c_1 c_2 \alpha - c_1 c_2^2 \beta + \alpha + 4c_2 \beta + c_2^2 \gamma_z}{3(c_1 - c_2)}, \quad (53)$$

$$\mathcal{A}_{\rho Q2} = \frac{c_2^3 \beta - \alpha + c_2 \gamma_\rho - 4c_2 \beta + c_2^2 \alpha - c_2^2 \gamma_z}{c_1 - c_2}. \quad (54)$$

In this case, the ratios of amplitudes are given by

$$R_\rho = \frac{A_{\rho Q}}{A_{\rho B}} \propto \frac{2\omega_B^2 - \omega_Q^2}{4\omega_B^2 - \omega_Q^2}, \quad (55)$$

$$R_z = \frac{A_{zQ}}{A_{zB}} \propto \frac{2\omega_B^2 - \omega_Q^2}{4\omega_B^2 - \omega_Q^2}. \quad (56)$$

Figure 13 compares analytical and numerical results for the mode coupling when initially only the breathing mode is excited, and then the quadrupole mode emerges due to the mode coupling. As for the case of the breathing mode frequency shift, there are no resonances, since  $\omega_B > \omega_Q$ , and the resonance condition  $2\omega_B = \omega_Q$  cannot be satisfied, as is confirmed by the graphs. Therefore, the amplitudes do not experience resonances in this case, contrary to what we have observed in figure 12. Again, this can be explained by the fact that amplitudes are functions of the breathing mode frequency, which does not experience any resonances, and hence the same is valid for the corresponding amplitude. Also, the condition  $\omega_B \sqrt{2} = \omega_Q$  cannot be satisfied, and therefore the amplitude of the quadrupole mode cannot be fully suppressed here, contrary to the case presented in figure 12. For a repulsive two-body interaction in figures 13(a)–(d), we see that the ratios  $R_\rho$  and  $R_z$  are below 10%, and the mode coupling mechanism is not able to produce a significant amplitude for the quadrupole mode. For the case of an attractive two-body interaction in figures 13(e)–(f), the ratio increases and the generated quadrupole mode amplitude is stronger. Here the agreement between analytical and numerical results is only qualitative, so that the perturbation theory would have to be carried out to higher orders in the small parameter  $\varepsilon$  in order to improve the agreement.

## 6. Conclusions

We have studied the dynamics and collective excitations of a BEC for different trap aspect ratios at zero temperature. In particular, we have investigated prominent resonant effects that arise due to two- and three-body interactions, and their delicate interplay. We have discussed the stability of a condensate in an axially symmetric harmonic trap for the experimentally most relevant setups: repulsive and attractive two-body interactions, attractive two-body and repulsive three-body interactions, and attractive two- and three-body interactions. We have shown that even a small repulsive three-body interaction is able to extend the stability region of the condensate beyond the critical number of atoms when the two-body interaction is attractive.

Using a perturbation theory and a Poincaré–Lindstedt analysis of a Gaussian variational approach for the condensate wavefunction, we have studied in detail the relation between resonant effects due to two- and three-body interactions, and the effects of the trap geometry. Within the variational approach and the Poincaré–Lindstedt method, we have analytically calculated frequency shifts and a mode coupling in order to identify geometric resonances of collective oscillation modes of an axially symmetric BEC. We have also shown that the observed geometric resonances can be suppressed if two- and three-body interactions are appropriately fine-tuned.

To verify the derived analytical results, we have used numerical simulations, which provide detailed excitation spectra of the BEC dynamics. We have numerically observed and analytically described several prominent nonlinear features of BEC systems: significant shifts in the frequencies of collective modes, generation of higher harmonics and linear combinations of collective modes, as well as resonant and non-resonant mode coupling. We have shown that, even if the system is excited so that the perturbation corresponds initially to the eigenvector of a particular mode, the nonlinear dynamics of the condensate will eventually excite also other modes due to the mode coupling. The presence of geometric resonances can significantly enhance this effect, as we have shown using the developed perturbation theory. All obtained analytical results are found to be in good agreement with the numerical results. Furthermore, the results for frequency shifts are shown to coincide with the earlier derived analytical results [18] within the hydrodynamic approach in the Thomas–Fermi approximation. In future work, we plan to extend the present analysis and also include the effects of quantum fluctuations [106].

## Acknowledgments

This work was supported in part by the Ministry of Education, Science, and Technological Development of the Republic of Serbia under projects no. ON171017, NAD-BEC and NAI-DBEC, by DAAD—German Academic and Exchange Service under projects NAD-BEC and NAI-DBEC, and by the European Commission under EU FP7 projects PRACE-1IP, PRACE-2IP, PRACE-3IP, HP-SEE and EGI-InSPIRE. Both AB and AP gratefully acknowledge a fellowship from the Hanse–Wissenschaftskolleg.

## References

- [1] Anderson M H, Ensher J R, Matthews M R, Wieman C E and Cornell E A 1995 *Science* **269** 198
- [2] Davis K B, Mewes M-O, Andrews M R, van Druten N J, Durfee D S, Kurn D M and Ketterle W 1995 *Phys. Rev. Lett.* **75** 3969
- [3] Bradley C C, Sackett C A and Hulet R G 1997 *Phys. Rev. Lett.* **78** 985
- [4] Gerton J M, Strelak D, Prodan I and Hulet R G 2000 *Nature* **408** 692
- [5] Cornish S L, Claussen N R, Roberts J L, Cornell E A and Wieman C E 2000 *Phys. Rev. Lett.* **85** 1795
- [6] Roberts J L, Claussen N R, Cornish S L, Donley E A, Cornell E A and Wieman C E 2001 *Phys. Rev. Lett.* **86** 4211
- [7] Jin D S, Ensher J R, Matthews M R, Wieman C E and Cornell E A 1996 *Phys. Rev. Lett.* **77** 420
- [8] Mewes M-O, Andrews M R, van Druten N J, Kurn D M, Durfee D S, Townsend C G and Ketterle W 1996 *Phys. Rev. Lett.* **77** 988
- [9] Stamper-Kurn D M, Miesner H-J, Inouye S, Andrews M R and Ketterle W 1998 *Phys. Rev. Lett.* **81** 500
- [10] Yang L, Wang X-R, Li K, Tan X-Z, Xiong H-W and Lu B-L 2009 *Chin. Phys. Lett.* **26** 076701
- [11] Stringari S 1996 *Phys. Rev. Lett.* **77** 2360
- [12] Edwards M, Ruprecht P A, Burnett K, Dodd R J and Clark C W 1996 *Phys. Rev. Lett.* **77** 1671
- [13] Edwards M, Dodd R J, Clark C W and Burnett K 1996 *J. Res. Natl. Inst. Stand. Technol.* **101** 553
- [14] Singh K G and Rokhsar D S 1996 *Phys. Rev. Lett.* **77** 1667
- [15] Pérez-García V M, Michinel H, Cirac J I, Lewenstein M and Zoller P 1996 *Phys. Rev. Lett.* **77** 5320
- [16] Pérez-García V M, Michinel H, Cirac J I, Lewenstein M and Zoller P 1997 *Phys. Rev. A* **56** 1424
- [17] You L, Hoston W and Lewenstein M 1997 *Phys. Rev. A* **55** R1581
- [18] Dalfovo F, Minniti C and Pitaevskii L 1997 *Phys. Rev. A* **56** 4855
- [19] Vidanović I, Balaž A, Al-Jibbouri H and Pelster A 2011 *Phys. Rev. A* **84** 013618
- [20] Hechenblaikner G, Maragò O M, Hodby E, Arlt J, Hopkins S and Foot C J 2000 *Phys. Rev. Lett.* **85** 692
- [21] Hechenblaikner G, Morgan S A, Hodby E, Maragò O M and Foot C J 2002 *Phys. Rev. A* **65** 033612
- [22] Pitaevskii L and Stringari S 1997 *Phys. Lett. A* **235** 398
- [23] Lee C, Huang J, Deng H, Dai H and Xu J 2012 *Front. Phys.* **7** 109
- [24] Pitaevskii L 1997 *Phys. Lett. A* **229** 406
- [25] Graham R, Walls D F and Collett M J 1998 *Phys. Rev. A* **57** 503
- [26] Castin Y and Dum R 1996 *Phys. Rev. Lett.* **77** 5315
- [27] García-Ripoll J J, Pérez-García V M and Torres P 1999 *Phys. Rev. Lett.* **83** 1715
- [28] García-Ripoll J J and Pérez-García V M 1999 *Phys. Rev. A* **59** 2220
- [29] Engels P, Atherton C and Hofer M A 2007 *Phys. Rev. Lett.* **98** 095301
- [30] Nicolin A I, Carretero-González R and Kevrekidis P G 2007 *Phys. Rev. A* **76** 063609
- [31] Pollack S E, Dries D, Junker M, Chen Y P, Corcovilos T A and Hulet R G 2009 *Phys. Rev. Lett.* **102** 090402
- [32] Nicolin A I 2011 *Phys. Rev. E* **84** 056202
- [33] Hamner C, Chang J J, Engels P and Hofer M A 2011 *Phys. Rev. Lett.* **106** 065302
- [34] Nicolin A I 2011 *Rom. Rep. Phys.* **63** 1329
- [35] Middelkamp S, Chang J J, Hamner C, Carretero-González R, Kevrekidis P G, Achilleos V, Frantzeskakis D J, Schmelcher P and Engels P 2011 *Phys. Lett. A* **375** 642
- [36] Nicolin A I 2012 *Physica A* **391** 1062

- [37] Balaž A and Nicolini A I 2012 *Phys. Rev. A* **85** 023613
- [38] Kobayakov D, Bychkov V, Lundh E, Bezett A and Marklund M 2012 *Phys. Rev. A* **86** 023614
- [39] Pepe F V, Facchi P, Florio G and Pascazio S 2012 *Phys. Rev. A* **86** 023629
- [40] Gaul C, Lima R P A, Diaz E, Müller C A and Dominguez-Adame F 2009 *Phys. Rev. Lett.* **102** 255303
- [41] Pollack S E, Dries D, Hulet R G, Magalhães K M F, Henn E A L, Ramos E R F, Caracanhas M A and Bagnato V S 2010 *Phys. Rev. A* **81** 053627
- [42] Sabari S, Raja R V J, Porsezian K and Muruganandam P 2010 *J. Phys. B: At. Mol. Opt. Phys.* **43** 125302
- [43] Gaul C, Diaz E, Lima R P A, Dominguez-Adame F and Müller C A 2011 *Phys. Rev. A* **84** 053627
- [44] Vidanović I, Al-Jibbouri H, Balaž A and Pelster A 2012 *Phys. Scr. T* **149** 014003
- [45] Hodby E, Maragò O M, Hechenblaikner G and Foot C J 2001 *Phys. Rev. Lett.* **86** 2196
- [46] Kasamatsu K, Tsubota M and Ueda M 2004 *Phys. Rev. A* **69** 043621
- [47] Ramos E R F, dos Santos F E A, Caracanhas M A and Bagnato V S 2012 *Phys. Rev. A* **85** 033608
- [48] Dalfovo F, Minniti C, Stringari S and Pitaevskii L 1997 *Phys. Lett. A* **227** 259
- [49] Leanhardt A E, Chikkatur A P, Kielpinski D, Shin Y, Gustavson T L, Ketterle W and Pritchard D E 2002 *Phys. Rev. Lett.* **89** 040401
- [50] Zhang W, Wright E M, Pu H and Meystre P 2003 *Phys. Rev. A* **68** 023605
- [51] Zhang A-X and Xue J-K 2007 *Phys. Rev. A* **75** 013624
- [52] Köhler T 2002 *Phys. Rev. Lett.* **89** 210404
- [53] Tolra B L, O'Hara K M, Huckans J H, Phillips W D, Rolston S L and Porto J V 2004 *Phys. Rev. Lett.* **92** 190401
- [54] Ruprecht P A, Holland M J, Burnett K and Edwards M 1995 *Phys. Rev. A* **51** 4704
- [55] Akhmediev N, Das M P and Vagov A V 1999 *Int. J. Mod. Phys. B* **13** 625
- [56] Gammal A, Frederico T, Tomio L and Chomaz Ph 2000 *J. Phys. B: At. Mol. Opt. Phys.* **33** 4053
- [57] Tomio L, Filho V S, Gammal A and Frederico T 2003 *Laser Phys.* **13** 582
- [58] Abdullaev F K, Gammal A, Tomio L and Frederico T 2001 *Phys. Rev. A* **63** 043604
- [59] Tewari S P, Silotia P, Saxena A and Gupta L K 2006 *Phys. Lett. A* **359** 658
- [60] Wamba E, Mohamadou A and Kofane T C 2008 *J. Phys. B: At. Mol. Opt. Phys.* **41** 225403
- [61] Abdullaev F K and Salerno M 2005 *Phys. Rev. A* **72** 033617
- [62] Chen B-L, Huang X-B, Kou S-P and Zhang Y 2008 *Phys. Rev. A* **78** 043603
- [63] Chen Y, Zhang K-Z and Chen Y 2009 *J. Phys. B: At. Mol. Opt. Phys.* **42** 185302
- [64] Zhou K, Liang Z and Zhang Z 2010 *Phys. Rev. A* **82** 013634
- [65] Silva-Valencia J and Souza A M C 2011 *Phys. Rev. A* **84** 065601
- [66] Sowiński T 2012 *Phys. Rev. A* **85** 065601
- [67] Singh M, Dhar A, Mishra T, Pai R V and Das B P 2012 *Phys. Rev. A* **85** 051604
- [68] Safavi-Naini A, von Stecher J, Capogrosso-Sansone B and Rittenhouse S T 2012 *Phys. Rev. Lett.* **109** 135302
- [69] Dasgupta R 2010 *Phys. Rev. A* **82** 063607
- [70] Roy U, Atre R, Sudheesh C, Kumar C N and Panigrahi P K 2010 *J. Phys. B: At. Mol. Opt. Phys.* **43** 025003
- [71] Ma J, Li Z and Xue J-K 2009 *Chin. Phys. B* **18** 4122
- [72] Josserand C, Pomeau Y and Rica S 1995 *Phys. Rev. Lett.* **75** 3150
- [73] Josserand C and Rica S 1997 *Phys. Rev. Lett.* **78** 1215
- [74] Berloff N G 2009 *Fluid Dyn. Res.* **41** 051403
- [75] Li H-C, Chen H-J and Xue J-K 2010 *Chin. Phys. Lett.* **27** 030304
- [76] Yong W-M, Wei X-F, Zhou X-Y and Xue J-K 2009 *Commun. Theor. Phys.* **51** 433
- [77] Peng P and Li G-Q 2009 *Chin. Phys. B* **18** 3221
- [78] Gross E P 1961 *Nuovo Cimento* **20** 454
- [79] Pitaevskii L P 1961 *Sov. Phys.—JETP* **13** 451
- [80] Pitaevskii L and Stringari S 2004 *Bose–Einstein Condensation* (Oxford: Clarendon)
- [81] Pethick C J and Smith H 2008 *Bose–Einstein Condensation in Dilute Gases* 2nd edn (Cambridge: Cambridge University Press)
- [82] Dalfovo F, Giorgini S, Pitaevskii L P and Stringari S 1999 *Rev. Mod. Phys.* **71** 463
- [83] Altin P A, Dennis G R, McDonald G D, Döring D, Debs J E, Close J D, Savage C M and Robins N P 2011 *Phys. Rev. A* **84** 033632
- [84] Efimov V 1971 *Sov. J. Nucl. Phys.* **12** 589
- [85] Efimov V 1979 *Sov. J. Nucl. Phys.* **29** 546
- [86] Braaten E and Nieto A 1999 *Eur. Phys. J. B* **11** 143
- [87] Gammal A, Frederico T and Tomio L 2001 *Phys. Rev. A* **64** 055602
- [88] Bulgac A 2002 *Phys. Rev. Lett.* **89** 050402
- [89] Trombettoni A and Smerzi A 2001 *Phys. Rev. Lett.* **86** 2353
- [90] Grimm R 2010 *Rev. Mod. Phys.* **82** 1225
- [91] Borzov D, Mashayekhi M S, Zhang S, Song J-L and Zhou F 2012 *Phys. Rev. A* **85** 023620
- [92] Bogoliubov N N and Mitropolsky Yu A 1961 *Asymptotic Methods in the Theory of Non-Linear Oscillations* (New York: Gordon and Breach)
- [93] Pelster A, Kleinert H and Schanz M 2003 *Phys. Rev. E* **67** 016604
- [94] Mickens R 1981 *An Introduction to Nonlinear Oscillations* (Cambridge: Cambridge University Press)
- [95] Minorsky N 1962 *Nonlinear Oscillations* (Princeton, NJ: Van Nostrand-Reinhold)
- [96] *Mathematica* symbolic calculation software package. Available at [www.wolfram.com/mathematica](http://www.wolfram.com/mathematica)
- [97] Muruganandam P and Adhikari S K 2009 *Comput. Phys. Commun.* **180** 1888
- [98] Vudragović D, Vidanović I, Balaž A, Muruganandam P and Adhikari S K 2012 *Comput. Phys. Commun.* **183** 2021
- [99] Vidanović I, Bogojević A, Balaž A and Belić A 2009 *Phys. Rev. E* **80** 066706
- [100] Balaž A, Vidanović I, Bogojević A and Pelster A 2010 *Phys. Lett. A* **374** 1539
- [101] Balaž A, Vidanović A, Bogojević A, Belić A and Pelster A 2011 *J. Stat. Mech.* **P03004**
- [102] Balaž A, Vidanović A, Bogojević A, Belić A and Pelster A 2011 *J. Stat. Mech.* **P03005**
- [103] Diakonov F K, Kalozoumis P A, Karanikas A I, Manifavas N and Schmelcher P 2012 *Phys. Rev. A* **85** 062110
- [104] Hu W H, Jin L and Song Z 2012 Dynamics of one-dimensional tight-binding models with arbitrary time-dependent external homogeneous fields arXiv:1205.6999
- [105] Balaž A, Vidanović I, Stojiljković D, Vudragović D, Belić A and Bogojević A 2012 *Commun. Comput. Phys.* **11** 739
- [106] Lima A R P and Pelster A 2012 *Phys. Rev. A* **86** 063609

## Spin modulation instabilities and phase separation dynamics in trapped two-component Bose condensates

Ivana Vidanović<sup>1,2,3</sup>, N J van Druten<sup>4</sup> and Masudul Haque<sup>2,5</sup>

<sup>1</sup> Scientific Computing Laboratory, Institute of Physics Belgrade, University of Belgrade, Pregrevica 118, 11080 Belgrade, Serbia

<sup>2</sup> Max-Planck-Institut für Physik komplexer Systeme, Nöthnitzer Straße 38, D-01187 Dresden, Germany

<sup>3</sup> Institut für Theoretische Physik, Goethe-Universität, D-60438 Frankfurt/Main, Germany

<sup>4</sup> Van der Waals-Zeeman Institute, University of Amsterdam, Science Park 904, 1098-XH Amsterdam, The Netherlands

E-mail: [haque@pks.mpg.de](mailto:haque@pks.mpg.de)

*New Journal of Physics* **15** (2013) 035008 (15pp)

Received 26 October 2012

Published 6 March 2013

Online at <http://www.njp.org/>

doi:10.1088/1367-2630/15/3/035008

**Abstract.** In the study of trapped two-component Bose gases, a widely used dynamical protocol is to start from the ground state of a one-component condensate and then switch half the atoms into another hyperfine state. The slightly different intra-component and inter-component interactions can then lead to highly non-trivial dynamics, especially in the density mismatch between the two components, commonly referred to as ‘spin’ density. We study and classify the possible subsequent dynamics, over a wide variety of parameters spanned by the trap strength and by the inter- to intra-component interaction ratio. A stability analysis suited to the trapped situation provides us with a framework to explain the various types of dynamics in different regimes.

<sup>5</sup> Author to whom any correspondence should be addressed.



Content from this work may be used under the terms of the [Creative Commons Attribution 3.0 licence](http://creativecommons.org/licenses/by/3.0/). Any further distribution of this work must maintain attribution to the author(s) and the title of the work, journal citation and DOI.



**Contents**

<b>1. Introduction</b>	<b>2</b>
<b>2. Geometry and formalism</b>	<b>4</b>
<b>3. Stability analysis and dynamical ‘phase diagram’</b>	<b>5</b>
<b>4. Dynamical features across the parameter space</b>	<b>7</b>
<b>5. Length scales of patterns</b>	<b>11</b>
<b>6. Conclusions and open problems</b>	<b>12</b>
<b>Acknowledgments</b>	<b>14</b>
<b>References</b>	<b>14</b>

**1. Introduction**

Two-component Bose–Einstein condensates (BECs) are increasingly appreciated as a rich and versatile source of intricate non-equilibrium pattern dynamics phenomena. In addition to experimental observations [1–13], pattern dynamics in two-component BECs has also attracted significant theoretical interest (see, e.g., [14–28] and references cited in [14]).

In a number of two-component BEC experiments reported over more than a decade, a standard technique has been to start from the equilibrium state of a single-component BEC, e.g. populating a single hyperfine state of  $^{87}\text{Rb}$  and then using a  $\pi/2$  pulse to switch half the atoms to a different hyperfine state [1–9]. This results in a binary condensate where the two intra-species interactions ( $g_{11}$  and  $g_{22}$ ) and one inter-species interaction ( $g_{12}$ ) are all slightly different from each other, but the starting state is the ground state determined by  $g_{11}$  alone. Since it has been realized several times in several different laboratory setups, this is a paradigm non-equilibrium initial state for binary condensate dynamics. A thorough and general analysis of the dynamics subsequent to such a  $\pi/2$  pulse is thus clearly important. In this paper, we present such an analysis, clarifying the combined role of the inter-species interaction ( $g_{12}$ ) and the strength  $\lambda$  of the trapping potential. We provide a stability analysis mapping out regions of the  $\lambda$ – $g_{12}$  parameter space hosting different types of dynamics. Since it is now routine to monitor real-time dynamics in such experiments (e.g. [6]), we also directly analyze the real-time evolution after a  $\pi/2$  pulse.

It is widely known that the ground state of a uniform two-species BEC is phase separated or miscible depending on whether or not the inter-species repulsion dominates over the self-repulsions of the two species, i.e. if

$$g_{11}g_{22} < (g_{12})^2, \quad (1)$$

then the ground state is phase separated [15]. This criterion is also a key ingredient in understanding dynamical features such as pattern dynamics in the density difference between the two species—such ‘spin patterns’ emerge when the phase separation condition is satisfied. (Since it is common to refer to the components of a two-component Bose gas as ‘spin’ states, e.g. [29–32], we refer to the density difference as ‘spin density’ and patterns in the density difference as ‘spin patterns’.) The emergence of spin patterns whenever equation (1) is satisfied can be understood as the onset of a modulation instability [16–18], identified by the appearance of an unstable mode in the excitation spectrum around a reference stationary state. For a

*homogeneous* situation, linear stability analysis shows that modulation instability sets in when the condition of equation (1) is satisfied [16–18].

The situation is different in the presence of a trapping potential. Phase separation in the ground state, as well as the appearance of modulation instability when starting from a mixed state, now requires larger inter-species repulsion [14, 19]. This suggests that the region of parameter space where pattern dynamics occurs also depends on the trap. A trap is almost always present in cold-atom experiments, and it is easy to imagine experiments where the trapping potential is not extremely shallow but varies between tight and shallow limits. (‘Tight’ and ‘shallow’ will be specified more precisely in section 2.) It is thus necessary to examine the relevance of equation (1) for trapped binary BECs. To this end, we explore different trap strengths spanning several orders of magnitude, and identify the appropriate extensions of equation (1) for the type of spin dynamics resulting from the  $\pi/2$  protocol described above.

We focus on the effects of two parameters. Firstly, we study the effects of changing cross-species interaction  $g_{12}$ , thus generalizing equation (1) for trapped situations. Secondly, we explore the role of the relative strength of the trap with respect to the interactions. Our analysis, performed for a one-dimensional (1D) geometry, sheds light on the situation where  $g_{11}$  and  $g_{22}$  are close but unequal: (a) the stability analysis is performed for  $g_{11} = g_{22}$  and their difference serves only to select appropriate instability modes; (b) the simulations are performed with  $g_{22}/g_{11} = 1.01$ .

We restrict ourselves to repulsive interactions ( $g_{ij} > 0$ ). Attractive interactions ( $g_{ij} < 0$ ) are known to cause collapse of the condensate for a large enough number of particles, even for a single-component BEC [33].

In section 2, we introduce the formalism and geometry. In section 3, we show the results from a linear stability analysis for a sequence of trap strengths, and identify and analyze relevant modulation instabilities. Through an analysis of unstable modes, we present a classification of the parameter space into dynamically distinct regions, in relation to the prototypical initial state explained above. This may be regarded as a dynamical ‘phase diagram’. A remarkable aspect is that the ‘phase transition’ line most relevant to spin pattern dynamics does not arise from the first modulation instability (studied in [14]). This first instability mode is antisymmetric in space, and as a result is not naturally excited in a symmetric trap with symmetric initial conditions. Complex dynamics (not due to collective modes but rather due to modulation instability) is generated only when the first *spatially symmetric* mode becomes unstable, which occurs at a higher value of  $g_{12}$ .

In section 4, we provide a relatively detailed account of the time evolution. For each trap strength  $\lambda$ , for values of  $g_{12}$  not much larger than  $g_{11}$ , we observe simple collective modes. Above a threshold value of  $g_{12}$ , the oscillation amplitude becomes sharply stronger, and at the same time the motion becomes notably aperiodic, signaling that the dynamics is more complex than a combination of a few modes. Dynamical spin patterns start appearing at this stage and become more pronounced as  $g_{12}$  is increased further. The threshold value at which the dynamics changes sharply corresponds to the second modulation instability line rather than the first, as we demonstrate through a careful choice of parameters in each region of the phase diagram derived from stability analysis.

Some further connections between the stability analysis and dynamical features, relating to the length scale of the generated patterns, appear in section 5. In the concluding section 6, we place our results in context and point out open questions.

## 2. Geometry and formalism

The relevant time-resolved experiments have been performed in both quasi-1D geometries (highly elongated traps with strong radial trapping) [6] and in a three-dimensional BEC of cylindrical symmetry with the radial variable playing an analogous role as the 1D coordinate [2, 5]. Since the basic phenomena are very similar, we expect the same theoretical framework to describe the essential features of each case. For definiteness, in this work we show results for 1D geometry. We expect the general picture emerging from this work to be qualitatively true also for other geometries exhibiting the same type of spin dynamics.

We will restrict ourselves to the mean field regime. Bosonic systems in elongated traps can of course also be in regimes beyond the applicability of mean field descriptions, e.g. when the particle number is small. In such a case a Lieb–Liniger or Tonks–Girardeau description might be more appropriate. Dynamics in such regimes is beyond the scope of this paper. The mean field regime is generally valid when the particle number is large enough [34].

In the mean field framework at zero temperature, the dynamics is described by two coupled Gross–Pitaevskii equations [35–37]:

$$i\partial_t\psi_1 = \left( -\frac{1}{2}\partial_x^2 + \frac{1}{2}\lambda^2x^2 + g_{11}|\psi_1|^2 + g_{12}|\psi_2|^2 \right) \psi_1, \quad (2)$$

$$i\partial_t\psi_2 = \left( -\frac{1}{2}\partial_x^2 + \frac{1}{2}\lambda^2x^2 + g_{12}|\psi_1|^2 + g_{22}|\psi_2|^2 \right) \psi_2. \quad (3)$$

Condensate wave functions  $\psi_1(x, t)$  and  $\psi_2(x, t)$  are normalized to unity, and  $\lambda$  is the strength of the harmonic trap. Factors of particle number and radial trapping frequency are absorbed as appropriate into the effective 1D interaction parameters  $g_{ij}$  [6, 37, 38]. We consider purely non-dissipative dynamics, i.e. we do not attempt to model experimental loss rates with a phenomenological dissipative term as was done in, e.g., [5–7].

The equations above are in a dimensionless form, because we measure lengths in units of trap oscillator length and time in units of inverse trapping frequency, for a hypothetical trap of unit strength ( $\lambda = 1$ ). The scale for trap strengths is itself fixed by imposing  $g_{11} = 1$ . With this convention, small values of  $\lambda$  correspond to a BEC in the Thomas–Fermi limit. For comparison, we note that the parameters of the experiment of [6] correspond to  $\lambda$  of the order of  $10^{-5}$  in these units. For the purposes of this paper, ‘tight’ and ‘shallow’ mean, respectively,  $\lambda \gtrsim 10^{-2}$  and  $\lambda \lesssim 10^{-4}$  in our units. Note that the trap oscillator strength is  $\lambda^{-1/2}$ .

Of course, one can switch between different units via the transformation:  $x \rightarrow x/l$ ,  $t \rightarrow t/l^2$ ,  $\lambda \rightarrow \lambda l^2$ ,  $g \rightarrow gl$  and  $\psi \rightarrow \psi\sqrt{l}$ , where  $l$  is an appropriately chosen scale.

The initial state after a  $\pi/2$  pulse involves both components occupying the ground state of a single-component system of interaction  $2g_{11}$ , because the atoms were all in the first hyperfine state before the pulse. We model this initial situation as a two-component BEC with  $g_{11} = g_{22} = g_{12}$ . The  $\pi/2$  pulse may then be regarded as a sudden change (a *quantum quench* [39]) of the interaction parameters  $g_{22}$  and  $g_{12}$ .

We use  $g_{11} = g_{22}$  for the stability analysis of section 3. For the explicit time evolution reported in section 4, we use  $g_{11}$  and  $g_{22}$  values close but unequal:  $g_{11} = 1$ ,  $g_{22} = 1.01$ . This choice of close values is convenient for illustrating the structure of the phase diagram, especially for shallow traps. In rubidium experiments the difference between  $g_{11}$  and  $g_{22}$  is somewhat larger (in the common case using  $^{87}\text{Rb}$  hyperfine states  $|1\rangle = |F = 1, m_F = -1\rangle$  and

$|2\rangle = |F = 2, m_F = 1\rangle$ ); however, our insights should be relevant to a broad regime of possible experiments. A full exploration of the regime of arbitrary differences ( $g_{11} - g_{22}$ ) remains an open task beyond the scope of the present paper.

Numerical simulations presented in section 4 were performed using a semi-implicit Crank–Nicolson method [40, 41].

### 3. Stability analysis and dynamical ‘phase diagram’

We provide in this section a stability analysis for  $g_{11} = g_{22}$  that maps out the regions of  $\lambda$ – $g_{12}$  parameter space which support pattern formation instabilities.

Ideally, one might wish to perform a stability analysis around the initial state. However, in contrast to the homogeneous case [16], we are faced with the situation that the initial state is not a stationary state of the final Hamiltonian. The choice of reference state is therefore a somewhat subtle aspect of the present analysis.

We use as the reference state  $\psi_0(x)$  the lowest-energy spatially symmetric stationary state of the case  $g_{11} = g_{22}$ , with parameter  $g_{12}$  set to its final value. (For large  $g_{12}$ , this is not the ground state for these parameters, which is phase-separated.) This reference state has the advantage of looking relatively similar to our actual initial state (two components totally overlapping in space), and of being a stationary state of the Hamiltonian for which we analyze linear stability. Our reference state can be regarded as placing both components in the single-component ground state for interaction  $g_{11} + g_{12}$ . We are not aware of a suitable stationary state even more similar to the actual initial state. We will see that our stability analysis around this reference state will predict remarkably well the main observed time-evolution features described in section 4.

Note that it is not natural to use  $g_{11} \neq g_{22}$ , because stationary states for such a case typically do not overlap completely in space. Instead, in our approach the difference between  $g_{11}$  and  $g_{22}$  will play the important role of selecting certain instability modes over others. For this reason, inferences from the present analysis apply only to small relative differences between  $g_{11}$  and  $g_{22}$ .

We linearize equations (2) and (3) around the reference stationary state  $\psi_0(x)$ :

$$\begin{aligned}\psi_1(x, t) &= [\psi_0(x) + \delta\psi_1(x, t)] \exp(-i\mu t), \\ \psi_2(x, t) &= [\psi_0(x) + \delta\psi_2(x, t)] \exp(-i\mu t),\end{aligned}\tag{4}$$

where  $\mu$  is the chemical potential corresponding to the reference state. By keeping only terms of the first order in  $\delta\psi_1(x, t)$  and  $\delta\psi_2(x, t)$ , we obtain a system of linear equations which can be cast in the form

$$\partial_t^2 \begin{pmatrix} \delta\psi_1 + \delta\psi_1^* \\ \delta\psi_2 + \delta\psi_2^* \end{pmatrix} + \mathcal{M} \begin{pmatrix} \delta\psi_1 + \delta\psi_1^* \\ \delta\psi_2 + \delta\psi_2^* \end{pmatrix} = 0.\tag{5}$$

Here  $\mathcal{M}$  is a matrix differential operator which, upon discretization or upon expansion in a set of orthogonal functions, becomes the so-called stability matrix (e.g. [22, 24]). We analyze below the eigenmodes of the stability matrix, which we have obtained by numerically calculating the reference stationary state  $\psi_0(x)$  and expanding in the basis of harmonic trap (non-interacting) eigenstates.

Since we use  $g_{11} = g_{22}$  for the stability analysis, eigenmodes will have well-defined ‘species parity’, i.e. will all be either even [ $\delta\psi_1(x, t) = \delta\psi_2(x, t)$ ] or odd [ $\delta\psi_1(x, t) = -\delta\psi_2(x, t)$ ] with respect to the interchange of species. Even modes describe in-phase motion of the two components and simply correspond to the excitation spectrum of a single-component

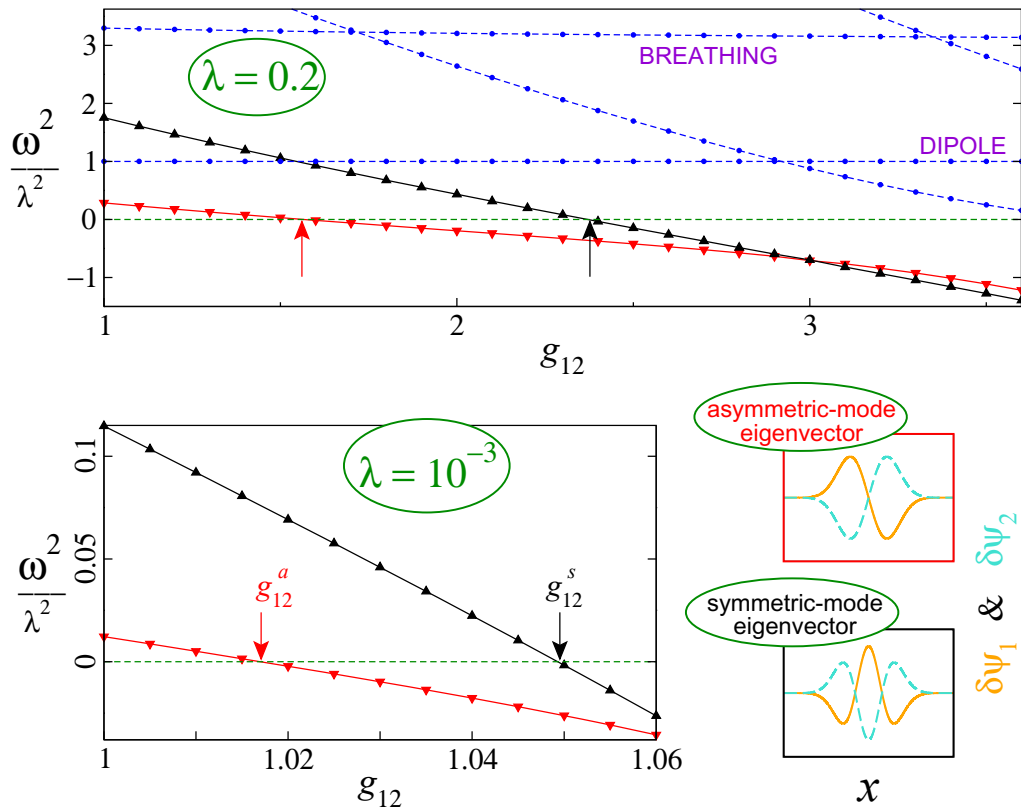


**Figure 1.** Results of stability analysis. Squared eigenvalues  $\omega^2$  of the stability matrix  $\mathcal{M}$  are plotted against  $g_{12}$ , for a tight trap (top) and for a shallow trap (bottom left). The arrows show the values of  $g_{12}$  for onset of the two instabilities, namely  $g_{12}^a$  (onset of spatially antisymmetric modulation instability) and  $g_{12}^s$  (onset of spatially symmetric instability). Typical eigenvectors corresponding to these two modes are shown in the panels on the lower right.

BEC with interaction constant  $g_{11} + g_{12}$ . Odd modes are more interesting—they describe out-of-phase motion of two components and are therefore reflected in the spin dynamics. Additionally, due to the spatial inversion symmetry  $x \rightarrow -x$ , the solutions will also have well-defined spatial reflection symmetry, and we can distinguish spatially symmetric and antisymmetric modes.

Typical eigenspectra are presented in figure 1. In the case of a tight trap  $\lambda = 0.2$ , we notice two modes whose frequencies are nearly constant. These are even modes encoding single-component or in-phase physics. The lower one is the dipole (Kohn) mode with frequency equal to the trap frequency  $\lambda$ . The second nearly constant mode is the breathing mode, which for elongated traps takes a value close to  $\omega^2 = 3\lambda^2$ . The breathing mode (oscillations of cloud size) is visible in the plots of figure 3 (section 4) as a fast oscillation of the total condensate widths.

The two lowest-lying eigenmodes are odd modes encoding out-of-phase physics. For  $g_{12} \gtrsim 1$ , their frequencies are significantly below the breathing mode, and therefore lead to relatively slow oscillations in the spin density. This will also be visible in the real-time dynamics presented in section 4 (the first two columns of figures 3 and 4). The forms of the corresponding eigenvectors are shown in the lower right of figure 1. The nature of the eigenvectors shows that the motion related to the lowest mode corresponds to the left–right oscillations of the

two species, while the next odd mode corresponds to spatially symmetric spin motion. The frequencies of these two modes become imaginary at certain values of  $g_{12}$ , thus leading to the onset of modulation instabilities. The antisymmetric mode becomes unstable at smaller value of  $g_{12}$  ( $g_{12}^a \approx 1.6$  for  $\lambda = 0.2$ ) in comparison with the symmetric mode ( $g_{12}^s \approx 2.4$  for  $\lambda = 0.2$ ). In a spatially symmetric trap, there is no natural mechanism for exciting the spatially antisymmetric mode. On the other hand, any difference between  $g_{11}$  and  $g_{22}$  naturally excites the second (spatially symmetric) mode. Thus, the second mode, occurring at larger  $g_{12}$ , is the relevant instability for understanding the dynamics observed in experiments and explored numerically in section 4.

We find similar excitation spectra for trap strengths  $\lambda$  spanning several orders of magnitude. The spatially antisymmetric mode becomes unstable before the spatially symmetric mode, and both instabilities get closer to 1 as the trap gets shallower. For example, for  $\lambda = 10^{-3}$  (also shown in figure 1) the lowest instability sets in for  $g_{12}^a \approx 1.02$ , while the next one appears at  $g_{12}^s \approx 1.05$ . The distinction between two instabilities becomes ever smaller as we go toward a uniform system  $\lambda \rightarrow 0$ , where the phase-separation condition, equation (1), becomes exact. Nevertheless, even for shallow traps, the issue is not purely academic as the precision in experimental measurement and control of scattering lengths continues to improve [6, 42].

In figure 2 (main panel), the results of the stability analyses are combined to present a dynamical ‘phase diagram’. The two lines show the two instabilities ( $g_{12}^a$  and  $g_{12}^s$ ) as a function of trap strength  $\lambda$ . For very shallow traps, the two transition lines merge as  $g_{12}^s \approx g_{12}^a \approx 1$ . The lower transition line ( $g_{12}^a$ ) was previously introduced in [14]. However, for a trap and initial state with left–right spatial symmetry, this is not the relevant dynamical transition line, because the first even mode only becomes unstable at some higher  $g_{12}$  value, given by the  $g_{12}^s$  line.

In section 4, we will see that spin pattern dynamics is indeed only generated when the inter-component repulsion  $g_{12}$  exceeds the second instability line ( $g_{12} > g_{12}^s$ ), and that crossing the first instability ( $g_{12}^a < g_{12} < g_{12}^s$ ) is not enough for pattern formation in a spatially symmetric trap.

#### 4. Dynamical features across the parameter space

In this section, we present and analyze the dynamics obtained from direct numerical simulation of the Gross–Pitaevskii equations (2) and (3), after the system is initially prepared in the ground state of the situation  $g_{11} = g_{22} = g_{12} = 1$ . The subsequent dynamics is performed with  $g_{11} = 1$ ,  $g_{22} = 1.01$ , and several different values of  $g_{12}$  for each trap strength  $\lambda$ .

It is difficult to show the full richness of pattern dynamics through plots of a few quantities. We choose to show the dynamics through two types of plots (figures 3 and 4). Figure 3 shows the time dependence of the root mean square widths of the two components

$$w_{1,2}^2(t) = \int_{-\infty}^{\infty} x^2 |\psi_{1,2}(x, t)|^2 dx, \quad (6)$$

while figure 4 shows density plots of the density difference (spin density),  $|\psi_1(x, t)|^2 - |\psi_2(x, t)|^2$ . In both figures, each row corresponds to a different trap strength ( $\lambda$ ), and we approach the shallow trap (Thomas–Fermi) limit going from top to bottom.

For each  $\lambda$  the four values of  $g_{12}$  from table 1 are used for figures 3 and 4. We have chosen  $g_{12}$  values such that the first panel in each row is in the parameter region where there are no instabilities, the second one is in the region where the only instability is the antisymmetric

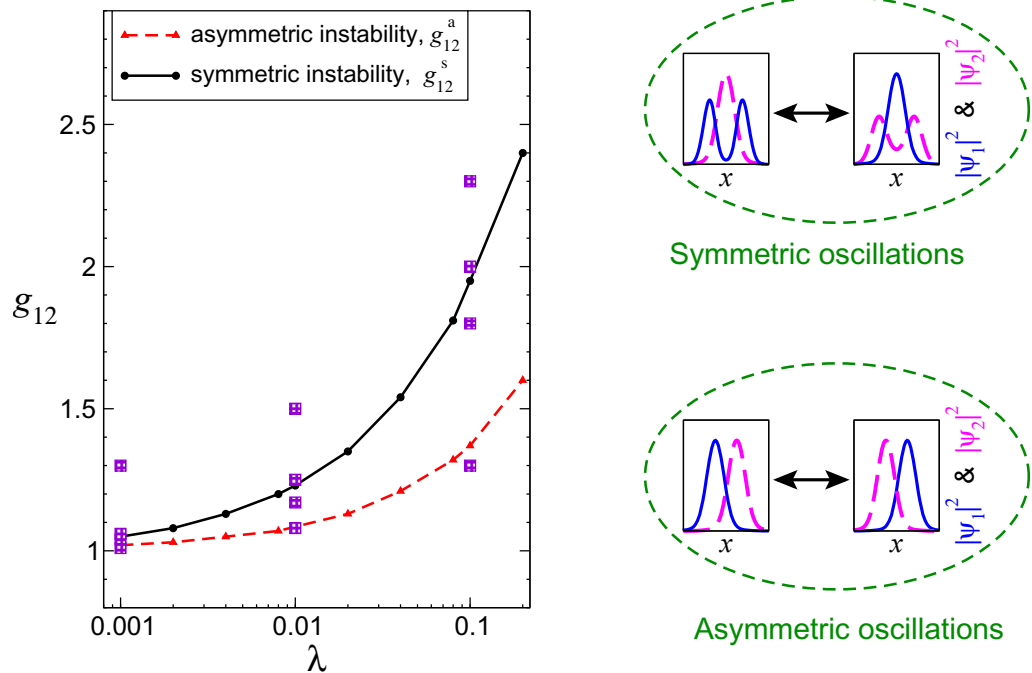


**Figure 2.** Left: the dynamical ‘phase diagram’ showing the critical values of  $g_{12}$  for the onset of the two types of modulation instability versus the trap strength  $\lambda$ . The instability lines are shown as straight lines joining numerically determined values. Right bottom: spatially asymmetric (left–right–left) oscillation mode, shown schematically through density profiles of the two components at two instants of an oscillation period. This type of mode is persistent everywhere above the  $g_{12}^a$  line. Right top: spatially symmetric (in–out–in) oscillation mode, shown schematically through density profiles of the two components at two instants of an oscillation period. This type of mode is persistent only above the higher  $g_{12}^s$  line. The spatially symmetric instability ( $g_{12}^s$  line) is the one relevant for experimental situations with symmetric traps. Squares mark values used in the dynamical simulations of figures 3 and 4 (table 1).

one, and the third on each row is at  $g_{12}$  values just above the second, relevant, instability. The fourth panel on each row is at higher  $g_{12}$  values. The choice of  $g_{12}$  values with respect to instability lines is clear in the tighter traps of the top three rows, as also shown by squares in figure 2. For shallow traps (lower rows), the instability lines are too close together and too close to  $g_{12} = 1$ , so making such choices is not meaningful. In the following, as we compare the features of the different columns, we implicitly exclude the lowest row (smallest  $\lambda$ ). This is also indicated by the fact that the schematic instability lines in figures 3 and 4 are not extended to the lowest row.

Broadly speaking, we note that there is only regular (collective-mode) dynamics in the second-column figures ( $g_{12}^a < g_{12} < g_{12}^s$ ) even though an instability is present. There is generally a sharp difference between the second and third figures in each row, indicating that the second instability ( $g_{12}^s$ ) is the relevant one. The fourth panel on each row is at higher  $g_{12}$  values, showing more rich dynamics.

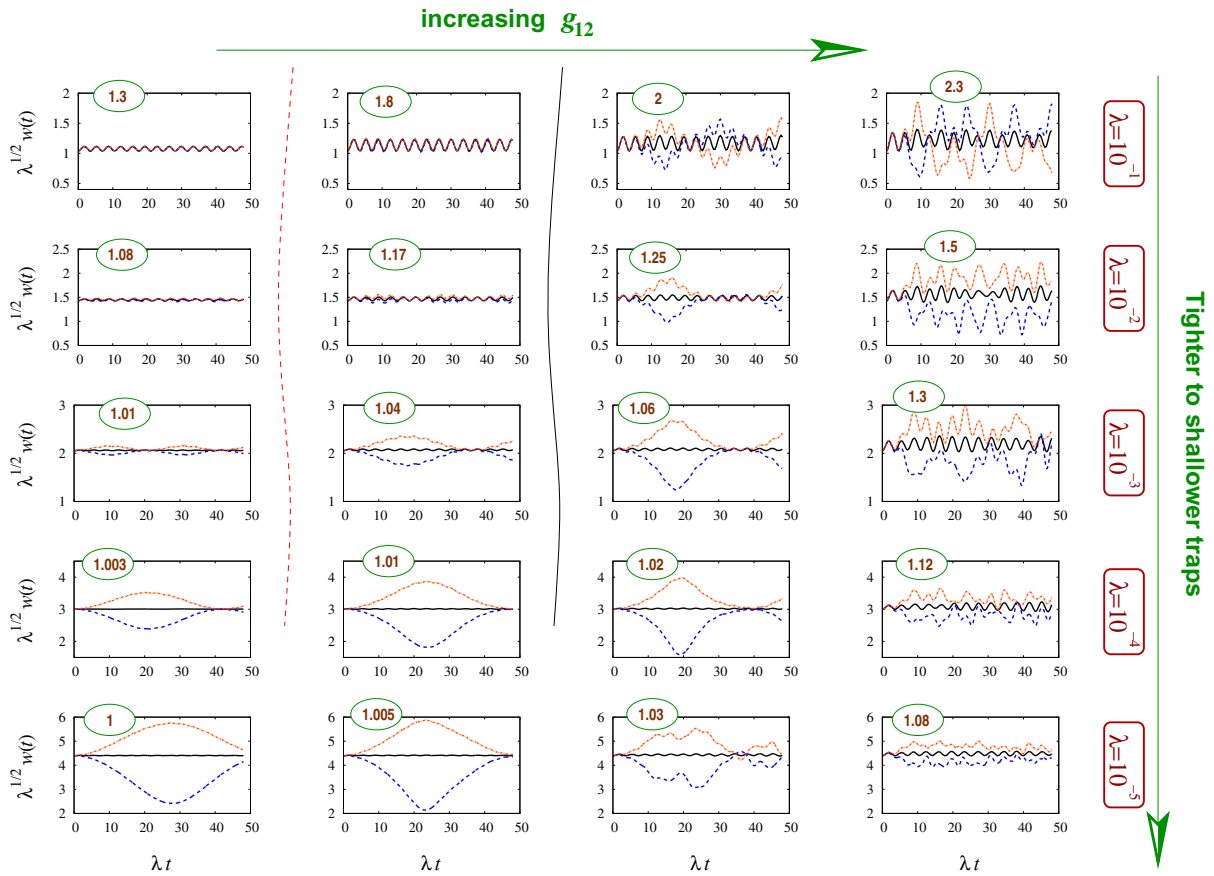


**Figure 3.** Time evolution of root-mean-square widths after  $\pi/2$  pulse (interaction quench). The first component width  $w_1(t)$  is shown as a blue dashed line, the second component width  $w_2(t)$  is shown as a red solid line (gray solid without color), and the total width  $w(t) = \sqrt{(w_1^2(t) + w_2^2(t))/2}$  is the black solid line intermediate between the other two. From top to bottom: tight to shallow traps. For each trap strength, four values of  $g_{12}$  (indicated near the top of each panel) from table 1 are used. The two lines separating the first and second columns (red dashed) and the second and third columns (black solid) indicate the ‘positions’ of instability lines, from figure 2. While the first two columns look qualitatively the same and show regular oscillatory dynamics, in the third column we observe aperiodic motion of stronger amplitude that we relate to the onset of spin pattern dynamics. The spin dynamics is even more pronounced in the fourth column.

In figure 3, we show the time dependence of the individual widths ( $w_1$ ,  $w_2$ ) and also of the total root-mean-square width,  $w(t) = \sqrt{(w_1^2(t) + w_2^2(t))/2}$ . Consistent with our observation that spatially symmetric modes (and not the antisymmetric ones) are naturally excited in the current setup, the dynamics shows signatures of the two most prominent spatially symmetric modes noted in figure 1. The breathing mode is the easiest to note and most ubiquitous—it shows up in almost every parameter choice as oscillations in the total density (in-phase in the two components), with a typical period given by  $2\pi/\sqrt{3}\lambda \approx 3.63/\lambda$ . This follows from the frequency of this mode being almost constant near  $\sqrt{3}\lambda$ .



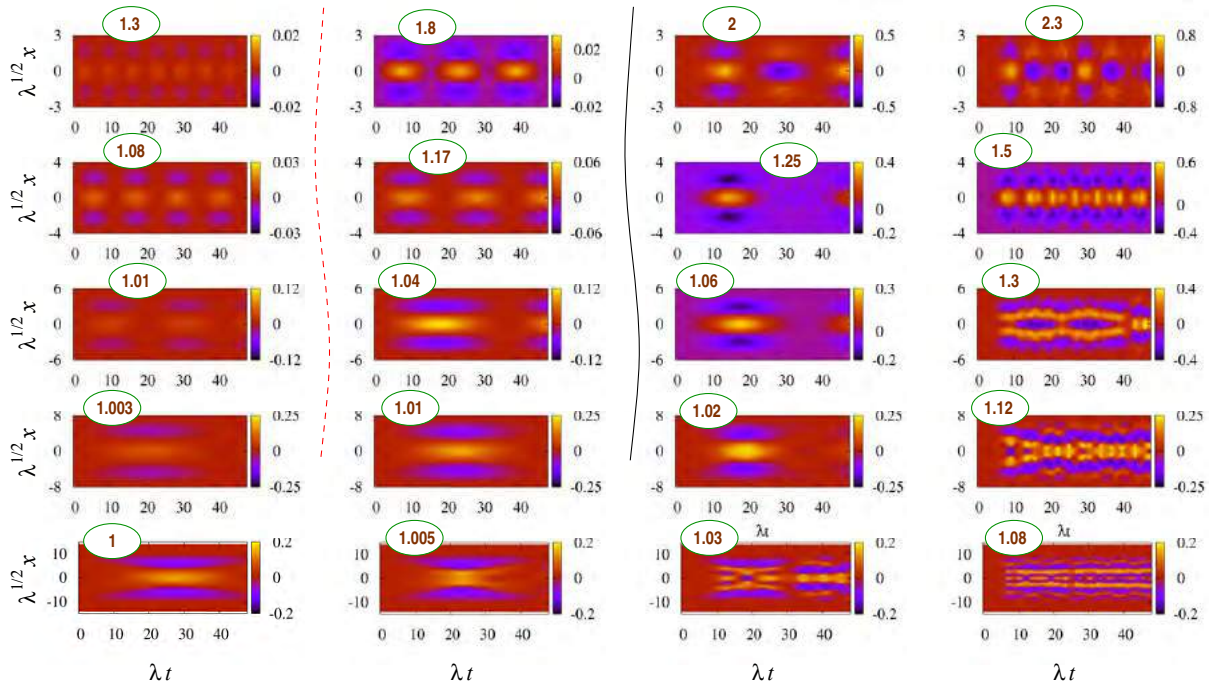


**Figure 4.** Spin dynamics subsequent to the  $\pi/2$  protocol, shown via the density difference  $\lambda^{-1/2} (|\psi_1(x, t)|^2 - |\psi_2(x, t)|^2)$ . Traps and  $g_{12}$  values are the same as in figure 3 and table 1:  $\lambda$  decreases from  $10^{-1}$  to  $10^{-5}$  from top to bottom and  $g_{12}$  values are indicated near the top of each panel. As in figure 3, the black solid line and the red dashed line indicate the instability lines from the ‘phase diagram’ of figure 2. Note the sharp change of color-scale ranges between the second and third columns in the upper rows, indicating that the dynamics changes dramatically only across the second instability line.

**Table 1.** Parameters from the first five columns are used for the plots in figures 3 and 4. The instability values  $g_{12}^a$  and  $g_{12}^s$  (introduced in figures 1 and 2 and discussed in section 3) are also given for each trap strength.

$\lambda$	$\frac{g_{12}^{(1)}}{\sqrt{g_{11}g_{22}}}$	$\frac{g_{12}^{(2)}}{\sqrt{g_{11}g_{22}}}$	$\frac{g_{12}^{(3)}}{\sqrt{g_{11}g_{22}}}$	$\frac{g_{12}^{(4)}}{\sqrt{g_{11}g_{22}}}$	$g_{12}^a$	$g_{12}^s$
$10^{-1}$	1.3	1.8	2	2.3	1.37	1.92
$10^{-2}$	1.08	1.17	1.25	1.5	1.085	1.23
$10^{-3}$	1.01	1.04	1.06	1.3	1.018	1.050
$10^{-4}$	1.003	1.01	1.02	1.12	1.004	1.011
$10^{-5}$	1	1.005	1.03	1.08	$\approx 1$	$\approx 1$

We also see out-of-phase motion of the two components, associated with the lower spatially symmetric mode in figure 1, which has odd species parity. In the first two columns of figure 3, corresponding to smaller values of  $g_{12}$  such that this mode has small real frequencies, this is excited as a regular ‘spin’ mode. For example, at  $\lambda = 10^{-3}$  and  $g_{12} = 1.04$ , we observe an out-of-phase oscillation with the period of approximately  $\approx 30$ , much slower than the breathing mode.

In addition, the oscillation period of the out-of-phase motion is slower in the second than in the first column of each row, corresponding to the decreasing frequency of the mode, as seen in stability analysis (figure 1). Once  $g_{12}$  becomes large enough that the instability threshold for this mode is crossed, the oscillation amplitudes increase sharply and the width dynamics becomes strongly aperiodic and irregular (the third column of figure 3). This signifies the onset of pattern dynamics, as opposed to the excitation of a regular collective mode around a stable state. Irregularity of the width dynamics at stronger  $g_{12}$  is even more apparent in the fourth column of figure 3.

It is noteworthy that the spatially antisymmetric modes play no role and do not show up in these dynamical simulations. We see no signature of the Kohn mode. Nor do we see any sharp change associated with the instability of the antisymmetric mode, i.e. there is no sharp difference between the first two columns of figure 3.

In figure 4, we show the dynamics of the ‘spin density’  $|\psi_1(x, t)|^2 - |\psi_2(x, t)|^2$ . The case of very shallow traps (last row) resembles the data in [17, 18]. As in figure 3, the first two columns show regular oscillations, corresponding to collective modes without instability. A sharp change occurs, not across the first instability line (between the first and second columns), but instead across the second instability line (the second and third columns), especially for tighter traps (top three rows) where the comparison with instability lines is meaningful. The sharp change can be noted through the color scales, which is dramatically different between the second and third columns in the upper rows.

## 5. Length scales of patterns

In homogeneous stability analysis, the length scale of patterns is inferred from the wavevector (momentum) at which an instability first occurs. Since we perform our stability analysis specifically for trapped systems, we do not have a momentum quantum number. Nevertheless, the eigenvectors of the unstable modes contain information about the form of patterns generated in the dynamics of the trapped system. This is illustrated in figure 5, where the eigenvectors of the lowest unstable spatially symmetric modes are shown for several values of  $g_{12}$ , together with the spin patterns generated in the non-equilibrium dynamics. There is a close match between the distance between nodes of the eigenvectors (rough analogue of ‘wavevector’) and the length scales involved in the patterns. As in previous figures, the lengths are shown scaled with the trap oscillator length,  $\lambda^{-1/2}$ , which plays the role of setting the overall length scale for the cloud.

In figure 4, we see that the patterns contain more spatial structure in shallow traps. The top two rows (tight traps) only show in–out–in type of patterns. This can be understood from the idea that the interactions induce length scales (‘healing lengths’) in the problem, which are smaller for larger interactions and which set the length scale of spatial structures. For tight traps, the healing length set by the interactions is large or comparable to the cloud size, so that only global dynamical patterns are generated. In such traps, generation of complex patterns with many spatial oscillations would require much higher values of  $(g_{12}/g_{11} - 1)$ . For shallow traps, the healing length becomes much smaller than the cloud size; as a result one can have a multitude of dynamical spin structures in the system, of the type seen in experiments and prior simulations [5, 6, 18]. This heuristic explanation can be made quantitative by counting the number of nodes appearing in the eigenmodes (as in figure 5). Generally, there are as many

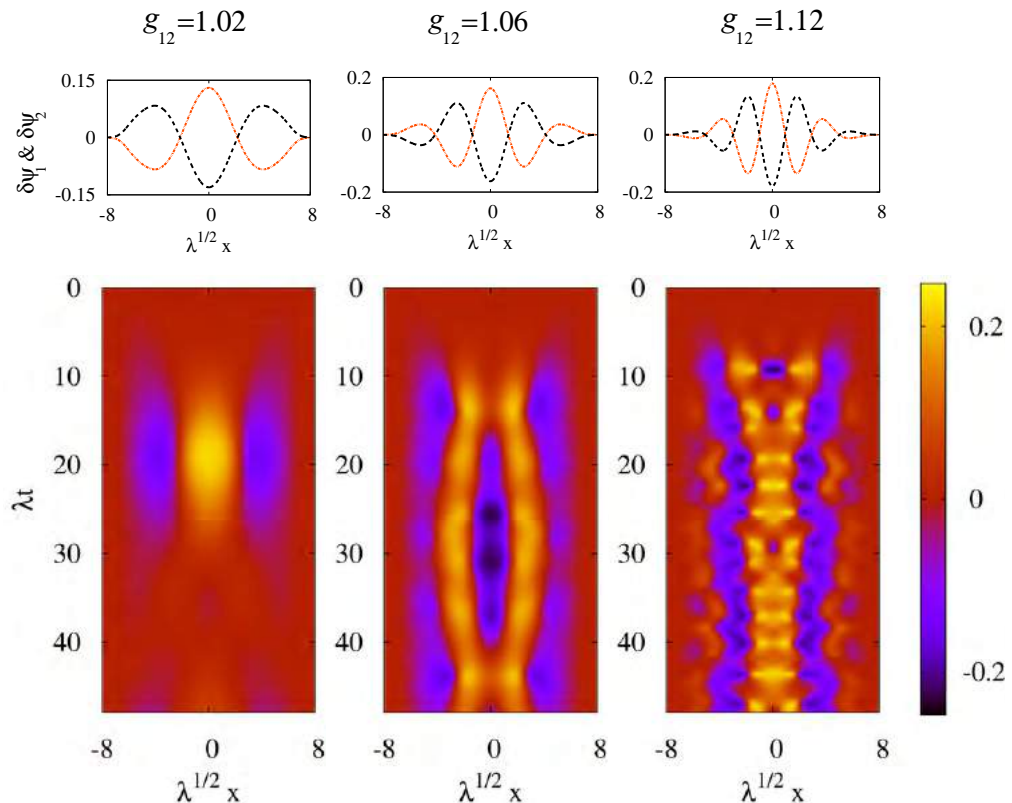


**Figure 5.** Top: eigenvectors of the most unstable spatially symmetric eigenmodes, from the stability analysis of section 3, for  $\lambda = 10^{-4}$ , and  $g_{12} = 1.02, 1.06$  and  $1.12$  from left to right. Below each eigenvector, the corresponding spin dynamics after the  $\pi/2$  protocol (parameters of section 4) is shown through the time evolution of  $|\psi_1(x, t)|^2 - |\psi_2(x, t)|^2$ . The number of nodes in the eigenvectors (top panels) corresponds closely to the number of nodes in the spin densities.

nodes in the eigenmodes as there are crossings between positive and negative spin densities seen in the dynamical patterns. Accordingly, as we have more nodes at larger  $g_{12}$ , we get more intricate dynamical patterns.

## 6. Conclusions and open problems

In this paper, we have analyzed a widely used dynamical protocol for two-component BECs, which involves starting from the ground state of one component and switching half the atoms to a different component through a  $\pi/2$  pulse. We have presented a stability analysis suitable to the trapped situation and also presented results from extensive dynamical simulations. Through an analysis of unstable modes, we have presented a classification of the parameter space into a number of dynamically distinct regions, in relation to the prototypical initial state. This may be regarded as a dynamical ‘phase diagram’.

In the ‘stable’ regime of parameter space (no modulation instabilities), our stability analysis explains the observed slow spin oscillations compared to the fast breathing mode oscillations

of the total density. We demonstrate that the important ‘phase transition’ line for spatially symmetric situations relevant to most experiments is not the first instability (studied in [14]), but a second transition line. The first instability is antisymmetric in space, and as a result is not naturally excited in a symmetric trap.

Our stability analysis is performed relative to a stationary state of the situation  $g_{11} = g_{22}$ . The  $\pi/2$  pulse of the experiments (in the cases where  $g_{11} \neq g_{22}$ ) can be considered as turning on a nonzero ( $g_{11} - g_{22}$ ), i.e. turning on ‘buoyancy’ such that one component gains more energy by being in the interior of the trap compared to the other. This helps to select instability modes which are symmetric in space.

Since we have used a stability analysis with  $g_{11} = g_{22}$  to analyze dynamics with  $g_{11} \neq g_{22}$ , an obvious question is how the ratio  $g_{22}/g_{11}$  affects the regime of applicability of this scheme. We expect that features of this ( $g_{11} = g_{22}$ ) stability analysis are useful for dynamical predictions as long as  $g_{12}/g_{11} - 1$  is roughly more than  $g_{22}/g_{11} - 1$ . For example, for shallow traps (small  $\lambda$ ), the instabilities occur at  $g_{12}/g_{11} - 1$  values comparable to 0.01, which is why the placement of parameters in the three dynamical regions of the ‘phase diagram’ (figure 2) is not meaningful for the smallest  $\lambda$  values (the lowest rows of figures 3 and 4).

For the stability analysis, we used a reference stationary state which is of course not the initial state: the initial state is the ground state for  $g_{11} = g_{22} = g_{12}$ , while the reference state is the lowest-energy spatially symmetric stationary state corresponding to the final value of  $g_{12}$ . The instability lines found in this stability analysis would describe even better a situation where the dynamics is triggered by a small quench of  $g_{12}$ , as opposed to the changes of  $g_{12}$  that we consider here, which can be relatively large. We have looked at some examples of this type of dynamics and indeed find instabilities matching the stability analysis extremely well. However, although the initial state in the  $\pi/2$  dynamics is somewhat different from the reference state of our stability analysis, our results show that this stability analysis does provide an excellent overall picture of the dynamics generated by the  $\pi/2$  protocol.

Our work opens up a number of questions deserving further study. Firstly, we have thoroughly explored the  $\lambda$ - $g_{12}$  parameter space, while assuming that the intra-component interactions  $g_{11}$  and  $g_{22}$  are unequal but close in value. The regime of large difference ( $g_{11} - g_{22}$ ) clearly might have other interesting dynamical features which are yet to be explored.

Secondly, in this work we have restricted ourselves to the mean field regime. While the mean field description captures well the richness of pattern formation phenomena (see [5, 14, 17, 18, 20] in addition to this work), it may be worth asking whether quantum effects beyond mean field might have interesting consequences for the pattern dynamics generated by a  $\pi/2$  pulse. For bosons in elongated traps, regimes other than mean field (such as the Lieb–Liniger or Tonks regimes) may occur naturally in experiments [29, 34, 43–45]. Dynamics subsequent to a  $\pi/2$  pulse in strongly interacting 1D gases outside the mean field regime is an open area for investigation.

Thirdly, we have assumed a spatially symmetric trap and an initial condition with spatial symmetry, and this plays a crucial role in the selection of instability channels. In a real-life experiment, the trap will have some left–right asymmetry. Also, thermal and quantum fluctuations can initiate spatially antisymmetric excitations. The extent to which a small spatial asymmetry affects spin dynamics remains unexplored; in such a case we would have some type of competition between the two types of instabilities. Navarro *et al* [14] have studied dynamical effects of fluctuations (noise), but the effects of thermal and quantum fluctuations are yet to be studied in the context of a  $\pi/2$  protocol.

Finally, one could consider time evolution and spatiotemporal patterns generated by a  $\pi/2$  pulse in the presence of an optical lattice, described by the dynamics of a two-component Bose–Hubbard model. This is a situation easy for us to imagine realizing experimentally. One could speculate that there is a complex interplay between spin dynamics and the spatial arrangement of Mott and superfluid regions.

## Acknowledgments

IV acknowledges discussions with A Balaž and support from the Ministry of Education and Science of the Republic of Serbia, under project no. ON171017. Numerical simulations were run on the AEGIS e-Infrastructure, supported in part by FP7 projects EGI-InSPIRE, PRACE-1IP, PRACE-2IP and HP-SEE. NJvD acknowledges support from FOM and NWO.

## References

- [1] Matthews M R, Hall D S, Jin D S, Ensher J R, Wieman C E, Cornell E A, Dalfovo F, Minniti C and Stringari S 1998 *Phys. Rev. Lett.* **81** 243
- [2] Hall D S, Matthews M R, Ensher J R, Wieman C E and Cornell E A 1998 *Phys. Rev. Lett.* **81** 1539
- [3] Miesner H-J, Stamper-Kurn D M, Stenger J, Inouye S, Chikkatur A P and Ketterle W 1999 *Phys. Rev. Lett.* **82** 2228
- [4] Lewandowski H J, Harber D M, Whitaker D L and Cornell E A 2002 *Phys. Rev. Lett.* **88** 070403
- [5] Mertes K M, Merrill J W, Carretero-González R, Frantzeskakis D J, Kevrekidis P G and Hall D S 2007 *Phys. Rev. Lett.* **99** 190402
- [6] Wicke P, Whitlock S and van-Druen N J 2010 arXiv:1010.4545
- [7] Anderson R P, Ticknor C, Sidorov A I and Hall B V 2009 *Phys. Rev. A* **80** 023603
- [8] Boehi P, Riedel M F, Hoffrogge J, Reichel J, Haensch T W and Treutlein P 2009 *Nature Phys.* **5** 592
- [9] Egorov M, Anderson R P, Ivannikov V, Opanchuk B, Drummond P, Hall B V and Sidorov A I 2011 *Phys. Rev. A* **84** 021605
- [10] Papp S B, Pino J M and Wieman C E 2008 *Phys. Rev. Lett.* **101** 040402
- [11] Myatt C J, Burt E A, Ghrist R W, Cornell E A and Wieman C E 1997 *Phys. Rev. Lett.* **78** 586
- [12] Modugno G, Modugno M, Riboli F, Roati G and Inguscio M 2002 *Phys. Rev. Lett.* **89** 190404
- [13] Hammer C, Chang J J, Engels P and Hofer M A 2011 *Phys. Rev. Lett.* **106** 065302
- [14] Navarro R, Carretero-González R and Kevrekidis P G 2009 *Phys. Rev. A* **80** 023613
- [15] Tin-Lun Ho Shenoy V B 1996 *Phys. Rev. Lett.* **77** 3276
- [16] Timmermans E 1998 *Phys. Rev. Lett.* **81** 5718
- [17] Kasamatsu K and Tsubota M 2004 *Phys. Rev. Lett.* **93** 100402
- [18] Kasamatsu K and Tsubota M 2006 *Phys. Rev. A* **74** 013617
- [19] Wen L, Liu W M, Cai Y, Zhang J M and Hu J 2012 *Phys. Rev. A* **85** 043602
- [20] Ronen S, Bohn J L, Halmó L E and Edwards M 2008 *Phys. Rev. A* **78** 053613
- [21] Sabbatini J, Zurek W H and Davis M J 2011 *Phys. Rev. Lett.* **107** 230402
- [22] Law C K, Pu H, Bigelow N P and Eberly J H 1997 *Phys. Rev. Lett.* **79** 3105
- [23] Busch Th, Cirac J I, Perez-Garcia V M and Zoller P 1997 *Phys. Rev. A* **56** 2978
- [24] Pu H and Bigelow N P 1998 *Phys. Rev. Lett.* **80** 1134
- [25] Graham R and Walls D 1998 *Phys. Rev. A* **57** 484
- [26] Sinatra A, Fedichev P O, Castin Y, Dalibard J and Shlyapnikov G V 1999 *Phys. Rev. Lett.* **82** 251
- [27] Li Y, Treutlein P, Reichel J and Sinatra A 2009 *Eur. Phys. J. B* **68** 365
- [28] Balaž A and Nicolin A 2012 *Phys. Rev. A* **85** 023613
- [29] Fuchs J N, Gangardt D M, Keilmann T and Shlyapnikov G V 2005 *Phys. Rev. Lett.* **95** 150402

- [30] Kleine A, Kollath C, McCulloch I P, Giamarchi T and Schollwöck U 2008 *Phys. Rev. A* **77** 013607
- [31] Gangardt D M and Kamenev A 2009 *Phys. Rev. Lett.* **102** 070402
- [32] Gu H-Q, An J-H and Jin K 2010 *J. Phys. B: At. Mol. Opt. Phys.* **43** 205308
- [33] Ruprecht P A, Holland M J, Burnett K and Edwards M 1995 *Phys. Rev. A* **51** 4704
- [34] Petrov D S, Shlyapnikov G V and Walraven J T M 2000 *Phys. Rev. Lett.* **85** 3745
- [35] Pitaevskii L P 1961 *Sov. Phys.—JETP* **13** 451
- [36] Gross E P 1961 *Nuovo Cimento* **20** 454
- [37] Salasnich L, Parola A and Reatto L 2002 *Phys. Rev. A* **65** 043614
- [38] Olshanii M 1998 *Phys. Rev. Lett.* **81** 938
- [39] Polkovnikov A, Sengupta K, Silva A and Vengalattore M 2011 *Rev. Mod. Phys.* **83** 863
- [40] Muruganandam P and Adhikari S K 2010 *Comput. Phys. Commun.* **180** 1888
- [41] Vudragović D, Vidanović I, Balaž A, Muruganandam P and Adhikari S K 2012 *Comput. Phys. Commun.* **183** 2021
- [42] Egorov M, Opanchuk B, Drummond P, Hall B V, Hannaford P and Sidorov A I 2012 arXiv:1204.1591
- [43] van Amerongen A H, van Es J J, Wicke P, Kheruntsyan K V and van Druten N J 2008 *Phys. Rev. Lett.* **100** 090402
- [44] Kinoshita T, Wenger T and Weiss D S 2004 *Science* **305** 1125
- [45] Haller E, Gustavsson M, Mark M J, Danzl J G, Hart R, Pupillo G and Nägerl H-C 2009 *Science* **325** 1224

**Dissipation through localized loss in bosonic systems with long-range interactions**

Ivana Vidanović, Daniel Cocks, and Walter Hofstetter

*Institut für Theoretische Physik, Johann-Wolfgang-Goethe-Universität, Max-von-Laue-Strasse 1, 60438 Frankfurt am Main, Germany*

(Received 31 January 2014; published 12 May 2014)

In recent years, controlled dissipation has proven to be a useful tool for the probing of a quantum system in an ultracold setup. In this paper we consider the dynamics of bosons induced by a dissipative local defect. We address superfluid and supersolid phases close to half filling that are ground states of an extended Bose-Hubbard Hamiltonian. To this end, we solve the master equation using the Gutzwiller approximation and find that in the superfluid phase repulsive nearest-neighbor interactions can lead to enhanced dissipation processes. On the other hand, our mean-field approach indicates that the effective loss rates are significantly suppressed deep in the supersolid phase where repulsive nearest-neighbor interactions play a dominant role. Our numerical results are explained by analytical arguments and, in particular, in the limit of strong dissipation we recover the quantum Zeno effect.

DOI: [10.1103/PhysRevA.89.053614](https://doi.org/10.1103/PhysRevA.89.053614)

PACS number(s): 03.75.Kk, 03.65.Yz, 67.85.De

**I. INTRODUCTION**

Dissipation arises in condensed matter systems through a variety of effects. Heating, impurities, and currents can often be included into these open systems only via dissipative processes. These can then contribute to the stabilization or destruction of particular equilibrium phases or produce relevant nonequilibrium physics such as resistive currents through materials. For many years, in the field of ultracold atoms, dissipation has been considered as one of the main obstacles in the preparation and manipulation of macroscopic quantum states. This point of view has changed recently, since it was realized that dissipation enables an additional way of tuning properties of the system. It has been predicted that the competition of unitary and dissipative dynamics leads to steady-state quantum phases [1–7] whose features have been compared to their equilibrium counterparts. Dissipation can be either engineered on purpose [1] or naturally present as, for example, heating processes via two-body loss [8–10], spontaneous decay of Rydberg atoms [11], or cavity loss [7].

Another beneficial aspect of controlled dissipation is that it can be exploited as a measurement tool. In this article, we choose to focus on the realization of dissipation via an electron beam [12–15] although our system can also be realized with an optical quantum gas microscope [16,17]. In all these experiments [12,16,17], application of a controlled loss process has opened the door to measurement of atoms in an optical lattice with single-site resolution. The electron beam experiment [15] operates in the following way: An electron source is focused into a very tight beam, such that electrons collide with atoms, imparting a very large amount of kinetic energy and expelling them from the trap. Both elastic and inelastic (i.e., ionizing) collisions occur and, by capturing the ions, the number of atoms in the focus of the beam can be determined. When applied in the presence of an optical lattice the loss can be made truly localized, i.e., acting on a single site, and then the effective loss rate reflects the initial local density per site in the system.

Although this measurement procedure is not described by the standard paradigm of projective measurement in quantum mechanics, it has still been shown to exhibit the quantum Zeno effect [18]. In a broader context [19], the quantum Zeno effect can be defined as a suppression of the unitary time evolution

by an interaction with the external environment. Typically, in cold atomic systems the effect is observed as a nonmonotonic behavior of the effective loss rate in the presence of an external periodic optical potential as a function of the bare loss (dissipation) strength: For weak dissipation, the effective loss rate is proportional to the dissipation strength, but in the regime of strong dissipation, the number of expelled particles decays as the dissipation gets stronger. The basic explanation of this nonintuitive phenomenon lies in the fact that the system protects itself from strong dissipation by approaching very closely a “dark” state that is unaffected by a loss process. The phenomenon has been theoretically addressed [20] and experimentally observed in three other setups in the cold atom context [21–23]. In the case of a two-body or three-body loss, it was shown that strong dissipation introduces effective hard-core repulsion into the physical system [20–22,24] precisely via the mentioned quantum Zeno effect. In recent experiments on polar molecules in three-dimensional optical lattices [23,25], the effect has been used to suppress molecular chemical reactions and to measure the density of the system.

Previous theoretical investigations of localized single-particle dissipation in bosonic systems have considered few-site Bose-Hubbard systems with large filling fractions [26–31]. It has been shown that the dynamics induced by local dissipation depends strongly on the initial state: A mean-field Gross-Pitaevskii-like description works well for initial states that are conventional homogeneous Bose-Einstein condensates. On the other hand, a beyond-mean-field treatment is necessary when the initial state is a Bose-Einstein condensate with a macroscopic occupation of the single-particle state corresponding to a nonzero momentum vector [27,30]. In that case, states with macroscopic entanglement naturally describe the long-time dynamics of the system. Localized dissipation of a one-dimensional strongly correlated system has also been addressed in a density-matrix renormalization-group (DMRG) study [32], where excitations created by dissipation as well as the quantum Zeno effect have been considered in detail.

In this paper we consider the dynamics induced by localized dissipation for bosons in a two-dimensional lattice at low filling fractions. To address the problem we apply the Gutzwiller (GW) mean-field approximation for the density matrix, which is expected to reasonably capture properties of

the system in higher dimensions. In our study we also include repulsive nearest-neighbor interactions, expected in systems of dipolar or Rydberg-dressed quantum gases [33] and polar molecules [23,25]. Usually in this context the main features of the quantum Zeno effect are explained by the balance of dissipation and hopping, and it is interesting to understand whether and how repulsive nearest-neighbor interactions can affect it. With long-range interactions, the model hosts not only Mott-insulator and superfluid phases, but also density-wave and supersolid ground states. In the following we choose the initial state as the ground state and then compare and contrast the response of superfluid and supersolid phases when exposed to localized dissipation. While the supersolid phase requires strong nearest-neighbor repulsion that is still difficult to reach experimentally, it is certainly important to find the fingerprints of weaker repulsive interaction in how a uniform superfluid responds to dissipation.

This paper has the following structure: In Sec. II we first briefly describe the zero-temperature phase diagram of the extended Hubbard model and introduce the quantum master equation that allows us to treat continuous dissipation. Our method of choice for solving the full problem is the Gutzwiller mean-field approximation, we discuss its advantages and shortcomings. However, before solving the full mean-field master equation, we consider in Sec. III two simpler, but closely related, quench-type processes that introduce local defects into the system. From these we learn about intrinsic time scales and about the dark state of the system. We then turn to continuous dissipation in Sec. IV and numerically study the response of different phases in the full range of dissipation strengths. Conveniently, our numerical results fit well into the analytical framework of Drummond and Walls [34] for a single dissipative cavity, and this enables an analytical insight into our problem. In particular, from the analytical solution we can directly obtain results in the limit of weak and strong dissipation. Furthermore, the analytical formula yields a very reasonable approximation of the numerical data for the whole range of the dissipation strength for the uniform superfluid. This is an important simplification that will allow for an easy and direct comparison of the theoretical prediction with experimental data, once they are available. We conclude with a discussion of our results.

## II. MODEL AND METHOD

We consider a two-dimensional (2D) bosonic gas, trapped in a significantly deep optical lattice described by a single-band Bose-Hubbard model, with local ( $U$ ) and nearest-neighbor ( $W$ ) interactions:

$$H = -J \sum_{\langle ij \rangle} (a_i^\dagger a_j + \text{H.c.}) + \frac{U}{2} \sum_i n_i(n_i - 1) - \sum_i \mu n_i + W \sum_{\langle ij \rangle} n_i n_j, \quad (1)$$

where  $\langle ij \rangle$  enumerates pairs of nearest neighbors  $i$  and  $j$ ,  $J$  is the hopping integral, and  $\mu$  is the chemical potential.

The ground state  $|\psi_0\rangle$  of the system without long-range interaction ( $W = 0$ ) is the well-known superfluid phase away from integer filling, or for strong enough hopping. At integer

filling and beneath a critical hopping value, a phase transition into the Mott-insulator state occurs [35–37]. The inclusion of long-range interaction has already been investigated in the context of dipolar gases [38–41] and new phases have been shown to appear: charge-density-wave (CDW) order for half-integer filling as well as supersolid (SS) order, which is characterized by both nonzero CDW order and a finite condensate order parameter. The CDW order parameter in this system is given by

$$C_{\text{DW}} = \frac{1}{N/2} \left| \sum_i (-1)^i \langle n_i \rangle \right| \quad (2)$$

and the condensate order parameter is defined locally on each site by  $\phi_i = \langle a_i \rangle$ .

To study the ground states and unitary dynamics of this model we use a Gutzwiller ansatz [35,42]:

$$|\psi_{\text{GW}}\rangle = \prod_{\otimes i} \sum_n c_{in}(t) |n\rangle_i,$$

which captures exactly the physics of the system in both the noninteracting and atomic limits. The energy functional and time evolution of the Gutzwiller ansatz treats the hopping at the mean-field level, while the long-range interaction provides a mean-field correction to the local chemical potential. Explicitly we solve

$$i \frac{d|\psi_{\text{GW}}\rangle}{dt} = \tilde{H} |\psi_{\text{GW}}\rangle, \quad \tilde{H} = \sum_i \tilde{H}_i$$

with the nonlinear effective ‘‘Hamiltonian’’

$$\tilde{H}_i = -J \sum_{j \in \langle ij \rangle} (\phi_j^* a_i + a_i^\dagger \phi_j) + \frac{U}{2} n_i(n_i - 1) - \left( \mu - W \sum_{j \in \langle ij \rangle} \langle n_j \rangle \right) n_i,$$

where  $\phi_j = \langle a_j \rangle$  is the local condensate order parameter. This ansatz restricts the validity of our dynamical simulations to phases with condensate order. One of its main recent applications has been in understanding properties of the amplitude mode. The description has been proven to be able to capture and explain the main experimental findings [43,44].

The ground-state phase diagram for varying chemical potential around half filling is shown in Fig. 1, for  $W = 0.25U$ . Numerically exact quantum Monte Carlo studies [40,41] have shown that mean-field calculations [39,45,46] overestimate the size of the supersolid region, yet the supersolid phase remains stable at fillings  $\gtrsim 0.5$  for  $zW \gtrsim U$  ( $z$  is the coordination number of the lattice) in the close vicinity of the density-wave regime. Therefore, in the following, we will consider parameter regimes within the uniform superfluid phase with and without long-range interaction and regimes deep within the supersolid phase, close to the density-wave lobe, where we expect that quantitatively correct predictions can be obtained based on mean-field GW considerations. For this to hold true, we are also limited to the zero-temperature case. Our units are set by the choice  $U = 1$ , unless otherwise stated. For the presentation of numerical data we chose a fixed noninteger



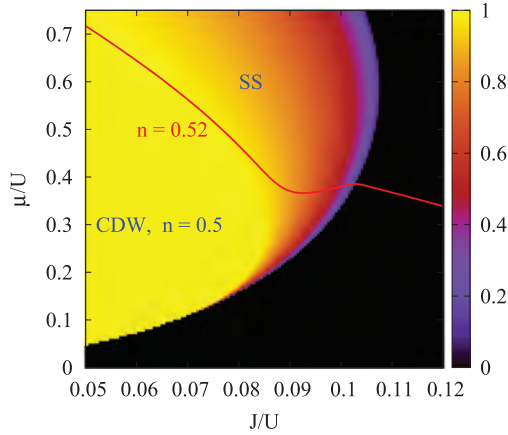


FIG. 1. (Color online) The ground-state phase diagram close to half filling within the Gutzwiller approximation for the extended Bose-Hubbard model (1) on the square lattice for  $W/U = 0.25$ . We plot the value of the CDW order parameter  $C_{DW}$ , Eq. (2). This quantity takes the following values:  $C_{DW} = 1$  in the density-wave phase,  $C_{DW} = 0$  in the uniform superfluid phase, and an intermediate value in the SS phase. A line of constant density  $n = 0.52$  is also shown.

density  $n = 0.52$ , and either  $W = 0$  or  $W = U/4$ , although we have also tested a range of other parameters.

The final ingredient in our simulation is a loss term that acts on a single site to remove individual particles. This has been considered before and can be shown, through a variety of representations of the loss process, to result [5,6,11] in the following Lindblad equation:

$$\frac{\partial \rho}{\partial t} = -i [H, \rho] + \frac{\Gamma}{2} (2a_l \rho a_l^\dagger - \{n_l, \rho\}), \quad (3)$$

where in our case a single site  $l$  is affected by the loss and we also apply the Gutzwiller ansatz to the density matrix  $\rho \equiv \prod_{\otimes i} \sum_{nm} c_{inm} |n\rangle_i \langle m|_i$ . The constant  $\Gamma$  describes the strength of dissipation and can be experimentally tuned by changing the strength of the applied electron beam [15].

To simulate the time evolution numerically, we will consider several different regimes of parameters  $J$ ,  $U$ ,  $W$ , and  $\Gamma$  for a finite system with open boundaries but without a trap. We first determine the ground state  $|\psi_0\rangle$  of  $\tilde{H}$  using imaginary time propagation. Finally, starting from  $\rho(t=0) = |\psi_0\rangle \langle \psi_0|$  we solve the master equation by propagating it in real time using standard differential equation solvers.

The accuracy of the above mean-field approximation improves as the coordination number of the lattice increases. For this reason, we would expect our final results for the uniform superfluid state to be even more accurate on the 3D lattice. On the other hand, the supersolid region in the phase diagram is expected to shrink as the dimension changes from two to three [41].

### III. WITHOUT DISSIPATION

Before discussing the solution of the master equation in its entirety, we first probe the unitary dynamics of the system due to the presence of a defect originating on the lossy site. To this end, we prepare the system in the ground state  $|\psi_0\rangle$  and either

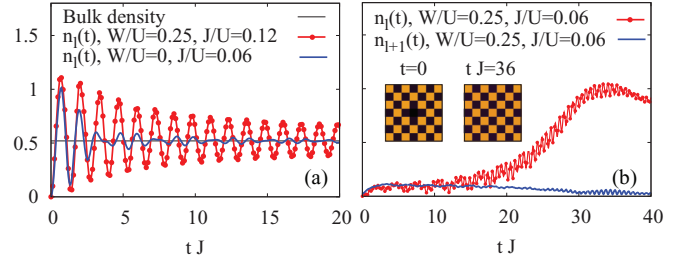


FIG. 2. (Color online) Time dependence of the density of the central site after it has been completely depopulated at  $t = 0$  for the uniform superfluid state (a) and SS state (b). The insets in (b) show the densities immediately after the defect has been introduced and at later moment when the system has recovered.

(a) completely depopulate the site  $l$  or (b) turn off the couplings to the neighboring sites and completely depopulate the site  $l$ . These are quench-type processes that give us an insight into the intrinsic relevant time scales of different phases.

In the first protocol we monitor the time dependence of the density of the central site after complete depopulation at  $t = 0$ , Fig. 2. In the superfluid phase [Fig. 2(a)] we observe persisting oscillations with the period  $1/J$ . The oscillation amplitude decays faster when there are no long-range interactions in the system. From the data presented in Fig. 2 we may conclude that the system recovers from the initial defect on a time scale approximately proportional to the inverse hopping rate. On the contrary, the healing time of the typical SS phase is much longer [see Fig. 2(b)], on the order of  $\sim 10/J$ . These time scales will have direct implications on the dynamics in the limit of weak dissipation strength.

In the second protocol we suddenly remove the four central links of the lattice at the same time as depopulating the central lattice site, Fig. 3. The recovery of the system with this type of defect is much more rapid than the sudden depopulation alone that we studied above, as can be seen in Fig. 4(a). In this figure, we show the change in the particle density on the sites next to the decoupled site  $[n_{l+1}(t)]$  as a function of time. As we see, without any nearest-neighbor repulsion, sites next to the defect lose some of their initial density, while strong enough nearest-neighbor repulsion leads to the opposite effect. The reason for the quick response is visible in the long-term behavior: The system approaches the ground

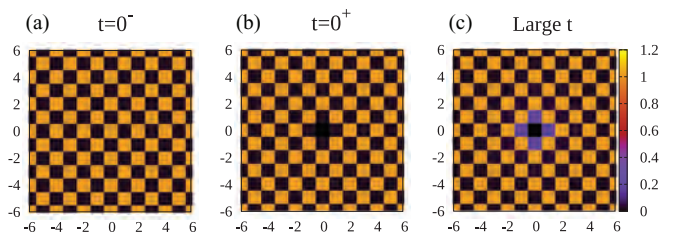


FIG. 3. (Color online) Density distributions realized by the quench-type process in which four central lattice links are suddenly removed and the central site is completely depopulated. The system is initially in the ground state in the SS phase (left), then the defect is introduced (middle), and finally, the system adjusts to this change (right). Parameters used are  $J = 0.06U$  and  $W = 0.25U$ .

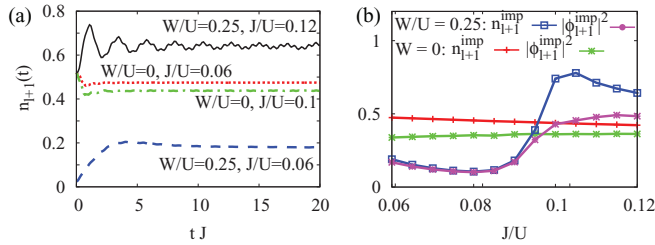


FIG. 4. (Color online) Left: Time dependence of the density on the nearest-neighbor site  $n_{l+1}(t)$  induced by the second quench protocol. Right: Saturated averaged values  $\lim_{t \rightarrow \infty} n_{l+1}(t)$  and  $\lim_{t \rightarrow \infty} |\phi_{l+1}(t)|$  as functions of  $J$  with and without repulsive nearest-neighbor interactions.

state with the four links removed (which we will refer to as  $|\psi_{\text{imp}}\rangle$ ). For nonzero  $W$  this state exhibits a “screening” effect [see Fig. 3(c)]. Simply, the density can become much larger at these neighboring sites, due to the lack of long-range repulsion from the central site and the bulk of the system is only weakly affected by the quench process.

We will show in the next section that the process of removing the central links is directly related to the limit of strong dissipation. For this reason it is important to understand in more detail how the saturated values of density and condensate order parameter of these nearest neighbors depend on  $J$ ,  $U$ , and  $W$ . As can be seen in Fig. 4(b), in the case of  $W = 0$  the condensate shows a monotonic increase in the order parameter on the neighboring sites with increasing  $J$ , but there is only a very weak dependence on  $J$  throughout the studied range. More complicated behavior is found for  $W = U/4$ . For the total initial density fixed at  $n = 0.52$  and  $J$  less than  $\approx 0.103U$ , the ground state is a supersolid and we always choose to remove links around the site of higher initial density. First we notice that saturated values of  $n_{l+1}$  are always higher than the initial values [see Fig. 4(a)] a result of the above-mentioned “screening.” Now, we compare what happens for  $J = 0.06U$  to  $J = 0.07U$ . Initial values of  $n_{l+1}$  are of the same order, but stronger effective repulsion in the first case yields a higher saturated value of  $n_{l+1}$ . In our simulations, the local condensate fractions  $f = |\phi_{l+1}|^2/n_{l+1}$  of neighboring sites are very high, i.e., close to 1, and the change in the density is followed by the related change in  $\phi_{l+1}$ . This explains the decrease of  $n_{l+1}$  and  $\phi_{l+1}$  with  $J$  observed for weak  $J$ . On the other hand, the initial value of  $n_{l+1}$  is significantly higher for  $J = 0.09U$  compared to  $J = 0.06U$ , corresponding to a smaller density-wave order parameter  $C_{\text{DW}}$ , and this leads also to the higher saturated value. Hence, the decrease in the initial value of the density-wave order parameter leads to the increasing saturated values for  $J = 0.08U - 0.1U$ . Finally, for strong enough  $J$ , the initial state is a uniform superfluid and exhibits similar qualitative behavior as found for  $W = 0$ .

#### IV. CONTINUOUS LOSS PROCESS

We now introduce dissipation by the use of the master equation (3). Similar to the above scenarios, we choose to affect only the central site of the lattice. This localized impurity produces several effects: a continuous loss of particles from the system, a disturbance of the bulk and a restructuring of

the density profile around the lossy site. In our finite-sized systems the disturbance in the bulk will eventually be reflected from the boundary but, as we are interested in the properties of an infinitely large system we consider only time scales smaller than this limit. Achieving larger times in our simulation hence requires larger systems. Although we consider a finite system and the only true “steady-state” solution is that of zero particle density, the solutions we obtain can be considered to be quasisteady state, as long as the loss rates are much smaller than the total number of particles.

#### A. Numerical results

We first present results for parameter regimes with and without long-range interaction, whose ground state is a homogeneous superfluid. Two examples, with snapshots of their time-dependent density profiles, are shown in Fig. 5, where we immediately see that the effect of long-range interaction is to enhance the charge-density-wave order in the bulk disturbance. To estimate the speed of propagation of this perturbation, we monitor the density of an arbitrary bulk site as a function of time as shown in Fig. 6. We choose a site which is ten sites away from the center and observe that it has a nearly constant density for initial times and then exhibits weak oscillations. The defect propagation velocity is obviously set by  $J$ , but it seems to be slightly higher in the presence of repulsive  $W$ .

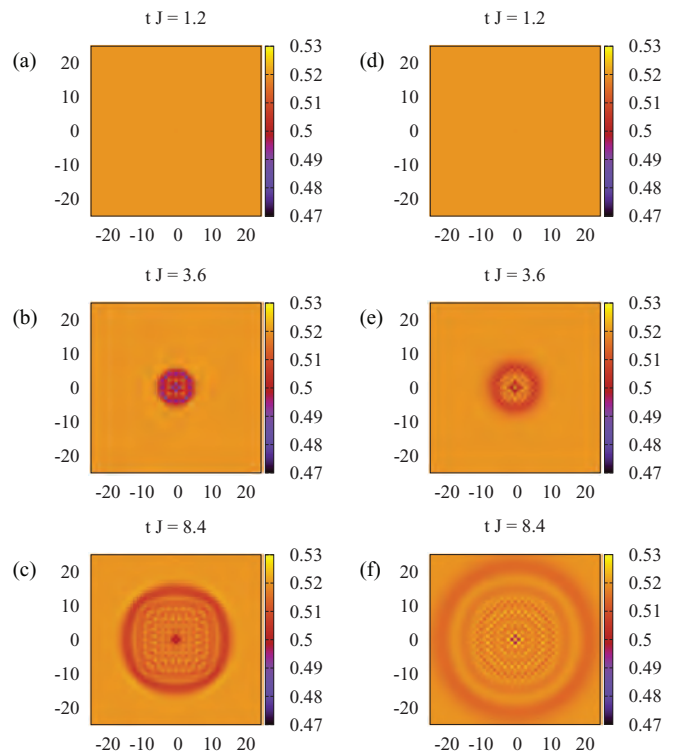


FIG. 5. (Color online) Real-space density profiles after time propagation showing the bulk properties, starting from an initial homogeneous superfluid. Parameters used are  $J/U = 0.12$ ,  $\Gamma = 0.2U$ , and  $W = 0$  (on the left) and  $W = 0.25U$  (on the right). Although the profiles share many similarities, note the enhancement of the charge-density-wave pattern in the bulk disturbance with the inclusion of long-range interactions.

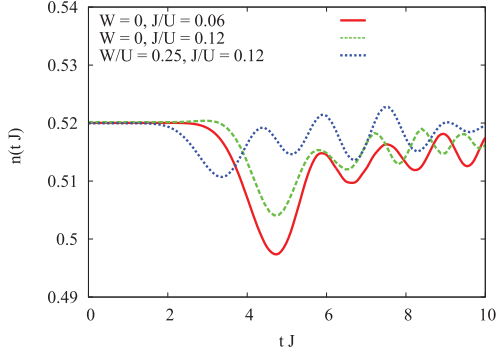


FIG. 6. (Color online) Density of a site in the bulk (ten sites away from the central lossy site) in the presence of continuous local dissipation,  $\Gamma = 0.2U$ .

Quantitatively, it is more useful to look at the density on both the lossy site and its neighbors, as shown in Figs. 7(a) and 7(b). We see here that these sites very quickly reach their steady-state values within a few hopping time scales, and that the steady-state particle density on the lossy site itself monotonically decreases with increasing  $\Gamma$ , approaching zero in the large- $\Gamma$  limit. This means that strong loss prevents hopping to the lossy site and is evidenced in our results in the limit  $\Gamma \gg 1$ , where we see that the steady-state density of neighboring sites approaches that of the ground state with central links removed,  $|\psi_{\text{imp}}\rangle$ , as discussed in Sec. III. As is to be expected, in the opposite limit  $\Gamma \rightarrow 0$  the saturated values of both lossy site and neighboring sites are close to their initial values.

We now turn to the supersolid phase, for which density profiles of lossy site and neighbours are presented in Figs. 7(c) and 7(d). We fix the lossy site to be an initially high density site of the checkerboard distribution. The most striking point

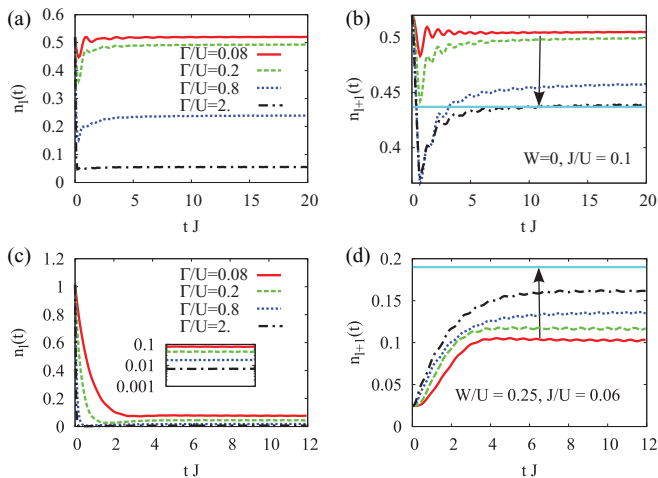


FIG. 7. (Color online) Temporal evolution of the local densities starting from an initially homogeneous superfluid  $W = 0$ ,  $J = 0.1U$  (top row) or starting from an initial supersolid state  $W = 0.25U$ ,  $J = 0.06U$  (bottom row). Left: Density of the lossy site as a function of time. Right: Density of the site next to the lossy site as a function of time. The horizontal line in the right plots shows the asymptotic value of  $n_{l+1}^{\text{imp}}$ , which is reached for strong  $\Gamma$ .

that we observe here is the behavior for weak loss. Even for loss rates of  $\Gamma = 0.02U$ , we see that the steady-state values are significantly altered compared to the initial values. This behavior can be related to the time scales considered in Sec. III, where we found that complete recovery of a supersolid state requires many hopping times. Instead, for the shorter time scales considered here, a steady state with different density distribution becomes the relevant one. For all values of  $\Gamma$  we observe an increase of the density on the neighboring site. This behavior reflects the “screening” effect that was found for the ground state with central links removed,  $|\psi_{\text{imp}}\rangle$ , as discussed in Sec. III, which we again obtain in the limit  $\Gamma \gg 1$ .

We must also mention that our results for weak loss may not truly reflect the limit of  $\Gamma \rightarrow 0$ . While in the superfluid the relaxation rate at which the density profiles return to equilibrium is related to  $J$ , yielding the criterion  $\Gamma < J$  which is satisfied in our simulations, relaxation rates in the supersolid phase are slower and may also depend on higher-order processes in perturbation theory (e.g.,  $J^2/W$ ). Unfortunately the rigorous investigation of even weaker loss rates requires accessing very large simulation times and consequently infeasibly large lattice sizes in order to neglect finite-size effects.

## B. Analytical insight

### 1. Density profiles

Within our approach, the study of local dissipation reduces to a set of coupled single-site Hamiltonians. In particular, the Hamiltonian of the central site that is directly exposed to the dissipation has an effective pumping term  $F(t)$ :

$$H_l = -(\mu - 4Wn_{l+1})a_l^\dagger a_l + \frac{U}{2}a_l^\dagger a_l^\dagger a_l a_l + F(t)a_l^\dagger + F^*(t)a_l, \quad (4)$$

where  $F(t) = -4J\phi_{l+1}(t)$  represents the incoming particles from the neighboring sites, obtained in the complete Gutzwiller simulation. From the numerical data presented in the previous section, we find that after an initial transient regime both  $n_{l+1}(t)$  and  $|\phi_{l+1}(t)|$  reach nearly constant values. Weak oscillations around averaged values are present even at later times, but this turns out to be a subleading effect and we may safely approximate  $n_{l+1}(t)$  and  $|\phi_{l+1}(t)|$  by constants. The local Hamiltonian (4) for constant  $F$  in the presence of dissipation has been explored in the context of isolated driven photonic cavities [34]. In that other context, the  $F$  terms represent the incident laser field, the dissipation  $\Gamma$  is a cavity dissipation rate, and a balance between unitary and dissipative dynamics leads to a local steady state. The exact solution for the single cavity is known [7,34] and it gives a steady-state density on the lossy site through

$$n_l = \langle a_l^\dagger a_l \rangle = \left| \frac{2F}{U} \right|^2 \frac{1}{|c|^2} \times \frac{\mathcal{F}(1+c, 1+c^*, 8|F/U|^2)}{\mathcal{F}(c, c^*, 8|F/U|^2)}, \quad (5)$$

where  $c = 2[-(\mu - 4Wn_{l+1}) - i\Gamma/2]/U$ ,

$$\mathcal{F}(c, d, z) = \sum_n \frac{\Gamma(c)\Gamma(d)}{\Gamma(c+n)\Gamma(d+n)} \times \frac{z^n}{n!}$$

is the hypergeometric function and  $\Gamma(x)$  is the Gamma function. Given the *a posteriori* numerical values of  $\phi_{l+1}$  and  $n_{l+1}$ , the analytical formula (5) matches very well with our numerical results for  $n_l$ . Equation (5) can be used to directly determine the particle number on the lossy site, given the condensate order parameter and density on the nearest neighbors.

To employ this analytical solution, we must, however, fix the chemical potential  $\mu$ . Although the value of  $\mu$  affects the propagation of the Hamiltonian only by a global phase factor, the analytical derivation of (5) relies on a time-independent value of  $F$ , which in turn requires  $\phi_i(t) = \phi_i$ . If we assume that our numerical results have reached a steady state, then it is clear that  $|\phi_i|$  must be time independent; however, the choice of  $\mu$  affects the time dependence of the phase of  $\phi_i$ . Fortunately, the value of  $\mu$  obtained by fixing the required particle number in the ground state has exactly this property, which one can see through  $d\langle\hat{a}_i\rangle_{|\psi_0\rangle}/dt = i\langle[\hat{H}, \hat{a}_i]\rangle_{|\psi_0\rangle} = 0$ . As this value of  $\mu$  reproduces the steady-state density profiles in both the limit of  $\Gamma \rightarrow 0$  (corresponding to the homogeneous ground state) and the limit of  $\Gamma \gg 1$  (corresponding to the ground state with central site and links removed), we can assume it is a good approximation for all values of  $\Gamma$  between these limits. Note that this value of  $\mu$  is independent of the description of the “bath” to which the master equation is coupled—any relative offset between the system and bath, e.g., a chemical potential difference, which would appear in the derivation of the master equation, has already been assumed to be absorbed into the parameter  $\Gamma$ .

## 2. Effective loss rates

The experimentally accessible quantity relevant to our simulations is the total number of expelled atoms  $N(t) = N_{\text{tot}}(t=0) - N_{\text{tot}}(t)$  per time. We determine this through

$$\frac{dN(t)}{dt} = -\text{Tr}\left(\hat{N}_{\text{tot}} \frac{d\rho}{dt}\right) = \Gamma n_l(t), \quad (6)$$

where  $\hat{N}_{\text{tot}} = \sum_i \hat{n}_i$  is the total number of particles and we have made use of the vanishing trace  $\text{Tr}([\hat{N}_{\text{tot}}, \hat{H}]\rho) = \langle[\hat{N}_{\text{tot}}, \hat{H}]\rangle = 0$ . Hence, we see that the global loss rate is determined by  $n_l(t)$ .

We show plots of the total number of particles lost in Fig. 8 and of the loss rate  $dN/dt$  in Fig. 9 for both the superfluid

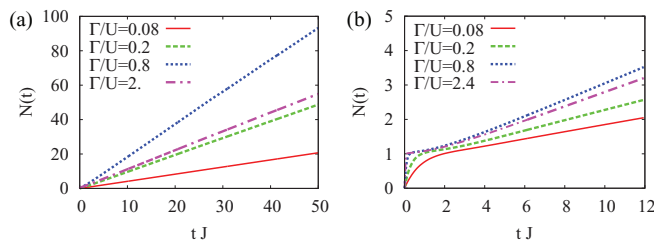


FIG. 8. (Color online) Time dependence of the total number of particles lost in the (a) superfluid phase ( $W = 0, J = 0.1U$ ) and (b) supersolid phase ( $W = 0.25U, J = 0.06U$ ). After a brief transient of strong loss as the central site is depleted, the system quickly reaches a quasisteady state, from which an approximately constant loss rate can be extracted.

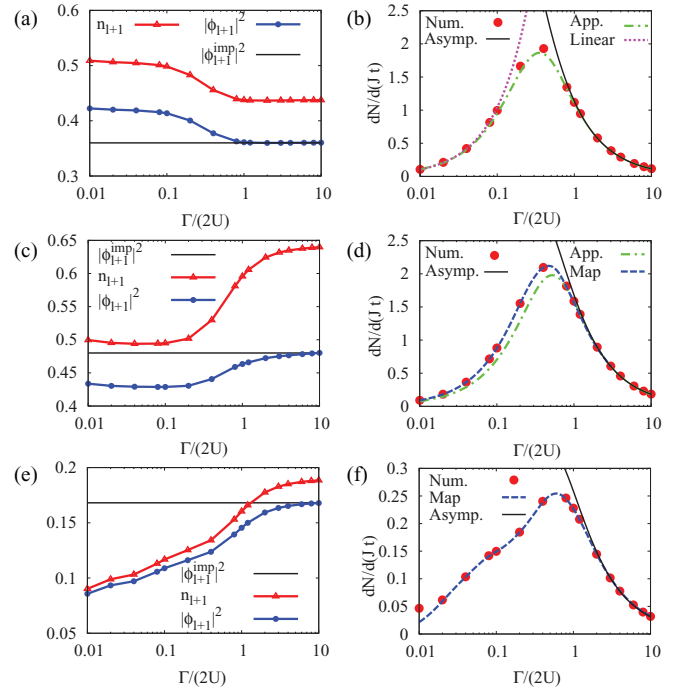


FIG. 9. (Color online) Off-site density and condensate order parameter (left column) and decay rate  $dN/dt$  (right column) as functions of dissipation strength for a homogeneous superfluid with (a),(b)  $W = 0, J = 0.1U$  and (c),(d)  $W = 0.25U, J = 0.12U$ , and (e),(f) supersolid with  $W = 0.25U, J = 0.06U$ . The quantum Zeno effect is apparent as the decay rate vanishes in the limit of strong dissipation in all cases. Using analytical arguments and the given off-site condensate order parameter, we can obtain near exact agreement with the numerical loss rate. For weak loss, there is a linear dependence on  $\Gamma$  [dotted line; for clarity, shown only in (b)] whereas for strong loss we observe the asymptotic form (7) (continuous line). The dashed blue line represents the full Eq. (5) used in (6), with off-site parameters taken directly from numerical simulations, as shown in the left column. The dot-dashed line gives a simplification—large  $\Gamma$  values for off-site parameters are used throughout the whole range of  $\Gamma$  in Eq. (5).

and supersolid phases. In all cases, initially the number of expelled particles grows rapidly as the lossy site is emptied. In the quasisteady state, when the dissipation is balanced by hopping, a constant current of expelled particles develops, and therefore constant loss rates  $dN/dt$  can be directly extracted from numerical data.

To prove that our system has indeed reached the local quasisteady state, we compare numerical results for effective loss rates with results obtained by using numerical values for off-site parameters (Fig. 9, left) in Eqs. (5) and (6). We find complete agreement as shown in Fig. 9, right, except for very weak dissipation in the supersolid phase. In this case, the dynamics is very slow and the system has not yet reached the steady state during the monitored time interval. But, although this mapping works perfectly, it still requires complete knowledge of the off-site expectation values. We can obtain a more applicable approximation through some further simplifications. In the case of uniform superfluid phases, we obtain nearly perfect agreement between analytical estimates

and the numerical simulations by using a constant  $\phi_{l+1}$  in the whole range of  $\Gamma$ , which is shown in Fig. 9 as the green (dot-dashed) line. The analytical estimate (5) has only one problem: We must know the value of  $\phi_{l+1}$  exactly. This is often not available *a priori* in experiment and is of course modified by the presence of the dissipation. However, we can easily perform a nondissipative Gutzwiller calculation for given experimental parameters, to determine the value of  $\phi_{l+1}$  in the ground state, and use this as an approximate value of  $\phi_{l+1}$  to estimate the steady-state loss rate. Similarly, we may also calculate the ground state with central links removed, which is relevant in the limit  $\Gamma \gg 1$ . In the case of the supersolid phase, we find stronger dependence of  $\phi_{l+1}$  and  $n_{l+1}$  on  $\Gamma$  that cannot be simply replaced by a constant value.

When describing the regime of strong dissipation, the analytical result (5) turns out to be very useful. Simply, by taking the limit  $\Gamma \rightarrow \infty$  in Eq. (5) and using (6) we obtain

$$\frac{dN}{dt} \approx 4z^2 |\phi_{l+1}^{\text{imp}}|^2 \frac{J^2}{\Gamma} \left( 1 + \frac{4(\mu - zWn_{l+1})^2}{\Gamma^2} \right)^{-1}, \quad (7)$$

where we have explicitly indicated that the condensate order parameter is to be taken from the ground-state solution with central links removed,  $\phi_{l+1}^{\text{imp}}$ , and  $z$  is the lattice coordination number. This limit can be seen in Fig. 9 where it agrees well with the full numerics for  $\Gamma > 1$ . In the opposite limit of  $\Gamma \rightarrow 0$ , the expected behavior is a linear dependence in  $\Gamma$  and this is clearly a good approximation, as can also be seen in Fig. 9.

The result captured in Eq. (7) describes the quantum Zeno regime and is to some extent general. The leading  $J^2/\Gamma$  dependence has been previously derived using an extended perturbative approach [20] and by considering simplified few-site Bose-Hubbard systems [27,29]. The essence of the formalism in [20] is to consider the dark state of the system which is, in our case,  $|\psi^{\text{imp}}\rangle$ . The nonzero decay rate of this state stems from the hopping events that couple it to states with finite density on the lossy site. This effect is captured, within the Gutzwiller ansatz, by Eq. (7). In the formalism of [20], however, the coupling is not the Gutzwiller mean-field hopping term but the original full hopping term. This leads us to conjecture that the loss rates beyond mean-field theory would depend also on the particle density of the neighboring sites, not only on the condensate density, and hence be larger than our results. Unfortunately, explicit calculations cannot be performed without knowledge of the exact state.

When considering local dissipation as a measurement tool, the main question is which properties of the observed system we can extract from the measured effective loss rates. The straightforward answer is given by Eq. (6)—effective loss rates are directly related to the density of the lossy site. In the limit of weak dissipation, this density closely corresponds to the initial bulk density. However, our results indicate that this limit is not always easy to reach, as for example in the case of the supersolid phase. On the other hand, in the large- $\Gamma$  limit the effective loss rate is proportional to  $J^2/\Gamma$  and related to the corresponding dark state. Within our description, further dependence on microscopic parameters of the model is contained in the proportionality constant  $|\phi_{l+1}^{\text{imp}}|^2$  and in the leading correction term  $(\mu - 4Wn_{l+1})^2$ . At approximately half

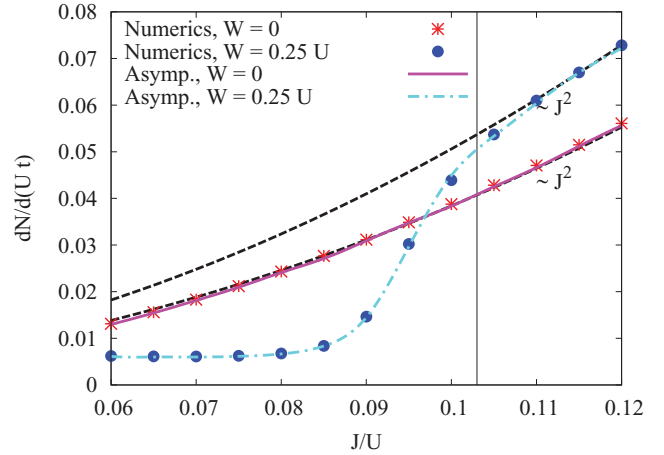


FIG. 10. (Color online) Loss rates  $dN/dt$  for large dissipation ( $\Gamma/U = 6$ ) for varying  $J$  obtained by numerical calculations within the Gutzwiller approximation and the analytical result in Eq. (7), which requires the knowledge of the condensate order parameter at the neighboring sites, taken directly from the numerical calculations of Sec. III. Dashed lines show the  $J^2$  dependence, while the vertical line marks the supersolid-superfluid transition.

filling, as considered throughout our paper, the correction term does not play a major role, yet at higher filling fractions it can become more pronounced. The influence of a similar term has been denoted as the nonlinear Zeno effect [27], since the dissipation rate is reduced by interactions. We again emphasize that the full interplay of  $U$  and  $\Gamma$  is captured by Eq. (5).

We now turn to further implications of Eq. (7) to understand how the effective loss rate in the large- $\Gamma$  limit is modified by the presence of interactions. The answer is directly based on the results for  $\phi_{l+1}^{\text{imp}}$  presented in Fig. 4(b) which we now use in combination with Eq. (7). Semianalytical results are in good agreement with full numerical calculations throughout the entire supersolid regime and through the transition to the superfluid phase with and without long-range interaction, as shown in Fig. 10. Here we take a fixed value of  $\Gamma/U = 6$  and vary  $J$  to show that the form of Eq. (7) fits the numerical data well. The trend of  $J^2$  is clearly visible for  $W = 0$  through the whole range of  $J$ . This is a direct consequence of the fact that we are close to half filling. Without long-range interactions, no quantum phase transition occurs at this filling, and hence the condensate fraction is only weakly dependent on  $J$ . Close to unity filling for example, the condensate fraction would depend more strongly on  $J$  and affect the  $J^2$  behavior. The  $J^2$  dependence is also apparent in the presence of repulsive interactions in the superfluid, where we find that effective loss rates are enhanced by  $W$ . On the contrary, deep in the supersolid phase the  $J^2$  dependence is strongly suppressed and effective loss rates are much weaker.

Based on the previous considerations, for a fixed value of  $J$  and  $\Gamma$  we expect an increase of the effective loss rate with increasing  $W$ , as shown in Fig. 11. However, eventually for strong enough  $W$ , in our mean-field calculations we reach the supersolid regime that finally leads to a suppression of the dissipative loss.

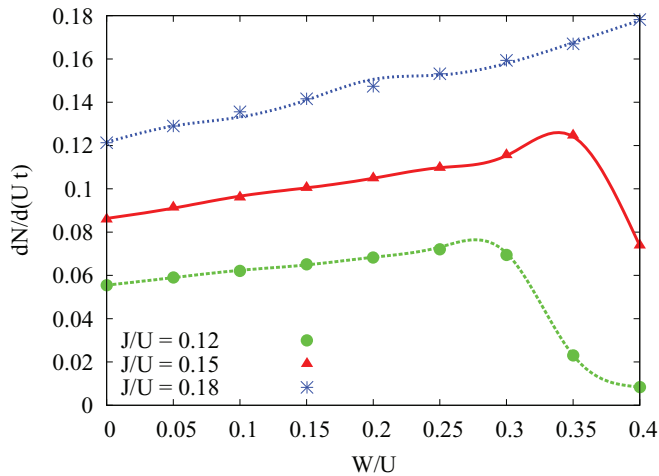


FIG. 11. (Color online) Loss rates  $dN/dt$  for large dissipation ( $\Gamma/U = 6$ ) for varying  $J$  and  $W$ , obtained by numerical Gutzwiller calculations.

## V. CONCLUSIONS

In this paper, we have addressed the dynamics of the extended Bose-Hubbard model induced by localized dissipation. We have solved the master equation using the mean-field Gutzwiller approximation and complemented our numerical study by the analytical description of Drummond and Walls. We have observed a regime of weak dissipation where effective loss rates are almost linearly proportional to the initial density and a regime of strong dissipation which exhibits the quantum Zeno effect, where stronger dissipation leads to smaller effective loss rates.

We have demonstrated that at the mean-field level, reasonably accurate loss rates in the quantum Zeno regime can be calculated without the need for explicit numerical solutions of the full dissipative problem. This can be achieved by taking a single result from the simpler nonlossy Hermitian calculation (regarding a quench-type process) as an input parameter for the analytical theory of Drummond and Walls [34]. In particular, in the case of a superfluid, this approximation turns out to be a very good description of the effective loss rates for the full regime of applied dissipation.

Based on these considerations, we have then estimated effects of nearest-neighbor repulsive interactions in the regime of strong dissipation: in the superfluid these interactions lead to enhanced effective loss rates due to a mechanism of screening of the local defect. On the other hand, when nearest-neighbor interactions are dominant over the hopping, and induce a supersolid phase, the process of dissipation is strongly suppressed and effective loss rates decrease.

We expect our mean-field results to be even more quantitatively accurate for the three-dimensional optical lattice and uniform superfluid phase. From comparison to [20] which introduces an effective model in the limit of strong dissipation, we expect that corrections to the mean-field theory would produce increased loss rates. Finally, we need to mention that time-dependent nonequilibrium calculations within mean-field theory are more accurate for superfluid rather than supersolid systems, due to the contribution of higher-order hopping processes.

## ACKNOWLEDGMENTS

The authors thank Herwig Ott for useful discussions. Support by the German Science Foundation DFG via Sonderforschungsbereich SFB/TR 49 and Forschergruppe FOR 801 is gratefully acknowledged.

- 
- [1] S. Diehl, A. Micheli, A. Kantian, B. Kraus, H. P. Büchler, and P. Zoller, *Nat. Phys.* **4**, 878 (2008).
  - [2] F. Verstraete, M. M. Wolf, and J. Ignacio Cirac, *Nat. Phys.* **5**, 633 (2009).
  - [3] D. Witthaut, F. Trimborn, and S. Wimberger, *Phys. Rev. Lett.* **101**, 200402 (2008).
  - [4] E. G. Dalla Torre, E. Demler, T. Giamarchi, and E. Altman, *Nat. Phys.* **6**, 806 (2010).
  - [5] S. Diehl, A. Tomadin, A. Micheli, R. Fazio, and P. Zoller, *Phys. Rev. Lett.* **105**, 015702 (2010).
  - [6] A. Tomadin, S. Diehl, and P. Zoller, *Phys. Rev. A* **83**, 013611 (2011).
  - [7] A. Le Boité, G. Orso, and C. Ciuti, *Phys. Rev. Lett.* **110**, 233601 (2013).
  - [8] D. Poletti, J.-S. Bernier, A. Georges, and C. Kollath, *Phys. Rev. Lett.* **109**, 045302 (2012).
  - [9] D. Poletti, P. Barmettler, A. Georges, and C. Kollath, *Phys. Rev. Lett.* **111**, 195301 (2013).
  - [10] D. Poletti, J.-S. Bernier, A. Georges, and C. Kollath, *arXiv:1212.4254*.
  - [11] T. E. Lee, H. Häffner, and M. C. Cross, *Phys. Rev. A* **84**, 031402 (2011).
  - [12] T. Gericke, P. Würtz, D. Reitz, T. Langen, and H. Ott, *Nat. Phys.* **4**, 949 (2008).
  - [13] P. Würtz, T. Langen, T. Gericke, A. Koglbauer, and H. Ott, *Phys. Rev. Lett.* **103**, 080404 (2009).
  - [14] V. Guarrera, P. Würtz, A. Ewerbeck, A. Vogler, G. Barontini, and H. Ott, *Phys. Rev. Lett.* **107**, 160403 (2011).
  - [15] G. Barontini, R. Labouvie, F. Stubenrauch, A. Vogler, V. Guarrera, and H. Ott, *Phys. Rev. Lett.* **110**, 035302 (2013).
  - [16] W. S. Bakr, J. I. Gillen, A. Peng, S. Fölling, and M. Greiner, *Nature (London)* **462**, 74 (2009).
  - [17] J. F. Sherson, C. Weitenberg, M. Endres, M. Cheneau, I. Bloch, and S. Kuhr, *Nature (London)* **467**, 68 (2010).
  - [18] B. Misra and E. C. G. Sudarshan, *J. Math. Phys.* **18**, 756 (1977).
  - [19] W. M. Itano, *arXiv:quant-ph/0612187*.
  - [20] J. J. García-Ripoll, S. Dürr, N. Syassen, D. M. Bauer, M. Lettner, G. Rempe, and J. I. Cirac, *New J. Phys.* **11**, 013053 (2009).
  - [21] N. Syassen, D. M. Bauer, M. Lettner, T. Volz, D. Dietze, J. J. García-Ripoll, J. I. Cirac, G. Rempe, and S. Dürr, *Science* **320**, 1329 (2008).
  - [22] M. J. Mark, E. Haller, K. Lauber, J. G. Danzl, A. Janisch, H. P. Büchler, A. J. Daley, and H.-C. Nägerl, *Phys. Rev. Lett.* **108**, 215302 (2012).

- [23] B. Yan, S. A. Moses, B. Gadway, J. P. Covey, K. R. A. Hazzard, A. M. Rey, D. S. Jin, and J. Ye, *Nature (London)* **501**, 521 (2013).
- [24] A. Privera, I. Titvinidze, S.-Y. Chang, S. Diehl, A. J. Daley, and W. Hofstetter, *Phys. Rev. A* **84**, 021601 (2011).
- [25] B. Zhu, B. Gadway, M. Foss-Feig, J. Schachenmayer, M. L. Wall, K. R. A. Hazzard, B. Yan, S. A. Moses, J. P. Covey, D. S. Jin, J. Ye, M. Holland, and A. M. Rey, *Phys. Rev. Lett.* **112**, 070404 (2014).
- [26] V. S. Shchesnovich and V. V. Konotop, *Phys. Rev. A* **81**, 053611 (2010).
- [27] V. S. Shchesnovich and D. S. Mogilevtsev, *Phys. Rev. A* **82**, 043621 (2010).
- [28] D. Witthaut, F. Trimborn, H. Hennig, G. Kordas, T. Geisel, and S. Wimberger, *Phys. Rev. A* **83**, 063608 (2011).
- [29] F. Trimborn, D. Witthaut, H. Hennig, G. Kordas, T. Geisel, and S. Wimberger, *Eur. Phys. J. D* **63**, 63 (2011).
- [30] G. Kordas, S. Wimberger, and D. Witthaut, *Europhys. Lett.* **100**, 30007 (2012).
- [31] G. Kordas, S. Wimberger, and D. Witthaut, *Phys. Rev. A* **87**, 043618 (2013).
- [32] P. Barmettler and C. Kollath, *Phys. Rev. A* **84**, 041606 (2011).
- [33] T. Lahaye, C. Menotti, L. Santos, M. Lewenstein, and T. Pfau, *Rep. Prog. Phys.* **72**, 126401 (2009).
- [34] P. D. Drummond and D. F. Walls, *J. Phys. A* **13**, 725 (1980).
- [35] M. P. A. Fisher, P. B. Weichman, G. Grinstein, and D. S. Fisher, *Phys. Rev. B* **40**, 546 (1989).
- [36] B. Capogrosso-Sansone, N. V. Prokof'ev, and B. V. Svistunov, *Phys. Rev. B* **75**, 134302 (2007).
- [37] B. Capogrosso-Sansone, Ş. G. Söyler, N. Prokof'ev, and B. Svistunov, *Phys. Rev. A* **77**, 015602 (2008).
- [38] K. Góral, L. Santos, and M. Lewenstein, *Phys. Rev. Lett.* **88**, 170406 (2002).
- [39] D. L. Kovrizhin, G. Venketeswara Pai, and S. Sinha, *Europhys. Lett.* **72**, 162 (2005).
- [40] P. Sengupta, L. P. Pryadko, F. Alet, M. Troyer, and G. Schmid, *Phys. Rev. Lett.* **94**, 207202 (2005).
- [41] T. Ohgoe, T. Suzuki, and N. Kawashima, *Phys. Rev. B* **86**, 054520 (2012).
- [42] K. V. Krutitsky and P. Navez, *Phys. Rev. A* **84**, 033602 (2011).
- [43] U. Bissbort, S. Götze, Y. Li, J. Heinze, J. S. Krauser, M. Weinberg, C. Becker, K. Sengstock, and W. Hofstetter, *Phys. Rev. Lett.* **106**, 205303 (2011).
- [44] M. Endres, T. Fukuhara, D. Pekker, M. Cheneau, P. Schauss, C. Gross, E. Demler, S. Kuhr, and I. Bloch, *Nature (London)* **487**, 454 (2012).
- [45] M. Iskin, *Phys. Rev. A* **83**, 051606 (2011).
- [46] T. Kimura, *Phys. Rev. A* **84**, 063630 (2011).

## Photonic currents in driven and dissipative resonator lattices

Thomas Mertz,<sup>1</sup> Ivana Vasić,<sup>2,1</sup> Michael J. Hartmann,<sup>3</sup> and Walter Hofstetter<sup>1</sup>

<sup>1</sup>*Institut für Theoretische Physik, Goethe-Universität, 60438 Frankfurt/Main, Germany*

<sup>2</sup>*Scientific Computing Laboratory, Institute of Physics Belgrade, University of Belgrade, 11080 Belgrade, Serbia*

<sup>3</sup>*Institute of Photonics and Quantum Sciences, Heriot-Watt University, Edinburgh EH14 4AS, Scotland, United Kingdom*

(Received 28 January 2016; published 5 July 2016)

Arrays of coupled photonic cavities driven by external lasers represent a highly controllable setup to explore photonic transport. In this paper we address (quasi)-steady states of this system that exhibit photonic currents introduced by engineering driving and dissipation. We investigate two approaches: in the first one, photonic currents arise as a consequence of a phase difference of applied lasers and, in the second one, photons are injected locally and currents develop as they redistribute over the lattice. Effects of interactions are taken into account within a mean-field framework. In the first approach, we find that the current exhibits a resonant behavior with respect to the driving frequency. Weak interactions shift the resonant frequency toward higher values, while in the strongly interacting regime in our mean-field treatment the effect stems from multiphotonic resonances of a single driven cavity. For the second approach, we show that the overall lattice current can be controlled by incorporating few cavities with stronger dissipation rates into the system. These cavities serve as sinks for photonic currents and their effect is maximal at the onset of quantum Zeno dynamics.

DOI: [10.1103/PhysRevA.94.013809](https://doi.org/10.1103/PhysRevA.94.013809)

### I. INTRODUCTION

Understanding the transport properties of photons in different media is a prerequisite for future applications, for example in quantum information processing. This subject has been addressed from various perspectives [1]. As one notable example we mention successful experimental realizations of photonic topological insulators, where emerging edge states provide robust transport channels [1–5]. Forthcoming experiments with arrays of coupled photonic cavities [1,6,7] are expected to feature strong interactions on a single-photon level. The latest theoretical and experimental progress in this direction is summarized in two recent review papers [8,9]. Transport measurements will be the most natural first experiments to carry out in these systems in order to explore how interactions affect the propagation of photons. First experimental results in this direction are already available [10,11].

Theoretically, arrays of coupled photonic cavities can be described by the Bose-Hubbard model [1,6,7]. However, photonic cavities exhibit dissipation due to intrinsic loss rates, which has to be compensated by driving the system with an external laser. Instead of equilibrium properties, stationary states that arise from the interplay of driving and dissipation are thus more naturally studied in this open quantum system [12–22]. The aim of our study is to explore steady states of the dissipative-driven two-dimensional Bose-Hubbard model which exhibit finite photonic currents and are generated by engineering the driving and dissipation. In particular, we will analyze how the emerging photonic currents are affected by the externally controllable parameters, such as intensity and frequency of the external laser pump, the loss rates, and the physical parameters of the underlying Bose-Hubbard model.

We note that transport measurements in cold atomic systems [23] have been reported recently [24–27] and that some of our conclusions may apply to corresponding bosonic systems of cold atoms as well. Different possibilities to control stationary flows of cold atoms by dissipation have been theoretically addressed in Refs. [28–32].

The structure of the paper is the following. The model we consider is described in Sec. II, where we also introduce two setups, which lead to stationary states with finite currents. In Sec. III we briefly outline the theoretical methods we employ in this work. In Sec. IV we explore properties of the currents first in the noninteracting limit, then at weak interactions, and finally in the regime of strong interactions, where we use the Gutzwiller mean-field approximation. In the end we summarize our main conclusions and outline open questions.

### II. THE MODEL

We study transparency in the dissipative-driven photonic Bose-Hubbard model, which describes the dynamics of photonic or polaritonic excitations in coupled cavity arrays; see Fig. 1 for a sketch of our setup. The key parameters of the Bose-Hubbard model are the hopping amplitude  $J$  and the on-site interaction  $U$ . The driving of the system via local excitation by external lasers can be described by  $F_l^* a_l \exp(i\omega_L t) + \text{H.c.}$ , where the amplitudes  $F_l$  are set by the laser intensity and  $a_l$  are the bosonic annihilation operators on site  $l$ . We describe the system in the corotating frame, by applying the unitary transformation  $U(t) = \exp(i\omega_L t \sum_l n_l)$ ,  $n_l = a_l^\dagger a_l$ . This transformation leads to an additional chemical potential term proportional to the detuning  $\Delta = \omega_L - \omega_C$  of the laser frequency with respect to the cavity mode  $\omega_C$ . The effective Hamiltonian of the model is [18,21]

$$\mathcal{H} = -\Delta \sum_l a_l^\dagger a_l - J \sum_{\langle l,j \rangle} (a_l^\dagger a_j + a_j^\dagger a_l) + \frac{U}{2} \sum_l n_l(n_l - 1) + \sum_l (F_l a_l^\dagger + F_l^* a_l), \quad (1)$$

where the sum over  $\langle l,j \rangle$  indicates that we only take into account tunneling between nearest-neighbor sites of the square lattice. In addition to the Hamiltonian time evolution we consider one-body loss described by a Lindblad master equation. The equations of motion for the density operator



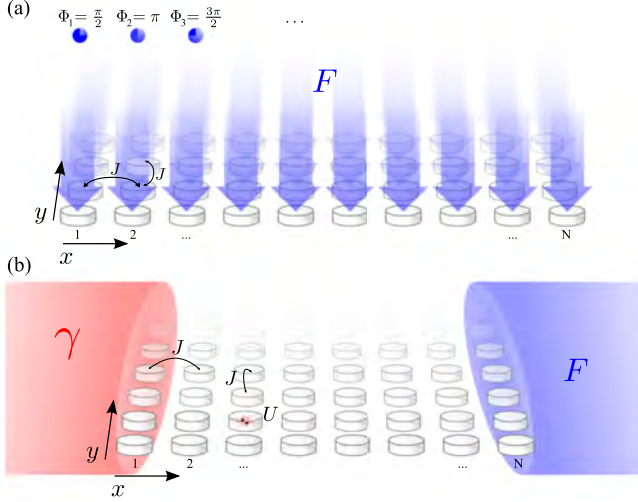


FIG. 1. (a) Sketch of the phase imprinting setup (6). (b) Sketch of the source-drain setup (7). Throughout this paper we assume translational invariance in the  $y$  direction, where all sites along the  $y$  axis behave in the same way.

$\rho$  of the dissipative model are given by

$$i \frac{d\rho}{dt} = [\mathcal{H}, \rho] + \mathcal{L}\rho, \quad (2)$$

where we set  $\hbar = 1$ . The dissipator  $\mathcal{L}$  is

$$\mathcal{L}\rho = i \sum_l \frac{\gamma_l}{2} (2a_l \rho a_l^\dagger - a_l^\dagger a_l \rho - \rho a_l^\dagger a_l), \quad (3)$$

where  $\gamma_l$  is the local dissipation rate.

In order to quantify the transparency of the material we calculate the (local) current density  $j$ , which is derived from the lattice continuity equation and provides a measure for the photon transport through the system. The current  $j_{lj}$  between sites  $l$  and  $j$  is given by

$$j_{lj} = -iJ(a_l^\dagger a_l - a_l^\dagger a_j), \quad (4)$$

and is the main quantity commonly used to describe transport in other lattice systems, as for example in Refs. [33–35]. From the experimental side, the two-point correlations  $\langle a_j^\dagger a_l \rangle$  have already been measured in superconducting circuits [36], implying that photonic bond currents may be directly accessible in forthcoming experiments. Another possibility for probing properties of a photonic flow is through a local loss of photons, which will be explained in the next section.

In our study we will investigate the photonic transport in the regime of finite local bosonic coherences given by  $|\langle a_l \rangle|$ . In this case it is reasonable to approximate the expectation value of the bond current from Eq. (4) by

$$\langle j_{lj} \rangle \approx -iJ(\langle a_j^\dagger \rangle \langle a_l \rangle - \langle a_l^\dagger \rangle \langle a_j \rangle), \quad (5)$$

where the local expectation values  $\langle a_l \rangle$  are calculated within a mean-field approximation. From the last equation it follows that the current is directly related to the phase ordering of the complex expectation values  $\langle a_l \rangle$  of lattice nearest neighbors, and that it is enhanced by strong bosonic coherences  $|\langle a_l \rangle|$ . In the following we consider different spatial distributions of the

dissipation rates  $\gamma_l$  and the driving amplitudes  $F_l$  in order to find an optimal regime where the steady states exhibit maximal bond currents. Due to the symmetry of the considered setups we assume translational invariance in the  $y$  direction, where all sites along the  $y$  axis behave in the same way. In this case there is no current in the  $y$  direction and the indices  $l$  and  $j$  label  $x$  coordinates of the lattice sites; see Fig. 1.

One possibility to realize steady states exhibiting a finite bond current is by engineering suitable phases of the coherent driving terms  $F_l$

$$F_l^{\text{PI}} = F \exp(i\Phi_l), \quad \Phi_l = \Phi^{\text{PI}}l, \quad \gamma_l^{\text{PI}} = \gamma_b, \quad (6)$$

that will be imprinted onto phases of  $\langle a_l \rangle$ , thus providing the finite current. This setup has been introduced in Ref. [14] and throughout the paper we designate it as phase imprinting (PI), Fig. 1(a). A second experimentally relevant protocol that leads to steady states with currents uses drives that inject photons into the lattice locally, e.g., by shining laser light on one side only, Fig. 1(b). Steady states in the presence of homogeneous dissipation in a one-dimensional lattice have been explored recently in such systems [21]. In particular, stronger loss rates at the opposite lattice side should serve as photonic sinks

$$F_l^{\text{SD}} = F \delta_{l,N}, \quad \gamma_l^{\text{SD}} = \gamma \delta_{l,1} + \gamma_b, \quad (7)$$

thus providing for a stable photonic flow. In both Eqs. (6) and (7), the index  $l$  stands for the site position along the  $x$  axis and there is no explicit dependence on the site position in the  $y$  direction. The aim of our study is to explicate how the emerging current intensity  $j$  is set by the laser amplitude  $F$  and intrinsic loss rates  $\gamma_l$ , as well as by the parameters of the underlying Hamiltonian in Eq. (1).

We note that the onset of particle currents in a bosonic system naturally raises questions about superfluidity in a dissipative-driven system [37–40]. A definite answer can be provided by studying how the presence of defects modifies the photonic flow or by analyzing asymptotics of long-range correlations in the system. These questions will be addressed in future work.

### III. METHODS

In the noninteracting limit  $U = 0$  we solve the exact equations of motion for the expectation values  $\phi_l = \langle a_l \rangle = \text{Tr} \rho a_l$ :

$$i \frac{d\phi_l}{d(tJ)} = -\frac{\Delta}{J} \phi_l - \sum_{\langle l,j \rangle} \phi_j + \frac{F_l}{J} - i \frac{\gamma_l}{2J} \phi_l, \quad (8)$$

where  $\langle l,j \rangle$  denotes summation over nearest-neighbor sites of the site  $l$ . We consider a two-dimensional lattice with  $N$  sites in the  $x$  direction and translational invariance in the  $y$  direction implemented using periodic boundary conditions, and the index  $l$  labels  $x$  coordinates of the lattice sites. In this notation we have for example  $\sum_{\langle l,j \rangle} \phi_j = 2\phi_l + \phi_{l-1} + \phi_{l+1}$ .

Using vector notation  $\vec{\phi} = (\phi_1, \dots, \phi_N)^T$ ,  $\vec{F} = (F_1, \dots, F_N)^T$  the steady-state solution can be written as [1,41]

$$\phi_l = -M_{lj}^{-1} F_j / J, \quad (9)$$

where  $M$  is a  $N \times N$  matrix with elements

$$M_{lj} = [-2 - \Delta/J - i\gamma_l/(2J)]\delta_{l,j} - \delta_{l-1,j} - \delta_{l+1,j}. \quad (10)$$

To simplify the notation, spatial indices will be omitted  $j_{lj} \rightarrow j$  from now on whenever the current throughout the lattice is constant and we implicitly assume the current between two nearest neighbors in the  $x$  direction.

At high densities, provided for example by strong driving, and for weak  $U$ , the interaction term may be treated at the mean-field level leading to nonlinearities for the  $\phi_l$  in their equations of motion:

$$i \frac{d\phi_l}{d(tJ)} = -\frac{\Delta}{J}\phi_l - \sum_{(l,j)} \phi_j + \frac{U}{J}|\phi_l|^2\phi_l + \frac{F_l}{J} - i \frac{\gamma_l}{2J}\phi_l. \quad (11)$$

To get an estimate of effects of quantum fluctuations on the mean-field predictions, we follow the approach described in Ref. [14]. Using a Fourier transform  $a_{l_x,l_y} = \frac{1}{\sqrt{N_x N_y}} \sum_{\vec{k}} e^{-i(k_x l_x + k_y l_y)} B_{\vec{k}}$  we rewrite the Hamiltonian (1) as

$$\begin{aligned} \mathcal{H} = & \sum_{\vec{k}} \omega_{\vec{k}} B_{\vec{k}}^\dagger B_{\vec{k}} + \sqrt{N_x N_y} F(B_{\Phi^{\text{PI}},0} + B_{\Phi^{\text{PI}},0}^\dagger) \\ & + \frac{U}{2N_x N_y} \sum_{\vec{k}_1, \vec{k}_2, \vec{k}_3, \vec{k}_4} \delta_{\vec{k}_1 + \vec{k}_2 + 2\pi(z,p), \vec{k}_3 + \vec{k}_4} B_{\vec{k}_1}^\dagger B_{\vec{k}_2}^\dagger B_{\vec{k}_3} B_{\vec{k}_4}, \end{aligned}$$

where  $\omega_{\vec{k}} = -\Delta - 2J(\cos k_x + \cos k_y)$ , and  $z$  and  $p$  are integers. In the next step, we expand operators around the mean-field solution as

$$B_{\vec{k}} = \sqrt{N_x N_y} \beta \delta_{k_x, \Phi^{\text{PI}}} \delta_{k_y, 0} + b_{\vec{k}}, \quad (12)$$

where  $|\beta|^2 = n^{\text{PI}}$  is the mean-field density. By taking into account fluctuations up to the second order we obtain an effective quadratic Hamiltonian

$$\tilde{\mathcal{H}} = \sum_{\vec{k}} \left[ (\omega_{\vec{k}} + 2n^{\text{PI}}U) b_{\vec{k}}^\dagger b_{\vec{k}} + \frac{U}{2} (\beta^{*2} b_{\vec{k}}^\dagger b_{\vec{k}\vec{k}} + \beta^2 b_{\vec{k}}^\dagger b_{\vec{k}\vec{k}}^\dagger) \right],$$

with  $kk_x = 2\pi z + 2\Phi^{\text{PI}} - k_x, kk_y = k_y$ . From the stationarity condition  $\frac{d}{dt} \langle b_{\vec{k}}^\dagger b_{\vec{k}} \rangle = 0$ ,  $\frac{d}{dt} \langle b_{\vec{k}}^\dagger b_{\vec{k}\vec{k}} \rangle = 0$ , we find closed-form equations for the second-order moments

$$iU\beta^{*2} \langle b_{\vec{k}}^\dagger b_{\vec{k}\vec{k}} \rangle - iU\beta^2 \langle b_{\vec{k}}^\dagger b_{\vec{k}\vec{k}}^\dagger \rangle - \gamma_b \langle b_{\vec{k}}^\dagger b_{\vec{k}} \rangle = 0, \quad (13)$$

$$\begin{aligned} & -i(\omega_{\vec{k}} + \omega_{\vec{k}\vec{k}} + 4n^{\text{PI}}U) \langle b_{\vec{k}}^\dagger b_{\vec{k}\vec{k}} \rangle - \gamma_b \langle b_{\vec{k}}^\dagger b_{\vec{k}\vec{k}} \rangle \\ & - iU\beta^2 (\langle b_{\vec{k}}^\dagger b_{\vec{k}} \rangle + \langle b_{\vec{k}\vec{k}}^\dagger b_{\vec{k}\vec{k}} \rangle + 1) = 0, \end{aligned} \quad (14)$$

that finally yield for  $m(\vec{k}) = \langle b_{\vec{k}}^\dagger b_{\vec{k}} \rangle$

$$m(\vec{k}) = \frac{2(Un^{\text{PI}})^2}{[(\omega_{\vec{k}} + \omega_{\vec{k}\vec{k}})^2 + 4n^{\text{PI}}U]^2 + \gamma_b^2 - 4(Un^{\text{PI}})^2}.$$

Fluctuation effects are quantified by the ratio

$$m/n^{\text{PI}} = \sum_{\vec{k}} m(\vec{k}) / (n^{\text{PI}} N_x N_y) \quad (15)$$

and the expansion up to second order in the fluctuations can be expected to be a good approximation as long as this ratio remains small,  $m/n^{\text{PI}} \ll 1$ .

When addressing the limit of strong interactions, we restrict our description to the well-established bosonic Gutzwiller approximation [13,17,42], where only local correlations are taken into account. The time-dependent variational Gutzwiller mixed state is a product of local mixed states. In other words the total density operator in the Gutzwiller approximation is given by a direct product of density operators  $\rho_i$  on the individual sites:

$$\rho_{\text{GW}}(t) = \prod_{\otimes l} \rho_l(t) = \prod_{\otimes l} \sum_{m,n < N_c} c_{nm}^l(t) |n\rangle_l \langle m|_l. \quad (16)$$

In our calculations we truncate the dimension of the local Hilbert space for every site at a finite value  $N_c = 10$ , which we choose large enough so that our results are independent of the choice of the cutoff. The accuracy and limitations of this approximation in describing dissipative systems have been discussed in Ref. [43]. In brief, by comparing Gutzwiller results with exact calculations on small lattices it is found that the method describes local quantities accurately, but it underestimates phase coherence between different sites. However, it is expected that the accuracy of the method improves as the lattice coordination number increases.

Projecting the Lindblad equation (2) onto the local occupation number bases we obtain equations of motion for the variational coefficients of the Gutzwiller state, which are  $N \times N_c$  coupled first-order differential equations:

$$\begin{aligned} i \frac{dc_{nm}^l(t)}{dt} = & \eta_l \sqrt{nc_{n-1,m}^l} + \eta_l^* \sqrt{n+1} c_{n+1,m}^l \\ & - \eta_l \sqrt{m+1} c_{n,m+1}^l - \eta_l^* \sqrt{m} c_{n,m-1}^l \\ & + i\gamma_l \sqrt{n+1} \sqrt{m+1} c_{n+1,m+1}^l \\ & + \left( \frac{U}{2} [n(n-1) - m(m-1)] \right. \\ & \left. - \Delta(n-m) - i \frac{\gamma_l}{2} (n+m) \right) c_{n,m}^l, \end{aligned} \quad (17)$$

where  $\eta_l = F_l - J \sum_{(l,j)} \phi_j$  takes into account the contribution of nearest-neighbor sites and the external driving term. After preparing the system in an initial state we propagate the equations of motion simultaneously to describe the subsequent nonequilibrium dynamics. We chose here to investigate the steady-state solutions by observing the long-time dynamics of the system.

## IV. RESULTS

In the following we present properties of photonic currents for the setups defined in Eqs. (6) and (7).

### A. Phase imprinting

In the noninteracting limit of the setup shown in Fig. 1(a), phases of the coherent driving terms  $F_l$  translate into phases of  $\phi_l$  according to Eq. (9) as

$$\phi_l = - \sum_k \frac{1}{\varepsilon_k - \Delta - i \frac{\gamma_b}{2}} k_l \sum_j k_j^* F_j, \quad (18)$$

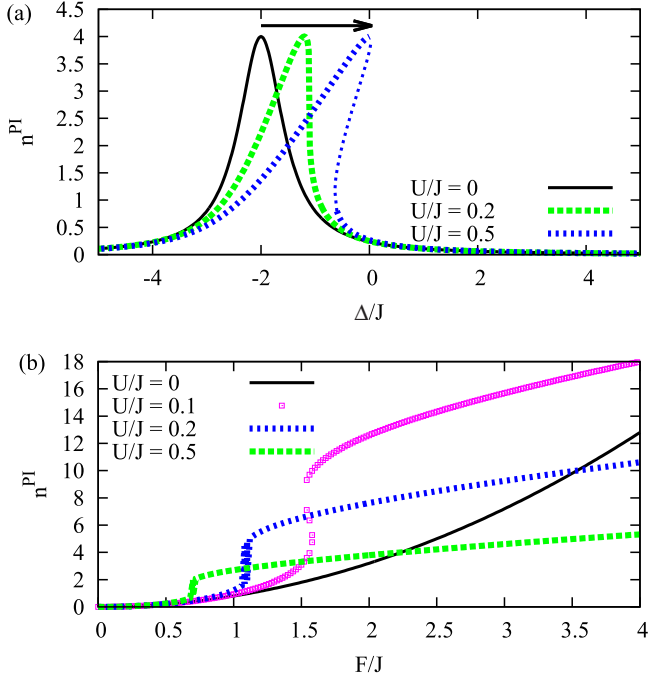


FIG. 2. The density  $n^{\text{PI}}$  [Eq. (22)] as a function of (a) detuning and (b) driving for the setup (6). Additional parameters used in the calculations:  $\Phi^{\text{PI}} = \pi/2$ , (a)  $F/J = 1$ ,  $\gamma_b/J = 1$ , (b)  $\Delta/J = -1$ ,  $\gamma_b/J = 1$ . The thin part of the dotted line in (a) corresponds to unstable solutions.

where  $\varepsilon_k$  and  $|k\rangle$  are eigenfrequencies and eigenmodes of

$$H_{lj}^0 = -2J\delta_{l,j} - J\delta_{l-1,j} - J\delta_{l+1,j}, \quad (19)$$

and we keep in mind that we work in a corotating frame. For a lattice obeying periodic boundary conditions in both  $x$  and  $y$  directions, we find homogeneous steady states with density

$$n^{\text{PI}} = \frac{F^2}{[2J(1 + \cos \Phi^{\text{PI}}) + \Delta]^2 + \frac{\gamma_b^2}{4}}, \quad (20)$$

and bond current

$$|j^{\text{PI}}| = 2Jn^{\text{PI}} \sin \Phi^{\text{PI}}. \quad (21)$$

The maximal current  $j^{\text{PI}} = 8JF^2/\gamma_b^2$  occurs at  $\Delta = -2J(1 + \cos \Phi^{\text{PI}})$ , and the highest ratio  $j^{\text{PI}}/(Jn^{\text{PI}}) = 2$  is found at  $\Phi^{\text{PI}} = \pi/2$ .

We now discuss effects of weak interactions on the currents for  $\Phi^{\text{PI}} = \pi/2$ . The lattice density is obtained from Eq. (11) by solving

$$n^{\text{PI}} = \frac{F^2}{(-2J - \Delta + n^{\text{PI}}U)^2 + \frac{\gamma_b^2}{4}}, \quad (22)$$

while the bond current is still given by Eq. (21). From Eq. (22) it is clear that the maximal current is the same as without interactions, only the resonance condition is changed to

$$\Delta_r^{\text{PI}} = -2J + 4U \frac{F^2}{\gamma_b^2}. \quad (23)$$

This effect is illustrated in Fig. 2(a), where we also see that in certain regimes the mean-field description predicts up to three

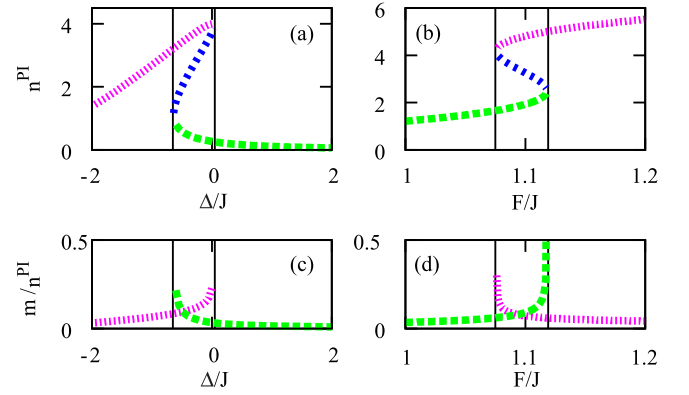


FIG. 3. Top: The density  $n^{\text{PI}}$  as a function of (a) detuning and (b) driving for phase imprinting  $\Phi^{\text{PI}} = \pi/2$ . Bottom: quantum fluctuations  $m/n^{\text{PI}}$ . Additional parameters used in the calculations: (a), (c)  $F/J = 1$ ,  $\gamma_b/J = 1$ ,  $U/J = 0.5$ , (b), (d)  $\Delta/J = -1$ ,  $\gamma_b/J = 1$ ,  $U/J = 0.2$ .

solutions for the same detuning  $\Delta$  [44]. From Fig. 2(b) it is evident that only in the limit of low filling we find  $j \sim F^2$  as in the case of  $U = 0$ . At a certain threshold value of  $F$ , the dependence becomes steep and finally turns into  $j \sim F^{2/3}$ . We note that even stronger switching from low to high occupation can be found for the nonlinear waveguide where normal modes synchronize during this switching process [45].

By inspecting the contribution of quantum fluctuations given in Eq. (15) for different solutions (22), we find that in the region of coexistence one branch of solutions is unstable [37,44] [the blue (middle) curve in Figs. 3(a) and 3(b)]. The two other branches exhibit stronger fluctuations in the intermediate regime [see Figs. 3(c) and 3(d)], indicating that the accuracy of the mean-field approach deteriorates and the exact solution may be a superposition of the two mean-field solutions. This conclusion is in agreement with a variational solution of Eq. (2) that captures beyond mean-field effects and exhibits a unique steady state [46].

In the limit of stronger interactions, in the Gutzwiller mean-field description (16) our system decomposes into single cavities with an effective driving

$$\eta = F - 2J\phi^{\text{PI}}(1 + \cos \Phi^{\text{PI}}), \quad (24)$$

which incorporates contributions from the nearest neighbors of every site of the square lattice. Our numerical results can be explained using an analytical result of Drummond and Walls [44] for a steady state of a single driven cavity. In the steady-state regime the value of the bosonic coherence  $\phi^{\text{PI}}$  satisfies the equation [17,18,44]

$$\phi^{\text{PI}} = \frac{\eta}{\Delta + i\gamma_b/2} \frac{\mathcal{F}(1 + c, c^*, 8|\eta/U|^2)}{\mathcal{F}(c, c^*, 8|\eta/U|^2)}. \quad (25)$$

The average density is given by

$$n^{\text{PI}} = \left| \frac{2\eta}{U} \right|^2 \frac{1}{|c|^2} \frac{\mathcal{F}(1 + c, 1 + c^*, 8|\eta/U|^2)}{\mathcal{F}(c, c^*, 8|\eta/U|^2)}, \quad (26)$$

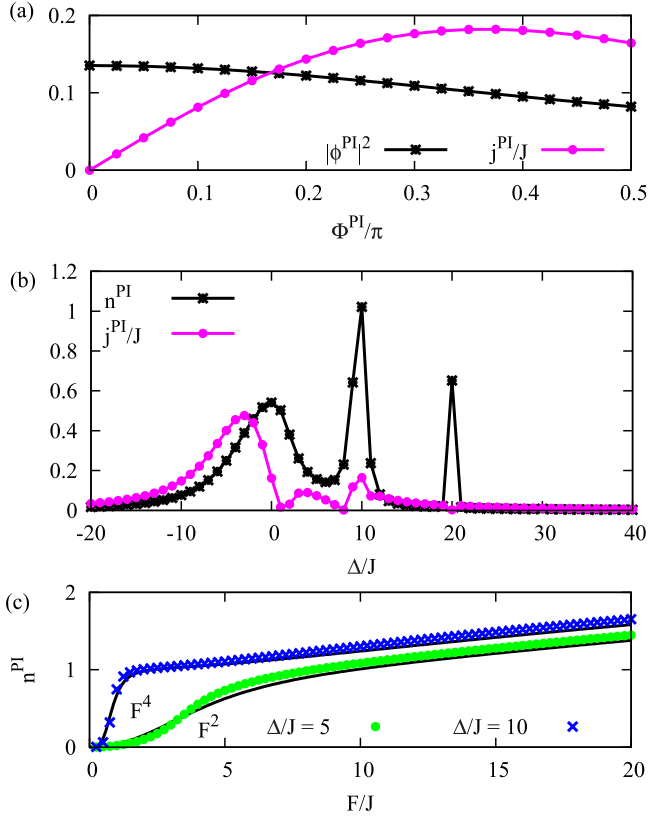


FIG. 4. The current  $j^{\text{PI}} = 2J|\phi^{\text{PI}}|^2 \sin \Phi^{\text{PI}}$  and local density  $n^{\text{PI}}$  in the steady state of the phase imprinting setup (6). Parameters:  $U/J = 20$ ,  $\gamma_b/J = 0.2$ , (a)  $\Delta/J = 10$ ,  $F/J = 2.4$ ,  $n^{\text{PI}} \approx 1$ , (b)  $F/J = 2.4$ ,  $\Phi^{\text{PI}} = \pi/2$ , (c)  $\Phi^{\text{PI}} = \pi/2$ . The black solid lines in (c) are the corresponding analytical results for  $J = 0$ .

where  $c = -2(\Delta + i\gamma_b/2)/U$ ,

$$\mathcal{F}(c, d, z) = \sum_n \frac{\Gamma(c)\Gamma(d)}{\Gamma(c+n)\Gamma(d+n)} \frac{z^n}{n!}$$

is the generalized hypergeometric function and  $\Gamma(x)$  is the gamma function. Our analysis is analogous to the analysis performed in Refs. [17,18], with the main difference that we introduce the parameter  $\Phi^{\text{PI}}$ , which is a necessary ingredient to obtain currents. The steady states we obtain by solving Eq. (25) are also found in real-time evolution of Eqs. (17) starting from an initial state with a strong bosonic coherence.

Our main results are summarized in Fig. 4. As the strong interaction  $U/J = 20$  tends to suppress bosonic coherences, the ratio of  $j^{\text{PI}}/(Jn^{\text{PI}})$  is an order of magnitude smaller compared to the noninteracting regime. The maximal ratio is found at  $\Phi^{\text{PI}} \approx 0.35\pi$ , since the bosonic coherence  $\phi^{\text{PI}}$  is higher for this value than at  $\Phi^{\text{PI}} = \pi/2$ , Fig. 4(a). The current  $j^{\text{PI}}$  is a nonmonotonous function of the detuning  $\Delta$ , Fig. 4(b). This behavior stems from multiphotonic resonances of the single cavity that occur at [18,44]

$$\Delta_r^{\text{PI}} = \frac{U}{2}(n-1), \quad n = 1, 2, \dots, \quad (27)$$

when the energy of  $n$  incoming photons is equal to the energy of  $n$  cavity photons. The number of resonances that can be resolved practically is set by the ratio  $F/U$ , which also

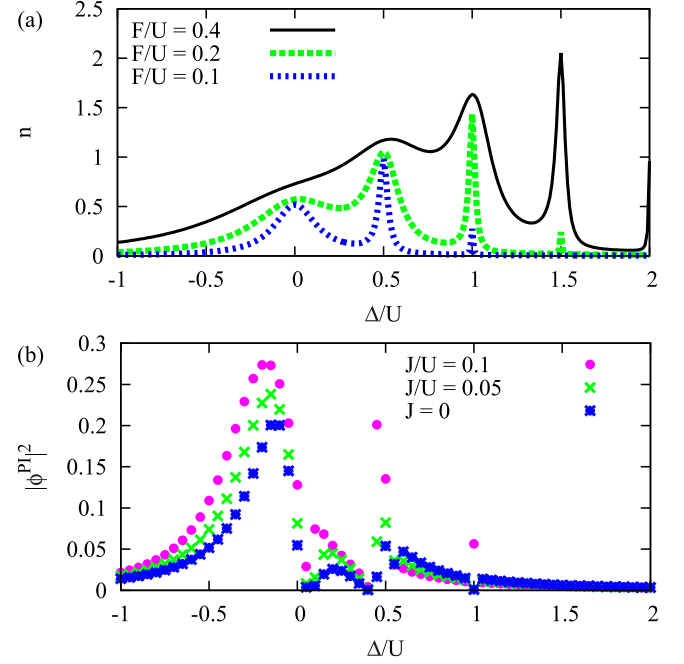


FIG. 5. (a) Analytical results from [44] for a steady state of a single driven cavity. (b) Bosonic coherence as a function of the detuning for several values of  $J$ . Parameters  $\gamma_b/U = 0.01$  and  $F/U = 0.12$ ,  $\Phi^{\text{PI}} = \pi/2$  in (b).

determines the maximal possible filling of the lattice. For very weak driving only low-lying resonances can be probed, as shown in Fig. 4(b) for  $F/U = 0.12$ . At stronger driving, low-order resonances are washed out—as can be seen from the analytical solution available for  $J = 0$ , see Fig. 5(a)—and replaced by a simpler dependence that is captured by Eq. (11). Yet, a few high-lying resonances can be resolved clearly even at strong  $F$ ; see Fig. 5(a). In the vicinity of the lowest-order resonance, maximal  $j^{\text{PI}}$  is found at some off-resonant negative value of  $\Delta$ , while higher-order resonances can appear either as peaks or dips in the current intensity. In Fig. 5(b) we observe a local maximum of the coherence at  $\Delta = U/2$ , while at  $\Delta = U$  there is a minimum at  $J/U = 0.05$  and maximum at  $J/U = 0.1$ . When  $J/U$  and  $F/U$  are comparable, a regime with multiple stable mean-field solutions can be found [17,18]; however, this topic is beyond the scope of this paper.

In order to infer the dependence of the current on the driving amplitude in the regime of strong  $U$ , we expand the analytical result [44] for  $J = 0$  in the limit of weak  $F$  and obtain

$$n \sim \frac{1}{U^6} [(\gamma_b^2 + 4\Delta^2)((U - 2\Delta)^2 + \gamma_b^2)F^2 + 8U(4\Delta - U)F^4 + \dots]. \quad (28)$$

If the dissipation rates are low ( $\gamma_b/U \ll 1$ ), at  $\Delta = U/2$  the term proportional to  $F^4$  will dominate the  $F^2$  term even at very weak  $F$ , as we clearly observe in Fig. 4(c) at  $\Delta/J = 10$ ,  $U/J = 20$ . Except for this special resonant case, we typically have an  $F^2$  dependence in the weak  $F$  limit. In the regime of strong  $F$ , we recover the result obtained in the previous section  $j \sim F^{2/3}$ .

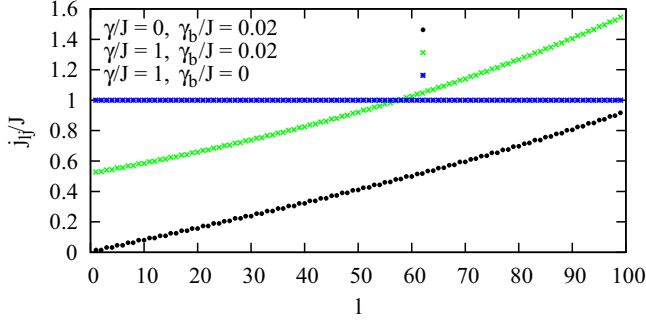


FIG. 6. The currents  $j_{l,l+1}$  between nearest-neighbor sites along the  $x$  direction for the source-drain setup (7). Parameters used:  $F/J = 1$ ,  $\Delta/J = -2$ .

### B. Source-drain setup

Typical spatial distributions of the bond currents in the noninteracting regime of the setup defined in Eq. (7) are presented in Fig. 6 for a lattice size of  $N = 100$  in the  $x$  direction and assuming translational invariance in the  $y$  direction, where a single site is repeated periodically. The driving is applied at the rightmost lattice sites, and in the presence of uniform dissipation rates the intensity of the bond currents decays roughly linearly as we approach the leftmost sites. In order to enhance overall currents, we consider the leftmost cavities to exhibit a stronger dissipation rate. In the idealized case of  $\gamma_b = 0$  we find a uniform current throughout the lattice. Hence, in the following we will explore the source-drain (SD) setup Eq. (7) with open boundary conditions in the  $x$  direction and periodic boundary conditions in the  $y$  direction. The differences of this setup with respect to the model studied in Ref. [21] are the following: we consider a two-dimensional lattice and we take into account spatially varying dissipation rates of cavities; see Eq. (7). Moreover, we investigate a regime of high lattice density and weak interactions, which was not addressed in Ref. [21].

In the steady-state regime with constant total number of photons, it holds true that

$$-2F \text{Im}\phi_N = \gamma n_1 + \gamma_b \sum_{j=1}^N n_j, \quad (29)$$

i.e., the flux of incoming particles on the right is equal to the flux of the particles leaving the system (continuity equation). In the special case of  $\gamma_b = 0$  we find a uniform current:

$$j^{\text{SD}} = \gamma n_1 = -2F \text{Im}\phi_N. \quad (30)$$

In the noninteracting limit of the setup (7), both the total density  $\sum_l \langle n_l \rangle$  and the intensity of the bond current are proportional to  $F^2$  according to Eq. (9). In Fig. 7(a) we show that the transport occurs if there is an eigenmode of  $H^0$  in Eq. (19) at the given value of  $\Delta$  to support it. In our case the range of resonant driving frequencies is  $\Delta \in [-4J, 0]$ , as the frequency of the lowest mode of a two-dimensional lattice is  $-4J$  and we only consider transport in the  $x$  direction. To infer effects of local dissipation  $\gamma$ , we invert the matrix  $M$  (10), first

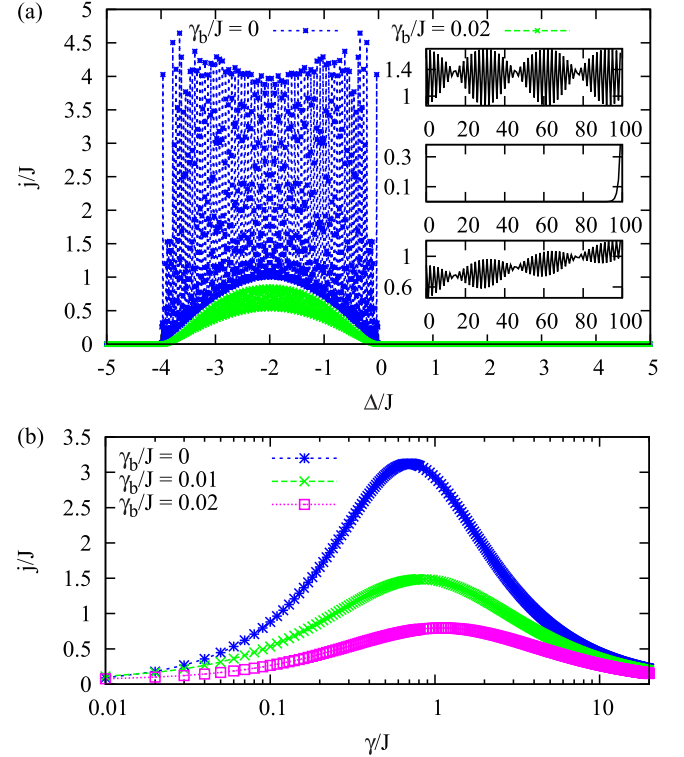


FIG. 7. The current (4) for the setup (7) as a function of (a) detuning and (b) local dissipation. Additional parameters: (a)  $\gamma/J = 1$ ,  $F/J = 1$ , (b)  $\Delta/J = -2.1$ ,  $F/J = 1$ . Insets in (a) show the spatial distribution of  $|\phi_l|$  over the site index  $l$  in the  $x$  direction. Typical distributions range from (top) “conducting” behavior ( $\Delta/J = -2.1, \gamma_b = 0$ ) to (center) the situation without bulk current ( $\Delta/J = 5, \gamma_b = 0.0$ ). Bottom: Conducting behavior with bulk dissipation ( $\Delta/J = -2.1, \gamma_b/J = 0.02$ ). The lattice consists of  $N = 100$  sites in the  $x$  direction.

for  $\gamma_b = 0$ . The bond current is given by

$$j = \gamma \frac{F^2}{J^2} \frac{p(2 + \frac{\Delta}{J})}{q(2 + \frac{\Delta}{J}) + \frac{\gamma^2}{4J^2} r(2 + \frac{\Delta}{J})}, \quad (31)$$

where  $p(x)$ ,  $q(x)$ , and  $r(x)$  are polynomials that can be expressed in terms of determinants of the matrix  $M$  and its submatrices with  $\gamma$  set to zero. The last dependence is plotted in Fig. 7(b) and we see that the bond current is maximal when the dissipation rate  $\gamma$  is of the same order of magnitude as the hopping rate  $J$ , i.e.,  $\gamma/J \sim 1$ . Beyond this value, the current is suppressed as the quantum Zeno effect takes place [43]. If the resonant condition  $\Delta = \varepsilon_n$  is fulfilled, the matrix  $M$  in Eq. (10) is singular for vanishing  $\gamma_b$  and we find  $j \sim \gamma^{-1}$ . As expected, the intensity of  $j$  is suppressed by the presence of finite bulk dissipation  $\gamma_b$ . In Fig. 7(b) at finite  $\gamma_b$  we plot the current between the leftmost site and its nearest neighbor in the  $x$  direction. The insets of Fig. 7(a) show density distributions in different regimes. In the conducting regime density profiles are typically nonuniform.

Now we address effects of weak interactions first with  $\gamma_b = 0$ . To access the steady states, we perform a real-time propagation of Eq. (11). This method raises an important question about if and how the steady states depend on the

chosen initial conditions [47]. For very weak  $U$ , such that  $nU/J \ll 1$ , the noninteracting steady states from the previous section provide a good starting point. States obtained in this way exhibit nonuniform density distributions. As  $U$  becomes stronger, our numerical results suggest that in the bulk of the system, where  $\gamma_l = 0$  and  $F_l = 0$ , the steady states are given by  $\phi_l = \sqrt{n^{\text{SD}}} \exp(i\Phi l)$ . The density is uniform in the bulk

$$n^{\text{SD}}(\Phi) = \frac{\Delta + 2J(1 + \cos \Phi)}{U}, \quad (32)$$

and so is the bond current

$$j^{\text{SD}}(\Phi) = 2Jn^{\text{SD}}(\Phi) \sin \Phi, \quad (33)$$

where  $\Phi$  is a constant phase difference between  $\phi_l$  of nearest neighbors. Unlike the phase imprinting setup, where the value of  $\Phi$  is fixed by the external drive, here the phase difference is set by the boundary conditions (30). In the following, we set the initial state for the real-time propagation of Eq. (11) to a steady state for fixed values of  $\Delta$ ,  $F$ , and  $\gamma$ , then adiabatically change one of the parameters and monitor how this change affects the steady state.

As in the phase imprinting setup, for very weak  $U$  it holds that  $j \sim F^2$ . In contrast, in the steady state (32) the driving  $F$  affects only the rightmost sites and not the bulk features. As  $F$  gets smaller, only the occupancy of the rightmost sites  $n_N$  decreases. Eventually, densities on the leftmost and rightmost lattice site become equal  $n_N \approx n_1$  and at this point the steady state is no longer supported. This occurs approximately at  $F^* = \frac{1}{2}\gamma\sqrt{n_1}$  and we have  $j \sim \theta(F - F^*)$ , where  $\theta(x)$  is a step function. With further decrease of the driving intensity  $F$ , our numerical results exhibit strong oscillations that persist up to the longest integration time. In this regime, numerical simulations fail to converge to a stationary regime and the average intensity of the bond current is zero.

The steady states (32) exist if  $\Delta \geq -4J$ . Above this threshold the lattice filling exhibits a roughly linear increase with  $\Delta$ . The detuning also affects the phase difference  $\Phi$ , as evidenced by the change in the ratio  $j/n$ ; see Fig. 8(a). The current per particle saturates at large  $\Delta$  and it turns out that at large enough  $\Delta$ , when the lattice filling is too high, the steady state is no longer supported for it requires stronger driving  $F$ .

In the source-drain setup the value of  $\Phi$  can be changed by tuning the intensity of the local dissipation  $\gamma$  [29]. Unlike  $F$ ,  $\gamma$  affects both the bulk density of a steady state as well as the strength of the bond current. For example, in the case presented in Fig. 8(b) an optimal ratio  $j/(Jn) \approx 1$  is found at  $\gamma/J \approx 2$ . By additionally optimizing the detuning  $\Delta$ , this ratio can be enhanced further; see Fig. 8(a). In a similar way as for the phase imprinting, effects of quantum fluctuations can be estimated and we find them to be reasonably small. Finally, we find that the states (32) are stable with respect to the bulk dissipation for moderate values of  $\gamma_b/J \sim 0.01$ .

We now investigate features of the current for stronger interactions at a fixed ratio  $U/J = 4$  as a function of the external system parameters  $\gamma, F$  ( $\gamma_b = 0$ ) by solving Eq. (17) for long times. In Fig. 9 we show the average current at large times  $tJ \sim 10^4$ , where we identify quasisteady states, which yield approximately constant current and particle densities  $j, n \approx \text{const}$ . We average these quantities over a large enough

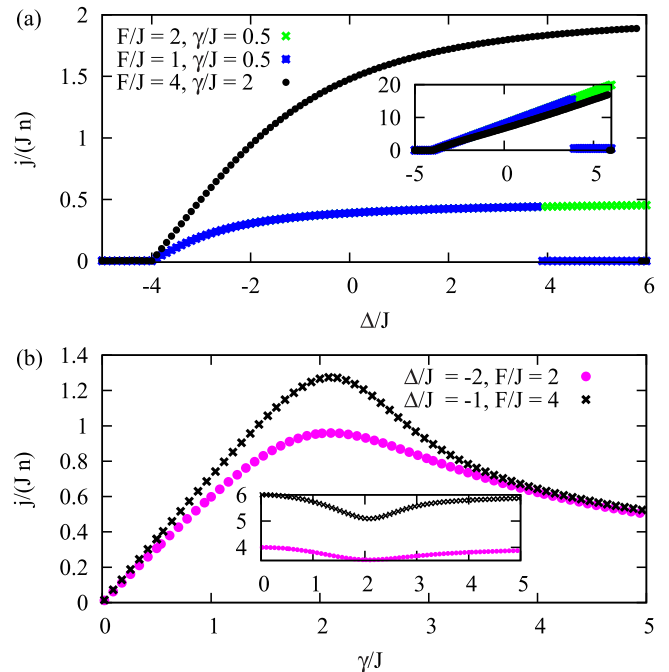


FIG. 8. The ratio  $j/(Jn)$  as a function of (a) detuning  $\Delta$  and (b) the dissipation  $\gamma$  for  $U/J = 0.5$ ,  $\gamma_b = 0$ , and  $N = 50$  for the source-drain setup (7). Insets of both plots show the local density  $n$  in the bulk.

time span, which evens out most of the oscillations, and we attribute any residual noise to lower-frequency components, which stem from our choice of the initial state. At small  $\gamma/J \lesssim 1$  the aforementioned quasisteady states exist and their current density increases almost linearly with  $\gamma/J$ . The current density is then only weakly dependent on the driving  $F/J$ . At  $\gamma_c/J \sim 1$  a sharp transition occurs and the existence of the quasisteady states is suddenly violated. What we find instead are oscillating mixed states with (almost) vanishing average current density, hence a nontransparent region.

We explain this observation with the quantum Zeno effect [48,49] by identifying the loss rate  $\gamma$  with the rate of a generalized measurement, which—repeated at high frequencies—stops the unitary time evolution and forces the system into the lossless steady state, where no significant particle transfer from the driven to the lossy site is observed. Following early theoretical considerations [50], the quantum Zeno effect was observed in experiments with cold ions [51] and ultracold atoms [52–55]. In the context of ultracold atoms, the interplay of interactions and dissipation has received a lot of attention [42,56–62]. Applying this principle to our system we first note that only the dissipative sites (in this case only the ones at the left boundary  $x = 0$ ) are being “measured,” which means that only the reduced density operators on these sites become time independent in the limit of frequent measurements, i.e., strong dissipation. In fact, in the limiting case the local density operators will be equal to the local vacuum. The rest of the system will henceforth pursue its own unitary time evolution, where the coupling to the dissipative site is simply disabled. This explains why we cannot find quasisteady states at large dissipation, because the only steady states under unitary time

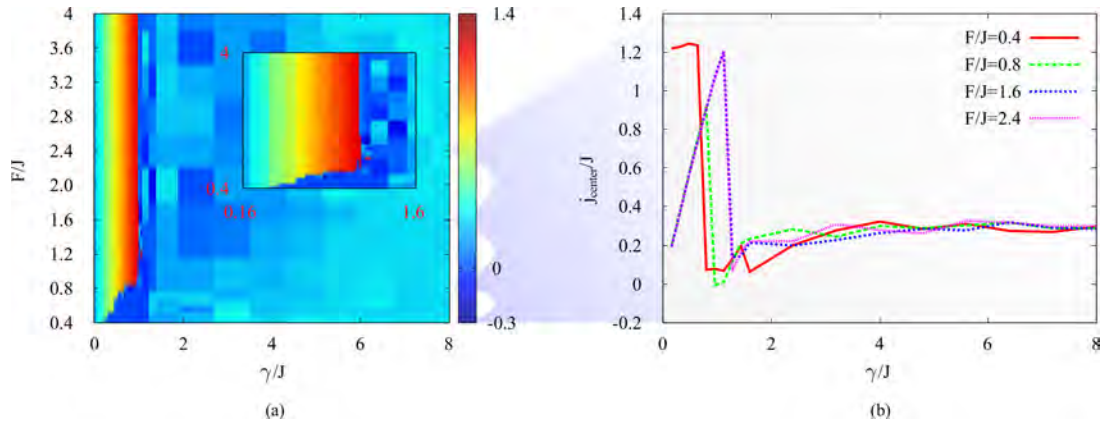


FIG. 9. (a) Average current  $j/J$  in the center of a system (7) of width  $N = 200$  sites in the  $x$  direction and translational invariance in the  $y$  direction at times  $tJ \sim 10^4$ . At  $\gamma_c/J \sim 1$  the current is suppressed due to the quantum Zeno effect. In (b) slices through the phase diagram at different driving strengths are shown. Parameters used are  $U/J = 4, \Delta/J = 2$ .

evolution are eigenstates of  $\mathcal{H}$  and for arbitrary initial states, composed of many different eigenstates of  $\mathcal{H}$ , observables do not converge.

The transition at  $\gamma_c/J \sim 1$  occurs at the point where the time scales of the local measurement  $\sim 1/\gamma$  and the competing hopping process at rate  $J$  are balanced. At this point the particle transfer is maximal since particle loss occurs at the same rate as the hopping, which fills up the dissipative sites again. If the dissipation is any stronger this filling process will be suppressed.

From this discussion it is already apparent that the dissipation is the prevalent ingredient for a description of the transport in this system. Microscopically, this can be understood from a wave picture, where excess currents are reflected from a hard wall and destructive interference of counterpropagating waves takes place. We confirm this assumption by examining snapshots of the current distribution at small times (see Fig. 10) before the quasisteady state regime has been reached. By observing the time evolution of easily identifiable current peaks we find that for weak  $\gamma$  only a small proportion of particles is reflected while the majority is transmitted to the lossy site and lost eventually, Fig. 10(a). However, for a large

enough ratio  $\gamma/J$ , currents are reflected—not at the system boundary, but at the lossy site, Fig. 10(b). Peaks traveling towards the dissipative edge will change the direction, i.e., the sign of the current, just before the dissipative site. As a consequence the dissipative site is effectively decoupled from the system.

The oscillations in the region with  $\gamma_c < \gamma \ll \infty$  can be explained in the wave picture as well. Since perfect destructive interference of reflected components would require suitable geometric conditions, which we do not alter throughout our simulations, the process of particles “bouncing” back and forth will lead to a small current distribution, which is difficult to average out completely.

The source-drain setup (7) is the simplest way to describe transport through the system, neglecting the penetration depth of the laser into the medium and de-excitations in the bulk. Typically, lattices are formed of identical cavities, the individual mode excitations of which have the same decay rates, so that a constant bulk decay rate is more realistic. In order to simulate the penetration of the laser into the medium we consider a decaying laser amplitude  $F$  as a function of the penetration depth. In the simplest case this would be a linear

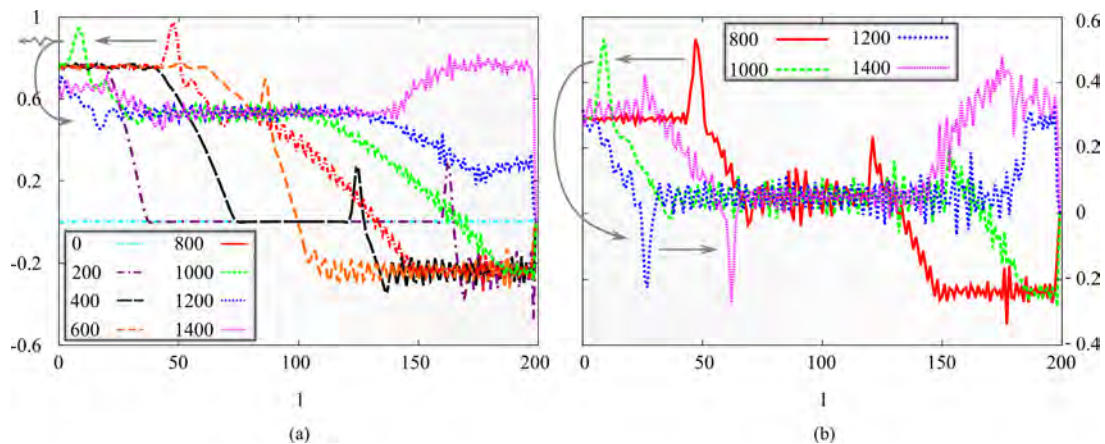


FIG. 10. Current distribution  $j_{l,l+1}/J$  at small times  $tJ \in [0, 1400]$  for the system of Fig. 9 at (a)  $\gamma/J = 0.8$  and (b)  $\gamma/J = 4$ . In (b) currents are reflected from the dissipative site as a consequence of quantum Zeno blocking. The initial dynamics for  $tJ \in [0, 600]$  are only shown in (a) for clarity. Relevant are the peaks in the current distribution; arrows are meant to guide the eye. Parameters used are  $U/J = 4, \Delta/J = 1, F/J = 2$ .

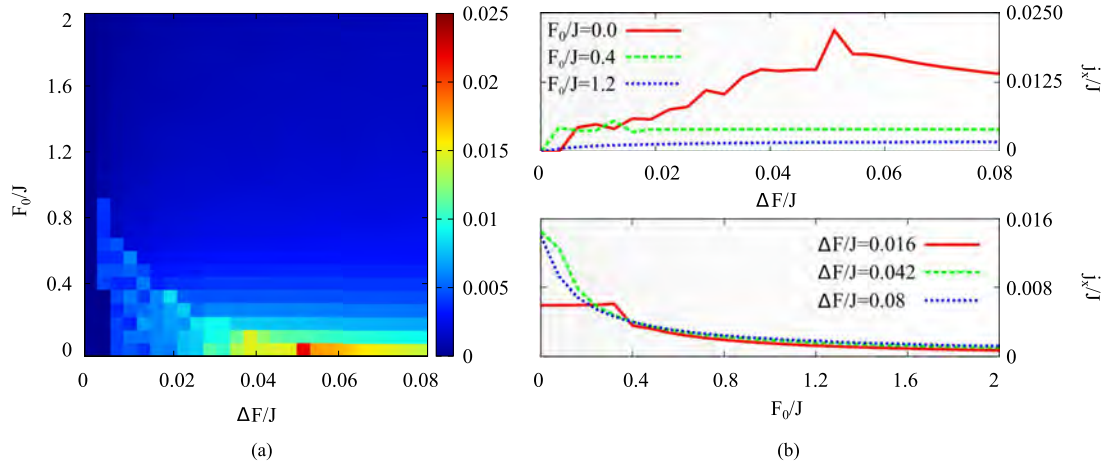


FIG. 11. (a) Average current  $j_x = 1/N \sum_l j_{l,l+1}$  as a function of the slope  $\Delta F$  of the driving laser amplitude (34) and the background amplitude  $F_0$ . Here, the system has a width of  $N = 200$  sites in the  $x$  direction and one site in the  $y$  direction, which is repeated via periodic boundary conditions. Cuts through the diagram are shown in (b), where we observe maximal current at a specific value of the slope  $\Delta F$  in the upper plot for small  $F_0$ . The maximum is shifted to the left with increasing  $F_0$ . Varying  $F_0$  at fixed  $\Delta F$  (lower plot) shows decreasing behavior of  $j_x$ . Parameters used are  $U/J = 4, \Delta/J = 1, \gamma/J = 0.2$ .

decay with bulk dissipation present:

$$F_l = F_0 + \Delta F(l - 1), \quad \gamma_l = \gamma, \quad (34)$$

where  $l$  denotes the site index in the  $x$  direction and no explicit  $y$  dependence is given, as before.

For the setup (34) we investigate the dependence of the currents on an overall laser field  $F_0$  and an “on top” gradient  $\Delta F$ . It turns out that the larger the offset field  $F_0$  the lower the overall current, Fig. 11(a). In Fig. 11(b) we observe a peak in the photon transport at  $F_0 = 0$  and a strongly suppressed transport for any other value of  $F_0$ . The effect can be understood by realizing that the off-set field corresponds to the phase imprinting with phase zero, i.e., we are pumping a mode that does not support any current. Effects of the gradient  $\Delta F$  are given in Fig. 11(b). At low  $\Delta F$ , the system compensates for the imbalance between neighboring sites via coherent transport of photons along the gradient and, as expected, the gradient enhances the current. However, at a certain value of the  $\Delta F$  the imbalance is so strong that the incoherent dynamics becomes the dominant process.

## V. CONCLUSIONS

Motivated by ongoing research interest in arrays of coupled photonic cavities, we have investigated different possibilities to optimize coherent transport in this setup. We have started from the noninteracting limit, where simple relations between the bond current and externally tunable parameters can be established. To address the role of interactions we have employed the Gutzwiller mean-field theory and a simpler Gross-Pitaevskii-like approach when possible.

In the case where bond currents are introduced by phase engineering of the external lasers, we have found that weak interactions shift the driving frequency that leads to a peak in the current toward higher values. On the other hand, in the strongly interacting regime of this setup, multiphotonic resonances of a single driven cavity lead to multiple peaks of

the current as a function of the driving frequency. The lattice filling is set by the strength of the applied driving field  $F$  and the dissipation rate  $\gamma_b$ , but interactions can modify the  $F^2$  proportionality into either a weaker  $F^{2/3}$  gain or an effectively stronger gain in the vicinity of multiphotonic resonances.

In the source-drain setup, local dissipation  $\gamma$  proves to be the tuning parameter that allows us to maximize the bond current. The optimal value of  $\gamma$  is set by the intrinsic hopping rate of the underlying Bose-Hubbard model. Further increase of  $\gamma$  leads to the quantum Zeno dynamics that suppresses uniform currents. The effects of the applied driving  $F$  turn out to be especially simple in the interacting case: the steady state is either stable at the specific value of  $F$  or its stationarity breaks down as stronger driving strength would be required to balance the dissipation.

The main approximation of our analysis is the employed mean-field approach together with the simplified form of the bond current, that limits to the regime of the strong bosonic coherences. The contribution of nontrivial correlations becomes important in the limit of very strong interactions and weak driving and this case should be treated in the future using beyond mean-field approximations [14,21,46,63,64]. However, we expect that the main effects we have identified at finite coherences will not be modified by the inclusion of higher-order terms. Another interesting research direction would be to connect our results with well-established results describing heat transport on the microscopic level [65].

## ACKNOWLEDGMENTS

The authors thank Daniel Cocks and Giuliano Orso for useful discussions. Support by the German Science Foundation Deutsche Forschungsgemeinschaft (DFG) via Sonderforschungsbereich Grant No. SFB/TR 49, Forschergruppe Grant No. FOR 801, and the high-performance computing center LOEWE-CSC is gratefully acknowledged. This work was supported in part by DAAD (German Academic and Exchange Service) under project BKMh. I.V. acknowledges support by



the Ministry of Education, Science, and Technological Development of the Republic of Serbia under Projects ON171017 and BKMH, and by the European Commission under H2020 Project VI-SEEM, Grant No. 675121. Numerical simulations were partly run on the PARADOX supercomputing facility at

the Scientific Computing Laboratory of the Institute of Physics Belgrade. M.J.H. acknowledges support by the DFG via Grant No. HA9953/3-1 and by the United Kingdom Engineering and Physical Sciences Research Council under Grant No. EP/N009428/1.

- 
- [1] I. Carusotto and C. Ciuti, *Rev. Mod. Phys.* **85**, 299 (2013).
- [2] Z. Wang, Y. Chong, J. D. Joannopoulos, and M. Soljacic, *Nature (London)* **461**, 772 (2009).
- [3] M. C. Rechtsman, J. M. Zeuner, Y. Plotnik, Y. Lumer, D. Podolsky, F. Dreisow, S. Nolte, M. Segev, and A. Szameit, *Nature (London)* **496**, 196 (2013).
- [4] M. Hafezi, S. Mittal, J. Fan, A. Migdall, and J. M. Taylor, *Nat. Photon.* **7**, 1001 (2013).
- [5] K. Le Hur, L. Henriot, A. Petrescu, K. Plekhanov, G. Roux, and M. Schiró, *arXiv:1505.00167*.
- [6] M. J. Hartmann, F. G. S. L. Brandão, and M. B. Plenio, *Nat. Phys.* **2**, 849 (2006).
- [7] A. A. Houck, H. E. Türeci, and J. Koch, *Nat. Phys.* **8**, 292 (2012).
- [8] C. Noh and D. G. Angelakis, *arXiv:1604.04433*.
- [9] M. J. Hartmann, *arXiv:1605.00383*.
- [10] M. Abbarchi, A. Amo, V. G. Sala, D. D. Solnyshkov, H. Flayac, L. Ferrier, I. Sagnes, E. Galopin, A. Lemaître, G. Malpuech, and J. Bloch, *Nat. Phys.* **9**, 275 (2013).
- [11] J. Raftery, D. Sadri, S. Schmidt, H. E. Türeci, and A. A. Houck, *Phys. Rev. X* **4**, 031043 (2014).
- [12] I. Carusotto, D. Gerace, H. E. Türeci, S. De Liberato, C. Ciuti, and A. Imamoglu, *Phys. Rev. Lett.* **103**, 033601 (2009).
- [13] A. Tomadin, V. Giovannetti, R. Fazio, D. Gerace, I. Carusotto, H. E. Türeci, and A. Imamoglu, *Phys. Rev. A* **81**, 061801 (2010).
- [14] M. J. Hartmann, *Phys. Rev. Lett.* **104**, 113601 (2010).
- [15] F. Nissen, S. Schmidt, M. Biondi, G. Blatter, H. E. Türeci, and J. Keeling, *Phys. Rev. Lett.* **108**, 233603 (2012).
- [16] J. Jin, D. Rossini, R. Fazio, M. Leib, and M. J. Hartmann, *Phys. Rev. Lett.* **110**, 163605 (2013).
- [17] A. Le Boité, G. Orso, and C. Ciuti, *Phys. Rev. Lett.* **110**, 233601 (2013).
- [18] A. Le Boité, G. Orso, and C. Ciuti, *Phys. Rev. A* **90**, 063821 (2014).
- [19] I. Pižorn, *Phys. Rev. A* **88**, 043635 (2013).
- [20] T. V. Lapyeva, A. A. Tikhomirov, O. I. Kanakov, and M. V. Ivanchenko, *Sci. Rep.* **5**, 13263 (2015).
- [21] A. Biella, L. Mazza, I. Carusotto, D. Rossini, and R. Fazio, *Phys. Rev. A* **91**, 053815 (2015).
- [22] U. Naether, F. Quijandría, J. J. García-Ripoll, and D. Zueco, *Phys. Rev. A* **91**, 033823 (2015).
- [23] I. Bloch, J. Dalibard, and W. Zwerger, *Rev. Mod. Phys.* **80**, 885 (2008).
- [24] J.-P. Brantut, J. Meineke, D. Stadler, S. Krinner, and T. Esslinger, *Science* **337**, 1069 (2012).
- [25] S. Krinner, D. Stadler, D. Husmann, J.-P. Brantut, and T. Esslinger, *Nature (London)* **517**, 64 (2015).
- [26] R. Labouvie, B. Santra, S. Heun, S. Wimberger, and H. Ott, *Phys. Rev. Lett.* **115**, 050601 (2015).
- [27] R. Labouvie, B. Santra, S. Heun, and H. Ott, *Phys. Rev. Lett.* **116**, 235302 (2016).
- [28] V. A. Brazhnyi, V. V. Konotop, V. M. Pérez-García, and H. Ott, *Phys. Rev. Lett.* **102**, 144101 (2009).
- [29] D. A. Zezyulin, V. V. Konotop, G. Barontini, and H. Ott, *Phys. Rev. Lett.* **109**, 020405 (2012).
- [30] M. Kreibich, J. Main, H. Cartarius, and G. Wunner, *Phys. Rev. A* **87**, 051601 (2013).
- [31] F. Single, H. Cartarius, G. Wunner, and J. Main, *Phys. Rev. A* **90**, 042123 (2014).
- [32] D. Haag, D. Dast, H. Cartarius, and G. Wunner, *Phys. Rev. A* **92**, 053627 (2015).
- [33] G. Benenti, G. Casati, T. Prosen, D. Rossini, and M. Žnidarič, *Phys. Rev. B* **80**, 035110 (2009).
- [34] T. Prosen and M. Žnidarič, *Phys. Rev. B* **86**, 125118 (2012).
- [35] J. J. Mendoza-Arenas, T. Grujic, D. Jaksch, and S. R. Clark, *Phys. Rev. B* **87**, 235130 (2013).
- [36] S. Philipp, P. Maurer, P. J. Leek, M. Baur, R. Bianchetti, J. M. Fink, M. Göppl, L. Steffen, J. M. Gambetta, A. Blais, and A. Wallraff, *Phys. Rev. Lett.* **102**, 200402 (2009).
- [37] I. Carusotto and C. Ciuti, *Phys. Rev. Lett.* **93**, 166401 (2004).
- [38] A. Janot, T. Hyart, P. R. Eastham, and B. Rosenow, *Phys. Rev. Lett.* **111**, 230403 (2013).
- [39] J. Ruiz-Rivas, E. del Valle, C. Gies, P. Gartner, and M. J. Hartmann, *Phys. Rev. A* **90**, 033808 (2014).
- [40] P.-E. Larré and I. Carusotto, *Phys. Rev. A* **91**, 053809 (2015).
- [41] T. Ozawa and I. Carusotto, *Phys. Rev. Lett.* **112**, 133902 (2014).
- [42] I. Vidanović, D. Cocks, and W. Hofstetter, *Phys. Rev. A* **89**, 053614 (2014).
- [43] G. Kordas, D. Witthaut, P. Buonsante, A. Vezzani, R. Burioni, A. I. Karanikas, and S. Wimberger, *EPJ ST* **224**, 2127 (2015).
- [44] P. D. Drummond and D. F. Walls, *J. Phys. A* **13**, 725 (1980).
- [45] M. Leib and M. J. Hartmann, *Phys. Rev. Lett.* **112**, 223603 (2014).
- [46] H. Weimer, *Phys. Rev. Lett.* **114**, 040402 (2015).
- [47] H. Spohn, *Lett. Math. Phys.* **2**, 33 (1977).
- [48] A. O. Caldeira and A. J. Leggett, *Ann. Phys.* **149**, 374 (1983).
- [49] J. I. Cirac, A. Schenzle, and P. Zoller, *Europhys. Lett.* **27**, 123 (1994).
- [50] B. Misra and E. C. G. Sudarshan, *J. Math. Phys.* **18**, 756 (1977).
- [51] W. M. Itano, D. J. Heinzen, J. J. Bollinger, and D. J. Wineland, *Phys. Rev. A* **41**, 2295 (1990).
- [52] N. Syassen, D. M. Bauer, M. Lettner, T. Volz, D. Dietze, J. J. García-Ripoll, J. I. Cirac, G. Rempe, and S. Dürr, *Science* **320**, 1329 (2008).
- [53] M. J. Mark, E. Haller, K. Lauber, J. G. Danzl, A. Janisch, H. P. Büchler, A. J. Daley, and H.-C. Nägerl, *Phys. Rev. Lett.* **108**, 215302 (2012).
- [54] G. Barontini, R. Labouvie, F. Stubenrauch, A. Vogler, V. Guarrera, and H. Ott, *Phys. Rev. Lett.* **110**, 035302 (2013).
- [55] B. Zhu, B. Gadway, M. Foss-Feig, J. Schachenmayer, M. L. Wall, K. R. A. Hazzard, B. Yan, S. A. Moses, J. P. Covey, D. S. Jin, J. Ye, M. Holland, and A. M. Rey, *Phys. Rev. Lett.* **112**, 070404 (2014).

- [56] Y. Khodorkovsky, G. Kurizki, and A. Vardi, *Phys. Rev. Lett.* **100**, 220403 (2008).
- [57] V. S. Shchesnovich and V. V. Konotop, *Phys. Rev. A* **81**, 053611 (2010).
- [58] V. S. Shchesnovich and D. S. Mogilevtsev, *Phys. Rev. A* **82**, 043621 (2010).
- [59] F. Trimborn, D. Witthaut, H. Hennig, G. Kordas, T. Geisel, and S. Wimberger, *Eur. Phys. J. D* **63**, 63 (2011).
- [60] P. Barmettler and C. Kollath, *Phys. Rev. A* **84**, 041606 (2011).
- [61] D. Poletti, J.-S. Bernier, A. Georges, and C. Kollath, *Phys. Rev. Lett.* **109**, 045302 (2012).
- [62] K. K. Rajagopal and S. Muniandy, *Physica A* **440**, 118 (2015).
- [63] U. Schollwöck, *Ann. Phys.* **326**, 96 (2011).
- [64] A. J. Daley, *Adv. Phys.* **63**, 77 (2014).
- [65] G. Benenti, G. Casati, T. Prosen, and K. Saito, [arXiv:1311.4430](https://arxiv.org/abs/1311.4430).

# Excitation spectra of a Bose-Einstein condensate with an angular spin-orbit coupling

Ivana Vasić and Antun Balaž

*Scientific Computing Laboratory, Center for the Study of Complex Systems, Institute of Physics Belgrade,  
University of Belgrade, Pregrevica 118, 11080 Belgrade, Serbia*

(Received 18 February 2016; published 21 September 2016)

A theoretical model of a Bose-Einstein condensate with angular spin-orbit coupling has recently been proposed and it has been established that a half-skyrmion represents the ground state in a certain regime of spin-orbit coupling and interaction. Here we investigate low-lying excitations of this phase by using the Bogoliubov method and numerical simulations of the time-dependent Gross-Pitaevskii equation. We find that a sudden shift of the trap bottom results in a complex two-dimensional motion of the system's center of mass that is markedly different from the response of a competing phase, and comprises two dominant frequencies. Moreover, the breathing mode frequency of the half-skyrmion is set by both the spin-orbit coupling and the interaction strength, while in the competing state it takes a universal value. Effects of interactions are especially pronounced at the transition between the two phases.

DOI: [10.1103/PhysRevA.94.033627](https://doi.org/10.1103/PhysRevA.94.033627)

## I. INTRODUCTION

Experimental realization of an effective spin-orbit coupling in ultracold atom systems [1–6] has allowed for new quantum phases to be explored. Bosonic systems with spin-orbit coupling are interesting as they have no direct analogs in condensed-matter systems and provide a new research playground. Different types of coupling based on atom-light interactions have been considered, e.g., Raman induced (as realized in the current experiments) and Rashba type [7]. Only recently bosonic systems with two-dimensional spin-orbit coupling have become experimentally available [8]. Ground-state phase diagrams that comprise a plane-wave, stripe, and nonmagnetic condensed phase have been predicted and probed [9–13]. Another type of condensate, a half-quantum vortex, is expected for harmonically trapped bosons with Rashba coupling [14–16]. A substantial progress in the field has been summarized in Refs. [7,17]. As a further extension of these ideas, in the very recent papers [18–23], a theoretical model of bosons with the coupling of spin and angular momentum has been introduced. From the experimental side, the proposal involves two copropagating Laguerre-Gauss laser beams that carry angular momentum and couple two internal states of bosonic atoms.

Since the first experimental realization of Bose-Einstein condensation, collective modes have been used to probe the macroscopic quantum state and to relate measurements to theoretical predictions [24]. Collective modes can reveal important information about system properties, such as role of interactions or quantum fluctuations. Experimentally, breathing mode and dipole mode excitations introduced through a quench of the harmonic trap are routinely accessible with great precision, thus providing an indispensable tool for probing the properties of a Bose-Einstein condensate. Along these lines, collective modes of bosons with the Raman-induced spin-orbit coupling have already been measured [3,4,20,25]. In the literature, several theoretical calculations of collective modes for different types of spin-orbit coupling are available [16,26–36]. In contrast to usual, harmonically trapped systems, spin-orbit coupled systems exhibit the absence of the Galilean invariance and, as a consequence, the Kohn theorem no longer

applies [7]. Another hallmark of these systems is that the motion in real space is coupled with spin dynamics.

In this paper we investigate collective modes of bosons with angular spin-orbit coupling that have not been addressed so far, and show that the two competing ground states can be directly distinguished according to their response to standard quenches of the underlying harmonic trap. The paper is organized as follows. In Sec. II we introduce the basic model and discuss its excitations in the noninteracting limit. In Sec. III we briefly describe methods that we use and summarize the ground-state phase diagram in the limit of weak interactions [18]. Finally, in Sec. IV we address breathing-mode and dipole mode excitations of the two relevant phases and in Sec. V we present our concluding remarks.

## II. NONINTERACTING MODEL

In recent Refs. [18–21] the following Hamiltonian for a two-component bosonic system has been introduced:

$$H_0 = \left( \frac{p^2}{2} + \frac{r^2}{2} \right) \mathcal{I}_2 + \frac{\Omega^2 r^2}{2} \begin{pmatrix} 1 & e^{-2i\phi} \\ e^{2i\phi} & 1 \end{pmatrix}, \quad (1)$$

where  $\mathcal{I}_2$  is a  $2 \times 2$  identity matrix and the effective spin 1/2 comes from the two bosonic components involved. The system is assumed to be effectively two dimensional (tightly trapped in the longitudinal direction) and the value of  $\Omega$  is proportional to the intensity of the applied Laguerre-Gauss laser beam. The last,  $\phi$ -dependent term, where  $\phi$  is the polar angle, provides the coupling between the spin and angular momentum, as can be explicated by using a proper unitary transformation [19]. We have assumed that the two lasers carry a unit of angular momentum in the opposite rotational directions. In Eq. (1) and in the following we use harmonic oscillator scales of the kinetic energy and the trap  $p^2/2m + m\omega^2 r^2/2$  as our units: the energy is expressed in terms of  $\hbar\omega$ , the unit length is the harmonic oscillator length scale  $\sqrt{\hbar/m\omega}$ , where  $m$  is the atomic mass, the unit momentum is  $\sqrt{\hbar m\omega}$ , and the time scale is given by  $\omega^{-1}$ . The frequency  $\Omega$  and all excitation frequencies are expressed in units of the harmonic oscillator frequency  $\omega$ .

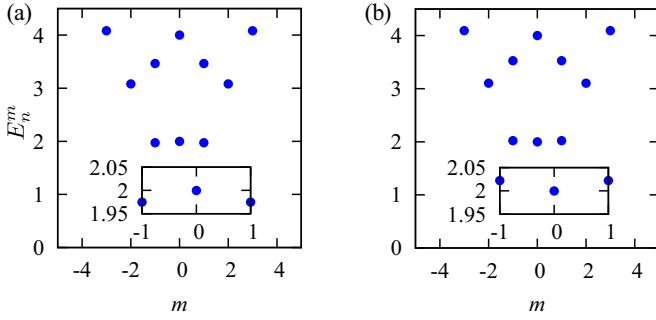


FIG. 1. Spectrum  $E_n^m$  of Hamiltonian (1) for (a)  $\Omega = 3.2$  and (b)  $\Omega = 3.5$ .

From the commutation relation  $[J_z, \mathcal{H}_0] = 0$ , where  $J_z = L_z \otimes \mathcal{I} + \mathcal{I} \otimes \sigma_z$  is the  $z$  component of the total angular momentum, it follows that the noninteracting eigenstates can be written in the form

$$\phi_m(r, \phi) = \frac{e^{im\phi}}{\sqrt{2\pi}} \begin{pmatrix} f_m(r)e^{-i\phi} \\ g_m(r)e^{i\phi} \end{pmatrix}, \quad (2)$$

where  $m$  as an eigenvalue of  $J_z$  takes integer values and  $r$  is the radial coordinate. By numerical calculation [18] it has been shown that the ground state moves from the  $m = 1$  into the  $m = 0$  subspace at  $\Omega_c \approx 3.35$ . The  $m = 1$  ground state exhibits a nontrivial spin texture that can be characterized by a topological number (a winding number of the spin vector). This state is called half-skyrmion and is degenerate, i.e., it has the same energy as the ground state in the  $m = -1$  subspace. The  $m = 0$  states comprises two vortices of opposite circulation.

We investigate excitations above the half-skyrmion and  $m = 0$  ground state, first at a single-particle level. The spectrum of the Hamiltonian (1) is shown in Fig. 1(a) for  $\Omega = 3.2$  and in Fig. 1(b) for  $\Omega = 3.5$ . In the first case, for  $\Omega = 3.2 < \Omega_c$  the ground state  $m = 1$  is doubly degenerate and the lowest  $m = 0$  state is close in energy,  $E_0^{m=0} - E_0^{m=1} \approx 2.5 \times 10^{-2}$ . For  $\Omega = 3.5 > \Omega_c$  the ground state corresponds to  $m = 0$ . In the following we will probe some features of these spectra by applying two experimentally relevant types of perturbations to a selected ground state.

To induce a breathing mode, we perturb the trap strength

$$H_{\text{pert}} = H_0 + \eta \frac{r^2}{2} \mathcal{I}_2. \quad (3)$$

From the time-dependent Schrödinger equation,

$$i \frac{\partial}{\partial t} \begin{pmatrix} \psi_1(t) \\ \psi_2(t) \end{pmatrix} = H_{\text{pert}} \begin{pmatrix} \psi_1(t) \\ \psi_2(t) \end{pmatrix}, \quad (4)$$

we calculate the time evolution of the width of the probability distribution,

$$\langle r^2(t) \rangle = \int_0^{2\pi} d\phi \int_0^\infty dr r^3 [|\psi_1(t)|^2 + |\psi_2(t)|^2], \quad (5)$$

as well as the spin dynamics captured by

$$\langle S_z(t) \rangle = \frac{1}{2} \int_0^{2\pi} d\phi \int_0^\infty dr r [|\psi_1(t)|^2 - |\psi_2(t)|^2]. \quad (6)$$

When changing the trap strength  $\eta$  in the Hamiltonian (3), we couple only states with the same value of  $m$ . In the limit

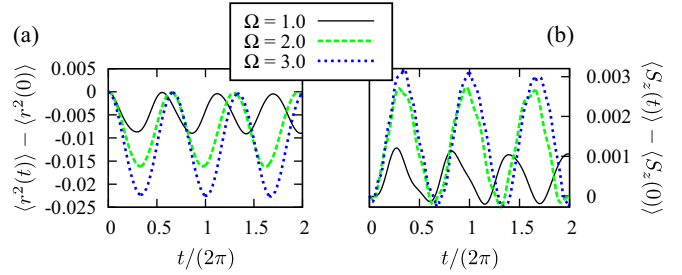


FIG. 2. Breathing mode oscillations of half-skyrmion state, evidenced by (a)  $\langle r^2(t) \rangle - \langle r^2(0) \rangle$  and (b)  $\langle S_z(t) \rangle - \langle S_z(0) \rangle$ . Motion is induced by changing harmonic trap potential as  $\frac{r^2}{2} \rightarrow 1.01 \frac{r^2}{2}$ .

of vanishing  $\Omega$ , the breathing mode frequency is  $\omega_B = 2$ . By increasing  $\Omega$ , while staying in a half-skyrmion state, we find that the breathing mode frequency decreases down to  $\omega_B \approx 1.5$  at the transition point, Fig. 2(a). Oscillations in the system size are accompanied by an oscillatory spin dynamics, as shown in Fig. 2(b).

In the  $m = 0$  subspace, by subtracting and summing the two coupled eigenequations, we find that the eigenproblem reduces to two independent harmonic oscillators,

$$\begin{aligned} \left( \mathcal{L} + \frac{(1 + 2\Omega^2)r^2}{2} \right) (f_0(r) + g_0(r)) &= E^{m=0} (f_0(r) + g_0(r)), \\ \left( \mathcal{L} + \frac{r^2}{2} \right) (f_0(r) - g_0(r)) &= E^{m=0} (f_0(r) - g_0(r)), \end{aligned}$$

with frequencies 1 and  $\sqrt{1 + 2\Omega^2}$ , and the azimuthal quantum number 1 in both cases as  $\mathcal{L} = -\frac{1}{2r} \frac{\partial}{\partial r} (r \frac{\partial}{\partial r}) + \frac{1}{2r^2}$ . Hence the  $m = 0$  energy levels are linear combinations of  $E_n^{m=0} = 2n$  and  $E_n^{m=0} = 2\sqrt{1 + 2\Omega^2}n$ ,  $n = 1, 2, \dots$ . In the region of interest, where  $\Omega$  is strong enough, the ground-state energy is exactly  $E_0^{m=0} = 2$  with a wave function

$$\phi_0 = \frac{1}{\sqrt{2\pi}} \begin{pmatrix} f_0(r)e^{-i\phi} \\ -f_0(r)e^{i\phi} \end{pmatrix}, \quad (7)$$

which is independent of  $\Omega$ . From this analysis it follows that the breathing mode frequency is  $\omega_B = 2$ , which is a well-known result for harmonically trapped bosons in two dimensions at the classical level [37]. Moreover, it is easy to show that the time evolution according to the perturbed Hamiltonian (3) is given by  $\phi_0(\mathbf{r}, t) = \begin{pmatrix} f_0(r, t)e^{-i\phi} \\ -f_0(r, t)e^{i\phi} \end{pmatrix}$ , leading to  $\langle S_z(t) \rangle = 0$ . Therefore, in this case oscillations in the system size are not followed by oscillations in  $\langle S_z(t) \rangle$ .

To excite a dipole mode, we consider a shift of the trap bottom in  $x$  direction,

$$H_{\text{pert}} = H_0 - \delta x \frac{r}{2} (e^{i\phi} + e^{-i\phi}) \mathcal{I}_2, \quad (8)$$

and monitor the motion of the center of mass of the system in that direction,

$$\langle x(t) \rangle = \int_0^{2\pi} d\phi \frac{(e^{i\phi} + e^{-i\phi})}{2} \int_0^\infty dr r^2 [|\psi_1(t)|^2 + |\psi_2(t)|^2], \quad (9)$$

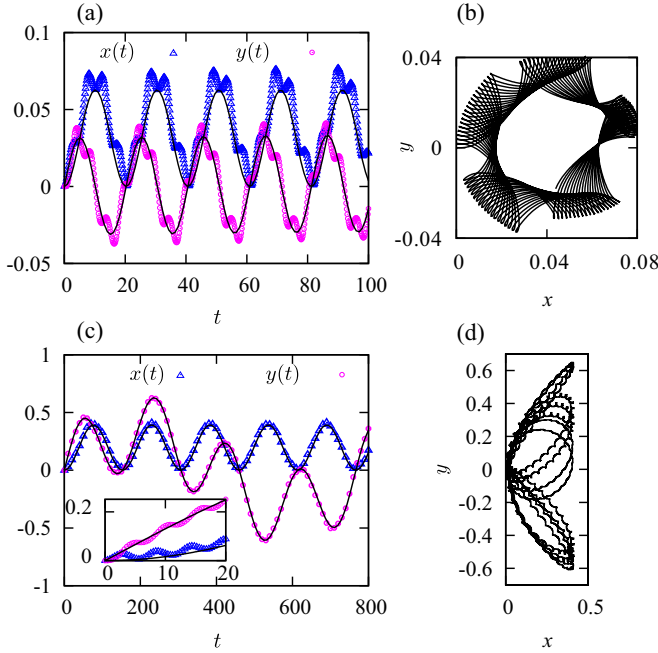


FIG. 3. Dipole mode oscillations of half-skyrmion state for  $\delta x = 0.02$  at (a),(b)  $\Omega = 2$  and (c),(d)  $\Omega = 3.2$ .

as well as  $\langle y(t) \rangle$ . In Fig. 3(a) for  $\Omega = 2$  we see that oscillations in  $x$  and  $y$  directions are coupled and that there are several frequencies involved. In Fig. 3(c) we observe that for  $\Omega = 3.2$  even a weak shift of  $\delta x = 0.02$  leads to very strong, slow oscillations in  $x$  and  $y$  directions. On top of this, we also find fast oscillations, as shown in the inset of the same figure. In Figs. 3(b) and 3(d) we show the resulting complex motion of the center of mass of the system, given by  $y(t)$  vs  $x(t)$ . These are all very distinct features not present in the conventional harmonically trapped system, where the same perturbation excites the Kohn mode—an oscillation with the trap frequency along  $x$  axis. In the following we discuss the origin of the complex dynamics.

First we note that the perturbation introduced in the Hamiltonian (8) couples the initial  $m = 1$  ground state with excited states corresponding to other eigenvalues of  $J_z$ , e.g.,  $\int_0^\infty dr r \int_0^{2\pi} d\phi \phi_1^*(r) H_{\text{pert}} \phi_0(r) \neq 0$ . In general, this effect may lead to the time-dependent expectation value  $\langle \psi(t) | J_z | \psi(t) \rangle = \langle J_z(t) \rangle$ . From the Heisenberg equations of motion  $i \frac{dJ_z(t)}{dt} = [J_z, H_{\text{pert}}]$  and from the commutation relation  $[J_z, x \otimes \mathcal{I}_2] = iy \otimes \mathcal{I}_2$ , we directly obtain that oscillating  $\langle J_z(t) \rangle$  implies a motion in  $y$  direction

$$\langle y(t) \otimes \mathcal{I}_2 \rangle = -\frac{1}{\delta x} \frac{d\langle J_z(t) \rangle}{dt}. \quad (10)$$

Now we discuss the emerging oscillation frequencies. In first order of perturbation theory, we would expect the dominant coupling of  $m = 1$  with  $m = 0$  and  $m = 2$  eigenstates, providing the two frequencies:

$$\omega_D^L = E_0^{m=0} - E_0^{m=1}, \quad \omega_D^H = E_0^{m=2} - E_0^{m=1}. \quad (11)$$

However, due to the degeneracy of the states  $m = -1$  and  $m = 1$ , the  $m = -1$  state has to be taken into account as well. The lowest frequencies can be described by using the perturbation

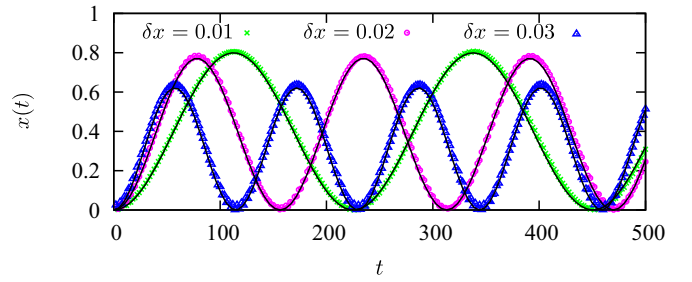


FIG. 4. Dipole mode oscillations for  $\Omega = 3.5$ , starting from  $m = 0$  ground state with different trap displacements  $\delta x$ . Black solid lines are results of the analytical calculation.

theory for degenerate states presented in Appendix A. Within this approach we find that the excitation frequencies are

$$\omega_1 = \sqrt{\omega_D^L{}^2 + 2(\delta x I_{10})^2}, \quad (12)$$

$$\omega_{2,3} = \left| \frac{\omega_D^L}{2} \pm \frac{1}{2} \sqrt{\omega_D^L{}^2 + 2(\delta x I_{10})^2} \right|, \quad (13)$$

together with  $\omega_D^H$ . Obviously, the excited frequencies are amplitude-dependent, and when  $\omega_D^L$  is low, i.e., close to the transition point, the contribution of the term proportional to the trap displacement  $\delta x$  is significant. This is another difference with respect to a standard harmonically trapped system. It arises due to the fact that by shifting the trap bottom, while keeping the term proportional to  $\Omega^2$  unchanged in the model (1), we lower the symmetry of the model and modify its energy levels. In the regime  $\omega_D^L \rightarrow 0$  it turns out that  $\omega_1$  corresponds to oscillations in  $x$  direction, while both  $\omega_2$  and  $\omega_3$  represent the motion in  $y$  direction. Results of the analytical calculation, Eqs. (A8) and (A7) from Appendix A, are given by the black solid lines in Figs. 3(a) and 3(c) and capture the low-lying frequencies or long-time dynamics quite well.

The response of a vortex–antivortex pair to the sudden shift of the trap is shown in Fig. 4. In this case, the perturbation couples the initial  $m = 0$  state symmetrically to excited states  $\pm m$ . Thus  $\langle J_z(t) \rangle = 0$  and the center of mass only oscillates in  $x$  direction. The two involved frequencies are

$$\omega_1 = \sqrt{\omega_D^L{}^2 + 2(\delta x I_{10})^2}, \quad \omega_D^H = E_1^{m=1} - E_0^{m=0}. \quad (14)$$

For  $\Omega = 3.5$ , we have  $\omega_D^L \approx 2.2 \times 10^{-2}$  and the increase of the excited frequency with the shift  $\delta x$  is clearly observable in the long-time dynamics; see Fig. 4.

Results of this section are summarized in Fig. 5, where we see that at the transition point,  $\Omega \approx 3.35$ ,  $\omega_D^L$  becomes gapless;  $\omega_B$  of the  $m = 1$  state decreases from  $\omega_B = 2$  down to  $\omega_B \approx 1.5$  and turns into  $\omega_D^H$  of  $m = 0$  state. On the other hand,  $\omega_B = 2$  on top of the  $m = 0$  ground state is unaffected by  $\Omega$ . We also keep in mind that, due to the degeneracy of the half-skyrmion, below the transition point we have a gapless quadrupole mode  $\omega_Q = E_0^{m=-1} - E_0^{m=1} = 0$  that indirectly affects dipole mode oscillations. For completeness, we note that the frequency  $\omega_D^H$  of the half-skyrmion turns into a quadrupole mode of  $m = 0$  state, but this excitation does not play an important role in the remaining discussion.

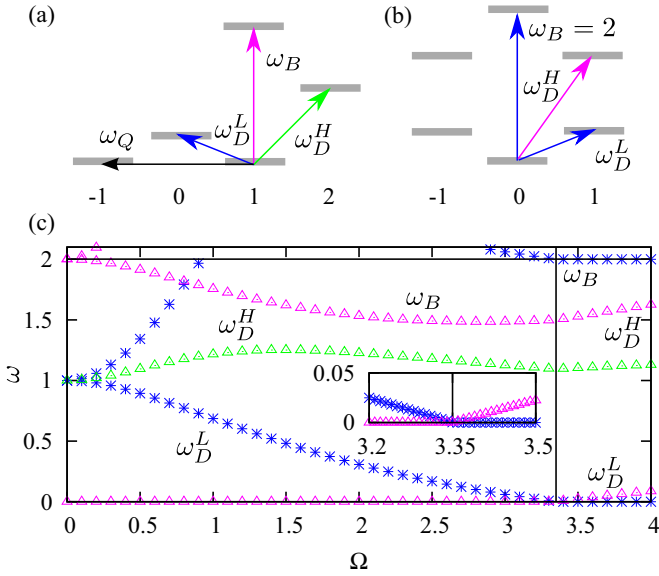


FIG. 5. Breathing-mode and dipole mode excitations at  $g = 0$  of (a)  $m = 1$  and (b)  $m = 0$  ground state. (c) Energy of excited states as a function of  $\Omega$ .

### III. WEAK INTERACTIONS

Now we consider weak spin-symmetric interactions, which are approximated by a contact potential [7,18,19]. The total Hamiltonian takes the form

$$\mathcal{H} = \int d\mathbf{r} \left[ \Psi^\dagger(\mathbf{r}) H_0 \Psi(\mathbf{r}) + \frac{g}{2} \sum_{a,b=1}^2 \Psi_a^\dagger(\mathbf{r}) \Psi_b^\dagger(\mathbf{r}) \Psi_b(\mathbf{r}) \Psi_a(\mathbf{r}) \right], \quad (15)$$

where  $\Psi(\mathbf{r})$  is a two-component spinor. Without interactions, the ground state of many bosons is degenerate for  $\Omega < \Omega_c$  as there are different possibilities to accommodate atoms into the two lowest degenerate noninteracting states. In general, the degeneracy of noninteracting eigenstates makes the occurrence of Bose-Einstein condensation more subtle [9,38]. In the case that we consider, it turns out that weak interactions promote condensation [7], as it is energetically favorable for the particles to condense into the same single-particle state in either the  $m = 1$  or the  $m = -1$  subspace [18,19]. As the many-body ground state is twofold degenerate, in the following we will consider a condensate formed in the  $m = 1$  subspace. For  $\Omega > \Omega_c$  and weak  $g$  there is a condensation into the  $m = 0$  state.

The total energy per particle of the condensed state with the order parameter  $[\psi_1(\mathbf{r}) \psi_2(\mathbf{r})]^T$  is given by

$$E_0 = \int d\mathbf{r} \left[ (\psi_1^* \psi_2^*) H_0 (\psi_1 \psi_2)^T + \frac{1}{2} g |\psi_1|^4 + \frac{1}{2} g |\psi_2|^4 + g |\psi_1|^2 |\psi_2|^2 \right]. \quad (16)$$

In order to find the ground state, we perform minimization of this functional with respect to  $\psi_1(\mathbf{r})$  and  $\psi_2(\mathbf{r})$ . As usual, we introduce a chemical potential  $\mu$  to enforce a normalization condition  $\int d\mathbf{r} [|\psi_1(\mathbf{r})|^2 + |\psi_2(\mathbf{r})|^2] = 1$ . In the ground state,

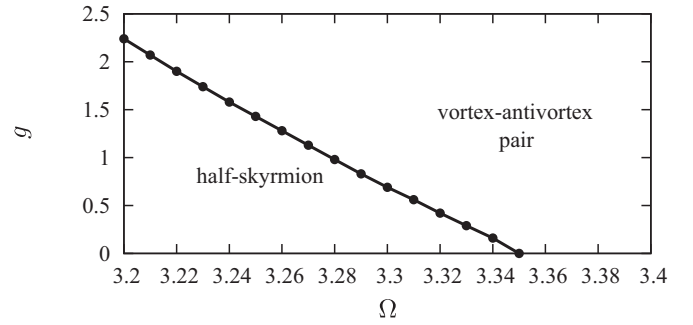


FIG. 6. Transition line between half-skyrmion and  $m = 0$  condensate, which was originally calculated in Ref. [18].

we have

$$\mu \psi_1^0 = \left[ \frac{p^2}{2} + \frac{r^2}{2} (1 + \Omega^2) + g (|\psi_1^0|^2 + |\psi_2^0|^2) \right] \psi_1^0 + \frac{r^2}{2} \Omega^2 e^{-2i\phi} \psi_2^0, \quad (17)$$

$$\mu \psi_2^0 = \left[ \frac{p^2}{2} + \frac{r^2}{2} (1 + \Omega^2) + g (|\psi_1^0|^2 + |\psi_2^0|^2) \right] \psi_2^0 + \frac{r^2}{2} \Omega^2 e^{2i\phi} \psi_1^0, \quad (18)$$

where the chemical potential  $\mu$  is given by  $\mu = \int d\mathbf{r} [(\psi_1^{0*} \psi_2^{0*}) H_0 (\psi_1^0 \psi_2^0)^T + g (|\psi_1^0|^2 + |\psi_2^0|^2)^2]$ . By comparing the ground-state energies of the condensed state in the two subspaces  $m = 0$  and  $m = 1$ , it has been established that even at  $\Omega < \Omega_c$  there is a transition into an  $m = 0$  condensate with increasing  $g$ , as shown in Fig. 6, which was originally calculated in Ref. [18].

In order to learn about low-energy excitations of the condensed phase, we use the Bogoliubov approach. It can be performed on the operator level, or starting from the time-dependent Gross-Pitaevskii equation for  $\psi_1(\mathbf{r}, t)$  and  $\psi_2(\mathbf{r}, t)$  [24]:

$$i \frac{\partial \psi_1}{\partial t} = \left[ \frac{p^2}{2} + \frac{r^2}{2} (1 + \Omega^2) \right] \psi_1 + \frac{1}{2} \Omega^2 r^2 e^{-2i\phi} \psi_2 + g |\psi_1|^2 \psi_1 + g |\psi_2|^2 \psi_1, \quad (19)$$

$$i \frac{\partial \psi_2}{\partial t} = \left[ \frac{p^2}{2} + \frac{r^2}{2} (1 + \Omega^2) \right] \psi_2 + \frac{1}{2} \Omega^2 r^2 e^{2i\phi} \psi_1 + g |\psi_2|^2 \psi_2 + g |\psi_1|^2 \psi_2. \quad (20)$$

In the following, we use the second approach.

Our first assumption is that the fluctuations  $\delta\psi_1(\mathbf{r}, t)$  and  $\delta\psi_2(\mathbf{r}, t)$  around the ground state,

$$\psi_1(\mathbf{r}, t) \approx [\psi_1^0(\mathbf{r}) + \delta\psi_1(\mathbf{r}, t)] \exp(-i\mu t), \quad (21)$$

$$\psi_2(\mathbf{r}, t) \approx [\psi_2^0(\mathbf{r}) + \delta\psi_2(\mathbf{r}, t)] \exp(-i\mu t), \quad (22)$$

are weak. At the zeroth order in the fluctuations, from Eqs. (19) and (20) we recover Eqs. (17) and (18). By keeping terms of the first order, we derive a set of linear equations that describe the

low-lying excitations of our system. To decouple the equations further, we proceed in a standard way and introduce

$$\delta\psi_1(\mathbf{r},t) = u_1(\mathbf{r})\exp(-i\omega t) + v_1^*(\mathbf{r})\exp(i\omega t), \quad (23)$$

$$\delta\psi_2(\mathbf{r},t) = u_2(\mathbf{r})\exp(-i\omega t) + v_2^*(\mathbf{r})\exp(i\omega t), \quad (24)$$

to obtain the generalized eigenproblem

$$\begin{aligned} \omega u_1 = & \left( \frac{p^2}{2} + \frac{r^2}{2}(1 + \Omega^2) + 2g|\psi_1^0|^2 + g|\psi_2^0|^2 - \mu \right) u_1 \\ & + \frac{r^2}{2}\Omega^2 e^{-2i\phi} u_2 + g(\psi_1^0)^2 v_1 \\ & + g\psi_1^0\psi_2^{0*} u_2 + g\psi_1^0\psi_2^0 v_2, \end{aligned} \quad (25)$$

$$\begin{aligned} -\omega v_1 = & \left( \frac{p^2}{2} + \frac{r^2}{2}(1 + \Omega^2) + 2g|\psi_1^0|^2 + g|\psi_2^0|^2 - \mu \right) v_1 \\ & + \frac{r^2}{2}\Omega^2 e^{2i\phi} v_2 + g(\psi_1^{0*})^2 u_1 \\ & + g\psi_1^{0*}\psi_2^0 v_2 + g\psi_1^{0*}\psi_2^{0*} u_2, \end{aligned} \quad (26)$$

$$\begin{aligned} \omega u_2 = & \left( \frac{p^2}{2} + \frac{r^2}{2}(1 + \Omega^2) + g|\psi_1^0|^2 + 2g|\psi_2^0|^2 - \mu \right) u_2 \\ & + \frac{r^2}{2}\Omega^2 e^{2i\phi} u_1 + g(\psi_2^0)^2 v_2 \\ & + g\psi_1^0\psi_2^0 v_1 + g\psi_1^{0*}\psi_2^0 u_1, \end{aligned} \quad (27)$$

$$\begin{aligned} -\omega v_2 = & \left( \frac{p^2}{2} + \frac{r^2}{2}(1 + \Omega^2) + g|\psi_1^0|^2 + 2g|\psi_2^0|^2 - \mu \right) v_2 \\ & + \frac{r^2}{2}\Omega^2 e^{-2i\phi} v_1 + g\psi_1^{0*}\psi_2^{0*} u_1 \\ & + g\psi_2^{0*}\psi_1^0 v_1 + g(\psi_2^{0*})^2 u_2. \end{aligned} \quad (28)$$

In general, the resulting eigenvalues form pairs  $-\omega_n, \omega_n$  and only positive frequencies correspond to physical excitations of the system.

To complement the Bogoliubov method, we numerically solve Eqs. (19) and (20) for different types of perturbations (3) and (8). For this purpose, the existing numerical codes for the two-dimensional time-dependent Gross-Pitaevskii equations [39–44] have been modified to include the spin-angular momentum coupling from Eq. (1).

#### IV. RESULTS

In this section we present and discuss excitation spectra and dynamical responses to perturbations (3) and (8) of the half-skyrmion and the  $m = 0$  condensate.

##### A. Half-skyrmion state

We first consider the case of  $\Omega < \Omega_c$  and weak interaction  $g$ , where all bosons condense into  $m = 1$  state. By inspecting Eqs. (25)–(28) for the  $\phi$ -dependent terms, where we take into account a nontrivial  $\phi$  dependence of the order parameters  $\psi_1(\mathbf{r})$  and  $\psi_2(\mathbf{r})$ , we can infer that the solution can be cast in

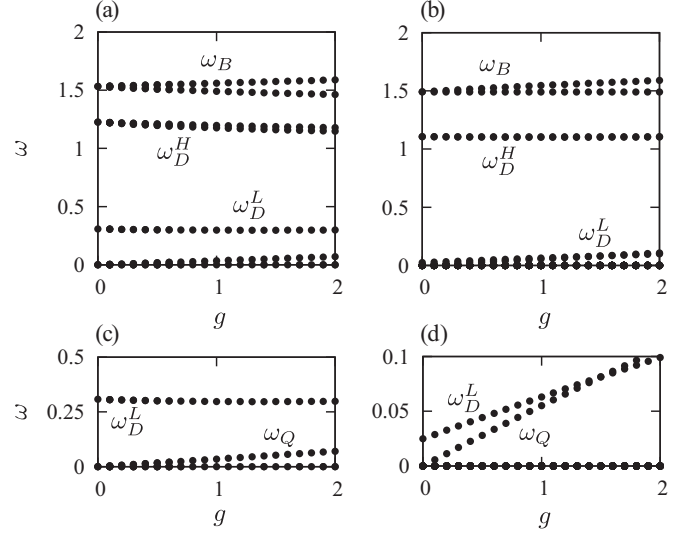


FIG. 7. Excitation spectra of half-skyrmion state for (a),(c)  $\Omega = 2$  and (b),(d)  $\Omega = 3.2$ . Results obtained by the Bogoliubov approach.

the form

$$\begin{pmatrix} u_1(\mathbf{r}) \\ v_1(\mathbf{r}) \\ u_2(\mathbf{r}) \\ v_2(\mathbf{r}) \end{pmatrix} = \sum_m \begin{pmatrix} u_1^{m-1}(r)r^{|m-1|} \exp[i(m-1)\phi] \\ v_1^{m-1}(r)r^{|m-1|} \exp[i(m-1)\phi] \\ u_2^{m+1}(r)r^{|m+1|} \exp[i(m+1)\phi] \\ v_2^{m-3}(r)r^{|m-3|} \exp[i(m-3)\phi] \end{pmatrix}. \quad (29)$$

The explicit form of the matrices, that are diagonalized, are given in Appendix B. The obtained spectrum shares many features with the noninteracting spectrum presented in Fig. 1(b), but it also exhibits important differences.

Excitation frequencies as a function of the interaction strength  $g$  are plotted in Fig. 7(a) for  $\Omega = 2$  and in Fig. 7(b) for  $\Omega = 3.2$ . The lowest excitation that does not change the relevant quantum number of the ground state is the breathing mode and its frequency increases for several percent with  $g$ . This is also confirmed by solving Eqs. (19) and (20) in order to obtain  $\langle r^2(t) \rangle$ , as shown in Fig. 8(a), and then inspecting corresponding Fourier transforms, Fig. 8(b).

The most obvious difference with respect to the noninteracting spectrum is that the quadrupole mode is now gapped: at finite interaction  $g$  it costs some energy to move a particle from the half-skyrmion  $m = 1$  condensate into the  $m = -1$

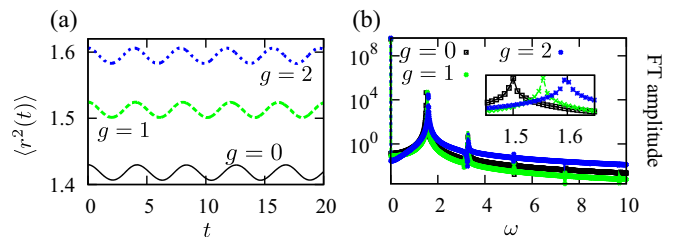


FIG. 8. Breathing mode oscillations in half-skyrmion phase: (a)  $\langle r^2(t) \rangle$  vs  $t$  and (b) corresponding Fourier transform. From the inset we observe increase of the breathing mode frequency with  $g$ . Motion is induced by changing harmonic trap potential as  $\frac{r^2}{2} \rightarrow 1.01 \frac{r^2}{2}$ ,  $\Omega = 3.2$ .

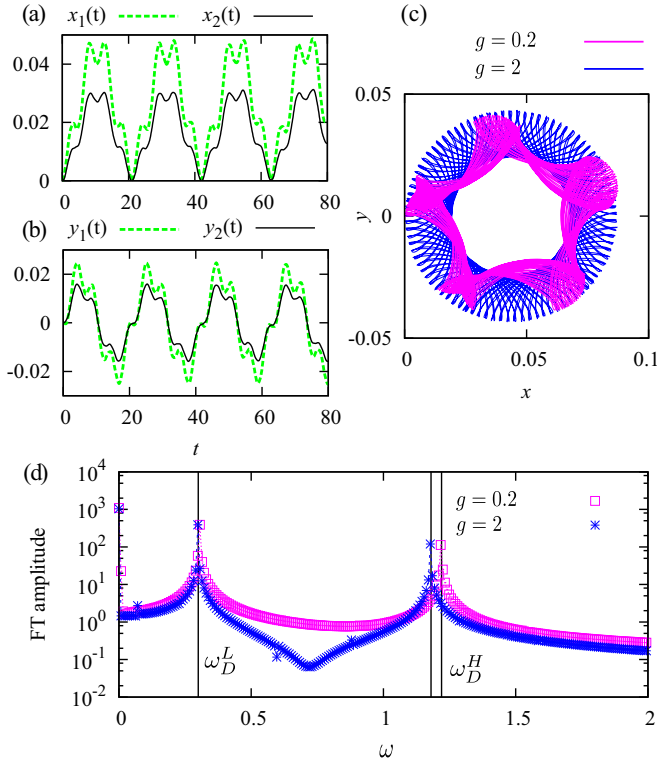


FIG. 9. Dipole mode oscillations of half-skyrmion state in interacting case for  $\Omega = 2$ . Motion is induced by shifting harmonic trap bottom for  $\delta x = 0.02$ . In (a) and (b)  $g = 1$ . In (c) motion of the center of mass,  $y(t)$  vs  $x(t)$ , is plotted. In (d) vertical lines give results for  $\omega_D^L$  and  $\omega_D^H$  obtained using the Bogoliubov method, and dots represent Fourier transform of  $x(t)$ .

state; see Fig. 7(c) and Fig. 7(d). This is directly reflected onto the dipole mode oscillations that take place in the  $xy$ -plane for the half-skyrmion state. For  $\Omega = 2$  both  $\omega_D^L$  and  $\omega_D^H$  are only weakly affected by  $g$ ; however, the fact that the quadrupole mode is gapped means that now a simpler perturbation theory applies. In the first order of this theory in  $\delta x$  the center-of-mass motion is given by

$$\langle x(t) \rangle \approx \frac{\delta x}{2} \left( \frac{I_{10}^2}{\omega_D^L} \cos \omega_D^L t + \frac{I_{12}^2}{\omega_D^H} \cos \omega_D^H t \right) + \text{const}, \quad (30)$$

$$\langle y(t) \rangle \approx \frac{\delta x}{2} \left( \frac{I_{10}^2}{\omega_D^L} \sin \omega_D^L t + \frac{I_{12}^2}{\omega_D^H} \sin \omega_D^H t \right), \quad (31)$$

where the values of  $I_{10}$  and  $I_{12}$  can be roughly approximated by using the noninteracting eigenstates from Eq. (2) as  $I_{10} = \int_0^\infty dr r^2 f_0^*(r)[f_1(r) - g_1(r)]$  and  $I_{12} = \int_0^\infty dr r^2 [f_1^*(r)f_2(r) + g_1^*(r)g_2(r)]$ . In Fig. 9(c) we see how the pattern in the  $xy$  plane becomes regular and symmetric as  $g$  is changed from  $g = 0.2$  to  $g = 2$ . The two bosonic components oscillate in phase in both directions; see Figs. 9(a) and 9(b). Results of the Bogoliubov approach, which are captured by Eqs. (25)–(28), match quite well to the numerical data obtained from direct numerical simulations of Eqs. (19) and (20); see Fig. 9(d).

Effects of interactions are more prominent close to  $\Omega_c$ . In this case the frequency  $\omega_D^L$  exhibits a strong increase with  $g$ ,

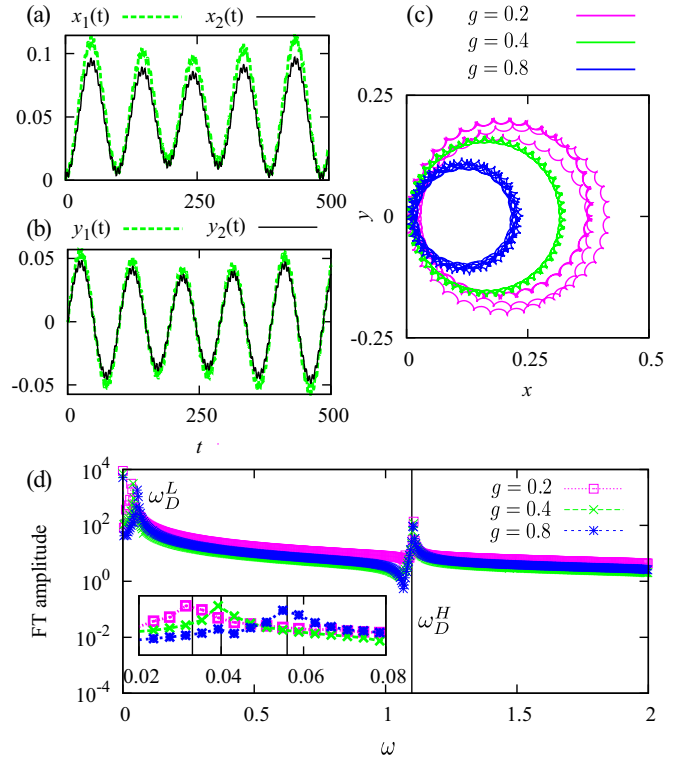


FIG. 10. Dipole mode oscillations of half-skyrmion state in interacting case for  $\Omega = 3.2$ . Motion is induced by shifting the harmonic trap bottom for  $\delta x = 0.01$ . In (a) and (b)  $g = 1$ . In (c) motion of the center of mass,  $y(t)$  vs  $x(t)$ , is plotted. The trajectory radius gets smaller with increasing  $g$ . In (d) vertical lines give results for  $\omega_D^L$  (in the inset) and  $\omega_D^H$  (in the main panel) obtained using the Bogoliubov method, and dots represent Fourier transform of  $x(t)$ .

as is depicted in Fig. 7(d). In Figs. 10(a) and 10(b) we see that the oscillations are still as strong as for  $g = 0$ , but the pattern is regular; compare Fig. 10(c) with Fig. 3(d). As the frequency  $\omega_D^L$  gets larger, the induced oscillation amplitude gets weaker and the induced frequency is less affected by the shift of the trap  $\delta x$ . In this case, the frequency  $\omega_D^H$  is found to be almost independent of  $g$ ; see Figs. 7(b) and 10(d).

## B. Vortex-antivortex pair

In a similar way we proceed in the case of  $\Omega > \Omega_c$ , where the bosons condense in the  $m = 0$  state. The solution of Eqs. (25)–(28) can now be cast in the form

$$\begin{pmatrix} u_1(\mathbf{r}) \\ v_1(\mathbf{r}) \\ u_2(\mathbf{r}) \\ v_2(\mathbf{r}) \end{pmatrix} = \sum_m \begin{pmatrix} u_1^{m-1}(r)r^{|m-1|} \exp[i(m-1)\phi] \\ v_1^{m+1}(r)r^{|m+1|} \exp[i(m+1)\phi] \\ u_2^{m+1}(r)r^{|m+1|} \exp[i(m+1)\phi] \\ v_2^{m-1}(r)r^{|m-1|} \exp[i(m-1)\phi] \end{pmatrix}. \quad (32)$$

Excitation frequencies as a function of the interaction strength  $g$  are plotted in Fig. 11. As anticipated in Sec. II, the breathing mode frequency of the  $m = 0$  state is independent of  $g$  and at the mean-field level we have  $\omega_B = 2$  [37].

In the dipole mode oscillations, the two bosonic components exhibit an out-of-phase oscillation in  $y$  direction, see Fig. 12(b), and consequently the center of mass only oscillates



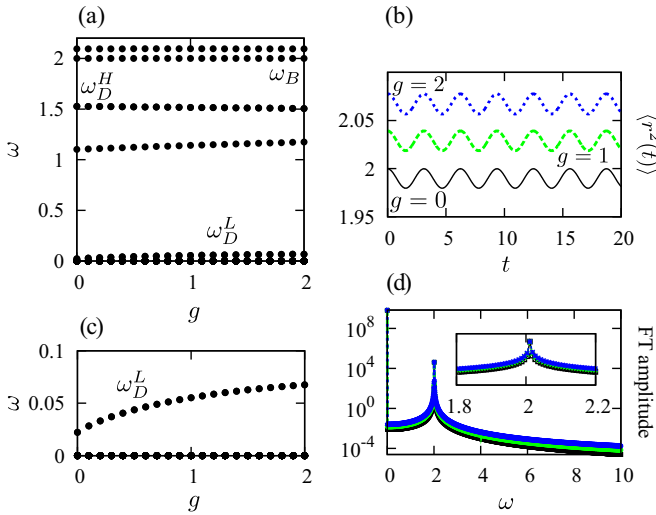


FIG. 11. Excitation spectra of the  $m = 0$  state for  $\Omega = 3.5$ , (a) and (c). Breathing mode oscillations for the  $m = 0$  solution: (b)  $\langle r^2(t) \rangle$  vs  $t$  and (d) corresponding Fourier transform. Motion is induced by changing harmonic trap potential as  $\frac{r^2}{2} \rightarrow 1.01 \frac{r^2}{2}$  for  $\Omega = 3.5$ .

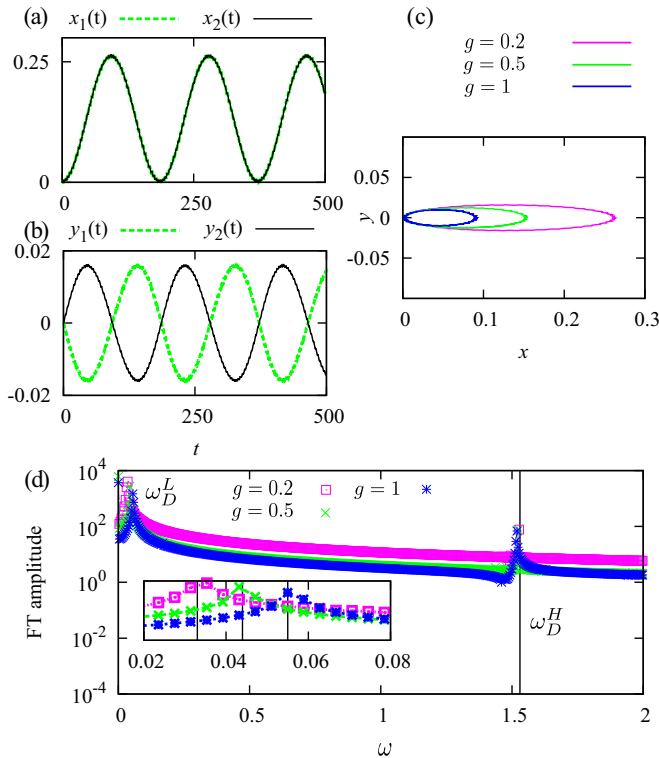


FIG. 12. Dipole mode oscillations of the  $m = 0$  solution in interacting case for  $\Omega = 3.5$ . Motion is induced by shifting harmonic trap bottom for  $\delta x = 0.01$ . In (a) and (b)  $g = 0.2$ . In (c) trajectory of the center of mass of a single bosonic component,  $y_1(t)$  vs  $x_1(t)$ , is plotted. In (d) vertical lines give results for  $\omega_D^L$  (in the inset) and  $\omega_D^H$  (in the main panel) obtained using Bogoliubov method and dots represent Fourier transform of  $x(t)$ .

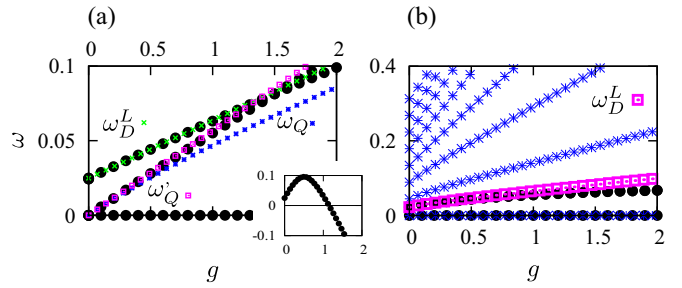


FIG. 13. Comparison of Bogoliubov analysis (black dots) and simplified diagonalization: (a)  $\Omega = 3.2$  and (b)  $\Omega = 3.5$ . Inset gives energy difference of  $m = 0$  state, which turns out to exhibit a condensate fraction significantly smaller than 1, and  $m = 15$  state, which corresponds to a half-skyrmion condensate.

in  $x$  direction with the frequency  $\omega_D^L$  that exhibits an increase with  $g$ ; see Fig. 11(b). The trajectory of the center of mass of each of the components is given by an ellipse, which is strongly elongated in  $x$  direction; see Fig. 12. A much weaker effect of  $g$  is observed in  $\omega_D^H$ , that is quite close to the numerical resolution of the applied methods.

### C. Discussion

The ground-state mean-field calculations indicate a first-order phase transition from a half-skyrmion state into  $m = 0$  condensate with increasing  $g$  at  $\Omega < \Omega_c$  and  $g = g_c$  [18] as shown in Fig. 6. Based on the Bogoliubov analysis we find that this  $m = 0$  state is dynamically unstable for  $\Omega < \Omega_c$  at  $g > g_c$  as it exhibits an imaginary excitation frequency. The results of the numerical simulations of Eqs. (19) and (20) also show a nonlinear behavior in this regime, such as mode coupling and the generation of higher harmonics. One way to resolve this issue is to use a method that is an alternative to the mean-field calculation, such as exact diagonalization. Although this method suffers from conceptual limitations in higher dimensions, if the two-body interactions are described by a contact potential (Dirac delta function) [45,46], we have implemented it with a finite-energy cutoff, as described in Ref. [47]. In particular, we perform a simplified diagonalization study for  $\Omega$  close to  $\Omega_c$  by taking into account only the three nearly degenerate noninteracting eigenstates. This analysis is sufficient to discuss the change in the ground state and the two lowest excitations  $\omega_Q$  and  $\omega_D^L$ .

A comparison of the results obtained by the simplified diagonalization and by the Bogoliubov method is given in Fig. 13 for  $N_p = 15$  particles used in the diagonalization, where we see that the two methods show good agreement in  $\omega_D^L$  in both phases. However, the frequency  $\omega_Q$  is overestimated in the Bogoliubov analysis. This can be understood as follows: when performing a diagonalization, the lowest-lying state in the sector  $m = N_p - 2$  is a linear combination of states  $|-11^{N_p-1}\rangle$  and  $|1^{N_p-2}00\rangle$ . However, the frequency  $\omega_Q$ , that we obtained using the Bogoliubov method, corresponds much better to the energy expectation value of  $|-11^{N_p-1}\rangle$ , from which we subtract  $E_0$ , as it neglects the two-particle excitations. An effect of similar origin is found for the  $m = 0$  condensate at  $\Omega > \Omega_c$ , where we find a series of two-particle excitations

$|0^{N_p}\rangle \rightarrow |0^{N_p-2}1-1\rangle \rightarrow |0^{N_p-4}11-1-1\rangle$  with the same quantum number as the ground state that we do not capture using the Bogoliubov method; see Fig. 13(b). In the inset of Fig. 13(a) we plot the energy difference between the two competing states for  $\Omega = 3.2$ . We find that the transition from the half-skyrmion condensate to  $m = 0$  state occurs at a lower value of  $g$  compared to the mean-field prediction, and that the  $m = 0$  state obtained in this way has a condensate fraction substantially lower than 1. For this reason in the region of the phase diagram  $\Omega < \Omega_{c,g} > g_c$  beyond-mean-field effects become important.

## V. CONCLUSIONS

Motivated by ongoing experimental efforts to realize and probe new quantum states, we have investigated the breathing mode and the dipole mode oscillations of the half-skyrmion bosonic condensed state. These excitations are routinely used in the experiments and we find that both of them distinguish the half-skyrmion phase from a competing  $m = 0$  state. In particular, the breathing mode frequency of the half-skyrmion state depends on the spin-orbit coupling and interaction strength, while it takes a universal value in the  $m = 0$  state at the classical level. As a response to the sudden shift of the harmonic trap, a center of mass of a half-skyrmion state exhibits a peculiar motion in the  $xy$  plane that involves the two dominant excitation frequencies  $\omega_D^L$  and  $\omega_D^H$ . In the noninteracting limit, the degeneracy of the  $m = 1$  half-skyrmion with  $m = -1$  state leads to complex motion patterns. Weak repulsive interactions make the quadrupole mode gapped and lead to simpler and symmetric patterns. These effects of interactions are stronger closer to the transition point between the two phases, where they prominently enhance the frequency  $\omega_D^L$ .

In future work, we plan to address bosonic excitations for spin-asymmetric interactions as well as to treat interactions for a spin-orbit-coupled system in more detail [48]. Another interesting direction would be to investigate the role of disorder [35,49–53], or the phenomenon of Faraday waves [54–56] in this type of system.

## ACKNOWLEDGMENTS

The authors thank Axel Pelster for useful discussions. This work was supported by the Ministry of Education, Science, and Technological Development of the Republic of Serbia under Projects No. ON171017 and No. OI1611005, and by the European Commission under H2020 project VI-SEEM, Grant No. 675121. Numerical simulations were performed on the PARADOX supercomputing facility at the Scientific Computing Laboratory of the Institute of Physics Belgrade.

## APPENDIX A: PERTURBATION THEORY FOR NEARLY DEGENERATE STATES

To describe the lowest excitation frequencies, we consider the lowest-lying states of the Hamiltonian (1), given in Eq. (2), for  $m = -1, 0, 1$ . The states  $m = \pm 1$  are degenerate and the state  $m = 0$  is close in energy; see Fig. 1. In the lowest order of the perturbation theory, the relevant part of the perturbed

Hamiltonian (8) can be approximated by

$$H_{\text{pert}}^{\text{red}} = \begin{pmatrix} a & c/2 & 0 \\ c/2 & b & -c/2 \\ 0 & -c/2 & a \end{pmatrix}, \quad (\text{A1})$$

where  $a = E_0^{m=-1} = E_0^{m=1}$ ,  $b = E_0^{m=0}$ ,  $c = \delta x I_{10} = \delta x \int_0^\infty dr r^2 f_0^*(r)[f_1(r) - g_1(r)]$ , and integrals over the angle  $\phi$  have already been performed. Functions  $f_0(r)$ ,  $f_1(r)$ , and  $g_1(r)$  are defined in Eq. (2). For completeness, other relevant operators in this subspace are approximated by

$$\begin{aligned} J_z^{\text{red}} &= \begin{pmatrix} -1 & 0 & 0 \\ 0 & 0 & 0 \\ 0 & 0 & 1 \end{pmatrix}, \\ x^{\text{red}} \otimes \mathcal{I}_2 &= \begin{pmatrix} 0 & -d/2 & 0 \\ -d/2 & 0 & d/2 \\ 0 & d/2 & 0 \end{pmatrix}, \\ y^{\text{red}} \otimes \mathcal{I}_2 &= \begin{pmatrix} 0 & id/2 & 0 \\ -id/2 & 0 & -id/2 \\ 0 & id/2 & 0 \end{pmatrix}, \end{aligned} \quad (\text{A2})$$

where  $d = I_{10}$ . The eigensystem of  $H_{\text{pert}}^{\text{red}}$  is given by

$$E_1 = a, \quad E_2 = \frac{a+b-z}{2}, \quad E_3 = \frac{a+b+z}{2}, \quad (\text{A3})$$

$$v_1 = \frac{1}{\sqrt{2}} \begin{pmatrix} 1 \\ 0 \\ 1 \end{pmatrix}, \quad v_2 = \frac{1}{\sqrt{n_2}} \begin{pmatrix} -1 \\ \frac{z-\omega_D^L}{c} \\ 1 \end{pmatrix}, \quad (\text{A4})$$

$$v_3 = \frac{1}{\sqrt{n_3}} \begin{pmatrix} -1 \\ -\frac{z+\omega_D^L}{c} \\ 1 \end{pmatrix},$$

where  $\omega_D^L = b - a$ ,  $z = \sqrt{\omega_D^{L2} + 2c^2}$ ,  $n_2 = 2z(z - \omega_D^L)/c^2$ , and  $n_3 = 2z(z + \omega_D^L)/c^2$ .

First we consider the case when the system is initially prepared in the half-skyrmion configuration  $|\psi(t=0)\rangle = (0 \ 0 \ 1)^T$ . With this initial condition, we have

$$\begin{aligned} |\psi(t)\rangle &\approx \frac{1}{2} \begin{pmatrix} 1 \\ 0 \\ 1 \end{pmatrix} e^{-iE_1 t} + \frac{1}{n_2} \begin{pmatrix} -1 \\ \frac{z-\omega_D^L}{c} \\ 1 \end{pmatrix} e^{-iE_2 t} \\ &\quad + \frac{1}{n_3} \begin{pmatrix} -1 \\ -\frac{z+\omega_D^L}{c} \\ 1 \end{pmatrix} e^{-iE_3 t}. \end{aligned} \quad (\text{A5})$$

From the last expression we can find all expectation values  $\langle O(t) \rangle = \langle \psi(t) | O | \psi(t) \rangle$ . We start from

$$\langle J_z(t) \rangle \approx \frac{2}{n_2} \cos(E_2 - E_1)t + \frac{2}{n_3} \cos(E_3 - E_1)t. \quad (\text{A6})$$

From Eq. (10) it follows directly

$$\begin{aligned} \langle y(t) \rangle &\approx \frac{2d}{c} \frac{E_2 - E_1}{n_2} \sin(E_2 - E_1)t + \frac{2d}{c} \frac{E_3 - E_1}{n_3} \sin(E_3 - E_1)t \\ &= \frac{\delta x I_{10}^2}{2\sqrt{\omega_D^L{}^2 + 2(\delta x I_{10})^2}} \left[ \sin\left(\frac{\sqrt{\omega_D^L{}^2 + 2(\delta x I_{10})^2} - \omega_D^L}{2}t\right) + \sin\left(\frac{\sqrt{\omega_D^L{}^2 + 2(\delta x I_{10})^2} + \omega_D^L}{2}t\right) \right]. \end{aligned} \quad (\text{A7})$$

When calculating the expectation value of  $x^{\text{red}}$ , we first note that  $x^{\text{red}}v_1 = 0$ ,  $v_1^T x^{\text{red}}v_{2,3} = 0$ . From here it follows that the expectation value will oscillate with the frequency  $E_3 - E_2$ . The straightforward calculation yields

$$\langle x(t) \rangle \approx \frac{\delta x I_{10}^2 \omega_D^L}{2(\omega_D^L{}^2 + 2(\delta x I_{10})^2)} [1 - \cos\sqrt{\omega_D^L{}^2 + 2(\delta x I_{10})^2}t]. \quad (\text{A8})$$

Results captured by Eqs. (A8) and (A7) are presented in Fig. 3, where we see that they reasonably agree with the full numerical calculation.

Next we consider the time evolution of the vortex-antivortex pair  $|\psi(t=0)\rangle = (0 \ 1 \ 0)^T$ . In this case

$$|\psi(t)\rangle \approx \frac{z - \omega_D^L}{cn_2} \begin{pmatrix} -1 \\ \frac{z - \omega_D^L}{c} \\ 1 \end{pmatrix} e^{-iE_2t} - \frac{z + \omega_D^L}{cn_3} \begin{pmatrix} -1 \\ -\frac{z + \omega_D^L}{c} \\ 1 \end{pmatrix} e^{-iE_3t}. \quad (\text{A9})$$

As the perturbation couples the  $m = 0$  state symmetrically to  $\pm m$  states, we find  $\langle J_z(t) \rangle = 0$  and the motion occurs only in the  $x$  direction, where we recover Eq. (A8).

## APPENDIX B: EXPLICIT FORM OF BOGOLIUBOV EQUATIONS

For a half-skyrmion ground state we rewrite linearized Eqs. (25)–(28) in the form of the eigenproblem of the matrix  $\mathcal{H}_{B_g,hs}$ ,

$$\mathcal{H}_{B_g,hs}^m \begin{pmatrix} u_1^{m-1}(\mathbf{r}) \\ v_1^{m-1}(\mathbf{r}) \\ u_2^{m+1}(\mathbf{r}) \\ v_2^{m-3}(\mathbf{r}) \end{pmatrix} = \omega \begin{pmatrix} u_1^{m-1}(\mathbf{r}) \\ v_1^{m-1}(\mathbf{r}) \\ u_2^{m+1}(\mathbf{r}) \\ v_2^{m-3}(\mathbf{r}) \end{pmatrix}, \quad (\text{B1})$$

where

$$\mathcal{H}_{B_g,hs} = \mathcal{H}_{B_g,hs}^0 + \mathcal{H}_{B_g,hs}^g - \mathcal{D}_\mu, \quad (\text{B2})$$

$\mathcal{H}_{B_g,hs}^{0,m}$

$$= \begin{pmatrix} \mathcal{H}_0^{m-1} + g|\psi_1^0|^2 + g|\psi_2^0|^2 & 0 & \frac{1}{2}\Omega^2 r^2 q_{13}(r) & 0 \\ 0 & -\mathcal{H}_0^{m-1} - g|\psi_1^0|^2 - g|\psi_2^0|^2 & 0 & -\frac{1}{2}\Omega^2 r^2 q_{24}(r) \\ \frac{1}{2}\Omega^2 r^2 q_{31}(r) & 0 & \mathcal{H}_0^{m+1} + g|\psi_2^0|^2 + g|\psi_1^0|^2 & 0 \\ 0 & -\frac{1}{2}\Omega^2 r^2 q_{41}(r) & 0 & -\mathcal{H}_0^{m-3} - g|\psi_2^0|^2 - g|\psi_1^0|^2 \end{pmatrix}, \quad (\text{B3})$$

and

$$\mathcal{H}_{B_g,hs}^{g,m} = g \begin{pmatrix} |\psi_1^0|^2 & (\psi_1^0)^2 & \psi_1^0 \chi_2^0 q_{13}(r) & \psi_1^0 \chi_2^0 q_{14}(r) \\ -(\psi_1^0)^2 & -|\psi_1^0|^2 & -\psi_1^0 \chi_2^0 q_{23}(r) & -\psi_1^0 \chi_2^0 q_{24}(r) \\ \psi_1^0 \chi_2^0 q_{31}(r) & \psi_1^0 \chi_2^0 q_{31}(r) & |\psi_2^0|^2 & (\chi_2^0)^2 q_{34}(r) \\ -\psi_1^0 \chi_2^0 q_{41}(r) & -\psi_1^0 \chi_2^0 q_{41}(r) & -(\chi_2^0)^2 q_{43}(r) & -|\psi_2^0|^2 \end{pmatrix}, \quad \mathcal{D}_\mu = \mu \begin{pmatrix} 1 & 0 & 0 & 0 \\ 0 & -1 & 0 & 0 \\ 0 & 0 & 1 & 0 \\ 0 & 0 & 0 & -1 \end{pmatrix}. \quad (\text{B4})$$

We have introduced the following functions:

$$\chi_2(r) = \psi_2(\mathbf{r}) \exp(-2i\phi), \quad (\text{B5})$$

$$\begin{aligned} q_{13}(r) &= r^{|m+1|-|m-1|}, & q_{14}(r) &= r^{|m-3|-|m-1|}, & q_{23}(r) &= r^{|m+1|-|m-1|}, & q_{24}(r) &= r^{|m-3|-|m-1|}, \\ q_{31}(r) &= r^{|m-1|-|m+1|}, & q_{34}(r) &= r^{|m-3|-|m+1|}, & q_{41}(r) &= r^{|m-1|-|m-3|}, & q_{43}(r) &= r^{|m+1|-|m-3|}, \end{aligned} \quad (\text{B6})$$

and  $\mathcal{H}_0^m = -\frac{1}{2}\left(\frac{2|m+1}{r}\frac{d}{dr} + \frac{d^2}{dr^2}\right) + \frac{1}{2}(1 + \Omega^2)r^2$ .

In a similar way we proceed in the case of  $m = 0$  ground state:

$$\mathcal{H}_{Bg,m0} = \mathcal{H}_{Bg,m0}^0 + \mathcal{H}_{Bg,m0}^g - \mathcal{D}_\mu, \quad (\text{B7})$$

with

$$\mathcal{H}_{Bg,m0}^{0,m} = \begin{pmatrix} \mathcal{H}_0^{m-1} + g|\psi_1^0|^2 + g|\psi_2^0|^2 & 0 & \frac{1}{2}\Omega^2 r^2 h(r) & 0 \\ 0 & -\mathcal{H}_0^{m+1} - g|\psi_1^0|^2 - g|\psi_2^0|^2 & 0 & -\frac{1}{2}\Omega^2 r^2 e(r) \\ \frac{1}{2}\Omega^2 r^2 e(r) & 0 & \mathcal{H}_0^{m+1} + g|\psi_2^0|^2 + g|\psi_1^0|^2 & 0 \\ 0 & -\frac{1}{2}\Omega^2 r^2 h(r) & 0 & -\mathcal{H}_0^{m-1} - g|\psi_2^0|^2 - g|\psi_1^0|^2 \end{pmatrix} \quad (\text{B8})$$

and

$$\mathcal{H}_{Bg,m0}^{g,m} = g|\psi_1^0|^2 \begin{pmatrix} 1 & h(r) & -h(r) & -1 \\ -e(r) & -1 & 1 & e(r) \\ -e(r) & -1 & 1 & e(r) \\ 1 & h(r) & -h(r) & -1 \end{pmatrix}, \quad (\text{B9})$$

where  $h(r) = r^{|m+1|-|m-1|}$  and  $e(r) = r^{|m-1|-|m+1|}$ .

- 
- [1] Y.-J. Lin, K. Jiménez-García, and I. B. Spielman, *Nature (London)* **471**, 83 (2011).
- [2] M. C. Beeler, R. A. Williams, K. Jiménez-García, L. J. Leblanc, A. R. Perry, and I. B. Spielman, *Nature (London)* **498**, 201 (2013).
- [3] J.-Y. Zhang, S.-C. Ji, Z. Chen, L. Zhang, Z.-D. Du, B. Yan, G.-S. Pan, B. Zhao, Y.-J. Deng, H. Zhai, S. Chen, and J.-W. Pan, *Phys. Rev. Lett.* **109**, 115301 (2012).
- [4] M. A. Khamehchi, Y. Zhang, C. Hamner, T. Busch, and P. Engels, *Phys. Rev. A* **90**, 063624 (2014).
- [5] L. W. Cheuk, A. T. Sommer, Z. Hadzibabic, T. Yefsah, W. S. Bakr, and M. W. Zwierlein, *Phys. Rev. Lett.* **109**, 095302 (2012).
- [6] J. Li, W. Huang, B. Shteynas, S. Burchesky, F. Cagrigli Top, E. Su, J. Lee, A. O. Jamison, and W. Ketterle, [arXiv:1606.03514](https://arxiv.org/abs/1606.03514) [cond-mat.quant-gas].
- [7] H. Zhai, *Rep. Prog. Phys.* **78**, 026001 (2015).
- [8] Z. Wu, L. Zhang, W. Sun, X.-T. Xu, B.-Z. Wang, S.-C. Ji, Y. Deng, S. Chen, X.-J. Liu, and J.-W. Pan, [arXiv:1511.08170](https://arxiv.org/abs/1511.08170) [cond-mat.quant-gas].
- [9] T. D. Stanescu, B. Anderson, and V. Galitski, *Phys. Rev. A* **78**, 023616 (2008).
- [10] C. Wang, C. Gao, C.-M. Jian, and H. Zhai, *Phys. Rev. Lett.* **105**, 160403 (2010).
- [11] T.-L. Ho and S. Zhang, *Phys. Rev. Lett.* **107**, 150403 (2011).
- [12] Y. Li, L. P. Pitaevskii, and S. Stringari, *Phys. Rev. Lett.* **108**, 225301 (2012).
- [13] S.-C. Ji, J.-Y. Zhang, L. Zhang, Z.-D. Du, W. Zheng, Y.-J. Deng, H. Zhai, S. Chen, and J.-W. Pan, *Nat. Phys.* **10**, 314 (2014).
- [14] S. Sinha, R. Nath, and L. Santos, *Phys. Rev. Lett.* **107**, 270401 (2011).
- [15] H. Hu, B. Ramachandhran, H. Pu, and X.-J. Liu, *Phys. Rev. Lett.* **108**, 010402 (2012).
- [16] B. Ramachandhran, B. Opanchuk, X.-J. Liu, H. Pu, P. D. Drummond, and H. Hu, *Phys. Rev. A* **85**, 023606 (2012).
- [17] V. Galitski and I. B. Spielman, *Nature (London)* **494**, 49 (2013).
- [18] Y.-X. Hu, C. Miniatura, and B. Grémaud, *Phys. Rev. A* **92**, 033615 (2015).
- [19] M. DeMarco and H. Pu, *Phys. Rev. A* **91**, 033630 (2015).
- [20] C. Qu, K. Sun, and C. Zhang, *Phys. Rev. A* **91**, 053630 (2015).
- [21] K. Sun, C. Qu, and C. Zhang, *Phys. Rev. A* **91**, 063627 (2015).
- [22] L. Chen, H. Pu, and Y. Zhang, *Phys. Rev. A* **93**, 013629 (2016).
- [23] C. Zhu, L. Dong, and H. Pu, *J. Phys. B: At. Mol. Opt. Phys.* **49**, 145301 (2016).
- [24] F. Dalfovo, S. Giorgini, L. P. Pitaevskii, and S. Stringari, *Rev. Mod. Phys.* **71**, 463 (1999).
- [25] C. Hamner, Y. Zhang, M. A. Khamehchi, M. J. Davis, and P. Engels, *Phys. Rev. Lett.* **114**, 070401 (2015).
- [26] E. van der Bijl and R. A. Duine, *Phys. Rev. Lett.* **107**, 195302 (2011).
- [27] Y. Zhang, L. Mao, and C. Zhang, *Phys. Rev. Lett.* **108**, 035302 (2012).
- [28] Y. Li, G. I. Martone, and S. Stringari, *EPL* **99**, 56008 (2012).
- [29] W. Zheng and Z. Li, *Phys. Rev. A* **85**, 053607 (2012).

- [30] Z. Chen and H. Zhai, *Phys. Rev. A* **86**, 041604 (2012).
- [31] G. I. Martone, Y. Li, L. P. Pitaevskii, and S. Stringari, *Phys. Rev. A* **86**, 063621 (2012).
- [32] Y. Li, G. I. Martone, L. P. Pitaevskii, and S. Stringari, *Phys. Rev. Lett.* **110**, 235302 (2013).
- [33] T. Ozawa, L. P. Pitaevskii, and S. Stringari, *Phys. Rev. A* **87**, 063610 (2013).
- [34] H. M. Price and N. R. Cooper, *Phys. Rev. Lett.* **111**, 220407 (2013).
- [35] S. Mardonov, M. Modugno, and E. Y. Sherman, *Phys. Rev. Lett.* **115**, 180402 (2015).
- [36] S. Mardonov, M. Modugno, and E. Y. Sherman, *J. Phys. B* **48**, 115302 (2015).
- [37] L. P. Pitaevskii and A. Rosch, *Phys. Rev. A* **55**, R853(R) (1997).
- [38] G. Möller and N. R. Cooper, *Phys. Rev. A* **82**, 063625 (2010).
- [39] P. Muruganandam and S. K. Adhikari, *Comput. Phys. Commun.* **180**, 1888 (2009).
- [40] D. Vudragović, I. Vidanović, A. Balaž, P. Muruganandam, and S. K. Adhikari, *Comput. Phys. Commun.* **183**, 2021 (2012).
- [41] R. K. Kumar, L. E. Young-S., D. Vudragović, A. Balaž, P. Muruganandam, and S. K. Adhikari, *Comput. Phys. Commun.* **195**, 117 (2015).
- [42] V. Lončar, A. Balaž, A. Bogojević, S. Škrbić, P. Muruganandam, and S. K. Adhikari, *Comput. Phys. Commun.* **200**, 406 (2016).
- [43] B. Satarić, V. Slavnić, A. Belić, A. Balaž, P. Muruganandam, and S. K. Adhikari, *Comput. Phys. Commun.* **200**, 411 (2016).
- [44] L. E. Young-S., D. Vudragović, P. Muruganandam, S. K. Adhikari, and A. Balaž, *Comput. Phys. Commun.* **204**, 209 (2016).
- [45] H. Saarikoski, S. M. Reimann, A. Harju, and M. Manninen, *Rev. Mod. Phys.* **82**, 2785 (2010).
- [46] B. D. Esry and C. H. Greene, *Phys. Rev. A* **60**, 1451 (1999).
- [47] T. Haugset and H. Haugerud, *Phys. Rev. A* **57**, 3809 (1998).
- [48] S. Gopalakrishnan, A. Lamacraft, and P. M. Goldbart, *Phys. Rev. A* **84**, 061604 (2011).
- [49] C. Krumnow and A. Pelster, *Phys. Rev. A* **84**, 021608 (2011).
- [50] B. Nikolić, A. Balaž, and A. Pelster, *Phys. Rev. A* **88**, 013624 (2013).
- [51] M. Ghabour and A. Pelster, *Phys. Rev. A* **90**, 063636 (2014).
- [52] T. Khellil and A. Pelster, *J. Stat. Mech.: Theory Exp.* (2016) 063301.
- [53] T. Khellil, A. Balaž, and A. Pelster, *New J. Phys.* **18**, 063003 (2016).
- [54] A. I. Nicolin, R. Carretero-González, and P. G. Kevrekidis, *Phys. Rev. A* **76**, 063609 (2007).
- [55] A. Balaž and A. I. Nicolin, *Phys. Rev. A* **85**, 023613 (2012).
- [56] A. Balaž, R. Paun, A. I. Nicolin, S. Balasubramanian, and R. Ramaswamy, *Phys. Rev. A* **89**, 023609 (2014).



## Chiral bosonic phases on the Haldane honeycomb lattice

Ivana Vasić,<sup>1</sup> Alexandru Petrescu,<sup>2,3</sup> Karyn Le Hur,<sup>3</sup> and Walter Hofstetter<sup>1</sup>

<sup>1</sup>*Institut für Theoretische Physik, Goethe-Universität, 60438 Frankfurt/Main, Germany*

<sup>2</sup>*Department of Physics, Yale University, New Haven, Connecticut 06520, USA*

<sup>3</sup>*Centre de Physique Theorique, Ecole Polytechnique, CNRS, 91128 Palaiseau Cedex, France*

(Received 4 September 2014; revised manuscript received 11 February 2015; published 3 March 2015)

Recent experiments in ultracold atoms and photonic analogs have reported the implementation of artificial gauge fields in lattice systems, facilitating the realization of topological phases. Motivated by such advances, we investigate the Haldane honeycomb lattice tight-binding model, for bosons with local interactions at the average filling of one boson per site. We analyze the ground-state phase diagram and uncover three distinct phases: a uniform superfluid (SF), a chiral superfluid (CSF), and a plaquette Mott insulator with local current loops (PMI). Nearest-neighbor and next-nearest-neighbor currents distinguish CSF from SF, and the phase transition between them is first order. We apply bosonic dynamical mean-field theory and exact diagonalization to obtain the phase diagram, complementing numerics with calculations of excitation spectra in strong and weak coupling perturbation theory. The characteristic density fluctuations, current correlation functions, and excitation spectra are measurable in ultracold atom experiments.

DOI: [10.1103/PhysRevB.91.094502](https://doi.org/10.1103/PhysRevB.91.094502)

PACS number(s): 67.85.Hj, 03.75.Lm, 03.75.Kk

### I. INTRODUCTION

Magnetic fields play a crucial role in condensed-matter physics, from the complete expulsion of magnetic fields in superconductors (Meissner effect) to the appearance of quantum Hall states. More generally, gauge fields play a central role in the description of macroscopic quantum phenomena. Lattice variants of the quantum Hall effect have attracted attention since the 1980s, beginning with the groundbreaking work by Hofstadter [1], followed by a complete characterization of magnetic bands via topological quantum numbers [2]. In 1988, Haldane [3] introduced a fermionic tight-binding model on the honeycomb lattice that breaks time-reversal symmetry without net magnetic flux through the unit cell. The model exhibits nontrivial topological properties as a result of next-nearest-neighbor tunneling processes. Time reversal symmetric extensions, 2D topological insulators [4,5] (for a review see Ref. [6]) have been experimentally realized in HgTe quantum wells [7]. Revived interest into these models stems from on-going experiments in photonic lattices [8–20], metamaterials [21,22], and optical lattices hosting ultracold atoms [23–29].

For ultracold atoms in optical lattices, artificial gauge fields producing complex hopping amplitudes have been realized by shaking the optical lattice, which results in a net Peierls phase [26,29] or by laser-assisted tunneling [27]. Two groups have recently reported the realization of a Hofstadter butterfly model [27,28], and very recently the first experimental realization of the Haldane model has been achieved [29]. Other ultracold atom experiments have also succeeded in realizing triangular flux lattices [26]. The current technologies allow to realize one-dimensional and two-dimensional lattice systems, which can be loaded with bosons or fermions. These recent developments constitute impressive steps towards simulating many-body physics, artificial gauge fields and spin-orbit couplings in optical lattices where interactions can be engineered and tuned in a precise manner.

In parallel, several theoretical works have focused on interaction-induced transitions from a topological into a

Mott insulator (MI) in fermionic systems [30–40]. Properties of lattice bosons exposed to artificial gauge fields have been addressed as well in different regimes. Lattices with staggered flux give rise to finite momentum Bose–Einstein condensates [41–43]. A related phenomenon has been identified in the presence of uniform flux and the excitation spectrum in the weakly interacting regime of this unusual superfluid phase has been calculated [44,45]. With stronger interactions, a superfluid to MI transition is expected to occur [41,42,46–52], and even more interestingly, the interplay of strong interactions and uniform lattice flux should lead to fractional Hall states [53] and topological transitions [54]. Another proposed setup for reaching the quantum Hall regime are optical flux lattices [55]. In low-dimensional lattices with staggered flux a new intermediate phase has been predicted—a chiral Mott state [56–58] that exhibits broken time-reversal symmetry without breaking U(1) symmetry. Bond-chirality and plaquette order have been shown to emerge in a system of two-dimensional hard-core bosons with frustrated ring exchange [59]. Topological transport in bosonic Mott states in the presence of spin orbit-coupling has been studied in Refs. [60,61]. Emergence of a chiral current and Meissner effect in bosonic ladders have been demonstrated experimentally [62] and theoretically analyzed [63–67]. While topological bosonic Mott insulators have been theoretically predicted in one dimension [68–70], an important open question in the field is the existence of bosonic topological Mott states in two spatial dimensions [71]. Multicomponent interacting bosonic systems exhibit spontaneous spin Hall effect [72], exotic magnetic order [73], and integer Hall effect [74]. A low-density ground state of spinor bosonic gases with isotropic Rashba spin-orbit coupling is proven to be a composite fermion state [75].

Recently several approaches for the realization of the Haldane model for integer quantum Hall effect without Landau levels [3] in an ultracold atom system were theoretically proposed [76–79]. In relation to this, the intricacies of the direct Peierls substitution for the Haldane model were addressed [80]. The very recent experiment [29] demonstrates

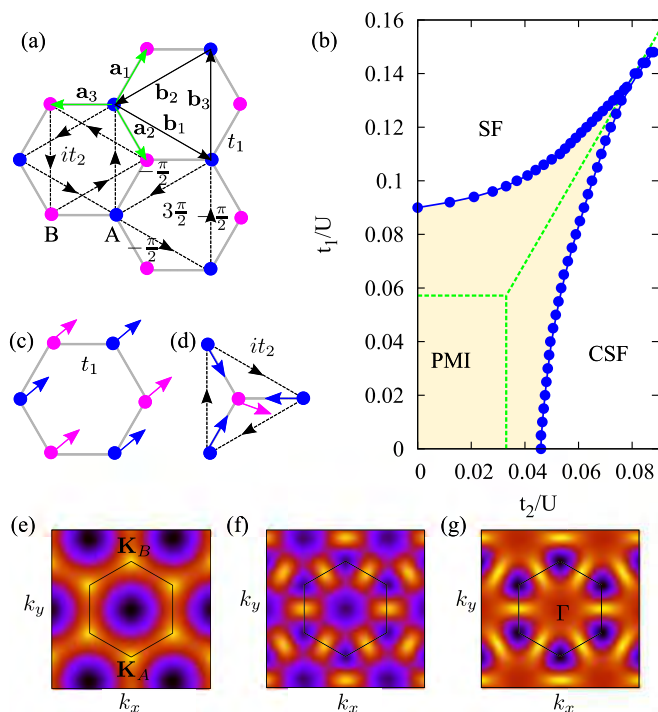


FIG. 1. (Color online) (a) Lattice vectors on the honeycomb lattice and hopping integrals the Haldane model of Eq. (1). (b) Phase diagram of the model (5) at unit filling, containing plaquette Mott insulator (PMI), uniform superfluid (SF) and chiral superfluid (CSF) phases. Solid (dashed) lines represent DMFT (Gutzwiller mean-field) results. (c) Local condensate order parameter in the uniform superfluid. (d) In CSF the condensate order parameters on sublattices  $A$  and  $B$  are determined up to a relative phase. (e)–(g) The lowest band of Eq. (1) for  $t_1 = 1$ ,  $\phi = \pi/2$ , and  $t_2 = 0, 1/\sqrt{3}, 1$ , from the left to the right. Band minima move from the center  $\Gamma$  to the corners  $\mathbf{K}_A$ ,  $\mathbf{K}_B$  of the first Brillouin zone (depicted as a solid line). At  $t_1 = \sqrt{3}t_2$ , there are three degenerate minima.

that time-periodic driving of a honeycomb optical lattice creates the prerequisite complex next-nearest-neighbor hopping. Topological transitions arising in the noninteracting Haldane model for fermions have been directly probed in this experimental setup.

Motivated by experimental possibilities and open theoretical questions on the emergence of new bosonic phases in the presence of gauge fields, we study the Haldane model for bosons at unit filling with a local repulsive Hubbard interaction. The Hamiltonian comprises three terms: a real nearest-neighbor hopping  $t_1$ , an imaginary next-nearest-neighbor hopping  $it_2$ , and the local repulsive interaction  $U$ . Each of the three terms favors one of the phases depicted in the diagram of Fig. 1(b), which is our main result. The  $t_1$ -dominated phase is a uniform superfluid (SF) with long-range phase correlations, whereas the  $t_2$ -dominated phase is a chiral superfluid (CSF) that exhibits phase modulation due to bosons condensing at nonzero momentum. The interactions dominated phase is a plaquette Mott insulator (PMI) characterized by local plaquette currents. We find that the excitation bands in both superfluid and Mott insulator phases are reminiscent of the single-particle spectrum of the Haldane model. For all considered phases, we

calculate experimentally accessible features such as density fluctuations, plaquette currents and excitation spectra.

The paper is organized as follows: we introduce the Haldane–Hubbard model in Sec. II. We discuss the weakly interacting limit and the distinction between the uniform superfluid and the chiral superfluid in Sec. III A, followed by a discussion of possible ground states and current expectation values in Sec. III B. To access the regime of stronger interactions, we start with a simple mean-field theory approach that leads to a phase diagram which captures all the important qualitative features in Sec. III C. To address effects beyond the mean-field approximation, in Sec. III D, we use bosonic dynamical mean-field theory (DMFT) [81–85] that gives information on the thermodynamic limit. We then compare such results to those extracted from the exact ground state found with the Lanczos algorithm for a finite system in Sec. III E. Within all these approaches, we compute the values of condensate order parameters, density fluctuations and plaquette currents in the ground state. We then turn to the excitation spectra of the superfluid (Sec. IV A) and of the Mott insulator (Sec. IV B) and characterize their main features. We conclude in Sec. V with a discussion of our results and indicate possible future research directions.

## II. MODEL

The Haldane Hamiltonian on the honeycomb lattice is given by [3]

$$\mathcal{H}_H = -t_1 \sum_{\langle i,j \rangle} \hat{b}_i^\dagger \hat{b}_j - t_2 \sum_{\langle\langle i,j \rangle\rangle} e^{i\phi_{ij}} \hat{b}_i^\dagger \hat{b}_j, \quad (1)$$

where  $\hat{b}_i$  is the annihilation operator at site  $i$ . The term proportional to  $t_1$  describes the graphene lattice with nonzero hopping elements only between nearest neighbors along vectors  $\mathbf{a}_1$ ,  $\mathbf{a}_2$ , and  $\mathbf{a}_3$  shown in Fig. 1(a). The  $t_2$  term was originally introduced by Haldane. It includes a complex phase  $\phi_{ij}$  for the tunneling between two next-nearest neighbors (sites belonging to the same sublattice) along  $\mathbf{b}_1 = \mathbf{a}_2 - \mathbf{a}_3$ ,  $\mathbf{b}_2 = \mathbf{a}_3 - \mathbf{a}_1$ , and  $\mathbf{b}_3 = \mathbf{a}_1 - \mathbf{a}_2$ . The absolute value of  $\phi_{ij}$  is constant throughout the lattice and its sign is shown in Fig. 1(a). As can be seen from the same figure, the net flux per unit cell is zero. In the following, we consider the case of  $|\phi_{ij}| = \pi/2$  and use the notation  $t_{ij}$  to shorten Eq. (1) to  $\mathcal{H}_H = -\sum_{i,j} t_{ij} \hat{b}_i^\dagger \hat{b}_j$ . We will add a label to make sublattice dependence explicit when necessary, for example,  $\hat{b}_i \rightarrow \hat{b}_{Ai}$ .

The single-particle Hamiltonian (1) can be described by the Chern numbers of its Bloch bands, a property which we briefly review here. In momentum space, (1) is rewritten as  $\mathcal{H}_H = \int_{\text{BZ}} d\mathbf{k} \psi(\mathbf{k})^\dagger \mathcal{H}_H(\mathbf{k}) \psi(\mathbf{k})$ , with

$$\mathcal{H}_H(\mathbf{k}) = -\mathbf{d}(\mathbf{k}) \cdot \hat{\sigma}. \quad (2)$$

The momenta  $\mathbf{k}$  belong to the first Brillouin zone, which is spanned by the vectors  $\mathbf{g}_1 = (2\pi/(3a), -2\pi/(a\sqrt{3}))$  and  $\mathbf{g}_2 = (2\pi/(3a), 2\pi/(a\sqrt{3}))$  in reciprocal space. We have introduced the field  $\psi(\mathbf{k}) = (b_A(\mathbf{k}), b_B(\mathbf{k}))^T$  of Fourier transforms of the annihilation operators on sublattices  $A$  and  $B$ . We wrote

$\mathcal{H}_H$  in the basis of Pauli matrices  $\hat{\sigma} = (\sigma_x, \sigma_y, \sigma_z)$  in terms of

$$\mathbf{d}(\mathbf{k}) = \left( t_1 \sum_i \cos \mathbf{k} \cdot \mathbf{a}_i, t_1 \sum_i \sin \mathbf{k} \cdot \mathbf{a}_i, -2t_2 \sum_i \sin \mathbf{k} \cdot \mathbf{b}_i \right). \quad (3)$$

The nontrivial topology of the Bloch bands translates to a nonzero winding number of the map  $\hat{\mathbf{d}} = \mathbf{d}/|\mathbf{d}|$  from the torus (the first Brillouin zone) to the unit sphere. Denoting by  $\partial_i$  the partial derivatives with respect to the two components of momentum  $k_i$ ,  $i = 1, 2$ , the winding number is [3]

$$\mathcal{C}_- = \frac{1}{4\pi} \int_{\text{BZ}} d\mathbf{k} \hat{\mathbf{d}} \cdot (\partial_1 \hat{\mathbf{d}} \times \partial_2 \hat{\mathbf{d}}). \quad (4)$$

Equation (4) represents the Chern number of the lower Bloch band, and it takes the value  $\mathcal{C}_- = 1$  at finite values of  $t_2$  and  $t_1$  when  $|\phi_{ij}| = \frac{\pi}{2}$ . For  $t_1 = 0$ , the two bands touch along the certain cuts of the Brillouin zone, and the spectrum is fully gapped as soon as  $t_1 > 0$ . The formula for the upper band is obtained by replacing  $\hat{\mathbf{d}}$  by  $-\hat{\mathbf{d}}$ , and leads to  $\mathcal{C}_+ = -1$ .

We focus here on the bosonic Haldane-Hubbard Hamiltonian

$$\mathcal{H} = \mathcal{H}_H + \frac{U}{2} \sum_i \hat{n}_i(\hat{n}_i - 1) - \mu \sum_i \hat{n}_i, \quad (5)$$

where  $U$  is a local (on-site) interaction and  $\mu$  is the chemical potential. Throughout this work, we will consider the zero temperature limit  $T = 0$ . In the following sections, we characterize different phases by the value of the condensate order parameter

$$\psi_i = \langle \hat{b}_i \rangle, \quad (6)$$

local density fluctuations

$$\Delta n_i = \langle \hat{n}_i^2 \rangle - \langle \hat{n}_i \rangle^2, \quad (7)$$

and emerging patterns of lattice currents. The expectation value of the current operator for the bond  $j \rightarrow i$  on the lattice is given by

$$J_{ij} = -i(t_{ji} \langle \hat{b}_j^\dagger \hat{b}_i \rangle - t_{ij} \langle \hat{b}_i^\dagger \hat{b}_j \rangle) = -2\text{Im}(t_{ij} \langle \hat{b}_i^\dagger \hat{b}_j \rangle), \quad (8)$$

as can be derived from the lattice continuity equation.

Implications of nontrivial Chern numbers (4) are most often discussed in the context of fermionic systems. In the seminal paper [2], the Hall conductance of noninteracting lattice fermions in the strong magnetic field has been expressed in terms of Chern numbers of occupied Bloch bands. The current cold-atom realization of the Haldane model [29] is based on the idea of Floquet topological insulators [86]. The definition and the meaning of topological invariants in these periodically driven systems have been in the focus of several studies [87–89]. Recently, the first photonic analogs of topologically nontrivial systems have been realized [20]: both in the classical regime [10,13] and in the quantum regime where arrays of coupled photonic cavities have been used [12]. These photonic experiments have probed the emerging edge states, as a clear indication of nontrivial topology. More recently, it has been theoretically proposed to directly measure topological invariants [16,90,91] in these systems. Topological transitions have been directly probed in quantum circuits of interacting superconducting qubits [92].

Photonic systems [12,14] typically work in the dissipative-driven regime. In the equilibrium situation that we consider throughout the paper, when a topological band is filled with weakly interacting bosons, the ground state can be a topologically trivial Bose-Einstein condensate [44,45,93,94]. Properties of the condensate are set by the features of band minima and are not affected by a nontrivial band topology expressed by Eq. (4). However, band topology does affect transport properties of bosons as well as properties of excitations [44,45,60,61,93,94]. Transport of lattice bosons has been used to probe a finite Berry curvature [95] and the Chern number of a topological band [96]. In contrast to weakly interacting bosons, strongly interacting (hard-core) bosons in topological flat bands at certain filling fractions are known to exhibit topologically nontrivial ground states [97]. In the next sections, we study the ground state and excitations of model (5).

### III. STUDY OF THE GROUND STATE

#### A. Weakly interacting bosons

In the weakly interacting limit, we expect bosons to condense. From the noninteracting model of Eq. (1), we can easily infer two limits that give rise to two types of superfluids: for  $t_2 = 0$  we obtain a honeycomb lattice and all bosons condense at the center of the Brillouin zone  $\Gamma$  at zero momentum. On the other hand, for  $t_1 = 0$ , the model turns into two decoupled triangular lattices, and we expect separate condensation of bosons on two sublattices.

To study the possible condensates at finite values of  $t_1$  and  $t_2$ , let us focus on the noninteracting Hamiltonian. The energy dispersion of the lowest band  $\epsilon_-(\mathbf{k})$  exhibits either a single minimum at  $\mathbf{k} = \Gamma$  for  $t_1 > \sqrt{3}t_2$  or degenerate minima at the two inequivalent corners of the Brillouin zone  $\mathbf{K}_A$  and  $\mathbf{K}_B$  for  $t_1 < \sqrt{3}t_2$  [see Figs. 1(e)–1(g)]. The momenta at the corners of the Brillouin zone satisfy

$$e^{i\mathbf{K}_A \cdot \mathbf{b}_i} = e^{i\frac{2\pi}{3}}, \quad e^{i\mathbf{K}_B \cdot \mathbf{b}_i} = e^{-i\frac{2\pi}{3}}, \quad (9)$$

for all  $i = 1, 2, 3$ . At these high-symmetry points, the Hamiltonian takes the following forms:

$$\mathcal{H}(\Gamma) = -3t_1\sigma_x \quad (10)$$

and

$$\mathcal{H}(\mathbf{K}_{A,B}) = \pm 3\sqrt{3}t_2\sigma_z. \quad (11)$$

The SF phase forms when  $t_1 > \sqrt{3}t_2$ . The condensate order parameter is  $\langle \hat{b}_i \rangle = \sqrt{n}$ , where  $n = N/N_{\text{sites}}$  is the filling. The ground-state energy obtained from the Gross-Pitaevskii (GP) energy functional [98]

$$E_0 = - \sum_{i,j} t_{ij} \psi_i^* \psi_j + \frac{1}{2} U \sum_i |\psi_i|^4 \quad (12)$$

is  $\frac{E_0}{N_{\text{sites}}} = (-3t_1n + \frac{1}{2}Un^2)$  and we find that the next-nearest-neighbor hopping is effectively canceled. Using Eq. (8), the next-nearest-neighbor bond current is

$$J_{AA}^{\text{SF}} = -2n t_2 \text{Im} \exp(-i\pi/2) = 2nt_2. \quad (13)$$

The CSF phase forms in the opposite case  $t_1 < \sqrt{3}t_2$ . Noninteracting bosons can condense in a state that is an



arbitrary linear combination of single-particle ground states at  $\mathbf{K}_A$  and  $\mathbf{K}_B$ , leading to large degeneracy. However, even weak repulsive interactions prefer a uniform density distribution on the two sublattices. To infer the low-energy description, we assume that only the minima of the lowest band are occupied and approximate operators according to Eq. (11) by

$$\begin{aligned}\hat{b}_{A,i} &\approx \frac{1}{\sqrt{N_{\text{sites}}/2}} e^{-i\mathbf{K}_A \mathbf{r}_i} \hat{b}_A(\mathbf{K}_A), \\ \hat{b}_{B,i} &\approx \frac{1}{\sqrt{N_{\text{sites}}/2}} e^{-i\mathbf{K}_B \mathbf{r}_i} \hat{b}_B(\mathbf{K}_B).\end{aligned}\quad (14)$$

The Hamiltonian (5) then turns into

$$\begin{aligned}\mathcal{H} &\approx -3\sqrt{3}t_2(\hat{b}_A^\dagger(\mathbf{K}_A)\hat{b}_A(\mathbf{K}_A) + \hat{b}_B^\dagger(\mathbf{K}_B)\hat{b}_B(\mathbf{K}_B)) \\ &+ \frac{U}{2}\hat{b}_A^\dagger(\mathbf{K}_A)\hat{b}_A(\mathbf{K}_A)\left(\frac{2}{N_{\text{sites}}}\hat{b}_A^\dagger(\mathbf{K}_A)\hat{b}_A(\mathbf{K}_A) - 1\right) \\ &+ \frac{U}{2}\hat{b}_B^\dagger(\mathbf{K}_B)\hat{b}_B(\mathbf{K}_B)\left(\frac{2}{N_{\text{sites}}}\hat{b}_B^\dagger(\mathbf{K}_B)\hat{b}_B(\mathbf{K}_B) - 1\right) \\ &- \mu(\hat{b}_A^\dagger(\mathbf{K}_A)\hat{b}_A(\mathbf{K}_A) + \hat{b}_B^\dagger(\mathbf{K}_B)\hat{b}_B(\mathbf{K}_B)),\end{aligned}\quad (15)$$

i.e., it describes two decoupled sublattices since the nearest-neighbor tunneling term vanishes:

$$\sum_{(i,j)} \hat{b}_i^\dagger \hat{b}_j \propto \sum_i \hat{b}_i^\dagger \sum_{j=1}^3 e^{-i\mathbf{K}_B \cdot (\mathbf{r}_i + \mathbf{a}_j)} \hat{b}_B(\mathbf{K}_B) = 0. \quad (16)$$

Thus we conclude that the ground state consists of two decoupled superfluids. The same observation follows directly from Eq. (12), i.e., at the mean-field level the ground-state consists of two separate condensates occupying the two sublattices.

The mean-field ground-state energy (12) is  $\frac{E_0}{N_{\text{sites}}} = (-3\sqrt{3}t_2n + \frac{1}{2}Un^2)$  and the corresponding momentum distributions are  $\rho_A(\mathbf{k}) \approx \frac{N}{2} \delta_{\mathbf{k},\mathbf{K}_A}$ ,  $\rho_B(\mathbf{k}) \approx \frac{N}{2} \delta_{\mathbf{k},\mathbf{K}_B}$ . For the operators  $\hat{b}_{A,i}$  on the same sublattice, we find from Eq. (9),

$$\begin{aligned}\langle \hat{b}_{A,i}^\dagger \hat{b}_{A,j} \rangle &= \psi_{A,i}^* \psi_{A,j} = \frac{2}{N_{\text{sites}}} \sum_{\mathbf{k}} e^{i\mathbf{k}(\mathbf{r}_i - \mathbf{r}_j)} \langle \hat{b}_A^\dagger(\mathbf{k}) \hat{b}_A(\mathbf{k}) \rangle \\ &= n \exp\left(i\frac{2\pi}{3}m\right),\end{aligned}\quad (17)$$

where  $m$  is an arbitrary integer. The condensate at nonzero momentum exhibits nonuniform phase differences between next-nearest neighbors [see Fig. 1(d)]. Phase ordering directly affects the next-nearest-neighbor current expectation value:

$$\begin{aligned}J_{AA}^{\text{CSF}} &= -2\text{Im}(t_2 e^{-i\pi/2} \langle \hat{b}_{A_i}^\dagger \hat{b}_{A_j} \rangle) \\ &= -2t_2 n \sin[-\pi/2 + \mathbf{K}_A \cdot (\mathbf{r}_i - \mathbf{r}_j)] = -nt_2.\end{aligned}\quad (18)$$

The aforementioned ‘‘decoupling of sublattices,’’ Eq. (16), is depicted in Fig. 1(d) as an arbitrary phase difference between order parameters on two sublattices.

At the critical hopping strength  $t_1 = \sqrt{3}t_2$ , there are three degenerate minima present in the dispersion relation, and in order to deduce the proper ground state at the mean-field level all three of them should be taken into account. However, the analysis of the mean-field energy functional indicates that condensation either at  $\Gamma$  or at both  $\mathbf{K}_A$  and  $\mathbf{K}_B$  is preferred, and

we do not find a density modulated phase in this case [44,45]. The fact that at the phase boundary between the two superfluids the current changes abruptly, Eqs. (13) and (18), hints towards a first-order phase transition between uniform and chiral superfluids in the weakly interacting limit.

## B. Josephson effect between sublattices

In Sec. III A, we distinguished SF and CSF phases through their patterns of the next-nearest-neighbor current  $J_{AA}$  (equivalently  $J_{BB}$ ), expressed in Eqs. (13) and (18), respectively. We now argue that the two superfluid phases have different expectation values of the nearest-neighbor current  $J_{AB}$ , which is a signature of Josephson-type phase coherence between sublattices  $A$  and  $B$ .

In the SF phase, the phases of bosons on the  $A$  and  $B$  sublattices are pinned and therefore the nearest-neighbor current vanishes:

$$J_{AB}^{\text{SF}} = 0. \quad (19)$$

This follows from the fact that the operator corresponding to the boson at the minimum of the lower band is  $\hat{b}_-(\mathbf{k} = \Gamma) = \frac{1}{\sqrt{2}}[\hat{b}_A(\Gamma) + \hat{b}_B(\Gamma)]$ . The ground-state energy is invariant to a  $\text{U}(1)$  rotation of the pinned phases on  $A$  and  $B$  sublattices, which corresponds to the existence of one Goldstone mode.

In the CSF phase, the boson annihilation operator corresponding to the band minimum obeys  $\hat{b}_-(\mathbf{K}_a) = \hat{b}_a(\mathbf{K}_a)$  for  $a = A$  or  $B$ . The twofold degeneracy of the band minimum leads us to the problem of coherence of a Bose-Einstein condensate in a double-well potential [72,99]. In the following, we prove that the presence of defects, or open boundary conditions, produces a condensate in which  $A$  and  $B$  sublattices are phase coherent. Secondly, we show that if discrete lattice symmetries are preserved, the ground state for weak  $U > 0$  consists of decoupled condensates on sublattices  $A$  and  $B$ .

We form first a condensate wave function from coherent superpositions of the degenerate minima

$$|\Phi'_{\text{CSF}}(\phi)\rangle = \frac{1}{\sqrt{N!}} \left[ \frac{1}{\sqrt{2}} \hat{b}_A^\dagger(\mathbf{K}_A) + \frac{e^{i\phi}}{\sqrt{2}} \hat{b}_B^\dagger(\mathbf{K}_B) \right]^N |0\rangle. \quad (20)$$

The nearest-neighbor current  $J_{AB}$  on the unit cell at coordinate  $\mathbf{r}_i$  has a well defined value  $\propto \sin[\phi - (\mathbf{K}_A - \mathbf{K}_B) \cdot \mathbf{r}_i]$ . Note that the ground state  $|\Phi'_{\text{CSF}}\rangle$  spontaneously breaks lattice translation and lattice inversion symmetries.

We form a second wave function for the chiral superfluid by uniformly superimposing all  $|\Phi'_{\text{CSF}}(\beta)\rangle$  for  $\beta$  between 0 and  $2\pi$ . This new wave function corresponds to decoupled condensates, and is both lattice translation and inversion symmetric:

$$|\Phi''_{\text{CSF}}\rangle = \frac{1}{(N/2)!} [\hat{b}_A^\dagger(\mathbf{K}_A)]^{N/2} [\hat{b}_B^\dagger(\mathbf{K}_B)]^{N/2} |0\rangle. \quad (21)$$

Note that now the nearest-neighbor current  $J_{AB}^{\text{CSF}}$  vanishes. This is due to the fact that the phases of the two sublattices can be rotated independently without changing the energy, which corresponds to the existence of two Goldstone modes.

First we discuss a finite size system with periodic boundary conditions. We find that the energy per site of  $|\Phi''_{\text{CSF}}\rangle$  is  $\frac{E_0''}{N_{\text{sites}}} = -3\sqrt{3}t_2n + (Un/2)(n + 1 - 2/N_{\text{sites}})$ . This is lower

by  $nU/(2N_{\text{sites}})$  than the energy of Eq. (20). Thus, if the system is finite, if the interactions are weakly repulsive and if all discrete lattice symmetries are preserved, then the variational ground state is  $|\Phi_{\text{CSF}}'\rangle$ . This is confirmed numerically using Lanczos methods for small translation and inversion symmetric clusters in Sec. III E. However, the fact that the states (20) and (21) become degenerate in the thermodynamic limit opens up a possibility of a ground state that breaks lattice symmetries [43]. We investigate this issue further in Secs. III E and IV A.

The ground state is significantly different if a defect is introduced in a finite lattice with periodic boundaries or in a finite lattice with open boundaries. In these cases, the double-well structure (15) does not apply anymore. For example, at the boundary of the lattice,  $A$  and  $B$  sublattice phases can be pinned since the number of  $B$  neighbors for any  $A$  site is 2 instead of 3. Once the phases are pinned at the boundary, the  $A$ - $B$  sublattice phase coherence proliferates into the bulk. Another possibility to establish phase coherence between  $A$  and  $B$  sublattices is to create a strong nearest-neighbor bond at a given unit cell (possibly imprinting a phase difference). As a consequence of long-range correlations between sites on the same sublattice,  $J_{AB}$  at any other bond acquires a definite value.

We conclude that

$$J_{AB}^{\text{CSF}} = 0 \quad (22)$$

in a finite system obeying lattice translation and inversion symmetries (i.e., a lattice on a torus with finitely many sites), whereas

$$J_{AB}^{\text{CSF}} \neq 0 \quad (23)$$

in the presence of defects or if the system has open boundaries, i.e., in realistic experimental conditions. Our qualitative remarks about the role of defects are substantiated with numerical results obtained by minimizing the GP energy functional (12) for finite lattices, presented in Fig. 2.

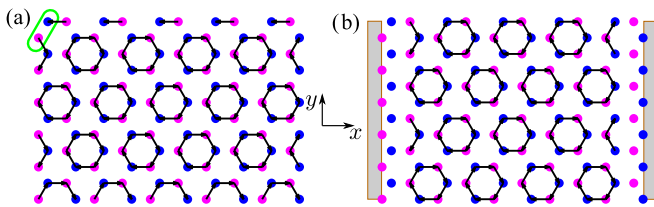


FIG. 2. (Color online) Aligning the phases of order parameters on the two sublattices:  $U = 1$ ,  $t_1 = 10$ ,  $t_2 = 10$ , and average filling  $n = 1$ . In (a), the top left link hosts a defect  $t_1 = 4t_2$ . In (b), we impose open boundary conditions in  $x$  direction. Arrows represent local (plaquette) currents with amplitude  $|J_{AB}| \approx |2t_1 n \sin \frac{2\pi}{3}| = \sqrt{3}nt_1$ . Weaker currents that should vanish in the bulk, far away from the defect are not plotted. Results are obtained by minimizing the energy functional (12) with respect to  $\psi_i$  for the 120 sites shown in the plot. In both plots, there are density modulations, for example, in (a) there are more particles sitting on the sites linked by  $4t_1$ .

### C. Mott insulator with plaquette currents

To address stronger interactions, we start with a mean-field decoupling of the tunneling term as  $\hat{b}_i^\dagger \hat{b}_j \approx \langle \hat{b}_i^\dagger \rangle \hat{b}_j + \hat{b}_i^\dagger \langle \hat{b}_j \rangle - \langle \hat{b}_i^\dagger \rangle \langle \hat{b}_j \rangle$  that is fully equivalent to applying a variational Gutzwiller ansatz  $|\psi_{\text{GW}}\rangle = \prod_{\otimes i} \sum_n c_{i,n} |n\rangle$  [100,101]. We obtain a mean-field Hamiltonian

$$\mathcal{H}_{\text{mf}} = \sum_i \mathcal{H}_{\text{mf}}^i + \text{const.}, \quad (24)$$

given by a sum of local terms

$$\mathcal{H}_{\text{mf}}^i = -\Psi_i^{\text{mf}} \hat{b}_i^\dagger - (\Psi_i^{\text{mf}})^* \hat{b}_i + \frac{U}{2} \hat{n}_i (\hat{n}_i - 1) - \mu \hat{n}_i, \quad (25)$$

where each lattice site is coupled to its neighbors only by a sum of condensate order parameters  $\Psi_i^{\text{mf}} = \sum_j t_{ij} \psi_j$ . The ground state is found by minimizing the expectation value of the Hamiltonian (24) with respect to the coefficients  $c_{i,n}$ . The approximation becomes an exact description both in the weakly interacting limit and in the atomic limit. A resulting mean-field phase diagram at unit filling is shown in Fig. 1(b) by dashed lines. It consists of the two superfluid phases discussed in the previous subsection and in addition it contains a Mott phase. The rectangular shape of the Mott domain implies that the ground-state energy of the uniform superfluid is unaffected by  $t_2$  and vice versa for the chiral superfluid.

However, the Mott state that we obtain within the mean-field approximation, given by Eqs. (24) and (25), is a simple product state  $\prod_{\otimes i} |n\rangle$  and is therefore featureless. To explore its properties in more detail we need a better approach. The random phase approximation (RPA) [102–104] is analytically tractable. It is a standard approach that shares some similarities with DMFT and we briefly outline it here.

In both approaches, we consider the single-particle Green's functions

$$G_{ij}(\tau_1 - \tau_2) = -\langle \mathcal{T} \hat{b}_i(\tau_1) \hat{b}_j^\dagger(\tau_2) \rangle \quad (26)$$

expressed in terms of Matsubara frequencies  $\omega_n = 2\pi n/\beta$ , where  $\beta$  is the inverse temperature ( $\beta \rightarrow \infty$ ) and  $G_{ij}(i\omega_n) = \int d\tau \exp(i\omega_n \tau) G_{ij}(\tau)$ . The main approximation of the two methods is that the self-energy is local. This is an exact property in the limit of infinite lattice coordination number.

In RPA, local self-energies are determined from the local Hamiltonian (25) [102–104]. Local Green's functions corresponding to the Hamiltonian (25) at  $T = 0$  when the ground state is  $\prod_{\otimes i} |n\rangle$  are given by

$$\mathcal{G}_{ii}^{\text{RPA}}(i\omega_n) = -\frac{n}{-(n-1)U + \mu + i\omega_n} + \frac{n+1}{-nU + \mu + i\omega_n}. \quad (27)$$

The corresponding self-energies are then calculated using the local Dyson equation

$$\Sigma_i^{\text{RPA}}(i\omega_n) = i\omega_n + \mu - (\mathcal{G}_{ii}^{\text{RPA}}(i\omega_n))^{-1}. \quad (28)$$

As already mentioned, the last result approximates the self-energy of the full lattice problem and is used in the lattice Dyson equation, written either in real

$$[G^{\text{RPA}}]_{ij}^{-1}(i\omega_n) = (i\omega_n + \mu)\delta_{ij} + t_{ij} - \delta_{ij} \Sigma_i^{\text{RPA}}(i\omega_n), \quad (29)$$

or  $k$  space

$$[G^{\text{RPA}}]^{-1}(i\omega_n, \mathbf{k}) = (i\omega_n + \mu - \Sigma_{ii}^{\text{RPA}}(i\omega_n))\mathcal{I} - \mathcal{H}_H(\mathbf{k}). \quad (30)$$

Starting from the Green's functions, Eq. (30), we first derive the excitation spectrum of the Mott state. By going into the basis in which  $\mathcal{H}_H(\mathbf{k})$  is diagonal and by applying analytical continuation  $i\omega_n \rightarrow \omega + i\delta$ , we can read off poles of the  $\mathbf{k}$ -dependent Green's function. The excitation spectrum of the Mott insulator is given by the particle-hole excitations [101–103]

$$\omega_{\pm, \alpha}(\mathbf{k}) = \frac{U}{2} \left[ (2n-1) - 2\frac{\mu}{U} + \frac{\epsilon_{\alpha}(\mathbf{k})}{U} \pm \sqrt{1 + 2(2n+1)\frac{\epsilon_{\alpha}(\mathbf{k})}{U} + \frac{\epsilon_{\alpha}(\mathbf{k})^2}{U^2}} \right], \quad (31)$$

where  $\alpha$  takes values  $\pm$  corresponding to the two noninteracting bands. A detailed study of the properties of excitations given by Eq. (31) is postponed to Sec. IV. Here, we only note that at filling  $n=1$  the gap in the spectrum closes at  $t_1^{\text{RPA},c} = U \frac{3-2\sqrt{2}}{3}$  for  $t_1 > \sqrt{3}t_2$  where the transition from the Mott insulator into the uniform superfluid occurs, while for  $t_1 < \sqrt{3}t_2$  the transition into the chiral superfluid is found for  $t_2^{\text{RPA},c} = U \frac{3-2\sqrt{2}}{3\sqrt{3}}$ . The two boundaries meet at the tricritical point with the line corresponding to a direct transition between the two superfluids, Fig. 1(b).

Another important feature of the Mott state are finite (nonvanishing) density fluctuations present at finite values of the hopping terms  $t_1$  and  $t_2$  (note that these are not captured by the oversimplified state  $\prod_{\otimes i} |n\rangle$ ). To understand how these fluctuations are affected by the complex hopping term ( $it_2$ ), we calculate local (plaquette) currents (8) between next-nearest neighbors. The expectation value  $\langle b_i^\dagger b_j \rangle$  can be expressed in terms of Green's functions

$$\langle b_i^\dagger b_j \rangle = -\frac{1}{\beta} \sum_n \exp(i\omega_n 0^+) G_{ji}(i\omega_n), \quad (32)$$

where  $\omega_n$  is Matsubara frequency. Deep in the Mott domain, an approximate result for  $G_{ij}$  can be derived from the strong-coupling expansion in hopping [104,105]. Here, we consider only contributions obtained by a formal matrix inversion of Eq. (29) and by keeping terms that are second order in  $t_{ij}$ . Directly from the second-order result for  $\langle b_i^\dagger b_j \rangle$  given in Refs. [104,105], we read off a general expression

$$\frac{J_{ij}^{(2)}}{U} = -2\text{Im} t_{ij} \left( \sum_k t_{jk} t_{ki} \right) \frac{3n(n+1)(2n+1)}{U^3} + \dots$$

In our case, we obtain the following perturbative result:

$$\frac{J_{AA}^{(2)}}{U} = \frac{36}{U^3} t_2 (t_1^2 - 2t_2^2). \quad (33)$$

On the other hand, at this order in perturbation theory, the current between nearest neighbors vanishes.

We finally note that correlations  $\langle J_{AA} J_{AA} \rangle$  between currents belonging to plaquettes that are separated [i.e., not connected by a kinetic term in  $\mathcal{H}_H$  of Eq. (2)] factorize and are proportional to the square of Eq. (33). Therefore the connected

correlation functions of plaquette currents vanish identically for separated plaquettes. This characterizes the Mott insulator phase as a state with local plaquette currents without long-range current-current correlations.

As mentioned at the beginning of the section, RPA is an exact description in the limit of infinite coordination number of the lattice. In the next section, we will use bosonic DMFT to include the next-order correction (i.e., a finite coordination number) and to go beyond RPA.

#### D. DMFT

Bosonic DMFT was originally introduced several years ago [81–85] in analogy to the well-established fermionic DMFT [106]. The method has been successfully applied in the context of topological band insulators with fermions [34,38,39,107]. Here, we use a spatially resolved version, the so-called real-space bosonic DMFT [108]. For completeness, we describe the method briefly.

The essence of DMFT is mapping of the full lattice problem onto a set of local problems. The next-order correction for the self-energy in Eq. (28) is still local in space [in our case, proportional to  $3(t_1^2 + 2t_2^2)$ ] as can be shown by a diagrammatic expansion [104]. To derive a proper local model that goes beyond the Hamiltonian (25), we perform an effective integration over all off-site degrees of freedom and keep only terms of suitable order. We find that the local Hamiltonian is given by a bosonic Anderson impurity model:

$$\mathcal{H}_{\text{AI}}^i = \sum_{l=0}^L (\epsilon_l \hat{a}_l^\dagger \hat{a}_l + V_l \hat{a}_l^\dagger \hat{b}_i + V_l^* \hat{a}_l \hat{b}_i^\dagger + W_l \hat{a}_l \hat{b}_i + W_l^* \hat{a}_l^\dagger \hat{b}_i^\dagger) - \psi_i^{\text{AI}*} \hat{b}_i - \psi_i^{\text{AI}} \hat{b}_i^\dagger + \frac{U}{2} \hat{n}_i (\hat{n}_i - 1) - \mu \hat{n}_i, \quad (34)$$

where index  $l$  counts Anderson orbitals and we allow for complex values of Anderson parameters  $V_l$  and  $W_l$ . The mapping is formally described in detail in Ref. [84]. At this point, it is useful to introduce hybridization functions of the Anderson impurity model:

$$\Delta_{11}(i\omega_n) = \sum_l \frac{|V_l|^2}{\epsilon_l - i\omega_n} + \frac{|W_l|^2}{\epsilon_l + i\omega_n},$$

$$\Delta_{12}(i\omega_n) = \sum_l \frac{V_l^* W_l}{\epsilon_l - i\omega_n} + \frac{V_l W_l^*}{\epsilon_l + i\omega_n}, \quad (35)$$

and  $\Delta_{21}(i\omega_n) = \Delta_{12}(i\omega_n)^*$ ,  $\Delta_{11}(i\omega_n) = \Delta_{22}(i\omega_n)^*$ . The term  $\psi_i^{\text{AI}}$  used in Eq. (34) incorporates a correction with respect to the mean-field result and it reads [84]

$$\psi_i^{\text{AI}} = \sum_j t_{ij} \psi_j - \Delta_{11}(0) \psi_i - \Delta_{12}(0) \psi_i^*.$$

We consider local Green's functions written in the Nambu notation to take into account off-diagonal terms:

$$G_{ii}(\tau_1 - \tau_2) = - \begin{pmatrix} \langle \mathcal{T} \hat{b}_i(\tau_1) \hat{b}_i^\dagger(\tau_2) \rangle & \langle \mathcal{T} \hat{b}_i(\tau_1) \hat{b}_i(\tau_2) \rangle \\ \langle \mathcal{T} \hat{b}_i^\dagger(\tau_1) \hat{b}_i^\dagger(\tau_2) \rangle & \langle \mathcal{T} \hat{b}_i^\dagger(\tau_1) \hat{b}_i(\tau_2) \rangle \end{pmatrix}.$$

The self-energy is obtained from the local Dyson equation

$$G_{ii}^{-1}(i\omega_n) = \begin{pmatrix} i\omega_n + \mu + \Delta_{11}(i\omega_n) - \Sigma_i^{11}(i\omega_n) & \Delta_{12}(i\omega_n) - \Sigma_i^{12}(i\omega_n) \\ \Delta_{21}(i\omega_n) - \Sigma_i^{21}(i\omega_n) & -i\omega_n + \mu + \Delta_{22}(i\omega_n) - \Sigma_i^{22}(i\omega_n) \end{pmatrix}. \quad (36)$$

In analogy to Eq. (29), the real-space Dyson equation takes the following form:

$$G_{ij,\text{lat}}^{-1}(i\omega_n) = \begin{pmatrix} (i\omega_n + \mu - \Sigma_i^{11}(i\omega_n))\delta_{ij} + t_{ij} & -\Sigma_i^{12}(i\omega_n)\delta_{ij} \\ -\Sigma_i^{21}(i\omega_n)\delta_{ij} & (-i\omega_n + \mu - \Sigma_i^{22}(i\omega_n))\delta_{ij} + t_{ij}^* \end{pmatrix}, \quad (37)$$

where we approximate the self-energy by a local contribution from Eq. (36). Finally, we need a criterion to set values of parameters  $\varepsilon_l$ ,  $V_l$ , and  $W_l$  in Eq. (34). To this end, a condition is imposed on the hybridization functions (35). These functions should be optimized such that the two Dyson equations (36) and (37), yield the same values of local Green's functions. Therefore local correlations are treated beyond the mean-field level.

In practice, we iterate a self-consistency loop to fulfill this condition, starting from arbitrary initial values. The local problem (34) is solved by exact diagonalization and we obtain results for the local density  $n_i = \langle \hat{n}_i \rangle$ , density fluctuations  $\Delta n_i = \langle \hat{n}_i^2 \rangle - \langle \hat{n}_i \rangle^2$ , and local condensate order parameter  $\psi_i = \langle \hat{b}_i \rangle$ . Here, we work with a finite lattice consisting of 72 sites that provides the proper sampling of the Brillouin zone that includes its corners [31]. To benchmark our code, we compare our results for hexagonal and triangular lattice (without flux) with accurate results available in the literature [109]. The deviation in the position of tip of the first Mott lobe is of the order of several percent and it is smaller for triangular than for hexagonal lattice, which can be justified by a higher coordination number of the former lattice.

The resulting phase diagram for the model (5) is given in Fig. 1(b). To have  $n = 1$  filling on the superfluid side we adjust the value of the chemical potential  $\mu$ . We find that the Mott domain is extended in comparison to the mean-field result and its ‘‘cusp’’ shape reveals the subtle interplay of two types of hopping, which goes beyond the simple mean-field picture. We can understand this point better by looking at density fluctuations, Fig. 3 and plaquette currents, Figs. 4 and 5.

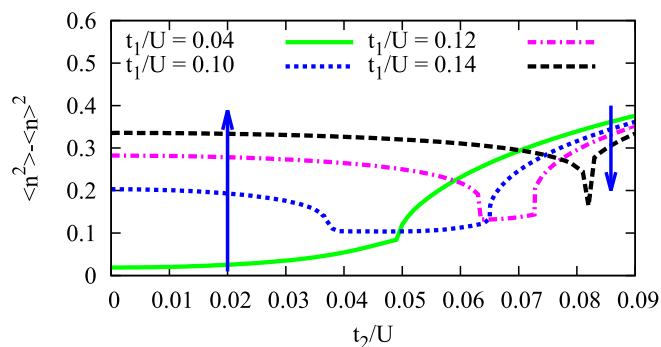


FIG. 3. (Color online) Local density fluctuations  $\langle \hat{n}_i^2 \rangle - \langle \hat{n}_i \rangle^2$  vs  $t_2$  at unit filling  $n = 1$ . We see a competing effect of  $t_1$  and  $t_2$ , as indicated by arrows: for small values of  $t_2$ ,  $t_1$  enhances fluctuations and drives the transition into SF. The opposite effect is found for strong enough  $t_2$  in CSF, where eventually the effect of  $t_1$  is washed out.

In Fig. 3, we show local density fluctuations for several cuts through the phase diagram. Weak density fluctuations are a hallmark of the Mott insulator phase, while stronger density fluctuations correspond to superfluid phases. In the CSF phase (rightmost part of the plot),  $t_1$  suppresses density fluctuations. This relates to the fact that  $t_1$  pushes the PMI-CSF phase boundary toward higher values of  $t_2$ , Fig. 1(b). Deep in the CSF phase ( $t_2/U > 0.08$ ) the effect is very weak (different curves become indistinguishable) in accordance with our mean-field results. At strong enough values of  $t_1$ , we enter the SF phase (curves in the upper left part of the plot). Finally, dips in the curves mark the reentrant transition from SF into PMI.

Next, we turn to bond currents between next-nearest neighbors, Figs. 4 and 5. In Fig. 4, we observe that in the PMI our numerical results are in good agreement with Eq. (33) and the current  $J_{AA}$  changes its sign smoothly here. In the limit of weak hopping the sign change occurs for  $t_1 = \sqrt{2}t_2$ , Fig. 4. At stronger values of  $t_1$  and  $t_2$ , there are more features showing up, Fig. 5. In agreement with Eqs. (13) and (18),  $J_{AA}$  is positive in the SF, and negative in the CSF. By increasing  $t_2$  and keeping  $t_1$  small enough (for example,  $t_1/U = 0.04$  in Fig. 5) we reach the point of the second order PMI-CSF transition. The aforementioned reentrant phase transition is marked by two second-order phase transitions from the SF into PMI and from the PMI into the CSF, for example for  $t_1/U = 0.10$ . It is interesting to note the nonmonotonic behavior—the absolute value of  $J_{AA}$  initially exhibits a linear increase with  $t_2$ , but

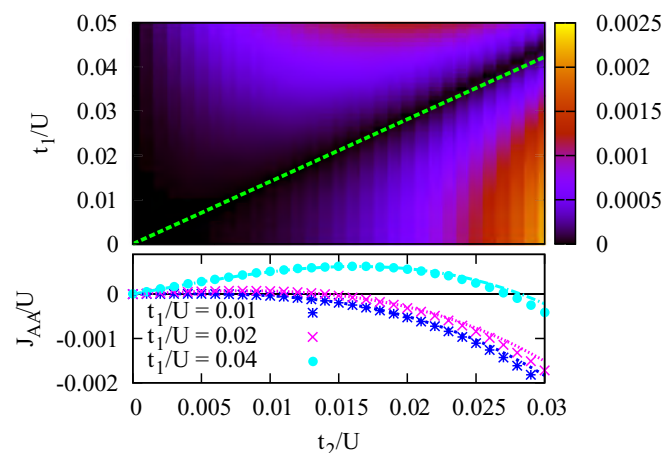


FIG. 4. (Color online) (Top) Absolute value of the next-nearest neighbor bond current  $|J_{AA}|/U$  deep in MI. The dashed line  $t_1 = \sqrt{2}t_2$  marks the region  $J_{AA} = 0$  according to Eq. (33). (Bottom) DMFT data for  $J_{AA}$  (dots) agree very well with the result Eq. (33) (lines) in this region of the phase diagram.

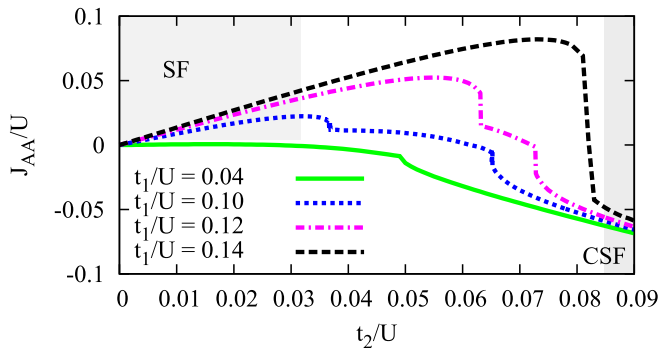


FIG. 5. (Color online) The  $J_{AA}$  current vs  $t_2$  for  $n = 1$  and several values of  $t_1$ . Deep in SF (upper left) the current is positive and exhibits linear increase with  $t_2$ . In CSF (bottom right), the current is negative, strongly dependent on  $t_2$  and only weakly affected by  $t_1$ . The absolute value  $|J_{AA}|$  is much weaker in MI (intermediate regions).

as we approach the Mott domain it decays due to a reduced value of the order parameter. At strong enough  $t_1$  and  $t_2$ , we expect the intermediate Mott domain to vanish and the first order phase transition described in Sec. III A to set in.

### E. Exact diagonalization

In this section, we use the ALPS implementation [110] of the Lanczos algorithm [111] in order to study the ground state of the interacting model in Eq. (5) at unit filling  $n = 1$ . We consider a lattice of  $3 \times 3$  unit cells, implying  $N_{\text{sites}} = 18$  and  $N = 18$  particles. The truncated boson Hilbert space contains states for which the number expectation value at any site is bounded above  $\langle n_i \rangle \leq 2$ . The Hilbert subspace with this constraint has dimension 4 4152 809. With periodic boundary conditions, total momentum  $\mathbf{Q} = \sum_{i=1}^N \mathbf{k}_i$  is a good quantum number and the dimension of the Hilbert space for each momentum sector is reduced by a factor of 9. The Brillouin zone contains  $3 \times 3$  points and includes the inequivalent points  $\Gamma$  and  $\mathbf{K}_A, \mathbf{K}_B$ , as shown in Fig. 7.

Since total particle number is conserved, the spontaneous breaking of the  $U(1)$  symmetry is not observable in the ground state. We rather identify the Mott insulator phase as the region of the  $(t_1/U, t_2/U)$  plane where number fluctuations at a site  $\langle n_i^2 \rangle - \langle n_i \rangle^2$  are small [see Fig. 6(d)].

As shown in Sec. III A, bond current expectation values distinguish the chiral superfluid from the uniform superfluid phase. The nearest-neighbor current  $J_{AB}$  vanishes identically at  $n = 1$ . The next-nearest-neighbor bond current  $J_{AA}$  as a function of  $t_1$  and  $t_2$  is consistent with the result from strong-coupling perturbation theory [Eq. (33)]. The next-nearest-neighbor current  $J_{AA}$  changes sign at  $t_1 = t_2 \sqrt{3}$ , and  $J_{BB}$  has analogous behavior [their common absolute value is plotted in Fig. 6(b)]. This is the exact phase boundary found previously in the weakly interacting regime and with DMFT for arbitrarily strong interactions. We thus confirm the existence of the PMI state with nonzero triangular plaquette currents at order  $t_1^2 t_2 / U^3$  but vanishing nearest-neighbor currents.

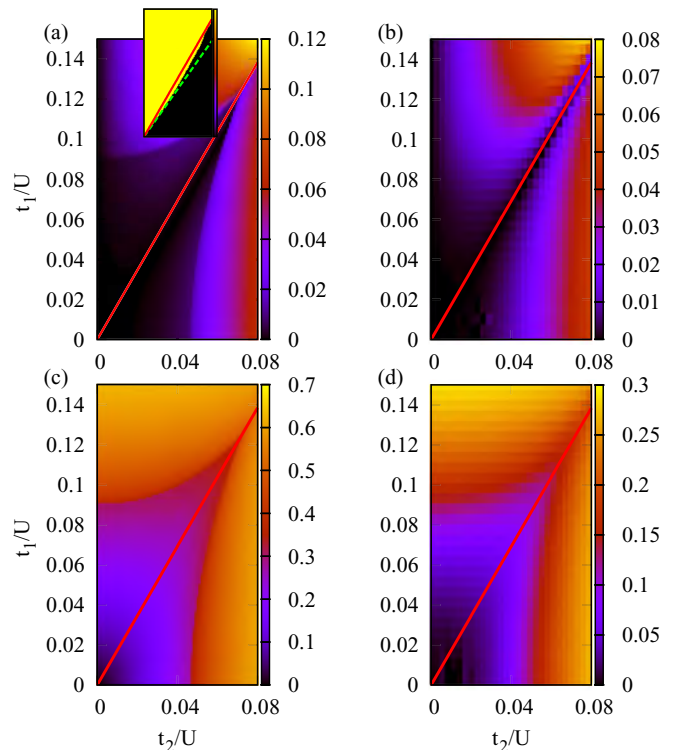


FIG. 6. (Color online) Comparison of DMFT [(a) and (c)] and ED results [(b) and (d)]. Absolute value of the current on the bond between two next-nearest neighbors  $|J_{AA}|/U$  is shown in (a) and (b). In (c) and (d), we plot local density fluctuations  $\langle \hat{n}_i^2 \rangle - \langle \hat{n}_i \rangle^2$ . The inset in (a) gives the sign of  $J_{AA}$ ; in the superfluid, the sign changes for  $t_1 = \sqrt{3}t_2$  (solid line), while deep in the Mott domain the boundary is given by  $t_1 = \sqrt{2}t_2$  (dashed line). DMFT data shown in these plots are for the fixed value of chemical potential  $\mu/U = 0.4$ , while ED results are at fixed filling  $n = 1$ . However, the main features discussed in the text are clearly visible.

To understand the momentum structure of the ground state, we consider the momentum distributions,

$$n_a(\mathbf{k}) \equiv \langle \hat{b}_a^\dagger(\mathbf{k}) \hat{b}_a(\mathbf{k}) \rangle = \sum_j e^{i\mathbf{k} \cdot \mathbf{r}_j} \langle \hat{b}_{a0}^\dagger \hat{b}_{aj} \rangle, \quad (38)$$

where  $a = A$  or  $B$  denotes the sublattice. In agreement with analytical results in the weakly interacting limit (Sec. III A), we find that in the SF the momentum distribution  $n_A(\mathbf{k}) + n_B(\mathbf{k})$  is sharply peaked at the  $\Gamma$  point. In the CSF phase,  $n_a(\mathbf{k})$  are peaked at  $\mathbf{K}_a$ , in agreement with the decoupled condensates wave function  $|\Phi_0'\rangle$  of Eq. (21). In the PMI,  $n_a(\mathbf{k})$  become more and more uniformly distributed as the hopping amplitudes  $t_1$  and  $t_2$  approach 0. Regarding the symmetries, we remark that the nine lattice translation symmetry operators and the lattice inversion symmetry are conserved by the ground state in the  $\mathbf{Q} = 0$  sector. Without breaking the discrete lattice symmetries it is impossible to obtain the coherent superposition  $|\Phi_0'\rangle$ .

In conclusion, we confirm by studying the exact ground state of the  $3 \times 3$  lattice all the qualitative features of the DMFT phase diagram [see Fig. 6 for a comparison]. We can distinguish between the SF and the CSF by studying momentum distributions and currents, and determine sharply the phase boundary between the two superfluids at the critical

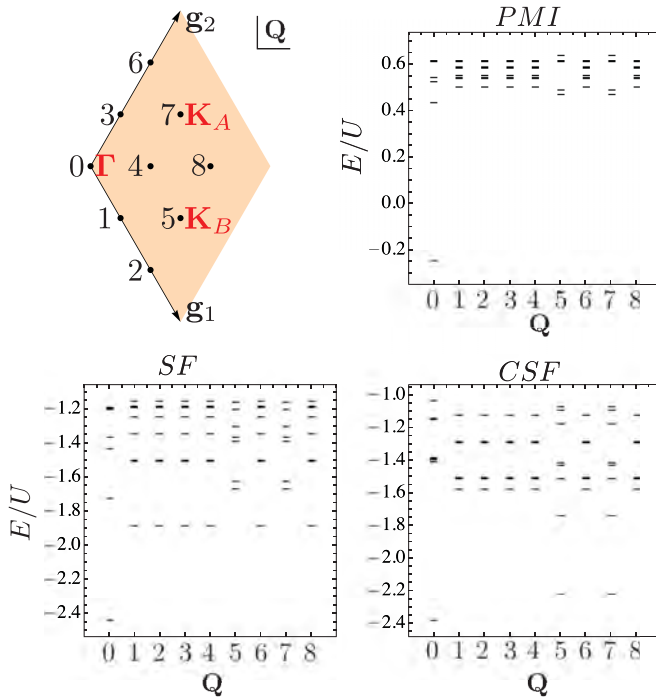


FIG. 7. (Color online) Low-lying energy levels in the spectra of the  $3 \times 3$  unit cell lattice at unit filling, for: PMI ( $t_1/U = 0.04$ ,  $t_2/U = 0.02$ ), SF ( $t_1/U = 0.14$ ,  $t_2/U = 0.02$ ), and CSF ( $t_1/U = 0.04$ ,  $t_2/U = 0.08$ ). The first eight energy levels in each sector of total momentum  $\mathbf{Q}$  are plotted. The nine momentum sectors in the Brillouin zone spanned by the vectors  $\mathbf{g}_1$  and  $\mathbf{g}_2$  are represented in the top left panel. For example, sectors labeled 0, 7, 5 correspond to  $\Gamma$ ,  $\mathbf{K}_A$ , and  $\mathbf{K}_B$ , respectively.

line  $t_1 = t_2\sqrt{3}$  by detecting the change in sign of the next-nearest-neighbor currents  $J_{AA}$  or  $J_{BB}$ .

We stress that the results obtained in this section are for a finite sized lattice Hamiltonian obeying translation and inversion symmetries. Consequently, the finite size ground state in the  $\mathbf{Q} = 0$  sector obeys these symmetries. For an infinite system obeying all symmetries, the ground state may be identified as a specific linear combination of degenerate ground states that breaks the symmetries [43]. To briefly explore this possibility, we plot the low-energy spectra for each phase, as shown in Fig. 7. In the CSF phase, there are two low-lying states in the  $\mathbf{Q} = \mathbf{K}_A$  and  $\mathbf{Q} = \mathbf{K}_B$  sectors, which may become degenerate with the ground state for an infinite system or as  $U \rightarrow 0$ . However, an analysis of the scaling of the gap with system size is limited by the large dimension of the Hilbert space at unit filling. Moreover, the  $U \rightarrow 0$  limit cannot be rigorously explored numerically due to the necessary truncation of the bosonic Hilbert space.

#### IV. EXCITATIONS

In this section, we study the excitation spectra in the superfluid phases (Sec. IV A) and in the Mott insulator (Sec. IV B).

##### A. Weakly interacting bosons

To compute the excitation spectrum in the weakly interacting limit, we start from the time-dependent GP equation [98]

$$i \frac{\partial \psi_i}{\partial t} = -t_1 \sum_{\langle i|j \rangle} \psi_j - it_2 \sum_{\langle\langle i|j \rangle\rangle} (\pm) \psi_j + U |\psi_i|^2 \psi_i, \quad (39)$$

where we make explicit with  $\langle i|j \rangle$  and  $\langle\langle i|j \rangle\rangle$  that index  $i$  is now fixed and we are summing over its neighbors. The  $\pm$  refers to the sign of the imaginary hopping term along the different directions (additionally, it takes opposite values for the two sublattices). We expand the order parameter in terms of fluctuations  $\delta_i$  around the mean-field solution  $\psi_i^0$  as

$$\psi_i = (\psi_i^0 + \delta_i) \exp(-i\mu t). \quad (40)$$

In the zeroth order in  $\delta_i$  we recover the ground-state equation

$$\mu \psi_i^0 = -t_1 \sum_{\langle i|j \rangle} \psi_j^0 - \sum_{\langle\langle i|j \rangle\rangle} it_2 (\pm) \psi_j^0 + U |\psi_i^0|^2 \psi_i^0, \quad (41)$$

that corresponds to the ground-state energy given by Eq. (12). By keeping terms of the order  $\delta_i$  we obtain an equation that allows the study of excitations:

$$i \frac{\partial \delta_i}{\partial t} = -\mu \delta_i - t_1 \sum_{\langle i|j \rangle} \delta_j - it_2 \sum_{\langle\langle i|j \rangle\rangle} (\pm) \delta_j + U (2|\psi_i^0|^2 \delta_i + (\psi_i^0)^2 \delta_i^*). \quad (42)$$

To decouple Eq. (42) further, we proceed in the standard way:

$$\delta_i = u_i \exp(-i\omega t) + v_i^* \exp(i\omega t), \quad (43)$$

and obtain the set of equations:

$$\begin{aligned} \omega u_i^A &= \delta u_i^A - t_1 \sum_{\langle i|j \rangle} u_j^B - it_2 \sum_{\langle\langle i|j \rangle\rangle} u_j^A (\pm) + U (\psi_i^0)^2 v_i^A, \\ -\omega v_i^A &= \delta v_i^A - t_1 \sum_{\langle i|j \rangle} v_j^B - it_2 \sum_{\langle\langle i|j \rangle\rangle} v_j^A (\mp) + U ((\psi_i^0)^2)^* u_i^A, \\ \omega u_i^B &= \delta u_i^B - t_1 \sum_{\langle i|j \rangle} u_j^A - it_2 \sum_{\langle\langle i|j \rangle\rangle} u_j^B (\mp) + U (\psi_i^0)^2 v_i^B, \\ -\omega v_i^B &= \delta v_i^B - t_1 \sum_{\langle i|j \rangle} v_j^A - it_2 \sum_{\langle\langle i|j \rangle\rangle} v_j^B (\pm) + U ((\psi_i^0)^2)^* u_i^B, \end{aligned} \quad (44)$$

where  $\delta = 2Un - \mu$ . In the next step, we rewrite Eq. (44) in the momentum basis and solve the emerging eigenproblem.

For the SF phase, the relevant matrix is of size  $4 \times 4$ , and since Eqs. (44) exhibit particle-hole symmetry we obtain two particle excitation branches, shown in Figs. 8(a) and 8(b). For the honeycomb lattice without flux, Fig. 8(a), we find a Goldstone mode and a Dirac cone inherited from the noninteracting dispersion relation, shown in the same figure by a solid line. As we increase  $t_2$  but remain in the same phase, the Goldstone mode persists and the sound velocity is unaffected by  $t_2$ . The gap between the two bands in Fig. 8(b) implies that the edge mode structure present in the noninteracting spectrum, arising due to a nontrivial topological index (4), remains intact in the presence of weak interactions [16].

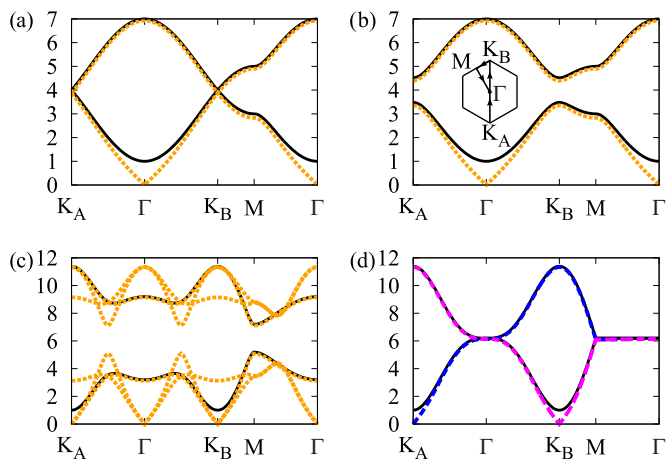


FIG. 8. (Color online) Bogoliubov dispersion relation  $\omega(\mathbf{k})/U$  for  $nU = 1$  and (a)  $t_1 = 1, t_2 = 0$ , (b)  $t_1 = 1, t_2 = 0.1$ , (c)  $t_1 = 1, t_2 = 1$ , (d)  $t_1 = 0, t_2 = 1$ . Black solid lines give the corresponding noninteracting dispersion relation shifted upwards by  $2Un - \mu$ . The inset in (b) defines the path in the Brillouin zone.

In CSF, the mean-field order parameter takes the form:

$$\psi_i^0 = \begin{cases} \sqrt{n} \exp(-i\mathbf{K}_A \mathbf{r}_i) \exp i\phi_A, & i \in A \\ \sqrt{n} \exp(-i\mathbf{K}_B \mathbf{r}_i) \exp i\phi_B, & i \in B \end{cases} \quad (45)$$

where we explicitly consider at the mean-field level two independent superfluids by introducing two angles  $\phi_A$  and  $\phi_B$ . The terms proportional  $(\psi_i^0)^2$  couple different momenta in Eq. (44) [44,45]. In the case of  $t_1 = 0$ ,  $u_{\mathbf{k}}^A$  couples to  $v_{\mathbf{k}-2\mathbf{K}_A}^A$  and  $u_{\mathbf{k}}^B$  couples to  $v_{\mathbf{k}-2\mathbf{K}_B}^B$ . (Vectors  $-\mathbf{K}_A$ ,  $\mathbf{K}_B$ , and  $2\mathbf{K}_A$  are equal up to reciprocal lattice vectors). Therefore we obtain two decoupled eigenproblems for

$$h^A(\mathbf{k}) = \begin{pmatrix} \delta - d_3(\mathbf{k}) & nU \\ -nU & -\delta - d_3(\mathbf{k} + \mathbf{K}_A) \end{pmatrix} \quad (46)$$

and

$$h^B(\mathbf{k}) = \begin{pmatrix} \delta + d_3(\mathbf{k}) & nU \\ -nU & -\delta + d_3(\mathbf{k} - \mathbf{K}_A) \end{pmatrix}, \quad (47)$$

where  $\mathbf{d}(\mathbf{k})$  is given in Eq. (3), that yield the following particle excitations:

$$\omega_A(\mathbf{k}) = \frac{1}{2}[-d_3(\mathbf{k}) - d_3(\mathbf{k} + \mathbf{K}_A) + \sqrt{(d_3(\mathbf{k}) - d_3(\mathbf{k} + \mathbf{K}_A) - 2\delta)^2 - 4n^2U^2}], \quad (48)$$

$$\omega_B(\mathbf{k}) = \frac{1}{2}[d_3(\mathbf{k}) + d_3(\mathbf{k} - \mathbf{K}_A) + \sqrt{(d_3(\mathbf{k}) - d_3(\mathbf{k} - \mathbf{K}_A) + 2\delta)^2 - 4n^2U^2}]. \quad (49)$$

These are shown in Fig. 8(d). We observe two Goldstone modes: one corresponding to the superfluid of sublattice A located around  $\mathbf{K}_A$  and the second one at  $\mathbf{K}_B$ . The inversion symmetry, present when both sublattices are taken into account, provides the particle-hole symmetry also in this case [45].

As the  $t_1$  term is turned on, the three momenta  $\mathbf{k}$ ,  $\mathbf{k} - \mathbf{K}_A$ , and  $\mathbf{k} + \mathbf{K}_A$  are coupled and the eigenproblem corresponding to Eq. (44) is of size  $12 \times 12$ . The related matrix is explicitly

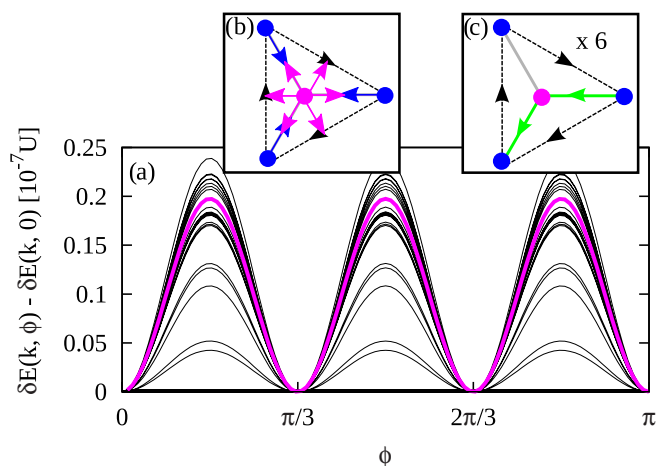


FIG. 9. (Color online) (a) Contribution of quantum fluctuations to the ground-state energy  $\delta E(\mathbf{k}, \phi) - \delta E(\mathbf{k}, 0)$ ,  $t_1 = t_2 = 1$ ,  $nU = 1$ ,  $\phi = \phi_A - \phi_B$ . For a single value of  $\mathbf{k}$ , we obtain the thick curve. The qualitative behavior of  $\delta E(\mathbf{k}, \phi)$  is similar throughout the Brillouin zone (thin lines). In (b), we illustrate the six configurations of order parameters on the two sublattices favoured by quantum fluctuations. In (c), the corresponding emerging plaquette currents are depicted.

given in the Appendix and it incorporates the angles  $\phi_A$  and  $\phi_B$ . An example of the result for the six particle bands is illustrated in Fig. 8(c) for  $\phi_A = \phi_B$ . We observe that the two Goldstone modes persist even at finite  $t_1$ . Some redundancies are present in Fig. 8(c), e.g.  $\mathbf{K}_A$ ,  $\Gamma$ , and  $\mathbf{K}_B$  correspond to the same point, since we have not reduced the Brillouin zone in accordance with the coupling between different momenta.

As mentioned many times throughout the paper, in the CSF at the mean-field level the two sublattices are fully decoupled. We now discuss the role of quantum fluctuations as a beyond mean-field effect that could lift the degeneracy of the mean-field solution and set the value of the phase difference  $\phi = \phi_A - \phi_B$ . The mechanism is known as ‘‘order by disorder’’ [112], and it has been discussed in the context of cold atoms [72,113–115]. The zero-point energy is given by

$$\delta E(\phi) = \sum_{\mathbf{k}} \delta E(\mathbf{k}, \phi) = \frac{1}{2} \sum_{\mathbf{k}, l} \omega_l(\mathbf{k}, \phi) \quad (50)$$

as can be derived using the Bogoliubov approach in the operator formalism [98,114,115]. The index  $l$  enumerates six particle bands. In Fig. 9(a), we show the typical behavior of  $\delta E(\mathbf{k}, \phi) - \delta E(\mathbf{k}, 0)$  throughout the Brillouin zone. The energy differences are typically small, but configurations with  $\phi = m \times \frac{\pi}{3}$ , where  $m$  is an integer [Fig. 9(b)] are preferred. Phase ordering between the sublattices leads to the current patterns shown in Fig. 9(c). These are similar to the patterns discussed in Sec. III B; out of the three nearest-neighbor links shown, one does not carry current and there are two possible directions for the current flow on the two other links. These current patterns are periodic with respect to an enlarged unit cell which consists of six sites. The dependence  $1 - \cos(6\phi)$  can be traced back to the eigenproblem of the matrix (A2). By inspecting the characteristic polynomial (A7), we find that the only contribution of the phase difference  $\phi$  is in the free term as

$\cos(6\phi)$  with proportionality constant  $t_1^6 U^6$ . The contribution vanishes exactly at  $\mathbf{K}_B$  and  $\mathbf{K}_A$ .

Our findings comply to the general rule stating that quantum fluctuations favor colinear (parallel or anti-parallel) order parameters [112]. As cold atoms represent highly tunable and clean systems, the effect could be possibly observed in an experiment. However, it may be difficult to distinguish it from the pinning that arises due to the boundary conditions or defects, discussed in Sec. III B. In addition, thermal effects may be important, but we do not discuss this point further.

## B. Excitations of the Mott phase

In this section, we study quasiparticle or quasihole excitations of the Mott insulator phase. We use the single particle Green's function  $G(i\omega_n, \mathbf{k})$  to compute quasiparticle and quasihole band dispersions. We characterize transport in excited bands through band Chern numbers [2]. We obtain  $G(i\omega_n, \mathbf{k})$  from DMFT and from the strong-coupling random phase approximation [116–118].

### 1. Strong-coupling expansion

We use the results of the strong-coupling expansion with RPA introduced in Sec. III C to study the spectrum of quasiparticle and quasihole excitations. We extend the approach of Sec. III C by grouping the sites on the lattice into identically shaped nonoverlapping clusters [116–118] (e.g., the collection of unit cells pointing along  $\mathbf{a}_1$  is a collection of two site clusters). Starting from the limit of decoupled clusters (intercluster hopping vanishes) we treat intercluster hopping perturbatively, summing all RPA contributions.

Let  $\mathcal{H}'_H$  be the sum of intercluster hopping terms in  $\mathcal{H}_H$ . Let  $\mathcal{H}_I \equiv \mathcal{H} - \mathcal{H}_H$  denote the interaction part of the Hamiltonian. The Hamiltonian of decoupled clusters is

$$\mathcal{H}_C = \mathcal{H}_I + \mathcal{H}_H - \mathcal{H}'_H = \sum_j \mathcal{H}_{C_j}. \quad (51)$$

The sum in the second equality is over decoupled cluster Hamiltonians  $\mathcal{H}_{C_j}$ .

We now define the local Green's function corresponding to one decoupled cluster. Let the ground state of  $\mathcal{H}_{C_j}$  be  $|\Phi_{0j}\rangle$  with ground-state energy  $E_0$ . Denote sites within a cluster using Latin indices  $a, b = A$  or  $B$ , such that  $\hat{b}_{aj}$  annihilates a quasiparticle at the  $a$ th site of the  $j$ th cluster. The local Green's function is

$$\begin{aligned} [G_{jj}^{\text{RPA}}(i\omega_n)]_{ab} = & -\langle \Phi_{0j} | \hat{b}_{bj}^\dagger \frac{1}{i\omega_n - E_0 + \mathcal{H}_{C_j}} \hat{b}_{aj} | \Phi_{0j} \rangle \\ & + \langle \Phi_{0j} | \hat{b}_{aj} \frac{1}{i\omega_n + E_0 - \mathcal{H}_{C_j}} \hat{b}_{bj}^\dagger | \Phi_{0j} \rangle, \end{aligned} \quad (52)$$

for each cluster  $j$ . In what follows, we assume that clusters are identical, and therefore we will drop the cluster index denoting the local Green's function simply by  $[G^{\text{RPA}}(i\omega_n)]_{ab}$ .

Note that Eq. (52) reduces to Eq. (27) of Sec. III C if we consider single-site clusters. The spectral function has a pole at  $nU - \mu$  with residue  $(n + 1)$  and a pole at  $(n - 1)U - \mu$  with residue  $-n$ . If the cluster comprises the unit cell, hybridization from the intracluster kinetic term results in pairs of quasiparticle and quasihole poles.

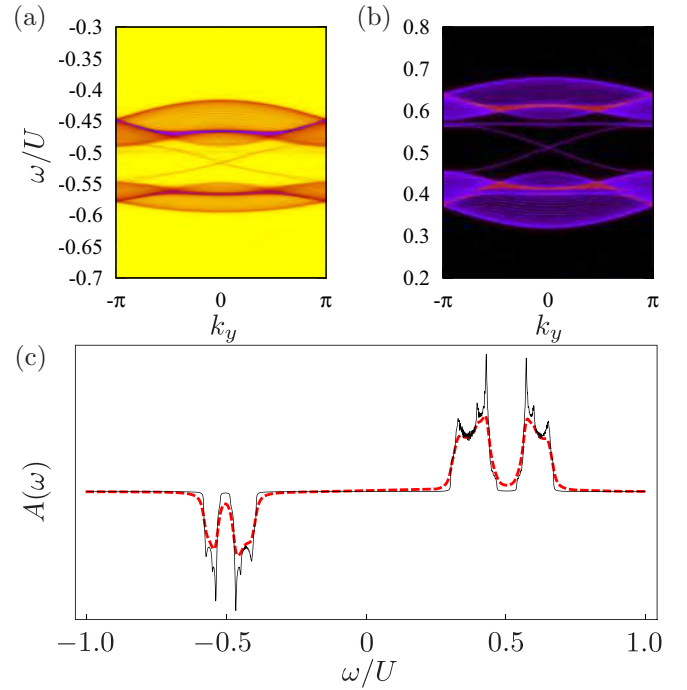


FIG. 10. (Color online) Typical spectral functions deep in the Mott domain, for  $t_1 = 3U/100$ ,  $t_2 = U/100$ ,  $\mu = U/2$ : (a) and (b) quasihole and quasiparticle branches of the spectral function obtained from DMFT for a cylinder geometry exhibiting edge modes for  $\delta = U/1000$ , (c) density of states  $A(\omega)$  (arbitrary units) in a torus geometry for two values of  $\delta$ :  $U/1000$  (solid black line) and  $U/100$  (thick dashed red line). Quasiparticle and quasihole bands are centered at  $U - \mu$  and  $-\mu$ , respectively.

We commit to clusters consisting of a single unit cell. In this case, the RPA approximation to the single particle Green's function is [117,118]

$$[G^{\text{RPA}}(i\omega_n, \mathbf{k})]^{-1} = [G^{\text{RPA}}(i\omega_n)]^{-1} - \mathcal{H}'_H(\mathbf{k}). \quad (53)$$

This is the equivalent of Eq. (30) in the cluster perturbation theory language. The difference is that now all three of  $[G^{\text{RPA}}(i\omega_n, \mathbf{k})]_{ab}$ ,  $[G^{\text{RPA}}(i\omega_n)]_{ab}$  and  $[\mathcal{H}'_H(\mathbf{k})]_{ab}$  are  $2 \times 2$  matrices acting on the sublattice basis. Tracing over sublattice indices in Eq. (53), we obtain the spectral function

$$A(\omega, \mathbf{k}) = -(1/\pi) \text{Tr} \text{Im} G^{\text{RPA}}(\omega, \mathbf{k}). \quad (54)$$

Since  $G^{\text{RPA}}(\omega, \mathbf{k})$  in Eq. (53) is a rational function, the spectral function  $A(\omega, \mathbf{k})$  is a sum of Lorentzians. Deep in the Mott phase, the strong-coupling spectral function agrees with that obtained from DMFT, plotted in Figs. 10(a) and 10(b) for a finite cylinder geometry. Note that the resolution of the edge states is dependent on the inverse lifetime  $\delta$ . In Fig. 10(c), we plot the density of states  $A(\omega) \equiv \int d^2\mathbf{k} A(\omega, \mathbf{k})$  for two values of  $\delta$ . The gap between quasiparticle (hole) bands disappears when the inverse lifetime approaches the bandwidth,  $\delta \sim t_1$ . In the opposite regime, a clear gap is present for  $\delta \ll t_1$ . We note finally that using larger clusters [117,118] yields a  $G^{\text{RPA}}$  whose qualitative features are similar to those of Eq. (53). In particular, this approach will not yield an estimate for the quasiparticle lifetime  $1/\delta$ .



## 2. Chern number of particle or hole excitations

We assume that  $\delta \ll t_1$ , such that the  $G^{\text{RPA}}(\omega, \mathbf{k})$  has well defined quasiparticle and quasihole peaks. We use Greek indices  $\alpha = +, -$  to denote the upper and lower subbands. We denote the quasiparticle dispersion relation as  $\omega_{+, \alpha}(\mathbf{k})$  and the quasihole dispersion relation  $\omega_{-, \alpha}(\mathbf{k})$ . Quasiparticle and quasihole poles arise from the equation

$$\lambda[\omega_{\pm, \alpha}(\mathbf{k}), \mathbf{k}] = 0, \quad (55)$$

where  $\lambda$  denotes any one of the two eigenvalues of  $[G^{\text{RPA}}(\omega, \mathbf{k})]^{-1}$  obtained from Eq. (53). We are interested in band Chern numbers, which arise from the Ishikawa-Matsuyama formula [119] of the many-body Hall conductivity

$$\sigma_{xy} = - \int \frac{d^2 \mathbf{k} d\omega}{8\pi^2} \epsilon^{ij} \text{Tr}[\partial_0 G \partial_i G^{-1} G \partial_j G^{-1}]. \quad (56)$$

The summation over indices  $i, j = 0, 1, 2$  is implicit and  $\epsilon^{ij}$  is the antisymmetric tensor. Integrations are performed over the Brillouin zone and over real frequencies  $\omega$ . We have denoted partial derivatives as  $\partial_j = \partial/\partial k_j$ , where  $k_0 \equiv \omega$ , and  $k_{1,2}$  denote momentum.

Let  $\mathcal{U}(\omega, \mathbf{k})$  be the unitary transformation that diagonalizes  $[G^{\text{RPA}}(\omega, \mathbf{k})]^{-1}$ , that is,

$$[G^{\text{RPA}}]_{ab}^{-1} = \sum_{\alpha\beta} \mathcal{U}_{a\alpha} \lambda_{\alpha} \delta_{\alpha\beta} \mathcal{U}_{\beta b}^{\dagger}. \quad (57)$$

We introduce the matrix of Berry gauge fields

$$\mathcal{A}_{\alpha\beta}^j = \sum_a i \mathcal{U}_{a\alpha} \partial_j \mathcal{U}_{\beta a}^{\dagger}, \quad \text{for } j = 0, 1, 2. \quad (58)$$

Note that the diagonal component  $\mathcal{A}_{\alpha\alpha}^j$  is the Berry gauge field associated with the  $\alpha$ th band. If the Green's function has only simple poles at  $\omega_{\pm, \alpha}(\mathbf{k})$ , then the frequency integral of Eq. (56) can be performed [60,61,120], leading to

$$\sigma_{xy} = - \sum_{\alpha\delta} \int \frac{d^2 \mathbf{k}}{2\pi} \epsilon^{ij} [\mathcal{A}_{\alpha\delta}^i \mathcal{A}_{\delta\alpha}^j + v_{-, \alpha}^i \mathcal{A}_{\alpha\delta}^j \mathcal{A}_{\delta\alpha}^0]_{\omega=\omega_{-, \alpha}(\mathbf{k})}. \quad (59)$$

The frequency integral of Eq. (56) amounts to evaluating the integrand of Eq. (59) at the two quasihole poles  $\omega_{-, \alpha}(\mathbf{k})$ . We have introduced band velocities

$$v_{-, \alpha}^j(\mathbf{k}) \equiv \partial_j \omega_{-, \alpha}(\mathbf{k}). \quad (60)$$

To further simplify Eq. (59), define the on-shell Berry gauge field for quasihole bands as

$$\mathcal{B}_{h, \alpha\beta}^i(\mathbf{k}) = \sum_a i \mathcal{U}_{a\alpha} [\omega_{-, \alpha}(\mathbf{k}), \mathbf{k}] \partial_i \mathcal{U}_{\beta a}^{\dagger} [\omega_{-, \beta}(\mathbf{k}), \mathbf{k}]. \quad (61)$$

Then  $\sigma_{xy}$  measures the flux of the on-shell Berry field strength through the Brillouin zone and splits into a sum over quasihole bands  $\sigma_{xy} = \sum_{\alpha=\pm} \mathcal{C}_{\alpha}$ , where

$$\mathcal{C}_{\alpha} = \frac{1}{2\pi} \int d^2 \mathbf{k} [\partial_1 \mathcal{B}_{h, \alpha\alpha}^2(\mathbf{k}) - \partial_2 \mathcal{B}_{h, \alpha\alpha}^1(\mathbf{k})]. \quad (62)$$

Direct evaluation of Eq. (62) gives  $\mathcal{C}_{\pm} = \pm 1$ . The total Hall conductivity of the two quasihole bands is hence  $\sigma_{xy} = 0$ . This corresponds to the Hall conductivity evaluated in the

Mott gap. Bulk-edge correspondence implies that edge modes exist in the gap between the two quasihole bands, Fig. 10. The quasiparticle bands have  $\mathcal{C}_{\pm} = \mp 1$ , which follows from an analogous calculation.

Small finite inverse lifetime  $\delta$  results in a shift of quasiparticle poles away from the real axis. The results of this subsection for  $\mathcal{C}_{\alpha}$  remain valid as long as a gap exists between quasiparticle bands. Figure 10 shows that whenever the inverse lifetime  $\delta$  is on the order of the kinetic energy strength  $t_1$ , the Mott gap and the two gaps between excited bands are smeared off. It is therefore necessary to require  $\delta \ll t_1$ . Moreover, this allows to resolve intra-gap edge modes from bulk states in the density of states.

The edge modes discussed in this section should be visible either in cold-atom experiments using Bragg spectroscopy [100,121] and photoemission spectroscopy [122] or in photonic systems, where the frequency of the incoming-wave can be adjusted. As mentioned in Sec. II, artificial gauge fields have already been synthesized in photonic systems [12]. The more challenging requirements are photon-photon interactions. However, on a single-cavity level it has been shown that photon-photon interactions can be induced by coupling an off-resonant superconducting qubit to a cavity [14,123].

## V. CONCLUSIONS

In this paper, we have investigated the bosonic Haldane-Hubbard model at unit filling. By combining several numerical and analytical approaches, we have mapped out the phase diagram as a function of two hopping amplitudes and local interaction and found that it consists of two competing types of superfluid and a Mott insulator supporting local plaquette currents. In particular, we found using methods beyond mean-field theory that there is a reentrant transition into the Mott insulator. We have discussed two distinct superfluid ground states. These are connected either by a first order transition in the weakly interacting regime, or via two second order Mott insulator transitions in the strongly interacting regime. Different physical properties of the phases are reflected in the ground-state density fluctuations and plaquette currents between next-nearest neighbors. All these observables are accessible in present-day ultracold atom experiments. In addition to the study of the ground states, we have addressed the excitation spectra in the weakly interacting superfluid and in the Mott domain and found that the corresponding quasiparticle or quasihole excitations consist of bands with nonzero Chern numbers which predict the existence of edge states in the gaps between excited bands.

We expect that our findings can be probed in the near future in ongoing experiments. This work paves the way to open questions about emergent phases at different filling fractions or in multicomponent systems, which we will address in future work. For example, related recent studies [97,124–128] of fermions on the half-filled honeycomb lattice have identified emergence of  $d$ -wave superconducting states close to the Mott transition. Recent work in Ref. [72] discusses a chiral spin superfluid phase of two-component bosons in a double-well potential realized on the honeycomb lattice. This shares some features with our proposal but is nevertheless different.

## ACKNOWLEDGMENTS

Support by the Deutsche Forschungsgemeinschaft (DFG) via Sonderforschungsbereich SFB/TR 49, Forschergruppe FOR 801 and the high-performance computing center LOEWE-CSC is gratefully acknowledged. A.P. acknowledges support from the High Performance Computing facilities of the Faculty of Arts and Sciences at Yale University. This work has also been supported from the Labex Palm, Paris-Saclay. We acknowledge discussions with S. M. Girvin, Markus Mueller, Arun Paramakanti, S. A. Parameswaran, N. Regnault, E. Demler, B. Halperin, F. Sols, and L. Tarruell. K.L.H. also acknowledges discussions at Canadian Institute for Advanced Research meetings in Canada.

## APPENDIX: EXCITATIONS OF THE CHIRAL SUPERFLUID

In this Appendix, we complement derivations of Sec. IV A. In the chiral superfluid at finite values of  $t_1$ , we have coupling of three momenta  $\mathbf{k}$ ,  $\mathbf{k} - \mathbf{K}_A$ , and  $\mathbf{k} + \mathbf{K}_A$  in Eq. (44). Accordingly, we introduce

$$\delta\psi(\mathbf{k}) = (u_{\mathbf{k}}^A, u_{\mathbf{k}-\mathbf{K}_A}^A, u_{\mathbf{k}+\mathbf{K}_A}^A, v_{\mathbf{k}}^A, v_{\mathbf{k}-\mathbf{K}_A}^A, v_{\mathbf{k}+\mathbf{K}_A}^A, u_{\mathbf{k}}^B, u_{\mathbf{k}-\mathbf{K}_A}^B, u_{\mathbf{k}+\mathbf{K}_A}^B, v_{\mathbf{k}}^B, v_{\mathbf{k}-\mathbf{K}_A}^B, v_{\mathbf{k}+\mathbf{K}_A}^B). \quad (\text{A1})$$

The dispersion relation  $\omega(\mathbf{k})$  is obtained by solving the eigenproblem of the  $12 \times 12$  matrix

$$h(\mathbf{k}) = \begin{pmatrix} h_{11} & h_{12} \\ h_{21} & h_{22} \end{pmatrix}, \quad (\text{A2})$$

where

$$h_{11} = \begin{pmatrix} \delta - d_3(\mathbf{k}) & 0 & 0 & 0 & 0 & nUe^{2i\phi_A} \\ 0 & \delta - d_3(\mathbf{k} - \mathbf{K}_A) & 0 & nUe^{2i\phi_A} & 0 & 0 \\ 0 & 0 & \delta - d_3(\mathbf{k} + \mathbf{K}_A) & 0 & nUe^{2i\phi_A} & 0 \\ 0 & -nUe^{-i2\phi_A} & 0 & -\delta - d_3(\mathbf{k}) & 0 & 0 \\ 0 & 0 & -nUe^{-i2\phi_A} & 0 & -\delta - d_3(\mathbf{k} - \mathbf{K}_A) & 0 \\ -nUe^{-i2\phi_A} & 0 & 0 & 0 & 0 & -\delta - d_3(\mathbf{k} + \mathbf{K}_A) \end{pmatrix}, \quad (\text{A3})$$

$$h_{22} = \begin{pmatrix} \delta + d_3(\mathbf{k}) & 0 & 0 & 0 & nUe^{2i\phi_B} & 0 \\ 0 & \delta + d_3(\mathbf{k} - \mathbf{K}_A) & 0 & 0 & 0 & nUe^{2i\phi_B} \\ 0 & 0 & \delta + d_3(\mathbf{k} + \mathbf{K}_A) & nUe^{2i\phi_B} & 0 & 0 \\ 0 & 0 & -nUe^{-i2\phi_B} & -\delta + d_3(\mathbf{k}) & 0 & 0 \\ -nUe^{-i2\phi_B} & 0 & 0 & 0 & -\delta + d_3(\mathbf{k} - \mathbf{K}_A) & 0 \\ 0 & -nUe^{-i2\phi_B} & 0 & 0 & 0 & -\delta + d_3(\mathbf{k} + \mathbf{K}_A) \end{pmatrix}, \quad (\text{A4})$$

$$h_{12} = \text{diag}(-d_1(\mathbf{k}) + id_2(\mathbf{k}), -d_1(\mathbf{k} - \mathbf{K}_A) + id_2(\mathbf{k} - \mathbf{K}_A), -d_1(\mathbf{k} + \mathbf{K}_A) + id_2(\mathbf{k} + \mathbf{K}_A), \\ d_1(\mathbf{k}) - id_2(\mathbf{k}), d_1(\mathbf{k} - \mathbf{K}_A) - id_2(\mathbf{k} - \mathbf{K}_A), d_1(\mathbf{k} + \mathbf{K}_A) - id_2(\mathbf{k} + \mathbf{K}_A)), \quad (\text{A5})$$

and

$$h_{21} = \text{diag}(-d_1(\mathbf{k}) - id_2(\mathbf{k}), -d_1(\mathbf{k} - \mathbf{K}_A) - id_2(\mathbf{k} - \mathbf{K}_A), -d_1(\mathbf{k} + \mathbf{K}_A) - id_2(\mathbf{k} + \mathbf{K}_A), \\ d_1(\mathbf{k}) + id_2(\mathbf{k}), d_1(\mathbf{k} - \mathbf{K}_A) + id_2(\mathbf{k} - \mathbf{K}_A), d_1(\mathbf{k} + \mathbf{K}_A) + id_2(\mathbf{k} + \mathbf{K}_A)). \quad (\text{A6})$$

Here,  $\delta = 2nU - \mu = Un + 3\sqrt{3}t_2$ .

The characteristic polynomial of the matrix (A2) is too long to be written down completely, so we explicitly show only the few most interesting terms:

$$p(x) = x^{12} + x^{10}[6n^2U^2 - 6\delta^2 - 2(\mathbf{d}(\mathbf{k})^2 + \mathbf{d}(\mathbf{k} - \mathbf{K}_A)^2 + \mathbf{d}(\mathbf{k} + \mathbf{K}_A)^2)] + \dots + ()x^2 + \delta^{12} \\ - 2n^6U^6 \cos(6\phi)(d_1(\mathbf{k})^2 + d_2(\mathbf{k})^2)(d_1(\mathbf{k} - \mathbf{K}_A)^2 + d_2(\mathbf{k} - \mathbf{K}_A)^2)(d_1(\mathbf{k} + \mathbf{K}_A)^2 + d_2(\mathbf{k} + \mathbf{K}_A)^2). \quad (\text{A7})$$

[1] D. R. Hofstadter, *Phys. Rev. B* **14**, 2239 (1976).  
 [2] D. J. Thouless, M. Kohmoto, M. P. Nightingale, and M. den Nijs, *Phys. Rev. Lett.* **49**, 405 (1982).  
 [3] F. D. M. Haldane, *Phys. Rev. Lett.* **61**, 2015 (1988).  
 [4] C. L. Kane and E. J. Mele, *Phys. Rev. Lett.* **95**, 226801 (2005).  
 [5] B. A. Bernevig, T. L. Hughes, and S.-C. Zhang, *Science* **314**, 1757 (2006).

[6] J. Cayssol, *C. R. Phys.* **14**, 760 (2013).  
 [7] M. König, S. Wiedmann, C. Brüne, A. Roth, H. Buhmann, L. W. Molenkamp, X.-L. Qi, and S.-C. Zhang, *Science* **318**, 766 (2007).  
 [8] F. D. M. Haldane and S. Raghu, *Phys. Rev. Lett.* **100**, 013904 (2008).  
 [9] S. Raghu and F. D. M. Haldane, *Phys. Rev. A* **78**, 033834 (2008).

- [10] Z. Wang, Y. Chong, J. D. Joannopoulos, and M. Soljacic, *Nature (London)* **461**, 772 (2009).
- [11] H. Hafezi, E. A. Demler, M. D. Lukin, and J. M. Taylor, *Nat. Phys.* **7**, 907 (2011).
- [12] M. Hafezi, S. Mittal, J. Fan, A. Migdall, and J. M. Taylor, *Nat. Photon.* **7**, 1001 (2013).
- [13] M. C. Rechtsman, J. M. Zeuner, Y. Plotnik, Y. Lumer, D. Podolsky, F. Dreisow, S. Nolte, M. Segev, and A. Szameit, *Nature (London)* **496**, 196 (2013).
- [14] I. Carusotto and C. Ciuti, *Rev. Mod. Phys.* **85**, 299 (2013).
- [15] J. Koch, A. A. Houck, K. L. Hur, and S. M. Girvin, *Phys. Rev. A* **82**, 043811 (2010).
- [16] A. Petrescu, A. A. Houck, and K. Le Hur, *Phys. Rev. A* **86**, 053804 (2012).
- [17] A. A. Houck, H. E. Türeci, and J. Koch, *Nat. Phys.* **8**, 292 (2012).
- [18] K. Fang, Z. Yu, and S. Fan, *Nat. Photon.* **6**, 782 (2012).
- [19] V. G. Sala, D. D. Solnyshkov, I. Carusotto, T. Jacqmin, A. Lemaitre, H. Tercas, A. Nalitov, M. Abbarchi, E. Galopin, I. Sagnes, J. Bloch, G. Malpuech, and A. Amo, [arXiv:1406.4816](https://arxiv.org/abs/1406.4816) [cond-mat].
- [20] L. Lu, J. D. Joannopoulos, and M. Soljačić, *Nat. Photon.* **8**, 821 (2014).
- [21] A. B. Khanikaev, S. H. Mousavi, W.-K. Tse, M. Kargarian, A. H. MacDonald, and G. Shvets, *Nat. Mater.* **12**, 233 (2013).
- [22] N. Jia, A. Sommer, D. Schuster, and J. Simon, [arXiv:1309.0878](https://arxiv.org/abs/1309.0878) [cond-mat.mes-hall].
- [23] Y.-J. Lin, K. Jiménez-García, and I. B. Spielman, *Nature (London)* **471**, 83 (2011).
- [24] J. Dalibard, F. Gerbier, G. Juzeliūnas, and P. Öhberg, *Rev. Mod. Phys.* **83**, 1523 (2011).
- [25] N. Goldman, G. Juzeliūnas, P. Öhberg, and I. B. Spielman, *Rep. Prog. Phys.* **77**, 126401 (2014).
- [26] J. Struck, M. Weinberg, C. Ölschläger, P. Windpassinger, J. Simonet, K. Sengstock, R. Höppner, P. Hauke, A. Eckardt, M. Lewenstein, and L. Mathey, *Nat. Phys.* **9**, 738 (2013).
- [27] M. Aidelsburger, M. Atala, M. Lohse, J. T. Barreiro, B. Paredes, and I. Bloch, *Phys. Rev. Lett.* **111**, 185301 (2013).
- [28] H. Miyake, G. A. Siviloglou, C. J. Kennedy, W. C. Burton, and W. Ketterle, *Phys. Rev. Lett.* **111**, 185302 (2013).
- [29] G. Jotzu, M. Messer, R. Desbuquois, M. Lebrat, T. Uehlinger, D. Greif, and T. Esslinger, *Nature (London)* **515**, 237 (2014).
- [30] S. Raghu, X.-L. Qi, C. Honerkamp, and S.-C. Zhang, *Phys. Rev. Lett.* **100**, 156401 (2008).
- [31] C. N. Varney, K. Sun, M. Rigol, and V. Galitski, *Phys. Rev. B* **82**, 115125 (2010).
- [32] D. Pesin and L. Balents, *Nat. Phys.* **6**, 376 (2010).
- [33] S. Rachel and K. Le Hur, *Phys. Rev. B* **82**, 075106 (2010).
- [34] W. Wu, S. Rachel, W.-M. Liu, and K. Le Hur, *Phys. Rev. B* **85**, 205102 (2012).
- [35] M. Hohenadler, T. C. Lang, and F. F. Assaad, *Phys. Rev. Lett.* **106**, 100403 (2011).
- [36] M. Hohenadler and F. F. Assaad, *J. Phys.: Condens. Matter* **25**, 143201 (2013).
- [37] A. Rüegg and G. A. Fiete, *Phys. Rev. Lett.* **108**, 046401 (2012).
- [38] D. Cocks, P. P. Orth, S. Rachel, M. Buchhold, K. Le Hur, and W. Hofstetter, *Phys. Rev. Lett.* **109**, 205303 (2012).
- [39] P. P. Orth, D. Cocks, S. Rachel, M. Buchhold, K. Le Hur, and W. Hofstetter, *J. Phys. B* **46**, 134004 (2013).
- [40] T. Liu, B. Doucot, and K. Le Hur, *Phys. Rev. B* **88**, 245119 (2013).
- [41] L.-K. Lim, C. M. Smith, and A. Hemmerich, *Phys. Rev. Lett.* **100**, 130402 (2008).
- [42] L.-K. Lim, A. Hemmerich, and C. M. Smith, *Phys. Rev. A* **81**, 023404 (2010).
- [43] G. Möller and N. R. Cooper, *Phys. Rev. A* **82**, 063625 (2010).
- [44] S. Powell, R. Barnett, R. Sensarma, and S. Das Sarma, *Phys. Rev. Lett.* **104**, 255303 (2010).
- [45] S. Powell, R. Barnett, R. Sensarma, and S. Das Sarma, *Phys. Rev. A* **83**, 013612 (2011).
- [46] M. P. A. Fisher, P. B. Weichman, G. Grinstein, and D. S. Fisher, *Phys. Rev. B* **40**, 546 (1989).
- [47] M. Greiner, O. Mandel, T. W. Hänsch, and I. Bloch, *Nature (London)* **419**, 51 (2002).
- [48] M. Niemeyer, J. K. Freericks, and H. Monien, *Phys. Rev. B* **60**, 2357 (1999).
- [49] R. O. Umucalilar and M. O. Oktel, *Phys. Rev. A* **76**, 055601 (2007).
- [50] D. S. Goldbaum and E. J. Mueller, *Phys. Rev. A* **77**, 033629 (2008).
- [51] S. Sinha and K. Sengupta, *Europhys. Lett.* **93**, 30005 (2011).
- [52] J. Yao and S. Zhang, *Phys. Rev. A* **90**, 023608 (2014).
- [53] A. Sterdyniak, N. Regnault, and G. Möller, *Phys. Rev. B* **86**, 165314 (2012).
- [54] S. D. Huber and N. H. Lindner, *Proc. Natl. Acad. Sci. USA* **108**, 19925 (2011).
- [55] N. R. Cooper and J. Dalibard, *Phys. Rev. Lett.* **110**, 185301 (2013).
- [56] A. Dhar, M. Maji, T. Mishra, R. V. Pai, S. Mukerjee, and A. Paramekanti, *Phys. Rev. A* **85**, 041602 (2012).
- [57] A. Dhar, T. Mishra, M. Maji, R. V. Pai, S. Mukerjee, and A. Paramekanti, *Phys. Rev. B* **87**, 174501 (2013).
- [58] M. P. Zaletel, S. A. Parameswaran, A. Rüegg, and E. Altman, *Phys. Rev. B* **89**, 155142 (2014).
- [59] D. Hueriga, J. Dukelsky, N. Laflorencie, and G. Ortiz, *Phys. Rev. B* **89**, 094401 (2014).
- [60] C. H. Wong and R. A. Duine, *Phys. Rev. Lett.* **110**, 115301 (2013).
- [61] C. H. Wong and R. A. Duine, *Phys. Rev. A* **88**, 053631 (2013).
- [62] M. Atala, M. Aidelsburger, M. Lohse, J. T. Barreiro, B. Paredes, and I. Bloch, *Nat. Phys.* **10**, 588 (2014).
- [63] E. Orignac and T. Giamarchi, *Phys. Rev. B* **64**, 144515 (2001).
- [64] A. Petrescu and K. Le Hur, *Phys. Rev. Lett.* **111**, 150601 (2013).
- [65] D. Hügél and B. Paredes, *Phys. Rev. A* **89**, 023619 (2014).
- [66] A. Tokuno and A. Georges, *New J. Phys.* **16**, 073005 (2014).
- [67] R. Wei and E. J. Mueller, *Phys. Rev. A* **89**, 063617 (2014).
- [68] S.-L. Zhu, Z.-D. Wang, Y.-H. Chan, and L.-M. Duan, *Phys. Rev. Lett.* **110**, 075303 (2013).
- [69] F. Grusdt, M. Höning, and M. Fleischhauer, *Phys. Rev. Lett.* **110**, 260405 (2013).
- [70] X. Deng and L. Santos, *Phys. Rev. A* **89**, 033632 (2014).
- [71] Z.-X. Liu, Z.-C. Gu, and X.-G. Wen, *Phys. Rev. Lett.* **113**, 267206 (2014).
- [72] X. Li, S. S. Natu, A. Paramekanti, and S. Das Sarma, *Nat. Commun.* **5**, 5174 (2014).
- [73] M. Piraud, Z. Cai, I. P. McCulloch, and U. Schollwöck, *Phys. Rev. A* **89**, 063618 (2014).
- [74] N. Regnault and T. Senthil, *Phys. Rev. B* **88**, 161106 (2013).

- [75] T. A. Sedrakyan, A. Kamenev, and L. I. Glazman, *Phys. Rev. A* **86**, 063639 (2012).
- [76] L. B. Shao, S.-L. Zhu, L. Sheng, D. Y. Xing, and Z. D. Wang, *Phys. Rev. Lett.* **101**, 246810 (2008).
- [77] T. D. Stanescu, V. Galitski, J. Y. Vaishnav, C. W. Clark, and S. Das Sarma, *Phys. Rev. A* **79**, 053639 (2009).
- [78] N. Goldman, E. Anisimovas, F. Gerbier, P. Öhberg, I. B. Spielman, and G. Juzeliūnas, *New J. Phys.* **15**, 013025 (2013).
- [79] E. Anisimovas, F. Gerbier, T. Andrijauskas, and N. Goldman, *Phys. Rev. A* **89**, 013632 (2014).
- [80] J. Ibañez-Azpiroz, A. Eiguren, A. Bergara, G. Pettini, and M. Modugno, *Phys. Rev. A* **90**, 033609 (2014).
- [81] K. Byczuk and D. Vollhardt, *Phys. Rev. B* **77**, 235106 (2008).
- [82] W.-J. Hu and N.-H. Tong, *Phys. Rev. B* **80**, 245110 (2009).
- [83] A. Hubener, M. Snoek, and W. Hofstetter, *Phys. Rev. B* **80**, 245109 (2009).
- [84] M. Snoek and W. Hofstetter, *Quantum Gases: Finite Temperature and Non-Equilibrium Dynamics* (Imperial College Press, London, 2013).
- [85] P. Anders, E. Gull, L. Pollet, M. Troyer, and P. Werner, *Phys. Rev. Lett.* **105**, 096402 (2010).
- [86] N. H. Lindner, G. Refael, and V. Galitski, *Nat. Phys.* **7**, 490 (2011); T. Kitagawa, E. Berg, M. Rudner, and E. Demler, *Phys. Rev. B* **82**, 235114 (2010); J. Cayssol, B. Dóra, F. Simon, and R. Moessner, *Phys. Status Solidi (RRL)* **7**, 101 (2013).
- [87] M. S. Rudner, N. H. Lindner, E. Berg, and M. Levin, *Phys. Rev. X* **3**, 031005 (2013).
- [88] D. Carpentier, P. Delplace, M. Fruchart, and K. Gawędzki, [arXiv:1407.7747](https://arxiv.org/abs/1407.7747) [cond-mat.mes-hall].
- [89] H. Dehghani, T. Oka, and A. Mitra, *Phys. Rev. B* **90**, 195429 (2014).
- [90] T. Ozawa and I. Carusotto, *Phys. Rev. Lett.* **112**, 133902 (2014).
- [91] M. Hafezi, *Phys. Rev. Lett.* **112**, 210405 (2014).
- [92] P. Roushan, C. Neill, Y. Chen, M. Kolodrubetz, C. Quintana, N. Leung, M. Fang, R. Barends, B. Campbell, Z. Chen, B. Chiaro, A. Dunsworth, E. Jeffrey, J. Kelly, A. Megrant, J. Mutus, P. O'Malley, D. Sank, A. Vainsencher, J. Wenner, T. White, A. Polkovnikov, A. N. Cleland, and J. M. Martinis, *Nature (London)* **515**, 241 (2014); M. D. Schroer, M. H. Kolodrubetz, W. F. Kindel, M. Sandberg, J. Gao, M. R. Vissers, D. P. Pappas, Anatoli Polkovnikov, and K. W. Lehnert, *Phys. Rev. Lett.* **113**, 050402 (2014).
- [93] L. J. LeBlanc, K. Jiménez-García, R. A. Williams, M. C. Beeler, A. R. Perry, W. D. Phillips, and I. B. Spielman, *Proc. Natl. Acad. Sci. USA* **109**, 10811 (2012).
- [94] H. M. Price and N. R. Cooper, *Phys. Rev. Lett.* **111**, 220407 (2013).
- [95] L. Duca, T. Li, M. Reitter, I. Bloch, M. Schleier-Smith, and U. Schneider, *Science* **347**, 288 (2015).
- [96] M. Aidelsburger, M. Lohse, C. Schweizer, M. Atala, J. T. Barreiro, S. Nascimbène, N. R. Cooper, I. Bloch, and N. Goldman, *Nat. Phys.* **11**, 162 (2015).
- [97] Z.-C. Gu, H.-C. Jiang, D. N. Sheng, H. Yao, L. Balents, and X.-G. Wen, *Phys. Rev. B* **88**, 155112 (2013).
- [98] L. Pitaevskii and S. Stringari, *Bose-Einstein Condensation* (Clarendon Press, Oxford, 2003).
- [99] A. J. Leggett, *Rev. Mod. Phys.* **73**, 307 (2001).
- [100] U. Bissbort, S. Götze, Y. Li, J. Heinze, J. S. Krauser, M. Weinberg, C. Becker, K. Sengstock, and W. Hofstetter, *Phys. Rev. Lett.* **106**, 205303 (2011).
- [101] K. V. Krutitsky and P. Navez, *Phys. Rev. A* **84**, 033602 (2011).
- [102] D. van Oosten, P. van der Straten, and H. T. C. Stoof, *Phys. Rev. A* **63**, 053601 (2001).
- [103] K. Sengupta and N. Dupuis, *Phys. Rev. A* **71**, 033629 (2005).
- [104] J. K. Freericks, H. R. Krishnamurthy, Y. Kato, N. Kawashima, and N. Trivedi, *Phys. Rev. A* **79**, 053631 (2009).
- [105] J. K. Freericks, H. R. Krishnamurthy, Y. Kato, N. Kawashima, and N. Trivedi, *Phys. Rev. A* **85**, 019913(E) (2012).
- [106] A. Georges, G. Kotliar, W. Krauth, and M. J. Rozenberg, *Rev. Mod. Phys.* **68**, 13 (1996).
- [107] A. Go, W. Witczak-Krempa, G. S. Jeon, K. Park, and Y. B. Kim, *Phys. Rev. Lett.* **109**, 066401 (2012).
- [108] Y. Li, M. R. Bakhtiari, L. He, and W. Hofstetter, *Phys. Rev. B* **84**, 144411 (2011).
- [109] N. Teichmann, D. Hinrichs, and M. Holthaus, *Europhys. Lett.* **91**, 10004 (2010).
- [110] B. Bauer, L. D. Carr, H. G. Evertz, A. Feiguin, J. Freire, S. Fuchs, L. Gamper, J. Gukelberger, E. Gull, S. Guertler, A. Hehn, R. Igarashi, S. V. Isakov, D. Koop, P. N. Ma, P. Mates, H. Matsuo, O. Parcollet, G. Pawłowski, J. D. Picon, L. Pollet, E. Santos, V. W. Scarola, U. Schollwöck, C. Silva, B. Surer, S. Todo, S. Trebst, M. Troyer, M. L. Wall, P. Werner, and S. Wessel, *J. Stat. Mech.* (2011) P05001.
- [111] J. Cullum and R. A. Willoughby, *Lanczos Algorithms for Large Symmetric Eigenvalue Computations: Vol. 1: Theory* (Birkhäuser, Boston, 1985).
- [112] C. L. Henley, *Phys. Rev. Lett.* **62**, 2056 (1989).
- [113] C. J. Pethick and H. Smith, *Bose-Einstein Condensation in Dilute Gases* (Cambridge University Press, Cambridge, UK, 2008).
- [114] R. Barnett, S. Powell, T. Graß, M. Lewenstein, and S. Das Sarma, *Phys. Rev. A* **85**, 023615 (2012).
- [115] Y.-Z. You, Z. Chen, X.-Q. Sun, and H. Zhai, *Phys. Rev. Lett.* **109**, 265302 (2012).
- [116] S. Pairault, D. Sénéchal, and A.-M. S. Tremblay, *Eur. Phys. J. B* **16**, 85 (2000).
- [117] D. Sénéchal, D. Perez, and M. Pioro-Ladrière, *Phys. Rev. Lett.* **84**, 522 (2000).
- [118] D. Sénéchal, D. Perez, and D. Plouffe, *Phys. Rev. B* **66**, 075129 (2002).
- [119] K. Ishikawa and T. Matsuyama, *Nucl. Phys. B* **280**, 523 (1987).
- [120] R. Shindou and L. Balents, *Phys. Rev. Lett.* **97**, 216601 (2006).
- [121] N. Goldman, J. Beugnon, and F. Gerbier, *Phys. Rev. Lett.* **108**, 255303 (2012).
- [122] J. T. Stewart, J. P. Gaebler, and D. S. Jin, *Nature (London)* **454**, 744 (2008).
- [123] A. J. Hoffman, S. J. Srinivasan, S. Schmidt, L. Spietz, J. Aumentado, H. E. Türeci, and A. A. Houck, *Phys. Rev. Lett.* **107**, 053602 (2011).
- [124] K. Le Hur and T. M. Rice, *Ann. Phys. (NY)* **324**, 1452 (2009).
- [125] W. Wu, M. M. Scherer, C. Honerkamp, and K. Le Hur, *Phys. Rev. B* **87**, 094521 (2013).
- [126] R. Nandkishore, L. S. Levitov, and A. V. Chubukov, *Nat. Phys.* **8**, 158 (2012).
- [127] A. M. Black-Schaffer and C. Honerkamp, *J. Phys.: Condens. Matter* **26**, 423201 (2014).
- [128] A. M. Black-Schaffer, W. Wu, and K. Le Hur, *Phys. Rev. B* **90**, 054521 (2014).

Organized by:



Department of Physics  
Faculty of Science,  
University of Zagreb

UNITY THROUGH  
KNOWLEDGE FUND



Institute of Physics,  
Zagreb

INSTITUT ZA FIZIKU

29 September – 1 October 2015

Zagreb, Croatia

Topological effects and synthetic gauge/magnetic fields for atoms and photons

**Invited speakers:**

Demetrios Christodoulides  
Klaus Sengstock  
Gennady Shvets  
Michael Fleischhauer  
Francesca Ferlino  
Gediminas Juzeliunas  
Fabrice Gerbier  
Alex Szameit  
Darrick Chang  
Mikael Rechtsman  
Zhigang Chen  
Thomas Pohl  
Marcello Dalmonte  
Thomas Gasenzer  
Netanel Lindner  
Giorgos Tsironis  
Ivana Vasić  
Gregor Jotzu

**Scientific organizing committee:**

Hrvoje Buljan  
Mordechai Segev  
Marin Soljačić

**Local organizing committee:**

Hrvoje Buljan  
Ticijana Ban  
Damir Aumiler  
Robert Pezer  
Karlo Lelas  
Neven Šantić  
Tena Dubček

*synthF*  
Zagreb

[synthetic.ifs.hr](http://synthetic.ifs.hr)



# Bosonic Phases On The Haldane Honeycomb Lattice

Vasić, I (1); Petrescu, A (2,3); Le Hur, K (2); Hofstetter, W (4);

Contact: ivana.vasic@ipb.ac.rs

(1) *Scientific Computing Laboratory, Institute of Physics Belgrade, University of Belgrade, Belgrade, Serbia*

(2) *Centre de Physique Theorique, Ecole Polytechnique, CNRS, 91128 Palaiseau Cedex, France*

(3) *Department of Physics, Yale University, New Haven, Connecticut 06520, USA*

(4) *Institute of Theoretical Physics, Goethe University, Frankfurt/Main, Germany*

Recent experiments [1] in ultracold atoms have reported the implementation of artificial gauge fields in lattice systems. Motivated by such advances, we investigate the Haldane honeycomb lattice tight-binding model [2], for bosons with local interactions at the average filling of one boson per site. We analyze the ground state phase diagram and uncover three distinct phases: a uniform superfluid, a chiral superfluid and a plaquette Mott insulator with local current loops. Nearest-neighbor and next-nearest neighbor currents distinguish CSF from SF, and the phase transition between them is first order. We apply bosonic dynamical mean field theory and exact diagonalization to obtain the phase diagram, complementing numerics with calculations of excitation spectra in strong and weak coupling perturbation theory. The characteristic density fluctuations and excitation spectra can be probed in future experiments.

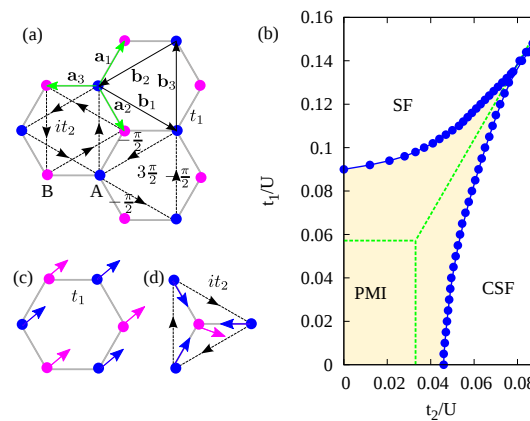


Figure 2.2: a) Lattice vectors and hopping integrals of the Haldane model. b) Phase diagram of the model at unit filling, containing plaquette Mott insulator (PMI), uniform superfluid (SF) and chiral superfluid (CSF) phases. c) Local condensate order parameter in the uniform superfluid; d) In CSF the condensate order parameters on sublattices A and B are determined up to a relative phase.

## References

- [1] G. Jotzu, M. Messer, R. Desbuquois, M. Lebrat, T. Uehlinger, D. Greif, T. Esslinger, *Nature (London)* **515**, 237 (2014).
- [2] I. Vasić, A. Petrescu, K. Le Hur, W. Hofstetter, *Phys. Rev. B* **91**, 094502 (2015).

XIX Symposium on  
Condensed Matter Physics  
SFKM 2015

---

**Book of Abstracts**

---



# Bosonic Phases On The Haldane Honeycomb Lattice

I. Vasić<sup>a</sup>, A. Petrescu<sup>bc</sup>, K. Le Hur<sup>b</sup> and W. Hofstetter<sup>d</sup>

<sup>a</sup>Scientific Computing Laboratory, Institute of Physics, University of Belgrade, Belgrade, Serbia

<sup>b</sup>Centre de Physique Theorique, Ecole Polytechnique, CNRS, 91128 Palaiseau Cedex, France

<sup>c</sup>Department of Physics, Yale University, New Haven, Connecticut 06520, USA

<sup>d</sup>Institute of Theoretical Physics, Goethe University, Frankfurt/Main, Germany

**Abstract.** Recent experiments [1] in ultracold atoms have reported the implementation of artificial gauge fields in lattice systems. Motivated by such advances, we investigate the Haldane honeycomb lattice tight-binding model [2], for bosons with local interactions at the average filling of one boson per site. We analyze the ground state phase diagram and uncover three distinct phases: a uniform superfluid, a chiral superfluid and a plaquette Mott insulator with local current loops. We apply bosonic dynamical mean field theory and exact diagonalization to obtain the phase diagram, complementing numerics with calculations of excitation spectra in strong and weak coupling perturbation theory. The characteristic density fluctuations and excitation spectra can be probed in future experiments.

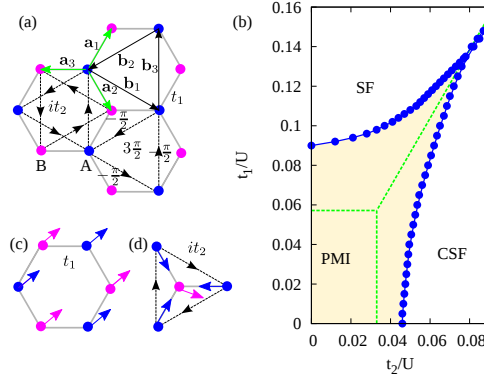


**FIGURE 1.** a) Lattice vectors and hopping integrals the Haldane model. b) Phase diagram of the model at unit filling, containing plaquette Mott insulator (PMI), uniform superfluid (SF) and chiral superfluid (CSF) phases. c) Local condensate order parameter in the uniform superfluid; d) In CSF the condensate order parameters on sublattices A and B are determined up to a relative phase.

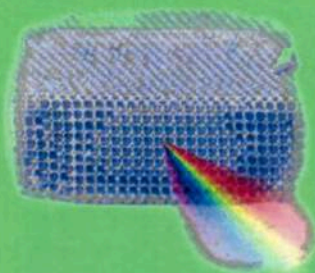
## REFERENCES

1. Jotzu, G., Messer, M., Desbuquois, R., Lebrat, M., Uehlinger, T., Greif, D., and Esslinger, T., *Nature (London)* **515**, 237-240 (2014).
2. Haldane, F. D. M., *Phys. Rev. Lett.* **61**, 2015 (1988).
3. Vasić, I., Petrescu, A., Le Hur, K., and Hofstetter, W., *Phys. Rev. B* **91**, 094502 (2015).



UNIVERZITET U BEOGRADU

Institut za fiziku



Konferencija

# Osma radionica fotonike (2015)

Zbornik apstrakata



Kopaonik, 8.–12. marta 2015.

## Chiral Bosonic Phases on the Haldane Honeycomb Lattice

Ivana Vasic<sup>1</sup>, Alex Petrescu<sup>2</sup>, Karyn Le Hur<sup>3</sup>, Walter Hofstetter<sup>4</sup>

<sup>1</sup>Scientific Computing Laboratory, Institute of Physics, Pregrevica 118, 11080 Belgrade, Serbia

<sup>2</sup>Department of Physics, Yale University, New Haven CT 06520, USA

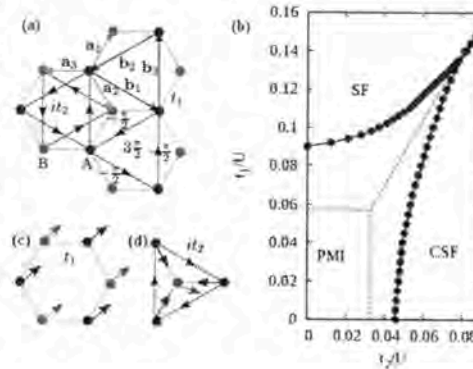
<sup>3</sup>Centre de Physique Theorique, Ecole Polytechnique, CNRS, 91128 Palaiseau Cedex, France

<sup>4</sup>ITP, Goethe University, 60438 Frankfurt/Main, Germany

Contact: I. Vasic (ivanavi@ipb.ac.rs)

**Abstract.** Recent experiments in ultracold atoms [1] and photonic analogs have reported the implementation of artificial gauge fields in lattice systems, facilitating the realization of topological phases. Motivated by such advances, we investigate the Haldane honeycomb lattice tight-binding model, for bosons with local interactions at the average filling of one boson per site [2]. We analyze the ground state phase diagram and uncover three distinct phases: a uniform superfluid *SF*, a chiral superfluid *CSF* and a plaquette Mott insulator with local current loops *PMI*. Nearest-neighbor and next-nearest neighbor currents distinguish *CSF* from *SF*, and the phase transition between them is first order. We apply bosonic dynamical mean field theory and exact diagonalization to obtain the phase diagram, complementing numerics with calculations of excitation spectra in strong and weak coupling perturbation theory. The characteristic density fluctuations, current correlation functions, and excitation spectra are measurable in ultracold atom experiments

Figure 1. **a)** Lattice vectors on the honeycomb lattice and hopping integrals the Haldane model. **b)** Phase diagram of the model at unit filling, containing plaquette Mott insulator (*PMI*), uniform superfluid (*SF*) and chiral superfluid (*CSF*) phases. Solid (dashed) lines represent DMFT (Gutzwiller mean-field) results. **c)** Local condensate order parameter in the uniform superfluid; **d)** In *CSF* the condensate order parameters on sublattices A and B are determined up to a relative phase.



### REFERENCES

- [1] G. Jotzu, M. Messer, R. Desbuquois, M. Lebrat, T. Uehlinger, D. Greif, and T. Esslinger, *Nature* (London) **515** (2014), 237.
- [2] I. Vasic, A. Petrescu, K. Le Hur, W. Hofstetter, arXiv: 1408.1411

**Bulletin of the American Physical Society****APS March Meeting 2016**

Volume 61, Number 2

Monday–Friday, March 14–18, 2016; Baltimore, Maryland

**Session L50: Cold Atomic Gases: Precision Measurement and Few-Body Physics**

11:15 AM–1:51 PM, Wednesday, March 16, 2016

Hilton Baltimore Room: Holiday Ballroom 1

Sponsoring Unit: DAMOP

Chair: Shina Tan, Georgia Institute of Technology

Abstract ID: BAPS.2016.MAR.L50.10

**Abstract: L50.00010 : The Bosonic Kane-Mele Hubbard model**

1:03 PM–1:15 PM

[Preview Abstract](#)[MathJax On | Off](#)   [← Abstract →](#)**Authors:**

Rajbir Nirwan

(Institut für Theoretische Physik, Goethe-Universität, 60438 Frankfurt/Main, Germany)

Ivana Vasic

(Scientific Computing Laboratory, Institute of Physics Belgrade, University of Belgrade, 11080 Belgrade, Serbia)

Alexandru Petrescu

(Department of Electrical Engineering, Princeton University, Princeton, New Jersey 08544, USA)

Karyn Le Hur

(Centre de Physique Théorique, Ecole Polytechnique and CNRS, Université Paris-Saclay, France)

Walter Hofstetter

(Institut für Theoretische Physik, Goethe-Universität, 60438 Frankfurt/Main, Germany)

We investigate the bosonic equivalent of the Kane-Mele model on the honeycomb lattice [1] including spin-orbit and interaction effects. This model is a generalization of the interacting bosonic Haldane model introduced in Ref. [2]. We also allow for an on-site conversion (coherent) term between the two species. We analyze the phase diagram using bosonic dynamical mean-field theory and analytical methods. In the Mott phase, a strong-coupling expansion is performed to investigate the magnetism and frustration effects. A connection is drawn with the quantum theory of an antiferromagnet on a triangular lattice in a magnetic field [3]. This model can be realized in ultra-cold atom systems with current technology. [1] C. L. Kane and E. Mele, *Phys. Rev. Lett.* 95, 226801 (2005). [2] I. Vasic, A. Petrescu, K. Le Hur and W. Hofstetter, *Phys. Rev. B* 91, 094502 (2015). [3] A. V. Chubukov and D. I. Golosov, *J. Phys. Cond. Matt.* 3 69 (1991).

To cite this abstract, use the following reference: <http://meetings.aps.org/link/BAPS.2016.MAR.L50.10>

---

WILHELM UND ELSE HERAEUS-STIFTUNG



616. WE-Heraeus-Seminar

**Ultracold Quantum Gases -  
Current Trends and  
Future Perspectives**

9 – 13 May 2016  
at the Physikzentrum Bad Honnef/Germany

## Excitation spectra of a Bose-Einstein condensate with an angular spin-orbit coupling

I. Vasić<sup>1</sup> and A. Balaž<sup>1</sup>

<sup>1</sup>Scientific Computing Laboratory, Institute of Physics Belgrade, University of Belgrade, Pregrevica 118, 11080 Belgrade, Serbia  
E-mail: ivana.vasic@ipb.ac.rs

A theoretical model of a Bose-Einstein condensate with an angular spin-orbit coupling has recently been proposed [1,2] and it has been established that a half-skyrmion represents the ground state in a certain regime of spin-orbit coupling and interaction. We investigate low-lying excitations of this phase by using the Bogoliubov method and numerical simulations of the time-dependent Gross-Pitaevskii equation [3]. We find that a sudden shift of the trap bottom results in a complex two-dimensional motion of the system's center of mass of the system that is markedly different from the response of a competing phase, and comprises two dominant frequencies. Moreover, the breathing mode frequency of the half-skyrmion is set by both the spin-orbit coupling and the interaction strength, while in the competing state it takes a universal value. Effects of interactions are especially pronounced at the transition between the two phases.

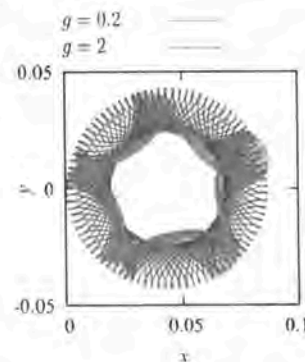


Fig. 1: Center-of-mass motion of a half-skyrmion for two different interaction strengths. Motion is induced by shifting harmonic trap bottom for  $dx=0.02$ .

### References

- [1] M. DeMarco and H. Pu, Phys. Rev. A **91**, 033630 (2015)
- [2] Y.-X. Hu, C. Miniatura, and B. Grémaud, Phys. Rev. A **92**, 033615 (2015)
- [3] I. Vasić and A. Balaž, arXiv:1602.03538

Kopfermann-Straße 1, 85748 Garching, Germany — <sup>2</sup>Fakultät für Physik, Ludwig-Maximilians-Universität München, Schellingstraße 4, 80799 München, Germany

Ultracold atoms in optical lattices provide an ideal testbed for the study of strongly correlated many-body systems. The detection and manipulation of single atoms in two-dimensional optical lattices offer a versatile toolbox to investigate condensed matter models. In our setup we are capable of such control and local detection at the single-atom level by fluorescence-imaging of a two-dimensional bosonic gas of Rubidium-87. In recent work we have investigated Rydberg gases, which feature strong van der Waals interactions and can be used for the study of strongly correlated long-range many-body systems. This has allowed us to observe crystalline states and to microscopically characterize Rydberg superatoms, as well as to detect spin correlations induced by Rydberg-dressed interactions. We have also explored the localization transition occurring in a disordered interacting bosonic system in two dimensions, in which a for large enough disorder strength non-thermal states prevail. To this end we prepare a highly-excited Mott insulator state and study its thermalization in the presence of a random disorder potential.

Q 27.8 Tue 16:30 Empore Lichthof

**Excitations of a Bose–Einstein condensate with angular spin-orbit coupling** — ●IVANA VASIĆ and ANTUN BALAZ — Scientific Computing Laboratory, Institute of Physics Belgrade, University of Belgrade, Pregrevica 118, 11080 Belgrade, Serbia

A theoretical model of a Bose–Einstein condensate with angular spin-orbit coupling has been recently introduced and it has been established that a half-skyrmion configuration represents the ground state in a certain regime of spin-orbit coupling and interaction. We investigate low-lying excitations of this phase by using the method of Bogoliubov and simulations of the time-dependent Gross–Pitaevskii equation. We find that a sudden shift of the trap bottom results in a complex motion of the center-of-mass of the system in the  $x$ - $y$  plane that is markedly different from a response of a competing phase. This behaviour of the half-skyrmion phase comprises a low-frequency interaction-dependent oscillation as well as a high-frequency contribution. Moreover, the breathing mode frequency of the half-skyrmion is set by the spin-orbit coupling and interaction strength, while it takes a universal value in the competing state.

Q 27.9 Tue 16:30 Empore Lichthof

**Observation of a superradiant Mott insulator in the Dicke-Hubbard model** — ●CHRISTOPH GEORGES, HANS KESSLER, JENS KLINDER, JOSE VARGAS, and ANDREAS HEMMERICH — Institut für Laserphysik, Universität Hamburg, Luruper Chaussee 149, D-22761 Hamburg, Germany

It is well known that the bosonic Hubbard model possesses a Mott insulator phase. Likewise, it is known that the Dicke model exhibits a self-organized superradiant phase. By implementing an optical lattice inside of a high finesse optical cavity both models are merged such that an extended Hubbard model with cavity-mediated infinite range interactions arises. In addition to a normal superfluid phase, two superradiant phases are found, one of them coherent and hence superfluid and one incoherent Mott insulating [1].

[1] J. Klinder et al., arXiv:1511.00850

Q 27.10 Tue 16:30 Empore Lichthof

**Direct Observation of Chiral Superfluid Order** — ●CARL HIPPLER, THORGE KOCK, HANNES WINTER, and ANDREAS HEMMERICH — Universität Hamburg

The overall goal of our experiment is to explore ultracold bosonic quantum gases in excited bands of an optical lattice. We investigate Rb-87 atoms in a bipartite interferometric lattice allowing us to change the lattice geometry dynamically. We observe the formation of a chiral superfluid order, arising from the interplay between the contact interaction of the atoms on each lattice site and the degeneracy of the  $p$  orbitals in the second Bloch band. A periodic pattern of locally alternating orbital currents and circular currents establishes in the lattice, time-reversal symmetry being spontaneously broken. We report on a technique that lets us directly observe the phase properties of the superfluid order parameter. Here, two independent atomic samples are produced in the second band at well separated spatial regions of the lattice and subsequently brought to interference.

Q 27.11 Tue 16:30 Empore Lichthof

**Laser using narrow band intercombination line of Calcium** — HANNES WINTER, ●TORBEN LASKE, and ANDREAS HEMMERICH — Institut für Laserphysik, Hamburg

We present our setup for realizing a superradiant laser [1] similar to the proposal to [2] using the narrow Calcium intercombination line  $4^1S_0 \leftrightarrow 4^3P_1$  as the laser transition. Such a laser operates in the bad-cavity regime, in which the coherence is not stored in the intra cavity light field but in the gain medium. The ultracold Calcium atoms are trapped in the Lamb-Dicke regime by a one dimensional intra cavity lattice to control the Doppler effect. Unlike conventional lasers, the expected frequency stability of this light source is not limited by mechanical fluctuations of the cavity length, which yields important implications for applications like time metrology.

[1] M. Holland and J. Thompson et al. Nature, 484(7392):78-81, (2012). [2] M. Holland et al., Phys. Rev. Lett. 102(16):163601, (2009).

Q 27.12 Tue 16:30 Empore Lichthof

**Towards an experimental realization of a periodic quantum Rabi model with ultracold atoms** — SIMONE FELICETTI<sup>1</sup>, ENRIQUE RICO<sup>1,2</sup>, CARLOS SABIN<sup>3</sup>, ●TILL OCKENFELS<sup>4</sup>, MARTIN LEDER<sup>4</sup>, CHRISTOPHER GROSSERT<sup>4</sup>, MARTIN WEITZ<sup>4</sup>, and ENRIQUE SOLANO<sup>1,2</sup> — <sup>1</sup>Department of Physical Chemistry, University of the Basque Country UPV/EHU, Bilbao, Spain — <sup>2</sup>IKERBASQUE, Basque Foundation for Science, Bilbao, Spain — <sup>3</sup>Instituto de Física Fundamental, CSIC, Madrid, Spain — <sup>4</sup>Institut für Angewandte Physik, Universität Bonn, Bonn

The quantum Rabi model [1,2,3] describes the interaction between a two-level quantum system and a single bosonic mode. Whereas the regime of ultra-strong coupling (USC) has just been recently investigated, and an experimental realization of the quantum Rabi model in the deep strong coupling (DSC) regime has so far been absent. We propose a setup to perform a full quantum simulation of the quantum Rabi model regarding an effective two-level quantum system, provided by the occupation of Bloch bands by ultra-cold atoms in tailored optical lattices [4], interacting with a quantum harmonic oscillator implemented with an optical dipole trap. This setup will enable us to study the crossover between USC and DSC regimes, where a pattern of collapse and revival is predicted.

[1] I.I. Rabi, Phys. Rev 49, 324 (1936).

[2] D. Braak, Phys. Rev. Lett. 107, 100401 (2011).

[3] J. Casanova et al., Phys. Rev. Lett. 105, 263603 (2010).

[4] T. Salger et al., Phys. Rev. Lett. 107, 240401 (2011).

Q 27.13 Tue 16:30 Empore Lichthof

**First order coherence of an ideal Bose gas of light** — ●TOBIAS DAMM<sup>1</sup>, JULIAN SCHMITT<sup>1</sup>, DAVID DUNG<sup>1</sup>, CHRISTIAN WAHL<sup>1</sup>, FRANK VEWINGER<sup>1</sup>, JAN KLAERS<sup>1,2</sup>, and MARTIN WEITZ<sup>1</sup> — <sup>1</sup>Institute of Applied Physics, University of Bonn — <sup>2</sup>Present address: Institute for Quantum Electronics, ETH Zürich

Bose-Einstein condensation in the gaseous regime has been observed with cold atoms, exciton-polaritons and more recently with photons in a dye-filled optical microcavity. The latter system is thermally equilibrated both below and above criticality due to repeated absorption and re-emission processes of the dye molecules.

In this work we report on the measurements of the first order coherence of the photon gas confined in a dye-filled optical microcavity below as well as above the phase transition to a photon condensate. Tunable Michelson and Mach-Zehnder interferometers are used to split up and recombine the cavity emission to obtain temporal and spatial coherence information respectively. The observed coherence times range from sub-picoseconds for noncritical system sizes up to microseconds for condensed systems. While below criticality the coherence length is in the micrometer regime, above criticality phase coherence is established macroscopically over the whole mode volume.

Q 27.14 Tue 16:30 Empore Lichthof

**Microstructuring of Trapping Potentials for Coupled Photon Condensates** — ●CHRISTIAN KURTSCHIED<sup>1</sup>, ERIK BUSLEY<sup>1</sup>, DAVID DUNG<sup>1</sup>, TOBIAS DAMM<sup>1</sup>, JULIAN SCHMITT<sup>1</sup>, FRANK VEWINGER<sup>1</sup>, JAN KLÄRS<sup>2</sup>, and MARTIN WEITZ<sup>1</sup> — <sup>1</sup>Institut für Angewandte Physik, Universität Bonn — <sup>2</sup>Institut für Quantenelektronik, ETH Zürich

We present recent work on multiple coupled photon condensates in a single optical microcavity. Unlike Bose-Einstein condensates of dilute atomic gases, the realization of a photon condensate is not feasible using a blackbody radiator by cooling, because the photons then simply

# PHOTONICA2015.

V International School and Conference on Photonics  
& COST actions: MP1204 and BM1205  
& the Second international workshop "Control of light and  
matter waves propagation and localization in photonic  
lattices"  
[www.vin.bg.ac.rs/photonica\\_2015](http://www.vin.bg.ac.rs/photonica_2015)

## *Book of Abstracts*



*Editors*

*Suzana Petrović, Goran Gligorić and Milutin Stepić*

Belgrade, 2015.

system of rate equations for all the relevant Landau levels, and obtain the necessary information about the carrier distribution among the levels, after which we are able to evaluate the permittivity component along the growth direction of the structure, as well as the range of frequencies at which the structure exhibits negative refraction for a predefined total electron sheet density.

## REFERENCES

- [1] C. Gmachl et al., Rep. Prog. Phys. 64, 1533 (2001).
- [2] A. Daničić et al., J. Phys. D 43, 045101 (2010).
- [3] S. Kumar, J. Sel. Top. Quant. Elec. 17, 38 (2011).
- [4] J. Radovanović et al., Appl. Phys. A 109, 763 (2012).

## Dissipation through localised loss in lattice bosonic systems

I. Vasić<sup>1</sup>, D. Cocks<sup>2</sup> and W. Hofstetter<sup>2</sup>

<sup>1</sup>*Scientific Computing Laboratory, Institute of Physics Belgrade, University of Belgrade, Pregrevica 118, 11080 Belgrade, Serbia*

<sup>2</sup>*Institut für Theoretische Physik, Johann Wolfgang Goethe-Universität, Max-von-Laue-Str. 1, 60438 Frankfurt/Main, Germany*  
e-mail: ivana.vasic@ipb.ac.rs

In the recent years, controlled dissipation has proven to be a useful tool for probing of a quantum system in the ultracold setup [1]. We consider dynamics of lattice bosons induced by a dissipative local defect [2]. We address superfluid and supersolid phases that are ground states of an extended Bose-Hubbard Hamiltonian. To this end, we solve the master equation using the Gutzwiller approximation and find that in the usual homogeneous superfluid phase repulsive interactions lead to enhanced dissipation process. On the other hand, our mean-field approach indicates that the effective loss rates are significantly suppressed deep in the supersolid phase where repulsive nearest neighbour interactions play a dominant role. Our numerical results are explained by an analytical insight and in particular, in the limit of strong dissipation we recover the quantum Zeno effect.

## REFERENCES

- [1] G. Barontini et al., Phys. Rev. Lett. 110, 035302 (2013).
- [2] I. Vidanović, D. Cocks, W. Hofstetter, Phys. Rev. A 89, 053614 (2014).



**Bulletin of the American Physical Society****APS March Meeting 2015**

Volume 60, Number 1

Monday–Friday, March 2–6, 2015; San Antonio, Texas

**Session J36: Bosons in Optical Lattices**

2:30 PM–5:30 PM, Tuesday, March 3, 2015

Room: 211

Sponsoring Unit: DAMOP  
Chair: Randall Hulet, Rice University

Abstract ID: BAPS.2015.MAR.J36.13

**Abstract: J36.00013 : Chiral Bosonic Phases on the Haldane Honeycomb Lattice**

4:54 PM–5:06 PM

[Preview Abstract](#)[MathJax On | Off](#) ← [Abstract](#) →**Authors:**Ivana Vasic  
(Institut fuer Theoretische Physik, Goethe-Universitaet, 60438 Frankfurt/Main, Germany)Alexandru Petrescu  
(Department of Physics, Yale University, New Haven, CT 06520, USA and Centre de Physique Theorique, Ecole Polytechnique, CNRS, 91128 Palaiseau, France)Karyn Le Hur  
(Centre de Physique Theorique, Ecole Polytechnique, CNRS, 91128 Palaiseau Cedex, France)Walter Hofstetter  
(Institut fuer Theoretische Physik, Goethe-Universitaet, 60438 Frankfurt/Main, Germany)

Motivated by its recent realization in an ultracold atom experiment [1], we investigate the honeycomb lattice tight-binding model introduced by Haldane [2], for bosons with local interactions at the average filling of one boson per site [3]. We uncover in the ground state phase diagram three phases: a uniform superfluid (SF), a chiral superfluid (CSF) and a plaquette Mott insulator with local current loops (PMI). Nearest-neighbor and next-nearest neighbor currents distinguish CSF from SF, and the phase transition between them is first order. We apply bosonic dynamical mean field theory and exact diagonalization to obtain the zero temperature phase diagram, complementing numerics with calculations of excitation spectra in strong and weak coupling perturbation theory. Furthermore, we explore the possibility of chiral Mott insulating phases at the average filling of one boson every two sites. The characteristic density fluctuations, current correlation functions, and excitation spectra are measurable in ultracold atom experiments. [1] G. Jotzu et al., arXiv:1406.7874 [2] F. D. M. Haldane, Phys. Rev. Lett. 61, 2015 (1988). [3] Ivana Vasic, Alexandru Petrescu, Karyn Le Hur, Walter Hofstetter, arXiv:1408.1411

To cite this abstract, use the following reference: <http://meetings.aps.org/link/BAPS.2015.MAR.J36.13>

## Q 62: Poster: Quantum Optics and Photonics III

Time: Thursday 17:00–19:00

Location: C/Foyer

Q 62.1 Thu 17:00 C/Foyer

**Towards imaging of single Rydberg Atoms** — ●VLADISLAV GAVRYUSEV, GEORG GÜNTER, GERHARD ZUERN, MIGUEL FERREIRA-CAO, GIULIA FARAONI, HANNA SCHEMPP, SHANNON WHITLOCK, and MATTHIAS WEIDEMÜLLER — Physikalisches Institut, Universität Heidelberg, Im Neuenheimer Feld 226, 69120 Heidelberg, Germany

Electronically highly excited (Rydberg) atoms constitute a system with long range interactions which allows to study many intriguing phenomena, ranging from quantum non-linear optics to dipole-mediated energy transport.

To optically image Rydberg atoms we use the interaction enhanced imaging technique [1] which exploits interaction-induced shifts on highly polarizable excited states of probe atoms, that can be spatially resolved via an electromagnetically induced transparency resonance. With this tool we observed by monitoring the Rydberg distribution the migration of Rydberg electronic excitations, driven by quantum-state changing interactions [2]. To push this technique to the level of individual Rydberg atom detection we developed a simple analytic Hard-Sphere model for light propagation through an atom cloud that takes into account interaction effects and technical noise sources. The model predicts a signal to noise ratio  $> 1$  and agrees with numerical non linear light propagation simulations. We will present our progress towards the observation of individual Rydberg atoms which would allow to study the spatial and temporal dynamics of the system.

[1] G. Günter et al., Phys. Rev. Lett. 108, 013002 (2012)

[2] G. Günter et al., Science 342, 954 (2013)

Q 62.2 Thu 17:00 C/Foyer

**Dipolar exchange in interacting Rydberg gases** — ●MIGUEL FERREIRA-CAO, GEORG GÜNTER, HANNA SCHEMPP, MARÍA M. VALADO, VLADISLAV GAVRYUSEV, GERHARD ZÜRN, SHANNON WHITLOCK, and MATTHIAS WEIDEMÜLLER — Physikalisches Institut, Universität Heidelberg, Im Neuenheimer Feld 226, 69120 Heidelberg, Germany

Dipolar exchange interactions play an important role in diverse systems ranging from polar molecules to molecular aggregates, light-harvesting complexes or quantum dots [1]. Ultracold Rydberg atoms offer an ideal system to study dipolar energy transport under the influence of a controlled environment [2].

We have performed measurements of microwave driven Rabi oscillations between Rydberg states with angular momentum state  $s$  and  $p$  in which interactions lead to reduced contrast for high Rydberg densities. This system constitutes a realization of a XY spin model with long-range and anisotropic spin-spin interactions [3,4]. The build-up of correlated phases of the spin distribution is an important aspect under investigation. Applying tomographic methods, future measurements can reveal the time-dependent properties of the many-body state.

[1] B. Yan et al., Nature 501, 521-525 (2013)

[2] G. Günter et al., Science 342, 954 (2013)

[3] D. Maxwell et al., Phys. Rev. Lett. 110, 103001 (2013)

[4] D. Barredo et al., arXiv:1408.1055 (2014)

Q 62.3 Thu 17:00 C/Foyer

**Rydberg dressing of ultracold Potassium atoms via electromagnetically induced transparency** — ●CHRISTOPH SCHWEIGER, NILS PEHOVIK, STEPHAN HELMRICH, ALDA ARIAS, and SHANNON WHITLOCK — Physikalisches Institut, Universität Heidelberg, Im Neuenheimer Feld 226, 69120 Heidelberg

We aim to use laser dressing of Rydberg states of ultracold potassium atoms to create and study novel strongly-correlated quantum gases with long-range interactions. Rydberg dressing, i.e. the small admixture of a Rydberg state to the ground state [1] can be realised via a single-photon transition or a two-photon transition in a three-level ladder scheme. We use a two-photon transition in an electromagnetically induced transparency (EIT) configuration to excite potassium-40 atoms to Rydberg states. The Rydberg state admixture and the lifetime of the dressed-states can be controlled by the ratio of the Rabi frequencies of the laser fields. We will describe a high-power narrow-linewidth laser system used to produce up to 2 W at a wavelength of 460 nm. It is stabilised using spectroscopy of Rydberg states using an EIT resonance using thermal atoms in a vapor cell. We will report our first experiments on EIT spectroscopy of potassium atoms, and discuss the prospects for creating long-range interacting fermionic

quantum gases via Rydberg dressing.

[1] Balewski, J.B. et al. "Rydberg dressing: Understanding of collective many-body effects and implications for experiments", arXiv:1312-6346, 2013

Q 62.4 Thu 17:00 C/Foyer

**Rydberg quantum optics in ultracold gases** — ●IVAN MIRRORODSKIY, HANNES GORNIACZYK, CHRISTOPH TRESP, SEBASTIAN WEBER, and SEBASTIAN HOFFERBERTH — 5. Physikalisches Institut, Universität Stuttgart, Germany

Mapping the strong interaction between Rydberg excitations in ultracold atomic ensembles onto single photons via electromagnetically induced transparency enables manipulation of light on the single photon level. We report the realization of a free-space single-photon transistor, where a single gate photon controls the transmission of more than 60 source photons. We show that this transistor can also be operated as a quantum device, where the gate input state is retrieved from the medium after the transistor operation. In addition, we demonstrate general theoretical techniques for the dynamic description of Rydberg pair state admixture at nonzero interaction angles with respect to the quantization axis. This model explains our experimental observation of dipolar dephasing of D-states.

Q 62.5 Thu 17:00 C/Foyer

**Towards a single-photon source based on Rydberg FWM in thermal microcells** — ●FABIAN RIPKA, YI-HSIN CHEN, ROBERT LÖW, and TILMAN PFAU — 5. Physikalisches Institut Universität Stuttgart, Stuttgart, Deutschland

Photonic quantum devices based on atomic vapors at room temperature combine the advantages of atomic vapors being intrinsically reproducible as well as semiconductor-based concepts being scalable and integrable. One key device in the field of quantum information are single-photon sources. A promising candidate for realizing an on-demand single-photon source relies on the combination of two atomic effects, namely four-wave mixing (FWM) and the Rydberg blockade.

Coherent dynamics to Rydberg states has been demonstrated in thermal vapor cells on nanosecond timescales [1] and van-der-Waals interaction has been observed [2], where the interaction strength exceeds the energy scale of thermal motion and is thus strong enough to enable quantum correlations. Subsequently, we observed both coherent dynamics and effects of dephasing due to Rydberg-Rydberg interaction also in a pulsed FWM scheme [3]. Both are essential effects for building up a single-photon source. As the next step, we are about to reduce the excitation volume towards below the Rydberg interaction range by use of high-NA optics and spatial confinement. First investigations on effects of the confinement on the FWM signal will be shown.

[1] Huber et al., PRL 107, 243001 (2011)

[2] Baluktsian et al., PRL 110, 123001 (2013)

[3] Huber et al., PRA 90, 053806 (2014)

Q 62.6 Thu 17:00 C/Foyer

**Dynamical Mean-Field Theory of Rydberg-dressed quantum gases in optical lattices** — ●ANDREAS GEISSLER<sup>1</sup>, MATHIEU BARBIER<sup>1</sup>, IVANA VASIC<sup>2</sup>, and WALTER HOFSTETTER<sup>1</sup> — <sup>1</sup>Goethe Universität, Frankfurt a. M., Germany — <sup>2</sup>University of Belgrade, Belgrade, Serbia

Recent experiments have shown that Rydberg-dressed quantum many body systems with large numbers of Rydberg excitations in an optical lattice are within reach. We have studied these strongly correlated systems for the bosonic case both within the Gutzwiller approximation (GA) and in a real-space bosonic extension of Dynamical Mean-Field Theory (RB-DMFT) for a two-species lattice Hamiltonian. While RB-DMFT becomes computationally demanding for high lattice fillings, the GA still allows for a thorough investigation of the phase space. We find new exotic quantum phases of lattice commensurate order, giving rise to a devil's staircase in the filling as a function of the chemical potential, long-range interaction and Rabi laser detuning. With increasing hopping, a nonzero condensate fraction starts to emerge, which can coexist with the spatial density-wave order, giving rise to a series of supersolid phases. Spontaneously broken lattice symmetries imply an anisotropic superfluid fraction. We obtain a rich phase diagram in our simulations for the chosen range of experimentally relevant

The impressive development of experimental techniques in ultracold quantum degenerate gases of alkaline-earth atoms in the last years has allowed investigation of strongly correlated systems. Long-lived metastable states in combination with a decoupled nuclear spin give the opportunity to study Hamiltonians beyond the possibilities of current alkali-based experiments such as: two-band Hubbard models, the Kondo lattice model as well as SU(N)-symmetric magnetic systems. From the experimental point of view Ytterbium is the most appropriate due to its large number of bosonic and fermionic (e.g.  $^{173}\text{Yb}$ ) isotopes with a wide range of interaction strengths. We study finite-temperature properties of four-component mixtures of ultracold fermions within the repulsive ( $U > 0$ ) Hubbard model, on the simple cubic lattice. We use the Real-Space Dynamical Mean-Field method, mostly for the half-filling case and at intermediate and strong couplings. We also investigate the case of different interspecies interactions and its influence on the possible magnetic orderings. Finally, we study the role of Hund's coupling (exchange interaction) in finite temperature magnetic phases, within two-band Hubbard model.

Q 15.29 Mon 17:00 C/Foyer

**Detection of topological order in interacting many-body systems using mobile impurities** — ●FABIAN GRUSDY<sup>1,2,3</sup>, NORMAN YAO<sup>3</sup>, DMITRY ABANIN<sup>3,4,5</sup>, and EUGENE DEMLER<sup>3</sup> — <sup>1</sup>Department of Physics and research center OPTIMAS, University of Kaiserslautern, Germany — <sup>2</sup>Graduate School Materials Science in Mainz, Kaiserslautern, Germany — <sup>3</sup>Department of Physics, Harvard University, Cambridge, Massachusetts 02138, USA — <sup>4</sup>Perimeter Institute for Theoretical Physics, Waterloo, Canada — <sup>5</sup>Institute for Quantum Computing, Waterloo, Canada

We present a scheme for the detection of topological order in interacting many-body systems. Our method is based on a generalization of single-particle interferometric schemes developed for the detection of topological invariants of band structures [Atala et al., *Nature Physics* 9, 795 (2013)]. We suggest to couple a spin-1/2 impurity to a (topological) excitation of the many-body system. Performing Ramsey interferometry in combination with Bloch oscillations of the resulting composite particle (a strong-coupling topological polaron) allows to directly detect many body-topological invariants. We demonstrate the feasibility of our scheme by discussing integer and fractional Chern insulators in two dimensions, and show how fractionalized excitations can be detected. We also consider one-dimensional systems and show how symmetry-protected topological invariants can be measured.

Q 15.30 Mon 17:00 C/Foyer

**Steady State Currents in the Driven Dissipative Bose-Hubbard Model** — ●THOMAS MERTZ<sup>1</sup>, IVANA VASIC<sup>1,2</sup>, DANIEL COCKS<sup>1,3</sup>, and WALTER HOFSTETTER<sup>1</sup> — <sup>1</sup>Institute for Theoretical Physics, Goethe-University, Frankfurt am Main, Germany — <sup>2</sup>Institute of Physics, University of Belgrade, Beograd, Serbia — <sup>3</sup>School of Engineering and Physical Sciences, James Cook University, Townsville, Australia

Non-equilibrium dynamics of interacting bosons has been explored intensely in recent experiments in both cold atoms and quantum optical systems. We study the driven Bose-Hubbard model with one-body loss in two dimensions for both spatially homogeneous and inhomogeneous coupling to the environment. We describe dissipation by coupling the system to a Markovian bath in terms of a Lindblad master equation for the reduced density operator. In our work we analyse the steady states of such systems, in particular we consider steady states that exhibit constant particle currents supported by inhomogeneous coupling to the environment. Furthermore, we investigate the effect of the bath parameters on the occurrence of constant currents.

Q 15.31 Mon 17:00 C/Foyer

**Superfluid Phases in the Presence of Artificial Gauge Fields** — ●RAJBIR NIRWAN<sup>1</sup>, IVANA VASIC<sup>1,2</sup>, ALEX PETRESCU<sup>3,4</sup>, KARYN LE HUR<sup>4</sup>, and WALTER HOFSTETTER<sup>1</sup> — <sup>1</sup>Institut für Theoretische Physik, Frankfurt, Germany — <sup>2</sup>Institute of Physics Belgrade, Belgrade, Serbia — <sup>3</sup>Department of Physics, Yale, USA — <sup>4</sup>Centre de Physique Theorique, Ecole Polytechnique, France

In recent years several experiments have reported the realization of artificial gauge fields in systems of cold atoms in optical lattices. One of the latest advances has been the realization of the Haldane model [1,2]. Motivated by these achievements, we investigate the Haldane model for bosons in the weakly interacting regime using the Gross Pitaevskii equation [3]. We study the ground state of the system and find two different superfluid phases. In the normal superfluid

phase the ground state of the system is a Bose-Einstein condensate at zero quasi-momentum. However, for sufficiently strong next-nearest neighbor hopping we find a chiral superfluid phase, where the ground state of the system consists of two condensates formed at finite quasi-momentum. In both cases we calculate the pattern of local mass currents and density distributions.

[1] F. D. M. Haldane, *Phys. Rev. Lett.* 61, 2015 (1988)

[2] G. Jotzu, M. Messer, R. Desbuquois, M. Lebrat, T. Uehlinger, D. Greif, and T. Esslinger, *Nature (London)* 515, 237 (2014)

[3] I. Vasic, A. Petrescu, K. Le Hur, W. Hofstetter, arXiv: 1408.1411

Q 15.32 Mon 17:00 C/Foyer

**Direct observation of chiral order in double layer superfluid** — ●ARNE EWERBECK, CARL HIPPLER, THORGE KOCK, ROBERT BÜCHNER, RAPHAEL EICHBERGER, MATTHIAS ÖLSCHLÄGER, WEN-MIN HUANG, LUDWIG MATHEY und ANDREAS HEMMERICH — Institut für Laseryphysik, Hamburg

A double layer chiral superfluid is formed in the second band of a bipartite optical square lattice. In an ballistic expansion process the two layers are superimposed. The Bragg maxima thus observed exhibit interference patterns, which provide direct information on the formation of chiral order and the presence and character of low energy excitations.

Q 15.33 Mon 17:00 C/Foyer

**Quasi-Condensation and Superfluidity in a Ring Trap** — HANSJÖRG POLSTER and ●CARSTEN HENKEL — University of Potsdam, Germany

Low-dimensional Bose gases suffer from large phase fluctuations that prevent the formation of a proper condensate as defined by Penrose and Onsager. We study a one-dimensional, phase-fluctuating gas in the cross-over region between the ideal gas and the quasi-condensate (weak interactions). Correlation functions of any order are found by mapping the quantum field theory to a random walk in the complex plane, making a classical field approximation [1]. We discuss in particular full distribution functions for the atomic density, including the formation of pairs and clusters at the onset of quasi-condensation. Currently we investigate the distribution function of the total particle current in a rotating ring trap [2] which provides insight into the superfluid behaviour of the gas.

[1] L. W. Gruenberg and L. Gunther, *Phys. Lett. A* 38 (1972) 463; D. J. Scalapino, M. Sears, and R. A. Ferrell, *Phys. Rev. B* 6 (1972) 3409

[2] I. Carusotto and Y. Castin, *C. R. Physique* 5 (2004) 107

Q 15.34 Mon 17:00 C/Foyer

**Failure of extended mean-field theories in one-dimensional Bose gases** — TIM SAUER and ●CARSTEN HENKEL — University of Potsdam, Germany

Due to large thermal fluctuations, low-dimensional Bose gases do not develop a proper condensate, and even the onset of quasi-condensation turns into a cross-over rather than a phase transition. This is actually a challenge to reproduce within a mean-field theory because the modeling of the system seems to require a larger number of relevant hydrodynamic fields. In other words, the statistics of the quantum field is far from Gaussian in the cross-over region. We outline a zoology of mean-field theories [1,2] and develop efficient analytical formulas using a high-temperature expansion. The problems of the theories are illustrated by studying the equation of state and density fluctuations.

[1] C. Mora and Y. Castin, *Phys. Rev. A* 67 (2003) 053615.

[2] R. Walsler, *Opt. Commun.* 243 (2004) 107

Q 15.35 Mon 17:00 C/Foyer

**Quench-condensation of one-dimensional Bose gases** — ●SEBASTIAN ERNE<sup>1,2,4</sup>, THOMAS GASENZER<sup>1,2,3</sup>, and JÖRG SCHMIEDMAYER<sup>4</sup> — <sup>1</sup>Institut für Theoretische Physik, Ruprecht-Karls-Universität Heidelberg, Philosophenweg 16, 69120 Heidelberg, Germany — <sup>2</sup>ExtreMe Matter Institute EMMI, GSI Helmholtzzentrum für Schwerionenforschung GmbH, Planckstraße 1, 64291 Darmstadt, Germany — <sup>3</sup>Kirchhoff-Institut für Physik, INF 227, 69120 Heidelberg, Germany — <sup>4</sup>Vienna Center for Quantum Science and Technology (VCQ), Atominstytut, TU Wien, Vienna, Austria

This work investigates the rapid cooling quench over the dimensional- and quasicondensate-cross-over. Following experiments performed by R. Bückler, W. Rohringer *et al* at the Atominstytut in Vienna, we study the relaxation of such a far-from equilibrium system. The early stage of condensate formation is dominated by solitonic excitations. The high

**Bulletin of the American Physical Society****45th Annual Meeting of the APS Division of Atomic, Molecular and Optical Physics**

Volume 59, Number 8

Monday–Friday, June 2–6, 2014; Madison, Wisconsin

**Session K1: Poster Session II (4:00pm - 6:00pm)**

4:00 PM, Wednesday, June 4, 2014

Room: Exhibit Hall

Abstract ID: BAPS.2014.DAMOP.K1.144

**Abstract: K1.00144 : Superfluid - Mott transition in the presence of artificial gauge fields**[Preview Abstract](#)MathJax On | [Off](#)   ← Abstract →**Authors:**

Ivana Vasic

(ITP, Goethe University, Frankfurt am Main)

Alex Petrescu

(Department of Physics, Yale University, New Haven, USA)

Karyn Le Hur

(Centre de Physique Theorique, Ecole Polytechnique, CNRS, Palaiseau Cedex, France)

Walter Hofstetter

(ITP, Goethe University, Frankfurt am Main)

Several recent cold atom experiments reported implementation of artificial gauge fields in optical lattice systems, paving the way toward observation of new phases of matter. Here we study the tight-binding model on the honeycomb lattice introduced by Haldane, for lattice bosons. We analyze the ground state topology and quasiparticle properties in the Mott phase by applying bosonic dynamical mean field theory, strong-coupling perturbation theory and exact diagonalization. The phase diagram also contains two different superfluid phases. The quasiparticle dynamics, number fluctuations, and local currents are measurable in cold atom experiments.

To cite this abstract, use the following reference: <http://meetings.aps.org/link/BAPS.2014.DAMOP.K1.144>

## Q 57: Quantum gases: Lattices II

Time: Friday 10:30–12:30

Location: UDL HS2002

Q 57.1 Fri 10:30 UDL HS2002

**Artificial graphene with tunable interactions** — ●MICHAEL MESSER<sup>1</sup>, THOMAS UEHLINGER<sup>1</sup>, GREGOR JOTZU<sup>1</sup>, DANIEL GREIF<sup>1</sup>, WALTER HOFSTETTER<sup>2</sup>, ULF BISSBORT<sup>2,3</sup>, and TILMAN ESSLINGER<sup>1</sup> — <sup>1</sup>Institute for quantum electronics, ETH Zurich, Zurich, Switzerland — <sup>2</sup>Institut für Theoretische Physik, Goethe Universität Frankfurt, Frankfurt, Germany — <sup>3</sup>Singapore university of technology and design, Singapore

We create an artificial graphene system with tunable interactions and study the crossover from metallic to Mott insulating regimes, both in isolated and coupled two-dimensional honeycomb layers. The artificial graphene consists of a two-component spin mixture of an ultracold atomic Fermi gas loaded into a honeycomb optical lattice. For strong repulsive interactions we observe a suppression of double occupancy and measure a gapped excitation spectrum. We present a quantitative comparison between our measurements and theory, making use of a novel numerical method to obtain Wannier functions for complex lattice structures. Extending our studies to time-resolved measurements, we investigate the equilibration of the double occupancy as a function of lattice loading time.

Q 57.2 Fri 10:45 UDL HS2002

**Realization of the Hofstadter Hamiltonian with ultracold atoms in optical lattices** — ●MICHAEL LOHSE<sup>1,2</sup>, MONIKA AIDELSBURGER<sup>1,2</sup>, MARCOS ATALA<sup>1,2</sup>, JULIO BARREIRO<sup>1,2</sup>, BELÉN PAREDES<sup>3</sup>, and IMMANUEL BLOCH<sup>1,2</sup> — <sup>1</sup>Fakultät für Physik, Ludwig-Maximilians-Universität, Schellingstrasse 4, 80799 München, Germany — <sup>2</sup>Max-Planck-Institut für Quantenoptik, Hans-Kopfermann-Strasse 1, 85748 Garching, Germany — <sup>3</sup>Instituto de Física Teórica CSIC/UAM C / Nicolás Cabrera, 13-15 Cantoblanco, 28049 Madrid, Spain

We developed a new experimental technique to simulate strong uniform artificial magnetic fields on the order of one flux quantum per plaquette with ultracold atoms in optical lattices. Using laser-assisted tunneling in a tilted optical lattice we engineer complex tunneling amplitudes - so called Peierls phases - whose value depends on the position in the lattice. Thereby, atoms hopping in the lattice accumulate a phase shift equivalent to the Aharonov-Bohm phase of charged particles in a magnetic field. We determine the local distribution of fluxes through the observation of cyclotron orbits of the atoms on isolated four-site square plaquettes. Furthermore, we show that for two atomic spin states with opposite magnetic moments, our system naturally realizes the time-reversal-symmetric Hamiltonian underlying the quantum spin Hall effect; i.e., two different spin components experience opposite directions of the magnetic field

Q 57.3 Fri 11:00 UDL HS2002

**Dynamical synthetic gauge fields using periodically modulated interactions** — SEBASTIAN GRESCHNER<sup>1</sup>, ●GAOYONG SUN<sup>1</sup>, DARIO POLETTI<sup>2</sup>, and LUIS SANTOS<sup>1</sup> — <sup>1</sup>Institut für Theoretische Physik, Leibniz Universität Hannover, Appelstr. 2, DE-30167 Hannover, Germany — <sup>2</sup>Engineering Product Development, Singapore University of Technology and Design, 20 Dover Drive, 138682 Singapore

We show that dynamical synthetic gauge fields may be engineered using periodically modulated interactions. We discuss two scenarios in one-dimensional lattices where periodic interactions may realize a quantum Peierls phase. We discuss how this dynamical gauge field may be probed in stroboscopic measurements of the momentum distribution in time-of-flight experiments. These measurements will show a density-dependent shift of the momentum distribution, revealing as well the quantum character of the created Peierls phase.

Q 57.4 Fri 11:15 UDL HS2002

**Superfluid - Mott transition in the presence of artificial gauge fields** — ●IVANA VIDANOVIC<sup>1</sup>, ALEX PETRESCU<sup>2</sup>, KARYN LE HUR<sup>3</sup>, and WALTER HOFSTETTER<sup>1</sup> — <sup>1</sup>Institut für Theoretische Physik, Johann Wolfgang Goethe-Universität, Frankfurt am Main, Germany — <sup>2</sup>Department of Physics, Yale University, New Haven, USA — <sup>3</sup>Centre de Physique Théorique, Ecole Polytechnique, CNRS, Palaiseau Cedex, France

Several recent cold atom experiments reported implementation of ar-

tificial gauge fields in optical lattice systems, paving the way toward observation of new phases of matter. Here we study the tight-binding model on the honeycomb lattice introduced by Haldane, for lattice bosons. We analyze the ground state topology and quasiparticle properties in the Mott phase by applying bosonic dynamical mean field theory, strong-coupling perturbation theory and exact diagonalization. The phase diagram also contains two different superfluid phases. The quasiparticle dynamics, number fluctuations, and local currents are measurable in cold atom experiments.

Q 57.5 Fri 11:30 UDL HS2002

**Landau-Stark states** — ●ANDREY R. KOLOVSKY — Kirensky Institute of Physics, 660036 Krasnoyarsk, Russia

The term "Landau-Stark states" refers to eigenstates of a charged particle in a 2D lattice in the presence of normal to the lattice plane magnetic and in-plane electric fields. I shall report the recent progress in understanding unusual properties of the Landau-Stark states [1,2] and discuss application of this newly developed theory to the Hall effect with cold atoms subjected to synthetic electric and magnetic fields [3].

[1] A.R.Kolovsky and G.Mantica, Cyclotron-Bloch dynamics of a quantum particle in a 2D lattice, Phys. Rev. E 83, 041123 (2011); Phys. Rev. E 86, 041146 (2012).

[2] A.R.Kolovsky and G.Mantica, Driven Harper model, Phys. Rev. B 86, 054306 (2012).

[3] A.R.Kolovsky, Master equation approach to conductivity of bosonic and fermionic carriers in one- and two-dimensional lattices, Annalen der Physik, DOI: 10.1002/andp201300169 (2013).

Q 57.6 Fri 11:45 UDL HS2002

**Observation of the Meissner effect in bosonic ladders** — ●MARCOS ATALA<sup>1,2</sup>, MICHAEL LOHSE<sup>1,2</sup>, MONIKA AIDELSBURGER<sup>1,2</sup>, JULIO BARREIRO<sup>1,2</sup>, BELÉN PAREDES<sup>3</sup>, and IMMANUEL BLOCH<sup>1,2</sup> — <sup>1</sup>Fakultät für Physik, Ludwig-Maximilians-Universität, Schellingstrasse 4, 80799 München, Germany — <sup>2</sup>Max-Planck-Institut für Quantenoptik, Hans-Kopfermann-Strasse 1, 85748 Garching, Germany — <sup>3</sup>Instituto de Física Teórica CSIC/UAM C / Nicolás Cabrera, 13-15 Cantoblanco, 28049 Madrid, Spain

We implemented a large uniform effective magnetic field with ultracold atoms using laser-assisted tunneling in a ladder created with an optical lattice. Depending on the ratio between the coupling along the rungs of the ladder and the one along the legs of the ladder, the system presents two different phases: the vortex phase, where the probability currents along the bonds have a vortex structure, and the Meissner phase where the currents form a single vortex of infinite length. In order to detect the probability currents associated to the different phases we populated the ground state of the flux ladder and subsequently projected the state into isolated double well potentials that allowed us to measure the average current direction and strength. We observed the different behavior of the current in both regimes. Furthermore, we also measured the time-of-flight momentum distribution of the ground state for different lattice parameters.

Q 57.7 Fri 12:00 UDL HS2002

**String order and correlated phases with periodically modulated interactions** — ●SEBASTIAN GRESCHNER<sup>1</sup>, LUIS SANTOS<sup>1</sup>, and DARIO POLETTI<sup>2</sup> — <sup>1</sup>Institut für Theoretische Physik, Leibniz Universität Hannover, Appelstr. 2, DE-30167 Hannover, Germany — <sup>2</sup>Engineering Product Development, Singapore University of Technology and Design, 20 Dover Drive, 138682 Singapore

The periodic modulation of certain parameters in optical lattice experiments opens interesting possibilities for the control and engineering of lattice gases. Periodically modulated interactions result in a non-linear hopping rate depending on the occupation differences at neighbouring sites [1]. In this way some type of correlated-hopping models [2] as well as dynamical synthetic gauge fields [3] can be engineered. We show how the combined periodic modulation of optical lattices and interactions may be used to realize a very broad class of correlated-hopping Hubbard models for ultracold fermions and bosons. We study the rich physics of this scenario, including pair-superfluidity, dimerized phases as well as exotic Mott-insulator states with a non-vanishing string-order. We also address different aspects of the experimental preparation, stability and detection.

tem. We observe effects that are not explained by thermal reaction rate theory.

Finally, we show multiple signatures of a stochastic resonance in our system, including an increased signal-to-noise ratio for added thermal noise and a measurement of the phase lag of the non-linear response.

Q 32.74 Wed 16:30 Spree-Palais

**Molecular dynamics of trapped cold gases on GPUs** — ●ROMAN NOLTE and REINHOLD WALSER — Institut für Angewandte Physik, Technische Universität Darmstadt

The understanding of classical molecular dynamics of  $N$  trapped interacting atoms is an important precursor in order to achieve quantum degeneracy. In the QUANTUS experiment, which explores quantum gases in microgravity in the ZARM droptower in Bremen, the evaporation time is a scarce resource. It is therefore of critical importance to understand the non-equilibrium dynamics with high precision.

In this contribution we present results of  $N$ -particle 3D molecular dynamics simulation performed on graphic cards (GPU). We investigated the dependence of relaxation on external parameters and the validity of common assumptions.

Q 32.75 Wed 16:30 Spree-Palais

**Dynamical Mean-Field Theory of Rydberg-dressed quantum gases in optical lattices** — ●ANDREAS GEISSLER, IVANA VIDANOVIC, and WALTER HOFSTETTER — Goethe Universität, Frankfurt, Hessen

As recent experiments have shown, it is now possible to investigate Rydberg-dressed quantum systems in optical lattices with a large number of Rydberg excitations. Here we investigate these strongly correlated systems for the bosonic case, by applying the real-space extension of bosonic dynamical mean-field theory (R-BDMFT) to the two-species lattice Hamiltonian in two and three dimensions. We find new exotic quantum phases of lattice commensurate order, giving rise to a devil's staircase in the filling as a function of the chemical potential. For increased hopping, a nonzero condensate fraction starts to emerge, which can coexist with the spatial density order, and thereby lead to a supersolid phase. A rich phase diagram is obtained in our simulations for experimentally realistic parameters.

Q 32.76 Wed 16:30 Spree-Palais

**Towards imaging of single Rydberg Atoms** — ●VLADISLAV GAVRYUSEV, GEORG GÜNTER, HANNA SCHEMPP, MARTIN ROBERT-DE SAINT-VINCENT, STEPHAN HELMRICH, CHRISTOPH S. HOFMANN, MIGUEL FERREIRA-CAO, SHANNON WHITLOCK, and MATTHIAS WEIDEMÜLLER — Physikalisches Institut, Universität Heidelberg, Im Neuenheimer Feld 226, 69120 Heidelberg, Germany

Electronically highly excited (Rydberg) atoms constitute a system with long range interactions which allows to study many intriguing phenomena, ranging from quantum non-linear optics to dipole-mediated energy transport.

We demonstrate optical imaging of Rydberg atoms using the interaction enhanced imaging technique [1], which allows to follow spatially the evolution of the system. This method exploits interaction-induced shifts on highly polarizable excited states of probe atoms, that can be spatially resolved via an electromagnetically induced transparency resonance. With this novel tool we observe the migration of Rydberg electronic excitations, driven by quantum-state changing interactions similar to Förster processes found in complex molecules. We find that the many-body dynamics of the energy transport is influenced by the environment, controlled through the laser parameters [2]. After having improved the optical resolution and CCD detector, we are progressing towards the observation of individual Rydberg atoms which would allow to resolve the spatial and temporal dynamics of the system.

[1] G. Günter et al., Phys. Rev. Lett. 108, 013002 (2012)

[2] G. Günter et al., Science 342, 954 (2013)

Q 32.77 Wed 16:30 Spree-Palais

**Atomic and photonic correlations in interacting Rydberg gases** — ●MIGUEL FERREIRA-CAO, VLADISLAV GAVRYUSEV, GEORG GÜNTER, HANNA SCHEMPP, MARTIN ROBERT-DE-SAINTE-VINCENT, CHRISTOPH S. HOFMANN, SHANNON WHITLOCK, and MATTHIAS WEIDEMÜLLER — Physikalisches Institut, Universität Heidelberg, Im Neuenheimer Feld 226, 69120 Heidelberg, Germany

Ultracold atomic gases involving strongly interacting Rydberg states in combination with electromagnetically induced transparency provide an excellent system to generate nonclassical states of light [1,2].

Recent experiments have delivered evidence of effective photon-

photon interactions and the corresponding atomic correlations [3,4]. Nonlocal effect such as self-focusing due to optical nonlinearities are predicted [5]. Strong antibunching of photons [2] as well as elastic interactions leading to bound state photons [6] are also evidenced.

We explore to which extent the emergence of photonic correlations can be related to atomic correlations through the full counting statistics of the Rydberg number [7] and direct Hanbury-Brown-Twiss measurements of photon correlations.

[1] Y. O. Dudin and A. Kuzmich, Science 336, 887 (2012)

[2] T. Peyronel et al., Nature 488, 57-60 (2012)

[3] D. Maxwell et al. Phys. Rev. Lett. 110, 103001 (2013)

[4] C.S. Hofmann et al., Phys. Rev. Lett. 110, 203601 (2013)

[5] S. Sevinçli et al. Phys. Rev. Lett. 107, 153001 (2011)

[6] O. Firstenberg et al., Nature 502, 71-75 (2013)

[7] H. Schempp et al. PRL accepted, arXiv:1308.0264 (2013)

Q 32.78 Wed 16:30 Spree-Palais

**Artificial Abelian gauge potentials induced by dipole-dipole interactions between Rydberg atoms** — ●ALEXANDRE CESA and JOHN MARTIN — Institut de Physique Nucléaire, Atomique et de Spectroscopie, Université de Liège, Bât. B15, B-4000 Liège, Belgium

We analyze the influence of dipole-dipole interactions between Rydberg atoms on the generation of Abelian artificial gauge potentials and fields. When two Rydberg atoms are driven by a uniform laser field, we show that the combined atom-atom and atom-field interactions give rise to nonuniform, artificial gauge potentials. We identify the mechanism responsible for the emergence of these gauge potentials. Analytical expressions for the latter indicate that the strongest artificial magnetic fields are reached in the regime intermediate between the dipole blockade regime and the regime in which the atoms are sufficiently far apart such that atom-light interaction dominates over atom-atom interactions. We discuss the differences and similarities of artificial gauge fields originating from resonant dipole-dipole and van der Waals interactions. We also give an estimation of experimentally attainable artificial magnetic fields resulting from this mechanism and we discuss their detection through the deflection of the atomic motion.

Q 32.79 Wed 16:30 Spree-Palais

**Coherent Rydberg dynamics and interaction in thermal vapor cells** — ●BERNHARD HUBER, ANDREAS KÖLLE, FABIAN RIPKA, ROBERT LÖW, and TILMAN PFAU — 5. Physikalisches Institut, Uni Stuttgart

Rydberg atoms are of great interest due to their prospects in quantum information. Coherent control of the strong Rydberg-Rydberg interaction allows for the realization of quantum operations and devices which have been demonstrated in ultracold experiments. Since then, coherent dynamics to Rydberg states has been demonstrated also in thermal vapor cells on nanosecond timescales [1] and van der Waals interatomic interaction has been observed [2], where the interaction strength exceeds the energy scale of thermal motion and is thus strong enough to enable quantum correlations.

We present our progress on implementing a non-classical light source from a thermal vapor cell based on four-wave-mixing and Rydberg interaction.

We observe coherent dynamics within a thermal ensemble of Rydberg atoms in a pulsed four-wave-mixing scheme and effects of dephasing due to Rydberg-Rydberg interaction. Furthermore we discuss our recent work on the reduction of the excitation volume to below the Rydberg interaction range (few  $\mu\text{m}$ ) in 3 dimensions by use of high-NA optics and spatial confinement. First results of Rydberg four-wave-mixing therein will be shown.

[1] Huber et al., PRL 107, 243001 (2011)

[2] Baluktsian et al., PRL 110, 123001 (2013)

Q 32.80 Wed 16:30 Spree-Palais

**Rydberg-Rydberg interactions in high density caesium vapour** — ●FABIAN RIPKA<sup>1</sup>, ALBAN URVOY<sup>1</sup>, MARGARITA RESCHKE<sup>1</sup>, DAVID PETER<sup>2</sup>, HARALD KÜBLER<sup>1</sup>, TILMAN PFAU<sup>1</sup>, and ROBERT LÖW<sup>1</sup> — <sup>1</sup>5. Physikalisches Institut, Universität Stuttgart, Pfaffenwaldring 57, 70550 Stuttgart Germany — <sup>2</sup>Institut für Theoretische Physik III, Universität Stuttgart, Pfaffenwaldring 57, 70550 Stuttgart Germany

Rydberg atoms are of growing interest, due to new physics provided by their exaggerated properties. For instance the van-der-Waals interaction between Rydberg atoms has been observed in thermal vapour [1] and is the foundation of several proposals for the realisation of quantum devices. It has also been demonstrated that a phase transition to collective behaviour of the Rydberg atoms can occur, leading to

in optical lattice potentials. To overcome the band gap between the lowest Bloch band and higher excited bands, we consider a scheme where the lattice is driven by an external time-periodic force. By the resulting AC-force on the particles, the bands are coupled coherently and thus hybridize. With the help of Floquet theory we derive effective time-independent Hubbard models describing the band-coupled system. Within this framework we study the melting of a bosonic Mott-insulator as a result of the coherent band coupling. We analyze the respective phase diagram of the bosonic ground state and in addition simulate an experimental protocol, in which the phase transition is achieved by an adiabatic tuning of the driving frequency.

Q 32.35 Wed 16:30 Spree-Palais

**Quantum dynamics of spin waves in ultracold bosonic systems** — ●FRAUKE SEESSELBERG<sup>1</sup>, SEBASTIAN HILD<sup>1</sup>, TAKESHI FUKUHARA<sup>1</sup>, PETER SCHAUSS<sup>1</sup>, JOHANNES ZEIER<sup>1</sup>, IMMANUEL BLOCH<sup>1,2</sup>, and CHRISTIAN GROSS<sup>1</sup> — <sup>1</sup>Max-Planck-Institut für Quantenoptik, Hans-Kopfermann-Straße 1, 85748 Garching, Germany — <sup>2</sup>Fakultät für Physik, Ludwig-Maximilians-Universität München, Schellingstraße 4, 80799 München, Germany

Ultracold quantum gases in optical lattices are promising candidates to simulate spin Hamiltonians, which describe a variety of different phenomena. Single-site resolved imaging of a single spin species allows for the spatially resolved measurement of spin-spin correlations. The atomic Mott insulator corresponds to a spin polarized state with very low entropy. Together with precise local or global spin manipulation, this allows for the study of the dynamics of precisely defined initial spin states.

We report on experiments studying the dynamics of bound and free magnons following local spin flips as well as globally imprinted spin spirals, which are highly excited states of the system. The ability to control the tunneling rate in the ultracold atomic gas allows us to study the scaling behavior of the spin spiral lifetime in one and two dimensions. The data is compared with theoretical predictions based on direct diagonalization.

Q 32.36 Wed 16:30 Spree-Palais

**Towards ultracold fermions in a 2D honeycomb lattice** — ●THOMAS PAINTNER, DANIEL HOFFMANN, MICHAEL GRIENER, JOCHEN GLEITER, WLADIMIR SCHOCH, WOLFGANG LIMMER, BENJAMIN DESSLER, and JOHANNES HECKER DENSCHLAG — Institut für Quantenmaterie, Universität Ulm, Deutschland

We are setting up a new experiment with ultracold fermionic atoms in a two-dimensional honeycomb lattice to investigate intriguing phenomena which are either related to relativistic quantum physics (e.g. Zitterbewegung, Klein tunnelling) or to condensed matter physics (quantum phases, quantum criticality). This system has the underlying geometry of graphene, but can be tuned and controlled in a much greater range. Fermionic <sup>6</sup>Li atoms are captured in a magneto-optical trap and loaded into a strong optical dipole trap. In the next steps, the atoms will be transferred optically into a glass cell and loaded into a 2D optical trap created by blue-detuned laser beam with a TEM<sub>01</sub> mode. We will present the experimental progress towards a two-dimensional degenerate Fermi gas, as well as results on the projection of a honeycomb potential created with a holographic phase plate.

Q 32.37 Wed 16:30 Spree-Palais

**Dissipation through localised loss in bosonic systems with long-range interactions** — ●IVANA VIDANOVIC, DANIEL COCKS, and WALTER HOFSTETTER — Institut für Theoretische Physik, Johann Wolfgang Goethe-Universität, Frankfurt am Main Germany

In the recent years, controlled dissipation has proven to be a useful tool for probing of a quantum system in the ultracold setup. In this paper we consider dynamics of bosons induced by a dissipative local defect. We address superfluid and supersolid phases that are ground states of an extended Bose-Hubbard Hamiltonian. To this end, we solve the master equation using the Gutzwiller approximation and find that in the usual homogeneous superfluid phase repulsive interactions lead to enhanced dissipation process. On the other hand, our mean-field approach indicates that the effective loss rates are significantly suppressed deep in the supersolid phase where repulsive nearest neighbour interactions play a dominant role. Our numerical results are explained by an analytical insight and in particular, in the limit of strong dissipation we recover the quantum Zeno effect.

Q 32.38 Wed 16:30 Spree-Palais

**Steady State Currents in the Driven Dissipative Bose-**

**Hubbard Model** — ●THOMAS MERTZ<sup>1</sup>, IVANA VIDANOVIC<sup>1</sup>, DANIEL COCKS<sup>1,2</sup>, and WALTER HOFSTETTER<sup>1</sup> — <sup>1</sup>Institute for Theoretical Physics, Goethe-University, Frankfurt am Main — <sup>2</sup>School of Engineering and Physical Sciences, James Cook University, Townsville, Australia

Non-equilibrium dynamics of interacting bosons has been explored intensely in recent experiments in both cold atoms and quantum optical systems. We study the driven Bose-Hubbard model with one-body loss in two dimensions for both spatially homogeneous and inhomogeneous coupling to the environment. We describe dissipation by coupling the system to a Markovian bath in terms of a Lindblad master equation for the reduced density operator. In our work we analyse the steady states of such systems, in particular we consider steady states that exhibit constant particle currents supported by inhomogeneous coupling to the environment. Furthermore, we investigate the effect of the bath parameters on the occurrence of constant currents.

Q 32.39 Wed 16:30 Spree-Palais

**Spectroscopy of ultracold Fermions in Triangular Optical Lattices using ultranarrow Optical Transitions** — ALEXANDER THOBE, ●BASTIAN HUNDT, ANDRÉ KOCHANKE, THOMAS PONATH, NIELS PETERSEN, CHRISTOPH BECKER, and KLAUS SENGSTOCK — Zentrum für Optische Quantentechnologien, Universität Hamburg, Luruper Chaussee 149, 22761 Hamburg, Germany

Quantum gases of two-electron atoms in optical lattices offer exciting new possibilities within the field of ultracold atoms. Especially the spin-independent ground state interaction, as well as the long lived metastable <sup>3</sup>P<sub>0,2</sub> states allow the realization of novel many-body Hamiltonians.

Here, we report on our recent experiments with ultracold Ytterbium quantum gases in a triangular optical lattice. In our 2D-/3D-MOT setup, we prepare quantum degenerate gases of fermionic <sup>173</sup>Yb with 1 to 6 spin components. In order to investigate the interaction properties of the metastable <sup>3</sup>P<sub>0</sub>-state, we perform spectroscopy on the narrow <sup>1</sup>S<sub>0</sub> – <sup>3</sup>P<sub>0</sub> clock transition of the ultracold atomic sample. To this end, we load the atoms into a triangular optical lattice at the magic wavelength, where the transition is probed with a stable laser system exhibiting a linewidth of a few Hz.

This work is supported by the DFG within the SFB 925 and GRK 1355, the EU FET-Open Scheme (iSense), and the Marie-Curie ITN on Quantum Sensor Technologies and Applications.

Q 32.40 Wed 16:30 Spree-Palais

**Dynamics of Quantum-Systems with Localized Dissipation** — ●RALF LABOUVIE, ANDREAS VOGLER, SIMON HEUN, BODHADITYA SANTRA, and HERWIG OTT — Fachbereich Physik and Research Center OPTIMAS, Technische Universität Kaiserslautern, 67663 Kaiserslautern, Germany

In our experiment, we are employing a tightly focussed scanning electron-beam on ultra-cold atoms to locally remove particles. This allows us to probe atomic density distributions with high temporal and spatial resolution. Furthermore, the electron-beam is a versatile tool to manipulate the atomic ensemble e.g. it yields the possibility for localized dissipative defects and therefore to create open quantum-systems. The obtained signal shows the system's reaction on the defect and allows to measure pair-correlations and Zeno-like behaviour. This method can also be used to engineer non-equilibrium states and investigate their time evolution e.g. tunnel dynamics in an one-dimensional optical lattice. In addition, subsequently obtained density-profiles allow for an in-vivo investigation of all the samples.

Q 32.41 Wed 16:30 Spree-Palais

**Realization of a finite-size optical lattice for cold fermionic atoms** — ●SIMON MURMANN<sup>1</sup>, ANDREA BERGSCHNEIDER<sup>1</sup>, VINCENT KLINKHAMER<sup>1</sup>, GERHARD ZÜRN<sup>1</sup>, THOMAS LOMPE<sup>1,2</sup>, and SELIM JOCHIM<sup>1</sup> — <sup>1</sup>Physikalisches Institut der Universität Heidelberg, INF 226, 69120 Heidelberg, Germany — <sup>2</sup>Department of Physics, Massachusetts Institute of Technology, Cambridge, MA, USA

We report on the realization of an experimental setup for the deterministic preparation of cold fermionic atoms in multiple-well potentials. Starting with a setup for the preparation of few-atom samples in the vibrational ground state of one tightly focused dipole trap, we expanded our experiment using an acousto-optic deflector (AOD) to split the trapping light into multiple orders forming one potential well each. Both depth and position of the individual wells can be changed independently, allowing the creation of a tunable finite-size optical lat-

tions. Finally, we will discuss different experimental routes to observe the predicted phase transition towards crystalline order.

A 34.21 Wed 16:30 Spree-Palais

**Coherently coupled two-component ultracold bosons** — ●ULRIKE BORNHEIMER, IVANA VIDANOVIC, and WALTER HOFSTETTER — Goethe Universität, Institut für Theoretische Physik, Max-von-Laue Straße 1, 60438 Frankfurt am Main

We investigate an ultracold, two-component bosonic gas in a cubic optical lattice. In addition to density-density interactions, the atoms are subject to coherent light matter interactions that couple different internal hyperfine states. In the strongly interacting Mott regime, the resulting Bose-Hubbard Model can be mapped onto an effective spin Hamiltonian. We examine the influence of the coherent coupling on the system and its' quantum phases by using Gutzwiller Mean Field as well as Bosonic Dynamical Mean Field Theory.

A 34.22 Wed 16:30 Spree-Palais

**Towards atom chips with submicron atom-surface separation** — ●AMRUTA GADGE<sup>1</sup>, ROBERT HOLLENSTEIN<sup>1,2</sup>, FRANCESCO INTRAVAIA<sup>1,3,4</sup>, JESSICA MACLEAN<sup>1</sup>, SAMANTA PIANO<sup>1</sup>, MARK FROMHOLD<sup>1</sup>, CHRISTIAN KOLLER<sup>1</sup>, and PETER KRUGER<sup>1</sup> — <sup>1</sup>Midlands Ultracold Atom Research Centre, School of Physics and Astronomy, University of Nottingham, Nottingham NG7 2RD, UK — <sup>2</sup>Vienna Center for Quantum Science and Technology, TU Wien, Atomistitut, Stadionallee 2 1020 Wien — <sup>3</sup>Institut fuer Physik, Humboldt-Universitaet zu Berlin, Newtonstr. 15, 12489 Berlin, Germany — <sup>4</sup>Max-Born-Institut, 12489 Berlin, Germany

Current atom chip technology enables trapping of atoms at distances of 10-100 microns from the surface. The limitation on the trapping distance arises from distance-dependent effects like surface forces, Johnson noise or fields generated from the adsorbates. Ultra-close trapping of atoms would improve the resolution of cold-atom based surface probes when they are used to map out current distributions and electric and magnetic fields. We are constructing an experimental system to trap atoms very close to the surface, considering relevant effects that can impede trapping at submicron distances. The basis of these experiments is an atom chip incorporating a thin film. We will position an ultracold cloud of Rb87 atoms, above a graphene sheet supported by a TEM grid, which will allow us to control and shift the cloud precisely to specific grid locations. We will compare the losses from the trap when the cloud is above the metal part and the hollow region of the grid. We will show theoretical calculations and experimental progress.

A 34.23 Wed 16:30 Spree-Palais

**Artificial gauge fields in a driven optical lattice** — ●MALTE WEINBERG<sup>1</sup>, CHRISTOPH ÖLSCHLÄGER<sup>1</sup>, JULIAN STRUCK<sup>1</sup>, JULIETTE SIMONET<sup>1</sup>, PATRICK WINDPASSINGER<sup>2</sup>, and KLAUS SENGSTOCK<sup>1</sup> — <sup>1</sup>Institut für Laserphysik, Universität Hamburg, Germany — <sup>2</sup>Institut für Physik, Johannes Gutenberg-Universität, Mainz, Germany

Atomic quantum gases are neutral, and therefore, not affected by external electromagnetic fields in the way electrons are. This constitutes a central issue towards the quantum simulation of solid state models involving an external magnetic field, e.g. the Quantum Spin Hall Effect. Therefore the experimental realization of artificial gauge fields in ultracold atomic systems shall put through quantum simulators of new kinds of exotic quantum matter.

In this perspective, driven optical lattices constitute a versatile tool, which allows controlling both phase and amplitude of the complex tunneling parameters and, thus, generating artificial gauge potentials [1]. By expanding this concept to a triangular lattice structure, it is possible to realize gauge invariant and fully tunable artificial magnetic fluxes that exhibit a staggered ordering [2].

[1] J. Struck et al., Phys. Rev. Lett. 108, 225304 (2012)

[2] J. Struck et al., Nat. Phys. 9, 738-743 (2013)

A 34.24 Wed 16:30 Spree-Palais

**Progress on the Fermi Quantum Microscope** — ●TIMON HILKER<sup>1</sup>, MARTIN BOLL<sup>1</sup>, AHMED OMRAN<sup>1</sup>, THOMAS REIMANN<sup>1</sup>, KONRAD VIEBAHN<sup>1</sup>, ALEXANDER KEESLING<sup>1</sup>, IMMANUEL BLOCH<sup>1,2</sup>, and CHRISTIAN GROSS<sup>1</sup> — <sup>1</sup>Max-Planck-Institut für Quantenoptik, Hans-Kopfermann-Str.1, 85748 Garching — <sup>2</sup>Ludwig-Maximilians-Universität München, Schellingstr. 4, 80799 München

Ultracold atoms in optical lattices have proven to be a powerful tool for investigating quantum many body systems. Recent experiments have demonstrated the power of single-site resolved detection in op-

tical lattices for the study of strongly correlated bosonic many body systems.

In our experiment we plan to apply similar techniques to fermionic systems. Here, we present our progress towards a fermionic many body system trapped in a 3D optical lattice. Li-6 atoms are cooled to degeneracy using a UV-MOT and a fast optical evaporation. We plan to achieve the imaging of single atoms resolved on individual sites of a 2D plane of the lattice by superimposing an additional small-scale pinning lattice onto the larger-scale physics lattice. This freezes out the distribution of atoms during imaging with a high resolution imaging system, which allows to separate the detector from the physical system under study. Different lattice geometries can thus be studied with single atom sensitivity. In this way we plan to probe the quantum phases of the Fermi-Hubbard Hamiltonian by local measurements, and investigate the underlying phenomena associated with condensed matter systems, e.g. quantum magnetism.

A 34.25 Wed 16:30 Spree-Palais

**Stochastic theory of thermal matter fields** — ●HOLGER HAUPTMANN<sup>1</sup>, SIGMUND HELLER<sup>1</sup>, HOLGER KANTZ<sup>2</sup>, and WALTER T. STRUNZ<sup>1</sup> — <sup>1</sup>Technische Universität Dresden — <sup>2</sup>Max-Planck-Institut für Physik komplexer Systeme

We study quasi one-dimensional ultracold Bose gases with repulsive self interaction. A nonlinear stochastic matter-field equation of generalized Gross-Pitaevskii type will be presented to describe Bose gases in the canonical ensemble (fixed particle number). This might be a more realistic experimental scenario than the grand-canonical approach. Applications of this equation to simulate recent experiments from the Schmiedmayer group [1] will be shown, especially the emergence of correlations in quantum many-body systems. Moreover, results for equilibrium coherence properties of one-dimensional Bose gases will be presented.

[1] Langen et al. Nature Physics 9, 640-643 (2013)

A 34.26 Wed 16:30 Spree-Palais

**Nonequilibrium BCS Dynamics of Ultracold Fermi Gases** — ●PETER KETTMANN<sup>1</sup>, SIMON HANNIBAL<sup>1</sup>, MIHAIL CROITORU<sup>2</sup>, ALEXEI VAGOV<sup>3</sup>, VOLLRATH MARTIN AXT<sup>3</sup>, and TILMANN KUHN<sup>1</sup> — <sup>1</sup>Institute of Solid State Theory, University of Münster — <sup>2</sup>Condensed Matter Theory, University of Antwerp — <sup>3</sup>Theoretical Physics III, University of Bayreuth

Ultracold Fermi gases are a convenient testbed for complex interacting Fermi systems like, e.g., superconductors. They are on the one hand easily accessible in experiment. On the other hand their interparticle interaction strength can be tuned to pass from a BCS to a BEC state. In this way, many-body effects in strongly correlated Fermi systems like high-Tc superconductors can be tested in a controlled way.

We investigate the BCS phase of an ultracold Fermi gas. In particular we calculate the nonequilibrium dynamics of a confined <sup>6</sup>Li gas after a sudden excitation, which can be achieved, e.g., by an abrupt change of an external magnetic field or the system confinement. We show that the dynamics of the BCS gap is given by a collective damped oscillation breaking down after a certain time. Afterwards a rather chaotic oscillation appears. We explain this behavior by expressing the quasi-particle equations of motion in terms of a set of coupled oscillators.

Studying systems with different parameters we see that the dynamics show a more or less pronounced initial part of the oscillation depending on the confinement. This is related to size-dependend superfluid resonances predicted by recent theoretical studies [1] and thus to the BCS-BEC crossover. [1] A. A. Shanenko et al., PRA 86, 033612 (2012)

A 34.27 Wed 16:30 Spree-Palais

**Narrow-line laser cooling of dysprosium into an optical dipole trap** — ●MATTHIAS SCHMITT, THOMAS MAIER, HOLGER KADAU, AXEL GRIESMAIER, and TILMAN PFAU — 5. Physikalisches Institut, Universität Stuttgart, Pfaffenwaldring 57, 70569 Stuttgart, Germany

We present our techniques to laser cool dysprosium on a narrow-line transition to achieve suitable conditions to directly load atoms into an optical dipole trap. Dysprosium is the element with the highest magnetic moment and offers a non-spherical symmetric groundstate <sup>5</sup>I<sub>g</sub>. This complex electronic structure leads to several possible cooling and optical pumping transitions. We use a broad cooling transition at 421 nm for Zeeman slowing and capture these atoms in a narrow-line magneto-optical trap using a transition at 626 nm. A transversal cooling stage before the Zeeman slower increases the capture rate by a factor of 4 and atom number by a factor of 3. By using a spectral



**Workshop on**  
**Ultracold Atoms and Gauge Theories**

*(Trieste, 13-17 May 2013)*

**POSTER SESSION**

(14 May, 18:30)

# *Collective modes of interacting bosons in artificial gauge fields*

**Ivana Vidanovic**,\* Ulf Bissbort, Walter Hofstetter

\* Scientific Computing Laboratory, Institute of Physics, Belgrade

Rapid experimental progress in the realization of artificial magnetic fields for cold neutral atoms heads toward the creation and direct observation of exotic quantum states under highly controllable experimental conditions. By combining mean-field and beyond mean-field approaches, we explore the Mott insulator and the superfluid phase of interacting lattice bosons in an artificial magnetic field.

We calculate ground states and excitation spectra of these phases. To demonstrate how the physical quantities of our system can be detected in experiments, we perform numerical calculations of the systems non-equilibrium behaviour under realistic perturbations.

## Q 31: Quantum gases: Optical lattices I

Time: Tuesday 14:00–16:15

Location: E 001

## Group Report

Q 31.1 Tue 14:00 E 001

**Observation of critical behavior at the non-equilibrium Dicke phase transition** — ●FERDINAND BRENNER<sup>1</sup>, RAFAEL MOTTLL<sup>1</sup>, RENATE LANDIG<sup>1</sup>, KRISTIAN BAUMANN<sup>2</sup>, TOBIAS DONNER<sup>1</sup>, and TILMAN ESSLINGER<sup>1</sup> — <sup>1</sup>Quantum Optics Group, ETH Zurich, Switzerland — <sup>2</sup>Department of Applied Physics, Stanford University

We experimentally study critical behavior of the Dicke phase transition, realized by Raman coupling motional degrees of freedom of a Bose-Einstein condensate to the field in a high-finesse optical cavity. We use the natural dissipation channel of the cavity to observe the incoherent fluctuation spectrum of the coupled system in real time. The corresponding measurement backaction introduces additional density fluctuations in the atomic gas and changes the critical behavior of the system. A correlation analysis of the light exiting the cavity reveals the diverging time scale of the fluctuation dynamics, in agreement with the experimentally observed mode softening in the excitation spectrum. We quantitatively compare our measurements with a theoretical model taking into account both cavity and atomic dissipation channels. Future directions of the experiment include Bose-Hubbard physics with cavity-mediated long-range interactions and self-organization in lower dimensions.

Q 31.2 Tue 14:30 E 001

**Semiclassical Study of Intrinsic Photoconductivity of Ultracold Fermions in Optical Lattices** — ●ALEXANDER ITIN<sup>1,2,3</sup>, JANNES HEINZE<sup>1</sup>, JASPER SIMON KRAUSER<sup>1</sup>, NICK FLÄSCHNER<sup>1</sup>, BASTIAN HUNDT<sup>1</sup>, SÖREN GÖTZE<sup>1</sup>, KLAUS SENGSTOCK<sup>1,2</sup>, CHRISTOPH BECKER<sup>1,2</sup>, and LUDWIG MATHEY<sup>1,2</sup> — <sup>1</sup>Institut für Laser-Physik, Universität Hamburg, Germany — <sup>2</sup>Zentrum für Optische Quantentechnologien, Universität Hamburg, Germany — <sup>3</sup>Space Research Institute, Moscow, Russia

We present theoretical analysis of recent experiments reported in [J. Heinze et al., arxiv:1208.4020v2]. Ultracold fermionic atoms in optical lattices were used to simulate the phenomenon of photoconductivity. Using amplitude modulations of the optical lattice, the analog of a persistent alternating photocurrent was induced in the atomic gas. A small fraction of the atoms was excited to the third band as a wavepacket with a well-defined quasimomentum, leaving a hole in the momentum distribution of atoms in the lowest band. The subsequent dynamics is due to an external harmonic trap. It was observed that the particle excitations in the third band exhibit long-lived oscillations with a frequency determined by the initial quasimomentum, while holes in the lowest band behave strikingly differently: an initial fast collapse was followed by periodic partial revivals. We explain both observations by a semiclassical approach to lattice dynamics. By using the Truncated Wigner Approximation and mapping the system onto a classical Hamiltonian resembling a nonlinear pendulum, both the long-lived particle oscillations and decaying hole revivals are understood quantitatively.

Q 31.3 Tue 14:45 E 001

**Motional coherence of fermions immersed in a bosonic bath** — ●RAPHAEL SCHELLE, ARNO TRAUTMANN, TOBIAS RENTROP, and MARKUS K. OBERTHALER — Kirchhoff-Institut für Physik, Universität Heidelberg, Im Neuenheimer Feld 227, 69120 Heidelberg

We study the impact of a Bose Einstein condensate of sodium atoms on the motional coherence of lithium atoms. For this purpose the lithium atoms are exposed to a species-selective lattice potential which allows to prepare the lithium atoms in a motional coherent state by control of the lattice position. We developed a spin echo technique in order to investigate the bath impact on the coherent evolution of the lithium atoms. The interaction between the two components induces a decay of the motional coherence and we extract the corresponding time scale by comparing the spin echo signal for freely evolving lithium atoms to the signal for atoms evolving within the bosonic bath. The observed coherence decay time is consistent with the time scale expected from relaxation measurements of motionally excited states.

Q 31.4 Tue 15:00 E 001

**Collective modes of interacting bosons in artificial gauge fields** — ●IVANA VIDANOVIC, ULF BISSBORT, and WALTER HOFSTETTER — Institut für Theoretische Physik, Johann Wolfgang Goethe-

Universität, 60438 Frankfurt/Main, Germany

Rapid experimental progress in the realization of artificial magnetic fields for cold neutral atoms heads toward the creation and direct observation of exotic quantum states under highly controllable experimental conditions. By combining mean-field and beyond mean-field approaches, we explore the phase diagram of strongly interacting lattice bosons in an artificial magnetic field. We calculate the ground state properties and excitation spectra of various phases. To demonstrate how the physical quantities of our system can be detected in experiments, we perform numerical calculations of the systems non-equilibrium behaviour under realistic perturbations.

Q 31.5 Tue 15:15 E 001

**Gapped chiral phases and spontaneous symmetry breaking for ultracold bosons in zig-zag optical lattices** — ●SEBASTIAN GRESCHNER, LUIS SANTOS, and TEMO VEKUA — Institut für theoretische Physik, Leibniz Universität Hannover, Appelstr. 2, 30167 Hannover, Germany

Ultracold bosons in (quasi)-one-dimensional zig-zag optical lattices - apart from being a theoretically well controllable test-bed to study the properties of possible quantum simulators of quantum antiferromagnetism - exhibit a wealth of interesting physical phenomena some of which are particular for one-dimensional systems [1]. In this talk we present the full phase diagram of ultracold bosons in zig-zag optical lattices for non-integer fillings. We comment on how interactions lead to a competition between spontaneous symmetry breaking chiral SF and two-component SF phases and analyse the emergence of insulating phases as well as gapped chiral phases exhibiting both local currents as well as a finite excitation gap. Some issues of phase preparation and detection are discussed.

[1] S. Greschner et al., arXiv:1202.5386 (2012)

Q 31.6 Tue 15:30 E 001

**Quantum simulation of curved spaces in optical lattices containing topological defects** — ●NIKODEM SZPAK — Fakultät für Physik, Universität Duisburg-Essen

We discuss the possibility of quantum simulation of relativistic fields living in curved spaces realized in optical lattices loaded with ultra-cold atoms. In the low energy regime their dynamics can be described by the Hubbard model which, under some circumstances, can be mapped onto a discrete version of a relativistic quantum field theory. Manipulation of the hopping constants and the lattice topology can lead to the coupling to an artificial Riemann-Cartan geometry containing curvature and torsion. We give examples of several lattice geometries and discuss the properties of the emergent curved spaces with the field theoretic effects, like scattering on curvature centers or vortices and birefringence on torsion lines.

Q 31.7 Tue 15:45 E 001

**Impact of inhomogeneities on antiferromagnetism in cold atom systems** — ●ELENA GORELIK and NILS BLÜMER — Institute of Physics, Johannes Gutenberg University, Mainz, Germany

The study of inhomogeneities in antiferromagnets (AF) is of considerable interest both in condensed matter physics and in the cold-atom context. In atomic clouds, the intrinsic inhomogeneity is due to the presence of a confinement potential, whereas in material context interfaces provide an example of the large-scale inhomogeneities. Localized inhomogeneities, in particular impurities, in both homogeneous and spatially variable background, play important role in the interplay of competing phases.

We employ the real-space extension of dynamical mean-field theory (RDMFT) combined with Hirsch-Fye quantum Monte Carlo (QMC) impurity solver [1,2] to explore the effect of single/multiple impurities on the formation of AF correlations. Both the dimensional aspects and the proximity effects are analyzed. In  $d = 2$ , RDMFT results are compared with those of direct calculations using the determinantal quantum Monte Carlo method.

[1] E. V. Gorelik, I. Titvinidze, W. Hofstetter, M. Snoek, and N. Blümer, Phys. Rev. Lett. **105**, 065301 (2010).[2] N. Blümer and E. V. Gorelik, Comp. Phys. Comm. **182**, 115 (2011).